frontiers | Research Topics

# Diabetes and cardiovascular disease: New therapeutic interventions

**Edited by**
Ludwig Weckbach, Michele D'Amico, Anca Hermenean and Maria Consiglia Trotta

**Coordinated by**
Bartolo Ferraro

**Published in**
Frontiers in Pharmacology

ISSN 1664-8714
ISBN 978-2-8325-5347-3
DOI 10.3389/978-2-8325-5347-3

## About Frontiers

Frontiers is more than just an open access publisher of scholarly articles: it is a pioneering approach to the world of academia, radically improving the way scholarly research is managed. The grand vision of Frontiers is a world where all people have an equal opportunity to seek, share and generate knowledge. Frontiers provides immediate and permanent online open access to all its publications, but this alone is not enough to realize our grand goals.

## Frontiers journal series

The Frontiers journal series is a multi-tier and interdisciplinary set of open-access, online journals, promising a paradigm shift from the current review, selection and dissemination processes in academic publishing. All Frontiers journals are driven by researchers for researchers; therefore, they constitute a service to the scholarly community. At the same time, the *Frontiers journal series* operates on a revolutionary invention, the tiered publishing system, initially addressing specific communities of scholars, and gradually climbing up to broader public understanding, thus serving the interests of the lay society, too.

## Dedication to quality

Each Frontiers article is a landmark of the highest quality, thanks to genuinely collaborative interactions between authors and review editors, who include some of the world's best academicians. Research must be certified by peers before entering a stream of knowledge that may eventually reach the public - and shape society; therefore, Frontiers only applies the most rigorous and unbiased reviews. Frontiers revolutionizes research publishing by freely delivering the most outstanding research, evaluated with no bias from both the academic and social point of view. By applying the most advanced information technologies, Frontiers is catapulting scholarly publishing into a new generation.

## What are Frontiers Research Topics?

Frontiers Research Topics are very popular trademarks of the *Frontiers journals series*: they are collections of at least ten articles, all centered on a particular subject. With their unique mix of varied contributions from Original Research to Review Articles, Frontiers Research Topics unify the most influential researchers, the latest key findings and historical advances in a hot research area.

Find out more on how to host your own Frontiers Research Topic or contribute to one as an author by contacting the Frontiers editorial office: frontiersin.org/about/contact

# Diabetes and cardiovascular disease: New therapeutic interventions

**Topic editors**
Ludwig Weckbach — LMU Munich University Hospital, Germany
Michele D'Amico — University of Campania Luigi Vanvitelli, Italy
Anca Hermenean — Vasile Goldis Western University of Arad, Romania
Maria Consiglia Trotta — University of Campania Luigi Vanvitelli, Italy

**Topic coordinator**
Bartolo Ferraro — Ludwig Maximilian University of Munich, Germany

**Citation**
Weckbach, L., D'Amico, M., Hermenean, A., Trotta, M. C., Ferraro, B., eds. (2024). *Diabetes and cardiovascular disease: New therapeutic interventions*. Lausanne: Frontiers Media SA. doi: 10.3389/978-2-8325-5347-3

# Table of contents

frontiers | Frontiers in Pharmacology

TYPE Editorial
PUBLISHED 12 August 2024
DOI 10.3389/fphar.2024.1472636



OPEN ACCESS

EDITED AND REVIEWED BY
Eliot Ohlstein,
Drexel University, United States

*CORRESPONDENCE
Bartolo Ferraro,
Bartolo.Ferraro@med.uni-muenchen.de
Maria Consiglia Trotta,
mariaconsiglia.trotta2@unicampania.it

RECEIVED 29 July 2024
ACCEPTED 05 August 2024
PUBLISHED 12 August 2024

CITATION
Trotta MC, D'Amico M, Weckbach LT, Hermenean A and Ferraro B (2024) Editorial: Diabetes and cardiovascular disease: new therapeutic interventions.
*Front. Pharmacol.* 15:1472636.
doi: 10.3389/fphar.2024.1472636



# Editorial: Diabetes and cardiovascular disease: new therapeutic interventions

Maria Consiglia Trotta[1]*, Michele D'Amico[1], Ludwig T. Weckbach[2,3,4,5], Anca Hermenean[6,7] and Bartolo Ferraro[3,4]*

[1]Department of Experimental Medicine, University of Campania "Luigi Vanvitelli", Naples, Italy, [2]German Center for Cardiovascular Research (DZHK), Partner Site Munich Heart Alliance, Munich, Germany, [3]Institute of Cardiovascular Physiology and Pathophysiology, Biomedical Center, Ludwig- Maximilian-University Munich, Munich, Germany, [4]Medizinische Klinik und Poliklinik I, Klinikum der Universität, Ludwig-Maximilians-University Munich, Munich, Germany, [5]Walter Brendel Centre of Experimental Medicine, Ludwig-Maximilians-University Munich, University Hospital, Munich, Germany, [6]Faculty of Medicine, Vasile Goldis Western University of Arad, Arad, Romania, [7]"Aurel Ardelean" Institute of Life Sciences, Vasile Goldis Western University of Arad, Arad, Romania

KEYWORDS

**diabetes, cardiovascular diseases, neuro-cardio-renal system, inflammation, therapies, drug discovery, experimental pharmacology**

Editorial on the Research Topic
Diabetes and cardiovascular disease: new therapeutic interventions

Diabetes mellitus (DM) is a chronic disease resulting from a deficiency in insulin production or the body's inability to effectively use this hormone. The consequent chronic hyperglycemia leads to the development of retinopathy, nephropathy, neuropathy, and cardiovascular diseases (Cho et al., 2022).

The optimal control of blood glucose levels can be achieved by modifying lifestyle factors in combination with antidiabetic drugs such as biguanides, dipeptidyl peptidase 4 inhibitors (DPP-4i), sulfonylureas, meglitinides, thiazolidinediones (TZDs), sodium-glucose cotransporter inhibitors (SGLT2i), α-glucosidase inhibitors, glucose-dependent insulinotropic polypeptide (GIP) receptor, glucagon-like peptide-1 receptor agonists (GLP-1RAs) and the various types of insulin (Shahcheraghi et al., 2021). However, some of these medications may have important cardiovascular side effects (Alvarez et al., 2015). Therefore, this Research Topic aimed to generate new therapeutic interventions capable of counteracting the negative effects of diabetes on the cardiovascular system.

In a multicenter observational study, Sardu et al. enrolled 334 diabetic patients with left bundle branch (LBB) block receiving LBB pacing for cardiac resynchronization therapy (CRT). The rate of CRT responders to LBB pacing was evaluated at 1-year follow-up, along with the causes of death, cardiac death, heart failure (HF) hospitalization events, and the expression of selected microRNAs. At 1-year follow-up, patients who responded to LBB pacing showed increased expression of several microRNAs, including miR-26, miR-29, miR-30, miR-92, and miR-145. Increased miR-30 expression was associated with significant improvement of cardiac function in patients with type 2 diabetes mellitus (T2DM), through a reversion of left ventricular remodelling. This would pave the way to test the effects of specific

treatment with mimic-miR on cardiac remodeling in patients treated with LBB pacing.

A network meta-analysis by Huang et al. reveals, for the first time, that different gliflozins have different impacts on various cardiovascular and respiratory outcomes. The study includes twenty-nine randomized controlled trials involving 100,740 subjects. The results of such meta-analysis show that sotagliflozin significantly reduced myocardial infarction, cardiac failure, chronic and congestive cardiac failure, complete atrioventricular block, and pneumonia; while empagliflozin reduced acute cardiac failure, acute respiratory failure, and hypertensive crisis. In addition, dapagliflozin reduced asthma and hypertensive emergency while canagliflozin significantly reduced respiratory tract infections.

An interesting comparison between SGLT2i and DPP4i effects on cardiovascular outcomes in diabetic patients has been performed by Chen et al. The analysis evidenced that a positive autonomic modulation emerged in patients treated with SGLT2i, showing also favorable cardiovascular and renal outcomes. On the contrary, detrimental effects on neuroelectrocardiography were evident in patients treated with DDP4i. Based on these data, SGLT2i could be recommended not only as a first/second-line medication in T2DM patients but also as an effective treatment for HF, independently from DM.

From a different perspective, Riemma et al. extensively described the beneficial effects of SGLT2i and GLP-1RAs in heart failure and cognitive impairment. The authors evidenced that, beyond their efficacy in gaining glycemic control in diabetic patients, both SGLT2i and GLP-1RAs exert cardioprotective and neuroprotective actions through the modulation of oxidative stress, inflammation, insulin signaling, and overload of ions. Therefore, the use of anti-diabetic drugs could be suggested to improve cardiometabolic profile and cognitive impairment in diabetic patients, independently from their anti-diabetic action.

The review by Fu et al. considered recent large-scale clinical trials and basic research articles on the use of SGLT2i, GLP-1RAs, and DPP-4i. It highlighted their cardiorenal protective effects, including the involvement of glucose-dependent and independent pathways, and underscored their clinical implications beyond glycemic management.

Xie et al. compared the effects of eplerenone, an aldosterone receptor antagonist, administered alone or in combination with ADAM17 knockdown in C57BL/6J mice receiving intraperitoneal streptozotocin (STZ) to mimic diabetic cardiomyopathy (DCM). The combined treatment significantly reduced cardiac hypertrophy, fibrosis, and dysfunction. Reduction of transforming growth factor beta 1 (TGF-β1)/Smad3 pathway was observed in both STZ-mice and cardiac fibroblasts exposed to high glucose levels. Therefore, the combination of eplerenone and ADAM17 knockdown could represent a potential therapeutic strategy in DCM, which requires further clinical investigations.

A different novel approach aimed at attenuating cardiac fibrosis induced by chronic diabetes was proposed by Trotta et al., through the formulation of a new drug delivery system (DDS) combining two anti-fibrotic molecules, chrysin (CHR) and the calixarene OTX008 (a Galectin-1 inhibitor) with sulfobutylated β-cyclodextrin (SBECD). The new DDS was tested in hyperglycemic H9c2 cardiomyocytes and STZ-CD1 mice. The treatment notably improved H9c2 cell morphology and viability. Moreover, it reduced Galectin-1 (a pro-fibrotic mediator) and TGF/Smad pathway both *in vitro* and in hearts from mice with chronic diabetes, showing an improved cardiac remodeling and extracellular matrix (ECM) composition. Overall, the novel DDS was able to increase CHR and OTX solubility/bioavailability *in vivo* and to counteract the cardiac fibrosis induced by prolonged hyperglycemia.

Through the prediction of pharmacokinetics, network pharmacology, and molecular docking, the study by Huang et al. identified the combination of rosmarinic acid, luteolin, and resveratrol as potent anti-diabetic molecules. Both *in vitro* α-Amylase inhibition assay and *in vivo* tests, such as oral starch tolerance test and oral glucose tolerance test in diet-induced obese diabetic mice, have demonstrated the predicted hypoglycemic effect of this mixture, capable of addressing the issue of low availability and enhance the efficacy of the single compounds. These promising results could have important implications for human health, although they need to be validated in clinical trials.

In another interesting study, An et al. investigated the impact of celastrol, a pentacyclic triterpene, on hyperglycemia-induced endothelial dysfunction. Low doses of celastrol were effective in attenuating superoxide and pro-inflammatory cytokines production in HUVEC cells exposed to high glucose and palmitic acid-containing media, by increasing the activity of nuclear factor (erythroid-derived 2)-like protein 2 (Nrf2). Furthermore, diabetic db/db mice treated with celastrol showed reduced blood glucose concentration and improved insulin sensitivity after fasting. The same mouse strain showed decreased capillary density in a wound healing model when injected intravenously with an adeno-associated virus (AAV9) harboring Nrf2 short hairpin (sh)RNA. Taken together, these findings may point at celastrol as a future new therapeutic approach for the short-term treatment of refractory diabetes-related skin ulcers and vascular defects.

The review by Zhang et al. focused on the importance of ferroptosis, a new form of cell death characterized by iron-dependent lipid peroxidation, in the pathogenesis of diabetic cardiovascular diseases (CVDs). The manuscript also summarizes the positive effects of traditional Chinese medicine in CVD prevention, by focusing on the regulation of ferroptosis by polyphenols, alkaloids, and saponins. This evidence provides a new scientific basis for innovative management of CVDs through modulation of ferroptosis.

Collectively, these studies tackle diabetes-induced cardiovascular complications from different perspectives and provide exciting new therapeutic approaches for their management.

## Author contributions

MT: Writing–original draft, Writing–review and editing. MD'A: Writing–review and editing. LW: Writing–review and editing. AH: Writing–review and editing. BF: Writing–review and editing, Writing–original draft.

## Funding

The author(s) declare that financial support was received for the research, authorship, and/or publication of this article. AH is supported by the Romanian Ministry of Research, Innovation, and Digitization, CNCS/CCCDI-UEFISCDI, project number PN-

III-P4-ID-PCE-2020-1772, within PNCDI III. LW is supported by the Else Kröner Fresenius Stiftung (Project 2023_EKEA.11).

## Conflict of interest

The authors declare that the research was conducted in the absence of any commercial or financial relationships that could be construed as a potential conflict of interest.

## Publisher's note



## References

Alvarez, C. A., Lingvay, I., Vuylsteke, V., Koffarnus, R. L., and McGuire, D. K. (2015). Cardiovascular risk in diabetes mellitus: complication of the disease or of antihyperglycemic medications. *Clin. Pharmacol. Ther.* 98(2), 145–161. doi:10.1002/cpt.143

Cho, Y., Park, H. S., Huh, B. W., Seo, S. H., Seo, D. H., Ahn, S. H., et al. (2022) Prevalence and risk of diabetic complications in young-onset versus late-onset type 2 diabetes mellitus. *Diabetes Metab.* 48(6), 101389. doi:10.1016/j.diabet.2022.101389

Shahcheraghi, S. H., Aljabali, A. A. A., Al Zoubi, M. S., Mishra, V., Charbe, N. B., Haggag, Y. A., et al. (2021). Overview of key molecular and pharmacological targets for diabetes and associated diseases. *Life Sci.* 278, 119632. doi:10.1016/j.lfs.2021.119632

frontiers | Frontiers in Pharmacology

TYPE Review
PUBLISHED 26 October 2023
DOI 10.3389/fphar.2023.1286718



OPEN ACCESS

EDITED BY
Michele D'Amico,
University of Campania Luigi Vanvitelli, Italy

REVIEWED BY
Xing Luo,
Harbin Medical University, China
Dario Siniscalco,
University of Campania Luigi Vanvitelli, Italy

*CORRESPONDENCE
Yabin Zhou,
zhouyabin@hotmail.com

†These authors have contributed equally to this work and share first authorship

RECEIVED 31 August 2023
ACCEPTED 16 October 2023
PUBLISHED 26 October 2023

CITATION
Zhang X, Sun J, Wang J, Meng T, Yang J and Zhou Y (2023), The role of ferroptosis in diabetic cardiovascular diseases and the intervention of active ingredients of traditional Chinese medicine.
*Front. Pharmacol.* 14:1286718.
doi: 10.3389/fphar.2023.1286718



# The role of ferroptosis in diabetic cardiovascular diseases and the intervention of active ingredients of traditional Chinese medicine

Xiaobing Zhang[1†], Jing Sun[2†], Jianying Wang[3†], Tianwei Meng[1†], Jianfei Yang[2] and Yabin Zhou[2*]

[1]Graduate School, Heilongjiang University of Chinese Medicine, Harbin, Heilongjiang, China, [2]Department of Cardiovascular Medicine, First Affiliated Hospital of Heilongjiang University of Chinese Medicine, Harbin, Heilongjiang, China, [3]Department of Endocrinology, Hanan Branch of the Second Affiliated Hospital of Heilongjiang University of Chinese Medicine, Harbin, Heilongjiang, China

Cardiovascular diseases (CVDs), encompassing ischaemic heart disease, cardiomyopathy, and heart failure, among others, are the most prevalent complications of diabetes and the leading cause of mortality in patients with diabetes. Cell death modalities, including apoptosis, necroptosis, and pyroptosis, have been demonstrated to be involved in the pathogenesis of CVDs. As research progresses, accumulating evidence also suggests the involvement of ferroptosis, a novel form of cell death, in the pathogenesis of CVDs. Ferroptosis, characterised by iron-dependent lipid peroxidation, which culminates in membrane rupture, may present new therapeutic targets for diabetes-related cardiovascular complications. Current treatments for CVDs, such as antihypertensive, anticoagulant, lipid-lowering, and plaque-stabilising drugs, may cause severe side effects with long-term use. Traditional Chinese medicine, with its broad range of activities and minimal side effects, is widely used in China. Numerous studies have shown that active components of Chinese medicine, such as alkaloids, polyphenols, and saponins, can prevent CVDs by regulating ferroptosis. This review summarises the recent findings on the regulatory mechanisms of active components of Chinese medicine against ferroptosis in CVDs, aiming to provide new directions and a scientific basis for targeting ferroptosis for the prevention and treatment of diabetic CVDs.

KEYWORDS

**ferroptosis, diabetes, cardiovascular diseases, traditional Chinese medicine, active ingredients, mechanism**

## 1 Introduction

Over the past 3 decades, the number of individuals with diabetes has quadrupled, with approximately 1 in 11 adults currently affected. According to estimates by the International Diabetes Federation, the number of individuals with diabetes is projected to rise to 642 million by 2040, with over 90% of cases to be type 2 diabetes mellitus (T2DM) (Zheng et al., 2018). Diabetes is a major risk factor for cardiovascular diseases (CVDs), which in turn are the primary cause of death in individuals with diabetes (Glovaci et al., 2019). Furthermore, once CVDs occur, diabetes exacerbates the progression and impacts prognosis of CVDs (Beckman and Creager, 2016). CVDs are the most prevalent complications of diabetes; they encompass a number of conditions in the heart or blood

vessels, such as ischaemic heart disease, cardiomyopathy, and heart failure (HF), and have become the most common cause of death globally (Townsend et al., 2022). Research shows that the number of people with CVDs increased from 271 million in 1990 to 523 million in 2019, i.e., nearly doubled; the number of deaths has also steadily increased, with approximately 18.6 million people having died from CVDs in 2019 (Roth et al., 2020). Therefore, there is an urgent need to identify potential pathogenic mechanisms of CVDs and find feasible treatment targets.

Cell death is a fundamental biological process, crucial in all aspects of embryonic development, growth, and aging (Bertheloot et al., 2021). Various forms of cell death, such as apoptosis, necroptosis, and pyroptosis, have been confirmed to be closely related to the pathogenesis of CVDs (Del Re et al., 2019). Increasing evidence shows that ferroptosis is also involved in the pathogenesis of CVDs (Fang et al., 2023). The concept of ferroptosis was first proposed by Dixon in 2012 (Dixon et al., 2012). Different from previously described forms of cell death, ferroptosis is a form of nonapoptotic cell death caused by iron-dependent lipid peroxidation, leading to membrane rupture (Chen et al., 2021a). This process can be inhibited by iron chelators or lipophilic antioxidants but not by inhibitors of apoptosis or necrosis (Stockwell et al., 2017; Hong et al., 2022). Cells undergoing ferroptosis show morphological characteristics such as mitochondrial shrinkage, outer membrane rupture, and a reduction or disappearance of mitochondrial cristae, while the cell nucleus is normal in size, without chromatin condensation (Mou et al., 2019; Lei et al., 2022). All these signs indicate that ferroptosis is a new form of cell death.

Therefore, studying the mechanism of ferroptosis may allow finding new targets for the treatment of CVDs. Currently, antihypertensive, anticoagulant, lipid-lowering, and plaque-stabilising drugs are commonly used in the clinical treatment of CVDs (Visseren et al., 2021). However, the side effects of long-term use of these drugs and the development of drug resistance show the urgent need to seek new treatment approaches. Traditional Chinese medicine (TCM) has a long history, and current evidence shows a definite efficacy of Chinese medicines in treating coronary atherosclerotic heart disease, HF, and other CVDs, with minimal toxic side effects (Hao et al., 2017; Meng et al., 2022). However, the mechanisms of CVDs are complex, and Chinese medicines comprise multiple components and have multiple targets. The specific role of ferroptosis in the treatment of CVDs with Chinese medicines is not yet clear. Therefore, this review discusses the mechanisms of ferroptosis and summarises the related mechanisms of active components of Chinese medicines in preventing and treating CVDs by targeting ferroptosis, in order to provide a new direction for the treatment of diabetic CVDs.

# 2 Ferroptosis and its regulatory mechanisms

The key to ferroptosis is the Fenton reaction caused by iron overload in cells, which leads to massive generation of hydroxyl radicals ($^{\bullet}$OH) and reactive oxygen species (ROS) and to the oxidation of polyunsaturated fatty acid (PUFA)-containing phospholipids (PUFA-PLs) (Lei et al., 2022). This process mainly involves metabolic pathways of iron, lipid, and amino acid metabolism (Shi et al., 2021). The specific details are shown in Figure 1.

## 2.1 Iron metabolism and ferroptosis

Iron is one of the essential trace elements in the human body. The ability of iron to provide or accept electrons in the intra- and extracellular environments makes it highly reactive and toxic (Ganz, 2013; Nemeth and Ganz, 2021). The maintenance of iron homeostasis is of great significance. Cells mainly take in iron through endocytosis. The complex formed by the binding of transferrin (TF), carrying two ferric ions (Fe3+), to TF receptor 1 (TFR1) on the cell membrane enters the cell through receptor-mediated endocytosis, which is dependent on the clathrin protein (Kawabata, 2019; Zeidan et al., 2021). Under acidic conditions of the endosome, Fe3+ separates from TF and is reduced to the ferrous ion (Fe2+) by six-transmembrane epithelial antigen of prostate 3 (STEAP3), and then Fe2+ is transported to the unstable iron pool in the cytoplasm by divalent metal transporter 1 (DMT1, also known as NRAMP2 and SLC11A2) (Vogt et al., 2021). The TF–TFR1 complex in the endosome is transported to the cell surface and reused by the cell (Kawabata, 2019). Knocking down TFR1 could inhibit cardiomyocyte ferroptosis induced by ischaemia/reperfusion (I/R) injury in rat hearts (Tang et al., 2021b). In addition, heat shock protein family B (small) member 1 (HSPB1) can inhibit the expression of TFR1 to reduce cellular iron levels. Overexpression of HSPB1 can inhibit erastin-induced ferroptosis (Sun et al., 2015).

Cytoplasmic iron can be utilised for the synthesis of haem and iron–sulphur clusters in mitochondria or stored in ferritin (Galaris et al., 2019), a complex composed of 24 ferritin heavy chain 1 (FTH1) and ferritin light chain (FTL) subunits. FTH1 possesses ferroxidase activity, which enables the conversion of Fe2+ to Fe3+ for storage (Ganz, 2013; Zhang N. et al., 2021), thereby preventing the Fenton reaction between Fe2+ and hydrogen peroxide and reducing ROS generation. Nuclear receptor coactivator 4 (NCOA4) interacts with FTH1, mediating the degradation of ferritin in autophagosomes to subsequently release its iron content into the labile iron pool, a process termed ferritinophagy (Muckenthaler et al., 2017; Ajoolabady et al., 2021). Specific knockout of the *Fth1* gene in mouse cardiomyocytes increases ROS accumulation, thereby increasing the sensitivity to ferroptosis (Fang X. et al., 2020). Conversely, knocking down NCOA4 can reduce intracellular iron levels and ROS accumulation, alleviating endothelial damage (Qin et al., 2021).

Hepcidin, a peptide hormone secreted by the liver, induces the degradation of ferroportin (FPN) (Nemeth and Ganz, 2021), the only known cellular iron export protein (Billesbølle et al., 2020). The hepcidin/FPN axis plays a crucial role in maintaining cellular iron homeostasis. Recent studies have shown that FPN is also present in cardiomyocytes. Specific knockout of *Fpn* in mouse cardiomyocytes leads to iron overload and severe cardiac damage, whereas mice with the hepcidin gene knocked out exhibit a milder phenotype and a longer survival time (Lakhal-Littleton et al., 2015; Lakhal-Littleton et al., 2016).

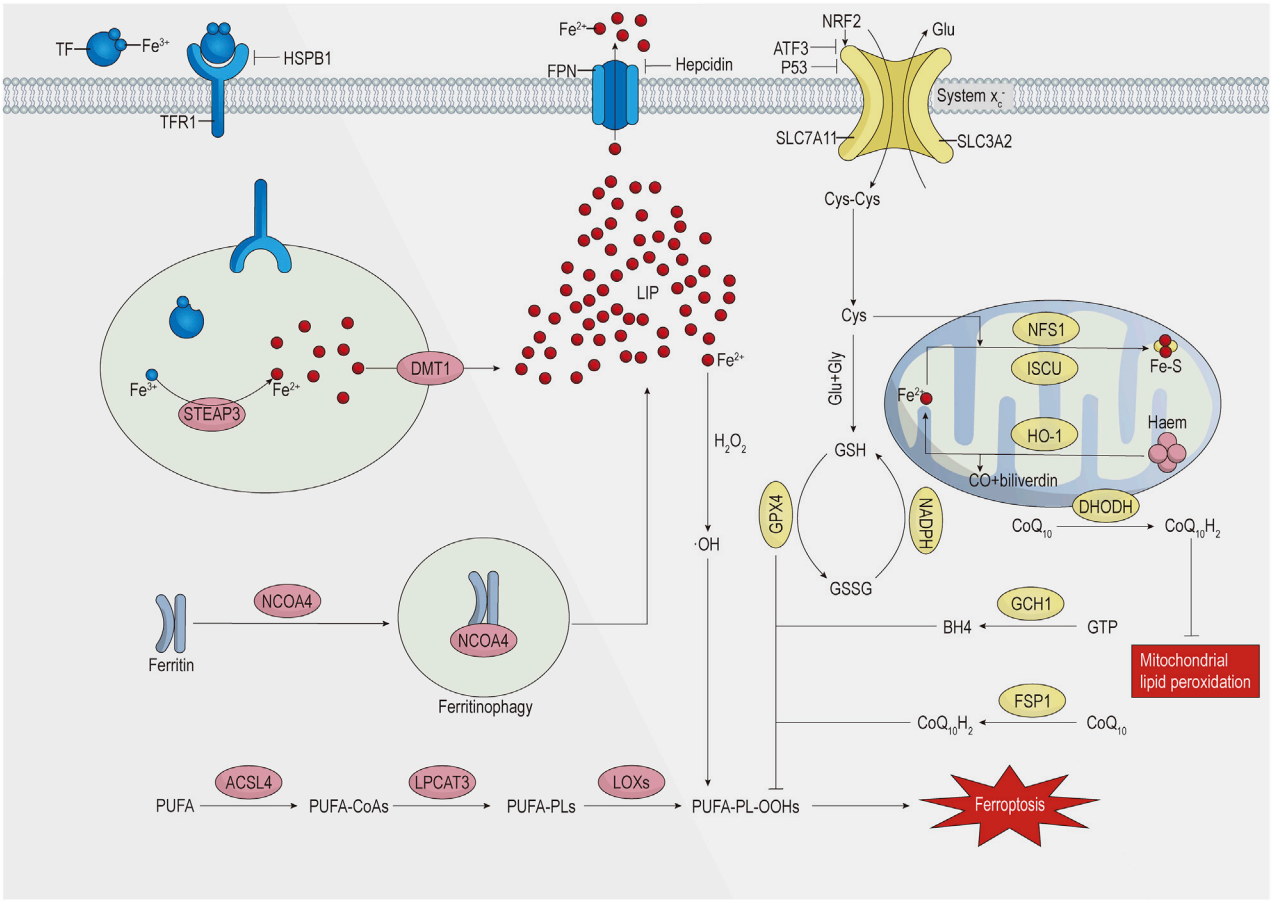


FIGURE 1
Schematic representation of the regulatory mechanism of ferroptosis.

The iron-responsive element/iron regulatory protein (IRE/IRP) regulatory system regulates iron homeostasis at the transcriptional level. When cells are iron deficient, IRP1 or IRP2 binds to the IREs in the 3′untranslated regions (UTRs) of *TFR1* mRNA and *DMT1* mRNA, stabilising transcription and enhancing translation. Conversely, IRP1 or IRP2 binds to the IREs in the 5′UTRs of *FTH1* mRNA and *FPN1* mRNA, inhibiting translation. When cellular iron is sufficient, IRP1 assembles a cubane Fe–S cluster, preventing its binding to IREs, while IRP2 is degraded, thereby inhibiting iron accumulation (Muckenthaler et al., 2008; Anderson and Frazer, 2017). Research has confirmed that overexpression of IRP1 significantly promotes melanoma cell ferroptosis induced by erastin and RSL3 (Yao et al., 2021).

Mitochondria are crucial for the synthesis of haem and iron–sulphur clusters, thus playing a vital role in maintaining cellular iron homeostasis (Ali et al., 2022). Mitoferrin 1 (also known as SLC25A37) and mitoferrin 2 (also known as SLC25A28) are key mitochondrial iron import proteins. Knocking down mitoferrin 1 can reduce mitochondrial iron levels, decrease ROS generation, and inhibit ferroptosis (Huang et al., 2018). Haem oxygenase 1 (HO-1) degrades haem into CO, $Fe^{2+}$, and biliverdin; HO-1 expression is regulated by nuclear factor-erythroid 2-related factor 2 (NRF2) (Zhang et al., 2020). However, whether HO-1 promotes or inhibits ferroptosis remains a matter of debate among researchers (Cai et al., 2022; Shi J. et al., 2023; Liu et al., 2023; Ni et al., 2023). Furthermore, several mitochondrial proteins involved in the synthesis of iron–sulphur clusters, such as cysteine desulfurase (NFS1), iron–sulphur cluster assembly enzyme (ISCU), CDGSH iron sulphur domain 1 (CISD1), and CDGSH iron sulphur domain 2 (CISD2), can inhibit ferroptosis by reducing mitochondrial $Fe^{2+}$ levels and decreasing ROS production (Chen et al., 2021a).

## 2.2 Lipid metabolism and ferroptosis

PLs are crucial components of the cell membrane, and the peroxidation of PUFA-PLs is a prerequisite for ferroptosis (Wu et al., 2021). Owing to the weak C–H bond at the *bis*-allylic position of PUFAs, they are susceptible to peroxidation (Stockwell, 2022). Increasing the cellular content of PUFAs increases the sensitivity to ferroptosis (Liang D. et al., 2022). However, free PUFAs cannot directly cause ferroptosis; they need to be integrated into PLs of the plasma membrane to drive ferroptosis (Li J. et al., 2020; Stockwell, 2022). Monounsaturated fatty acids (MUFAs) can compete with PUFAs for the incorporation into PLs. Since MUFAs lack a *bis*-allylic structure, they are less prone to peroxidation (Naowarojna et al., 2023). Increasing the MUFA content can reduce the sensitivity

to ferroptosis (Das, 2019). Acyl-coenzyme A (CoA) synthetase long-chain family member 3 (ACSL3) mediates the activation of MUFAs and inserts them into PLs (Pope and Dixon, 2023). The absence of ACSL3 can increase the sensitivity of melanoma cells to ferroptosis (Ubellacker et al., 2020).

Unlike ACSL3, acyl-CoA synthetase long-chain family member 4 (ACSL4) is capable of catalysing the binding of PUFAs (particularly arachidonic and adrenic acids) to CoA to generate PUFA-CoAs. Subsequently, lysophosphatidylcholine acyltransferase 3 (LPCAT3) incorporates them into PLs, forming PUFA-PLs (primarily arachidonic acid-phosphatidylethanolamines and adrenic acid-phosphatidylethanolamines) (Lin Z. et al., 2021; Lei et al., 2022). ACSL4 and LPCAT3 are key drivers in the production of ferroptotic lipids (Jiang et al., 2021; Stockwell, 2022), while the inactivation of ACSL4 or LPCAT3 reduces or inhibits ferroptosis. For instance, the knockout of *Acsl4* significantly reduces ferroptosis in mice with acute kidney injury (Wang Y. et al., 2022), while inhibition of LPCAT3 protects human cells from ferroptosis (Reed et al., 2022).

PUFA-PLs form hydroperoxides (PUFA-PL-OOHs) through nonenzymatic or enzymatic oxidation reactions (Jiang et al., 2021; Shi et al., 2021). Nonenzymatic oxidation reactions are primarily triggered by the Fenton reaction product $^{\bullet}OH$, and unlike strictly controlled enzymatic reactions, they are poorly controlled and prone to chain reactions (Shi et al., 2021). Lipoxygenases (LOXs) are a class of non-haem iron oxidoreductases that mediate enzymatic reactions in lipid oxidation (Chen et al., 2021b). Knocking out LOXs can inhibit erastin-induced ferroptosis (Yang et al., 2016). As the peroxidation reaction continues and a large number of secondary products are generated, the integrity of the cell membrane is compromised, triggering ferroptosis.

## 2.3 Amino acid metabolism and ferroptosis

The glutathione (GSH) peroxidase 4 (GPX4)-mediated GSH metabolic pathway is a crucial defence mechanism against ferroptosis (Seibt et al., 2019). GPX4 can reduce PUFA-PL-OOHs to nontoxic PUFA-PL alcohols (PUFA-PL-OHs), protecting the cell membrane from oxidative damage, while reduced GSH is converted into oxidised GSH (GSSG) (Imai et al., 2017). GPX4 is a selenoprotein, and its expression is regulated by the selenium content (Forcina and Dixon, 2019). Overexpression of GPX4 can inhibit RSL3-induced ferroptosis, whereas inhibition of GPX4 increases cell sensitivity to ferroptosis (Yang et al., 2014). However, some tumour cells can still resist ferroptosis after inhibition of GPX4, which indicates the existence of GPX4-independent defence pathways against ferroptosis (Bersuker et al., 2019).

GSH, a key substrate of GPX4, is a tripeptide antioxidant composed of cysteine, glutamic acid, and glycine. Reduced nicotinamide adenine dinucleotide phosphate (NADPH) can maintain GSH levels (Lu, 2009). Depletion of GSH inactivates GPX4, triggering ferroptosis (Sun et al., 2018). Cysteine is considered the rate-limiting precursor for GSH synthesis (Shi Y. et al., 2023). Although cysteine can be synthesised through the transsulphuration pathway, most cells primarily obtain cysteine through the cystine–glutamate antiporter (system $x_c^-$) (Fang et al., 2023). System $x_c^-$belongs to the heterodimeric amino acid transporter (HAT) family and is composed of the light chain subunit SLC7A11 (also known as xCT) and the heavy chain subunit SLC3A2 (also known as 4F2HC) (Liu M.-R. et al., 2021). SLC7A11 mainly mediates the transport function of the complex, while SLC3A2 primarily stabilises the complex structure and ensures proper membrane localisation (Liu M.-R. et al., 2021; Fang et al., 2023). Extracellular cystine and intracellular glutamate are exchanged at a 1:1 ratio through system $x_c^-$, with cystine being converted into cysteine in the cell to participate in GSH synthesis (Lewerenz et al., 2013). SLC7A11 has multiple regulatory factors. Activating transcription factor 3 (ATF3) can inhibit SLC7A11 activity, deplete GSH, and thus promote erastin-induced ferroptosis (Wang et al., 2020). p53, a tumour suppressor protein, can also inhibit SLC7A11 expression, increasing cell sensitivity to ferroptosis (Jiang et al., 2015). NRF2 can promote SLC7A11 expression, and knocking down NRF2 promotes the occurrence of ferroptosis (Dong et al., 2020). Additionally, as the extracellular concentration of glutamate increases, it can inhibit system $x_c^-$, thereby inducing ferroptosis, which indicates that glutamate is also a regulatory factor in ferroptosis (Fan et al., 2023).

## 2.4 Other defensive mechanisms against ferroptosis

As mentioned above, there are GPX4-independent defence mechanisms against ferroptosis. Ferroptosis suppressor protein 1 (FSP1) can convert $CoQ_{10}$ (also known as ubiquinone) into $CoQ_{10}H_2$ (also known as ubiquinol). As a lipophilic antioxidant, $CoQ_{10}H_2$ can prevent lipid peroxidation and inhibit ferroptosis (Li et al., 2023). Similarly, dihydroorotate dehydrogenase (DHODH) converts CoQ10 on the inner mitochondrial membrane into $CoQ_{10}H_2$, thus inhibiting mitochondrial ferroptosis (Lei et al., 2022; Stockwell, 2022). GTP cyclohydrolase 1 (GCH1) mediates the generation of tetrahydrobiopterin (BH4). BH4 inhibits ferroptosis by capturing lipid free radicals. Additionally, GCH1 can increase the abundance of $CoQ_{10}H_2$ and consume PUFA-PLs to prevent ferroptosis (Jiang et al., 2021; Stockwell, 2022). These pathways provide potential targets for intervening in ferroptosis.

# 3 Ferroptosis and diabetes

Increasing evidence suggests that ferroptosis plays a significant role in the development and progression of T2DM and its complications (Deng et al., 2023). Maintaining iron homeostasis is crucial for the endocrine system, as iron metabolism is involved in various glucose pathways, including insulin secretion, hepatic metabolism, and lipid metabolism (Backe et al., 2016; Zhang Z. et al., 2021; Gao et al., 2022). Iron overload is a known risk factor for T2DM (Simcox and McClain, 2013), as excessive $Fe^{2+}$ triggers the Fenton reaction, resulting in the production of large amounts of ROS. Owing to the weak antioxidant capacity of pancreatic β cells and low expression and activity of superoxide dismutase (SOD) and

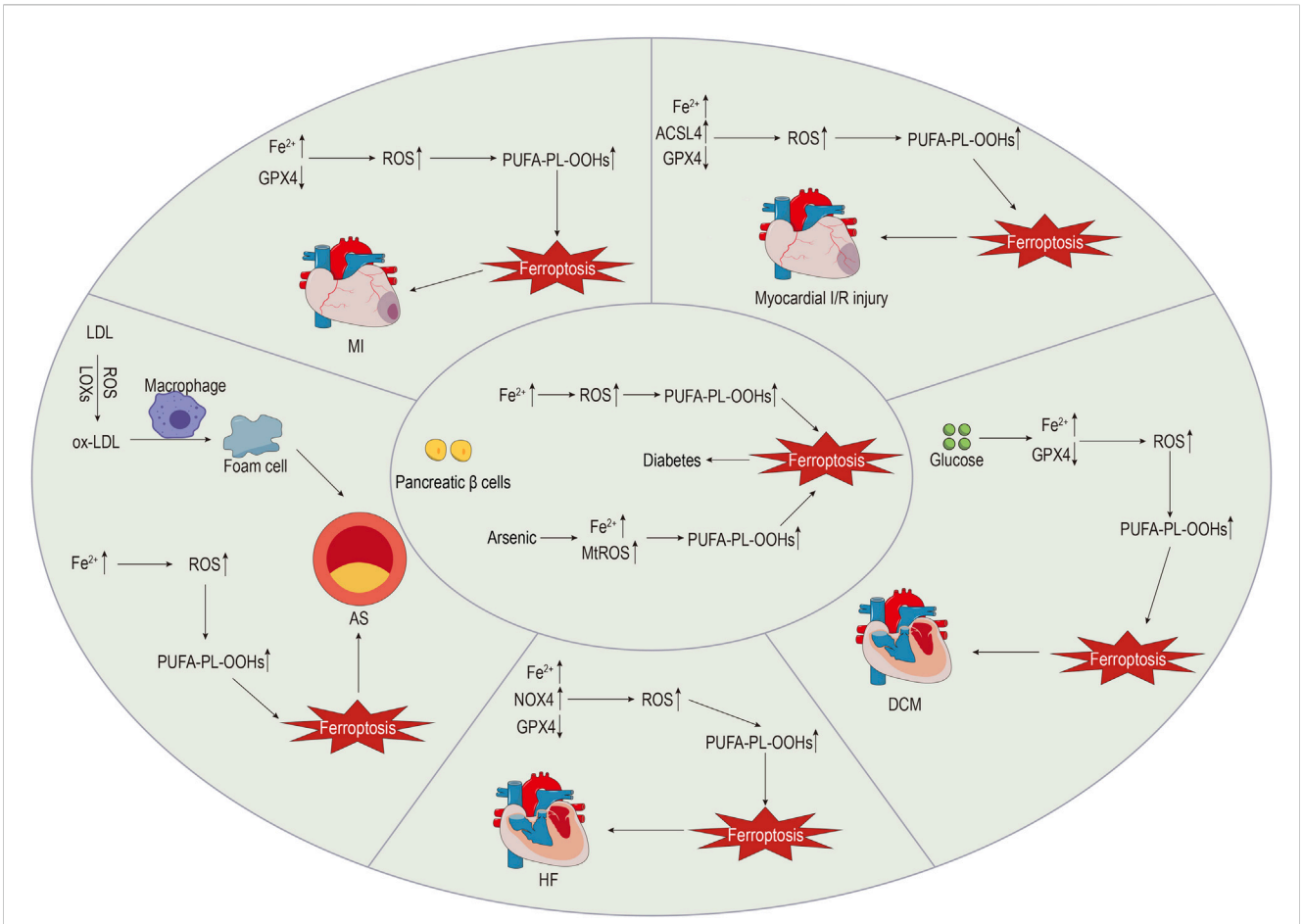


FIGURE 2
The role of ferroptosis in diabetes and CVDs.

GPX4, these cells are susceptible to oxidative stress-induced damage (Wang and Wang, 2017). Ferroptosis of pancreatic β cells leads to reduced insulin synthesis and secretion, ultimately triggering diabetes (Xie et al., 2023). Abnormalities in Fe–S cluster regulation in mitochondria also contribute to ferroptosis of pancreatic β cells, leading to the development of diabetes (Miao et al., 2023). Additionally, chronic arsenic exposure has been identified as a high-risk factor for T2DM (Yang and Yang, 2022), as it causes mitochondrial damage in pancreatic β cells, resulting in excessive mitochondrial ROS production, which triggers ferroptosis and impairs insulin secretion (Xie et al., 2023). The existence of ferroptosis has been confirmed in both *in vivo* and *in vitro* models of $NaAsO_2$-induced pancreatic β-cell injury (Wei et al., 2020).

# 4 Ferroptosis and CVDs

The intricate mechanisms of CVDs make them the most prevalent cause of death. Evidence suggests that ferroptosis plays a role in the pathophysiology of CVDs, including atherosclerosis (AS), myocardial infarction (MI), myocardial I/R injury, cardiomyopathy, and HF (Wu et al., 2021). The specific details are shown in Figure 2.

Investigating the role of ferroptosis in CVDs may reveal novel therapeutic targets.

## 4.1 Ferroptosis and AS

AS is the most common macrovascular complication of diabetes, and it serves as the pathological basis for various CVDs, significantly impacting the quality of life of affected individuals (Katakami, 2018). Dysfunction of vascular endothelial and smooth muscle cells, which is a key characteristic of AS, disrupts vascular homeostasis, with long-term hyperglycaemia and insulin resistance exacerbating this process through oxidative stress and inflammatory reactions (Jyotsna et al., 2023). The deposition of lipids or fibrous material in the arterial intima gradually forms atherosclerotic plaques. The rupture of unstable plaques leads to thrombosis, ultimately resulting in vascular stenosis or occlusion (Libby et al., 2019). The pathological features of AS mainly include lipid metabolism disorders, oxidative stress, endothelial cell injury, and inflammation (Wang et al., 2021). As early as in 1994, studies indicated that iron overload exacerbated endothelial injury, thereby causing AS (Jacob, 1994). Chronic iron overload increases ROS levels in the aorta and induces oxidative stress, which leads to endothelial cell damage and promotes AS

progression (Marques et al., 2019). LOXs participate in lipid peroxidation, and upregulation of 12/15-LOX expression promotes the deposition of low-density lipoprotein (LDL) beneath the vascular endothelium, where it is oxidised (Li et al., 2018). Macrophages then engulf oxidised LDL, forming foam cells and further promoting AS development (Wang et al., 2021; Ma et al., 2022). Macrophages also engulf senescent red blood cells, generating haem, which is degraded into $Fe^{2+}$ under the action of HO-1. Iron overload and ferroptosis in macrophages accelerate AS progression (Ma et al., 2022). Research by Xu et al. (Xu et al., 2023) demonstrated that inhibiting macrophage ferroptosis through the NRF2 pathway significantly delayed the development of AS. A study by Bai et al. (Bai et al., 2020) showed that the inhibitor of ferroptosis ferrostatin-1 could alleviate AS injury in $ApoE^{-/-}$ mice that were fed a high-fat diet. Moreover, ferrostatin-1 could reduce iron accumulation in $ApoE^{-/-}$ mice, increase the expression of SLC7A11 and GPX4, and enhance the vitality of mouse arterial endothelial cells. This suggests that the use of ferroptosis inhibitors may be a new direction for AS treatment. Moreover, recent studies have discovered that ferrostatin-1 inhibits ferroptosis in vascular smooth muscle cells of high-fat diet-fed mice through a pathway independent of p53/SLC7A11/GPX4, thereby improving AS lesions (You et al., 2023). Further research has indicated that NRF2/FSP1 may be a key antioxidant target for suppressing ferroptosis in vascular smooth muscle cells, thereby providing new strategies for AS treatment (You et al., 2023). Additionally, high levels of uric acid have been shown to promote AS by inducing ferroptosis through the inhibition of the NRF2/SLC7A11/GPX4 signalling pathway (Yu et al., 2022).

## 4.2 Ferroptosis and MI

Chronic hyperglycaemia and insulin resistance negatively impact lipid metabolism, accelerating the progression of AS and increasing plaque instability (Chen et al., 2022). Following plaque rupture, thrombosis occludes the coronary artery, leading to sustained myocardial ischaemia and local myocardial necrosis (Wang and Kang, 2021). MI remains a common cause of HF, with a relatively high mortality rate, particularly in patients with concomitant diabetes (Miki et al., 2012). In MI mouse models, FTH1 levels are significantly reduced, and punctate iron deposition appears in the infarcted area (Omiya et al., 2009), suggesting a possible link between MI and ferroptosis. Using proteomic analysis, Park et al. (Park et al., 2019) found that in MI mouse models, the levels of GPX4 were significantly decreased. Specific knockout or inhibition of GPX4 leads to lipid peroxidation, promoting H9c2 cell ferroptosis, which elucidates the potential mechanism of ferroptosis in the occurrence and development of MI. A deeper understanding of the disease mechanisms can aid in discovering new treatments. By exploring the protective mechanism of mesenchymal stem cell (MSC)-derived exosomes in acute MI mouse models, Song et al. (Song et al., 2021) found that DMT1 expression was upregulated, $Fe^{2+}$ levels increased, and GSH levels and GPX4 activity both decreased. Further research found that MSC-derived exosomes inhibited ferroptosis by targeting DMT1 expression, which reduced myocardial injury, thus demonstrating the tremendous potential of MSC-derived exosomes for MI treatment.

## 4.3 Ferroptosis and myocardial I/R injury

Prompt restoration of the blood supply to the infarcted area is the preferred treatment for MI that significantly reduces mortality. Meanwhile, prolonged myocardial ischaemia can lead to more severe myocardial injury after reperfusion, a process known as myocardial I/R injury (He et al., 2022). Both preclinical and clinical data indicate that diabetes increases susceptibility to myocardial I/R injury, attenuating protective effects of the heart and influencing patient prognosis (Russo et al., 2017), while exacerbating myocardial I/R injury through oxidative stress and other mechanisms (Zhao et al., 2017). Currently, there are no effective clinical methods to avoid myocardial I/R injury, but recent research on the mechanisms of ferroptosis and myocardial I/R injury may provide new strategies for treating myocardial I/R injury (Zhao K. et al., 2023). Tang et al. (Tang et al., 2021a) subjected rat hearts to ischaemia and reperfusion for different durations and observed that ACSL4, iron, and malondialdehyde (MDA) levels gradually increased with the reperfusion time, while GPX4 levels decreased, suggesting that myocardial cell ferroptosis mainly occurs during the reperfusion stage. This discovery could provide a basis for precise treatment of myocardial I/R injury. Cai et al. (Cai et al., 2023) used a mouse model with ligation of the left anterior descending coronary artery and similarly found that myocardial cells underwent ferroptosis during prolonged reperfusion. Researchers also found that ALOX15 expression was specifically increased in a damaged myocardium, while inhibiting ALOX15 expression could reduce myocardial cell ferroptosis, protecting the damaged myocardium. GPX4 is a key endogenous inhibitor of ferroptosis, and Sun et al. (Sun et al., 2021) found using their established rat model of myocardial I/R injury that during I/R, intracellular $Fe^{2+}$ levels increased, GPX4 and FTH1 expression decreased, and downregulating GPX4 promoted myocardial cell ferroptosis, exacerbating myocardial injury. Additionally, research has found that myocardial I/R injury is related to endoplasmic reticulum stress (ERS), and erastin can exacerbate ERS by inducing ferroptosis. Conversely, inhibiting ERS can alleviate ferroptosis and myocardial injury (Li W. et al., 2020; Miyamoto et al., 2022). In summary, ferroptosis plays a crucial role in the pathogenesis of myocardial I/R injury and may provide new targets for treating myocardial I/R injury.

## 4.4 Ferroptosis and cardiomyopathy

Diabetic cardiomyopathy (DCM) is a severe complication of diabetes, unrelated to hypertension and coronary artery disease (Guo et al., 2022). Long-term hyperglycaemia and hyperinsulinaemia, induced by diabetes, impair capillaries, leading to myocardial fibrosis and hypertrophy. Oxidative stress and inflammatory reactions associated with diabetes also contribute to these processes (Nakamura et al., 2022). Additionally, diabetes disrupts lipid metabolism, causing excessive uptake of fatty acids by the heart. Once the storage and oxidation capacities are exceeded, this excess becomes lipotoxic, resulting in myocardial hypertrophy and dysfunction (Nakamura and Sadoshima, 2020). Research shows that ferroptosis participates in the pathophysiological process of DCM, which is mainly manifested as high ROS production and a

decreased antioxidant capacity (Zhao Y. et al., 2023). Sun et al. (Sun et al., 2023) found that exogenous spermine could alleviate DCM by reducing ROS production and inhibiting ferroptosis. Wang et al. (Wang X. et al., 2022) found that sulphoraphane could activate the NRF2 signalling pathway, increase the levels of ferritin and SLC7A11 to inhibit ferroptosis, and protect cardiomyocytes. The above research indicates that the inhibition of ferroptosis is promising for the prevention and treatment of DCM.

### 4.5 Ferroptosis and HF

HF is a severe cardiac disease due to myocardial injury, wherein the cardiac output cannot meet the needs of the body, and HF is the final stage of various CVDs (Xie et al., 2022). There is a close relationship between HF and diabetes, which serves as an independent risk factor for HF. HF can develop not only from ischaemic heart disease associated with diabetes but also from DCM based on metabolic disorders, such as glucotoxicity and lipotoxicity (Nakamura et al., 2022). Research has shown that both iron deficiency and iron overload can lead to HF, and myocardial cells are highly susceptible to iron overload (Li et al., 2021). Ferroptosis of myocardial cells results in severe cardiac dysfunction, as the loss of terminally differentiated myocardial cells is irreversible. Early inhibition of ferroptosis of myocardial cells can help maintain cardiac function and delay the progression of HF (Zhang et al., 2019; Yang X. et al., 2022). In a rat model of HF induced by aortic stenosis, Liu et al. (Liu et al., 2018) found a significant increase in NADPH oxidase 4 (NOX4) levels in myocardial cells, along with decreased levels of GPX4 and FTH1. However, puerarin, an antioxidant, could reverse these phenomena, providing a promising therapeutic approach for HF. In a rat model of HF induced by aortic constriction, Chen et al. (Chen et al., 2019) found that knocking down Toll-like receptor 4 (TLR4) or NOX4 could inhibit ferroptosis and delay rat HF, suggesting potential therapeutic targets. Resveratrol is a polyphenolic substance that can inhibit the p53 pathway, reduce the degradation of SLC7A11, and increase GSH and GPX4 levels to reduce ferroptosis and improve heart function (Zhang et al., 2023).

## 5 Clinical applications of ferroptosis

Despite significant progress in the basic research of ferroptosis, the path to clinical applications has not been straightforward (von Samson-Himmelstjerna et al., 2022). Currently, the clinical applications of ferroptosis for disease diagnosis and treatment are still in their infancy.

The lack of specific biomarkers for ferroptosis has been a major limiting factor in the development of this field (Fang et al., 2023). Currently, the biomarkers used in clinical practice, such as serum iron, serum ferritin, TF, and soluble TF receptor, are nonspecific (Leng et al., 2021). Among them, serum iron is used most commonly, and monitoring its levels serves as an important indicator for assessing ferroptosis. A retrospective study has shown that elevated serum levels of iron are associated with increased severity of AS (Ozdemir, 2020). A cohort study has demonstrated a significant correlation between elevated serum ferritin levels and an increased risk of T2DM (Díaz-López et al., 2020). MDA, a lipid peroxidation product, can also be used to predict ferroptosis (Wang K. et al., 2022). Research has shown that serum MDA levels are the strongest predictor of CVD in patients on dialysis, and there is a positive correlation between serum MDA levels and the incidence of CVDs (Boaz et al., 1999). GPX4 and ACSL4 are proteins that are relatively stable in serum and have the advantages of easy measurement and sensitivity, making them recognised biomarkers for ferroptosis (Wang K. et al., 2022).

Regulators of ferroptosis include inducers and inhibitors. Based on different mechanisms of action, ferroptosis inducers can be roughly divided into iron metabolism inducers, system $x_c^-$ inhibitors, and GPX4 inhibitors, which are mostly used in the treatment of tumours and neurological diseases (Xia et al., 2021). Ferroptosis inhibitors have the potential to treat CVDs and mainly include iron chelators and lipophilic antioxidants. Deferoxamine and deferasirox are iron chelators with a strong affinity for iron that are commonly used in clinical practice (Chen et al., 2023). Studies have shown that deferoxamine can increase GPX4 expression, alleviate ferroptosis, and reduce the MI area (Tu et al., 2021). In addition, dexrazoxane is the only iron chelator approved by the US Food and Drug Administration for preventing doxorubicin-induced cardiotoxicity in patients with cancer (Fang et al., 2023) by exerting a cardioprotective effect via inhibition of ferroptosis (Fang et al., 2019). Ferrostatin-1 and liproxstatin-1 are both lipophilic antioxidants, and ferrostatin-1 is the first-generation ferroptosis inhibitor (Dixon et al., 2012) that reduces myocardial I/R injury by inhibiting lipid peroxidation and improving cardiac function in diabetic mice (Li et al., 2020). Liproxstatin-1 has a similar mechanism of action and can alleviate myocardial I/R injury in mice by reducing mitochondrial ROS production and maintaining GPX4 activity (Feng et al., 2019).

## 6 Intervention with active ingredients of TCMs in ferroptosis to treat CVDs

TCM has a wealth of clinical experience in treating CVDs, and its formulations have the advantages of low toxicity and low side effects, a wide application range, and low prices. TCMs are natural compound libraries, and many active ingredients of TCMs have been confirmed to be useful for the treatment of CVDs, with their mechanisms being related to ferroptosis. Therefore, we summarised the mechanisms of various active ingredients of TCMs in the treatment of CVDs in Table 1. Figure 3 shows the chemical structures of natural medicines.

### 6.1 Alkaloids

Alkaloids are a class of nitrogen-containing organic compounds, many of which have complex cyclic structures and are mostly alkaline or neutral (Li X. et al., 2022). Alkaloids have powerful anti-inflammatory, antibacterial, antioxidant, and antitumor effects (Liu et al., 2019), and play an important role in the treatment of CVDs. Matrine is an alkaloid isolated from TCMs such as *Sophora flavescens* Aiton and *Euchresta japonica* Hook. f. ex Regel, and it has been confirmed to alleviate oxidative stress and cell death in various

**TABLE 1 Mechanisms of active ingredients of traditional Chinese medicine regulating ferroptosis.**

| Active ingredients | | Mechanism and effect | Models | | Ref |
|---|---|---|---|---|---|
| | | | *In Vivo* | *In Vitro* | |
| Alkaloids | Matrine | Active the PI3K/AKT signalling pathway, upregulate the expression of GPX4, downregulate the expression of ACSL4 | C57BL/6 mice | – | Xiao et al. (2023) |
| | Berberine | Upregulate the expression of NRF2, FTH1 and GPX4, downregulate the expression of TFR1 and p53 | C57BL/6j mice | H9c2 cells | Song et al. (2023) |
| Polyphenols | Baicalin | Downregulate the expression of TFR1, NCOA4 and ACSL4, reduce ferritinophagy | SD rats | H9c2 cells | Fan et al. (2021) |
| | | Upregulate the expression of GPX4 | *ApoE*$^{-/-}$ mice | – | Wu et al. (2018) |
| | Naringenin | Upregulate the expression of NRF2, SLC7A11, GPX4, FTH1 and FPN | SD rats | H9c2 cells | Xu et al. (2021) |
| | Puerarin | Upregulate the expression of FTH1 and GPX4, downregulate the expression of NOX4, reduce lipid peroxidation | SD rats | H9c2 cells | Liu et al. (2018) |
| | | Active the AMPK signalling pathway, upregulate the expression of GPX4 and ferritin, downregulate the expression of ACSL4 and TFR1 | SD rats | – | Zhou et al. (2022) |
| | | Upregulate the levels of GSH and GPX4, downregulate the levels of ROS and MDA | C57BL/6 mice | H9c2 cells | Ding et al. (2023) |
| | Cyanidin-3-glucoside | Upregulate the expression of FTH1 and GPX4, downregulate the expression of NCOA4 and TFR1, reduce ferritinophagy | SD rats | H9c2 cells | Shan et al. (2021) |
| | Icariin | Active the NRF2/HO-1 signalling pathway, upregulate the levels of GPX4, downregulate the levels of $Fe^{2+}$ and ACSL4 | – | H9c2 cells | Liu et al. (2021b) |
| | | Active the SIRT1/NRF2/HO-1 signalling pathway, upregulate the expression of GPX4 and SLC7A11, downregulate the expression of ACSL4 and p53 | C57BL/6 mice | HL-1 atrial myocytes | Yu et al. (2023) |
| | | Upregulate the expression of GPX4 and FTH1, downregulate the expression of TFR1 | *ApoE*$^{-/-}$ mice | HUVECs | Wang et al. (2023) |
| | Salvianolic acid B | Active the NRF2 signalling pathway, upregulate the expression of SLC7A11, GPX4, FPN and FTH1 | SD rats | – | Shen et al. (2022a) |
| | Curcumin | Active the NRF2/HO-1 signalling pathway, upregulate the expression of GPX4 | New Zealand rabbits | H9c2 cells | Wei et al. (2022) |
| | | Upregulate the expression of GPX4, downregulate the expression of ACSL4 | Wistar rats | – | Kar et al. (2023) |
| | Resveratrol | Upregulate the expression of FTH1 and GPX4, downregulate the expression of TFR1 | SD rats | H9c2 cells | Li et al. (2022a) |
| | | Upregulate the levels of GSH, upregulate the expression of GPX4 and SLC7A11, downregulate the levels of $Fe^{2+}$, MDA and ROS | SD rats | H9c2 cells | Liu et al. (2022) |
| Saponins | Ginsenoside Re | Upregulate the levels of GSH, upregulate the expression of SLC7A11, downregulate the expression of miR-144-3p | WKY rats | H9c2 cells | Ye et al. (2023) |
| | Astragaloside IV | Active the NRF2 signalling pathway, upregulate the expression of GPX4, downregulate the expression of NOX | SD rats | – | Luo et al. (2021) |
| | Ophiopogonin D | Upregulate the expression of GPX4 and FTH1, downregulate the expression of TFR1, COX2, NOX1 and ACSL4 | – | H9c2 cells | Lin et al. (2021a) |
| | Saikosaponin A | Upregulate the levels of GSH, upregulate the expression of GPX4 and SOD, downregulate the levels of MDA, downregulate the expression of ACSL4 | – | HUVECs | Huang et al. (2022) |

(Continued on following page)

**TABLE 1 (*Continued*) Mechanisms of active ingredients of traditional Chinese medicine regulating ferroptosis.**

| Active ingredients | | Mechanism and effect | Models | | Ref |
|---|---|---|---|---|---|
| | | | *In Vivo* | *In Vitro* | |
| | Aralosides and Araloside A | Upregulate the expression of NR3C1 and SLC7A11, downregulate the expression of p53 | – | AC16 cells | Liang et al. (2022b) |
| Others | Tanshinone IIA | Active the NRF2/HO-1 signalling pathway, upregulate the expression of GSH-Px, downregulate the levels of MDA | – | H9c2 cells | Yang et al. (2020) |
| | | Active the NRF2 signalling pathway, upregulate the levels of GSH and SLC7A11, downregulate the levels of ROS | – | HCAECs | He et al. (2021) |
| | Geniposide | Active the GRSF1/GPX4 signalling pathway, upregulate the expression of FTH1, downregulate the expression of TFR1 | SD rats | Primary cardiomyocytes, H9c2 cells | Shen et al. (2022b) |
| | Thymoquinone | Active the NRF2/HO-1 signalling pathway, upregulate the expression of GPX4 and FTH1 | C57BL/6j mice | – | Luo (2022) |

CVDs (Sun et al., 2022). In a mouse model of sepsis-induced myocardial injury, matrine protects the damaged myocardium by activating the PI3K/AKT pathway to upregulate GPX4 expression and downregulate ACSL4 expression to inhibit ferroptosis (Xiao et al., 2023). Berberine is an isoquinoline alkaloid extracted from TCMs such as *Coptis chinensis* Franch. and *Phellodendron amurense* Rupr. (Song et al., 2023), and it has strong anti-inflammatory and antioxidant activities and cardiovascular protective effects (Cicero and Baggioni, 2016). Yang et al. (Yang K.-T. et al., 2022) found that in a cardiomyocyte ferroptosis model induced by erastin and RSL3, berberine could reduce the accumulation of ROS and lipid peroxidation. *In vivo* experiments also showed that berberine reduced the levels of MDA and iron in rats, downregulated the expression of TFR1 and p53, and upregulated the expression of NRF2, FTH1, and GPX4 to reduce cardiotoxicity (Song et al., 2023).

## 6.2 Polyphenols

Polyphenolic compounds are widely present in plants and have diverse structures, but all consist of a phenyl ring combined with one or more hydroxyl groups. According to their structures, polyphenols can be divided into flavonoids, phenolic acids, stilbenes, and lignans (Cheng et al., 2017; Singla et al., 2019; Lesjak et al., 2022). Polyphenols have anti-inflammatory and antioxidant capacities, contribute to cardiovascular health, and can neutralise free radicals by providing electrons or hydrogen atoms to reduce oxidative damage. Polyphenols are also metal chelators, which can chelate $Fe^{2+}$, inhibit the Fenton reaction, and reduce the production of ROS (Cheng et al., 2017).

Flavonoid compounds typically possess a C6–C3–C6 backbone structure and are subdivided into flavones, flavonols, flavanones, flavanols, isoflavones, and anthocyanins, among others (Serafini et al., 2010; Khoddami et al., 2013). Baicalin, a flavonoid glycoside isolated from the roots and stems of the TCM *Scutellaria baicalensis* Georgi, inhibits TFR1 and NCOA4 expression, reducing ferroptosis and ACSL4 expression and thereby alleviating myocardial I/R injury (Fan et al., 2021). Furthermore, baicalin exerts antioxidant effects by enhancing GPX4 activity and thereby mitigating AS (Wu et al., 2018). Naringenin is a flavanone compound, and Xu et al. (Xu et al., 2021) found that in a rat myocardial I/R injury model, naringin increased the expression of NRF2, SLC7A11, GPX4, FTH1, and FPN, inhibited ferroptosis, and alleviated myocardial I/R injury. In hypoxia/reoxygenation-induced H9c2 cells, erastin reversed the protective effect of naringenin on the cells. Puerarin, an isoflavone extracted from the TCM Puerariae Lobatae Radix, has been widely used in the treatment of CVDs (Zhou et al., 2014). Puerarin increases FTH1 and GPX4 expression, reduces NOX4 expression, decreases lipid peroxidation, and inhibits myocardial cell loss in HF (Liu et al., 2018). Zhou et al. (Zhou et al., 2022) found that puerarin activated the AMPK signalling pathway, increased GPX4 and ferritin expression, reduced ACSL4 and TFR1 expression, inhibited ferroptosis, and protected against sepsis-induced myocardial injury. Moreover, puerarin was shown to inhibit ferroptosis and reduce myocardial I/R injury by decreasing ROS and MDA production and increasing GSH and GPX4 levels (Ding et al., 2023). Cyanidin-3-glucoside, a natural anthocyanin, possesses potent antioxidant activity due to two hydroxyl groups on its B-ring (Tan et al., 2019). Cyanidin-3-glucoside downregulates NCOA4 and TFR1 expression, upregulates FTH1 and GPX4 expression, inhibits ferroptosis, and thus alleviates myocardial I/R injury (Shan et al., 2021). Icariin, an isopentenyl flavonoid compound, is the main active ingredient of the TCM *Epimedium brevicornum* Maxim. (He et al., 2020). Liu et al. (Liu X.-J. et al., 2021) found that icariin activated the NRF2/HO-1 signalling pathway, reduced $Fe^{2+}$ and ACSL4 levels, increased GPX4 levels, and alleviated myocardial cell ferroptosis. Yu et al. (Yu et al., 2023) found that icariin alleviated ethanol-induced atrial remodelling and reduced susceptibility to atrial fibrillation by activating the SIRT1/NRF2/HO-1 signalling pathway, increasing GPX4 and SLC7A11 expression, and inhibiting ACSL4 and p53 expression. Additionally, icariin delays AS by increasing

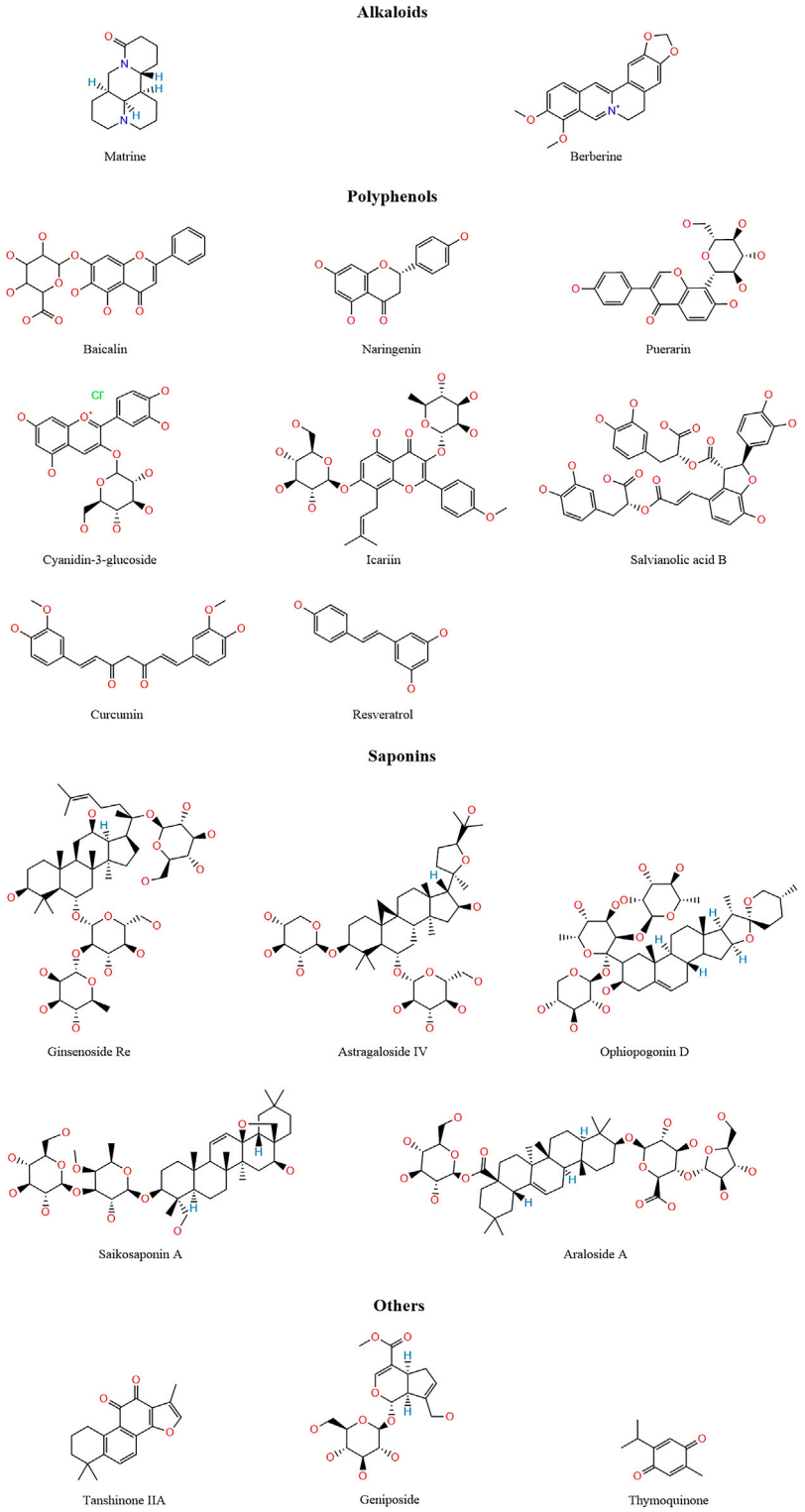


FIGURE 3
The structure of active ingredients of traditional Chinese medicine.

GPX4 and FTH1 expression and reducing TFR1 expression (Wang et al., 2023).

Salvianolic acid B, a phenolic acid compound, is the main active ingredient of the TCM *Salvia miltiorrhiza* Bunge and has been widely used to treat cardiovascular and cerebrovascular diseases (Shi et al., 2019). Shen et al. (Shen et al., 2022a) established a MI model by ligating the left anterior descending coronary artery in rats and found that salvianolic acid B activated the NRF2 signalling pathway,

increased SLC7A11, GPX4, FPN, and FTH1 expression, inhibited ferroptosis, and alleviated MI.

Curcumin, a diphenylheptane compound derived from the rhizome of the plant *Curcuma longa* L., has been confirmed to possess anti-inflammatory, antioxidant, hypoglycaemic, wound-healing, antibacterial, and antitumour activities (Lesjak et al., 2022). In a diabetic rabbit model, curcumin inhibits diabetes-induced myocardial cell ferroptosis by activating the NRF2/HO-1 signalling pathway and increasing GPX4 expression (Wei et al., 2022). Kar et al. (Kar et al., 2023) found that curcumin inhibited myocardial cell ferroptosis and alleviated I/R injury by reducing ACSL4 expression and increasing GPX4 expression.

Resveratrol, a member of the stilbene family, is a natural polyphenol that protects the cardiovascular system against vascular wall oxidation, inflammation, and thrombosis (Bonnefont-Rousselot, 2016; Lesjak et al., 2022). Both *in vivo* and *in vitro* experiments have shown that resveratrol inhibits ferroptosis and protects against myocardial I/R injury by reducing $Fe^{2+}$ levels, downregulating TFR1 expression, and increasing FTH1 and GPX4 expression (Li T. et al., 2022). In a rat MI model, resveratrol alleviates MI-related myocardial injury and fibrosis by increasing GSH levels, upregulating GPX4 and SLC7A11 expression, and reducing $Fe^{2+}$ and MDA levels and ROS accumulation (Liu et al., 2022).

## 6.3 Saponins

Saponins are a class of natural glycosides that are divided into triterpenoid and steroid saponins and are widely found in TCMs such as *Panax ginseng* C. A. Mey., *Astragalus membranaceus* var. *mongholicus* (Bunge) P. K. Hsiao, *B. chinensis* DC., and *Anemarrhena asphodeloides* Bunge. Saponins possess various biological activities, including anti-inflammatory, antiviral, immunomodulatory, cardiovascular protective, and anticancer effects (Xu et al., 2016). Ginsenoside Re, an active ingredient of the TCM *P. ginseng*, protects against myocardial I/R injury by inhibiting miR-144-3p expression, upregulating SLC7A11 expression, and increasing GSH levels to inhibit ferroptosis (J et al., 2023). Astragaloside IV activates the NRF2 signalling pathway, thereby increasing GPX4 expression, and reduces the expression of the positive regulator of ferroptosis NOX, thereby inhibiting Adriamycin-induced myocardial ferroptosis (Luo et al., 2021). Ophiopogonin D inhibits the expression of the ferroptosis-related proteins TFR1, cyclooxygenase 2 (COX2), NOX1, and ACSL4, increases GPX4 and FTH1 expression, and alleviates ferroptosis in rat myocardial cells (Lin Y. et al., 2021). Saikosaponin A, a triterpenoid saponin isolated from the TCM *Bupleurum chinensis*, increases GSH levels and SOD activity, reduces MDA levels, upregulates GPX4 expression, downregulates ACSL4 expression, and inhibits ferroptosis in a concentration-dependent manner, thus showing promise as a novel option for AS prevention and treatment (Huang et al., 2022). Aralosides and Araloside A inhibit hypoxia/reoxygenation-induced ferroptosis in AC16 cardiomyocytes by upregulating NR3C1 and SLC7A11 expression and downregulating p53 expression (Liang F. et al., 2022).

## 6.4 Others

Tanshinone IIA, a natural diterpene quinone compound, exhibits various biological activities, including anti-atherosclerosis effects, and alleviates angina and MI (Fang Z.-Y. et al., 2020). In a rat cardiomyocyte model of $H_2O_2$-induced oxidative damage, tanshinone IIA protects cardiomyocytes by activating the NRF2/HO-1 signalling pathway, enhancing GSH-Px activity, and reducing MDA activity (Yang et al., 2020). Tanshinone IIA also activates the NRF2 signalling pathway, increases GSH and SLC7A11 levels, reduces ROS production, protects the vascular endothelium, and delays AS development (He et al., 2021). Geniposide, a natural iridoid glycoside compound mainly derived from the TCM *Gardenia jasminoides* J. Ellis (Zhou et al., 2019), alleviates myocardial injury caused by MI by activating the GRSF1/GPX4 signalling pathway, increasing FTH1 expression, and reducing TFR1 expression (Shen et al., 2022b). Thymoquinone, a monoterpenoid compound (Kohandel et al., 2021; Talebi et al., 2021), activates the NRF2/HO-1 signalling pathway, increases GPX4 and FTH1 expression, and inhibits the cardiotoxic effects of doxorubicin (Luo, 2022).

# 7 Conclusion and outlook

Although CVDs are multifactorial and complex diseases involving multiple mechanisms, diabetes is a major risk factor. Increasing evidence suggests that ferroptosis plays an important role in diabetes and its cardiovascular complications (Yang and Yang, 2022), thus providing new therapeutic targets for diabetes-related cardiovascular complications.

In this review, we summarised the prerequisites for driving ferroptosis, including iron overload, ROS generation, and lipid peroxidation, as well as the defence mechanisms against ferroptosis, including the GPX4/GSH, FSP1/$CoQ_{10}H_2$, DHODH/$CoQ_{10}H_2$, and GCH1/BH4 systems. These genes could potentially serve as therapeutic targets for diabetic CVDs. Despite certain advancements in the study of ferroptosis mechanisms, challenges remain; in particular, specific biomarkers are currently lacking for ferroptosis, and many studies assess ferroptosis based on $Fe^{2+}$ levels, ROS accumulation, and GPX4 expression. However, there are other forms of iron-dependent cell death that are distinct from ferroptosis, and ROS accumulation also occurs in oxidative stress. Therefore, finding specific biomarkers for ferroptosis is of great value. Furthermore, diabetic CVDs involve various mechanisms, including inflammation, oxidative stress, necrosis, apoptosis, pyroptosis, and ferroptosis. Identifying which mechanism dominates the development of disease and finding how to combine medications are problems that need to be solved in the future. Lastly, various organelles and proteins participate in the regulation of ferroptosis, increasing the difficulty of selecting targets for inhibiting ferroptosis. Different diseases have different therapeutic targets. Promoting ferroptosis in tumour cells helps inhibit and kill tumours, but normal cells, such as cardiomyocytes, pancreatic β-cells, and neurons, are also sensitive to ferroptosis. Determining how to selectively regulate ferroptosis is a major issue that requires extensive future research.

TCM has a long history of treating CVDs and has achieved a significant efficacy. The active ingredients of TCMs have various biological functions, and the discovery and continuous exploration

of ferroptosis mechanisms provide a new theoretical basis for the treatment of CVDs with TCMs. Research findings on the treatment of CVDs through ferroptosis-related mechanisms by active ingredients of TCMs, such as alkaloids, polyphenols, and saponins, are summarised in Table 1. These compounds can act on various ferroptosis-related signalling pathways or regulatory proteins, protecting cardiomyocytes or vascular endothelial cells from ferroptosis. However, there are many problems to be solved in the treatment of CVDs by regulating ferroptosis with TCMs. First, the extraction and purification of active ingredients of TCMs are relatively complex processes that are affected by the environment, the quality of medicinal materials, and the process flow. Second, the treatment of diseases with TCMs does not depend on a specific active ingredient but often involves multiple ingredients working together, making it difficult to elucidate their mechanisms of action. Third, most of the current research on the mechanisms of active ingredients of TCMs intervening in ferroptosis is concentrated on animal- and cell-based experiments, while there is a lack of high-quality clinical research, especially randomised controlled trials. Fourth, MI has a sudden onset and a certain intervention time window, which raises a question whether TCMs targeting ferroptosis can exert their effects in time. Fifth, although the side effects of TCMs are small, chronic diseases such as chronic HF require long-term medication, and its safety still needs a large amount of clinical research for evaluation.

In conclusion, ferroptosis participates in the development of diabetes and CVDs, and a large amount of evidence shows that targeting ferroptosis in the treatment of CVDs by active ingredients of TCMs has certain advantages. In the future, it is necessary to continue research to improve the understanding of the signalling pathways and mechanisms related to ferroptosis, to provide new directions for the development of ferroptosis inhibitors, and thus provide new strategies for the treatment of diabetic CVDs.

## Author contributions

XZ: Formal Analysis, Investigation, Writing–original draft. JS: Formal Analysis, Investigation, Writing–review and editing. JW: Conceptualization, Investigation, Writing–review and editing. JY: Supervision, Writing–review and editing. TM: Software, Writing–review and editing. YZ: Supervision, Writing–review and editing.

## Funding

The author(s) declare financial support was received for the research, authorship, and/or publication of this article. This article is supported by 2019 Heilongjiang University of Chinese Medicine Research Fund Project (2019XY04).

## Conflict of interest

The authors declare that the research was conducted in the absence of any commercial or financial relationships that could be construed as a potential conflict of interest.

## Publisher's note



## References

Ajoolabady, A., Aslkhodapasandhokmabad, H., Libby, P., Tuomilehto, J., Lip, G. Y. H., Penninger, J. M., et al. (2021). Ferritinophagy and ferroptosis in the management of metabolic diseases. *Trends Endocrinol. metabolism TEM* 32 (7), 444–462. doi:10.1016/j.tem.2021.04.010

Ali, M. Y., Oliva, C. R., Flor, S., and Griguer, C. E. (2022). Mitoferrin, cellular and mitochondrial iron homeostasis. *Cells* 11 (21), 3464. doi:10.3390/cells11213464

Anderson, G. J., and Frazer, D. M. (2017). Current understanding of iron homeostasis. *Am. J. Clin. Nutr.* 106 (6), 1559S–1566S. doi:10.3945/ajcn.117.155804

Backe, M. B., Moen, I. W., Ellervik, C., Hansen, J. B., and Mandrup-Poulsen, T. (2016). Iron regulation of pancreatic beta-cell functions and oxidative stress. *Annu. Rev. Nutr.* 36, 241–273. doi:10.1146/annurev-nutr-071715-050939

Bai, T., Li, M., Liu, Y., Qiao, Z., and Wang, Z. (2020). Inhibition of ferroptosis alleviates atherosclerosis through attenuating lipid peroxidation and endothelial dysfunction in mouse aortic endothelial cell. *Free Radic. Biol. Med.* 160, 92–102. doi:10.1016/j.freeradbiomed.2020.07.026

Beckman, J. A., and Creager, M. A. (2016). Vascular complications of diabetes. *Circulation Res.* 118 (11), 1771–1785. doi:10.1161/CIRCRESAHA.115.306884

Bersuker, K., Hendricks, J. M., Li, Z., Magtanong, L., Ford, B., Tang, P. H., et al. (2019). The CoQ oxidoreductase FSP1 acts parallel to GPX4 to inhibit ferroptosis. *Nature* 575 (7784), 688–692. doi:10.1038/s41586-019-1705-2

Bertheloot, D., Latz, E., and Franklin, B. S. (2021). Necroptosis, pyroptosis and apoptosis: an intricate game of cell death. *Cell. Mol. Immunol.* 18 (5), 1106–1121. doi:10.1038/s41423-020-00630-3

Billesbølle, C. B., Azumaya, C. M., Kretsch, R. C., Powers, A. S., Gonen, S., Schneider, S., et al. (2020). Structure of hepcidin-bound ferroportin reveals iron homeostatic mechanisms. *Nature* 586 (7831), 807–811. doi:10.1038/s41586-020-2668-z

Boaz, M., Matas, Z., Biro, A., Katzir, Z., Green, M., Fainaru, M., et al. (1999). Serum malondialdehyde and prevalent cardiovascular disease in hemodialysis. *Kidney Int.* 56 (3), 1078–1083. doi:10.1046/j.1523-1755.1999.00613.x

Bonnefont-Rousselot, D. (2016). Resveratrol and cardiovascular diseases. *Nutrients* 8 (5), 250. doi:10.3390/nu8050250

Cai, W., Liu, L., Shi, X., Liu, Y., Wang, J., Fang, X., et al. (2023). Alox15/15-HpETE aggravates myocardial ischemia-reperfusion injury by promoting cardiomyocyte ferroptosis. *Circulation* 147 (19), 1444–1460. doi:10.1161/CIRCULATIONAHA.122.060257

Cai, X., Hua, S., Deng, J., Du, Z., Zhang, D., Liu, Z., et al. (2022). Astaxanthin activated the Nrf2/HO-1 pathway to enhance autophagy and inhibit ferroptosis, ameliorating acetaminophen-induced liver injury. *ACS Appl. Mater. interfaces* 14 (38), 42887–42903. doi:10.1021/acsami.2c10506

Chen, X., Kang, R., Kroemer, G., and Tang, D. (2021a). Broadening horizons: the role of ferroptosis in cancer. *Nat. Rev. Clin. Oncol.* 18 (5), 280–296. doi:10.1038/s41571-020-00462-0

Chen, X., Li, J., Kang, R., Klionsky, D. J., and Tang, D. (2021b). Ferroptosis: machinery and regulation. *Autophagy* 17 (9), 2054–2081. doi:10.1080/15548627.2020.1810918

Chen, X., Xu, S., Zhao, C., and Liu, B. (2019). Role of TLR4/NADPH oxidase 4 pathway in promoting cell death through autophagy and ferroptosis during heart failure. *Biochem. biophysical Res. Commun.* 516 (1), 37–43. doi:10.1016/j.bbrc.2019.06.015

Chen, Y.-C., Jandeleit-Dahm, K., and Peter, K. (2022). Sodium-glucose Co-transporter 2 (SGLT2) inhibitor dapagliflozin stabilizes diabetes-induced atherosclerotic plaque instability. *J. Am. Heart Assoc.* 11 (1), e022761. doi:10.1161/JAHA.121.022761

Chen, Y., Li, X., Wang, S., Miao, R., and Zhong, J. (2023). Targeting iron metabolism and ferroptosis as novel therapeutic approaches in cardiovascular diseases. *Nutrients* 15 (3), 591. doi:10.3390/nu15030591

Cheng, Y.-C., Sheen, J.-M., Hu, W. L., and Hung, Y.-C. (2017). Polyphenols and oxidative stress in atherosclerosis-related ischemic heart disease and stroke. *Oxidative Med. Cell. Longev.* 2017, 8526438. doi:10.1155/2017/8526438

Cicero, A. F. G., and Baggioni, A. (2016). Berberine and its role in chronic disease. *Adv. Exp. Med. Biol.* 928, 27–45. doi:10.1007/978-3-319-41334-1_2

Das, U. N. (2019). Saturated fatty acids, MUFAs and PUFAs regulate ferroptosis. *Cell Chem. Biol.* 26 (3), 309–311. doi:10.1016/j.chembiol.2019.03.001

Del Re, D. P., Amgalan, D., Linkermann, A., Liu, Q., and Kitsis, R. N. (2019). Fundamental mechanisms of regulated cell death and implications for heart disease. *Physiol. Rev.* 99 (4), 1765–1817. doi:10.1152/physrev.00022.2018

Deng, Q., Zhu, Y., Zhang, M., Fei, A., Liang, J., Zheng, J., et al. (2023). Ferroptosis as a potential new therapeutic target for diabetes and its complications. *Endocr. Connect.* 12 (3), e220419. doi:10.1530/EC-22-0419

Díaz-López, A., Iglesias-Vázquez, L., Pallejà-Millán, M., Rey Reñones, C., Flores Mateo, G., and Arija, V. (2020). Association between iron status and incident type 2 diabetes: a population-based cohort study. *Nutrients* 12 (11), 3249. doi:10.3390/nu12113249

Ding, Y., Li, W., Peng, S., Zhou, G., Chen, S., Wei, Y., et al. (2023). Puerarin protects against myocardial ischemia/reperfusion injury by inhibiting ferroptosis. *Biol. Pharm. Bull.* 46 (4), 524–532. doi:10.1248/bpb.b22-00174

Dixon, S. J., Lemberg, K. M., Lamprecht, M. R., Skouta, R., Zaitsev, E. M., Gleason, C. E., et al. (2012). Ferroptosis: an iron-dependent form of nonapoptotic cell death. *Cell* 149 (5), 1060–1072. doi:10.1016/j.cell.2012.03.042

Dong, H., Qiang, Z., Chai, D., Peng, J., Xia, Y., Hu, R., et al. (2020). Nrf2 inhibits ferroptosis and protects against acute lung injury due to intestinal ischemia reperfusion via regulating SLC7A11 and HO-1. *Aging* 12 (13), 12943–12959. doi:10.18632/aging.103378

Fan, G., Liu, M., Liu, J., and Huang, Y. (2023). The initiator of neuroexcitotoxicity and ferroptosis in ischemic stroke: glutamate accumulation. *Front. Mol. Neurosci.* 16, 1113081. doi:10.3389/fnmol.2023.1113081

Fan, Z., Cai, L., Wang, S., Wang, J., and Chen, B. (2021). Baicalin prevents myocardial ischemia/reperfusion injury through inhibiting ACSL4 mediated ferroptosis. *Front. Pharmacol.* 12, 628988. doi:10.3389/fphar.2021.628988

Fang, X., Ardehali, H., Min, J., and Wang, F. (2023). The molecular and metabolic landscape of iron and ferroptosis in cardiovascular disease. *Nat. Rev. Cardiol.* 20 (1), 7–23. doi:10.1038/s41569-022-00735-4

Fang, X., Cai, Z., Wang, H., Han, D., Cheng, Q., Zhang, P., et al. (2020a). Loss of cardiac ferritin H facilitates cardiomyopathy via slc7a11-mediated ferroptosis. *Circulation Res.* 127 (4), 486–501. doi:10.1161/CIRCRESAHA.120.316509

Fang, X., Wang, H., Han, D., Xie, E., Yang, X., Wei, J., et al. (2019). Ferroptosis as a target for protection against cardiomyopathy. *Proc. Natl. Acad. Sci. U. S. A.* 116 (7), 2672–2680. doi:10.1073/pnas.1821022116

Fang, Z.-Y., Zhang, M., Liu, J.-N., Zhao, X., Zhang, Y.-Q., and Fang, L. (2020b). Tanshinone IIA: a review of its anticancer effects. *Front. Pharmacol.* 11, 611087. doi:10.3389/fphar.2020.611087

Feng, Y., Madungwe, N. B., Imam Aliagan, A. D., Tombo, N., and Bopassa, J. C. (2019). Liproxstatin-1 protects the mouse myocardium against ischemia/reperfusion injury by decreasing VDAC1 levels and restoring GPX4 levels. *Biochem. Biophysical Res. Commun.* 520 (3), 606–611. doi:10.1016/j.bbrc.2019.10.006

Forcina, G. C., and Dixon, S. J. (2019). GPX4 at the crossroads of lipid homeostasis and ferroptosis. *Proteomics* 19 (18), e1800311. doi:10.1002/pmic.201800311

Galaris, D., Barbouti, A., and Pantopoulos, K. (2019). Iron homeostasis and oxidative stress: an intimate relationship. *Biochimica Biophysica Acta. Mol. Cell Res.* 1866 (12), 118535. doi:10.1016/j.bbamcr.2019.118535

Ganz, T. (2013). Systemic iron homeostasis. *Physiol. Rev.* 93 (4), 1721–1741. doi:10.1152/physrev.00008.2013

Gao, H., Jin, Z., Bandyopadhyay, G., Wang, G., Zhang, D., Rocha, K. C. E., et al. (2022). Aberrant iron distribution via hepatocyte-stellate cell axis drives liver lipogenesis and fibrosis. *Cell Metab.* 34 (8), 1201–1213.e5. doi:10.1016/j.cmet.2022.07.006

Glovaci, D., Fan, W., and Wong, N. D. (2019). Epidemiology of diabetes mellitus and cardiovascular disease. *Curr. Cardiol. Rep.* 21 (4), 21. doi:10.1007/s11886-019-1107-y

Guo, Y., Zhang, W., Zhou, X., Zhao, S., Wang, J., Guo, Y., et al. (2022). Roles of ferroptosis in cardiovascular diseases. *Front. Cardiovasc. Med.* 9, 911564. doi:10.3389/fcvm.2022.911564

Hao, P., Jiang, F., Cheng, J., Ma, L., Zhang, Y., and Zhao, Y. (2017). Traditional Chinese medicine for cardiovascular disease: evidence and potential mechanisms. *J. Am. Coll. Cardiol.* 69 (24), 2952–2966. doi:10.1016/j.jacc.2017.04.041

He, C., Wang, Z., and Shi, J. (2020). Pharmacological effects of icariin. *Adv. Pharmacol. (San Diego, Calif.)* 87, 179–203. doi:10.1016/bs.apha.2019.10.004

He, J., Liu, D., Zhao, L., Zhou, D., Rong, J., Zhang, L., et al. (2022). Myocardial ischemia/reperfusion injury: mechanisms of injury and implications for management (Review). *Exp. Ther. Med.* 23 (6), 430. doi:10.3892/etm.2022.11357

He, L., Liu, Y.-Y., Wang, K., Li, C., Zhang, W., Li, Z.-Z., et al. (2021). Tanshinone IIA protects human coronary artery endothelial cells from ferroptosis by activating the NRF2 pathway. *Biochem. biophysical Res. Commun.* 575, 1–7. doi:10.1016/j.bbrc.2021.08.067

Hong, M., Rong, J., Tao, X., and Xu, Y. (2022). The emerging role of ferroptosis in cardiovascular diseases. *Front. Pharmacol.* 13, 822083. doi:10.3389/fphar.2022.822083

Huang, J., Chen, S., Hu, L., Niu, H., Sun, Q., Li, W., et al. (2018). Mitoferrin-1 is involved in the progression of alzheimer's disease through targeting mitochondrial iron metabolism in a *Caenorhabditis elegans* model of alzheimer's disease. *Neuroscience* 385, 90–101. doi:10.1016/j.neuroscience.2018.06.011

Huang, Z., Wu, M., Xu, F., Gong, J., Xiong, T., Wang, X., et al. (2022). Saikosaponin A inhibits oxidative stress and ferroptosis and reduces the injury of human umbilical vein endothelial cells induced by hydrogen peroxide. *Chin. J. Arteriosclerosis* 30 (1), 43–48.

Imai, H., Matsuoka, M., Kumagai, T., Sakamoto, T., and Koumura, T. (2017). Lipid peroxidation-dependent cell death regulated by GPx4 and ferroptosis. *Curr. Top. Microbiol. Immunol.* 403, 143–170. doi:10.1007/82_2016_508

Jacob, H. S. (1994). Newly recognized causes of atherosclerosis: the role of microorganisms and of vascular iron overload. *J. Laboratory Clin. Med.* 123 (6), 808–816.

Jiang, L., Kon, N., Li, T., Wang, S.-J., Su, T., Hibshoosh, H., et al. (2015). Ferroptosis as a p53-mediated activity during tumour suppression. *Nature* 520 (7545), 57–62. doi:10.1038/nature14344

Jiang, X., Stockwell, B. R., and Conrad, M. (2021). Ferroptosis: mechanisms, biology and role in disease. *Nat. Rev. Mol. Cell Biol.* 22 (4), 266–282. doi:10.1038/s41580-020-00324-8

Jyotsna, F., Ahmed, A., Kumar, K., Kaur, P., Chaudhary, M. H., Kumar, S., et al. (2023). Exploring the complex connection between diabetes and cardiovascular disease: analyzing approaches to mitigate cardiovascular risk in patients with diabetes. *Cureus* 15 (8), e43882. doi:10.7759/cureus.43882

Kar, F., Yıldız, F., Hacioglu, C., Kar, E., Donmez, D. B., Senturk, H., et al. (2023). LoxBlock-1 or Curcumin attenuates liver, pancreas and cardiac ferroptosis, oxidative stress and injury in Ischemia/reperfusion-damaged rats by facilitating ACSL/GPx4 signaling. *Tissue & Cell* 82, 102114. doi:10.1016/j.tice.2023.102114

Katakami, N. (2018). Mechanism of development of atherosclerosis and cardiovascular disease in diabetes mellitus. *J. Atheroscler. thrombosis* 25 (1), 27–39. doi:10.5551/jat.RV17014

Kawabata, H. (2019). Transferrin and transferrin receptors update. *Free Radic. Biol. Med.* 133, 46–54. doi:10.1016/j.freeradbiomed.2018.06.037

Khoddami, A., Wilkes, M. A., and Roberts, T. H. (2013). Techniques for analysis of plant phenolic compounds. *Molecules* 18 (2), 2328–2375. doi:10.3390/molecules18022328

Kohandel, Z., Farkhondeh, T., Aschner, M., and Samarghandian, S. (2021). Anti-inflammatory effects of thymoquinone and its protective effects against several diseases. *Biomed. Pharmacother. = Biomedecine Pharmacother.* 138, 111492. doi:10.1016/j.biopha.2021.111492

Lakhal-Littleton, S., Wolna, M., Carr, C. A., Miller, J. J. J., Christian, H. C., Ball, V., et al. (2015). Cardiac ferroportin regulates cellular iron homeostasis and is important for cardiac function. *Proc. Natl. Acad. Sci. U. S. A.* 112 (10), 3164–3169. doi:10.1073/pnas.1422373112

Lakhal-Littleton, S., Wolna, M., Chung, Y. J., Christian, H. C., Heather, L. C., Brescia, M., et al. (2016). An essential cell-autonomous role for hepcidin in cardiac iron homeostasis. *eLife* 5, e19804. doi:10.7554/eLife.19804

Lei, G., Zhuang, L., and Gan, B. (2022). Targeting ferroptosis as a vulnerability in cancer. *Nat. Rev. Cancer* 22 (7), 381–396. doi:10.1038/s41568-022-00459-0

Leng, Y., Luo, X., Yu, J., Jia, H., and Yu, B. (2021). Ferroptosis: a potential target in cardiovascular disease. *Front. Cell Dev. Biol.* 9, 813668. doi:10.3389/fcell.2021.813668

Lesjak, M., Simin, N., and Srai, S. K. S. (2022). Can polyphenols inhibit ferroptosis? *Antioxidants (Basel, Switz.* 11 (1), 150. doi:10.3390/antiox11010150

Lewerenz, J., Hewett, S. J., Huang, Y., Lambros, M., Gout, P. W., Kalivas, P. W., et al. (2013). The cystine/glutamate antiporter system x(c)(-) in health and disease: from molecular mechanisms to novel therapeutic opportunities. *Antioxidants Redox Signal.* 18 (5), 522–555. doi:10.1089/ars.2011.4391

Li, C., Chen, J. W., Liu, Z. H., Shen, Y., Ding, F. H., Gu, G., et al. (2018). CTRP5 promotes transcytosis and oxidative modification of low-density lipoprotein and the development of atherosclerosis. *Atherosclerosis* 278, 197–209. doi:10.1016/j.atherosclerosis.2018.09.037

Li, J., Cao, F., Yin, H.-L., Huang, Z.-J., Lin, Z.-T., Mao, N., et al. (2020a). Ferroptosis: past, present and future. *Cell death Dis.* 11 (2), 88. doi:10.1038/s41419-020-2298-2

Li, N., Jiang, W., Wang, W., Xiong, R., Wu, X., and Geng, Q. (2021). Ferroptosis and its emerging roles in cardiovascular diseases. *Pharmacol. Res.* 166, 105466. doi:10.1016/j.phrs.2021.105466

Li, T., Tan, Y., Ouyang, S., He, J., and Liu, L. (2022a). Resveratrol protects against myocardial ischemia-reperfusion injury via attenuating ferroptosis. *Gene* 808, 145968. doi:10.1016/j.gene.2021.145968

Li, W., Li, W., Leng, Y., Xiong, Y., and Xia, Z. (2020b). Ferroptosis is involved in diabetes myocardial ischemia/reperfusion injury through endoplasmic reticulum stress. *DNA Cell Biol.* 39 (2), 210–225. doi:10.1089/dna.2019.5097

Li, W., Liang, L., Liu, S., Yi, H., and Zhou, Y. (2023). FSP1: a key regulator of ferroptosis. *Trends Mol. Med.* 29 (9), 753–764. doi:10.1016/j.molmed.2023.05.013

Li, X., Geng-Ji, J.-J., Quan, Y.-Y., Qi, L.-M., Sun, Q., Huang, Q., et al. (2022b). Role of potential bioactive metabolites from traditional Chinese medicine for type 2 diabetes mellitus: an overview. *Front. Pharmacol.* 13, 1023713. doi:10.3389/fphar.2022.1023713

Liang, D., Minikes, A. M., and Jiang, X. (2022a). Ferroptosis at the intersection of lipid metabolism and cellular signaling. *Mol. Cell* 82 (12), 2215–2227. doi:10.1016/j.molcel.2022.03.022

Liang, F., Lu, W., Zhou, T., and Wang, Y. (2022b). Effects of aralosides and its component Araloside A on hypoxia/reoxygenation induced ferroptosis of myocardial cells based on NR3C1/p53/SLC7A11 pathway. *Chin. J. Inf. Traditional Chin. Med.* 29 (5), 63–68. doi:10.19879/j.cnki.1005-5304.202110061

Libby, P., Buring, J. E., Badimon, L., Hansson, G. K., Deanfield, J., Bittencourt, M. S., et al. (2019). Atherosclerosis. *Nat. Rev. Dis. Prim.* 5 (1), 56. doi:10.1038/s41572-019-0106-z

Lin, Y., Yang, C. Q., Lian, W. Y., Xiao, C. R., Tan, H. L., Gao, Y., et al. (2021a). Ophiopogonin D interferes with ferroptosis to reduce the damage of cardiomyocytes induced by ophiopogonin D. *Acta Pharm. Sin.* 56 (8), 2241–2247. doi:10.16438/j.0513-4870.2021-0419

Lin, Z., Liu, J., Kang, R., Yang, M., and Tang, D. (2021b). Lipid metabolism in ferroptosis. *Adv. Biol.* 5 (8), e2100396. doi:10.1002/adbi.202100396

Liu, B., Zhao, C., Li, H., Chen, X., Ding, Y., and Xu, S. (2018). Puerarin protects against heart failure induced by pressure overload through mitigation of ferroptosis. *Biochem. Biophysical Res. Commun.* 497 (1), 233–240. doi:10.1016/j.bbrc.2018.02.061

Liu, C., Yang, S., Wang, K., Bao, X., Liu, Y., Zhou, S., et al. (2019). Alkaloids from traditional Chinese medicine against hepatocellular carcinoma. *Biomed. Pharmacother. = Biomedecine Pharmacother.* 120, 109543. doi:10.1016/j.biopha.2019.109543

Liu, J., Zhang, M., Qin, C., Wang, Z., Chen, J., Wang, R., et al. (2022). Resveratrol attenuate myocardial injury by inhibiting ferroptosis via inducing KAT5/GPX4 in myocardial infarction. *Front. Pharmacol.* 13, 906073. doi:10.3389/fphar.2022.906073

Liu, M.-R., Zhu, W.-T., and Pei, D.-S. (2021a). System Xc-: a key regulatory target of ferroptosis in cancer. *Investig. New Drugs* 39 (4), 1123–1131. doi:10.1007/s10637-021-01070-0

Liu, M., Wen, H., Zuo, L., Song, X., Geng, Z., Ge, S., et al. (2023). Bryostatin-1 attenuates intestinal ischemia/reperfusion-induced intestinal barrier dysfunction, inflammation, and oxidative stress via activation of Nrf2/HO-1 signaling. *FASEB J.* 37 (6), e22948. doi:10.1096/fj.202201540R

Liu, X.-J., Lv, Y.-F., Cui, W.-Z., Li, Y., Liu, Y., Xue, Y.-T., et al. (2021b). Icariin inhibits hypoxia/reoxygenation-induced ferroptosis of cardiomyocytes via regulation of the Nrf2/HO-1 signaling pathway. *FEBS open bio* 11 (11), 2966–2976. doi:10.1002/2211-5463.13276

Lu, S. C. (2009). Regulation of glutathione synthesis. *Mol. Aspects Med.* 30 (1-2), 42–59. doi:10.1016/j.mam.2008.05.005

Luo, L.-F., Guan, P., Qin, L.-Y., Wang, J.-X., Wang, N., and Ji, E.-S. (2021). Astragaloside IV inhibits adriamycin-induced cardiac ferroptosis by enhancing Nrf2 signaling. *Mol. Cell. Biochem.* 476 (7), 2603–2611. doi:10.1007/s11010-021-04112-6

Luo, W. (2022). "The protective effect and mechanism of thymoquinone on doxorubicin-induced cardiotoxicity,". Master (Nanchang, China: Nanchang Univ).

Ma, J., Zhang, H., Chen, Y., Liu, X., Tian, J., and Shen, W. (2022). The role of macrophage iron overload and ferroptosis in atherosclerosis. *Biomolecules* 12 (11), 1702. doi:10.3390/biom12111702

Marques, V. B., Leal, M. A. S., Mageski, J. G. A., Fidelis, H. G., Nogueira, B. V., Vasquez, E. C., et al. (2019). Chronic iron overload intensifies atherosclerosis in apolipoprotein E deficient mice: role of oxidative stress and endothelial dysfunction. *Life Sci.* 233, 116702. doi:10.1016/j.lfs.2019.116702

Meng, T., Li, X., Li, C., Liu, J., Chang, H., Jiang, N., et al. (2022). Natural products of traditional Chinese medicine treat atherosclerosis by regulating inflammatory and oxidative stress pathways. *Front. Pharmacol.* 13, 997598. doi:10.3389/fphar.2022.997598

Miao, R., Fang, X., Zhang, Y., Wei, J., Zhang, Y., and Tian, J. (2023). Iron metabolism and ferroptosis in type 2 diabetes mellitus and complications: mechanisms and therapeutic opportunities. *Cell Death Dis.* 14 (3), 186. doi:10.1038/s41419-023-05708-0

Miki, T., Itoh, T., Sunaga, D., and Miura, T. (2012). Effects of diabetes on myocardial infarct size and cardioprotection by preconditioning and postconditioning. *Cardiovasc. Diabetol.* 11, 67. doi:10.1186/1475-2840-11-67

Miyamoto, H. D., Ikeda, M., Ide, T., Tadokoro, T., Furusawa, S., Abe, K., et al. (2022). Iron overload via heme degradation in the endoplasmic reticulum triggers ferroptosis in myocardial ischemia-reperfusion injury. *JACC. Basic Transl. Sci.* 7 (8), 800–819. doi:10.1016/j.jacbts.2022.03.012

Mou, Y., Wang, J., Wu, J., He, D., Zhang, C., Duan, C., et al. (2019). Ferroptosis, a new form of cell death: opportunities and challenges in cancer. *J. Hematol. Oncol.* 12 (1), 34. doi:10.1186/s13045-019-0720-y

Muckenthaler, M. U., Galy, B., and Hentze, M. W. (2008). Systemic iron homeostasis and the iron-responsive element/iron-regulatory protein (IRE/IRP) regulatory network. *Annu. Rev. Nutr.* 28, 197–213. doi:10.1146/annurev.nutr.28.061807.155521

Muckenthaler, M. U., Rivella, S., Hentze, M. W., and Galy, B. (2017). A red carpet for iron metabolism. *Cell* 168 (3), 344–361. doi:10.1016/j.cell.2016.12.034

Nakamura, K., Miyoshi, T., Yoshida, M., Akagi, S., Saito, Y., Ejiri, K., et al. (2022). Pathophysiology and treatment of diabetic cardiomyopathy and heart failure in patients with diabetes mellitus. *Int. J. Mol. Sci.* 23 (7), 3587. doi:10.3390/ijms23073587

Nakamura, M., and Sadoshima, J. (2020). Cardiomyopathy in obesity, insulin resistance and diabetes. *J. Physiology* 598 (14), 2977–2993. doi:10.1113/JP276747

Naowarojna, N., Wu, T. W., Pan, Z., Li, M., Han, J. R., and Zou, Y. (2023). Dynamic regulation of ferroptosis by lipid metabolism. *Antioxidants redox Signal.* 39 (1-3), 59–78. doi:10.1089/ars.2023.0278

Nemeth, E., and Ganz, T. (2021). Hepcidin-ferroportin interaction controls systemic iron homeostasis. *Int. J. Mol. Sci.* 22 (12), 6493. doi:10.3390/ijms22126493

Ni, M., Zhou, J., Zhu, Z., Xu, Q., Yin, Z., Wang, Y., et al. (2023). Shikonin and cisplatin synergistically overcome cisplatin resistance of ovarian cancer by inducing ferroptosis via upregulation of HMOX1 to promote Fe2+ accumulation. *Phytomedicine Int. J. Phytotherapy Phytopharm.* 112, 154701. doi:10.1016/j.phymed.2023.154701

Omiya, S., Hikoso, S., Imanishi, Y., Saito, A., Yamaguchi, O., Takeda, T., et al. (2009). Downregulation of ferritin heavy chain increases labile iron pool, oxidative stress and cell death in cardiomyocytes. *J. Mol. Cell. Cardiol.* 46 (1), 59–66. doi:10.1016/j.yjmcc.2008.09.714

Ozdemir, B. (2020). Correlation of C-reactive protein and serum iron levels with syntax score. *Archives Razi Inst.* 75 (3), 413–418. doi:10.22092/ari.2020.128122.1404

Park, T.-J., Park, J. H., Lee, G. S., Lee, J.-Y., Shin, J. H., Kim, M. W., et al. (2019). Quantitative proteomic analyses reveal that GPX4 downregulation during myocardial infarction contributes to ferroptosis in cardiomyocytes. *Cell death Dis.* 10 (11), 835. doi:10.1038/s41419-019-2061-8

Pope, L. E., and Dixon, S. J. (2023). Regulation of ferroptosis by lipid metabolism. *Trends Cell Biol.* S0962-8924 00086–00087. doi:10.1016/j.tcb.2023.05.003

Qin, X., Zhang, J., Wang, B., Xu, G., Yang, X., Zou, Z., et al. (2021). Ferritinophagy is involved in the zinc oxide nanoparticles-induced ferroptosis of vascular endothelial cells. *Autophagy* 17 (12), 4266–4285. doi:10.1080/15548627.2021.1911016

Reed, A., Ichu, T.-A., Milosevich, N., Melillo, B., Schafroth, M. A., Otsuka, Y., et al. (2022). LPCAT3 inhibitors remodel the polyunsaturated phospholipid content of human cells and protect from ferroptosis. *ACS Chem. Biol.* 17 (6), 1607–1618. doi:10.1021/acschembio.2c00317

Roth, G. A., Mensah, G. A., Johnson, C. O., Addolorato, G., Ammirati, E., Baddour, L. M., et al. (2020). Global burden of cardiovascular diseases and risk factors, 1990-2019: update from the GBD 2019 study. *J. Am. Coll. Cardiol.* 76 (25), 2982–3021. doi:10.1016/j.jacc.2020.11.010

Russo, I., Penna, C., Musso, T., Popara, J., Alloatti, G., Cavalot, F., et al. (2017). Platelets, diabetes and myocardial ischemia/reperfusion injury. *Cardiovasc. Diabetol.* 16 (1), 71. doi:10.1186/s12933-017-0550-6

Seibt, T. M., Proneth, B., and Conrad, M. (2019). Role of GPX4 in ferroptosis and its pharmacological implication. *Free Radic. Biol. Med.* 133, 144–152. doi:10.1016/j.freeradbiomed.2018.09.014

Serafini, M., Peluso, I., and Raguzzini, A. (2010). Flavonoids as anti-inflammatory agents. *Proc. Nutr. Soc.* 69 (3), 273–278. doi:10.1017/S002966511000162X

Shan, X., Lv, Z.-Y., Yin, M.-J., Chen, J., Wang, J., and Wu, Q.-N. (2021). The protective effect of cyanidin-3-glucoside on myocardial ischemia-reperfusion injury through ferroptosis. *Oxidative Med. Cell. Longev.* 2021, 8880141. doi:10.1155/2021/8880141

Shen, Y., Shen, X., Wang, S., Zhang, Y., Wang, Y., Ding, Y., et al. (2022a). Protective effects of Salvianolic acid B on rat ferroptosis in myocardial infarction through upregulating the Nrf2 signaling pathway. *Int. Immunopharmacol.* 112, 109257. doi:10.1016/j.intimp.2022.109257

Shen, Y., Wang, X., Shen, X., Wang, Y., Wang, S., Zhang, Y., et al. (2022b). Geniposide possesses the protective effect on myocardial injury by inhibiting oxidative stress and ferroptosis via activation of the grsf1/GPx4 Axis. *Front. Pharmacol.* 13, 879870. doi:10.3389/fphar.2022.879870

Shi, J., Wang, Q.-H., Wei, X., Huo, B., Ye, J.-N., Yi, X., et al. (2023a). Histone acetyltransferase P300 deficiency promotes ferroptosis of vascular smooth muscle cells by activating the HIF-1α/HMOX1 axis. *Mol. Med. Camb. Mass* 29 (1), 91. doi:10.1186/s10020-023-00694-7

Shi, M., Huang, F., Deng, C., Wang, Y., and Kai, G. (2019). Bioactivities, biosynthesis and biotechnological production of phenolic acids in Salvia miltiorrhiza. *Crit. Rev. Food Sci. Nutr.* 59 (6), 953–964. doi:10.1080/10408398.2018.1474170

Shi, Y., Shi, X., Zhao, M., Chang, M., Ma, S., and Zhang, Y. (2023b). Ferroptosis: a new mechanism of traditional Chinese medicine compounds for treating acute kidney injury. *Biomed. Pharmacother.* 163, 114849. doi:10.1016/j.biopha.2023.114849

Shi, Z., Zhang, L., Zheng, J., Sun, H., and Shao, C. (2021). Ferroptosis: biochemistry and biology in cancers. *Front. Oncol.* 11, 579286. doi:10.3389/fonc.2021.579286

Simcox, J. A., and McClain, D. A. (2013). Iron and diabetes risk. *Cell Metab.* 17 (3), 329–341. doi:10.1016/j.cmet.2013.02.007

Singla, R. K., Dubey, A. K., Garg, A., Sharma, R. K., Fiorino, M., Ameen, S. M., et al. (2019). Natural polyphenols: chemical classification, definition of classes, subcategories, and structures. *J. AOAC Int.* 102 (5), 1397–1400. doi:10.5740/jaoacint.19-0133

Song, C., Li, D., Zhang, J., and Zhao, X. (2023). Berberine hydrochloride alleviates imatinib mesylate - induced cardiotoxicity through the inhibition of Nrf2-dependent ferroptosis. *Food & Funct.* 14 (2), 1087–1098. doi:10.1039/d2fo03331c

Song, Y., Wang, B., Zhu, X., Hu, J., Sun, J., Xuan, J., et al. (2021). Human umbilical cord blood-derived MSCs exosome attenuate myocardial injury by inhibiting ferroptosis in acute myocardial infarction mice. *Cell Biol. Toxicol.* 37 (1), 51–64. doi:10.1007/s10565-020-09530-8

Stockwell, B. R. (2022). Ferroptosis turns 10: emerging mechanisms, physiological functions, and therapeutic applications. *Cell* 185 (14), 2401–2421. doi:10.1016/j.cell.2022.06.003

Stockwell, B. R., Friedmann Angeli, J. P., Bayir, H., Bush, A. I., Conrad, M., Dixon, S. J., et al. (2017). Ferroptosis: a regulated cell death nexus linking metabolism, redox biology, and disease. *Cell* 171 (2), 273–285. doi:10.1016/j.cell.2017.09.021

Sun, J., Xu, J., Liu, Y., Lin, Y., Wang, F., Han, Y., et al. (2023). Exogenous spermidine alleviates diabetic cardiomyopathy via suppressing reactive oxygen species, endoplasmic reticulum stress, and Pannexin-1-mediated ferroptosis. *Biomol. Biomed.* 23, 825–837. doi:10.17305/bb.2022.8846

Sun, W., Shi, R., Guo, J., Wang, H., Shen, L., Shi, H., et al. (2021). miR-135b-3p promotes cardiomyocyte ferroptosis by targeting GPX4 and aggravates myocardial ischemia/reperfusion injury. *Front. Cardiovasc. Med.* 8, 663832. doi:10.3389/fcvm.2021.663832

Sun, X.-Y., Jia, L.-Y., Rong, Z., Zhou, X., Cao, L.-Q., Li, A.-H., et al. (2022). Research advances on matrine. *Front. Chem.* 10, 867318. doi:10.3389/fchem.2022.867318

Sun, X., Ou, Z., Xie, M., Kang, R., Fan, Y., Niu, X., et al. (2015). HSPB1 as a novel regulator of ferroptotic cancer cell death. *Oncogene* 34 (45), 5617–5625. doi:10.1038/onc.2015.32

Sun, Y., Zheng, Y., Wang, C., and Liu, Y. (2018). Glutathione depletion induces ferroptosis, autophagy, and premature cell senescence in retinal pigment epithelial cells. *Cell Death Dis.* 9 (7), 753. doi:10.1038/s41419-018-0794-4

Talebi, M., Talebi, M., Farkhondeh, T., and Samarghandian, S. (2021). Biological and therapeutic activities of thymoquinone: focus on the Nrf2 signaling pathway. *Phytotherapy Res. PTR* 35 (4), 1739–1753. doi:10.1002/ptr.6905

Tan, J., Li, Y., Hou, D.-X., and Wu, S. (2019). The effects and mechanisms of cyanidin-3-glucoside and its phenolic metabolites in maintaining intestinal integrity. *Antioxidants (Basel, Switz.* 8 (10), 479. doi:10.3390/antiox8100479

Tang, L.-J., Luo, X.-J., Tu, H., Chen, H., Xiong, X.-M., Li, N.-S., et al. (2021a). Ferroptosis occurs in phase of reperfusion but not ischemia in rat heart following ischemia or ischemia/reperfusion. *Naunyn-Schmiedeberg's archives Pharmacol.* 394 (2), 401–410. doi:10.1007/s00210-020-01932-z

Tang, L.-J., Zhou, Y.-J., Xiong, X.-M., Li, N.-S., Zhang, J.-J., Luo, X.-J., et al. (2021b). Ubiquitin-specific protease 7 promotes ferroptosis via activation of the p53/TfR1 pathway in the rat hearts after ischemia/reperfusion. *Free Radic. Biol. Med.* 162, 339–352. doi:10.1016/j.freeradbiomed.2020.10.307

Townsend, N., Kazakiewicz, D., Lucy Wright, F., Timmis, A., Huculeci, R., Torbica, A., et al. (2022). Epidemiology of cardiovascular disease in Europe. *Nat. Rev. Cardiol.* 19 (2), 133–143. doi:10.1038/s41569-021-00607-3

Tu, H., Zhou, Y.-J., Tang, L.-J., Xiong, X.-M., Zhang, X.-J., Ali Sheikh, M. S., et al. (2021). Combination of ponatinib with deferoxamine synergistically mitigates ischemic heart injury via simultaneous prevention of necroptosis and ferroptosis. *Eur. J. Pharmacol.* 898, 173999. doi:10.1016/j.ejphar.2021.173999

Ubellacker, J. M., Tasdogan, A., Ramesh, V., Shen, B., Mitchell, E. C., Martin-Sandoval, M. S., et al. (2020). Lymph protects metastasizing melanoma cells from ferroptosis. *Nature* 585 (7823), 113–118. doi:10.1038/s41586-020-2623-z

Visseren, F. L. J., Mach, F., Smulders, Y. M., Carballo, D., Koskinas, K. C., Bäck, M., et al. (2021). 2021 ESC Guidelines on cardiovascular disease prevention in clinical practice. *Eur. Heart J.* 42 (34), 3227–3337. doi:10.1093/eurheartj/ehab484

Vogt, A.-C. S., Arsiwala, T., Mohsen, M., Vogel, M., Manolova, V., and Bachmann, M. F. (2021). On iron metabolism and its regulation. *Int. J. Mol. Sci.* 22 (9), 4591. doi:10.3390/ijms22094591

von Samson-Himmelstjerna, F. A., Kolbrink, B., Riebeling, T., Kunzendorf, U., and Krautwald, S. (2022). Progress and setbacks in translating a decade of ferroptosis research into clinical practice. *Cells* 11 (14), 2134. doi:10.3390/cells11142134

Wang, J., and Wang, H. (2017). Oxidative stress in pancreatic beta cell regeneration. *Oxidative Med. Cell. Longev.* 2017, 1930261. doi:10.1155/2017/1930261

Wang, K., Chen, X.-Z., Wang, Y.-H., Cheng, X.-L., Zhao, Y., Zhou, L.-Y., et al. (2022a). Emerging roles of ferroptosis in cardiovascular diseases. *Cell death Discov.* 8 (1), 394. doi:10.1038/s41420-022-01183-2

Wang, L., Liu, Y., Du, T., Yang, H., Lei, L., Guo, M., et al. (2020). ATF3 promotes erastin-induced ferroptosis by suppressing system Xc. *Cell Death Differ.* 27 (2), 662–675. doi:10.1038/s41418-019-0380-z

Wang, X.-D., and Kang, S. (2021). Ferroptosis in myocardial infarction: not a marker but a maker. *Open Biol.* 11 (4), 200367. doi:10.1098/rsob.200367

Wang, X., Chen, X., Zhou, W., Men, H., Bao, T., Sun, Y., et al. (2022b). Ferroptosis is essential for diabetic cardiomyopathy and is prevented by sulforaphane via AMPK/NRF2 pathways. *Acta Pharm. Sin. B* 12 (2), 708–722. doi:10.1016/j.apsb.2021.10.005

Wang, X., Zhang, M., Mao, C., Zhang, C., Ma, W., Tang, J., et al. (2023). Icariin alleviates ferroptosis-related atherosclerosis by promoting autophagy in xo-LDL -induced vascular endothelial cell injury and atherosclerotic mice. *Phytotherapy Res.* 37, 3951–3963. doi:10.1002/ptr.7854

Wang, Y., Zhang, M., Bi, R., Su, Y., Quan, F., Lin, Y., et al. (2022c). ACSL4 deficiency confers protection against ferroptosis-mediated acute kidney injury. *Redox Biol.* 51, 102262. doi:10.1016/j.redox.2022.102262

Wang, Y., Zhao, Y., Ye, T., Yang, L., Shen, Y., and Li, H. (2021). Ferroptosis signaling and regulators in atherosclerosis. *Front. Cell Dev. Biol.* 9, 809457. doi:10.3389/fcell.2021.809457

Wei, S., Qiu, T., Yao, X., Wang, N., Jiang, L., Jia, X., et al. (2020). Arsenic induces pancreatic dysfunction and ferroptosis via mitochondrial ROS-autophagy-lysosomal pathway. *J. Hazard. Mater.* 384, 121390. doi:10.1016/j.jhazmat.2019.121390

Wei, Z., Shaohuan, Q., Pinfang, K., and Chao, S. (2022). Curcumin attenuates ferroptosis-induced myocardial injury in diabetic cardiomyopathy through the Nrf2 pathway. *Cardiovasc. Ther.* 2022, 3159717. doi:10.1155/2022/3159717

Wu, X., Li, Y., Zhang, S., and Zhou, X. (2021). Ferroptosis as a novel therapeutic target for cardiovascular disease. *Theranostics* 11 (7), 3052–3059. doi:10.7150/thno.54113

Wu, Y., Wang, F., Fan, L., Zhang, W., Wang, T., Du, Y., et al. (2018). Baicalin alleviates atherosclerosis by relieving oxidative stress and inflammatory responses via inactivating the NF-κB and p38 MAPK signaling pathways. *Biomed. Pharmacother. = Biomedecine Pharmacother.* 97, 1673–1679. doi:10.1016/j.biopha.2017.12.024

Xia, J., Si, H., Yao, W., Li, C., Yang, G., Tian, Y., et al. (2021). Research progress on the mechanism of ferroptosis and its clinical application. *Exp. Cell Res.* 409 (2), 112932. doi:10.1016/j.yexcr.2021.112932

Xiao, Y., Yu, Y., Hu, L., Yang, Y., Yuan, Y., Zhang, W., et al. (2023). Matrine alleviates sepsis-induced myocardial injury by inhibiting ferroptosis and apoptosis. *Inflammation* 46, 1684–1696. doi:10.1007/s10753-023-01833-2

Xie, D., Li, K., Feng, R., Xiao, M., Sheng, Z., and Xie, Y. (2023). Ferroptosis and traditional Chinese medicine for type 2 diabetes mellitus. *Diabetes, Metabolic Syndrome Obes.* 16, 1915–1930. doi:10.2147/DMSO.S412747

Xie, L.-H., Fefelova, N., Pamarthi, S. H., and Gwathmey, J. K. (2022). Molecular mechanisms of ferroptosis and relevance to cardiovascular disease. *Cells* 11 (17), 2726. doi:10.3390/cells11172726

Xu, J., Han, X., Xia, N., Zhao, Q., and Cheng, Z. (2023). IL-37 suppresses macrophage ferroptosis to attenuate diabetic atherosclerosis via the NRF2 pathway. *Exp. Ther. Med.* 25 (6), 289. doi:10.3892/etm.2023.11988

Xu, S., Wu, B., Zhong, B., Lin, L., Ding, Y., Jin, X., et al. (2021). Naringenin alleviates myocardial ischemia/reperfusion injury by regulating the nuclear factor-erythroid factor 2-related factor 2 (Nrf2)/System xc-/glutathione peroxidase 4 (GPX4) axis to inhibit ferroptosis. *Bioengineered* 12 (2), 10924–10934. doi:10.1080/21655979.2021.1995994

Xu, X.-H., Li, T., Fong, C. M. V., Chen, X., Chen, X.-J., Wang, Y.-T., et al. (2016). Saponins from Chinese medicines as anticancer agents. *Mol. (Basel, Switz.* 21 (10), 1326. doi:10.3390/molecules21101326

Yang, G., Wang, F., Wang, Y., Yu, X., Yang, S., Xu, H., et al. (2020). Protective effect of tanshinone IIA on H2O2-induced oxidative stress injury in rat cardiomyocytes by activating Nrf2 pathway. *J. Recept. Signal Transduct. Res.* 40 (3), 264–272. doi:10.1080/10799893.2020.1731535

Yang, K.-T., Chao, T.-H., Wang, I.-C., Luo, Y.-P., Ting, P.-C., Lin, J.-H., et al. (2022a). Berberine protects cardiac cells against ferroptosis. *Tzu chi Med. J.* 34 (3), 310–317. doi:10.4103/tcmj.tcmj_236_21

Yang, W. S., Kim, K. J., Gaschler, M. M., Patel, M., Shchepinov, M. S., and Stockwell, B. R. (2016). Peroxidation of polyunsaturated fatty acids by lipoxygenases drives ferroptosis. *Proc. Natl. Acad. Sci. U. S. A.* 113 (34), E4966–E4975. doi:10.1073/pnas.1603244113

Yang, W. S., SriRamaratnam, R., Welsch, M. E., Shimada, K., Skouta, R., Viswanathan, V. S., et al. (2014). Regulation of ferroptotic cancer cell death by GPX4. *Cell* 156 (1-2), 317–331. doi:10.1016/j.cell.2013.12.010

Yang, X.-D., and Yang, Y.-Y. (2022). Ferroptosis as a novel therapeutic target for diabetes and its complications. *Front. Endocrinol.* 13, 853822. doi:10.3389/fendo.2022.853822

Yang, X., Kawasaki, N. K., Min, J., Matsui, T., and Wang, F. (2022b). Ferroptosis in heart failure. *J. Mol. Cell. Cardiol.* 173, 141–153. doi:10.1016/j.yjmcc.2022.10.004

Yao, F., Cui, X., Zhang, Y., Bei, Z., Wang, H., Zhao, D., et al. (2021). Iron regulatory protein 1 promotes ferroptosis by sustaining cellular iron homeostasis in melanoma. *Oncol. Lett.* 22 (3), 657. doi:10.3892/ol.2021.12918

Ye, J., Lyu, T. J., Li, L. Y., Liu, Y., Zhang, H., Wang, X., et al. (2023). Ginsenosi*de re* attenuates myocardial ischemia/reperfusion induced ferroptosis via miR-144-3p/SLC7A11. *Phytomedicine* 113, 154681. doi:10.1016/j.phymed.2023.154681

You, J., Ouyang, S., Xie, Z., Zhi, C., Yu, J., Tan, X., et al. (2023). The suppression of hyperlipid diet-induced ferroptosis of vascular smooth muscle cells protests against atherosclerosis independent of p53/SCL7A11/GPX4 axis. *J. Cell. Physiology* 238 (8), 1891–1908. doi:10.1002/jcp.31045

Yu, L.-M., Dong, X., Huang, T., Zhao, J.-K., Zhou, Z.-J., Huang, Y.-T., et al. (2023). Inhibition of ferroptosis by icariin treatment attenuates excessive ethanol consumption-induced atrial remodeling and susceptibility to atrial fibrillation, role of SIRT1. *Apoptosis Int. J. Program. Cell death* 28 (3-4), 607–626. doi:10.1007/s10495-023-01814-8

Yu, W., Liu, W., Xie, D., Wang, Q., Xu, C., Zhao, H., et al. (2022). High level of uric acid promotes atherosclerosis by targeting NRF2-mediated autophagy dysfunction and ferroptosis. *Oxidative Med. Cell. Longev.* 2022, 9304383. doi:10.1155/2022/9304383

Zeidan, R. S., Han, S. M., Leeuwenburgh, C., and Xiao, R. (2021). Iron homeostasis and organismal aging. *Ageing Res. Rev.* 72, 101510. doi:10.1016/j.arr.2021.101510

Zhang, H., Zhabyeyev, P., Wang, S., and Oudit, G. Y. (2019). Role of iron metabolism in heart failure: from iron deficiency to iron overload. *Biochimica Biophysica Acta (BBA) - Mol. Basis Dis.* 1865 (7), 1925–1937. doi:10.1016/j.bbadis.2018.08.030

Zhang, N., Yu, X., Xie, J., and Xu, H. (2021a). New insights into the role of ferritin in iron homeostasis and neurodegenerative diseases. *Mol. Neurobiol.* 58 (6), 2812–2823. doi:10.1007/s12035-020-02277-7

Zhang, W., Qian, S., Tang, B., Kang, P., Zhang, H., and Shi, C. (2023). Resveratrol inhibits ferroptosis and decelerates heart failure progression via Sirt1/p53 pathway activation. *J. Cell. Mol. Med.* 27, 3075–3089. doi:10.1111/jcmm.17874

Zhang, X., Yu, Y., Lei, H., Cai, Y., Shen, J., Zhu, P., et al. (2020). The nrf-2/HO-1 signaling Axis: a ray of hope in cardiovascular diseases. *Cardiol. Res. Pract.* 2020, 5695723. doi:10.1155/2020/5695723

Zhang, Z., Funcke, J.-B., Zi, Z., Zhao, S., Straub, L. G., Zhu, Y., et al. (2021b). Adipocyte iron levels impinge on a fat-gut crosstalk to regulate intestinal lipid absorption and mediate protection from obesity. *Cell Metab.* 33 (8), 1624–1639.e9. doi:10.1016/j.cmet.2021.06.001

Zhao, D., Yang, J., and Yang, L. (2017). Insights for oxidative stress and mTOR signaling in myocardial ischemia/reperfusion injury under diabetes. *Oxidative Med. Cell. Longev.* 2017, 6437467. doi:10.1155/2017/6437467

Zhao, K., Chen, X., Bian, Y., Zhou, Z., Wei, X., and Zhang, J. (2023a). Broadening horizons: the role of ferroptosis in myocardial ischemia–reperfusion injury. *Naunyn-Schmiedeberg's Archives Pharmacol.* 396, 2269–2286. doi:10.1007/s00210-023-02506-5

Zhao, Y., Pan, B., Lv, X., Chen, C., Li, K., Wang, Y., et al. (2023b). Ferroptosis: roles and molecular mechanisms in diabetic cardiomyopathy. *Front. Endocrinol.* 14, 1140644. doi:10.3389/fendo.2023.1140644

Zheng, Y., Ley, S. H., and Hu, F. B. (2018). Global aetiology and epidemiology of type 2 diabetes mellitus and its complications. *Nat. Rev. Endocrinol.* 14 (2), 88–98. doi:10.1038/nrendo.2017.151

Zhou, B., Zhang, J., Chen, Y., Liu, Y., Tang, X., Xia, P., et al. (2022). Puerarin protects against sepsis-induced myocardial injury through AMPK-mediated ferroptosis signaling. *Aging* 14 (8), 3617–3632. doi:10.18632/aging.204033

Zhou, Y.-X., Zhang, H., and Peng, C. (2014). Puerarin: a review of pharmacological effects. *Phytotherapy Res. PTR* 28 (7), 961–975. doi:10.1002/ptr.5083

Zhou, Y.-X., Zhang, R.-Q., Rahman, K., Cao, Z.-X., Zhang, H., and Peng, C. (2019). Diverse pharmacological activities and potential medicinal benefits of geniposide. *Evidence-Based Complementary Altern. Med. eCAM* 2019, 4925682. doi:10.1155/2019/4925682

10.3389/fphar.2023.1286718

# Glossary

| | |
|---|---|
| **$^{\bullet}OH$** | Hydroxyl radicals |
| **ACSL4** | Acyl-coenzyme A synthetase long chain family member 4 |
| **AS** | Atherosclerosis |
| **ATF3** | Activating transcription factor 3 |
| **BH4** | Tetrahydrobiopterin |
| **CoA** | Acyl-coenzyme A |
| **CVDs** | Cardiovascular diseases |
| **DCM** | Diabetic cardiomyopathy |
| **DHODH** | Dihydroorotate dehydrogenase |
| **DMT1** | Divalent metal transporter 1 |
| **ERS** | Endoplasmic reticulum stress |
| **$Fe^{2+}$** | Ferrous iron |
| **$Fe^{3+}$** | Ferric iron |
| **FPN** | Ferroportin |
| **FSP1** | Ferroptosis suppressor protein 1 |
| **FTH1** | Ferritin heavy chain 1 |
| **FTL** | Ferritin light chain |
| **GCH1** | GTP cyclohydrolase 1 |
| **GPX4** | Glutathione peroxidase 4 |
| **GSH** | Glutathione |
| **GSSG** | Oxidized glutathione |
| **HF** | Heart failure |
| **HO-1** | Haem oxygenase 1 |
| **HSPB1** | Heat shock protein family B (small) member 1 |
| **I/R** | Ischemia/reperfusion |
| **IRE** | Iron-responsive element |
| **IRP** | Iron-regulatory protein |
| **LOXs** | Lipoxygenases |
| **LPCAT3** | Lysophosphatidylcholine acyltransferase 3 |
| **MDA** | Malondialdehyde |
| **MI** | Myocardial infarction |
| **MUFAs** | Monounsaturated fatty acids |
| **NADPH** | Reduced nicotinamide adenine dinucleotide phosphate |
| **NCOA4** | Nuclear receptor coactivator 4 |
| **NOX4** | NADPH oxidase 4 |
| **NRF2** | Nuclear factor-erythroid 2-related factor 2 |
| **PLs** | Phospholipids |
| **PUFA-PL-OHs** | PUFA phospholipid alcohols |
| **PUFA-PL-OOHs** | PUFA phospholipid hydroperoxides |
| **PUFA-PLs** | Phospholipids containing polyunsaturated fatty acids |
| **PUFAs** | Polyunsaturated fatty acids |
| **ROS** | Reactive oxygen species |
| **STEAP3** | Six-transmembrane epithelial antigen of prostate 3 |
| **System $x_c^-$** | The cystine-glutamate antiporter |
| **T2DM** | Type 2 diabetes mellitus |
| **TF** | Transferrin |
| **TFR1** | Transferrin receptor protein 1 |
| **TCM** | Traditional Chinese medicine |
| **UTRs** | Untranslated regions |

frontiers | Frontiers in Pharmacology

TYPE Original Research
PUBLISHED 18 December 2023
DOI 10.3389/fphar.2023.1332212



OPEN ACCESS

EDITED BY
Nirmal Parajuli,
Henry Ford Health System, United States

REVIEWED BY
Elsa Ching Chan,
Centre for Eye Research Australia, Australia
Debora Collotta,
University of Turin, Italy, Italy

*CORRESPONDENCE
Anca Hermenean,
hermenean.anca@uvvg.ro

†These authors have contributed equally to this work and share first authorship

‡These authors have contributed equally to this work and share last authorship

RECEIVED 02 November 2023
ACCEPTED 04 December 2023
PUBLISHED 18 December 2023

CITATION
Trotta MC, Herman H, Ciceu A, Mladin B, Rosu M, Lepre CC, Russo M, Bácskay I, Fenyvesi F, Marfella R, Hermenean A, Balta C and D'Amico M (2023), Chrysin-based supramolecular cyclodextrin-calixarene drug delivery system: a novel approach for attenuating cardiac fibrosis in chronic diabetes.
*Front. Pharmacol.* 14:1332212.
doi: 10.3389/fphar.2023.1332212



# Chrysin-based supramolecular cyclodextrin-calixarene drug delivery system: a novel approach for attenuating cardiac fibrosis in chronic diabetes

Maria Consiglia Trotta[1†], Hildegard Herman[2†], Alina Ciceu[2], Bianca Mladin[2], Marcel Rosu[2], Caterina Claudia Lepre[2,3], Marina Russo[4,5], Ildikó Bácskay[6,7], Ferenc Fenyvesi[6], Raffaele Marfella[8], Anca Hermenean[2,9]*, Cornel Balta[2‡] and Michele D'Amico[1‡]

[1]Department of Experimental Medicine, University of Campania "Luigi Vanvitelli", Naples, Italy, [2]"Aurel Ardelean" Institute of Life Sciences, Vasile Goldis Western University of Arad, Arad, Romania, [3]PhD Course in Translational Medicine, University of Campania "Luigi Vanvitelli", Naples, Italy, [4]PhD Course in National Interest in Public Administration and Innovation for Disability and Social Inclusion, Department of Mental, Physical Health and Preventive Medicine, University of Campania "Luigi Vanvitelli", Naples, Italy, [5]School of Pharmacology and Clinical Toxicology, University of Campania "Luigi Vanvitelli", Naples, Italy, [6]Department of Molecular and Nanopharmaceutics, Faculty of Pharmacy, University of Debrecen, Debrecen, Hungary, [7]Institute of Healthcare Industry, University of Debrecen, Debrecen, Hungary, [8]Department of Advanced Medical and Surgical Sciences, University of Campania "Luigi Vanvitelli", Naples, Italy, [9]Department of Histology, Faculty of Medicine, Vasile Goldis Western University of Arad, Arad, Romania

**Introduction:** Cardiac fibrosis is strongly induced by diabetic conditions. Both chrysin (CHR) and calixarene OTX008, a specific inhibitor of galectin 1 (Gal-1), seem able to reduce transforming growth factor beta (TGF-β)/SMAD pro-fibrotic pathways, but their use is limited to their low solubility. Therefore, we formulated a dual-action supramolecular system, combining CHR with sulfobutylated β-cyclodextrin (SBECD) and OTX008 (SBECD + OTX + CHR). Here we aimed to test the anti-fibrotic effects of SBECD + OTX + CHR in hyperglycemic H9c2 cardiomyocytes and in a mouse model of chronic diabetes.

**Methods:** H9c2 cardiomyocytes were exposed to normal (NG, 5.5 mM) or high glucose (HG, 33 mM) for 48 h, then treated with SBECD + OTX + CHR (containing OTX008 0.75–1.25–2.5 μM) or the single compounds for 6 days. TGF-β/SMAD pathways, Mitogen-Activated Protein Kinases (MAPKs) and Gal-1 levels were assayed by Enzyme-Linked Immunosorbent Assays (ELISAs) or Real-Time Quantitative Reverse Transcription Polymerase chain reaction (qRT-PCR). Adult CD1 male mice received a single intraperitoneal (i.p.) administration of streptozotocin (STZ) at a dosage of 102 mg/kg body weight. From the second week of diabetes, mice received 2 times/week the following i.p. treatments: OTX (5 mg/kg)-SBECD; OTX (5 mg/kg)-SBECD-CHR, SBECD-CHR, SBECD. After a 22-week period of diabetes, mice were euthanized and cardiac tissue used for tissue staining, ELISA, qRT-PCR aimed to analyse TGF-β/SMAD, extracellular matrix (ECM) components and Gal-1.

**Results:** In H9c2 cells exposed to HG, SBECD + OTX + CHR significantly ameliorated the damaged morphology and reduced TGF-β1, its receptors

(TGFβR1 and TGFβR2), SMAD2/4, MAPKs and Gal-1. Accordingly, these markers were reduced also in cardiac tissue from chronic diabetes, in which an amelioration of cardiac remodeling and ECM was evident. In both settings, SBECD + OTX + CHR was the most effective treatment compared to the other ones.

**Conclusion:** The CHR-based supramolecular SBECD-calixarene drug delivery system, by enhancing the solubility and the bioavailability of both CHR and calixarene OTX008, and by combining their effects, showed a strong anti-fibrotic activity in rat cardiomyocytes and in cardiac tissue from mice with chronic diabetes. Also an improved cardiac tissue remodeling was evident. Therefore, new drug delivery system, which could be considered as a novel putative therapeutic strategy for the treatment of diabetes-induced cardiac fibrosis.

KEYWORDS

**chrysin, cyclodextrin, calixarene, drug delivery system, cardiac fibrosis, chronic diabetes**

# 1 Introduction

Cardiac fibrosis is a prominent outcome in heart-related disorders, exhibited by various cardiac regions (Tian et al., 2017; Ytrehus et al., 2018). The main cells involved in development of cardiac fibrosis are activated myofibroblasts originating from the epicardium (Tao et al., 2013), the endocardium (Wessels et al., 2012), and the cardiac neural crest (Ali et al., 2014a). Other cells, like macrophages and endothelial cells, also participate in cardiac fibrogenesis via unique molecular pathways (Jiang et al., 2021).

The activation of cardiac myofibroblasts leads to an increased deposition the extracellular matrix (ECM), which amplifies cardiac dysfunction, leads to interstitial fibrosis and can consequently cause heart failure (González et al., 2018; Jiang et al., 2021). However, although cardiac fibrosis is frequently associated with myocardial infarction, it characterizes also idiopathic dilated cardiomyopathy, hypertensive heart disease, and diabetic hypertrophic cardiomyopathy (Jellis et al., 2010; Disertori et al., 2017). Particularly, the first asymptomatic stage of diabetic cardiomyopathy is characterized by myocardial fibrosis, worsened by hyperglycaemia (Jia et al., 2018).

To this regard, Galectin 1 (Gal-1) protein has recently emerged as a promising target for treating diabetes-induced fibrosis. Indeed, it has been found upregulated in kidneys from mice with type 1 and type 2 diabetes (Kuo et al., 2020), contributing to the progression of kidney fibrosis (Liu et al., 2015). Similarly, Gal-1 increase has been shown in cardiac disorders promoted by fibrotic processes, such as heart failure and acute myocardial infarction (Talman and Ruskoaho, 2016; Seropian et al., 2018). Interestingly, the Gal-1 inhibition by OTX008 compound has been effective in counteracting the buildup of Gal-1 under high glucose conditions. Indeed, a previous study reproducing *in vitro* diabetic retinopathy reported a reduction of Transforming Growth Factor beta 1 (TGF-β1) in human retinal pigment epithelial cells cultured in high glucose and treated with OTX008 (Trotta et al., 2022). On another side, we previously identified the anti-fibrotic properties of another mediator, the flavonoid chrysin (CHR), tested in a rodent model of carbon tetrachloride ($CCl_4$)-induced liver fibrosis (Balta et al., 2015; 2018). Therefore, both OTX008 and CHR could have anti-fibrotic effects even in cardiac damage induced by high glucose levels. However, their low solubility in water could affect their *in vivo* administration (Dong et al., 2021; Hermenean et al., 2023).

In this context, we previously formulated a dual-action supramolecular system to improve CHR and OTX008 solubility, aiming at reducing fibrosis in chronic diabetes. Particularly, we first combined CHR with sulfobutylated β-cyclodextrin (SBECD) to improve its limited solubility in water; then we integrated calixarene OTX008, known for its Gal-1 inhibitory properties, into our drug delivery system (Hermenean et al., 2023). This CHR-based supramolecular cyclodextrin-calixarene delivery system was characterized in the context of rat embryonic cardiomyocytes (H9c2) cell viability, ascertaining its safety. Therefore, it could be considered as a promising therapeutic candidate for addressing cardiac fibrosis in chronic diabetes (Hermenean et al., 2023).

To this regard, the present study aimed to explore the potential cardioprotective benefits of the novel CHR-based supramolecular cyclodextrin-calixarene delivery system, by hypothesizing an amplified anti-fibrotic efficacy due to the integration of readily soluble CHR, able to counteract fibrosis, with the selective Gal-1 inhibitor OTX008. Therefore, we investigated the effects of the new drug delivery system in hyperglycemic H9c2 cardiomyocytes and in a mouse model of chronic diabetes, by analyzing the main profibrotic pathways: TGF-β1/SMAD, able to activate myofibroblasts and to increase fibrotic genes, along with ECM deposition (Ma et al., 2018; Saadat et al., 2021); p38, which mediates SMAD-independent TGF-β responses leading to cardiac remodeling, ECM deposition and metalloproteinases (MMPs) modulation (Turner and Blythe, 2019); Erk1/2 mitogen-activated protein kinases (MAPKs), contributing to cardiac fibrosis in diabetic cardiomyopathy (Xu et al., 2016).

# 2 Materials and methods

## 2.1 Materials

OTX008 (Calixarene 0118) was purchased from Selleck Chemicals GmbH, while CHR (5,7-Dihydroxyflavone) from Alfa Aesar (by ThermoFisher Scientific, Kandel, Germany). Sulfobutylated β-cyclodextrin sodium salt (SBECD) (DS~6) was produced by Cyclolab Ltd. (Budapest, Hungary).

The experimental methods used to obtain the novel CHR complex in OTX-SBECD have been previously detailed and established (Hermenean et al., 2023). Comprehensive phase-solubility evaluations elucidated the mechanisms behind solubility augmentation and complexation. Molecular associations within the cyclodextrin-calixarene-CHR ternary system were assessed via dynamic light-scattering, as well as nuclear magnetic resonance, differential scanning calorimetry, and computational studies, as documented by Hermenean et al. (2023).

## 2.2 *In vitro* setting

As previously described (Hermenean et al., 2023), embryonic rat cardiac H9c2 (2-1) cells (ECACC, United Kingdom) were cultured at 37°C under an atmosphere of 5% $CO_2$, in Dulbecco's modified Eagle's medium (DMEM; Aurogene, Italy). This growth medium contained 5.5 mM D-glucose, 1% L-Glutamine (L-Glu; AU-X0550 Aurogene, Italy), 10% heat inactivated fetal bovine serum (FBS; AU-S181H Aurogene, Italy) and 1% penicillin/streptomycin (P/S) solution (AU-L0022 Aurogene, Italy). H9c2 cells were seeded at a specific density for each assay before being exposed to NG, high glucose (HG; 33 mM D-glucose) or NG + 27.5 mM mannitol (M; as osmotic control) for 48 h (Hermenean et al., 2023). Cells were then treated in NG or HG medium for 6 days (Hermenean et al., 2023) with the following substances:

- CHR 0.399 mg/mL dissolved in NaCl (CHR);
- SBECD 7.3 m/m% dissolved in NaCl (SBECD);
- SBECD + 0.095 mg/mL CHR dissolved in NaCl (SBECD + CHR);
- as vehicle for OTX008, dimethyl sulfoxide 2.5% (DMSO);
- OTX008 (0.75–1.25–2.50 μM);
- SBECD-OTX008 (2.5–1.25–0.75 μM) dissolved in NaCl (SBECD + OTX);
- SBECD-OTX008 (2.5–1.25–0.75 μM)-CHR dissolved in NaCl (SBECD + OTX + CHR).

Three independent experiments were done, each performed in triplicates ($N$ = 3). Cell morphology was observed at the optical microscope.

### 2.2.1 RNA isolation and real-time quantitative reverse transcription polymerase chain reaction (qRT-PCR)

H9c2 cells were seeded in 6-well plates ($1 \times 10^5$ cells/well) (Liu et al., 2020), exposed to NG or HG medium for 48 h and then treated for 6 days as previously described. Total RNA was purified from H9c2 lysates with an appropriate isolation kit (217004 Qiagen, Italy). RNA concentration and purity was determined by using the NanoDrop 2000c Spectrophotometer (Thermo Fisher Scientific, Italy). Genomic DNA (gDNA) contaminations were eliminated from RNA samples before the Reverse Transcription (RT) step, carried out on the Gene AMP PCR System 9700 (Applied Biosystems, Italy) by using the QuantiTect Reverse Transcription kit (205311 Qiagen, Italy), according to the protocol "Reverse Transcription with Elimination of Genomic DNA for Quantitative, Real-Time PCR." The final step for Real Time PCR (qPCR) analysis was carried out in triplicate on the CFX96 Real-time System C1000 Touch Thermal Cycler (Biorad, Italy). This was performed according to the protocol "Two-Step RT-PCR (Standard Protocol)," by using the QuantiTect SYBR Green PCR Kit (204143 Qiagen, Italy) and specific QuantiTect Primer Assays (249900 Qiagen, Italy) for TGF-β1 (QT00187796 Qiagen, Italy), TGFβ receptor 1 (TGFβR1; QT00190953 Qiagen, Italy), TGFβ receptor 2 (TGFβR2; QT00182315 Qiagen, Italy), Erk1 (or MAPK3—QT00176330 Qiagen, Italy) and Erk2 (or MAPK1—QT00190379 Qiagen, Italy) genes. Relative quantization of gene expression was performed by using the $2^{-\Delta\Delta Ct}$ method, by using rat Glyceraldehyde 3-phosphate dehydrogenase (GAPDH; QT01082004 Qiagen, Italy) as housekeeping control gene.

### 2.2.2 Enzyme-linked immunosorbent assays (ELISAs)

Cell-biased ELISA assays were performed to analyze the cellular levels of rat p38 MAPK (phosphorylated/total) (CBEL-P38-1 RayBiotech, GA, United States), Smad2 (LS-F1057-1 LSBio, MA, United States) and Smad4 (LS-F2315-1 LSBio, MA, United States) according to the manufacturer's protocols. Competitive ELISA test was used to quantify the cellular levels of Gal-1 (abx256936 abbexa, United Kingdom), according to the manufacturer's instructions.

## 2.3 Animals and experimental protocol

Animal experimental procedures were approved by the Ethical Commettee of Vasile Goldis Western University of Arad (Approval number 20, 12/06/2020) and the National Sanitary Veterinary and Food Safety Authority (Certificate number 001/04.02.2021) and were performed according to the guidelines of the Declaration of Helsinki, in compliance with European and national guidelines for research on laboratory animals.

Adult CD1 male mice sourced from the Animal facility of the "Vasile Goldiș" Western University of Arad served as the experimental subjects. These animals were maintained under standardized housing conditions, in compliance with both national and European standards and guidelines. Diabetes was elicited in mice via a single intraperitoneal (i.p.) administration of streptozotocin (STZ) at a dosage of 102 mg/kg body weight. The STZ was freshly prepared in a 50 mM citrate buffer solution (pH 4.5). Post 2 weeks of the STZ administration, fasting blood glucose levels were ascertained. Mice registering blood glucose concentrations exceeding 200 mg/dL were categorized as diabetic and were maintained for a duration of 20 weeks prior to initiating interventions. Post the 20-week period, the chronic diabetic mice, coupled with 10 age-matched healthy counterparts, were randomly assigned into seven distinct groups ($N$ = 10 per group):

- Group 1 (Control): Healthy mice serving as the baseline control.
- Group 2 (Diabetes): Chronic diabetic mice, which were euthanized following the 22-week period.
- Group 3 (OTX-SBECD): Chronic diabetic mice at 20 weeks, administered with 5 mg/kg of OTX complexed with SBECD
- Group 4 (OTX-SBECD-CHR): Chronic diabetic mice at 20 weeks, given 5 mg/kg of OTX complexed with SBECD, along with chrysin.

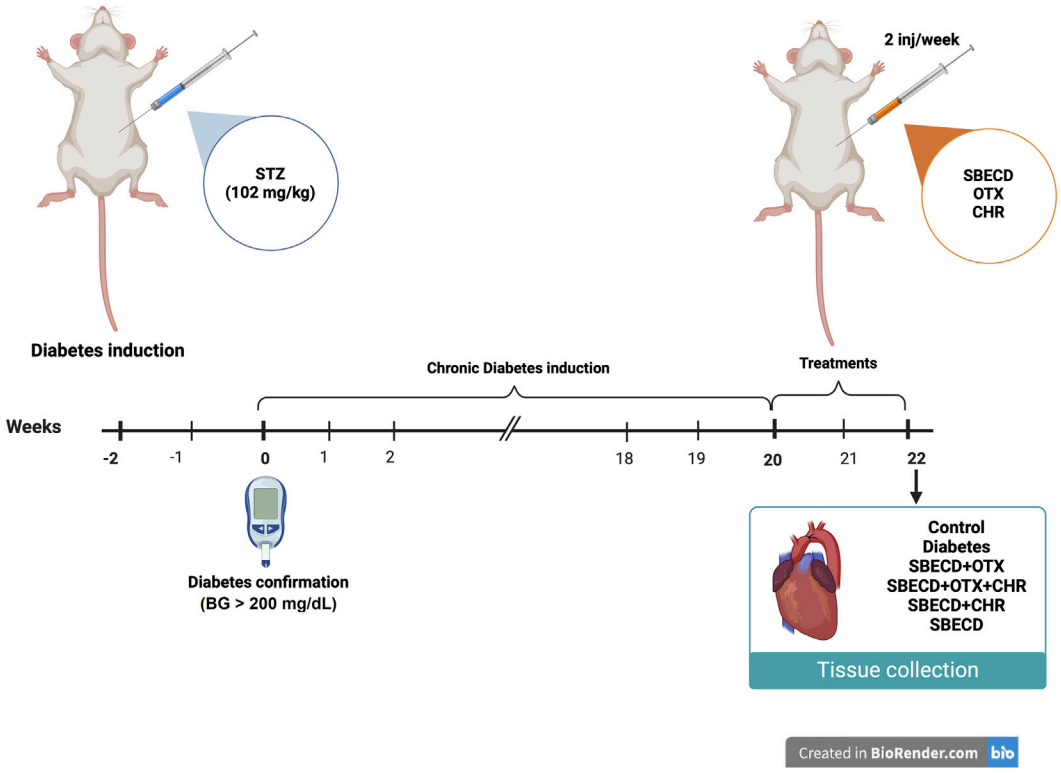


FIGURE 1
*In vivo* experimental design. This figure was created with BioRender.com.

- Group 5 (SBECD-CHR): Chronic diabetic mice at 20 weeks, treated with CHR complexed with SBECD.
- Group 6 (SBECD): Chronic diabetic mice at 20 weeks, receiving the uncomplexed SBECD.

After 20 weeks of chronic diabetes, treatments were administered 2 times/week for 2 weeks by i.p. injections. Figure 1 provides a schematic representation of the experimental protocol.

### 2.3.1 Histology

Cardiac specimens were promptly fixed using a 4% paraformaldehyde solution buffered in phosphate buffered saline (PBS) and subsequently embedded in paraffin for processing. Following this, tissue sections were stained with Gomori's trichrome using the stain kit (38016SS1 Leica, United States). The entire staining procedure adhered closely to the guidelines specified by the Bio-Optica staining kit (Italy). Once stained, the histological slides were examined under an Olympus BX43 microscope (Germany). High-resolution images of the representative sections were captured for documentation and detailed analysis using an Olympus XC30 digital camera (Germany).

### 2.3.2 Immunohistochemistry

Prior to undertaking immunohistochemistry, heart sections, embedded in paraffin and measuring 5 µm in thickness, underwent deparaffinization and rehydration through established techniques. For antigen detection, sections were treated with primary antibodies—rabbit polyclonal TGF-β1 (sc-146 Santa Cruz Biotechnology, TX, United States), Smad2/3 (sc-133098 Santa Cruz Biotechnology, TX, United States), and α-smooth muscle actin (αSMA, ab32575 abcam, United Kingdom), all at a 1:200 dilution. This was followed by an overnight incubation at 4°C. The Novocastra Peroxidase/DAB kit (Leica Biosystems, Germany) was then employed, consistent with the manufacturer's directives, to visualize the immunoreactions. For negative controls, primary antibodies were substituted with irrelevant immunoglobulins of the same isotype, and the specimens were observed under bright-field microscopy. Quantitative analysis was performed by determining the ratio of the positively stained area to the total section area using the Image J software.

### 2.3.3 *In vivo* qRT-PCR evaluations

qRT-PCR was performed to evaluate the mRNA expression levels of TGF-β1, Smad 2/3, Smad 7, Collagen I (Col I), αSMA, MMPs and TIMP metallopeptidase inhibitor 1 (TIMP1). The extraction of total RNA was facilitated using the SV Total RNA isolation kit (Promega, Italy). Following extraction, the integrity and concentration of the RNA samples were gauged via a NanoDrop One spectrophotometer (Thermo Scientific, MA, United States). Subsequently, reverse transcription of the RNA was carried out employing the First Strand cDNA Synthesis Kit (Thermo Scientific, MA, United States). The Maxima SYBR Green/ROX qPCR Master Mix (Life Technologies, CA, United States) was utilized for the RT-PCR, executed on an Mx3000PTM RT-PCR system (Agilent, CA, United States). Every sample underwent triplicate runs for accuracy.

**TABLE 1 Primer sequences for *in vivo* RT-PCR.**

| Target | Sense | Antisense |
|---|---|---|
| TGF-β1 | 5′ TTTGGAGCCTGGACACACAGTAC 3′ | 5′ TGTGTTGGTTGTAGAGGGCAAGGA 3′ |
| α-SMA | 5′ CCGACCGAATGCAGAAG GA 3′ | 5′ ACAGAGTATTTGCGCTCCGAA 3′ |
| Smad 2 | 5′ GTTCCTGCCTTTGCTGAGAC 3′ | 5′ TCTCTTTGCCAGGAATGCTT 3′ |
| Smad 3 | 5′ TGCTGGTGACTGGATAGCAG 3′ | 5′ CTCCTTGGAAGGTGCTGAAG 3′ |
| Smad 7 | 5′ GCTCACGCACTCGGTGCTCA 3′ | 5′ CCAGGCTCCAGAAGAAGTTG 3′ |
| Col I | 5′ CAGCCGCTTCACCTACAGC 3′ | 5′ TTTTGTATTCAATCACTGTCTTGCC 3′ |
| MMP1 | 5′ GCAGCGTCAAGTTTAACTGGAA 3′ | 5′AACTACATTTAGGGGAGAGGTGT 3′ |
| MMP2 | 5′ CAG GGA ATG AGT ACT GGG TCT ATT 3′ | 5′ ACT CCA GTT AAA GGC AGC ATC TAC 3′ |
| MMP3 | 5′ ACCAACCTATTCCTGGTTGCTGCT 3′ | 5′ ATGGAAACGGGACAAGTCTGTGGA 3′ |
| MMP9 | 5′ AAT CTC TTC TAG AGA CTG GGA AGG AG 3′ | 5′ AGC TGA TTG ACT AAA GTA GCT GGA 3′ |
| Timp1 | 5′ GGTGTGCACAGTGTTTCCCTGTTT 3′ | 5′TCCGTCCACAAACAGTGAGTGTCA 3′ |
| GAPDH | 5′ CGACTTCAACAGCAACTCCCACTCTTCC-3′ | 5′ TGGGTGGTCCAGGGTTTCTTACTCCTT 3′ |

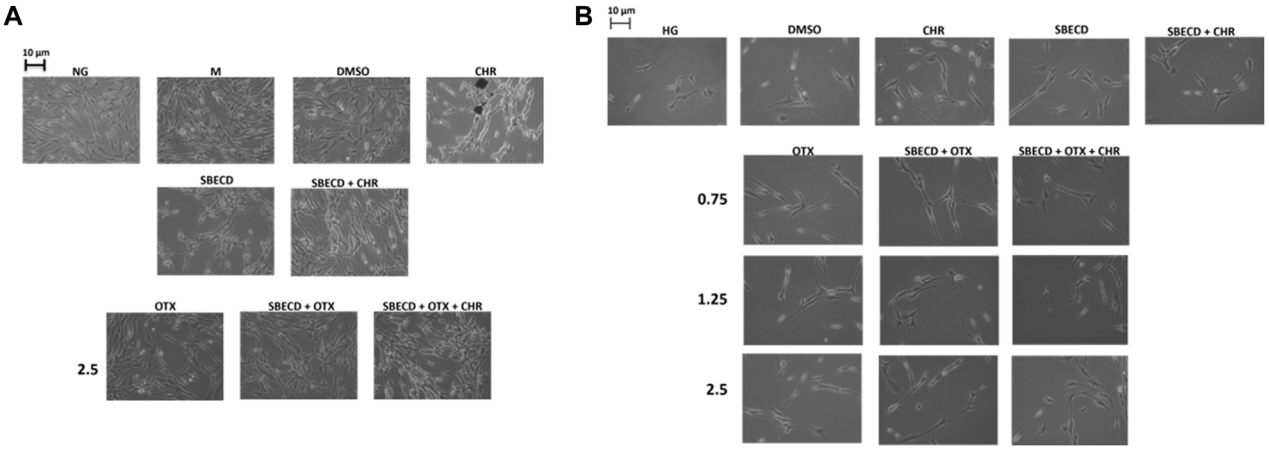


FIGURE 2
CHR-based supramolecular drug delivery system preserved H9c2 morphology in high glucose. **(A)** Representative optic microscope observations of H9c2 cells cultured in normal glucose (NG) for 48 h and exposed for 6 days to the highest dose (2.5 µM) of OTX008 alone or in the different combinations considered, or **(B)** cultured in high glucose (HG) for 48 h and treated for 6 days with 3 doses (0.75–1.25–2.5 µM) of OTX008 alone or in the different combinations considered. Magnification = ×20; scale bar = 10 µm. *N* = 3 per group (three independent experiments, each performed in triplicate). NG: 5.5 mM D-glucose; M: NG + 27.5 mM mannitol; DMSO: dimethyl sulfoxide 2.5%; CHR: 5,7-Dihydroxyflavone 0.399 mg/mL; SBECD: Sulfobutylated β-cyclodextrin sodium salt 7.3 m/m%; SBECD + CHR: SBECD + 0.095 mg/mL CHR; OTX: calixarene OTX008—Calixarene 0118—(0.75–1.25–2.5): OTX008 (0.75–1.25–2.5 µM); SBECD + OTX: SBECD-OTX008 (2.5–1.25–0.75 µM); SBECD + OTX + CHR: SBECD-OTX008 (2.5–1.25–0.75 µM)-CHR; HG: 33 mM D-glucose.

Detailed primer sequences are presented in Table 1. Serving as a reference gene, the expression of GAPDH was also gauged, following the identical experimental guidelines. The relative shifts in gene expression were ascertained employing the $2^{-\Delta\Delta Ct}$ methodology, as documented in reference (Jiang et al., 2021).

### 2.3.4 Determination of Gal-1 protein levels

Gal-1 protein levels were assessed in mice cardiac tissues by ELISA assay (EM1051 FineTest, China), according to the manufacturer's protocol.

## 2.4 Statistical analysis

Data analyses were performed using GraphPad Prism 9.4.0. Results are expressed as mean ± SD. Statistical analysis was performed by employing one-way analysis of variance (ANOVA) with the Bonferroni correction. The strength of association between 2 factors was assessed by Pearson correlation analysis, by determining Pearson correlation coefficient (r). For both ANOVA and Pearson correlation analysis, a $p$-value of $<0.05$ was considered significant.

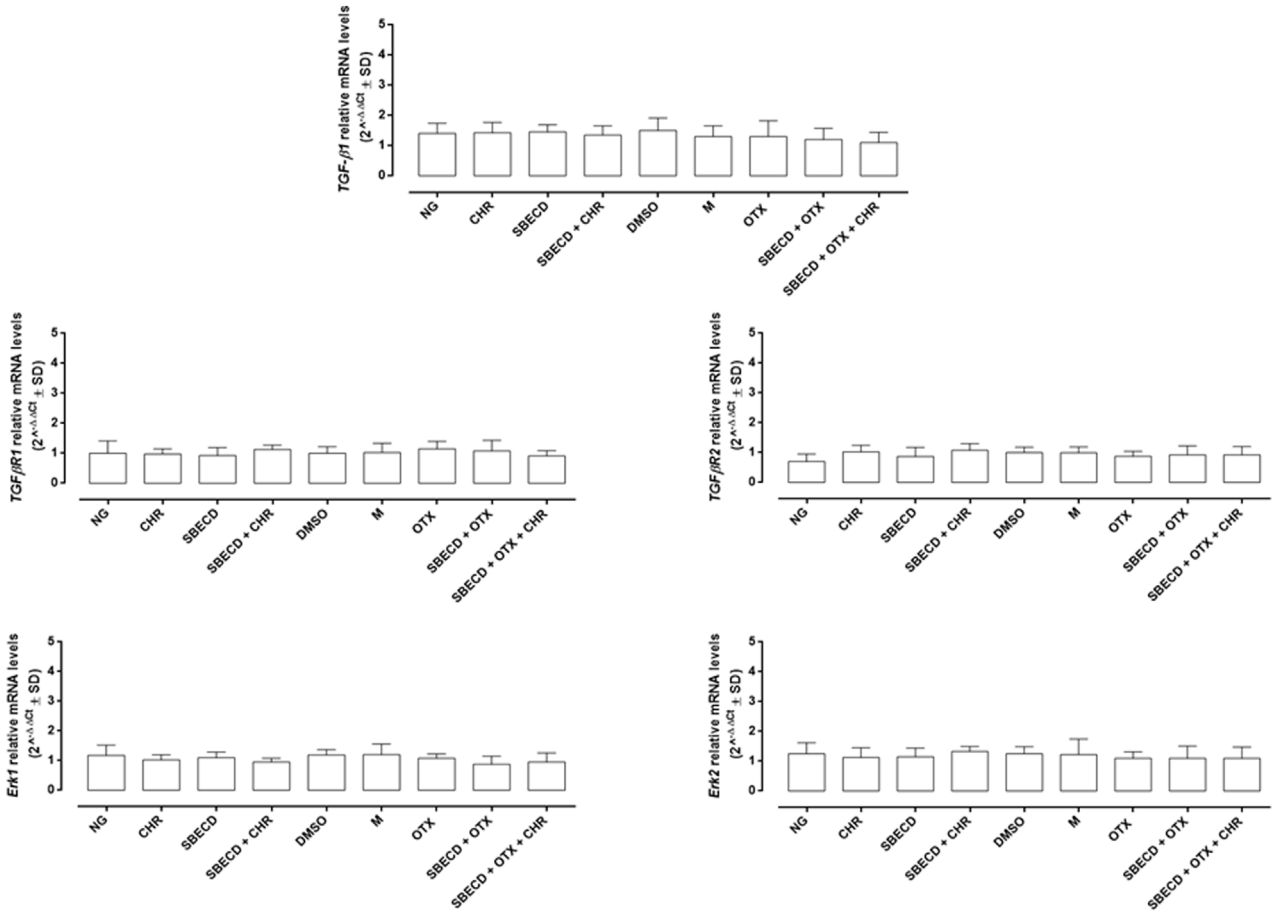


FIGURE 3
CHR-based supramolecular drug delivery system does not affect TGF-β signaling and MAPKs in H9c2 cardiomyocytes cultured in normal glucose. TGF-β1, TGFβR1, TGFβR2, Erk1 and Erk2 mRNA levels ($2^{-\Delta\Delta Ct}$ ± SD) were determined by qRT-PCR, using GAPDH as gene control. *N* = 3 per group (three independent experiments, each performed in triplicate). NG: 5.5 mM D-glucose; M: NG + 27.5 mM mannitol; DMSO: dimethyl sulfoxide 2.5%; CHR: 5,7-Dihydroxyflavone 0.399 mg/mL; SBECD: Sulfobutylated β-cyclodextrin sodium salt 7.3 m/m%; SBECD + CHR: SBECD + 0.095 mg/mL CHR; OTX: calixarene OTX008—Calixarene 0118—(2.5 μM); SBECD + OTX: SBECD-OTX008 (2.5 μM); SBECD + OTX + CHR: SBECD-OTX008 (2.5 μM)-CHR.

# 3 Results

## 3.1 CHR-based supramolecular drug delivery system ameliorates the damaged morphology in H9c2 cells exposed to high glucose

In normal glucose (NG) condition, the physiological elongated morphology exhibited by H9c2 cells was not affected by the treatments with OTX (2.5 μM) alone or combined with SBECD/SBECD + CHR (Figure 2A). H9c2 morphology was not altered also by the single treatments with CHR, SBECD, SBECD + CHR, DMSO or mannitol (M) (Figure 2A). This was in accordance with our previous data showing a normal viability of these cardiomyocytes in normal glucose when treated with the same compounds (Hermenean et al., 2023). Conversely, H9c2 exposed to high glucose (HG) evidenced a markedly reduced cell viability (Hermenean et al., 2023) and were less elongated, showing a shrunken shape and hypertrophy (Figure 2B). In HG, the treatments with CHR, SBECD and SBECD + CHR did not alter cell viability (Hermenean et al., 2023) and partially recovered the H9c2 damaged cell morphology. This was markedly ameliorated by OTX (0.75–1.25–2.5 μM) alone or in the different formulations with SBECD/SBECD + CHR (Figure 2B), accordingly with the higher increase in cell viability showed by SBECD + OTX and SBECD + OTX + CHR (2.5 μM) (Hermenean et al., 2023).

## 3.2 CHR-based supramolecular drug delivery system reduces the pro-fibrotic pathways in H9c2 cells exposed to high glucose

The main pro-fibrotic pathways, the canonical (involving TGF-β1, TGFβR1/2, Smad2/4) and non-canonical one (involving p38, Erk1/2 mitogen-activated protein kinases) were not altered in H9c2 cells cultured in normal glucose and exposed to the different treatments (Figure 3; Table 2). Conversely, HG

**TABLE 2** Smad2/4 and p38 protein levels in H9c2 cells cultured in normal glucose and exposed to the different treatments.

| | NG | CHR | SBECD | SBECD + CHR | DMSO | M | OTX | SBECD + OTX | SBECD + OTX + CHR |
|---|---|---|---|---|---|---|---|---|---|
| Smad2 | 0.9 ± 0.2 | 1.1 ± 0.2 | 1.0 ± 0.2 | 1.0 ± 0.2 | 1.0 ± 0.2 | 0.8 ± 0.3 | 1.0 ± 0.1 | 1.0 ± 0.1 | 1.0 ± 0.3 |
| Smad4 | 1.0 ± 0.2 | 1.1 ± 0.2 | 1.1 ± 0.2 | 1.0 ± 0.1 | 1.0 ± 0.2 | 1.0 ± 0.3 | 1.1 ± 0.1 | 1.2 ± 0.3 | 1.1 ± 0.2 |
| P-p38/p38 | 1.1 ± 0.2 | 1.0 ± 0.2 | 1.0 ± 0.2 | 1.0 ± 0.2 | 1.1 ± 0.2 | 1.0 ± 0.2 | 1.0 ± 0.2 | 0.9 ± 0.2 | 0.9 ± 0.4 |

Smad2, Smad4 relative protein levels and P-p38/p38 MAPK ratio (optical density values at 450 nm ± SD) were determined by cell-biased ELISA. $N = 3$ per group (three independent experiments, each performed in triplicate). NG: 5.5 mM D-glucose; M: NG + 27.5 mM mannitol; DMSO: dimethyl sulfoxide 2.5%; CHR: 5,7-Dihydroxyflavone 0.399 mg/mL; SBECD: Sulfobutylated β-cyclodextrin sodium salt 7.3 m/m%; SBECD + CHR: SBECD + 0.095 mg/mL CHR; OTX: calixarene OTX008—Calixarene 0118—(2.5 μM); SBECD + OTX: SBECD-OTX008 (2.5 μM); SBECD + OTX + CHR: SBECD-OTX008 (2.5 μM)-CHR.

exposure significantly increased both the pro-fibrotic pathways in H9c2 cells ($p < 0.0001$ vs. NG) (Figures 4, 5; Table 3). Interestingly, SBECD, CHR and SBECD + CHR were able to significantly reduce TGF-β1 and TGFβR1/2 expression levels in H9c2 cells exposed to HG, but not the other pro-fibrotic targets. In HG, the three doses of OTX (0.75–1.25 and 2.5 μM) tested alone or in combination with SBECD or SBECD + CHR were able to significantly decrease the canonical and non-canonical fibrotic pathways, but only the two formulations combined with OTX 2.5 μM (SBECD + OTX 2.5 and SBECD + OTX 2.5 + CHR) were able to further decrease the pro-fibrotic pathways compared to same dose of OTX tested alone (Figures 4, 5; Table 3).

## 3.3 CHR-based supramolecular drug delivery system downregulates the main pro-fibrotic signalling pathways in cardiac tissues

αSMA gene expression is a marker of activated myofibroblasts in tissue remodeling (Shinde et al., 2017). For the diabetes group, there was a notable increase in αSMA gene expression, as demonstrated by RT-PCR analysis, when compared to the control group ($p < 0.001$). All treatments resulted in significant decreases in this expression relative to the Diabetes group. Among these, the SBECD + OTX + CHR treatment yielded the most substantial decrease, as illustrated in Figure 6. Immunohistochemical studies revealed enhanced staining for the cardiac tissue samples from the Diabetes group, but this expression was almost returned to control levels after SBECD + OTX + CHR treatment.

TGF-β1 plays a crucial role in promoting tissue fibrosis, operating primarily via the phosphorylation of Smad 2/3. In contrast, Smad 7, a Smad inhibitor, works by downregulating Smad 2/3 and targeting the TGF-β1 receptor (Biernacka et al., 2011). In comparison to the control, chronic diabetes led to a significant increase in TGF-β1 gene expression and intense immunopositivity. Treatments with SBECD + OTX, SBECD + OTX + CHR, and SEBCD + CHR lowered TGF-β1 levels by 1.97-fold, 19.11-fold, and 6.62-fold, respectively, when compared to the Diabetes group. The same pattern was obtained for Smad2 and Smad3. In contrast, the mRNA expression of Smad7 was significantly upregulated in SBECD + OTX + CHR group by 12.7-fold compared to diabetes (Figure 6).

## 3.4 CHR-based supramolecular drug delivery system suppresses the secretion and deposition of collagen in cardiac tissues

Cardiac tissue displayed an increase in collagen production and accumulation as determined by Gomori's Trichrome staining in chronic Diabetes group (Figure 7). An RT-PCR examination revealed a significant rise in the expression of Col-1 gene in the diabetes group relative to the control group ($p < 0.001$). Post-treatment, there was a marked reduction in gene expression levels when compared to the diabetes group, with SBECD + OTX + CHR treatment resulting in a decrease by 23.76 times compared to diabetic animals (Figure 7).

TIMP-1 acts as a natural inhibitor, preventing MMPs from breaking down the ECM. To study how the CHR-based cyclodextrin-calixarene supramolecular system affects ECM in the fibrotic heart tissue of diabetic mice, we evaluated the mRNA levels of TIMP-1 and MMPs using RT-PCR. The results indicated that the diabetes group exhibited considerably elevated expression levels of TIMP-1, MMP-2, -3, and -9 genes when contrasted with the control group ($p < 0.001$). The applied treatments effectively reduced these mRNA expressions compared to the diabetes group ($p < 0.001$). However, MMP-1 mRNA expression was notably increased following the treatments relative to the diabetes group ($p < 0.001$). Specifically, in the SBECD + OTX + CHR treatment group, TIMP-1, MMP-2, MMP-3, and MMP-9 expressions dropped approximately by about 29.04, 15.12, 58.77, and 19.41 times, respectively, compared to the diabetes group. Conversely, MMP-1 gene expression raised significantly after treatment with SBECD + OTX + CHR compared to diabetes ($p < 0.001$) (Figure 7).

## 3.5 CHR-based supramolecular drug delivery system modulates Gal-1 levels in H9c2 cells and in cardiac tissues

Gal-1 protein levels were significantly elevated in H9c2 cells exposed to HG (481 ± 26 pg/mL, $p < 0.01$ vs NG) compared to control group (163 ± 38 pg/mL) and were not significantly modulated by CHR (480 ± 108 pg/mL), SBECD + CHR (420 ± 96 pg/mL) and SBECD (534 ± 79 pg/mL) in hyperglycaemic conditions (Figure 7A). All the doses of OTX (0.75–1.25–2.5 μM) alone or in combination with SBECD or SBECD + CHR were able to significantly downregulate Gal-1

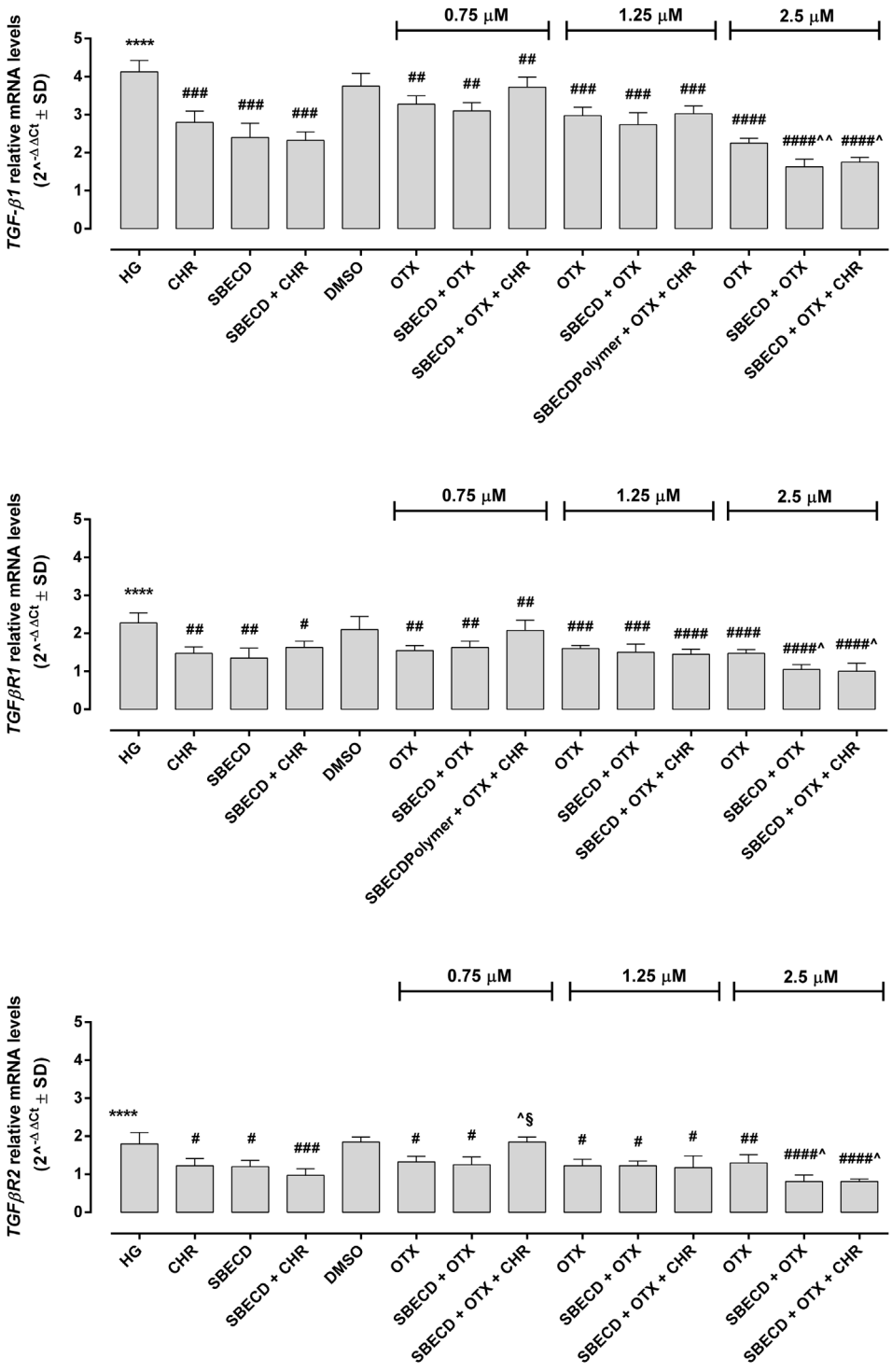


FIGURE 4
CHR-based supramolecular drug delivery system downregulates TGF-β signaling in H9c2 cardiomyocytes exposed to high glucose. TGF-β1, TGFβR1 and TGFβR2 mRNA levels ($2^{-\Delta\Delta Ct} \pm$ SD) were determined by qRT-PCR, using GAPDH as gene control. *N* = 3 per group (three independent experiments, each performed in triplicate). HG: 33 mM D-glucose; M: NG + 27.5 mM mannitol; DMSO: dimethyl sulfoxide 2.5%; CHR: 5,7-Dihydroxyflavone 0.399 mg/mL; SBECD: Sulfobutylated β-cyclodextrin sodium salt 7.3 m/m%; SBECD + CHR: SBECD + 0.095 mg/mL CHR; OTX (0.75–1.25–2.5): calixarene OTX008—Calixarene 0118—(0.75–1.25–2.5 μM); SBECD + OTX (0.75–1.25–2.5): SBECD-OTX008 (0.75–1.25–2.5 μM); SBECD + OTX (0.75–1.25–2.5)+ CHR: SBECD-OTX008 (0.75–1.25–2.5 μM)-CHR. ****$p < 0.0001$ vs. NG; $^{\#}p < 0.5$, $^{\#\#}p < 0.01$, $^{\#\#\#}p < 0.001$ and $^{\#\#\#\#}p < 0.0001$ vs. HG; $^{\wedge}p < 0.05$ and $^{\wedge\wedge}p < 0.01$ vs. OTX; $^{\S}p < 0.05$ vs. SBECD + OTX (same dose).

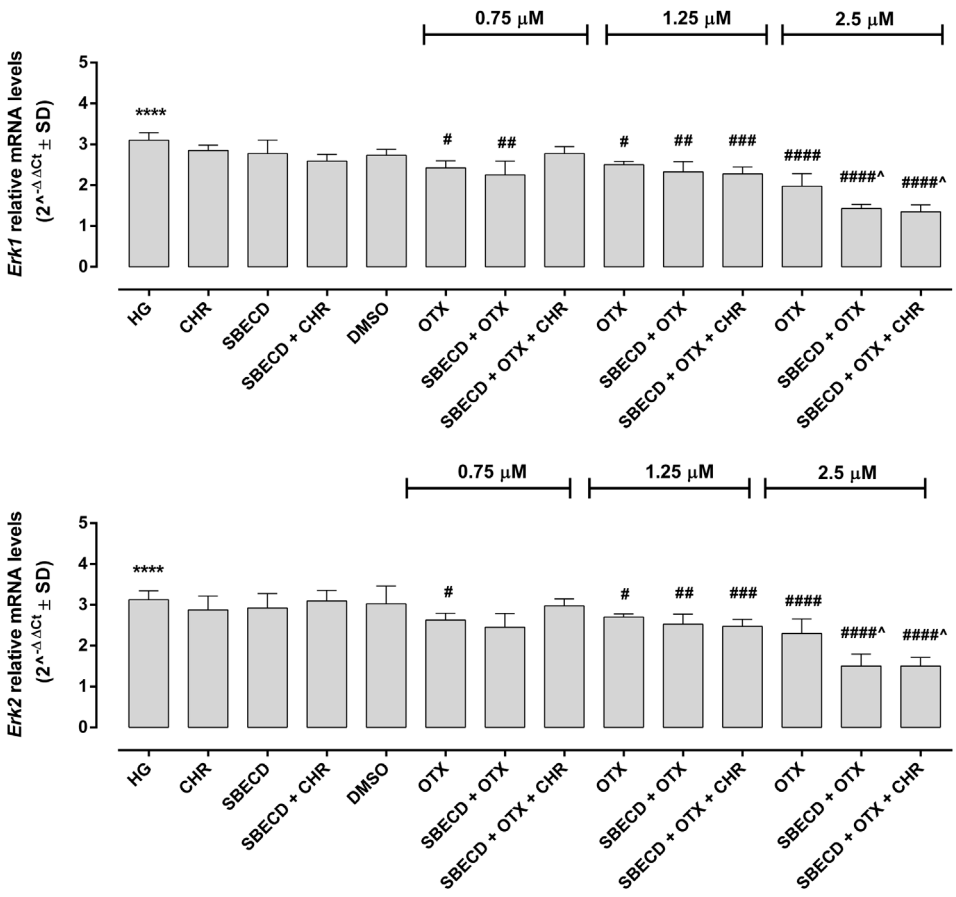


FIGURE 5
CHR-based supramolecular drug delivery system downregulates MAPKs in H9c2 cardiomyocytes exposed to high glucose. Erk1 and Erk2 mRNA levels ($2^{-\Delta\Delta Ct}$ ± SD) were determined by qRT-PCR, using GAPDH as gene control. *N* = 3 per group (three independent experiments, each performed in triplicate). HG: 33 mM D-glucose; M: NG + 27.5 mM mannitol; DMSO: dimethyl sulfoxide 2.5%; CHR: 5,7-Dihydroxyflavone 0.399 mg/mL; SBECD: Sulfobutylated β-cyclodextrin sodium salt 7.3 m/m%; SBECD + CHR: SBECD + 0.095 mg/mL CHR; OTX (0.75–1.25–2.5): calixarene OTX008—Calixarene 0118—(0.75–1.25–2.5 μM); SBECD + OTX (0.75–1.25–2.5): SBECD-OTX008 (0.75–1.25–2.5 μM); SBECD + OTX (0.75–1.25–2.5)+ CHR: SBECD-OTX008 (0.75–1.25–2.5 μM)-CHR. ****$p < 0.0001$ vs. NG; $^{\#}p < 0.5$, $^{\#\#}p < 0.01$, $^{\#\#\#}p < 0.001$ and $^{\#\#\#\#}p < 0.0001$ vs. HG; $^{\wedge}p < 0.05$ vs. OTX (same dose).

protein levels ($p < 0.001$) in H9c2 cells exposed to high glucose (Figure 8B). Moreover, at the doses of 1.25 and 2.5 μM, SBECD + OTX + CHR further reduced Gal-1 protein levels in H9c2 cells compared to OTX at the same doses ($p < 0.05$) (Figure 8B).

Consistent with the *in vitro* findings, after 22 weeks of hyperglycaemia, the cardiac Gal-1 protein levels in chronic diabetes animals showed a significant rise (8,068 ± 71 pg/mL, $p <$ 0.01 vs. Control). In contrast, non-diabetic mice exhibited levels of 5,075 ± 233 pg/mL. After 2 weeks of treatments, there was a significant decrease in its levels ($p < 0.001$) (Figure 8C).

## 4 Discussion

Cardiac fibrosis is a defining feature of diabetic cardiomyopathy. This condition is marked by the accumulation of ECM proteins in the cardiac interstitium, leading to perivascular fibrosis and left ventricular (LV) hypertrophy, which frequently results in heart failure (Russo and Frangogiannis, 2016; Jia et al., 2018).

Hyperglycaemia or diabetes has been widely documented to impact the development of cardiac fibrosis, both in preclinical and clinical scenarios. Specifically, rodent models mimicking type I and type II diabetes exhibited a marked cardiomyocyte hypertrophy and myocardial fibrosis, accompanied by the increase of pro-fibrotic genes (Ares-Carrasco et al., 2009; Huynh et al., 2010; 2012; Li et al., 2010; Biernacka et al., 2011; Gonzalez-Quesada et al., 2013; Hao et al., 2015). Similarly, diabetic patients showed extensive interstitial, perivascular and replacement fibrosis (Regan et al., 1977; Kwong et al., 2008; Turkbey et al., 2011), coupled with capillary basement membrane thickening, type I and III collagen accumulation and cardiomyocyte hypertrophy (Fischer et al., 1984; Nunoda et al., 1985; Sutherland et al., 1989; Van Hoeven and Factor, 1990; Shimizu et al., 1993; Kawaguchi et al., 1997; Van Heerebeek et al., 2008; Falcão-Pires et al., 2011). These changes are underlined by the activation of TGF-β pathway following hyperglycaemia (Shamhart et al., 2014), as documented by TGF-β upregulation in the hearts of diabetic rodents exhibiting cardiac fibrosis

**TABLE 3 Smad2/4 and p38 protein levels in H9c2 cells cultured in high glucose and exposed to the different treatments.**

| | Smad2 | Smad4 | P-p38/p38 |
|---|---|---|---|
| HG | 1.9 ± 0.1**** | 2.3 ± 0.3**** | 2.5 ± 0.2**** |
| CHR | 1.9 ± 0.2 | 2.2 ± 0.3 | 2.6 ± 0.2 |
| SBECD | 1.7 ± 0.2 | 2.4 ± 0.4 | 2.7 ± 0.2 |
| SBECD + CHR | 1.8 ± 0.2 | 2.2 ± 0.2 | 2.5 ± 0.1 |
| DMSO | 1.9 ± 0.2 | 2.2 ± 0.2 | 2.4 ± 0.2 |
| OTX (0.75) | 1.4 ± 0.1# | 1.6 ± 0.1## | 1.6 ± 0.1## |
| SBECD + OTX (0.75) | 1.3 ± 0.1# | 1.6 ± 0.2## | 1.7 ± 0.1## |
| SBECD + OTX (0.75) + CHR | 1.9 ± 0.2#°§ | 2.0 ± 0.1 | 2.1 ± 0.1 |
| OTX (1.25) | 1.5 ± 0.1# | 1.5 ± 0.2#### | 1.8 ± 0.1### |
| SBECD + OTX (1.25) | 1.4 ± 0.1## | 1.3 ± 0.2#### | 1.8 ± 0.1#### |
| SBECD + OTX (1.25) + CHR | 1.5 ± 0.2# | 1.7 ± 0.1## | 2.3 ± 0.2°§ |
| OTX (2.5) | 1.5 ± 0.1## | 1.7 ± 0.3## | 1.9 ± 0.1### |
| SBECD + OTX (2.5) | 1.1 ± 0.1####° | 1.3 ± 0.1####°° | 1.3 ± 0.1####°° |
| SBECD + OTX (2.5) + CHR | 1.1 ± 0.1####°° | 1.7 ± 0.1####° | 1.4 ± 0.2####° |

Smad2, Smad4 relative protein levels and P-p38/p38 MAPK ratio (optical density values at 450 nm ± SD) were determined by cell-biased ELISA. $N = 3$ per group (three independent experiments, each performed in triplicate). HG: 33 mM D-glucose; M: NG + 27.5 mM mannitol; DMSO: dimethyl sulfoxide 2.5%; CHR: 5,7-Dihydroxyflavone 0.399 mg/mL; SBECD: Sulfobutylated β-cyclodextrin sodium salt 7.3 m/m%; SBECD + CHR: SBECD + 0.095 mg/mL CHR; OTX (0.75–1.25–2.5): calixarene OTX008—Calixarene 0118—(0.75–1.25–2.5 μM); SBECD + OTX (0.75–1.25–2.5): SBECD-OTX008 (0.75–1.25–2.5 μM); SBECD + OTX (0.75–1.25–2.5)+ CHR: SBECD-OTX008 (0.75–1.25–2.5 μM)-CHR. ****$p < 0.0001$ vs. NG; #$p < 0.5$, ##$p < 0.01$, ###$p < 0.001$ and ####$p < 0.0001$ vs. HG; °$p < 0.05$ and °°$p < 0.01$ vs. OTX; §$p < 0.05$ vs. SBECD + OTX (same dose).

(Carroll and Tyagi, 2005; Westermann et al., 2007; Senador et al., 2009; Abed et al., 2013).

It is well known that TGF-β isoforms play a central role in the genesis of tissue fibrosis (Biernacka et al., 2011). Specifically, TGF-β1 promotes pro-fibrotic responses in cardiomyocytes through both Smad-dependent and independent signalling (Dobaczewski et al., 2010; Biernacka et al., 2011; Rahaman et al., 2014). Indeed, TGF-β1/Smad pathway plays a crucial role in the activation of myofibroblasts, stimulation of ECM deposition through Col-I synthesis and modulation of MMP activity (Uchinaka et al., 2014; Hanna et al., 2021). On the other hand, TGF-β1 is also able to increasing reactive oxygen species (ROS), consequently activating p38 and Erk1/2 MAPKs (Sano et al., 2001; Wu et al., 2022), leading to collagen deposition in heart tissue (See et al., 2004; Johnston and Gillis, 2022). Importantly, in our prior research, we found a significant reduction in the TGF-β1/Smad pathway in a mouse model of liver fibrosis when treated with CHR (Balta et al., 2015; Balta et al., 2018). This 5,7-dihydroxyflavone was characterized by antioxidant, antitumor, anti-hypercholesterolemic and anti-inflammatory activities (Bae et al., 2011; Brechbuhl et al., 2012; Ali et al., 2014b; Anandhi et al., 2014; Samarghandian et al., 2016; Phan et al., 2021). Our data are in line with other research that identified CHR-mediated inhibition of pro-fibrotic pathways in rat myocardial injury, renal fibrosis and osteoarthritis, by reducing TGF-β1/Smad3, p38, Erk1/2, MMP2 and PERK/TXNIP/NLRP3 signalling (Rani et al., 2015; Nagavally et al., 2021; Ding et al., 2023). Additionally, by using a different pharmacological approach, we demonstrated that TGF-β/Smad pathway can be reduced in human retinal pigment epithelial cells exposed to high glucose by using calixarene OTX008, a selective inhibitor Gal-1 (Trotta et al., 2022). This particular galectin, expressed under normal and pathological conditions, plays a pivotal role in the pathogenesis of fibrosis (Hermenean et al., 2022) and is upregulated in heart failure and acute myocardial infarction (Talman and Ruskoaho, 2016; Seropian et al., 2018). Particularly, Gal-1 is constitutively expressed in cardiomyocytes close to sarcomeric actin, with its expression and secretion increased after cardiac injury promoted by hypoxia, inflammation and fibrosis (Seropian et al., 2018). While its early upregulation can be considered a homeostatic response to prevent cardiac remodeling induced by inflammation, prolonged Gal-1 increase could negatively influence cardiac structure and function (Ou et al., 2021). Interestingly, Gal-1 blocking/silencing by OTX008 has been shown to inhibit TGF-β in various studies, including a cell model of hypoxia-induced pulmonary fibrosis (Kathiriya et al., 2017), a mouse model of liver fibrosis (Jiang et al., 2018), dendritic cells derived from patients with chronic lymphocytic leukaemia (Kostic et al., 2021) and tumour cells (Leung et al., 2014; Koonce et al., 2017).

Worth of note, CHR and Gal-1 have roles that extend beyond influencing pro-fibrotic pathways; they also have implications in the onset and progression of diabetes. Particularly, as evidenced in preclinical studies, CHR seems to attenuate the diabetes-related tissue damage by ameliorating blood glucose levels, insulin resistance and inflammatory state in diabetic animals, by reducing Vascular Endothelial Growth Factor (VEGF) in preclinical models of diabetic retinopathy and by decreasing advanced glycosylation end products (AGEs), TGF-β1/Smad and Col-I deposition in diabetic hearts (Li et al., 2014; Farkhondeh et al., 2019; Zhou et al., 2021a; Salama et al., 2022). This protective effect of

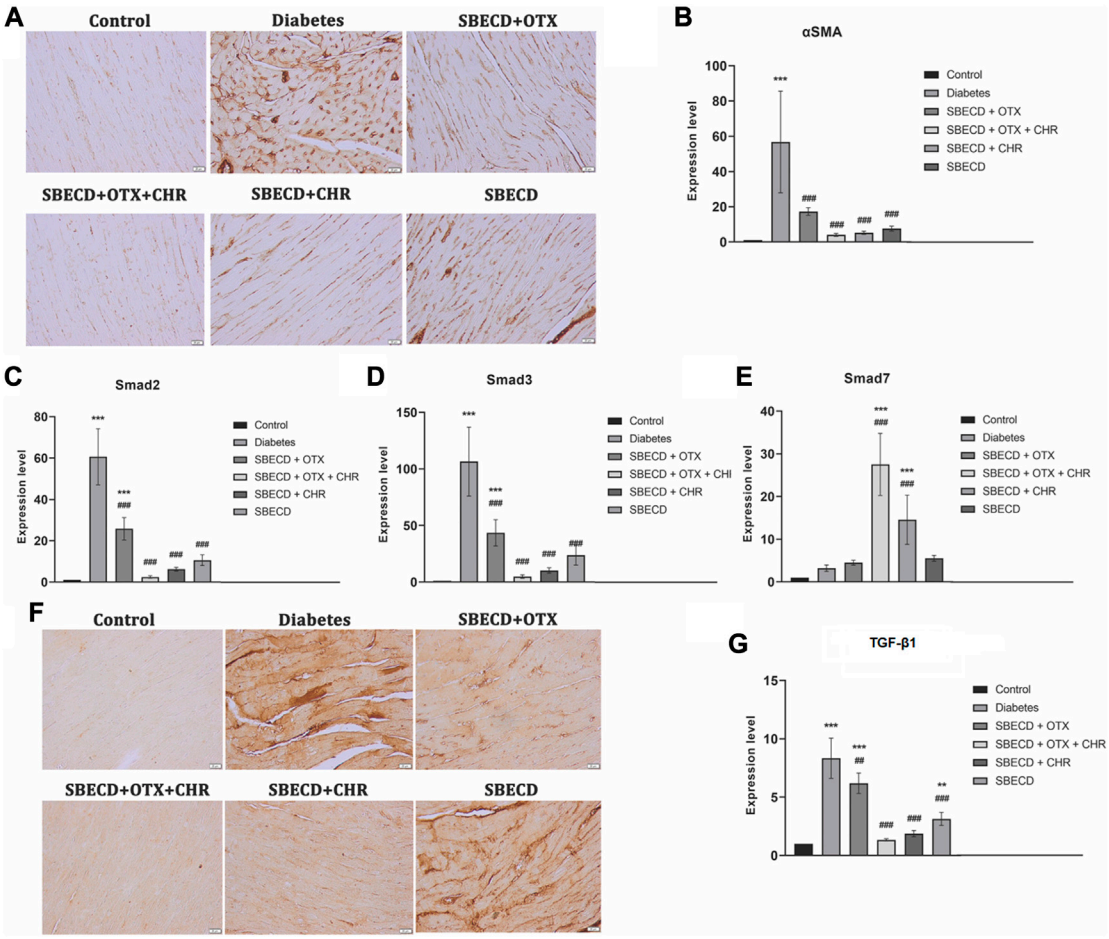


FIGURE 6
CHR-based supramolecular drug delivery system downregulates the main pro-fibrotic signaling pathways in cardiac tissues. **(A)** Immunohistochemical expression of α-SMA, Scale bar: 20 μm; **(B)** RT-PCR analysis of α-SMA gene expression. **(C)** RT-PCR analysis of Smad2 gene expression; **(D)** RT-PCR analysis of Smad3 gene expression; **(E)** RT-PCR analysis of Smad7 gene expression; **(F)** Immunohistochemical expression of TGF-β1, Scale bar: 20 μm; **(G)** RT-PCR analysis of TGF-β1 gene expression. *N* = 10 mice per group. Control: non-diabetic mice; Diabetes: diabetic mice; SBECD: sulfobutylated β-cyclodextrin; OTX: calixarene OTX008 - Calixarene 0118; CHR: 5,7-Dihydroxyflavone; ***$p < 0.001$ vs. Control; $^{###}p < 0.001$ and $^{##}p < 0.01$ vs. Diabetes.

CHR is further highlighted by its potential in improving conditions related to diabetes, such as fibrosis (Kang et al., 2023) and cardiometabolic diseases (Talebi et al., 2022). On the other hand, Gal-1 levels have been observed to be elevated in serum of diabetic patients and associated to a reduction of renal function and insulin resistance (Fryk et al., 2016; Drake et al., 2022). Its inhibition, specifically with OTX008, has been proposed in preclinical studies as a possible therapeutic target to treat diabetic renal fibrosis (Al-Obaidi et al., 2019) and proliferative diabetic retinopathy (Abu El-Asrar et al., 2020; Trotta et al., 2022).

Considering their individual protective effects against diabetes-related damage, the co-administration of CHR and calixarene OTX008 presents a potential approach for addressing diabetic fibrosis. However, both CHR and OTX008 showed a lower solubility in water, affecting their bioavailability and absorption (Dong et al., 2021; Hermenean et al., 2023). Indeed, the two compounds are soluble in organic solvents, such as DMSO or dimethylformamide (DMF), which are not suitable for *in vivo* administration at high doses due to their hepatotoxicity (Mathew et al., 1980; Dong et al., 2021; Hermenean et al., 2023). Therefore, we previously developed a dual-action supramolecular drug delivery system, in order to have a water soluble ternary complex. A key step was enhancing CHR's water solubility. To achieve this, CHR was combined with SBECD, a recognized cyclodextrin derivative known for its safety, polyanionic nature and excellent solubilization properties (Fenyvesi et al., 2020). Then, OTX008 was incorporated in this novel CHR-based supramolecular cyclodextrin-calixarene drug delivery system that synergistically combined cyclodextrin and calixarene. Crucially, safety tests conducted on H9c2 cardiomyocytes revealed no detrimental impacts on cell viability when exposed to this drug delivery system (Hermenean et al., 2023). Moreover, the drug delivery system not only was able to improve H9c2 cell viability in high glucose, but also surpassed the performance of OTX008 when used on its own (Hermenean et al., 2023). This highlights the potential therapeutic promise of this combined approach in diabetic fibrosis treatment.

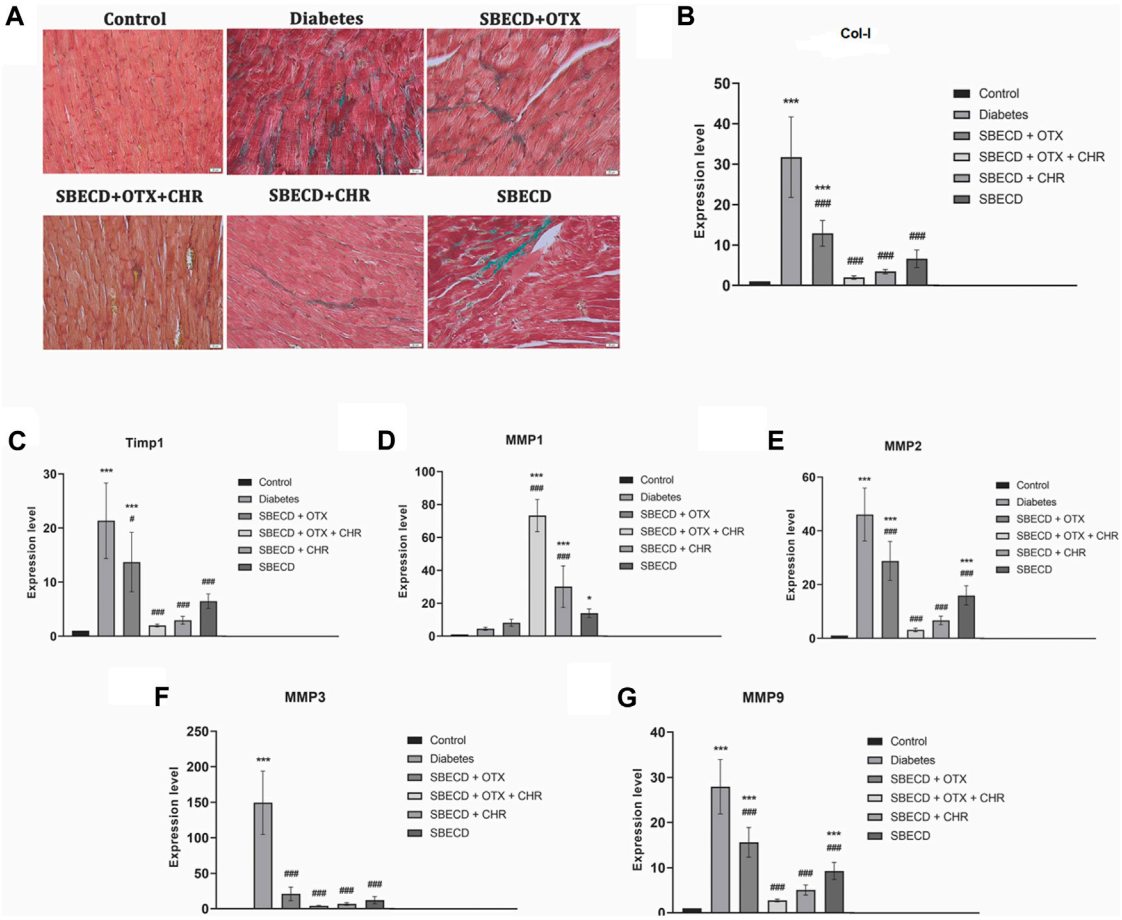


FIGURE 7
CHR-based supramolecular drug delivery system suppresses the secretion and deposition of collagen in cardiac tissues. **(A)** Collagen staining with Gomori's Trichrome kit; green—collagen deposition; **(B)** RT-PCR analysis of Col-I gene expression; **(C)** RT-PCR analysis of Timp-1 gene expression; **(D)** RT-PCR analysis of MMP1 gene expression; **(E)** RT-PCR analysis of MMP2 gene expression; **(F)** RT-PCR analysis of MMP3 gene expression; **(G)** RT-PCR analysis of MMP9 gene expression. N = 10 mice per group. Control: non-diabetic mice; Diabetes: diabetic mice; SBECD: sulfobutylated β-cyclodextrin; OTX: calixarene OTX008—Calixarene 0118; CHR: 5,7-Dihydroxyflavone; ***$p < 0.001$ compared to control; $^{\#}p < 0.05$ and $^{\#\#\#}p < 0.001$ vs. Diabetes.

In this study was characterized the anti-fibrotic effects of the CHR-based supramolecular cyclodextrin-calixarene drug delivery system in H9c2 cells exposed to high glucose. The system demonstrated its strongest anti-fibrotic effects, particularly when paired with the higher dose of OTX008. This lead to a significant reduction of Gal-1 levels, implying a possible modulation of cardiac inflammatory process but primarily leading to the suppression of both canonical and non-canonical profibrotic pathways, in line with previous studies (Leung et al., 2014; Kathiriya et al., 2017; Koonce et al., 2017; Jiang et al., 2018; Kostic et al., 2021; Trotta et al., 2022). Of note, the inhibition of TGF-β1 and its receptors in H9c2 cardiomyocytes could attenuate the fibrotic process by reducing the TGF-β1-induced myofibroblasts activation through Smad2/3 (Yan et al., 2018). Such findings signify the drug delivery system's ability to counteract the pathological changes instigated by high glucose in cardiomyocytes, as evidenced by the restored morphology of these cells.

Although the CHR-based supramolecular SBECD-calixarene drug delivery system showed were very similar anti-fibrotic actions compared to the combination of OTX008 with SBECD *in vitro*, its higher efficacy in counteracting Gal-1 and the fibrotic pathways was evident in cardiac tissues from mice developing chronic diabetes. Indeed, this dual-action supramolecular drug delivery system led to a marked downregulation of Gal-1, implying an amelioration of cardiac remodeling and inflammatory state, as well as a reduction of profibrotic pathways. To this regard, the decrement of TGF-β1/Smad2/3 pathway in hearts from mice with chronic diabetes may lead to a reduced myofibroblasts transformation and an attenuated cardiac hypertrophic response, though the inhibitions of fibrosis-mediating genes (Fiaschi et al., 2014; Khalil et al., 2017; Yan et al., 2018). Also the increase in cardiac Smad7 levels observed in diabetic mice treated with the SBECD-calixarene drug delivery system could contribute to the reduction of fibrotic process, since Smad7 is a negative regulator of TGF-β signalling in heart, as well as an inhibitor of cardiac remodeling (Chen et al., 2009; Wei et al., 2013). Lastly, the reduction of p38 and Erk1/2 MAPK cardiac levels, associated to abnormal ECM deposition (Tang et al., 2007; Aguilar et al., 2014), confirmed the anti-fibrotic effects of the new drug delivery system treatment.

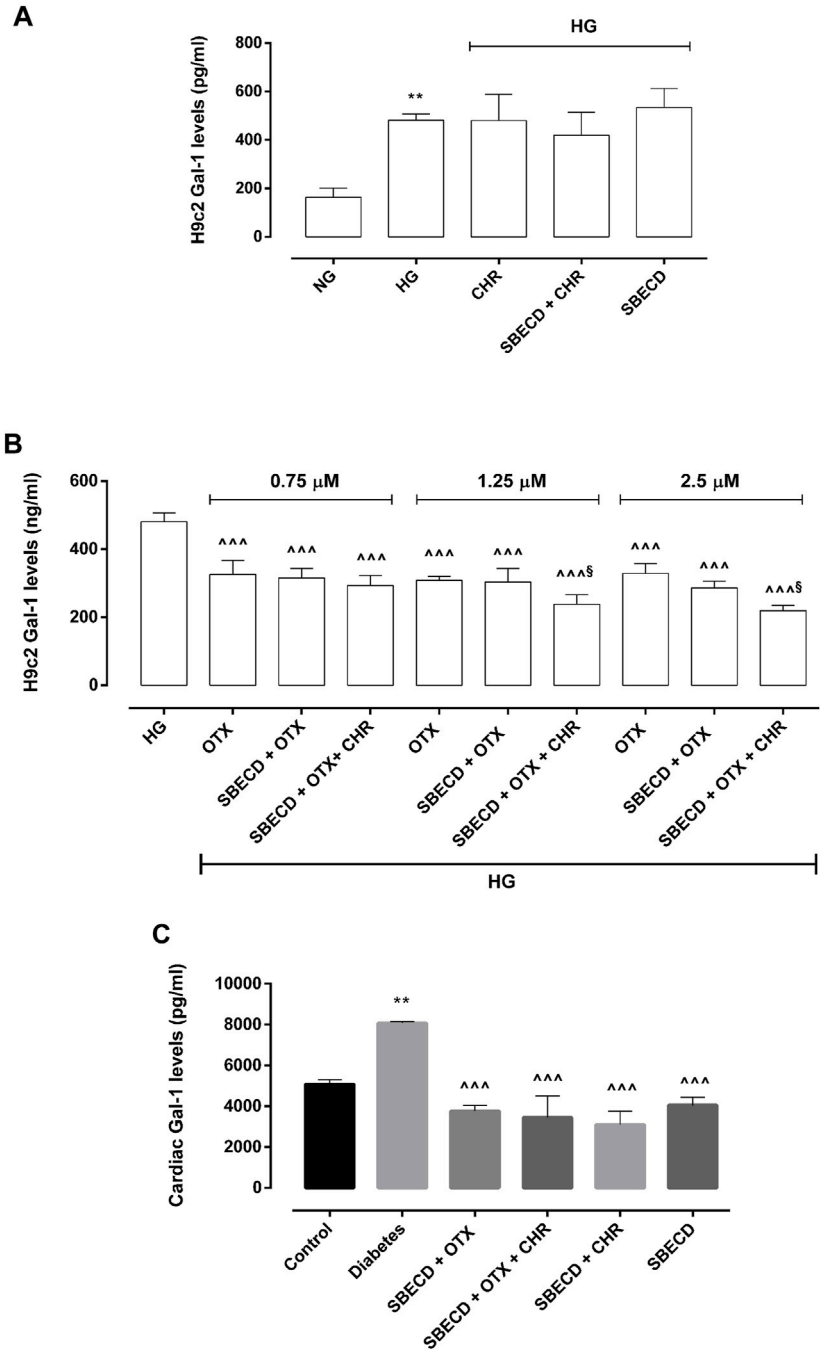


FIGURE 8
CHR-based supramolecular drug delivery system reduces Gal-1 in H9c2 cells exposed to high glucose and in cardiac tissues. **(A)** Gal-1 protein levels (pg/mL ± SD), determined by ELISA, in H9c2 cells cultured in normal glucose (NG) or high glucose (HG) for 48 h and exposed to CHR, SBECD + CHR and SBECD for 6 days in HG; **(B)** Gal-1 protein levels (pg/mL ± SD) in H9c2 cells cultured in HG for 48 h and treated with OTX008 (0.75–1.25–2.5 μM) alone or combined with SBECD/SBECD + CHR; *N* = 3 per group (three independent experiments, each performed in triplicate). NG: 5.5 mM D-glucose; HG: 33 mM D-glucose; CHR: 5,7-Dihydroxyflavone 0.399 mg/mL; SBECD: Sulfobutylated β-cyclodextrin sodium salt 7.3 m/m%; SBECD + CHR: SBECD + 0.095 mg/mL CHR; OTX: calixarene OTX008—Calixarene 0118—(0.75–1.25–2.5): OTX008 (0.75–1.25–2.5 μM); SBECD + OTX: SBECD-OTX008 (2.5–1.25–0.75 μM); SBECD + OTX + CHR: SBECD-OTX008 (2.5–1.25–0.75 μM)-CHR; $^{**}p < 0.01$ vs. NG; $^{\wedge\wedge\wedge}p < 0.001$ vs. HG; $^{\S}p < 0.05$ vs. OTX; **(C)** Gal-1 protein levels (pg/mL ± SD) determined by ELISA in cardiac tissues. *N* = 10 mice per group. Control: non-diabetic mice; Diabetes: diabetic mice; SBECD: sulfobutylated β-cyclodextrin; OTX: calixarene OTX008—Calixarene 0118; CHR: 5,7-Dihydroxyflavone. $^{**}p < 0.01$ vs. Control; $^{\wedge\wedge\wedge}p < 0.001$ vs. Diabetes.

Along with reduced TGF-β/Smad pathway, a decrease in αSMA levels was observed in diabetic hearts treated with the new drug delivery system. This marker of activated myofibroblasts (Shinde et al., 2017) is higher in cardiomyocytes exposed to high glucose and underwent to myofibroblast conversion, followed by subsequent changes and remodeling in the extracellular matrix (Levick and Widiapradja, 2020). Accordingly, Timp1, an MMP inhibitor stimulated by high glucose levels (Mclennan et al., 2000), was

reduced by the treatment with the novel drug delivery system, along with MMP2, 3 and 9 genes, which are typically elevated in diabetic disorders (Zhou et al., 2021b). Under normal physiological circumstances in the heart, MMP1 plays a crucial role in breaking down collagen types I, II, and III, as well as basement membrane proteins (Fan et al., 2012). Our research revealed a decline in MMP1 expression in cardiac tissue subjected to prolonged exposure to high glucose concentrations. This aligns with prior findings where patients with end-stage dilated cardiomyopathy exhibited reduced MMP1 levels in their left ventricular myocardial tissue samples (Thomas et al., 1998). The therapeutic interventions succeeded in elevating MMP1 gene expression, thereby aiding in restoring balance to the matrix components and reverting the cardiac normal architecture. Moreover, the CHR-based supramolecular SBECD-calixarene drug delivery system was the most effective in reducing cardiac Col-I expression and tissue deposition. It is well known that fibrotic heart exhibits Col-I deposition in the cardiac interstitial space, associated with heart dysfunction, dynamic alterations and cardiac remodeling (Kong et al., 2014). Its accumulation induced by high glucose is known to be a factor in myocardial fibrosis, impaired relaxation and mitochondrial degeneration in patients with diabetic cardiomyopathy (Sakakibara et al., 2011; Levick and Widiapradja, 2020). Therefore, Col-I inhibition obtained with the new drug delivery system could be considered a novel strategic therapeutic tool to counteract cardiac fibrosis.

Overall, the CHR-based supramolecular SBECD-calixarene drug delivery system enhanced the solubility and the bioavailability of both CHR and calixarene OTX008. By combining the effects of the two drugs, it showcased a strong anti-fibrotic response in rat cardiomyocytes, as well as in cardiac tissue from mice with chronic diabetes. These evidenced also an improved cardiac tissue remodeling after the treatment with the dual-action supramolecular drug delivery system, which could be considered as a novel putative therapeutic strategy for the treatment of diabetes-induced cardiac fibrosis.

## Data availability statement

The original contributions presented in the study are included in the article/supplementary material, further inquiries can be directed to the corresponding author.

## Ethics statement

The animal study was approved by Ethical Commettee of Vasile Goldis Western University of Arad (Approval number 20, 12/06/2020) and National Sanitary Veterinary and Food Safety Authority (Certificate number 001/04.02.2021). The study was conducted in accordance with the local legislation and institutional requirements.

## Author contributions

MT: Conceptualization, Writing–original draft. HH: Conceptualization, Writing–original draft. AC: Investigation, Methodology, Writing–review and editing. BM: Investigation, Methodology, Writing–review and editing. MRo: Investigation, Methodology, Writing–review and editing. CL: Investigation, Methodology, Writing–review and editing. MRu: Investigation, Methodology, Writing–review and editing. IB: Investigation, Methodology, Writing–review and editing. FF: Investigation, Methodology, Writing–review and editing. RM: Data curation, Formal Analysis, Writing–review and editing. AH: Conceptualization, Data curation, Formal Analysis, Project administration, Writing–original draft, Writing–review and editing. CB: Writing–review and editing. MD'A: Writing–review and editing.

## Funding

The authors declare financial support was received for the research, authorship, and/or publication of this article. This research was funded by a grant of the Ministry of Research, Innovation and Digitization, CNCS/CCCDI—UEFISCDI, project number PN-III-P4-ID-PCE-2020-1772, within PNCDI III.

## Conflict of interest

The authors declare that the research was conducted in the absence of any commercial or financial relationships that could be construed as a potential conflict of interest.

The authors declared that they were an editorial board member of Frontiers, at the time of submission. This had no impact on the peer review process and the final decision.

## Publisher's note



## References

Abed, H. S., Samuel, C. S., Lau, D. H., Kelly, D. J., Royce, S. G., Alasady, M., et al. (2013). Obesity results in progressive atrial structural and electrical remodeling: implications for atrial fibrillation. *Heart rhythm.* 10, 90–100. doi:10.1016/j.hrthm.2012.08.043

Abu El-Asrar, A. M., Ahmad, A., Allegaert, E., Siddiquei, M. M., Alam, K., Gikandi, P. W., et al. (2020). Galectin-1 studies in proliferative diabetic retinopathy. *Acta Ophthalmol.* 98, e1–e12. doi:10.1111/aos.14191

Aguilar, H., Fricovsky, E., Ihm, S., Schimke, M., Maya-Ramos, L., Aroonsakool, N., et al. (2014). Role for high-glucose-induced protein *O* -GlcNAcylation in stimulating cardiac fibroblast collagen synthesis. *Am. J. Physiology-Cell Physiology* 306, C794–C804. doi:10.1152/ajpcell.00251.2013

Ali, N., Rashid, S., Nafees, S., Hasan, S. K., and Sultana, S. (2014a). Beneficial effects of Chrysin against Methotrexate-induced hepatotoxicity via attenuation of oxidative stress and apoptosis. *Mol. Cell. Biochem.* 385, 215–223. doi:10.1007/s11010-013-1830-4

Ali, S. R., Ranjbarvaziri, S., Talkhabi, M., Zhao, P., Subat, A., Hojjat, A., et al. (2014b). Developmental Heterogeneity of Cardiac Fibroblasts Does Not Predict Pathological Proliferation and Activation. *Circ. Res.* 115, 625–635. doi:10.1161/CIRCRESAHA.115.303794

Al-Obaidi, N., Mohan, S., Liang, S., Zhao, Z., Nayak, B. K., Li, B., et al. (2019). Galectin-1 is a new fibrosis protein in type 1 and type 2 diabetes. *FASEB J.* 33, 373–387. doi:10.1096/fj.201800555RR

Anandhi, R., Thomas, P. A., and Geraldine, P. (2014). Evaluation of the anti-atherogenic potential of chrysin in Wistar rats. *Mol. Cell. Biochem.* 385, 103–113. doi:10.1007/s11010-013-1819-z

Ares-Carrasco, S., Picatoste, B., Benito-Martín, A., Zubiri, I., Sanz, A. B., Sánchez-Niño, M. D., et al. (2009). Myocardial fibrosis and apoptosis, but not inflammation, are present in long-term experimental diabetes. *Am. J. Physiology-Heart Circulatory Physiology* 297, H2109–H2119. doi:10.1152/ajpheart.00157.2009

Bae, Y., Lee, S., and Kim, S.-H. (2011). Chrysin suppresses mast cell-mediated allergic inflammation: involvement of calcium, caspase-1 and nuclear factor-κB. *Toxicol. Appl. Pharmacol.* 254, 56–64. doi:10.1016/j.taap.2011.04.008

Balta, C., Ciceu, A., Herman, H., Rosu, M., Boldura, O. M., and Hermenean, A. (2018). Dose-dependent antifibrotic effect of chrysin on Regression of liver fibrosis: the role in extracellular matrix remodeling. *Dose-Response* 16, 1559325818789835. doi:10.1177/1559325818789835

Balta, C., Herman, H., Boldura, O. M., Gasca, I., Rosu, M., Ardelean, A., et al. (2015). Chrysin attenuates liver fibrosis and hepatic stellate cell activation through TGF-β/Smad signaling pathway. *Chemico-Biological Interact.* 240, 94–101. doi:10.1016/j.cbi.2015.08.013

Biernacka, A., Dobaczewski, M., and Frangogiannis, N. G. (2011). TGF-β signaling in fibrosis. *Growth factors.* 29, 196–202. doi:10.3109/08977194.2011.595714

Brechbuhl, H. M., Kachadourian, R., Min, E., Chan, D., and Day, B. J. (2012). Chrysin enhances doxorubicin-induced cytotoxicity in human lung epithelial cancer cell lines: the role of glutathione. *Toxicol. Appl. Pharmacol.* 258, 1–9. doi:10.1016/j.taap.2011.08.004

Carroll, J., and Tyagi, S. (2005). Extracellular matrix remodeling in the heart of the Homocysteinemic obese rabbit. *Am. J. Hypertens.* 18, 692–698. doi:10.1016/j.amjhyper.2004.11.035

Chen, Q., Chen, H., Zheng, D., Kuang, C., Fang, H., Zou, B., et al. (2009). Smad7 is Required for the development and function of the heart. *J. Biol. Chem.* 284, 292–300. doi:10.1074/jbc.M807233200

Ding, L., Liao, T., Yang, N., Wei, Y., Xing, R., Wu, P., et al. (2023). Chrysin ameliorates synovitis and fibrosis of osteoarthritic fibroblast-like synoviocytes in rats through PERK/TXNIP/NLRP3 signaling. *Front. Pharmacol.* 14, 1170243. doi:10.3389/fphar.2023.1170243

Disertori, M., Masè, M., and Ravelli, F. (2017). Myocardial fibrosis predicts ventricular tachyarrhythmias. *Trends Cardiovasc. Med.* 27, 363–372. doi:10.1016/j.tcm.2017.01.011

Dobaczewski, M., Bujak, M., Li, N., Gonzalez-Quesada, C., Mendoza, L. H., Wang, X.-F., et al. (2010). Smad3 signaling critically Regulates fibroblast phenotype and function in healing myocardial infarction. *Circ. Res.* 107, 418–428. doi:10.1161/CIRCRESAHA.109.216101

Dong, X., Cao, Y., Wang, N., Wang, P., and Li, M. (2021). Systematic study on solubility of chrysin in different organic solvents: the synergistic effect of multiple intermolecular interactions on the dissolution process. *J. Mol. Liq.* 325, 115180. doi:10.1016/j.molliq.2020.115180

Drake, I., Fryk, E., Strindberg, L., Lundqvist, A., Rosengren, A. H., Groop, L., et al. (2022). The role of circulating galectin-1 in type 2 diabetes and chronic kidney disease: evidence from cross-sectional, longitudinal and Mendelian randomisation analyses. *Diabetologia* 65, 128–139. doi:10.1007/s00125-021-05594-1

Falcão-Pires, I., Hamdani, N., Borbély, A., Gavina, C., Schalkwijk, C. G., Van Der Velden, J., et al. (2011). Diabetes Mellitus Worsens Diastolic Left Ventricular Dysfunction in Aortic Stenosis Through Altered Myocardial Structure and Cardiomyocyte Stiffness. *Circulation* 124, 1151–1159. doi:10.1161/CIRCULATIONAHA.111.025270

Fan, D., Takawale, A., Lee, J., and Kassiri, Z. (2012). Cardiac fibroblasts, fibrosis and extracellular matrix remodeling in heart disease. *Fibrogenes. Tissue Repair* 5, 15. doi:10.1186/1755-1536-5-15

Farkhondeh, T., Samarghandian, S., and Roshanravan, B. (2019). Impact of chrysin on the molecular mechanisms underlying diabetic complications. *J. Cell. Physiology* 234, 17144–17158. doi:10.1002/jcp.28488

Fenyvesi, F., Nguyen, T. L. P., Haimhoffer, Á., Rusznyák, Á., Vasvári, G., Bácskay, I., et al. (2020). Cyclodextrin Complexation improves the solubility and Caco-2 Permeability of chrysin. *Materials* 13, 3618. doi:10.3390/ma13163618

Fiaschi, T., Magherini, F., Gamberi, T., Lucchese, G., Faggian, G., Modesti, A., et al. (2014). Hyperglycemia and angiotensin II cooperate to enhance collagen I deposition by cardiac fibroblasts through a ROS-STAT3-dependent mechanism. *Biochimica Biophysica Acta (BBA) - Mol. Cell. Res.* 1843, 2603–2610. doi:10.1016/j.bbamcr.2014.07.009

Fischer, V. W., Barner, H. B., and Larose, L. S. (1984). Pathomorphologic aspects of muscular tissue in diabetes mellitus. *Hum. Pathol.* 15, 1127–1136. doi:10.1016/S0046-8177(84)80307-X

Fryk, E., Sundelin, J. P., Strindberg, L., Pereira, M. J., Federici, M., Marx, N., et al. (2016). Microdialysis and proteomics of subcutaneous interstitial fluid reveals increased galectin-1 in type 2 diabetes patients. *Metabolism* 65, 998–1006. doi:10.1016/j.metabol.2016.04.003

González, A., Schelbert, E. B., Díez, J., and Butler, J. (2018). Myocardial interstitial fibrosis in Heart Failure: Biological and Translational Perspectives. *J. Am. Coll. Cardiol.* 71, 1696–1706. doi:10.1016/j.jacc.2018.02.021

Gonzalez-Quesada, C., Cavalera, M., Biernacka, A., Kong, P., Lee, D.-W., Saxena, A., et al. (2013). Thrombospondin-1 Induction in the Diabetic Myocardium Stabilizes the Cardiac Matrix in Addition to Promoting Vascular Rarefaction Through Angiopoietin-2 Upregulation. *Circ. Res.* 113, 1331–1344. doi:10.1161/CIRCRESAHA.113.302593

Hanna, A., Humeres, C., and Frangogiannis, N. G. (2021). The role of Smad signaling cascades in cardiac fibrosis. *Cell. Signal.* 77, 109826. doi:10.1016/j.cellsig.2020.109826

Hao, P.-P., Yang, J.-M., Zhang, M.-X., Zhang, K., Chen, Y.-G., Zhang, C., et al. (2015). Angiotensin-(1–7) treatment mitigates right ventricular fibrosis as a distinctive feature of diabetic cardiomyopathy. *Am. J. Physiology-Heart Circulatory Physiology* 308, H1007–H1019. doi:10.1152/ajpheart.00563.2014

Hermenean, A., Dossi, E., Hamilton, A., Trotta, M. C., Russo, M., Lepre, C. C., et al. (2023). Chrysin directing an enhanced solubility through the formation of a supramolecular cyclodextrin-calixarene drug delivery system: a potential strategy in antifibrotic diabetes therapeutics. *Pharmacol. Toxicol.* doi:10.1101/2023.10.03.560552

Hermenean, A., Oatis, D., Herman, H., Ciceu, A., D'Amico, G., and Trotta, M. C. (2022). Galectin 1—a key player between tissue repair and fibrosis. *IJMS* 23, 5548. doi:10.3390/ijms23105548

Huynh, K., Kiriazis, H., Du, X.-J., Love, J. E., Jandeleit-Dahm, K. A., Forbes, J. M., et al. (2012). Coenzyme Q10 attenuates diastolic dysfunction, cardiomyocyte hypertrophy and cardiac fibrosis in the db/db mouse model of type 2 diabetes. *Diabetologia* 55, 1544–1553. doi:10.1007/s00125-012-2495-3

Huynh, K., McMullen, J. R., Julius, T. L., Tan, J. W., Love, J. E., Cemerlang, N., et al. (2010). Cardiac-specific IGF-1 receptor Transgenic expression Protects against cardiac fibrosis and diastolic dysfunction in a mouse model of diabetic cardiomyopathy. *Diabetes* 59, 1512–1520. doi:10.2337/db09-1456

Jellis, C., Martin, J., Narula, J., and Marwick, T. H. (2010). Assessment of Nonischemic myocardial fibrosis. *J. Am. Coll. Cardiol.* 56, 89–97. doi:10.1016/j.jacc.2010.02.047

Jia, G., Hill, M. A., and Sowers, J. R. (2018). Diabetic Cardiomyopathy: An Update of Mechanisms Contributing to This Clinical Entity. *Circ. Res.* 122, 624–638. doi:10.1161/CIRCRESAHA.117.311586

Jiang, W., Xiong, Y., Li, X., and Yang, Y. (2021). Cardiac Fibrosis: Cellular Effectors, Molecular Pathways, and Exosomal Roles. *Front. Cardiovasc. Med.* 8, 715258. doi:10.3389/fcvm.2021.715258

Jiang, Z., Shen, Q., Chen, H., Yang, Z., Shuai, M., and Zheng, S. (2018). Galectin-1 gene silencing inhibits the activation and proliferation but induces the apoptosis of hepatic stellate cells from mice with liver fibrosis. *Int. J. Mol. Med.* 43, 103–116. doi:10.3892/ijmm.2018.3950

Johnston, E. F., and Gillis, T. E. (2022). Regulation of collagen deposition in the trout heart during thermal acclimation. *Curr. Res. Physiology* 5, 99–108. doi:10.1016/j.crphys.2022.02.004

Kang, Y.-H., Park, S.-H., Sim, Y. E., Oh, M.-S., Suh, H. W., Lee, J.-Y., et al. (2023). Highly water-soluble diacetyl chrysin ameliorates diabetes-associated renal fibrosis and retinal microvascular abnormality in db/db mice. *Nutr. Res. Pract.* 17, 421–437. doi:10.4162/nrp.2023.17.3.421

Kathiriya, J. J., Nakra, N., Nixon, J., Patel, P. S., Vaghasiya, V., Alhassani, A., et al. (2017). Galectin-1 inhibition attenuates profibrotic signaling in hypoxia-induced pulmonary fibrosis. *Cell. Death Discov.* 3, 17010. doi:10.1038/cddiscovery.2017.10

Kawaguchi, M., Techigawara, M., Ishihata, T., Asakura, T., Saito, F., Maehara, K., et al. (1997). A comparison of ultrastructural changes on endomyocardial biopsy specimens obtained from patients with diabetes mellitus with and without hypertension. *Heart Vessels* 12, 267–274. doi:10.1007/BF02766802

Khalil, H., Kanisicak, O., Prasad, V., Correll, R. N., Fu, X., Schips, T., et al. (2017). Fibroblast-specific TGF-β–Smad2/3 signaling underlies cardiac fibrosis. *J. Clin. Investigation* 127, 3770–3783. doi:10.1172/JCI94753

Kong, P., Christia, P., and Frangogiannis, N. G. (2014). The pathogenesis of cardiac fibrosis. *Cell. Mol. Life Sci.* 71, 549–574. doi:10.1007/s00018-013-1349-6

Koonce, N., Griffin, R., and Dings, R. (2017). Galectin-1 Inhibitor OTX008 Induces Tumor Vessel Normalization and Tumor Growth Inhibition in Human Head and Neck Squamous Cell Carcinoma Models. *IJMS* 18, 2671. doi:10.3390/ijms18122671

Kostic, M., Dzopalic, T., Marjanovic, G., Urosevic, I., and Milosevic, I. (2021). Immunomodulatory effects of galectin-1in patients with chronic lymphocytic leukemia. *cejoi* 46, 54–62. doi:10.5114/ceji.2021.105246

Kuo, C.-S., Chou, R.-H., Lu, Y.-W., Tsai, Y.-L., Huang, P.-H., and Lin, S.-J. (2020). Increased circulating galectin-1 levels are associated with the progression of kidney function decline in patients undergoing coronary angiography. *Sci. Rep.* 10, 1435. doi:10.1038/s41598-020-58132-1

Kwong, R. Y., Sattar, H., Wu, H., Vorobiof, G., Gandla, V., Steel, K., et al. (2008). Incidence and Prognostic implication of Unrecognized myocardial scar characterized by cardiac magnetic resonance in diabetic patients without clinical evidence of myocardial infarction. *Circulation* 118, 1011–1020. doi:10.1161/CIRCULATIONAHA.107.727826

Leung, L. Y., Chan, C. P. Y., Leung, Y. K., Jiang, H. L., Abrigo, J. M., Wang, D. F., et al. (2014). Comparison of miR-124-3p and miR-16 for early diagnosis of hemorrhagic and ischemic stroke. *Clin. Chim. Acta* 433, 139–144. doi:10.1016/j.cca.2014.03.007

Levick, S. P., and Widiapradja, A. (2020). The diabetic cardiac fibroblast: mechanisms underlying phenotype and function. *IJMS* 21, 970. doi:10.3390/ijms21030970

Li, J., Zhu, H., Shen, E., Wan, L., Arnold, J. M. O., and Peng, T. (2010). Deficiency of Rac1 Blocks NADPH oxidase activation, inhibits Endoplasmic Reticulum stress, and reduces myocardial remodeling in a mouse model of type 1 diabetes. *Diabetes* 59, 2033–2042. doi:10.2337/db09-1800

Li, R., Zang, A., Zhang, L., Zhang, H., Zhao, L., Qi, Z., et al. (2014). Chrysin ameliorates diabetes-associated cognitive deficits in Wistar rats. *Neurol. Sci.* 35, 1527–1532. doi:10.1007/s10072-014-1784-7

Liu, L., Liu, F., Sun, Z., Peng, Z., You, T., and Yu, Z. (2020). LncRNA NEAT1 promotes apoptosis and inflammation in LPS-induced sepsis models by targeting miR-590-3p. *Exp. Ther. Med.* 20, 3290–3300. doi:10.3892/etm.2020.9079

Liu, Y., Long, L., Yuan, F., Liu, F., Liu, H., Peng, Y., et al. (2015). High glucose-induced Galectin-1 in human podocytes implicates the involvement of Galectin-1 in diabetic nephropathy. *Cell. Biol. Int.* 39, 217–223. doi:10.1002/cbin.10363

Ma, Z.-G., Yuan, Y.-P., Wu, H.-M., Zhang, X., and Tang, Q.-Z. (2018). Cardiac fibrosis: new insights into the pathogenesis. *Int. J. Biol. Sci.* 14, 1645–1657. doi:10.7150/ijbs.28103

Mathew, T., Karunanithy, R., Yee, M. H., and Natarajan, P. N. (1980). Hepatotoxicity of dimethylformamide and dimethylsulfoxide at and above the levels used in some aflatoxin studies. *Lab. Investig.* 42, 257–262.

Mclennan, S. V., Fisher, E., Martell, S. Y., Death, A. K., Williams, P. F., Lyons, J. G., et al. (2000). Effects of glucose on matrix metalloproteinase and plasmin activities in mesangial cells: possible role in diabetic nephropathy. *Kidney Int.* 58, S81–S87. doi:10.1046/j.1523-1755.2000.07713.x

Nagavally, R. R., Sunilkumar, S., Akhtar, M., Trombetta, L. D., and Ford, S. M. (2021). Chrysin ameliorates Cyclosporine-A-induced renal fibrosis by inhibiting TGF-β1-induced epithelial–Mesenchymal Transition. *IJMS* 22, 10252. doi:10.3390/ijms221910252

Nunoda, S., Genda, A., Sugihara, N., Nakayama, A., Mizuno, S., and Takeda, R. (1985). Quantitative approach to the histopathology of the biopsied right ventricular myocardium in patients with diabetes mellitus. *Heart Vessels* 1, 43–47. doi:10.1007/BF02066486

Ou, D., Ni, D., Li, R., Jiang, X., Chen, X., and Li, H. (2021). Galectin-1 alleviates myocardial ischemia-reperfusion injury by reducing the inflammation and apoptosis of cardiomyocytes. *Exp. Ther. Med.* 23, 143. doi:10.3892/etm.2021.11066

Phan, T. H. G., Paliogiannis, P., Nasrallah, G. K., Giordo, R., Eid, A. H., Fois, A. G., et al. (2021). Emerging cellular and molecular determinants of idiopathic pulmonary fibrosis. *Cell. Mol. Life Sci.* 78, 2031–2057. doi:10.1007/s00018-020-03693-7

Rahaman, S. O., Grove, L. M., Paruchuri, S., Southern, B. D., Abraham, S., Niese, K. A., et al. (2014). TRPV4 mediates myofibroblast differentiation and pulmonary fibrosis in mice. *J. Clin. Investig.* 124, 5225–5238. doi:10.1172/JCI75331

Rani, N., Bharti, S., Bhatia, J., Tomar, A., Nag, T. C., Ray, R., et al. (2015). Inhibition of TGF-β by a novel PPAR-γ agonist, chrysin, salvages β-receptor stimulated myocardial injury in rats through MAPKs-dependent mechanism. *Nutr. Metab. (Lond)* 12, 11. doi:10.1186/s12986-015-0004-7

Regan, T. J., Lyons, M. M., Ahmed, S. S., Levinson, G. E., Oldewurtel, H. A., Ahmad, M. R., et al. (1977). Evidence for cardiomyopathy in Familial diabetes mellitus. *J. Clin. Investig.* 60, 884–899. doi:10.1172/JCI108843

Russo, I., and Frangogiannis, N. G. (2016). Diabetes-associated cardiac fibrosis: cellular effectors, molecular mechanisms and therapeutic opportunities. *J. Mol. Cell. Cardiol.* 90, 84–93. doi:10.1016/j.yjmcc.2015.12.011

Saadat, S., Noureddini, M., Mahjoubin-Tehran, M., Nazemi, S., Shojaie, L., Aschner, M., et al. (2021). Pivotal role of TGF-β/Smad signaling in cardiac fibrosis: non-coding RNAs as Effectual Players. *Front. Cardiovasc. Med.* 7, 588347. doi:10.3389/fcvm.2020.588347

Sakakibara, M., Hirashiki, A., Cheng, X. W., Bando, Y., Ohshima, K., Okumura, T., et al. (2011). Association of diabetes mellitus with myocardial collagen accumulation and relaxation impairment in patients with dilated cardiomyopathy. *Diabetes Res. Clin. Pract.* 92, 348–355. doi:10.1016/j.diabres.2011.02.023

Salama, A., Asaad, G., and Shaheen, A. (2022). Chrysin ameliorates STZ-induced diabetes in rats: possible impact of modulation of TLR4/NF-κβ pathway. *Res. Pharma Sci.* 17, 1–11. doi:10.4103/1735-5362.329921

Samarghandian, S., Azimi-Nezhad, M., Samini, F., and Farkhondeh, T. (2016). Chrysin treatment improves diabetes and its complications in liver, brain, and pancreas in streptozotocin-induced diabetic rats. *Can. J. Physiol. Pharmacol.* 94, 388–393. doi:10.1139/cjpp-2014-0412

Sano, M., Fukuda, K., Sato, T., Kawaguchi, H., Suematsu, M., Matsuda, S., et al. (2001). ERK and p38 MAPK, but not NF-kappaB, are critically involved in reactive oxygen species-mediated induction of IL-6 by angiotensin II in cardiac fibroblasts. *Circulation Res.* 89, 661–669. doi:10.1161/hh2001.098873

See, F., Thomas, W., Way, K., Tzanidis, A., Kompa, A., Lewis, D., et al. (2004). p38 mitogen-activated protein kinase inhibition improves cardiac function and attenuates left ventricular remodeling following myocardial infarction in the rat. *J. Am. Coll. Cardiol.* 44, 1679–1689. doi:10.1016/j.jacc.2004.07.038

Senador, D., Kanakamedala, K., Irigoyen, M. C., Morris, M., and Elased, K. M. (2009). Cardiovascular and autonomic phenotype of *db*/*db* diabetic mice. *Exp. Physiol.* 94, 648–658. doi:10.1113/expphysiol.2008.046474

Seropian, I. M., González, G. E., Maller, S. M., Berrocal, D. H., Abbate, A., and Rabinovich, G. A. (2018). Galectin-1 as an emerging mediator of Cardiovascular inflammation: mechanisms and therapeutic opportunities. *Mediat. Inflamm.* 2018, 8696543–8696611. doi:10.1155/2018/8696543

Shamhart, P. E., Luther, D. J., Adapala, R. K., Bryant, J. E., Petersen, K. A., Meszaros, J. G., et al. (2014). Hyperglycemia enhances function and differentiation of adult rat cardiac fibroblasts. *Can. J. Physiol. Pharmacol.* 92, 598–604. doi:10.1139/cjpp-2013-0490

Shimizu, M., Umeda, K., Sugihara, N., Yoshio, H., Ino, H., Takeda, R., et al. (1993). Collagen remodelling in myocardia of patients with diabetes. *J. Clin. Pathology* 46, 32–36. doi:10.1136/jcp.46.1.32

Shinde, A. V., Humeres, C., and Frangogiannis, N. G. (2017). The role of α-smooth muscle actin in fibroblast-mediated matrix contraction and remodeling. *Biochimica Biophysica Acta (BBA) - Mol. Basis Dis.* 1863, 298–309. doi:10.1016/j.bbadis.2016.11.006

Sutherland, C. G. G., Fisher, B. M., Frier, B. M., Dargie, H. J., More, I. A. R., and Lindop, G. B. M. (1989). Endomyocardial biopsy pathology in insulin-dependent diabetic patients with abnormal ventricular function. *Histopathology* 14, 593–602. doi:10.1111/j.1365-2559.1989.tb02200.x

Talebi, M., Talebi, M., Farkhondeh, T., Simal-Gandara, J., Kopustinskiene, D. M., Bernatoniene, J., et al. (2022). Promising protective effects of chrysin in cardiometabolic diseases. *CDT* 23, 458–470. doi:10.2174/1389450122666211005113234

Talman, V., and Ruskoaho, H. (2016). Cardiac fibrosis in myocardial infarction—from repair and remodeling to regeneration. *Cell. Tissue Res.* 365, 563–581. doi:10.1007/s00441-016-2431-9

Tang, M., Zhang, W., Lin, H., Jiang, H., Dai, H., and Zhang, Y. (2007). High glucose promotes the production of collagen types I and III by cardiac fibroblasts through a pathway dependent on extracellular-signal-regulated kinase 1/2. *Mol. Cell. Biochem.* 301, 109–114. doi:10.1007/s11010-006-9401-6

Tao, G., Miller, L. J., and Lincoln, J. (2013). Snai1 is important for avian epicardial cell transformation and motility: the Role of Snai1 in the Avian Epicardium. *Dev. Dyn.* 242, 699–708. doi:10.1002/dvdy.23967

Thomas, C. V., Coker, M. L., Zellner, J. L., Handy, J. R., Crumbley, A. J., and Spinale, F. G. (1998). Increased matrix metalloproteinase activity and selective upregulation in LV myocardium from patients with end-stage dilated cardiomyopathy. *Circulation* 97, 1708–1715. doi:10.1161/01.CIR.97.17.1708

Tian, J., An, X., and Niu, L. (2017). Myocardial fibrosis in congenital and pediatric heart disease. *Exp. Ther. Med.* 13, 1660–1664. doi:10.3892/etm.2017.4224

Trotta, M. C., Petrillo, F., Gesualdo, C., Rossi, S., Corte, A. D., Váradi, J., et al. (2022). Effects of the Calix[4]arene derivative compound OTX008 on high glucose-stimulated ARPE-19 cells: Focus on galectin-1/TGF-β/EMT pathway. *Molecules* 27, 4785. doi:10.3390/molecules27154785

Turkbey, E. B., Backlund, J.-Y. C., Genuth, S., Jain, A., Miao, C., Cleary, P. A., et al. (2011). Myocardial structure, function, and scar in patients with type 1 diabetes mellitus. *Circulation* 124, 1737–1746. doi:10.1161/CIRCULATIONAHA.111.022327

Turner, L., and Blythe, H. (2019). Cardiac fibroblast p38 MAPK: a Critical regulator of myocardial remodeling. *JCDD* 6, 27. doi:10.3390/jcdd6030027

Uchinaka, A., Kawaguchi, N., Mori, S., Hamada, Y., Miyagawa, S., Saito, A., et al. (2014). Tissue inhibitor of metalloproteinase-1 and -3 improves cardiac function in an ischemic cardiomyopathy model rat. *Tissue Eng. Part A* 20, 3073–3084. doi:10.1089/ten.tea.2013.0763

Van Heerebeek, L., Hamdani, N., Handoko, M. L., Falcao-Pires, I., Musters, R. J., Kupreishvili, K., et al. (2008). Diastolic Stiffness of the failing diabetic heart: Importance of fibrosis, advanced Glycation end products, and Myocyte resting Tension. *Circulation* 117, 43–51. doi:10.1161/CIRCULATIONAHA.107.728550

Van Hoeven, K. H., and Factor, S. M. (1990). A comparison of the pathological spectrum of hypertensive, diabetic, and hypertensive-diabetic heart disease. *Circulation* 82, 848–855. doi:10.1161/01.CIR.82.3.848

Wei, L.-H., Huang, X.-R., Zhang, Y., Li, Y.-Q., Chen, H., Yan, B. P., et al. (2013). Smad7 inhibits angiotensin II-induced hypertensive cardiac remodelling. *Cardiovasc. Res.* 99, 665–673. doi:10.1093/cvr/cvt151

Wessels, A., Van Den Hoff, M. J. B., Adamo, R. F., Phelps, A. L., Lockhart, M. M., Sauls, K., et al. (2012). Epicardially derived fibroblasts preferentially contribute to the parietal leaflets of the atrioventricular valves in the murine heart. *Dev. Biol.* 366, 111–124. doi:10.1016/j.ydbio.2012.04.020

Westermann, D., Rutschow, S., Jäger, S., Linderer, A., Anker, S., Riad, A., et al. (2007). Contributions of inflammation and cardiac matrix metalloproteinase activity to cardiac failure in diabetic cardiomyopathy: the role of angiotensin type 1 receptor antagonism. *Diabetes* 56, 641–646. doi:10.2337/db06-1163

Wu, M., Xing, Q., Duan, H., Qin, G., and Sang, N. (2022). Suppression of NADPH oxidase 4 inhibits PM2.5-induced cardiac fibrosis through ROS-P38 MAPK pathway. *Sci. Total Environ.* 837, 155558. doi:10.1016/j.scitotenv.2022.155558

Xu, Z., Sun, J., Tong, Q., Lin, Q., Qian, L., Park, Y., et al. (2016). The role of ERK1/2 in the development of diabetic cardiomyopathy. *IJMS* 17, 2001. doi:10.3390/ijms17122001

Yan, Z., Shen, D., Liao, J., Zhang, Y., Chen, Y., Shi, G., et al. (2018). Hypoxia suppresses TGF-B1-induced cardiac Myocyte myofibroblast transformation by inhibiting Smad2/3 and Rhoa signaling pathways. *Cell. Physiol. Biochem.* 45, 250–257. doi:10.1159/000486771

Ytrehus, K., Hulot, J.-S., Perrino, C., Schiattarella, G. G., and Madonna, R. (2018). Perivascular fibrosis and the microvasculature of the heart. Still hidden secrets of pathophysiology? *Vasc. Pharmacol.* 107, 78–83. doi:10.1016/j.vph.2018.04.007

Zhou, P., Yang, C., Zhang, S., Ke, Z.-X., Chen, D.-X., Li, Y.-Q., et al. (2021a). The Imbalance of MMP-2/TIMP-2 and MMP-9/TIMP-1 contributes to collagen deposition disorder in diabetic non-Injured Skin. *Front. Endocrinol.* 12, 734485. doi:10.3389/fendo.2021.734485

Zhou, Y.-J., Xu, N., Zhang, X.-C., Zhu, Y.-Y., Liu, S.-W., and Chang, Y.-N. (2021b). Chrysin improves glucose and Lipid Metabolism disorders by regulating the AMPK/PI3K/AKT signaling pathway in insulin-Resistant HepG2 cells and HFD/STZ-Induced C57BL/6J mice. *J. Agric. Food Chem.* 69, 5618–5627. doi:10.1021/acs.jafc.1c01109

frontiers | Frontiers in Pharmacology

TYPE Review
PUBLISHED 06 February 2024
DOI 10.3389/fphar.2024.1349069



OPEN ACCESS

EDITED BY
Maria Consiglia Trotta,
University of Campania Luigi Vanvitelli, Italy

REVIEWED BY
Aikaterini Andreadi,
University of Rome Tor Vergata, Italy
Maria Antonietta Riemma,
University of Campania Luigi Vanvitelli, Italy

*CORRESPONDENCE
Zhong-Xiuzi Gao,
gaozhongxiuzi@zzu.edu.cn
Peng Wu,
wupengcg@zzu.edu.cn
Zhang-Suo Liu,
zhangsuoliu@zzu.edu.cn

†These authors have contributed equally to this work

RECEIVED 06 December 2023
ACCEPTED 26 January 2024
PUBLISHED 06 February 2024

CITATION
Fu W-J, Huo J-L, Mao Z-H, Pan S-K, Liu D-W, Liu Z-S, Wu P and Gao Z-X (2024), Emerging role of antidiabetic drugs in cardiorenal protection.
*Front. Pharmacol.* 15:1349069.
doi: 10.3389/fphar.2024.1349069



# Emerging role of antidiabetic drugs in cardiorenal protection

Wen-Jia Fu[1,2,3,4†], Jin-Ling Huo[1,2,3,4†], Zi-Hui Mao[1,2,3,4], Shao-Kang Pan[1,2,3,4], Dong-Wei Liu[1,2,3,4], Zhang-Suo Liu[1,2,3,4*], Peng Wu[1,2,3,4*] and Zhong-Xiuzi Gao[1,2,3,4*]

[1]Traditional Chinese Medicine Integrated Department of Nephrology, The First Affiliated Hospital of Zhengzhou University, Zhengzhou, China, [2]Institute of Nephrology, Zhengzhou University, Zhengzhou, China, [3]Henan Province Research Center for Kidney Disease, Zhengzhou, China, [4]Key Laboratory of Precision Diagnosis and Treatment for Chronic Kidney Disease in Henan Province, Zhengzhou, China

The global prevalence of diabetes mellitus (DM) has led to widespread multi-system damage, especially in cardiovascular and renal functions, heightening morbidity and mortality. Emerging antidiabetic drugs sodium-glucose cotransporter 2 inhibitors (SGLT2i), glucagon-like peptide-1 receptor agonists (GLP-1RAs), and dipeptidyl peptidase-4 inhibitors (DPP-4i) have demonstrated efficacy in preserving cardiac and renal function, both in type 2 diabetic and non-diabetic individuals. To understand the exact impact of these drugs on cardiorenal protection and underlying mechanisms, we conducted a comprehensive review of recent large-scale clinical trials and basic research focusing on SGLT2i, GLP-1RAs, and DPP-4i. Accumulating evidence highlights the diverse mechanisms including glucose-dependent and independent pathways, and revealing their potential cardiorenal protection in diabetic and non-diabetic cardiorenal disease. This review provides critical insights into the cardiorenal protective effects of SGLT2i, GLP-1RAs, and DPP-4i and underscores the importance of these medications in mitigating the progression of cardiovascular and renal complications, and their broader clinical implications beyond glycemic management.

KEYWORDS

**diabetes mellitus, cardiorenal protection, SGLT2 inhibitors, GLP-1 receptor agonists, DPP-4 inhibitors**

## 1 Introduction

Diabetes mellitus (DM) is the most common metabolic disorder worldwide. It is reported that the prevalence of diabetes will increase to 12.2% (789.2 million) by 2045 (Sun et al., 2022). Type 2 diabetes mellitus (T2DM) is particularly prone to a range of complications, including macrovascular disease (cardiovascular and cerebrovascular disease), which is mainly characterized by atherosclerosis of large blood vessels, as well as microvascular disease (diabetic retinopathy and diabetic kidney disease), which often manifests as microvascular endothelial dysfunction and microthrombosis (Li et al., 2023; Mauricio et al., 2023). The driving factors for cardiovascular complications in diabetic patients including glucotoxicity, lipotoxicity, and hypertension (Kenny and Abel, 2019). Meanwhile, diabetic kidney disease (DKD) is the most common cause of death among microvascular complications of diabetes and is closely associated with cardiovascular outcomes (Blazek and Bakris, 2023). Currently, there has been a paradigm shift in the management of diabetes and its complications, with a focus on not only controlling blood glucose levels but also addressing the associated cardiovascular and renal risks.

In recent years, new classes of anti-diabetic medications such as sodium-glucose cotransporter 2 inhibitors (SGLT2i), glucagon-like peptide-1 receptor agonists (GLP-1RAs), and dipeptidyl peptidase-4 inhibitors (DPP-4i), have shown efficacy in reducing cardiovascular events, slowing the progression of DKD, and improving overall cardiovascular and renal health in diabetic patients (Yin et al., 2022; Guo et al., 2023; Klen and Dolžan, 2023; Panico et al., 2023). More importantly, these medications exhibit cardiorenal protective effects beyond glycemic control and have the potential to ameliorate non-diabetic cardiovascular and renal diseases.

Research have shown that these three classes of drugs can reduce oxidative stress and inflammation through various mechanisms, including reducing cell damage caused by advanced glycation end products, improving mitochondrial function, and inhibiting the production of reactive oxygen species. This suggests that these medications may have therapeutic potential beyond lowering glucose levels (Andreadi et al., 2023; Balogh et al., 2023). Understanding the mechanisms of these drugs is crucial for developing targeted therapies and improving the quality of life for millions of individuals affected by diabetes-related complications.

# 2 Emerging antidiabetic drugs

## 2.1 SGLT2i

Sodium-glucose cotransporter 2 (SGLT2) is located in the proximal tubules of the kidney and is responsible for reabsorbing 80%–90% of urine glucose. Studies have shown that SGLT2 expression is upregulated in the tubular tissues of T2DM and type 1 diabetes mellitus (T1DM) patients (Rahmoune et al., 2005). SGLT2i reduce glucose reabsorption by inhibiting this protein. Interestingly, this effect is independent of insulin secretion and β-cell function, largely reducing the burden on β-cells and the risk of hypoglycemia (Abdul-Ghani et al., 2013). The reduced glucose reabsorption also results in less fluid retention and better control of overweight and hypertension, which often accompany T2DM. Over the past decade, SGLT2i have become a hot topic in scientific and clinical research and a breakthrough in the field of new hypoglycemic agents because of their unique therapeutic effect on diabetes. Representative drugs include empagliflozin, canagliflozin, dapagliflozin, sotagliflozin, ertugliflozin, etc.

## 2.2 GLP-1RAs

Glucagon-like peptide-1 (GLP-1) is an incretin hormone that is secreted in large amounts by L cells located in the intestinal crypt when the intestine is stimulated by nutrients (Müller et al., 2019). The action of GLP-1 depends on the location of its receptors. GLP-1 receptors belong to the G protein-coupled receptors family and are widely distributed in various tissues of the body. In pancreatic α cells, GLP-1 can reduce the secretion of glucagon, while in β cells, it can increase the secretion of insulin, improve the body's insulin sensitivity, and even promote the proliferation of β cells (Graaf et al., 2016). What's more, GLP-1, which is located in the brain, suppresses appetite and reduces food intake, leading to weight loss, which is as important as glycemic control in patients with T2DM (Baggio and Drucker, 2014). GLP-1RAs are a new class of antidiabetic drugs that were first approved for the treatment of diabetes in 2005. The representative drugs are exenatide, dulaglutide, liraglutide, and semaglutide.

## 2.3 DPP-4i

Dipeptidyl peptidase-4 (DPP-4) is an enzyme that can rapidly cleave GLP-1, which is a hormone with a very short half-life (Tschöp et al., 2023). DPP-4i can effectively prolong the half-life of GLP-1, increase insulin in the body, and reduce blood glucose over a long period (Capuano et al., 2013). The representative drugs are sitagliptin, linagliptin, and saxagliptin.

# 3 Cardiorenal protection of SGLT2i, GLP-1RAs, and DPP-4i

The American Diabetes Association (ADA) recommends that SGLT2i and GLP-1RAs be used in combination with metformin as first-line initial therapy in patients at high risk of heart failure (HF), atherosclerotic cardiovascular disease (ASCVD), and chronic kidney disease (CKD). In patients with T2DM, GLP-1RAs are even more effective than insulin in some cases. For patients with established ASCVD, SGLT2i and GLP-1RAs can be used as additional agents alone, independent of metformin (Committee ADAPP, 2022b). Compared with the former two agents, DPP-4i are slightly inferior, and studies on cardiac and renal outcomes are limited. DPP-4i can be considered in patients with GLP-1RAs intolerance. Furthermore, the ADA also states that SGLT2i should be administered as early as possible in patients with stage CKD2 or worse, regardless of blood glucose. GLP-1RAs are principally used to delay cardiovascular disease, which may also delay CKD progression (Committee ADAPP, 2022a).

Similarly, the 2022 Kidney Disease: Improving Global Outcomes (KDIGO) guidelines also recommend SGLT2i therapy in patients with T2DM and CKD. Long-acting GLP-1RAs are recommended when ideal glycemic targets are not achieved with the combination of metformin and SGLT2i. Notably, when GLP-1RAs combined with insulin or sulfonylureas, reduced dose of these drugs is recommended to avoid hypoglycemia. Some DPP-4i, such as saxagliptin and sitagliptin, are accessible to patients with an estimated glomerular filtration rate (eGFR) of less than 30 mL/min/1.73 $m^2$ or who are receiving dialysis, and offer a viable alternative for individuals who are not utilizing GLP-1RAs (de Boer et al., 2022).

In general, SGLT2i and GLP-1RAs have significant beneficial effects on renal and cardiac outcomes, while the cardiorenal protective effect of DPP-4i needs to be further explored and clarified. We reviewed the real-world clinical data and the literature on potential mechanisms to gain insight into the pleiotropic effects of emerging antidiabetic agents.

TABLE 1 Summary of CV outcome-related trials using SGLT2i, GLP-1RAs, DPP-4i.

| Trial | Drug | Study design | Patient characteristics | Treatment dose (median duration) | Primary CV outcome | HR (95%CI), *p*-value |
|---|---|---|---|---|---|---|
| DAPA-HF (McMurray et al., 2019) | Dapagliflozin | randomized, double-blind, placebo-controlled study | Aged>18, NYHA class II, III, or IV symptoms, EF of 40% or less (with or without T2D) (N = 4744) | 10 mg/d (18 months) | a composite of worsening HF or death from CV causes | 0.74 (0.65–0.85) $p < 0.001$ |
| DELIVER (Solomon et al., 2022) | Dapagliflozin | phase 3, double-blind, randomized, controlled trial | Aged>40, HF and a LVEF of more than 40% (with or without T2D) (N = 6263) | 10 mg/d (2.3 years) | worsening HF or CV death | 0.82 (0.73–0.92) $p < 0.001$ |
| DECLARE-TIMI 58 (Wiviott et al., 2019) | Dapagliflozin | phase 3, double-blind, randomized, controlled trial | Aged>40, T2D, eGFR ≥60 mL/min also had multiple risk factors for ASCVD or had established ASCVD (N = 17160) | 10 mg/d (4.2 years) | MACE (defined as CV death, myocardial infarction, or ischemic stroke). Efficacy outcomes were MACE and a composite of CV death or hospitalization for HF | 95%CI < 1.3; $p < 0.001$ for noninferiority, 0.83 (0.73–0.95) $p = 0.005$ for efficacy |
| EMPEROR-Preserved (Anker et al., 2021) | Empagliflozin | randomized, double-blind, placebo-controlled, event-driven trial | Aged>18, II–IV HF and an EF ≥ 40%, NT-proBNP ≥300 pg/mL (with or without T2D) (N = 5988) | 10 mg/d (26.2 months) | a composite of CV death or hospitalization for HF | 0.79 (0.69–0.90), $p < 0.001$ |
| MK-8835-004 (Cannon et al., 2020) | Ertugliflozin | double-blind, randomized, placebo-controlled, noninferiority trial | Aged>40, T2D and established ASCVD (N = 8246) | 5 or 15 mg/d (3.1 years) | MACE (a composite of death from CV causes, nonfatal myocardial infarction, or nonfatal stroke) | 0.97 (0.85–1.11), $p < 0.001$ for noninferiority |
| SOLOIST-WHF (Bhatt et al., 2021) | Sotagliflozin | phase 3, double-blind, randomized, placebo-controlled trial | aged 18 to 85, T2D and had been hospitalized because of the presence of signs and symptoms of HF and received treatment with intravenous diuretic therapy (N = 1222) | 200 mg/d (9.2 months) | the total number of deaths from cardiovascular causes and hospitalizations and urgent visits for HF (first and subsequent events) | 0.67 (0.52–0.85), $p < 0.001$ |
| EMPULSE (Voors et al., 2022) | Empagliflozin | randomized, double-blind, placebo-controlled study | with a primary diagnosis of acute denovo or decompensated CHF regardless of LVEF (N = 530) | 10 mg/d (3–90 days) | clinical benefit, defined as a hierarchical composite of death from any cause, number of HF events and time to first HF event, or a 5 point or greater difference in change from baseline in the KCCQ-TSS at 90 days | stratified win ratio, 1.36 (1.09–1.68), $p = 0.0054$ |
| ELIXA (Pfeffer et al., 2015) | Lixisenatide | randomized, double-blind, placebo-controlled study | had T2D and had an acute coronary event within 180 days before screening (N = 6068) | 10μg–20 μg/d (s.c) (25 months) | death from CV causes, nonfatal myocardial infarction, nonfatal stroke, or hospitalization for unstable angina | 1.02 (0.89–1.17), $p < 0.001$ for noninferiority, $p = 0.81$ for surperiority |
| LEADER (Marso et al., 2016a) | Liraglutide | randomized, double-blind, placebo-controlled study | T2D, aged≥50 (at least one CV condition) or aged≥60 (at least one CV risk factor) (N = 9340) | 1.8 mg/d (s.c.) (3.5 years) | the first occurrence of death from CV causes, nonfatal (including silent) myocardial infarction, or nonfatal stroke | 0.87 (0.78–0.97), $p < 0.001$ for noninferiority; $p = 0.01$ for superiority |
| SUSTAIN-6 (Marso et al., 2016b) | Semaglutide | randomized, double-blind, placebo-controlled study | T2D, aged≥50 (established CVD, CHF, or CKD of stage 3 or higher) or aged≥60 (at least one CV risk factor (N = 3297) | 0.5/1.0 mg/(s.c.) (2.1 years) | the first occurrence of death from CV causes, nonfatal myocardial infarction (including silent), or nonfatal stroke | 0.74 (0.58–0.95), $p < 0.001$ for noninferiority; $p = 0.02$ for superiority |

(Continued on following page)

TABLE 1 (*Continued*) Summary of CV outcome-related trials using SGLT2i, GLP-1RAs, DPP-4i.

| Trial | Drug | Study design | Patient characteristics | Treatment dose (median duration) | Primary CV outcome | HR (95%CI), *p*-value |
|---|---|---|---|---|---|---|
| PIONEER6 (Husain et al., 2019) | Semaglutide | randomized, double-blind, placebo-controlled study | T2D, aged≥50 (established CVD, CHF, or CKD of stage 3 or higher) or aged≥60 (at least one CV risk factor) (N = 3183) | 14 mg/d (oral) (15.9 months) | the first occurrence of MACE, a composite of death from CV causes, nonfatal myocardial infarction, or nonfatal stroke | 0.79 (0.57–1.11), $p <$ 0.001 for noninferiority |
| EXSCEL (Holman et al., 2017) | Exenatide | randomized, double-blind, placebo-controlled study | T2D, had previous CV events (70%), would not have had previous CV events (30%) (N = 14752) | 2 mg once weekly (s.c.) (3.2 years) | first occurrence of any composite outcome of death from CV causes, nonfatal myocardial infarction, or nonfatal stroke | 0.91 (0.83–1.00), $p <$ 0.001 for noninferiority, $p =$ 0.06 for superiority |
| Harmony Outcomes (Hernandez et al., 2018) | Albiglutide | randomized, double-blind, placebo-controlled study | T2D, ≥40, established disease of the coronary, cerebrovascular, or peripheral arterial circulation (N = 9463) | 30–50 mg once weekly (s.c.) (1.5 years) | the first occurrence of cardiovascular death, myocardial infarction, or stroke | 0·78 (0·68–0·90), $p <$ 0·0001 for noninferiority, $p =$ 0·0006 for superiority |
| REWIND (Gerstein et al., 2019) | Dulaglutide | randomized, double-blind, placebo-controlled study | T2D, aged≥50 had to have vascular disease; aged≥55 had to have MI, or lower extremity artery stenosis exceeding 50%, LVH, eGFR <60 mL/min/1.73m$^2$, aged≥60 had to have at least two of tobacco use, dyslipidaemia (N = 9901) | 1.5 mg once weekly (s.c.) (5.4 years) | the first occurrence of any component of the composite outcome, which comprised non-fatal myocardial infarction, non-fatal stroke, and death from cardiovascular causes or unknown causes | 0.88 (0·79 to 0·99), $p =$ 0·026 |
| EXAMINE (White et al., 2013) | Alogliptin | randomized, double-blind, placebo-controlled study | T2D and had had an acute coronary syndrome within 15–90 days before randomization (N = 5380) | 6.25–25 mg/d (533 days)[a] | a composite of death from CV causes, nonfatal myocardial infarction, or nonfatal stroke | 0.96 (≤1.16), $p <$ 0.001 for noninferiority $p =$ 0.32 for superiority |
| SAVOR-TIMI53 (Scirica et al., 2013) | Saxagliptin | phase 4, double-blind, randomized, placebo-controlled trial | T2D, ≥55 (men); ≥60 (women)and either a history of established CVD or multiple risk factors for vascular disease (N = 16492) | 5 mg/d (2.1 years) | a composite of CV death, nonfatal myocardial infarction, or nonfatal ischemic stroke | 1.00 (0.89–1.12), $p =$ 0.99 for superiority, $p <$ 0.001 for noninferiority |
| TECOS (Green et al., 2015) | Sitagliptin | randomized, double-blind, placebo-controlled study | T2D with established CVD and were aged≥50 when treated with stable oral anti-hyperglycemic agents or insulin (N = 14671) | 50–100 mg/d (3.3 years)[#] | a composite of CV death, nonfatal myocardial infarction, nonfatal stroke, or hospitalization for unstable angina | 0.98 (0.88–1.09), $p <$ 0.001 for noninferiority, $p =$ 0.65 for superiority |
| CARMELINA (Rosenstock et al., 2019) | Linagliptin | randomized, double-blind, placebo-controlled study | T2D, HbA1c values of 6.5%–10.0% inclusive, and high cardiovascular and renal risk (N = 6979) | 5 mg/d (oral) (2.2 years) | the time to first occurrence of CV death, nonfatal myocardial infarction, or nonfatal stroke | 1.02 (0.89–1.17), $p <$ .001 for noninferiority, $p =$ 0.74 for superiority |

EF: ejection fraction, LVEF: left ventricular ejection fraction, HbA1c: Hemoglobin A1c, CHF: chronic heart failure, LVH: left ventricular hypertrophy, MI: myocardial ischaemia, KCCQ-TSS: kansas city cardiomyopathy questionnaire total symptom score, ASCVD: atherosclerotic cardiovascular disease, CVD: cardiovascular disease, MACE: major adverse cardiovascular events, HF: heart failure, CV: cardiovascular, NYHA: new york heart association, T2D: Type 2 Diabetes.

[a]25 mg/d for GFR≥60 mL/min/1.73 m$^2$, 125 mg for GFR, of 30–60 mL/min/1.73 m$^2$, 625 mg for GFR ≤30 mL/min/1,73 m$^2$; # 50 mg/d for eGFR, was ≥30 and <50 mL/min/1.73 m$^2$.

## 3.1 Cardiovascular protection

### 3.1.1 SGLT2i

#### 3.1.1.1 Clinical trial

SGLT2i have demonstrated superiority over placebo in most cardiovascular outcome trials. In 2019, the DAPA-HF trial, which recruited 4744 patients with HF and reduced ejection fraction, indicated that once-daily dapagliflozin (10 mg) lowered the risk of composite cardiovascular outcomes when compared to placebo (HR, 0.74 [95% CI, 0.65 to 0.85]; $p < 0.001$) (Table 1) (McMurray et al., 2019). Furthermore, in a 2022 trial, dapagliflozin exhibited significant cardioprotective effects (DELIVER) on patients with HF with mild reduced ejection fraction or preserved left ventricular ejection fraction (>40%) (HR, 0.82 [95% CI, 0.73 to 0.92]; $p < 0.001$) (Solomon et al., 2022). These results are consistent with those of the empagliflozin and ertugliflozin outcomes trials in HF with a

preserved ejection fraction (EMPEROR-Preserved trial, MK-8835-004 trial) (Cannon et al., 2020; Anker et al., 2021). However, the protective effect of SGLT2i appeared to vary based on gender; a study from Australia indicates that older men with baseline HF benefit more from SGLT2i than women (subdistribution HR, 0.78 [95% CI, 0.66 to 0.93] for men; subdistribution HR, 0.99 [95% CI, 0.77 to 1.28] for women). On the contrary, SGLT2i were observed to improve the outcomes of women with baseline ASCVD (subdistribution HR, 0.98 [95% CI, 0.74 to 0.73] for men; subdistribution HR, 0.36 [95% CI, 0.18 to 0.71] for women) (Sharma et al., 2023). In another study, the effect of canagliflozin on cardiovascular events did not differ by age or sex (HR, 0.71 [95% CI, 0.54 to 0.95] for women; HR, 0.69 [95% CI, 0.56 to 0.84] for men; $p$ = 0.8 for interaction) (Yi et al., 2023). The disparate findings of these two reports are intriguing. The absence of beneficial effects of SGLT2i in women with baseline HF may, in part, be attributed to the limited number of women in this specific subgroup. Notably, given the age-related increase in cardiovascular disease (CVD) risk in both genders, particularly among post-menopausal women (Zhao et al., 2018), further investigations focusing on sex differences and involving a substantial number of patients are warranted to ascertain the potential sex-specific benefits of SGLT2i and elucidate the mechanisms involved. In addition, SGLT2i also have a significant advantage in acute HF, suggesting a lower risk of hospitalization (Park et al., 2023). Sotagliflozin has been shown to significantly reduce cardiovascular death-related events in T2DM patients with recent worsening HF (HR, 0.67 [95% CI, 0.52 to 0.85]; $p < 0.001$) (SOLOIST-WHF trial) (Bhatt et al., 2021). Empagliflozin was also associated with a greater reduction in the rate of worsening HF events (HR, 1.36 [95% CI, 1.09 to 1.68]; $p = 0.0054$) (EMPULSE trial) (Voors et al., 2022).

#### 3.1.1.2 Basic research

SGLT2i exhibit superior efficacy in improving cardiovascular diseases, regardless of the presence of diabetes. *In vivo* experiments revealed that dapagliflozin reduced interleukin (IL)-1β expression and can downregulate the activity of [$Na^+$] and [$Ca^{2+}$]-related ion channels to alleviate mitochondrial reactive oxygen species, thereby improving angiotensin II (Ang II)-induced diabetic cardiomyopathy in *db/db* mice (Table 3) (Arow et al., 2020). Consistently, an *in vivo* study focusing on diabetic cardiomyopathy in T1DM rats revealed that dapagliflozin markedly reduced oxidative stress (Rosa et al., 2022). Notably, SGLT2i can restore and maintain sinus rhythm after ablation of atrial fibrillation in T2DM patients (Abu-Qaoud et al., 2023). Interestingly, empagliflozin was found to block the binding of CpG islands in the promoter regions of nuclear factor kappa-B (NF-κB) and superoxide dismutase 2 (SOD2) to ten-eleven translocation (TET2) in cardiomyocytes under high glucose conditions, preventing gene demethylation and alleviating myocardial injury (Scisciola et al., 2023).

In addition to their protective effect against diabetes-induced cardiomyopathy, SGLT2i also have a beneficial effect on other cardiovascular diseases, including ASCVD, which is primarily caused by hypertension-induced inflammation. SGLT2 receptor expression is present in macrophages, which are major players in the inflammatory response. Adenosine 5′-monophosphate-activated protein kinase (AMPK) is a key energy regulator that inhibits the pro-inflammatory effects of macrophages (Packer, 2020a; Jansen et al., 2020). In an atherosclerosis model characterized by a high-fat diet, empagliflozin inhibited NF-κB expression in plaque and reduced the viability of macrophages in *Apoe*$^{-/-}$ mice. Most importantly, it was able to restore p-AMPK expression in macrophages (Fu et al., 2022). Heme oxygenase-1 (HO-1) can protect the cardiovascular system by increasing the bioavailability of NO in endothelial cells. Canagliflozin can increase the expression of HO-1 in endothelial cells and attenuate the adhesion of monocytes to endothelial cells (Peyton et al., 2022). Vascular calcification is a common pathological process in ASCVD. Chen *et al.* demonstrated for the first time that canagliflozin could reduce vascular smooth muscle cells (VSMCs) calcification by down-regulating the expression of NOD-like receptor thermal protein domain associated protein 3 (NLRP3) (Chen et al., 2023). There are many ion channels in cardiomyocytes, such as $Na^+/H^+$ exchanger 1 (NHE1) and $Na^+/Ca^{2+}$ exchanger (NCX). Pathological conditions that lead to excessive activation or inhibition of ion channels significantly impact the systolic and diastolic movements of the heart. Various hormones (Ang II, aldosterone) released during HF or myocardial ischemia (MI) can activate NHE1, inhibit NCX, and lead to intracellular calcium overload, which in turn activates NHE1 and exacerbates calcium overload (Figure 1A) (Kim et al., 2017). Studies have shown that dapagliflozin, empagliflozin, and canagliflozin can inhibit NHE1 to improve endothelial permeability induced by mechanical stretch (Li X. et al., 2021). These studies confirmed that SGLT2i can protect both static and dynamic endothelial cell function (Juni et al., 2021).

Notably, dapagliflozin also inhibits the mitogen-acticated protein kinase/activator protein-1 (MAPK/AP-1) pathway in an NHE1-dependent way to alleviate obesity-induced myocardial inflammation (Lin et al., 2022). Similarly, empagliflozin can improve myocardial injury in obese mice by regulating the AMPK/mammalian target of rapamycin (mTOR) pathway to maintain redox balance (Sun et al., 2020). In addition, empagliflozin also inhibited the overstimulated autophagy in cardiomyocytes by inhibiting the AMPK/glycogen synthase kinase 3β (GSK3β) pathway and NHE1 (Chung et al., 2023; Madonna et al., 2023). These findings highlight the multiple mechanisms by which SGLT2i contribute to the reduction of obesity-related myocardial complications.

SGLT2i also offer promising insights into preventing cardiac toxicity associated with antineoplastic agents. For example, dapagliflozin alleviated adriamycin-induced myocardial injury by inhibiting the phosphoinositide 3-kinase (PI3K)/protein kinase B (PKB)/nuclear factor erythroid 2-related factor 2 (Nrf2) pathway (Hsieh et al., 2022). Empagliflozin could significantly enhance the adriamycin-induced reduction of cardiomyocyte viability and inhibit the expression of NLRP3 and myeloid differentiation factor 88 (MyD88) (Quagliariello et al., 2021). Furthermore, empagliflozin was found to ameliorate sunitinib- and trastuzumab-induced cardiovascular complications by regulating the AMPK/mTOR pathway and ferroptosis (Ren et al., 2021; Min et al., 2023).

In conclusion, the cardiovascular protective effects of SGLT2i in relation to diabetes have been extensively explored. Additionally, SGLT2i have also shown multiple protective mechanisms in animal models of ASCVD, and it has been applied for the treatment of HF (Heidenreich et al., 2022). However, there is still new potential for

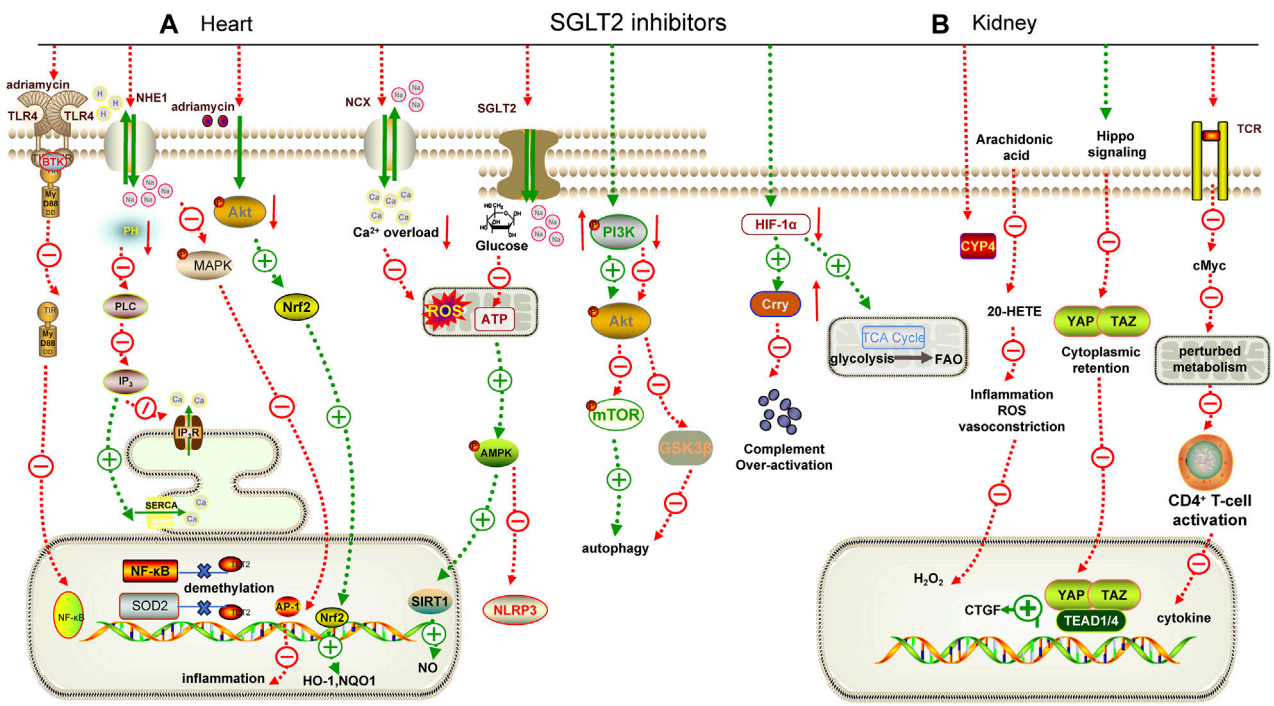


FIGURE 1
Mechanisms underlying the cardiorenal effects of SGLT2 inhibitors. **(A)** for heart; **(B)** for kidney. AMPK: adenosine monophosphate-activated protein kinase, TLR4: Toll-like receptor 4, MyD88: myeloid differentiation factor 88, NF-κB: nuclear factor-κB, PLC: phospholipase C, $IP_3$: inositol 1,4,5-triphosphate, $IP_3R$: inositol 1,4,5-triphosphate receptor, SERCA: sarcoplasmic reticulum $Ca^{2+}$-ATPase, MAPK: mitogen-acticated protein kinase, AP-1: activator protein-1, Nrf2: nuclear factor erythroid2-related factor 2, SIRT1: sirtuin 1, PI3K: phosphatidylinositol 3-kinase, mTOR: mammalian target of rapamycin, GSK3β: glycogen synthase kinase 3β, HIF-1α: hypoxia-inducible factor 1-alpha, TCR: T cell receptor, CTGF: connective tissue growth factor, YAP: yes associated protein 1, TAZ: transcriptional coactivator PDZ-binding motif, RTK: receptor tyrosine kinase, NOQ1: NADH dehydrogenase quinone 1, SOD2: superoxide dismutase 2.

clinical translation. SGLT2i have demonstrated remarkable advantages in obesity-related, antibiotic-induced, and antineoplastic drug-induced cardiotoxicity (Ren et al., 2021; Min et al., 2023). It is worth noting that although canagliflozin can exhibit anti-inflammatory effects in endothelial cells, recent reports have raised concerns about its specific impact on endothelial cells, which may elevate the risk of amputation (Peyton et al., 2022). Therefore, establishing SGLT2i as routine therapy for diseases beyond diabetes still has a way to go.

## 3.1.2 GLP-1RAs

### 3.1.2.1 Clinical trial

Although the previous ELIXA trial did not show superiority of lixisenatide in reducing the rate of major adverse cardiovascular events (MACE) (Table 1) (Pfeffer et al., 2015; Husain et al., 2019), GLP-1RAs has been gradually shown its advantage in improving cardiovascular outcomes in recent trials. Cardiovascular mortality among patients with T2DM and high cardiovascular risk was found to be lower with liraglutide than with placebo (HR, 0.87 [95% CI, 0.78 to 0.97]; $p$ = 0.01) (LEADER) (Marso et al., 2016a). The SUSTAIN-6 trial, which involved 3,297 patients with T2DM and high cardiovascular risk, found that twice-weekly semaglutide significantly reduced the incidence of MACE (HR, 0.74 [95% CI, 0.58 to 0.95]; $p$ = 0.02) (Marso et al., 2016b). In the Harmony Outcomes trial, the rate of MACE in T2DM patients with the addition of albiglutide (30–50 mg once-weekly) was lower than the placebo group (HR, 0.78 [95% CI, 0.68 to 0.90]; $p$ = 0.0006) (Hernandez et al., 2018). Lastly, the REWIND trial revealed a reduction in MACE with once-weekly dulaglutide in T2DM patients (HR, 0.88 [95% CI, 0.79 to 0.99]; $p$ = 0.026) (Gerstein et al., 2019).

### 3.1.2.2 Basic research

Extensive basic studies overwhelmingly support the observed beneficial effects of GLP-1RAs in clinical trials. Diabetes is often accompanied by lipid metabolism disorders, causing mitochondrial dysfunction. Studies have shown that liraglutide can inhibit the diacylglycerol/protein kinase C (DAG/PKC) pathway by activating AMPK, and upregulate Sirtuin 1 (SIRT1) to inactivate acetyl-CoA carboxylase phosphorylation, thereby reducing lipid-overloaded cardiomyocyte injury in streptozotocin-induced diabetic rats (Figure 2A) (Table 3)(Inoue et al., 2015). Similarly, liraglutide also increased adiponectin secretion and restored peroxisome proliferator-activated receptor gamma coactivator-1α (PGC-1α) expression by upregulating AMPK, which ameliorated IL-1β-induced mitochondrial damage in HL-1 cells (Zhang et al., 2020). Dulaglutide reduced the expression of NLRP3, IL-1β, and endoplasmic reticulum stress-related proteins induced by high glucose in human umbilical vein endothelial cells (HUVECs) via upregulating SIRT1 (Luo et al., 2019). Moreover, liraglutide enhanced the angiogenic potential of CD34 hematopoietic stem cells under high glucose conditions by activating the protective

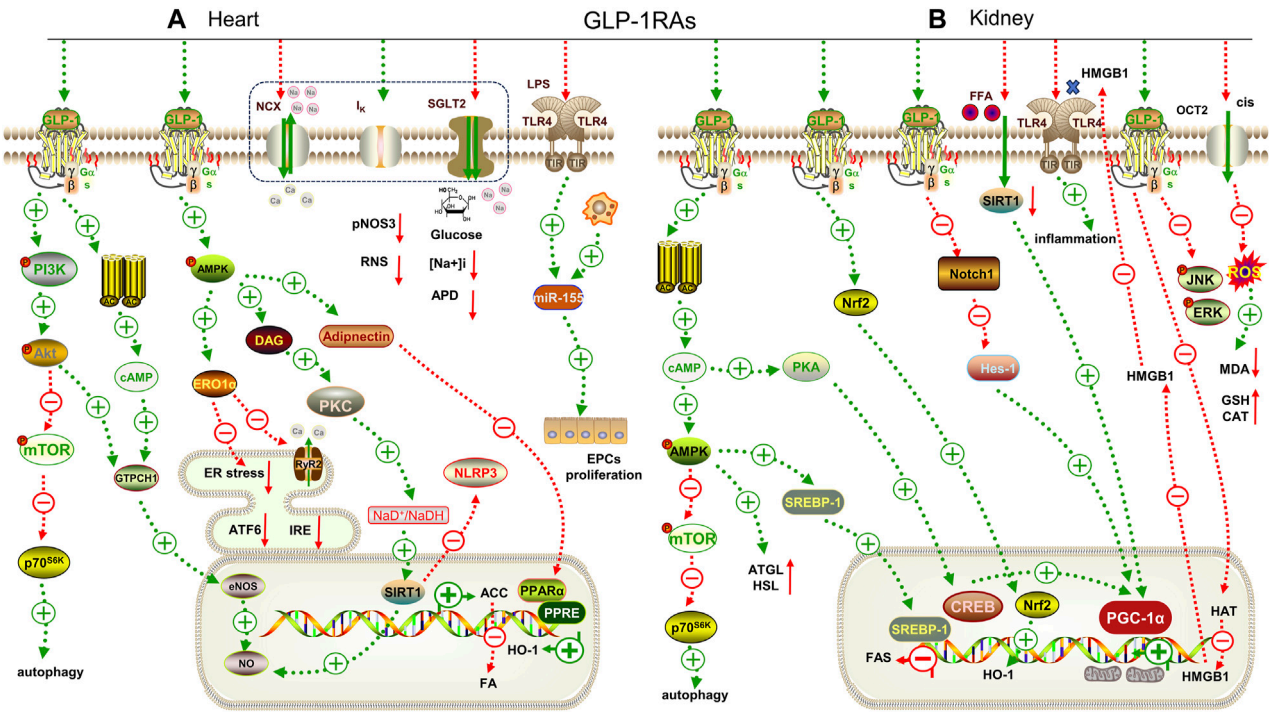


FIGURE 2
Mechanisms underlying the cardiorenal effects of GLP-1RAs. **(A)** for heart; **(B)** for kidney. GTPCH1: GTPcyclohydrolase I, eNOS: endothelial nitric oxide synthase, ERO1α: endoplasmic oxidoreductin 1 like protein, ATF6: activating transcription factor 6, IRE: inositol-requiring enzyme, RyR2: ryanodine receptor 2, DAG: diacylglycerol, PPARα: peroxisome proliferator-activated receptor α, ATGL: adipose triglyceride lipase, HSL: hormone-sensitive lipase, SREBP-1: sterol regulatory element binding protein-1, FAS: fatty acid synthase, CREB: cAMP-response element binding protein, PGC-1α: peroxisome proliferator-activated receptor gamma coactivator-1alpha, Notch1: Notch homolog 1, Hes-1: hairy and enhancer of split-1, MDA: malondialdehyde. GSH: glutathione. pNOS3: phospho-endothelial nitric oxide, RNS: nitrogen species, APD: action potential duration, HMGB1: high mobility group protein 1, CAT: catalase, HAT: histone acrtyltransferases, LPS: lipopolysaccharide, ACC: acetyl CoA carboxylase.

PI3K/PKB pathway and stimulating mitochondrial respiration (Sforza et al., 2022). Exenatide protects against high glucose-induced myocardial injury by inhibiting the NF-κB pathway and reducing the expression of tumor necrosis factor α (TNF-α) and monocyte chemotactic protein-1 (MCP-1) (Fu et al., 2020).

GLP-1RAs exhibit similar potential to SGLT2i in improving ASCVD. Liraglutide has been shown to attenuate plaque formation in *Apoe*$^{-/-}$ mice by inducing cell cycle arrest in VSMCs in an AMPK-dependent or AMPK-independent manner (Jojima et al., 2017; Koshibu et al., 2019). Moreover, in the same mouse model, liraglutide was able to induce plaque regression by modulating bone marrow-derived macrophages to convert to anti-inflammatory phenotypes in the established plaque (Bruen et al., 2019).

GLP-1RAs have also demonstrated their potential in improving various other types of heart disease, including obesity-related, senile, and inflammatory heart disease, as well as improving the function of donor hearts after isolation. For example, liraglutide alleviates vascular inflammation in obesity by upregulating pAMPK expression and promoting Nrf2 nuclear translocation (Liu et al., 2023). It has also been shown to restore autophagy by inhibiting the mTOR/phosphoprotein 70 ribosomal protein S6 kinase (p70S6K) pathway caused by abdominal aortic coarctation (Zheng et al., 2020), regulate iNCX, delayed after potassium channel ($I_k$) and ryanodine receptor 2 (RyR2) channels in the myocardium, and restore mitochondrial membrane depolarization to protect the aged heart (Durak and Turan, 2023). Recent studies have also shown that acute administration of exenatide can increase NO to maintain good diastolic function after reperfusion in isolated hearts (Kadowaki et al., 2023). Furthermore, semaglutide can reduce lipopolysaccharides (LPS)-induced miR-155 secretion from macrophage exosomes to protect endothelial progenitor cell function (Pan et al., 2023). These findings highlight the multifaceted beneficial effects of GLP-1RAs on the cardiovascular system.

Currently, the superiority of GLP-1RAs in cardiovascular protection is primarily focused on diabetes-related conditions, as demonstrated above. However, recent findings have revealed that apart from their hypoglycemic effects, GLP-1RAs also have therapeutic efficacy in weight loss (Campbell et al., 2023). Basic research show their potential anti-inflammatory effects in obesity-related heart disease and advantages in ASCVD and aged animal models (Withaar et al., 2023). Despite the lack of clinical evidence, these findings suggest that GLP-1RAs may be used as a second or third-line therapy for non-diabetes-related cardiovascular diseases in the future.

## 3.1.3 DPP-4i

### 3.1.3.1 Clinical trial

Most of the cardiovascular outcome trials of DPP-4i have demonstrated cardiovascular safety rather than superiority. The EXAMINE trial, which included 5380 T2DM patients with a

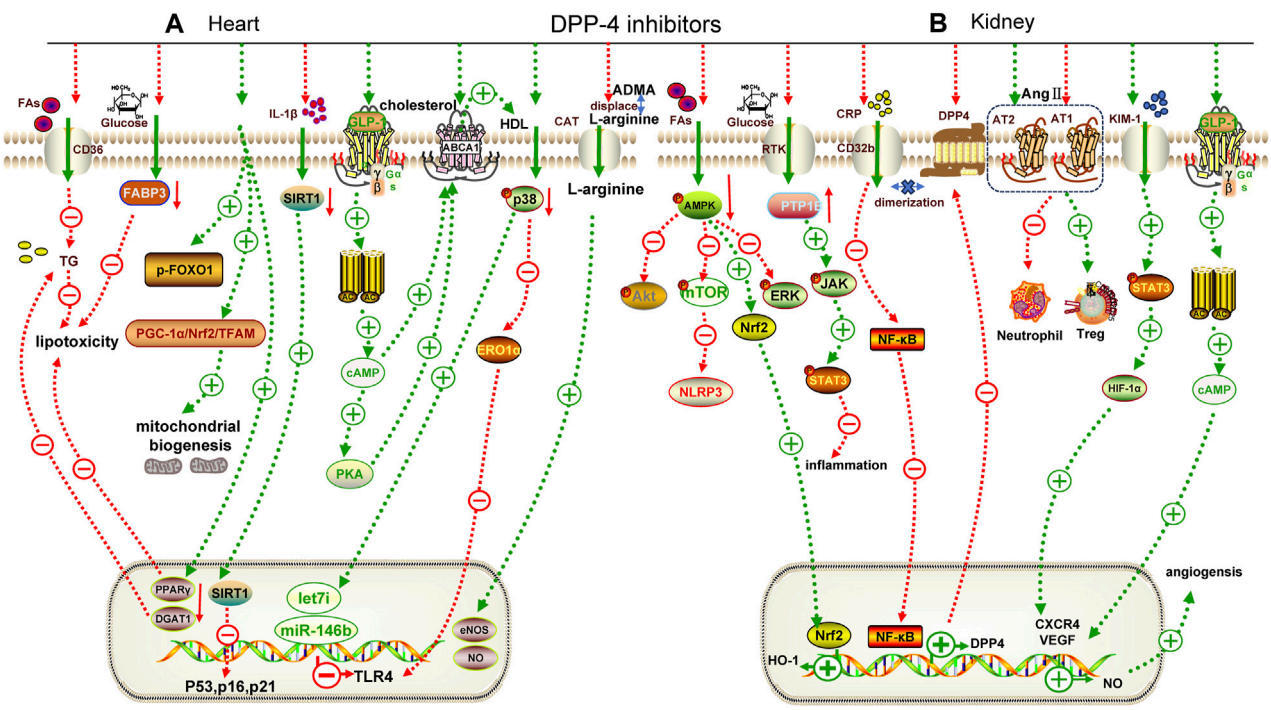


FIGURE 3
Mechanisms underlying the cardiorenal effects of DPP-4 inhibitors. **(A)** for heart; **(B)** for kidney. TG: triglyceride, FABP3: fatty acid binding protein 3, p-FOXO1: phospho-Forkhead box protein O1, ABCA1: adenosine triphosphate transporter A1, PTP1B: protein tyrosine phosphatase, CRP: C-reactive protein, KIM-1: kidney injury molecule 1, CXCR4: chemokine receptor 4, AT1: angiotensin receptor 1, AT2: angiotensin receptor 2, ERK: extracellular regulated protein kinase, DGAT1: diacylglycerol acyltransferase 1, CAT: cationic amino acid transporters, HDL: high density lipoprotein, TFAM: mitochondrial transcription factor A, eNOS: endothelial nitric oxide synthase, DGAT1: diacylglycerol o-acyltransferase 1, PPARγ: peroxisome proliferator activated receptor γ, JAK: janus tyrosine kinase, STAT3: signal transducer and activator of transcription 3.

recent acute coronary event, showed that the rate of MACE with the addition of alogliptin was not superior to that of placebo (HR, 0.96 [upper boundary of the one-sided repeated CI, 1.16]; $p < 0.001$ for non-inferiority) (Table 1) (White et al., 2013). In the SAVOR-TIMI 53 trial, saxagliptin did not increase the rate of MACE in the elderly and very elderly patients (HR, 1.00 [95% CI, 0.89 to 1.12]; $p = 0.99$), but saxagliptin was surprisingly associated with an increased risk for HF hospitalization, thus its use requires detailed evaluation (HR, 1.27 [95% CI, 1.07 to 1.51]; $p = 0.007$) (Scirica et al., 2013; Leiter et al., 2015). The TECOS trial showed that sitagliptin did not increase the rate of MACE and hospitalizations for HF in patients with T2DM, even in high-risk patients (HR, 0.98 [95% CI, 0.88 to 1.09]; $p = 0.65$) (Green et al., 2015; McGuire et al., 2016). Similarly, sitagliptin was not superior to placebo in terms of efficacy in T2DM patients with ASCVD (Nauck et al., 2019). The CARMELINA trial indicated that linagliptin added to usual treatment resulted in a non-inferior risk of MACE in T2DM patients with high cardiovascular risk (HR, 1.02 [95% CI, 0.89 to 1.17]; $p = 0.74$) (Rosenstock et al., 2019). However, a trial from Thailand showed that linagliptin was superior in reducing 10-year cardiovascular risk score in patients with a baseline risk greater than 20%, with enhanced outcomes in older patients (Poonchuay et al., 2022).

### 3.1.3.2 Basic research

While clinical trials have not demonstrated significant advantages of DPP-4i, basic research has revealed their cardioprotective effect. The normal diastolic and systolic functions of the heart depend on the energy provided by a large number of mitochondria and fatty acid oxidation in cardiomyocytes. Evogliptin (an oral hypoglycemic drug approved for the treatment of T2DM in South Korea in 2015) can restore the expression of the mitochondrial-synthesis-related pathway, PGC-1α/Nrf2/mitochondrial transcription factor A (TFAM), to promote normal mitochondrial synthesis (Gureev et al., 2019) and inhibit the expression of lipid transmembrane transporters (fatty acid binding protein 3, FABP3) (Zhang et al., 2015) and synthetic proteins (Forkhead box protein O1, FOXO1; peroxisome proliferator activated receptor γ, PPARγ; diacylglycerol o-acyltransferase 1, DGAT1) (Kyriazis et al., 2021) to block the over-activated lipid pathway in *db/db* mice (Figure 3A) (Pham et al., 2023). Further studies have shown that sitagliptin combined with insulin can improve diabetic cardiomyopathy by reducing the expression of inflammatory factors to a greater extent (Table 3) (Wadie et al., 2022).

In addition, DPP-4i have shown significant advantages in non-diabetic cardiovascular diseases, particularly ASCVD. Trelagliptin inhibits IL-1β-induced MCP-1 expression in human aortic endothelial cells by inhibiting the NF-κB pathway, preventing monocyte infiltration during atherosclerosis (Meng et al., 2020). Alogliptin has been shown to reduce IL-1β-induced inflammatory cytokine expression in VSMCs by restoring SIRT1 expression and downregulating senescence-related markers (p16, p21 and p53) to prevent premature smooth muscle cell senescence and enhance

TABLE 2 Summary of renal outcome-related trials using SGLT2i, GLP-1RAs, DPP-4i.

| Trial | Drug | Study design | Patient characteristics | Treatment dose (median duration) | Primary renal outcome | HR (95%CI), *p*-value |
|---|---|---|---|---|---|---|
| DAPA-CKD (Heerspink et al., 2020) | Dapagliflozin | randomized, double-blind, placebo-controlled study | with or without T2D who had an eGFR of 25–75 mL/min/1.73m$^2$ and a UACR of 200–5000(N = 4744) | 10 mg once daily (2.4 years) | The first occurrence of any of the following: a decline of at least 50% in the eGFR (confirmed by a second Scr measurement after ≥28 days), the onset of ESKD (defined as maintenance dialysis for ≥28 days, kidney transplantation, or an eGFR of <15 mL/min/1.73 m$^2$ confirmed by a second measurement after ≥28 days), or death from renal or cardiovascular causes | 0.61 (0.51–0.72), $p$ < 0.001 |
| DIAMOND (Cherney et al., 2020) | Dapagliflozin | randomized, double-blind, placebo-controlled study | aged 18–75 years, with CKD, without T2D, with a 24 h urinary protein excretion >500–3500 mg, eGFR≥25 mL/min/1.73m$^2$, and who were on stable RAS blockade (N = 58) | 10 mg/d (treat 6 weeks with 6-week washout in between) | The percentage change from baseline in 24 h proteinuria during dapagliflozin treatment relative to placebo | dapagliflozin *versus* placebo was −6·6 mL/min/1·73 m$^2$ (−9·0 to −4·2; $p$ < 0·0001) |
| CREDENCE (Perkovic et al., 2019) | Canagliflozin | randomized, double-blind, placebo-controlled study | aged ≥30, had T2DM, also required to have CKD (defined as an eGFR of 30 to <90 mL/min/1.73m$^2$), UACR>300 to 5000(N = 4401) | 100 mg once daily (2.62 years) | A composite of ESKD, doubling of the Scr level from baseline (average of randomization and pre-randomization value) sustained for at least 30 days according to central laboratory assessment, or death from renal or cardiovascular disease | 0.70 (0.59–0.82), $p$ = 0.00001 |
| EMPA-KIDNEY (Herrington et al., 2023) | Empagliflozin | randomized, double-blind, placebo-controlled study | with or without T2DM, eGFR of at least 20 but less than 45 mL/min/1.73m$^2$, regardless of the level of albuminuria, or with an eGFR of at least 45 but less than 90 mL/min/1.73m$^2$ with UACR of at least 200 at the screening visit (N = 6609) | 10 mg once daily (2 years) | The first occurrence of ESRD or death from cardiovascular causes; the initiation of maintenance dialysis or receipt of a kidney transplant, a sustained decrease in the eGFR to less than 10 mL/min/1.73m$^2$, a sustained decrease from baseline in the eGFR of at least 40%, or death from renal causes | 0.72 (0.6–0.82), $p$ < 0.001 |
| LEADER (Mann et al., 2017) prespecified secondary analysis | Liraglutide | randomized, double-blind, placebo-controlled study | aged ≥50, T2D with at least one cardiovascular coexisting condition or an age of 60 years or more with at least one cardiovascular risk factor (N = 9340) | 1.8 mg once daily (s.c.) (3.5 years) | The composite renal outcome consisted of new-onset persistent macroalbuminuria, persistent doubling of the serum creatinine level and an eGFR of 45 or less mL/minute/1.73m$^2$, the need for continuous RRT with no reversible cause of the renal disease, or death from renal disease | 0.78 (0.67–0.92), $p$ = 0.003 |
| AMPLITUDE-O (Gerstein et al., 2021) | Efpeglenatide | randomized, double-blind, | aged ≥18, T2D, had a history of cardiovascular disease or ≥50 (men); ≥55 (women) and had | 2 mg/week for 4 weeks, then 4 mg/week for 4 weeks, and | A composite renal outcome incident macroalbuminuria | 0.68 (0.57–0.79), $p$ < 0.001 |

(Continued on following page)

TABLE 2 (*Continued*) Summary of renal outcome-related trials using SGLT2i, GLP-1RAs, DPP-4i.

| Trial | Drug | Study design | Patient characteristics | Treatment dose (median duration) | Primary renal outcome | HR (95%CI), *p*-value |
|---|---|---|---|---|---|---|
| | | placebo-controlled study | kidney disease defined as an eGFR of 25.0–59.9 mL/min/1.73m$^2$, and at least one additional cardiovascular risk factor (N = 4076) | then 6 mg/week until the end (1.81 years) | defined as a UACR>300, plus an increase in the UACR of ≥30% from baseline, a sustained decrease in the eGFR of ≥40% for ≥30 days, renal-replacement therapy for ≥90 days, or a sustained eGFR of <15 mL/min/1.73m$^2$ for ≥30 days | |
| FLOW (Rossing et al., 2023) | Semaglutide | phase 3b, randomized, double-blind, placebo-controlled study | aged ≥18 years or ≥20 years in Japan with pre-existing CKD with high albuminuria, low eGFR, T2D, HbA1c ≤ 10% (<86 mmol/mol) and on stable treatment with the maximum labelled or tolerated dose of a RAAS blocking agent (N = 3534) | 0.25 mg/week for 4 weeks, then 0.5 mg/week for 4 weeks, and then 1.0 mg/week until the end (s.c.) | Ongoing | Ongoing |
| GUARD (Yoon et al., 2017) | Gemigliptin | randomized, double-blind, placebo-controlled study | aged 19–75 years, diagnosed with T2D, and confirmed to have moderate (eGFR: 30–59 mL/min/1.73m$^2$) to severe (eGFR: 15–29 mL/min/1.73m$^2$) (N = 132) | 50 mg daily (12 weeks) | Changes in eGFR, UACR at Week 12 | gemigliptin group, the mean decrease in UACR was significant, MA (−41.9 mg/g creatinine, $p = 0.03$) and macroalbuminuria (−528.9 mg/g creatinine, $p < 0.001$) |
| GUARD-extension (Han et al., 2018) | Gemigliptin | randomized, double-blind, placebo-controlled study | Patients who had completed the 12-week study and consented to participate in the extended study were enrolled. (N = 102) | 50 mg of gemigliptin daily; 5 mg of linagliptin daily | Changes in eGFR, UACR at Week 52 | eGFR decreased by 3.86 mL/min/1.73m$^2$ in the gemigliptin group and 1.85 mL/min/1.73m$^2$ in the placebo/linagliptin group. The UACR did not change significantly in either group between baseline and week 52 |

UACR: urine albumin creatine ratio, CKD: chronic kidney disease, eGFR: estimated Glomerular Filtration Rate, ESKD: End-Stage Kidney Disease, T2D: Type 2 Diabetes, MA: microalbuminuria, RAS: renin angiotensin system, SCr: Serum Creatine rate, RRT: renal replacement therapy.

plaque progression (Zhao et al., 2021). Reverse cholesterol transport is an important mechanism for improving ASCVD, which is mainly mediated by high-density lipoprotein (HDL)-associated cyclic adenosine monophosphate (cAMP) and can activate adenosine triphosphate transporter A1 (ABCA1) to promote HDL formation. Sitagliptin increases intracellular cAMP levels by indirectly activating GLP-1R and up-regulating ABCA1 expression, thereby promoting reverse cholesterol transport in macrophages and reducing foam cell generation (Komatsu et al., 2023). In an MI model of *db/db* mice, linagliptin upregulated the expression of microRNAs (miR-146b and Let-7i) in cardiomyocytes by reducing p38 phosphorylation, thereby inhibiting toll-like receptor 4 (TLR4) upregulation (Birnbaum et al., 2019).

DPP-4i also offer benefits in improving metabolic syndrome. Plasma asymmetrical dimethylarginine (ADMA) is increased in fructose-induced metabolic syndrome, which can inhibit NO by replacing L-arginine, the substrate of NO synthase, and aggravate endothelial dysfunction. Sitagliptin reduces endothelial dysfunction by increasing the activity of dimethylarginine dimethylaminohydrolase 1 (DDAH1) (an enzyme that degrades ADMA) in the kidney to degrade ADMA, thereby increasing plasma NO levels (Wójcicka et al., 2023).

Although published clinical trials have not demonstrated the superior cardiovascular benefits of DPP-4i in diabetic population, extensive basic researches have highlighted its protective effects on the cardiovascular system in animal models of metabolic syndrome, ASCVD, and MI. These findings emphasize the necessity for further exploration into the potential clinical application of DPP-4i.

## 3.2 Renal protection

### 3.2.1 SGLT2i

#### 3.2.1.1 Clinical trial

SGLT2i have demonstrated significant advantages in kidney- and cardiovascular system-related clinical trials. Dapagliflozin has been shown to reduce HF hospitalization rates in T2DM patients

(DECLARE-TIMI 58) (HR, 0.83 [95% CI, 0.73 to 0.95]; $p = 0.005$) (Wiviott et al., 2019). In the DAPA-CKD trial, dapagliflozin exhibited superior efficacy in mitigating sustained eGFR decline of at least 50% in both diabetic and non-diabetic patients with CKD (Table 2) (HR, 0.61 [95% CI, 0.51 to 0.72]; $p < 0.001$) (Heerspink et al., 2020). The analysis of the DAPA-CKD trial also demonstrated the superior benefits of dapagliflozin in reducing albuminuria and improving eGFR in T2DM patients (Heerspink et al., 2021; Jongs et al., 2021). In addition, the analysis of the DELIVER trial (Solomon et al., 2022) also showed that dapagliflozin significantly slowed the decline in eGFR from the baseline (difference in eGFR decline from baseline was 0.5, [95% CI, 0.1–0.9 mL/min/1.73 $m^2$ per year]; $p = 0.01$) (Mc Causland et al., 2023). However, the failure of dapagliflozin to improve GFR in the DIAMOND trial, which focused on patients with non-T2DM CKD (difference in mean proteinuria change from baseline was 0.9%, [95% CI, −16.6 to 22.1]; $p = 0.93$), suggests that the specific effects of dapagliflozin on GFR need to be further investigated (Cherney et al., 2020). In the CREDENCE trial, canagliflozin significantly reduced the rates of end-stage renal disease (ESRD) and doubled serum creatinine (HR, 0.70 [95% CI, 0.59 to 0.82]; $p = 0.00001$) (Perkovic et al., 2019). Lastly, empagliflozin (10 mg/day) was significantly superior to placebo in slowing kidney disease in the EMPA-KIDNEY trial (HR, 0.72 [95% CI, 0.6 to 0.82]; $p < 0.001$) (Herrington et al., 2023).

#### 3.2.1.2 Basic research

Promising results have been obtained from basic research on the role of SGLT2i in alleviating kidney injury. High glucose stimulation induces heightened energy consumption in HK-2 cells, leading to a decrease in the intracellular adenosine-diphosphate/adenosine-triphosphate (ADP/ATP) ratio. This disruption affects the AMPK/mTOR pathway, resulting in reduced autophagy and inhibited energy production (Figure 1B) (Xiao et al., 2011; Packer, 2020b). Dapagliflozin may reverse this process (Xu et al., 2021). Cytochrome P4 (CYP4) is highly expressed in diabetic kidney and can metabolize arachidonic acid into 20-hydroxy-eicosapentaenoic acid (20-HETE), which promotes the formation of superoxide. Dapagliflozin can reduce the inflammation of DKD by targeting the CYP4/20-HETE pathway (Dia et al., 2023). In addition, dapagliflozin could appropriately restore fatty acid metabolism to improve the activation of hypoxia-inducible factor-1α (HIF-1α) and metabolite accumulation caused by mitochondrial tricarboxylic acid (TCA) cycle over-activation under DKD, suggesting that SGLT2i could prevent tubular cell metabolic shift and associate with inflammation (Ke et al., 2022). The Hippo-yes associated protein 1/transcriptional coactivator (YAP/TAZ) pathway plays an important role in fibrosis. Dapagliflozin can inhibit the nuclear translocation of YAP/TAZ, thereby reducing the transcription of its downstream pro-fibrotic target genes connective tissue growth factor (CTGF) to improve DKD fibrosis (Table 3) (Feng et al., 2023). Empagliflozin can also delay DKD fibrosis by preventing reprogramming of serine-threonine metabolism (Lu et al., 2022).

In recent years, the role of SGLT2i in mediating immune response has attracted great attention. Canagliflozin has been shown to inhibit $CD4^+$T cell activation and reduce cancer myelocytomatosis oncogene (cMyc) to prevent metabolic reprogramming and immune inflammation (Jenkins et al., 2023). Consistently, a study by Zhao et al. revealed that empagliflozin can inhibit the over-activated SGLT2 in lupus kidney glomeruli, prevent the activation of mechanistic target of rapamycin complex 1 (mTORC1), and delay glomerular injury in lupus kidney (Zhao et al., 2023). Also, the expression of complement receptor type 1-related protein y (Crry), a key complement regulator, was upregulated by dapagliflozin, inhibiting HIF-1α accumulation under high glucose to alleviate immune inflammatory injury in *db/db* mice (Chang et al., 2021).

SGLT2i have a significant protective effect on DKD. Immune-related nephropathy is identified as a major contributor to CKD, and several basic studies have confirmed the positive role of SGLT2i in regulating the immune system. As a result, Säemann et al. advocate for the inclusion of patients with autoimmune diseases in large-scale renal outcome trials (Säemann and Kronbichler, 2022). Currently, relevant clinical trials have confirmed the acceptable safety profile of SGLT2i in the treatment of lupus nephritis, but further evaluation is needed to assess its efficacy (Wang et al., 2022).

### 3.2.2 GLP-1RAs

#### 3.2.2.1 Clinical trial

Most clinical trials of GLP-1RAs have been *post hoc* and prespecified analyses, highlighting their role in reducing eGFR and urine albumin creatine ratio (UACR). A prespecified analysis of renal outcomes in the LEADER trial showed a significant improvement in macroalbuminuria with liraglutide (HR, 0.78 [95% CI, 0.67 to 0.92]; $p = 0.003$) (Table 2) (Mann et al., 2017). In a *post hoc* analysis of the (SUSTAIN1-7) trial, semaglutide has a significant effect on reducing UACR but decreasing eGFR only in an early stage in T2DM patients with established CKD (Mann et al., 2020). Similarly, in the pooled analysis of SUSTAIN 6 and LEADER, both liraglutide and semaglutide reduced albuminuria by 24% over 2 years (95% CI, 20%–27%; $p < 0.001$), with a greater delay in the continuous decline of eGFR at an eGFR of 30–60 mL/min/1.73 $m^2$ (Shaman et al., 2022). In addition, a pooled analysis of the SUSTAIN 6 and PIONEER 6 trials showed that although the improvement in eGFR slope was not significant in subgroups, semaglutide still reduced the eGFR slope in an overall population analysis (Tuttle et al., 2023). Of note, in a *post hoc* analysis of the STEP1-3 trial in obese patients, a higher dose (2.4 mg) of once-weekly semaglutide reduced UACR by 20.6%, while there was no difference between semaglutide and placebo in the eGFR slope at week 68 (Heerspink et al., 2023). A direct, specific trial is underway to assess whether semaglutide can delay DKD (FLOW) in older patients who have had T2DM for nearly two decades, which will provide novel insights into the long-term renal effects of GLP-1RAs (Rossing et al., 2023).

#### 3.2.2.2 Basic research

Similar to SGLT2i, GLP-1RAs have shown hopeful results in delaying the progression of kidney disease, regardless of diabetes status. Nrf2 expression was significantly upregulated by liraglutide, activating the AMPK/mTOR pathway and thereby alleviating DKD (Figure 2B) (Table 3) (Yang et al., 2020). Further, Nrf2 can regulate the disorder of lipid metabolism through the AMPK pathway to reduce ectopic lipid deposition in renal tubules in DKD (Su et al., 2020). Notably, co-administration of exenatide and adipose-derived mesenchymal stem cells (ADMSCs) significantly improved the renal function of DKD (Habib et al., 2021).

TABLE 3 Summary of *in vitro* and *in vivo* models using SGLT2i, GLP-1RAs, and DPP-4i.

| Drug | Animal treatment | Mice type | Cell type | Mechanism | References |
|---|---|---|---|---|---|
| dapagliflozin | Ang II (cardiomyopathy) | db/db mice | primary SD rat ventricular myocytes | anti-oxidative stress | Arow et al. (2020) |
| dapagliflozin | STZ (T1D cardiomyopathy) | Wistar rats | - | anti-oxidative stress | Rosa et al. (2022) |
| empagliflozin | HFD (atherosclerosis) | Apoe$^{-/-}$ mice | RAW264.7 cell | anti-inflammatory | Fu et al. (2022) |
| dapagliflozin | HFD (obesity-related cardiac dysfunction) | C57 mice | rat cardiomyocyte H9c2 cells | anti-inflammatory | Lin et al. (2022) |
| empagliflozin | Isoproterenol (HF) | Wistar rats | human atrial fibroblasts | anti-fibrosis | Chung et al. (2023) |
| dapagliflozin | DOX (cardiomyopathy) | SD rat | rat cardiomyocyte H9c2 cells | anti-oxidative stress/ inflammatory/fibrosis | Hsieh et al. (2022) |
| empagliflozin | sunitinib (cardiomyopathy) | C57 mice | rat cardiomyocyte H9c2 cells | inhibition of autophagy | Ren et al. (2021) |
| empagliflozin | trastuzumab (cardiomyopathy) | C57 mice | primary C57 mice myocytes | ferroptosis | Min et al. (2023) |
| dapagliflozin | STZ + HFD (DKD) | SD rat | HK-2 cell | anti-fibrosis | Feng et al. (2023) |
| empagliflozin | LPS (acute septic renal injury) | C57 mice | - | anti-inflammatory | (Maayah et al., 2021) |
| empagliflozin | lupus-prone mice (lupus nephrities) | MRL/lpr mice | podocyte | anti-inflammatory | Zhao et al. (2023) |
| liraglutide | STZ (T1D cardiomyopathy) | Wistar rats | - | anti-oxidative stress | Inoue et al. (2015) |
| liraglutide | - | - | hematopoietic stem progenitor cells (HSPCs) | enhanced angiogenic potential | Sforza et al. (2022) |
| liraglutide | STZ (atherosclerosis) | Apoe$^{-/-}$ mice | human umbilical vein endothelial cells (HUVECs) | anti-inflammatory | Koshibu et al. (2019) |
| liraglutide | AAC (myocardial fibrosis) | SD rat | - | anti-fibrosis | Zheng et al. (2020) |
| semaglutide | - | - | endothelial progenitor cells (EPCs)/ RAW264.7 cell | anti-inflammatory | Pan et al. (2023) |
| liraglutide | HFD (DKD) | zucker diabetic fatty rats | Hkc8/HEK293 cells | anti-oxidative stress | Yang et al. (2020) |
| liraglutide | HSD (DKD) | zucker fatty rats | - | anti-inflammatory | Sukumaran et al. (2019) |
| exenatide | HFD (obesity-related kidney dysfunction) | C57 mice | HK-2 cell | anti-oxidative stress/apoptosis | Wang et al. (2021) |
| liraglutide | IRI-AKI | C57 mice | HK-2 cell | anti-inflammatory | Li et al. (2021a) |
| liraglutide | GM-AKI | SD rat | - | anti-oxidative stress/apoptosis/ inflammatory | Elkhoely (2023) |
| liraglutide | Cis-AKI | SD rat | - | anti-oxidative stress/apoptosis/ inflammatory | Sharaf et al. (2023) |
| sitagliptin | STZ (T1D cardiomyopathy) | SD rat | - | anti-inflammatory | Wadie et al. (2022) |
| trelagliptin | IL-1β (atherosclerosis) | - | human aortic endothelial cells (HAECs) | anti-inflammatory | Meng et al. (2020) |
| linagliptin | IRI-MI | db/db mice | primary human cardiofbroblasts (HCF)/ cardiomyocytes (HCM) | anti-inflammatory | Birnbaum et al. (2019) |
| sitagliptin | STZ (DKD) | Wistar rats | - | anti-inflammatory | Al-Qabbaa et al. (2023) |
| linagliptin | STZ (DKD) | CD-1 mice | human dermal microvascular endothelial cells (HMVECs) | anti-fibrosis | Kanasaki et al. (2014) |
| saxagliptin | Ang II (hypertensive nephropathy) | C57 mice | T35OK-ANG II type 1 A receptor ($AT_{1A}R$) (OK) cells (opossum-derived proximal tubule cells) | anti-inflammatory | Nistala et al. (2021) |
| saxagliptin | GM-AKI | SD rat | - | anti-oxidative stress/apoptosis/ inflammatory | Mayer et al. (2021) |

HFD: high-fat diet, HF:heart failure, T1D: type 1 diabete, DOX: doxorubicin, STZ: streptozotocin, LPS: lipopolysaccharide, AAC: abdominal aortic constriction. HSD: high-salt diet, IRI: ischemia-reperfusion injury, GM: gentamicin, Cis: cisplatin, AKI: acute kidney injury, MI: myocardial infarction, DKD: diabetic kidney disease.

Additionally, GLP-1RAs may have therapeutic promise in renal injury caused by hypertension, obesity or ischemia reperfusion. Studies have shown that liraglutide can reduce blood pressure by increasing the expression of endothelial nitric oxide synthase (eNOS) and vascular endothelial growth factor (VEGF), thereby improving the vasoconstriction of intrarenal arterioles. It can also reduce the infiltration of macrophages into renal vascular endothelial cells and alleviate renal vascular inflammation in obese rats induced by a high-salt diet (Sukumaran et al., 2019). Exenatide can stabilize mitochondrial membrane potential and reduce palmitate-induced reactive oxygen species production in HK-2 cells through the upregulation of SIRT1 (Wang et al., 2021). High mobility group box 1 protein (HMGB1) is a damage-associated molecular pattern, which is released from the nucleus to the cytoplasm during renal ischemia and then binds to its receptors, such as TLR-4, to promote the inflammatory cascade. Liraglutide can downregulate the expression of HMGB1 receptors and prevent acetylation of HMGB1 by increasing histone acrtyltransferases (HAT) activity, thereby reducing neutrophil infiltration and delaying renal ischemia-reperfusion injury *in vivo* and *in vitro* (Li Y. et al., 2021).

GLP-1RAs have also been shown to have a positive role in reducing the nephrotoxic effects of antibiotics and antitumor drugs. Liraglutide can mediate mitochondrial biogenesis by regulating the protein kinase A/cyclic-AMP response binding protein (PKA/CREB) and notch homolog 1/hairy and enhancer of split-1 (Notch/Hes-1) pathways and up-regulating the expression of PGC-1α to activate Nrf2, thereby improving the nephrotoxicity induced by glucocorticoids (Elkhoely, 2023). Cisplatin, a common and effective chemotherapeutic agent, often causes irreversible acute kidney injury (AKI). Organic cations transporter 2 (OCT2) is located on the basement membrane of renal tubules and is responsible for the absorption of cisplatin. The MAPK pathway plays a pivotal role in cisplatin-induced AKI. Liraglutide can reduce renal injury by inhibiting the expression of OCT2 and c-Jun N-terminal kinase/extracellular regulated protein kinase (JNK/ERK), thereby restoring the oxidative/antioxidant balance (Sharaf et al., 2023). Additionally, liraglutide also inhibited the release of HMGB1 to reduce cisplatin-induced apoptosis in HK-2 cells (Xu et al., 2023).

These basic studies demonstrate that GLP-1RAs offer significant protection against obesity-related kidney disease, in addition to their benefits in improving DKD. Exenatide is even more effective than simvastatin in treating obesity-induced tubular epithelial cell lipotoxicity (Wang et al., 2021). The fact that GLP-1RAs has also become a second-line therapy for CKD expands its clinical benefits range besides weight loss (Navaneethan et al., 2023). Moreover, it has been reported that liraglutide, either alone or in combination with rabeprazole, can protect against cisplatin-induced nephrotoxicity (Sharaf et al., 2023), highlighting the potential of GLP-1RAs for further validation in clinical trials investigating nephrotoxicity associated with antineoplastic drugs.

### 3.2.3 DPP-4i

#### 3.2.3.1 Clinical trial

The outcomes of clinical trials assessing the impact of DPP-4i on renal outcomes remain controversial. Initial findings indicated the potential benefits of DPP-4i in ameliorating DKD. In a retrospective analysis of four clinical datasets concerning linagliptin, it was observed that treatment with linagliptin led to a significant reduction in UACR after 12–24 weeks (Groop et al., 2013). Other studies showed that linagliptin reduced the probability of first adverse kidney events (HR, 0.84 [95% CI, 0.72–0.97]; $p = 0.02$) and new-onset albuminuria (HR, 0.82 [95% CI, 0.69–0.98]; $p = 0.03$) (Cooper et al., 2015). In the GUARD study, gemigliptin improved microalbuminuria (decrease in UACR was −41.9 mg/g creatinine; $p = 0.03$) and macroalbuminuria (decrease in UACR was −528.9 mg/g creatinine; $p < 0.001$) in both the short-term 12-week observation and the 40-week extension study (Table 2) (Yoon et al., 2017; Han et al., 2018). Analysis of the SAVOR-TIMI 53 trial found that saxagliptin improved UACR in patients with renal insufficiency (the difference in UACR change was −19.3 mg/g; $p = 0.033$) (Mosenzon et al., 2017). In the CARMELINA trial, linagliptin had a significant advantage in reducing UACR in T2DM patients with or without nephrotic range proteinuria (reduction of UACR ≥50%; HR, 1.15 [95% CI, 1.07 to 1.25] from baseline) (Wanner et al., 2021). In line with the CARMELINA trial, the EXAM trial showed that alogliptin may benefit patients with eGFR ≥60 mL/min/1.73 $m^2$ (HR, 0.81 [95% CI, 0.65 to 0.99] for eGFR ≥60 mL/min/1.73 $m^2$; HR, 1.2 [95% CI, 0.95 to 1.53] for eGFR <60 mL/min/1.73 $m^2$) (Ferreira et al., 2020). However, there is contrary evidence to the above results. In the TECOS trial, sitagliptin did not significantly improve CKD progression, regardless of the baseline eGFR level (Cornel et al., 2016). The secondary analysis of CARMELINA also proved that linagliptin was not significantly different from placebo in improving renal outcomes (Perkovic et al., 2020). Postprandial glomerular hyperfiltration may be one of the renal risk factors in diabetic patients. Compared with glimepiride, linagliptin does not improve postprandial hemodynamics, and may even moderately induce postprandial glomerular hyperfiltration (Muskiet et al., 2020; Muskiet et al., 2022).

#### 3.2.3.2 Basic research

Inconsistent with clinical trials, preclinical data have unequivocally demonstrated the beneficial effects of DPP-4i in alleviating DKD. High glucose activates the C-reactive protein (CRP)/FcγRIIb (CD32b)/NF-κB pathway, which enriches DPP-4 and forms a dimer with CD32b to maintain its expression, thereby forming an inflammatory cycle and aggravating the injury. Linagliptin can block this cycle (Tang et al., 2021). Omarigliptin can improve high glucose-induced glomerular endothelial cell inflammation by activating the AMPK/mTOR pathway and negatively regulating the NLRP3 inflammasome (Figure 3B) (Li L. et al., 2021). Protein tyrosine phosphatase 1B (PTP1B) participates in the inflammatory response by negatively regulating the janus tyrosine kinase/signal transducer and activator of transcription (JAK/STAT) pathway. Sitagliptin reduces renal inflammation in streptozotocin-induced rats by inhibiting PTP1B (Table 3) (Al-Qabbaa et al., 2023). Linagliptin alleviate renal fibrosis in streptozotocin-induced mice by increasing the expression of microRNA 29. Upregulation of microRNA 29 directly inhibited the expression of fibrosis genes (Kanasaki et al., 2014).

DPP-4i may also alleviate renal dysfunction induced by AngII. The expression of Ang II receptor 2 (AT2R), which can antagonize

Ang Ⅱ receptor 1 (AT1R)-mediated inflammatory responses, was upregulated by linagliptin to alleviate Ang Ⅱ-induced renal fibrosis (Bai et al., 2020). Additionally, saxagliptin can mediate innate and adaptive immune inflammation, inhibit the activity of pro-inflammatory cells ($CD8^+$T cells, neutrophils), and convert them into anti-inflammatory cells (M2 macrophages and Treg cells) to reduce Ang Ⅱ-induced hypertensive nephropathy (Nistala et al., 2021). In addition, saxagliptin can also activate multiple pathways, such as GLP-1/cAMP/VEGF, kidney injury molecule-1 (KIM-1)/STAT3/HIF-1α/VEGF/eNOS, to increase the expression of NO and repair damaged blood vessels caused by inflammation after renal ischemia/reperfusion (Kamel et al., 2019).

Additionally, DPP-4i play a significant role in improving antibiotic-induced nephrotoxicity and nephritis. Saxagliptin can reduce the expression of malondialdehyde and increase the expression of glutathione to regulate the disorder of renal inflammation and oxidative stress caused by gentamicin (Helal et al., 2018). Interestingly, linagliptin also accelerated glomerular crescentic degeneration in anti-glomerular basement membrane (GBM) nephritis (Mayer et al., 2021).

Basic research are still ongoing to explore the potential benefits and mechanisms of DPP-4i in improving DKD. Additionally, DPP-4i can improve hypertensive nephropathy through immune mechanisms independent of blood pressure reduction (Nistala et al., 2021), and promote the regression of crescents in anti-GBM nephritis, thereby providing a clinical translation point for their future use in immune system diseases.

## 4 Conclusion

Patients with T2DM often suffer from adverse cardiovascular and renal outcomes. Accumulating evidence suggest that SGLT2i and GLP-1RAs have cardiorenal protective effects including glucose-dependent and independent pathways. They not only protect against heart and kidney diseases through classical anti-inflammatory, anti-oxidative stress, and anti-fibrosis pathways but are also implicated in non-classical epigenetics, mitochondrial energy metabolism, and immune complement pathways. They have also demonstrated positive effects on immune diseases and cardiovascular and renal toxicity caused by antineoplastic drugs and antibiotics. Although basic research indicate the beneficial effects of DPP-4i, most clinical studies have only demonstrated their non-inferiority, underscoring the necessity for further exploration. Therefore, more direct and larger clinical trials (involving a larger proportion of CVD/CKD patients without diabetes) are needed to assess this drug.

By exploring the cardiorenal protective effects of drugs, we can identify common mechanisms that contribute to cardiorenal injury in various diseases. These findings will establish a theoretical and experimental basis for developing novel clinical drugs. Additionally, a drug that can effectively treat both heart and kidney diseases has significant practical implications, including reducing the medication burden on patients, lowering adverse reactions, enhancing patient compliance, and alleviating financial strain and so on. Therefore, further research should investigate new mechanistic pathways to explore the effectiveness of second-generation anti-glucose drugs.

## Author contributions

W-JF: Writing–original draft. J-LH: Writing–original draft. Z-HM: Writing–review and editing. S-KP: Writing–review and editing. D-WL: Writing–review and editing. Z-SL: Conceptualization, Writing–review and editing. PW: Conceptualization, Funding acquisition, Supervision, Writing–review and editing. Z-XG: Conceptualization, Funding acquisition, Supervision, Writing–review and editing.

## Funding

The author(s) declare financial support was received for the research, authorship, and/or publication of this article. This work was supported by the Natural Science Foundation of Henan Province (222300420089 to PW), National Natural Science Foundation of China (32371170 to Z-XG, 31971065 to PW, and 82300323 to J-LH), and Scientific Research and Innovation Team of the First Affiliated Hospital of Zhengzhou University (QNCXTD2023006 to PW).

## Acknowledgments

The authors would like to thank Editage for professional editing.

## Conflict of interest

The authors declare that the research was conducted in the absence of any commercial or financial relationships that could be construed as a potential conflict of interest.

## Publisher's note



## References

Abdul-Ghani, M. A., DeFronzo, R. A., and Norton, L. (2013). Novel hypothesis to explain why SGLT2 inhibitors inhibit only 30-50% of filtered glucose load in humans. *Diabetes* 62 (10), 3324–3328. doi:10.2337/db13-0604

Abu-Qaoud, M. R., Kumar, A., Tarun, T., Abraham, S., Ahmad, J., Khadke, S., et al. (2023). Impact of SGLT2 inhibitors on AF recurrence after catheter ablation in Patients with type 2 diabetes. *JACC Clin. Electrophysiol.* 9 (10), 2109–2118. doi:10.1016/j.jacep.2023.06.008

Al-Qabbaa, S. M., Qaboli, S. I., Alshammari, T. K., Alamin, M. A., Alrajeh, H. M., Almuthnabi, L. A., et al. (2023). Sitagliptin mitigates diabetic nephropathy in a rat model of streptozotocin-induced type 2 diabetes: possible role of PTP1B/JAK-STAT pathway. *Int. J. Mol. Sci.* 24 (7), 6532. doi:10.3390/ijms24076532

Andreadi, A., Muscoli, S., Tajmir, R., Meloni, M., Muscoli, C., Ilari, S., et al. (2023). Recent pharmacological options in type 2 diabetes and synergic mechanism in cardiovascular disease. *Int. J. Mol. Sci.* 24 (2), 1646. doi:10.3390/ijms24021646

Anker, S. D., Butler, J., Filippatos, G., Ferreira, J. P., Bocchi, E., Böhm, M., et al. (2021). Empagliflozin in heart failure with a preserved ejection fraction. *N. Engl. J. Med.* 385 (16), 1451–1461. doi:10.1056/NEJMoa2107038

Arow, M., Waldman, M., Yadin, D., Nudelman, V., Shainberg, A., Abraham, N. G., et al. (2020). Sodium-glucose cotransporter 2 inhibitor Dapagliflozin attenuates diabetic cardiomyopathy. *Cardiovasc. Diabetol.* 19 (1), 7. doi:10.1186/s12933-019-0980-4

Baggio, L. L., and Drucker, D. J. (2014). Glucagon-like peptide-1 receptors in the brain: controlling food intake and body weight. *J. Clin. investigation* 124 (10), 4223–4226. doi:10.1172/jci78371

Bai, F., Zhang, L. H., Zhang, W. W., Zheng, R. H., Eskew, J. R., Bennett, J., et al. (2020). Conservation of glucagon like peptide-1 level with liraglutide and linagilptin protects the kidney against angiotensin II-induced tissue fibrosis in rats. *Eur. J. Pharmacol.* 867, 172844. doi:10.1016/j.ejphar.2019.172844

Balogh, D. B., Wagner, L. J., and Fekete, A. (2023). An overview of the cardioprotective effects of novel antidiabetic classes: focus on inflammation, oxidative stress, and fibrosis. *Int. J. Mol. Sci.* 24 (9), 7789. doi:10.3390/ijms24097789

Bhatt, D. L., Szarek, M., Steg, P. G., Cannon, C. P., Leiter, L. A., McGuire, D. K., et al. (2021). Sotagliflozin in patients with diabetes and recent worsening heart failure. *N. Engl. J. Med.* 384 (2), 117–128. doi:10.1056/NEJMoa2030183

Birnbaum, Y., Tran, D., Bajaj, M., and Ye, Y. (2019). DPP-4 inhibition by linagliptin prevents cardiac dysfunction and inflammation by targeting the Nlrp3/ASC inflammasome. *Basic Res. Cardiol.* 114 (5), 35. doi:10.1007/s00395-019-0743-0

Blazek, O., and Bakris, G. L. (2023). Slowing the progression of diabetic kidney disease. *Cells* 12 (15), 1975. doi:10.3390/cells12151975

Bruen, R., Curley, S., Kajani, S., Lynch, G., O'Reilly, M. E., Dillon, E. T., et al. (2019). Liraglutide attenuates preestablished atherosclerosis in apolipoprotein E-deficient mice via regulation of immune cell phenotypes and proinflammatory mediators. *J. Pharmacol. Exp. Ther.* 370 (3), 447–458. doi:10.1124/jpet.119.258343

Campbell, J. E., Müller, T. D., Finan, B., DiMarchi, R. D., Tschöp, M. H., and D'Alessio, D. A. (2023). GIPR/GLP-1R dual agonist therapies for diabetes and weight loss-chemistry, physiology, and clinical applications. *Cell metab.* 35 (9), 1519–1529. doi:10.1016/j.cmet.2023.07.010

Cannon, C. P., Pratley, R., Dagogo-Jack, S., Mancuso, J., Huyck, S., Masiukiewicz, U., et al. (2020). Cardiovascular outcomes with ertugliflozin in type 2 diabetes. *N. Engl. J. Med.* 383 (15), 1425–1435. doi:10.1056/NEJMoa2004967

Capuano, A., Sportiello, L., Maiorino, M. I., Rossi, F., Giugliano, D., and Esposito, K. (2013). Dipeptidyl peptidase-4 inhibitors in type 2 diabetes therapy--focus on alogliptin. *Drug Des. Dev. Ther.* 7, 989–1001. doi:10.2147/dddt.S37647

Chang, D. Y., Li, X. Q., Chen, M., and Zhao, M. H. (2021). Dapagliflozin ameliorates diabetic kidney disease via upregulating crry and alleviating complement over-activation in db/db mice. *Front. Pharmacol.* 12, 729334. doi:10.3389/fphar.2021.729334

Chen, A., Lan, Z., Li, L., Xie, L., Liu, X., Yang, X., et al. (2023). Sodium-glucose cotransporter 2 inhibitor canagliflozin alleviates vascular calcification through suppression of nucleotide-binding domain, leucine-rich-containing family, pyrin domain-containing-3 inflammasome. *Cardiovasc. Res.* 119 (13), 2368–2381. doi:10.1093/cvr/cvad119

Cherney, D. Z. I., Dekkers, C. C. J., Barbour, S. J., Cattran, D., Abdul Gafor, A. H., Greasley, P. J., et al. (2020). Effects of the SGLT2 inhibitor dapagliflozin on proteinuria in non-diabetic patients with chronic kidney disease (DIAMOND): a randomised, double-blind, crossover trial. *lancet Diabetes and Endocrinol.* 8 (7), 582–593. doi:10.1016/s2213-8587(20)30162-5

Chung, C. C., Lin, Y. K., Chen, Y. C., Kao, Y. H., Yeh, Y. H., Trang, N. N., et al. (2023). Empagliflozin suppressed cardiac fibrogenesis through sodium-hydrogen exchanger inhibition and modulation of the calcium homeostasis. *Cardiovasc. Diabetol.* 22 (1), 27. doi:10.1186/s12933-023-01756-0

Committee ADAPP (2022a). 11. Chronic kidney disease and risk management: standards of medical care in diabetes-2022. *Diabetes care* 45 (Suppl. 1), S175–s184. doi:10.2337/dc22-S011

Committee ADAPP (2022b). 9. Pharmacologic approaches to glycemic treatment: standards of medical care in diabetes-2022. *Diabetes care* 45 (Suppl. 1), S125–s143. doi:10.2337/dc22-S009

Cooper, M. E., Perkovic, V., McGill, J. B., Groop, P. H., Wanner, C., Rosenstock, J., et al. (2015). Kidney disease end points in a pooled analysis of individual patient-level data from a large clinical trials program of the dipeptidyl peptidase 4 inhibitor linagliptin in type 2 diabetes. *Am. J. kidney Dis.* 66 (3), 441–449. doi:10.1053/j.ajkd.2015.03.024

Cornel, J. H., Bakris, G. L., Stevens, S. R., Alvarsson, M., Bax, W. A., Chuang, L. M., et al. (2016). Effect of sitagliptin on kidney function and respective cardiovascular outcomes in type 2 diabetes: outcomes from TECOS. *Diabetes care* 39 (12), 2304–2310. doi:10.2337/dc16-1415

de Boer, I. H., Khunti, K., Sadusky, T., Tuttle, K. R., Neumiller, J. J., Rhee, C. M., et al. (2022). Diabetes management in chronic kidney disease: a consensus report by the American diabetes association (ADA) and kidney disease: improving global outcomes (KDIGO). *Diabetes care* 45 (12), 3075–3090. doi:10.2337/dci22-0027

Dia, B., Alkhansa, S., Njeim, R., Al Moussawi, S., Farhat, T., Haddad, A., et al. (2023). SGLT2 inhibitor-dapagliflozin attenuates diabetes-induced renal injury by regulating inflammation through a CYP4A/20-HETE signaling mechanism. *Pharmaceutics* 15 (3), 965. doi:10.3390/pharmaceutics15030965

Durak, A., and Turan, B. (2023). Liraglutide provides cardioprotection through the recovery of mitochondrial dysfunction and oxidative stress in aging hearts. *J. physiology Biochem.* 79 (2), 297–311. doi:10.1007/s13105-022-00939-9

Elkhoely, A. (2023). Liraglutide ameliorates gentamicin-induced acute kidney injury in rats via PGC-1α-mediated mitochondrial biogenesis: involvement of PKA/CREB and Notch/Hes-1 signaling pathways. *Int. Immunopharmacol.* 114, 109578. doi:10.1016/j.intimp.2022.109578

Feng, L., Chen, Y., Li, N., Yang, X., Zhou, L., Li, H., et al. (2023). Dapagliflozin delays renal fibrosis in diabetic kidney disease by inhibiting YAP/TAZ activation. *Life Sci.* 322, 121671. doi:10.1016/j.lfs.2023.121671

Ferreira, J. P., Mehta, C., Sharma, A., Nissen, S. E., Rossignol, P., and Zannad, F. (2020). Alogliptin after acute coronary syndrome in patients with type 2 diabetes: a renal function stratified analysis of the EXAMINE trial. *BMC Med.* 18 (1), 165. doi:10.1186/s12916-020-01616-8

Fu, J., Xu, H., Wu, F., Tu, Q., Dong, X., Xie, H., et al. (2022). Empagliflozin inhibits macrophage inflammation through AMPK signaling pathway and plays an anti-atherosclerosis role. *Int. J. Cardiol.* 367, 56–62. doi:10.1016/j.ijcard.2022.07.048

Fu, Z., Mui, D., Zhu, H., and Zhang, Y. (2020). Exenatide inhibits NF-κB and attenuates ER stress in diabetic cardiomyocyte models. *Aging* 12 (9), 8640–8651. doi:10.18632/aging.103181

Gerstein, H. C., Colhoun, H. M., Dagenais, G. R., Diaz, R., Lakshmanan, M., Pais, P., et al. (2019). Dulaglutide and cardiovascular outcomes in type 2 diabetes (REWIND): a double-blind, randomised placebo-controlled trial. *Lancet* 394 (10193), 121–130. doi:10.1016/s0140-6736(19)31149-3

Gerstein, H. C., Sattar, N., Rosenstock, J., Ramasundarahettige, C., Pratley, R., Lopes, R. D., et al. (2021). Cardiovascular and renal outcomes with efpeglenatide in type 2 diabetes. *N. Engl. J. Med.* 385 (10), 896–907. doi:10.1056/NEJMoa2108269

Graaf, C., Donnelly, D., Wootten, D., Lau, J., Sexton, P. M., Miller, L. J., et al. (2016). Glucagon-like peptide-1 and its class B G protein-coupled receptors: a long march to therapeutic successes. *Pharmacol. Rev.* 68 (4), 954–1013. doi:10.1124/pr.115.011395

Green, J. B., Bethel, M. A., Armstrong, P. W., Buse, J. B., Engel, S. S., Garg, J., et al. (2015). Effect of sitagliptin on cardiovascular outcomes in type 2 diabetes. *N. Engl. J. Med.* 373 (3), 232–242. doi:10.1056/NEJMoa1501352

Groop, P. H., Cooper, M. E., Perkovic, V., Emser, A., Woerle, H. J., and von Eynatten, M. (2013). Linagliptin lowers albuminuria on top of recommended standard treatment in patients with type 2 diabetes and renal dysfunction. *Diabetes care* 36 (11), 3460–3468. doi:10.2337/dc13-0323

Guo, X., Sang, C., Tang, R., Jiang, C., Li, S., Liu, N., et al. (2023). Effects of glucagon-like peptide-1 receptor agonists on major coronary events in patients with type 2 diabetes. *Diabetes, Obes. metabolism* 25 (Suppl. 1), 53–63. doi:10.1111/dom.15043

Gureev, A. P., Shaforostova, E. A., and Popov, V. N. (2019). Regulation of mitochondrial biogenesis as a way for active longevity: interaction between the Nrf2 and PGC-1α signaling pathways. *Front. Genet.* 10, 435. doi:10.3389/fgene.2019.00435

Habib, H. A., Heeba, G. H., and Khalifa, M. M. A. (2021). Effect of combined therapy of mesenchymal stem cells with GLP-1 receptor agonist, exenatide, on early-onset nephropathy induced in diabetic rats. *Eur. J. Pharmacol.* 892, 173721. doi:10.1016/j.ejphar.2020.173721

Han, S. Y., Yoon, S. A., Han, B. G., Kim, S. G., Jo, Y. I., Jeong, K. H., et al. (2018). Comparative efficacy and safety of gemigliptin versus linagliptin in type 2 diabetes patients with renal impairment: a 40-week extension of the GUARD randomized study. *Diabetes, Obes. metabolism* 20 (2), 292–300. doi:10.1111/dom.13059

Heerspink, H. J. L., Apperloo, E., Davies, M., Dicker, D., Kandler, K., Rosenstock, J., et al. (2023). Effects of semaglutide on albuminuria and kidney function in people with overweight or obesity with or without type 2 diabetes: exploratory analysis from the STEP 1, 2, and 3 trials. *Diabetes care* 46 (4), 801–810. doi:10.2337/dc22-1889

Heerspink, H. J. L., Jongs, N., Chertow, G. M., Langkilde, A. M., McMurray, J. J. V., Correa-Rotter, R., et al. (2021). Effect of dapagliflozin on the rate of decline in kidney function in patients with chronic kidney disease with and without type 2 diabetes: a prespecified analysis from the DAPA-CKD trial. *lancet Diabetes and Endocrinol.* 9 (11), 743–754. doi:10.1016/s2213-8587(21)00242-4

Heerspink, H. J. L., Stefánsson, B. V., Correa-Rotter, R., Chertow, G. M., Greene, T., Hou, F. F., et al. (2020). Dapagliflozin in patients with chronic kidney disease. *N. Engl. J. Med.* 383 (15), 1436–1446. doi:10.1056/NEJMoa2024816

Heidenreich, P. A., Bozkurt, B., Aguilar, D., Allen, L. A., Byun, J. J., Colvin, M. M., et al. (2022). 2022 AHA/ACC/HFSA guideline for the management of heart failure: a

report of the American college of cardiology/American heart association joint committee on clinical practice guidelines. *Circulation* 145 (18), e895–e1032. doi:10.1161/CIR.0000000000001063

Helal, M. G., Zaki, M., and Said, E. (2018). Nephroprotective effect of saxagliptin against gentamicin-induced nephrotoxicity, emphasis on anti-oxidant, anti-inflammatory and anti-apoptic effects. *Life Sci.* 208, 64–71. doi:10.1016/j.lfs.2018.07.021

Hernandez, A. F., Green, J. B., Janmohamed, S., D'Agostino, R. B., Granger, C. B., Jones, N. P., et al. (2018). Albiglutide and cardiovascular outcomes in patients with type 2 diabetes and cardiovascular disease (Harmony Outcomes): a double-blind, randomised placebo-controlled trial. *Lancet* 392 (10157), 1519–1529. doi:10.1016/s0140-6736(18)32261-x

Herrington, W. G., Staplin, N., Wanner, C., Green, J. B., Hauske, S. J., Emberson, J. R., et al. (2023). Empagliflozin in patients with chronic kidney disease. *N. Engl. J. Med.* 388 (2), 117–127. doi:10.1056/NEJMoa2204233

Holman, R. R., Bethel, M. A., Mentz, R. J., Thompson, V. P., Lokhnygina, Y., Buse, J. B., et al. (2017). Effects of once-weekly exenatide on cardiovascular outcomes in type 2 diabetes. *N. Engl. J. Med.* 377 (13), 1228–1239. doi:10.1056/NEJMoa1612917

Hsieh, P. L., Chu, P. M., Cheng, H. C., Huang, Y. T., Chou, W. C., Tsai, K. L., et al. (2022). Dapagliflozin mitigates doxorubicin-caused myocardium damage by regulating AKT-mediated oxidative stress, cardiac remodeling, and inflammation. *Int. J. Mol. Sci.* 23 (17), 10146. doi:10.3390/ijms231710146

Husain, M., Birkenfeld, A. L., Donsmark, M., Dungan, K., Eliaschewitz, F. G., Franco, D. R., et al. (2019). Oral semaglutide and cardiovascular outcomes in patients with type 2 diabetes. *N. Engl. J. Med.* 381 (9), 841–851. doi:10.1056/NEJMoa1901118

Inoue, T., Inoguchi, T., Sonoda, N., Hendarto, H., Makimura, H., Sasaki, S., et al. (2015). GLP-1 analog liraglutide protects against cardiac steatosis, oxidative stress and apoptosis in streptozotocin-induced diabetic rats. *Atherosclerosis* 240 (1), 250–259. doi:10.1016/j.atherosclerosis.2015.03.026

Jansen, T., Kvandová, M., Daiber, A., Stamm, P., Frenis, K., Schulz, E., et al. (2020). The AMP-activated protein kinase plays a role in antioxidant defense and regulation of vascular inflammation. *Antioxidants* 9 (6), 525. doi:10.3390/antiox9060525

Jenkins, B. J., Blagih, J., Ponce-Garcia, F. M., Canavan, M., Gudgeon, N., Eastham, S., et al. (2023). Canagliflozin impairs T cell effector function via metabolic suppression in autoimmunity. *Cell metab.* 35 (7), 1132–1146.e9. doi:10.1016/j.cmet.2023.05.001

Jojima, T., Uchida, K., Akimoto, K., Tomotsune, T., Yanagi, K., Iijima, T., et al. (2017). Liraglutide, a GLP-1 receptor agonist, inhibits vascular smooth muscle cell proliferation by enhancing AMP-activated protein kinase and cell cycle regulation, and delays atherosclerosis in ApoE deficient mice. *Atherosclerosis* 261, 44–51. doi:10.1016/j.atherosclerosis.2017.04.001

Jongs, N., Greene, T., Chertow, G. M., McMurray, J. J. V., Langkilde, A. M., Correa-Rotter, R., et al. (2021). Effect of dapagliflozin on urinary albumin excretion in patients with chronic kidney disease with and without type 2 diabetes: a prespecified analysis from the DAPA-CKD trial. *lancet Diabetes and Endocrinol.* 9 (11), 755–766. doi:10.1016/s2213-8587(21)00243-6

Juni, R. P., Al-Shama, R., Kuster, D. W. D., van der Velden, J., Hamer, H. M., Vervloet, M. G., et al. (2021). Empagliflozin restores chronic kidney disease-induced impairment of endothelial regulation of cardiomyocyte relaxation and contraction. *Kidney Int.* 99 (5), 1088–1101. doi:10.1016/j.kint.2020.12.013

Kadowaki, S., Siraj, M. A., Chen, W., Wang, J., Parker, M., Nagy, A., et al. (2023). Cardioprotective actions of a glucagon-like peptide-1 receptor agonist on hearts donated after circulatory death. *J. Am. Heart Assoc.* 12 (3), e027163. doi:10.1161/jaha.122.027163

Kamel, N. M., Abd El Fattah, M. A., El-Abhar, H. S., and Abdallah, D. M. (2019). Novel repair mechanisms in a renal ischaemia/reperfusion model: subsequent saxagliptin treatment modulates the pro-angiogenic GLP-1/cAMP/VEGF, ANP/eNOS/NO, SDF-1α/CXCR4, and Kim-1/STAT3/HIF-1α/VEGF/eNOS pathways. *Eur. J. Pharmacol.* 861, 172620. doi:10.1016/j.ejphar.2019.172620

Kanasaki, K., Shi, S., Kanasaki, M., He, J., Nagai, T., Nakamura, Y., et al. (2014). Linagliptin-mediated DPP-4 inhibition ameliorates kidney fibrosis in streptozotocin-induced diabetic mice by inhibiting endothelial-to-mesenchymal transition in a therapeutic regimen. *Diabetes* 63 (6), 2120–2131. doi:10.2337/db13-1029

Ke, Q., Shi, C., Lv, Y., Wang, L., Luo, J., Jiang, L., et al. (2022). SGLT2 inhibitor counteracts NLRP3 inflammasome via tubular metabolite itaconate in fibrosis kidney. *FASEB J.* 36 (1), e22078. doi:10.1096/fj.202100909RR

Kenny, H. C., and Abel, E. D. (2019). Heart failure in type 2 diabetes mellitus. *Circulation Res.* 124 (1), 121–141. doi:10.1161/circresaha.118.311371

Kim, Y. M., Kim, S. J., Tatsunami, R., Yamamura, H., Fukai, T., and Ushio-Fukai, M. (2017). ROS-induced ROS release orchestrated by Nox4, Nox2, and mitochondria in VEGF signaling and angiogenesis. *Am. J. physiology Cell physiology* 312 (6), C749–C764. doi:10.1152/ajpcell.00346.2016

Klen, J., and Dolžan, V. (2023). SGLT2 inhibitors in the treatment of diabetic kidney disease: more than just glucose regulation. *Pharmaceutics* 15 (7), 1995. doi:10.3390/pharmaceutics15071995

Komatsu, T., Abe, S., Nakashima, S., Sasaki, K., Higaki, Y., Saku, K., et al. (2023). Dipeptidyl peptidase-4 inhibitor sitagliptin phosphate accelerates cellular cholesterol efflux in THP-1 cells. *Biomolecules* 13 (2), 228. doi:10.3390/biom13020228

Koshibu, M., Mori, Y., Saito, T., Kushima, H., Hiromura, M., Terasaki, M., et al. (2019). Antiatherogenic effects of liraglutide in hyperglycemic apolipoprotein E-null mice via AMP-activated protein kinase-independent mechanisms. *Am. J. physiology Endocrinol. metabolism* 316 (5), E895–E907. doi:10.1152/ajpendo.00511.2018

Kyriazis, I. D., Hoffman, M., Gaignebet, L., Lucchese, A. M., Markopoulou, E., Palioura, D., et al. (2021). KLF5 is induced by FOXO1 and causes oxidative stress and diabetic cardiomyopathy. *Circulation Res.* 128 (3), 335–357. doi:10.1161/circresaha.120.316738

Leiter, L. A., Teoh, H., Braunwald, E., Mosenzon, O., Cahn, A., Kumar, K. M., et al. (2015). Efficacy and safety of saxagliptin in older participants in the SAVOR-TIMI 53 trial. *Diabetes care* 38 (6), 1145–1153. doi:10.2337/dc14-2868

Li, L., Qian, K., Sun, Y., Zhao, Y., Zhou, Y., Xue, Y., et al. (2021b). Omarigliptin ameliorated high glucose-induced nucleotide oligomerization domain-like receptor protein 3 (NLRP3) inflammasome activation through activating adenosine monophosphate-activated protein kinase α (AMPKα) in renal glomerular endothelial cells. *Bioengineered* 12 (1), 4805–4815. doi:10.1080/21655979.2021.1957748

Li, X., Römer, G., Kerindongo, R. P., Hermanides, J., Albrecht, M., Hollmann, M. W., et al. (2021). Sodium glucose Co-transporter 2 inhibitors ameliorate endothelium barrier dysfunction induced by cyclic stretch through inhibition of reactive oxygen species. *Int. J. Mol. Sci.* 22 (11), 6044. doi:10.3390/ijms22116044

Li, Y., Liu, Y., Liu, S., Gao, M., Wang, W., Chen, K., et al. (2023). Diabetic vascular diseases: molecular mechanisms and therapeutic strategies. *Signal Transduct. Target. Ther.* 8 (1), 152. doi:10.1038/s41392-023-01400-z

Li, Y., Xu, B., Yang, J., Wang, L., Tan, X., Hu, X., et al. (2021a). Liraglutide protects against lethal renal ischemia-reperfusion injury by inhibiting high-mobility group box 1 nuclear-cytoplasmic translocation and release. *Pharmacol. Res.* 173, 105867. doi:10.1016/j.phrs.2021.105867

Lin, K., Yang, N., Luo, W., Qian, J. F., Zhu, W. W., Ye, S. J., et al. (2022). Direct cardio-protection of Dapagliflozin against obesity-related cardiomyopathy via NHE1/MAPK signaling. *Acta Pharmacol. Sin.* 43 (10), 2624–2635. doi:10.1038/s41401-022-00885-8

Liu, J., Aylor, K. W., and Liu, Z. (2023). Liraglutide and exercise synergistically attenuate vascular inflammation and enhance metabolic insulin action in early diet-induced obesity. *Diabetes* 72 (7), 918–931. doi:10.2337/db22-0745

Lu, Y. P., Zhang, Z. Y., Wu, H. W., Fang, L. J., Hu, B., Tang, C., et al. (2022). SGLT2 inhibitors improve kidney function and morphology by regulating renal metabolic reprogramming in mice with diabetic kidney disease. *J. Transl. Med.* 20 (1), 420. doi:10.1186/s12967-022-03629-8

Luo, X., Hu, Y., He, S., Ye, Q., Lv, Z., Liu, J., et al. (2019). Dulaglutide inhibits high glucose-induced endothelial dysfunction and NLRP3 inflammasome activation. *Archives Biochem. biophysics* 671, 203–209. doi:10.1016/j.abb.2019.07.008

Madonna, R., Moscato, S., Cufaro, M. C., Pieragostino, D., Mattii, L., Del Boccio, P., et al. (2023). Empagliflozin inhibits excessive autophagy through the AMPK/GSK3β signalling pathway in diabetic cardiomyopathy. *Cardiovasc. Res.* 119 (5), 1175–1189. doi:10.1093/cvr/cvad009

Mann, J. F. E., Hansen, T., Idorn, T., Leiter, L. A., Marso, S. P., Rossing, P., et al. (2020). Effects of once-weekly subcutaneous semaglutide on kidney function and safety in patients with type 2 diabetes: a post-hoc analysis of the SUSTAIN 1-7 randomised controlled trials. *lancet Diabetes and Endocrinol.* 8 (11), 880–893. doi:10.1016/s2213-8587(20)30313-2

Mann, J. F. E., Ørsted, D. D., Brown-Frandsen, K., Marso, S. P., Poulter, N. R., Rasmussen, S., et al. (2017). Liraglutide and renal outcomes in type 2 diabetes. *N. Engl. J. Med.* 377 (9), 839–848. doi:10.1056/NEJMoa1616011

Marso, S. P., Bain, S. C., Consoli, A., Eliaschewitz, F. G., Jódar, E., Leiter, L. A., et al. (2016b). Semaglutide and cardiovascular outcomes in patients with type 2 diabetes. *N. Engl. J. Med.* 375 (19), 1834–1844. doi:10.1056/NEJMoa1607141

Marso, S. P., Daniels, G. H., Brown-Frandsen, K., Kristensen, P., Mann, J. F., Nauck, M. A., et al. (2016a). Liraglutide and cardiovascular outcomes in type 2 diabetes. *N. Engl. J. Med.* 375 (4), 311–322. doi:10.1056/NEJMoa1603827

Mauricio, D., Gratacòs, M., and Franch-Nadal, J. (2023). Diabetic microvascular disease in non-classical beds: the hidden impact beyond the retina, the kidney, and the peripheral nerves. *Cardiovasc. Diabetol.* 22 (1), 314. doi:10.1186/s12933-023-02056-3

Mayer, A. L., Scheitacker, I., Ebert, N., Klein, T., Amann, K., and Daniel, C. (2021). The dipeptidyl peptidase 4 inhibitor linagliptin ameliorates renal injury and accelerated resolution in a rat model of crescentic nephritis. *Br. J. Pharmacol.* 178 (4), 878–895. doi:10.1111/bph.15320

Mc Causland, F. R., Claggett, B. L., Vaduganathan, M., Desai, A. S., Jhund, P., de Boer, R. A., et al. (2023). Dapagliflozin and kidney outcomes in patients with heart failure with mildly reduced or preserved ejection fraction: a prespecified analysis of the DELIVER randomized clinical trial. *JAMA Cardiol.* 8 (1), 56–65. doi:10.1001/jamacardio.2022.4210

McGuire, D. K., Van de Werf, F., Armstrong, P. W., Standl, E., Koglin, J., Green, J. B., et al. (2016). Association between sitagliptin use and heart failure hospitalization and related outcomes in type 2 diabetes mellitus: secondary analysis of a randomized clinical trial. *JAMA Cardiol.* 1 (2), 126–135. doi:10.1001/jamacardio.2016.0103

McMurray, J. J. V., Solomon, S. D., Inzucchi, S. E., Køber, L., Kosiborod, M. N., Martinez, F. A., et al. (2019). Dapagliflozin in patients with heart failure and reduced ejection fraction. *N. Engl. J. Med.* 381 (21), 1995–2008. doi:10.1056/NEJMoa1911303

Meng, J., Zhang, W., Wang, C., Xiong, S., Wang, Q., Li, H., et al. (2020). The dipeptidyl peptidase (DPP)-4 inhibitor trelagliptin inhibits IL-1β-induced endothelial inflammation and monocytes attachment. *Int. Immunopharmacol.* 89 (Pt B), 106996. doi:10.1016/j.intimp.2020.106996

Min, J., Wu, L., Liu, Y., Song, G., Deng, Q., Jin, W., et al. (2023). Empagliflozin attenuates trastuzumab-induced cardiotoxicity through suppression of DNA damage and ferroptosis. *Life Sci.* 312, 121207. doi:10.1016/j.lfs.2022.121207

Mosenzon, O., Leibowitz, G., Bhatt, D. L., Cahn, A., Hirshberg, B., Wei, C., et al. (2017). Effect of saxagliptin on renal outcomes in the SAVOR-TIMI 53 trial. *Diabetes care* 40 (1), 69–76. doi:10.2337/dc16-0621

Müller, T. D., Finan, B., Bloom, S. R., D'Alessio, D., Drucker, D. J., Flatt, P. R., et al. (2019). Glucagon-like peptide 1 (GLP-1). *Mol. Metab.* 30, 72–130. doi:10.1016/j.molmet.2019.09.010

Muskiet, M. H. A., Tonneijck, L., Smits, M. M., Kramer, M. H. H., Ouwens, D. M., Hartmann, B., et al. (2020). Effects of DPP-4 inhibitor linagliptin versus sulfonylurea glimepiride as add-on to metformin on renal physiology in overweight patients with type 2 diabetes (renalis): a randomized, double-blind trial. *Diabetes care* 43 (11), 2889–2893. doi:10.2337/dc20-0902

Muskiet, M. H. A., Tonneijck, L., Smits, M. M., Kramer, M. H. H., Ouwens, D. M., Hartmann, B., et al. (2022). Postprandial renal haemodynamic effects of the dipeptidyl peptidase-4 inhibitor linagliptin versus the sulphonylurea glimepiride in adults with type 2 diabetes (RENALIS): a predefined substudy of a randomized, double-blind trial. *Diabetes, Obes. metabolism* 24 (1), 115–124. doi:10.1111/dom.14557

Nauck, M. A., McGuire, D. K., Pieper, K. S., Lokhnygina, Y., Strandberg, T. E., Riefflin, A., et al. (2019). Sitagliptin does not reduce the risk of cardiovascular death or hospitalization for heart failure following myocardial infarction in patients with diabetes: observations from TECOS. *Cardiovasc. Diabetol.* 18 (1), 116. doi:10.1186/s12933-019-0921-2

Navaneethan, S. D., Zoungas, S., Caramori, M. L., Chan, J. C. N., Heerspink, H. J. L., Hurst, C., et al. (2023). Diabetes management in chronic kidney disease: synopsis of the 2020 KDIGO clinical practice guideline. *Ann. Intern Med.* 176 (3), 385–394. doi:10.7326/M20-5938

Nistala, R., Meuth, A. I., Smith, C., An, J., Habibi, J., Hayden, M. R., et al. (2021). DPP4 inhibition mitigates ANG II-mediated kidney immune activation and injury in male mice. *Am. J. physiology Ren. physiology* 320 (3), F505–f517. doi:10.1152/ajprenal.00565.2020

Packer, M. (2020a). SGLT2 inhibitors produce cardiorenal benefits by promoting adaptive cellular reprogramming to induce a state of fasting mimicry: a paradigm shift in understanding their mechanism of action. *Diabetes care* 43 (3), 508–511. doi:10.2337/dci19-0074

Packer, M. (2020b). Interplay of adenosine monophosphate-activated protein kinase/sirtuin-1 activation and sodium influx inhibition mediates the renal benefits of sodium-glucose co-transporter-2 inhibitors in type 2 diabetes: a novel conceptual framework. *Diabetes, Obes. metabolism* 22 (5), 734–742. doi:10.1111/dom.13961

Pan, X., Yang, L., Wang, S., Liu, Y., Yue, L., and Chen, S. (2023). Semaglutide alleviates inflammation-Induced endothelial progenitor cells injury by inhibiting MiR-155 expression in macrophage exosomes. *Int. Immunopharmacol.* 119, 110196. doi:10.1016/j.intimp.2023.110196

Panico, C., Bonora, B., Camera, A., Chilelli, N. C., Prato, G. D., Favacchio, G., et al. (2023). Pathophysiological basis of the cardiological benefits of SGLT-2 inhibitors: a narrative review. *Cardiovasc. Diabetol.* 22 (1), 164. doi:10.1186/s12933-023-01855-y

Park, S., Jeong, H. E., Lee, H., You, S. C., and Shin, J. Y. (2023). Association of sodium-glucose cotransporter 2 inhibitors with post-discharge outcomes in patients with acute heart failure with type 2 diabetes: a cohort study. *Cardiovasc. Diabetol.* 22 (1), 191. doi:10.1186/s12933-023-01896-3

Perkovic, V., Jardine, M. J., Neal, B., Bompoint, S., Heerspink, H. J. L., Charytan, D. M., et al. (2019). Canagliflozin and renal outcomes in type 2 diabetes and nephropathy. *N. Engl. J. Med.* 380 (24), 2295–2306. doi:10.1056/NEJMoa1811744

Perkovic, V., Toto, R., Cooper, M. E., Mann, J. F. E., Rosenstock, J., McGuire, D. K., et al. (2020). Effects of linagliptin on cardiovascular and kidney outcomes in people with normal and reduced kidney function: secondary analysis of the CARMELINA randomized trial. *Diabetes care* 43 (8), 1803–1812. doi:10.2337/dc20-0279

Peyton, K. J., Behnammanesh, G., Durante, G. L., and Durante, W. (2022). Canagliflozin inhibits human endothelial cell inflammation through the induction of heme oxygenase-1. *Int. J. Mol. Sci.* 23 (15), 8777. doi:10.3390/ijms23158777

Pfeffer, M. A., Claggett, B., Diaz, R., Dickstein, K., Gerstein, H. C., Køber, L. V., et al. (2015). Lixisenatide in patients with type 2 diabetes and acute coronary syndrome. *N. Engl. J. Med.* 373 (23), 2247–2257. doi:10.1056/NEJMoa1509225

Pham, T. K., Nguyen, T. H. T., Yi, J. M., Kim, G. S., Yun, H. R., Kim, H. K., et al. (2023). Evogliptin, a DPP-4 inhibitor, prevents diabetic cardiomyopathy by alleviating cardiac lipotoxicity in db/db mice. *Exp. Mol. Med.* 55 (4), 767–778. doi:10.1038/s12276-023-00958-6

Poonchuay, N., Wattana, K., and Uitrakul, S. (2022). Efficacy of linagliptin on cardiovascular risk and cardiometabolic parameters in Thai patients with type 2 diabetes mellitus: a real-world observational study. *Diabetes and metabolic syndrome* 16 (5), 102498. doi:10.1016/j.dsx.2022.102498

Quagliariello, V., De Laurentiis, M., Rea, D., Barbieri, A., Monti, M. G., Carbone, A., et al. (2021). The SGLT-2 inhibitor empagliflozin improves myocardial strain, reduces cardiac fibrosis and pro-inflammatory cytokines in non-diabetic mice treated with doxorubicin. *Cardiovasc. Diabetol.* 20 (1), 150. doi:10.1186/s12933-021-01346-y

Rahmoune, H., Thompson, P. W., Ward, J. M., Smith, C. D., Hong, G., and Brown, J. (2005). Glucose transporters in human renal proximal tubular cells isolated from the urine of patients with non-insulin-dependent diabetes. *Diabetes* 54 (12), 3427–3434. doi:10.2337/diabetes.54.12.3427

Ren, C., Sun, K., Zhang, Y., Hu, Y., Hu, B., Zhao, J., et al. (2021). Sodium-glucose CoTransporter-2 inhibitor empagliflozin ameliorates sunitinib-induced cardiac dysfunction via regulation of AMPK-mTOR signaling pathway-mediated autophagy. *Front. Pharmacol.* 12, 664181. doi:10.3389/fphar.2021.664181

Rosa, C. M., Campos, D. H. S., Reyes, D. R. A., Damatto, F. C., Kurosaki, L. Y., Pagan, L. U., et al. (2022). Effects of the SGLT2 inhibition on cardiac remodeling in streptozotocin-induced diabetic rats, a model of type 1 diabetes mellitus. *Antioxidants* 11 (5), 982. doi:10.3390/antiox11050982

Rosenstock, J., Perkovic, V., Johansen, O. E., Cooper, M. E., Kahn, S. E., Marx, N., et al. (2019). Effect of linagliptin vs placebo on major cardiovascular events in adults with type 2 diabetes and high cardiovascular and renal risk: the CARMELINA randomized clinical trial. *Jama* 321 (1), 69–79. doi:10.1001/jama.2018.18269

Rossing, P., Baeres, F. M. M., Bakris, G., Bosch-Traberg, H., Gislum, M., Gough, S. C. L., et al. (2023). The rationale, design and baseline data of FLOW, a kidney outcomes trial with once-weekly semaglutide in people with type 2 diabetes and chronic kidney disease. *Nephrol. Dial. Transplant.* 38 (9), 2041–2051. doi:10.1093/ndt/gfad009

Säemann, M., and Kronbichler, A. (2022). Call for action in ANCA-associated vasculitis and lupus nephritis: promises and challenges of SGLT-2 inhibitors. *Ann. rheumatic Dis.* 81 (5), 614–617. doi:10.1136/annrheumdis-2021-221474

Scirica, B. M., Bhatt, D. L., Braunwald, E., Steg, P. G., Davidson, J., Hirshberg, B., et al. (2013). Saxagliptin and cardiovascular outcomes in patients with type 2 diabetes mellitus. *N. Engl. J. Med.* 369 (14), 1317–1326. doi:10.1056/NEJMoa1307684

Scisciola, L., Taktaz, F., Fontanella, R. A., Pesapane, A., Surina, Cataldo, V., et al. (2023). Targeting high glucose-induced epigenetic modifications at cardiac level: the role of SGLT2 and SGLT2 inhibitors. *Cardiovasc. Diabetol.* 22 (1), 24. doi:10.1186/s12933-023-01754-2

Sforza, A., Vigorelli, V., Rurali, E., Perrucci, G. L., Gambini, E., Arici, M., et al. (2022). Liraglutide preserves CD34(+) stem cells from dysfunction Induced by high glucose exposure. *Cardiovasc. Diabetol.* 21 (1), 51. doi:10.1186/s12933-022-01486-9

Shaman, A. M., Bain, S. C., Bakris, G. L., Buse, J. B., Idorn, T., Mahaffey, K. W., et al. (2022). Effect of the glucagon-like peptide-1 receptor agonists semaglutide and liraglutide on kidney outcomes in patients with type 2 diabetes: pooled analysis of SUSTAIN 6 and LEADER. *Circulation* 145 (8), 575–585. doi:10.1161/circulationaha.121.055459

Sharaf, G., E M, E. M., and El-Sayed, E. K. (2023). Augmented nephroprotective effect of liraglutide and rabeprazole via inhibition of OCT2 transporter in cisplatin-induced nephrotoxicity in rats. *Life Sci.* 321, 121609. doi:10.1016/j.lfs.2023.121609

Sharma, A., Wood, S., Bell, J. S., De Blasio, M. J., Ilomäki, J., and Ritchie, R. H. (2023). Sex differences in risk of cardiovascular events and mortality with sodium glucose co-transporter-2 inhibitors versus glucagon-like peptide 1 receptor agonists in Australians with type 2 diabetes: a population-based cohort study. *Lancet regional health West. Pac.* 33, 100692. doi:10.1016/j.lanwpc.2023.100692

Solomon, S. D., McMurray, J. J. V., Claggett, B., de Boer, R. A., DeMets, D., Hernandez, A. F., et al. (2022). Dapagliflozin in heart failure with mildly reduced or preserved ejection fraction. *N. Engl. J. Med.* 387 (12), 1089–1098. doi:10.1056/NEJMoa2206286

Su, K., Yi, B., Yao, B. Q., Xia, T., Yang, Y. F., Zhang, Z. H., et al. (2020). Liraglutide attenuates renal tubular ectopic lipid deposition in rats with diabetic nephropathy by inhibiting lipid synthesis and promoting lipolysis. *Pharmacol. Res.* 156, 104778. doi:10.1016/j.phrs.2020.104778

Sukumaran, V., Tsuchimochi, H., Sonobe, T., Shirai, M., and Pearson, J. T. (2019). Liraglutide improves renal endothelial function in obese zucker rats on a high-salt diet. *J. Pharmacol. Exp. Ther.* 369 (3), 375–388. doi:10.1124/jpet.118.254821

Sun, H., Saeedi, P., Karuranga, S., Pinkepank, M., Ogurtsova, K., Duncan, B. B., et al. (2022). IDF Diabetes Atlas: global, regional and country-level diabetes prevalence estimates for 2021 and projections for 2045. *Diabetes Res. Clin. Pract.* 183, 109119. doi:10.1016/j.diabres.2021.109119

Sun, X., Han, F., Lu, Q., Li, X., Ren, D., Zhang, J., et al. (2020). Empagliflozin ameliorates obesity-related cardiac dysfunction by regulating sestrin2-mediated AMPK-mTOR signaling and redox homeostasis in high-fat diet-induced obese mice. *Diabetes* 69 (6), 1292–1305. doi:10.2337/db19-0991

Tang, P. M., Zhang, Y. Y., Hung, J. S., Chung, J. Y., Huang, X. R., To, K. F., et al. (2021). DPP4/CD32b/NF-κB circuit: a novel druggable target for inhibiting CRP-driven diabetic nephropathy. *Mol. Ther. J. Am. Soc. Gene Ther.* 29 (1), 365–375. doi:10.1016/j.ymthe.2020.08.017

Tschöp, M., Nogueiras, R., and Ahrén, B. (2023). Gut hormone-based pharmacology: novel formulations and future possibilities for metabolic disease therapy. *Diabetologia* 66 (10), 1796–1808. doi:10.1007/s00125-023-05929-0

Tuttle, K. R., Bosch-Traberg, H., Cherney, D. Z. I., Hadjadj, S., Lawson, J., Mosenzon, O., et al. (2023). *Post hoc* analysis of SUSTAIN 6 and PIONEER 6 trials suggests that people with type 2 diabetes at high cardiovascular risk treated with semaglutide experience more stable kidney function compared with placebo. *Kidney Int.* 103 (4), 772–781. doi:10.1016/j.kint.2022.12.028

Voors, A. A., Angermann, C. E., Teerlink, J. R., Collins, S. P., Kosiborod, M., Biegus, J., et al. (2022). The SGLT2 inhibitor empagliflozin in patients hospitalized for acute heart failure: a multinational randomized trial. *Nat. Med.* 28 (3), 568–574. doi:10.1038/s41591-021-01659-1

Wadie, W., Ahmed, G. S., Shafik, A. N., and El-Sayed, M. (2022). Effects of insulin and sitagliptin on early cardiac dysfunction in diabetic rats. *Life Sci.* 299, 120542. doi:10.1016/j.lfs.2022.120542

Wang, H., Li, T., Sun, F., Liu, Z., Zhang, D., Teng, X., et al. (2022). Safety and efficacy of the SGLT2 inhibitor dapagliflozin in patients with systemic lupus erythematosus: a phase I/II trial. *RMD open* 8 (2), e002686. doi:10.1136/rmdopen-2022-002686

Wang, Y., He, W., Wei, W., Mei, X., Yang, M., and Wang, Y. (2021). Exenatide attenuates obesity-induced mitochondrial dysfunction by activating SIRT1 in renal tubular cells. *Front. Endocrinol.* 12, 622737. doi:10.3389/fendo.2021.622737

Wanner, C., Cooper, M. E., Johansen, O. E., Toto, R., Rosenstock, J., McGuire, D. K., et al. (2021). Effect of linagliptin versus placebo on cardiovascular and kidney outcomes in nephrotic-range proteinuria and type 2 diabetes: the CARMELINA randomized controlled trial. *Clin. kidney J.* 14 (1), 226–236. doi:10.1093/ckj/sfaa225

White, W. B., Cannon, C. P., Heller, S. R., Nissen, S. E., Bergenstal, R. M., Bakris, G. L., et al. (2013). Alogliptin after acute coronary syndrome in patients with type 2 diabetes. *N. Engl. J. Med.* 369 (14), 1327–1335. doi:10.1056/NEJMoa1305889

Withaar, C., Meems, L. M. G., Nollet, E. E., Schouten, E. M., Schroeder, M. A., Knudsen, L. B., et al. (2023). The cardioprotective effects of semaglutide exceed those of dietary weight loss in mice with HFpEF. *JACC Basic Transl. Sci.* 8 (10), 1298–1314. doi:10.1016/j.jacbts.2023.05.012

Wiviott, S. D., Raz, I., Bonaca, M. P., Mosenzon, O., Kato, E. T., Cahn, A., et al. (2019). Dapagliflozin and cardiovascular outcomes in type 2 diabetes. *N. Engl. J. Med.* 380 (4), 347–357. doi:10.1056/NEJMoa1812389

Wójcicka, G., Pradiuch, A., Fornal, E., Stachniuk, A., Korolczuk, A., Marzec-Kotarska, B., et al. (2023). The effect of exenatide (a GLP-1 analogue) and sitagliptin (a DPP-4 inhibitor) on asymmetric dimethylarginine (ADMA) metabolism and selected biomarkers of cardiac fibrosis in rats with fructose-induced metabolic syndrome. *Biochem. Pharmacol.* 214, 115637. doi:10.1016/j.bcp.2023.115637

Xiao, B., Sanders, M. J., Underwood, E., Heath, R., Mayer, F. V., Carmena, D., et al. (2011). Structure of mammalian AMPK and its regulation by ADP. *Nature* 472 (7342), 230–233. doi:10.1038/nature09932

Xie, Y., Bowe, B., Xian, H., Loux, T., McGill, J. B., and Al-Aly, Z. (2023). Comparative effectiveness of SGLT2 inhibitors, GLP-1 receptor agonists, DPP-4 inhibitors, and sulfonylureas on risk of major adverse cardiovascular events: emulation of a randomised target trial using electronic health records. *lancet Diabetes and Endocrinol.* 11 (9), 644–656. doi:10.1016/s2213-8587(23)00171-7

Xu, C., Lu, C., Wang, Z., Hu, X., Li, S., Xie, Y., et al. (2023). Liraglutide abrogates nephrotoxic effects of chemotherapies. *Pharmacol. Res.* 189, 106680. doi:10.1016/j.phrs.2023.106680

Xu, J., Kitada, M., Ogura, Y., Liu, H., and Koya, D. (2021). Dapagliflozin restores impaired autophagy and suppresses inflammation in high glucose-treated HK-2 cells. *Cells* 10 (6), 1457. doi:10.3390/cells10061457

Yang, S., Lin, C., Zhuo, X., Wang, J., Rao, S., Xu, W., et al. (2020). Glucagon-like peptide-1 alleviates diabetic kidney disease through activation of autophagy by regulating AMP-activated protein kinase-mammalian target of rapamycin pathway. *Am. J. physiology Endocrinol. metabolism* 319 (6), E1019–E1030. doi:10.1152/ajpendo.00195.2019

Yi, T. W., Smyth, B., Di Tanna, G. L., Arnott, C., Cardoza, K., Kang, A., et al. (2023). Kidney and cardiovascular effects of canagliflozin according to age and sex: a *post hoc* analysis of the CREDENCE randomized clinical trial. *Am. J. kidney Dis.* 82 (1), 84–96.e1. doi:10.1053/j.ajkd.2022.12.015

Yin, R., Xu, Y., Wang, X., Yang, L., and Zhao, D. (2022). Role of dipeptidyl peptidase 4 inhibitors in antidiabetic treatment. *Mol.* 27 (10), 3055. doi:10.3390/molecules27103055

Yoon, S. A., Han, B. G., Kim, S. G., Han, S. Y., Jo, Y. I., Jeong, K. H., et al. (2017). Efficacy, safety and albuminuria-reducing effect of gemigliptin in Korean type 2 diabetes patients with moderate to severe renal impairment: a 12-week, double-blind randomized study (the GUARD Study). *Diabetes, Obes. metabolism* 19 (4), 590–598. doi:10.1111/dom.12863

Zhang, L., Tian, J., Diao, S., Zhang, G., Xiao, M., and Chang, D. (2020). GLP-1 receptor agonist liraglutide protects cardiomyocytes from IL-1β-induced metabolic disturbance and mitochondrial dysfunction. *Chemico-biological Interact.* 332, 109252. doi:10.1016/j.cbi.2020.109252

Zhang, Y., Bao, M., Dai, M., Wang, X., He, W., Tan, T., et al. (2015). Cardiospecific CD36 suppression by lentivirus-mediated RNA interference prevents cardiac hypertrophy and systolic dysfunction in high-fat-diet induced obese mice. *Cardiovasc. Diabetol.* 14, 69. doi:10.1186/s12933-015-0234-z

Zhao, D., Guallar, E., Ouyang, P., Subramanya, V., Vaidya, D., Ndumele, C. E., et al. (2018). Endogenous sex hormones and incident cardiovascular disease in post-menopausal women. *J. Am. Coll. Cardiol.* 71 (22), 2555–2566. doi:10.1016/j.jacc.2018.01.083

Zhao, J., He, X., Zuo, M., Li, X., and Sun, Z. (2021). Anagliptin prevented interleukin 1β (IL-1β)-induced cellular senescence in vascular smooth muscle cells through increasing the expression of sirtuin1 (SIRT1). *Bioengineered* 12 (1), 3968–3977. doi:10.1080/21655979.2021.1948289

Zhao, X. Y., Li, S. S., He, Y. X., Yan, L. J., Lv, F., Liang, Q. M., et al. (2023). SGLT2 inhibitors alleviated podocyte damage in lupus nephritis by decreasing inflammation and enhancing autophagy. *Ann. rheumatic Dis.* 82 (10), 1328–1340. doi:10.1136/ard-2023-224242

Zheng, R. H., Zhang, W. W., Ji, Y. N., Bai, X. J., Yan, C. P., Wang, J., et al. (2020). Exogenous supplement of glucagon like peptide-1 protects the heart against aortic banding induced myocardial fibrosis and dysfunction through inhibiting mTOR/p70S6K signaling and promoting autophagy. *Eur. J. Pharmacol.* 883, 173318. doi:10.1016/j.ejphar.2020.173318

frontiers | Frontiers in Pharmacology

TYPE Original Research
PUBLISHED 10 May 2024
DOI 10.3389/fphar.2024.1364827



OPEN ACCESS

EDITED BY
Anca Hermenean,
Vasile Goldis Western University of Arad, Romania

REVIEWED BY
Syed Anees Ahmed,
East Carolina University, United States
Andrea Elia,
Temple University, United States
Vajir M. Malek,
City of Hope, United States

*CORRESPONDENCE
Yun Zhang,
zhangyun@sdu.edu.cn
Wenhai Sui,
swh@email.sdu.edu.cn
Fei Xue,
xuefei93xf@163.com

RECEIVED 03 January 2024
ACCEPTED 20 March 2024
PUBLISHED 10 May 2024

CITATION
Xie L, Zang D, Yang J, Xue F, Sui W and Zhang Y (2024), Combination of ADAM17 knockdown with eplerenone is more effective than single therapy in ameliorating diabetic cardiomyopathy.
*Front. Pharmacol.* 15:1364827.
doi: 10.3389/fphar.2024.1364827



# Combination of ADAM17 knockdown with eplerenone is more effective than single therapy in ameliorating diabetic cardiomyopathy

Lin Xie[1], Dejin Zang[1], Jianmin Yang[1], Fei Xue[1]*, Wenhai Sui[1]* and Yun Zhang[1,2]*

[1]National Key Laboratory for Innovation and Transformation of Luobing Theory, The Key Laboratory of Cardiovascular Remodeling and Function Research, Chinese Ministry of Education, Chinese National Health Commission and Chinese Academy of Medical Sciences, Department of Cardiology, Qilu Hospital of Shandong University, Jinan, China, [2]Cardiovascular Disease Research Center of Shandong First Medical University, Central Hospital Affiliated to Shandong First Medical University, Jinan, China

**Background:** The renin-angiotensin-aldosterone system (RAAS) members, especially Ang II and aldosterone, play key roles in the pathogenesis of diabetic cardiomyopathy (DCM). Angiotensin-converting enzyme inhibitors or angiotensin-receptor blockers combined with aldosterone receptor antagonists (mineralocorticoid receptor antagonists) have substantially improved clinical outcomes in patients with DCM. However, the use of the combination has been limited due to its high risk of inducing hyperkalemia.

**Methods:** Type 1 diabetes was induced in 8-week-old male C57BL/6J mice by intraperitoneal injection of streptozotocin at a dose of 55 mg/kg for 5 consecutive days. Adeno-associated virus 9-mediated short-hairpin RNA (shRNA) was used to knock down the expression of ADAM17 in mice hearts. Eplerenone was administered via gavage at 200 mg/kg daily for 4 weeks. Primary cardiac fibroblasts were exposed to high glucose (HG) *in vitro* for 24 h to examine the cardiac fibroblasts to myofibroblasts transformation (CMT).

**Results:** Cardiac collagen deposition and CMT increased in diabetic mice, leading to cardiac fibrosis and dysfunction. In addition, ADAM17 expression and activity increased in the hearts of diabetic mice. ADAM17 inhibition and eplerenone treatment both improved diabetes-induced cardiac fibrosis, cardiac hypertrophy and cardiac dysfunction, ADAM17 deficiency combined with eplerenone further reduced the effects of cardiac fibrosis, cardiac hypertrophy and cardiac dysfunction compared with single therapy *in vivo*. High-glucose stimulation promotes CMT *in vitro* and leads to increased ADAM17 expression and activity. ADAM17 knockdown and eplerenone pretreatment can reduce the CMT of fibroblasts that is induced by high glucose levels by inhibiting TGFβ1/Smad3 activation; the combination of the two can further reduce CMT compared with single therapy *in vitro*.

**Conclusion:** Our findings indicated that ADAM17 knockout could improve diabetes-induced cardiac dysfunction and remodeling through the inhibition of RAAS overactivation when combined with eplerenone treatment, which reduced TGF-β1/Smad3 pathway activation-mediated CMT. The combined intervention of ADAM17 deficiency and eplerenone therapy provided

additional cardiac protection compared with a single therapy alone without disturbing potassium level. Therefore, the combination of ADAM17 inhibition and eplerenone is a potential therapeutic strategy for human DCM.

KEYWORDS

diabetic cardiomyopathy, ADAM17, eplerenone, RAAS, fibrosis

## Introduction

The prevalence of diabetes mellitus (DM) has been continually increasing in the past decade, imposing a heavy burden on global public health. Cardiovascular complications secondary to DM have become a major challenge in the field of cardiovascular medicine (Bugger and Abel, 2014). Diabetic cardiomyopathy (DCM) was initially described as a human pathophysiological condition in which heart failure occurred in the absence of coronary artery disease, hypertension, and valvular heart disease, which considerably contribute to the increased mortality of diabetes mellitus worldwide (Dillmann, 2019). Despite numerous studies on DCM, there are few effective therapies. In addition, the pathology and molecular mechanism of DCM are yet unclear, which hinders the development of effective therapeutic targets. Therefore, further studies on novel therapeutic approaches of DCM treatments are necessary.

DCM initially presents with cardiac hypertrophy, diastolic dysfunction and partially reduced systolic function which leading to clinical restrictions due to heart failure symptoms (Dannenberg et al., 2021). DCM is characterized by myocardial hypertrophy, fibrosis and inflammation, as well as cardiomyocyte death (Boudina and Abel, 2007). There is ample evidence that patients with DM exhibit significant myocardial fibrosis, but no evidence-based therapies have been shown to have a beneficial effect on cardiac fibrosis in patients with diabetes (Dannenberg et al., 2021). Mechanistically, there are several pathological changes associated with DM that leading to cardiac functional alterations, such as metabolic disorders, oxidative stress, inflammatory response, altered calcium signaling, and activation of the renin-angiotensin-aldosterone system (RAAS) play major roles. RAAS

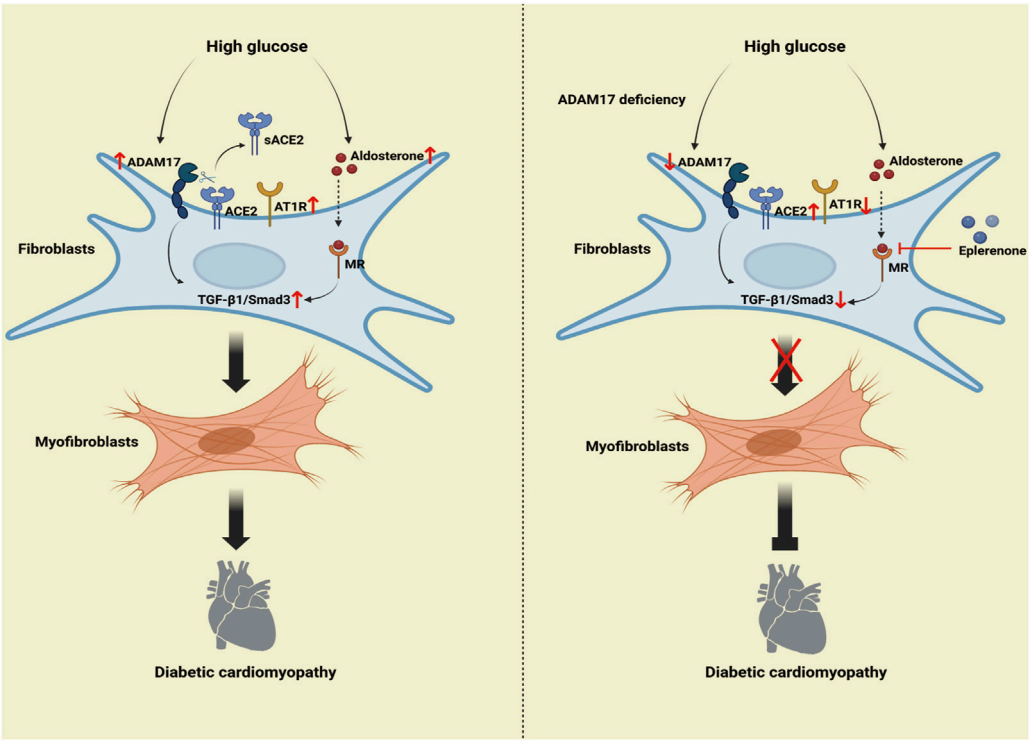


GRAPHICAL ABSTRACT
Mechanism of the roles of combination of ADAM17 knockdown and eplerenone treatment in DCM-induced cardiac fibrosis. The high-glucose activated RAAS increased ADAM17 activity, ACE2 shedding, and AT1R expression, thereby activating TGF-β1/Smad3 signaling in cardiac fibroblasts, which increased myofibroblast transformation and cardiac collagen deposition in DCM. The overactivated RAAS increased aldosterone expression, so aldosterone then bound to aldosterone receptors to further promote TGF-β1/Smad3 pathway-mediated myofibroblast transformation.
ADAM17 deletion weakened ACE2 shedding and AT1R expression, inactivated TGF-β1/Smad3 signaling in myocardial fibroblasts, and resulted in reduced myofibroblast transformation and cardiac collagen deposition in DCM. Moreover, eplerenone acted as an aldosterone receptor antagonist to reduce the aldosterone activation of TGF-β1. Eplerenone combined with ADAM17 deficiency can further reduce the fibroblast transformation and collagen deposition caused by diabetes and improve the cardiac fibrosis and cardiac remodeling caused by DCM compared with when either of the two is used as monotherapy.

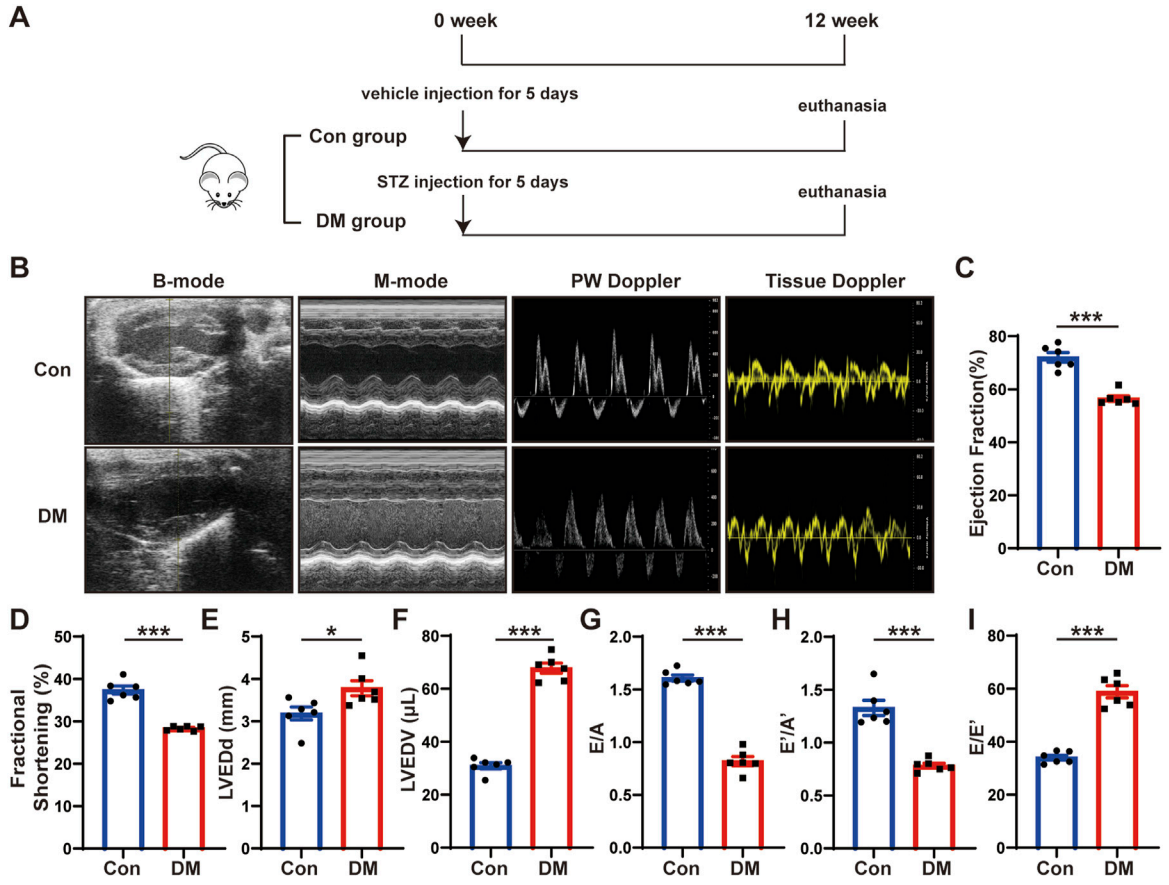


FIGURE 1
Time line of experimental studies *in vivo* and echocardiographic measurements of control and diabetic mice hearts. **(A)** Animal grouping and time line in first part of experimental studies *in vivo*. **(B)** Representative two-dimensional echocardiograms (first row), M-mode echocardiograms (second row), pulse-wave Doppler mode of mitral inflow (third row), and tissue Doppler mode of mitral annulus (fourth row). **(C)** Measurements of left ventricular ejection fraction (LVEF) in two groups of mice. **(D)** Measurements of fractional shortening (FS) in two groups of mice. **(E)** Measurements of left ventricular end-diastolic diameter (LVEDd) in two groups of mice. **(F)** Measurements of left ventricular end-diastolic volume (LVEDV) in two groups of mice. **(G)** Measurements of ratio of early to late left ventricular filling velocity (E/A) in two groups of mice. **(H)** Measurements of ratio of early to late diastolic peak annular velocity (E'/A') in two groups of mice. **(I)** Measurements of the ratio of early diastolic transmittal inflow velocity to early diastolic mitral annulus velocity (E/E') in two groups of mice. Values shown were mean and SEM ($n$ = 6 in each group). *$p$ < 0.05; ***$p$ < 0.001.

members, especially Ang II and aldosterone, play key roles in cardiac fibrosis in DCM (Cambier et al., 2018; Wu et al., 2018). The administration of angiotensin-converting enzyme inhibitors (ACEIs) and angiotensin-receptor blockers (ARBs), as well as aldosterone receptor antagonists (mineralocorticoid receptor antagonists, MRAs), have substantially improved clinical outcomes in patients with DCM, however, these classic treatment are inadequate in counteracting an overactivated RAAS in patients with DCM due to their inherent limitations (Agarwal et al., 2021; Adamo et al., 2022). Therefore, new approaches are urgently needed to counteract RAAS overactivation in patients with DCM.

Eplerenone, a selective aldosterone receptor antagonist (Pitt et al., 2023), has fewer side effects for it is more selective to aldosterone receptors than spironolactone (Agarwal et al., 2021). Moreover, the RAAS plays an important role in the development of diabetic cardiomyopathy (Collier and McDonald, 2012). In a hyperglycemic environment, the local RAAS is often directly overactivated (Dillmann, 2019), causing aldosterone accumulation, which promotes the Ang II activity and fibrosis in the diabetic myocardium by upregulating profibrotic and oxidative mediators (Pitt et al., 2003; Brown, 2013). Improvement in left ventricular hypertrophy and structural remodeling through the use of MRAs has been confirmed in clinical research (Maron and Leopold, 2010; Leung et al., 2013). Johansen *et al.* found that eplerenone suppresses interstitial fibrosis in the subcutaneous adipose tissue of patients with type 2 diabetes (Johansen et al., 2021). Mahajan *et al.* found that eplerenone improved hemodynamic and ventricular dysfunction in streptozotocin (STZ)-isoproterenol-challenged rats (Mahajan et al., 2018). Overall, the potential utility of eplerenone for DCM treatment has been demonstrated in both by clinical and basic research. However, the mechanisms underlying the cardioprotective effects of eplerenone on DCM remain unclear.

A disintegrin and metalloproteinase-17 (ADAM17), also known as tumor necrosis factor-alpha-converting enzyme, is a membrane-bound enzyme that proteolytically releases multiple cell surface proteins such as cytokines and cytokine receptors to regulate their bioavailability (Scheller et al., 2011). In recent years, ADAM17 has been implicated in many etiological factors and in playing an important role in organ interstitial fibrosis, including

liver fibrosis (Cai et al., 2020), lung fibrosis (Liu et al., 2018), kidney fibrosis (Kefaloyianni et al., 2016), and vascular fibrosis (Takayanagi et al., 2016). Furthermore, ADAM17 silencing prevents Ang II-induced cardiac hypertrophy and fibrosis in mice (Wang et al., 2009). ADAM17 acts by regulating angiotensin-converting enzyme-2 (ACE2) shedding, as a member of the RAAS. ACE2 cleaves Ang II to produce angiotensin-(1–7) (Ang 1–7) and thus acts as a negative regulator of the RAAS (Simões e Silva and Teixeira, 2016). Our previous studies showed that ADAM17 increased cardiac fibrosis by regulating ACE2 shedding in diabetic mice (Cheng et al., 2022). ACE2 overexpression improved left ventricular remodeling and function in a rat model of DCM (Dong et al., 2012). Several ADAM17 inhibitors have been screened for cancer research, but the high homology between metalloproteinases active sites has limited the development of highly specific ADAM17 small molecule inhibitors, and the clinical use has been limited due to its potential side effects (Rossello et al., 2016).

Myocardial fibrosis, a pathological change in DCM, contributes to the development of myocardial remodeling (Jia et al., 2018). Approximately 60%–70% of the cells in the heart are cardiac fibroblasts, which normally remain stationary and secrete extracellular collagen, which maintains the structural integrity and normal function of the heart. In DCM, cardiac fibroblasts to myofibroblasts transformation (CMT) is the initial step in myocardial fibrosis (Zhou et al., 2018). Myofibroblasts highly express α-smooth muscle actin (α-SMA) (He et al., 2018). Fibroblast activation protein (FAP), a membrane-bound proline-specific serine protease, is not expressed in normal fibroblasts but is expressed in myofibroblasts, so is a specific marker of myofibroblasts (Goldsmith et al., 2014). In addition, the TGF-β1/Smad3 pathway regulated cardiac fibrosis in mice with myocardial infarction by regulating the CMT. Targeting CMT, which is regulated by TGF-β1, may offer new hope for preventing DCM.

In large-scale clinical trials, the addition of aldosterone receptor antagonists to standard medical therapies, including ACEIs or ARBs, has beneficial effects on the prognosis of patients experiencing heart failure (Nagatomo et al., 2014). However, this treatment increases the risk of hyperkalemia (Leung et al., 2013). ADAM17 knockout and eplerenone can be used to effectively treat DCM. However, whether combination therapy is more effective than single therapy and whether this combination therapy causes adverse side effects, such as hyperkalemia, remains unclear. To test this hypothesis, we investigated the mechanism through which ADAM17 knockout combined with eplerenone therapy ameliorates left ventricular remodeling and function in a mouse model of DCM *in vivo* and whether ADAM17 knockout combined with eplerenone treatment reduces CMT in rat cardiac fibroblasts *in vitro*.

# Materials and methods

## Ethics statement

All animal experimental protocols complied with the Animal Management Rules of the Chinese Ministry of Health (Document no. 55, 2001) and conformed to National Institutes of Health (NIH) guidelines (the Guide for the Care and Use of Laboratory Animals; NIH Publication No. 85-23, revised 1996). All mice were maintained under specific pathogen-free, environmentally controlled (Temperature: 20°C–25°C; humidity: 50% ± 5%) barrier conditions in individual ventilated cages and were fed with sterile food and water.

## Materials

Streptozotocin (STZ) was purchased from MCE (USA). Eplerenone was purchased from BOC Sciences (USA). Masson's trichrome, Sirius red and hematoxylin and eosin (H&E) staining kits were purchased from Solarbio (Beijing, China). Fluorescein isothiocyanate-conjugated wheat germ agglutinin (FITC-conjugated WGA) staining was purchased from Sigma-Aldrich (USA). *In situ* cell death detection kit was purchased from Roche (USA). The SensoLyte 520 TACE (α-secretase) activity assay kit was purchased from AnaSpec, Fremont (CA). RNeasy mini kit was purchased from Qiagen (Germany). The primary antibodies used are listed in Supplementary Table S3 and the primer sequences were listed in Supplementary Table S4.

## Adeno-associated virus 9 mediated gene knockdown

A type 9 adeno-associated virus (AAV9) has been reported to be the most effective virus for cardiac genetic intervention (Pacak et al., 2006). To knock down ADAM17 in the myocardium in C57BL/6J male mice, a AAV9 serotype system carrying scramble shRNA (shNC) and ADAM17 shRNA (shA17) was constructed by Genechem Technologies (Shanghai, China). Each mouse was injected with 200 μL of AAV9-shNC or AAV9-shA17 at a titer of $5 \times 10^{11}$ vg through tail vein.

## Animal model and grouping

The animal experiments were divided into two parts. In the first part of the *in vivo* experiments (Figure 1A), eight-week-old male C57BL/6J mice, purchased from Vital River Laboratory Animal Technology Co., Ltd. (Beijing, China), were used. After 1 week of adaptive feeding, the mice were randomly divided into two groups: a control group and a diabetes mellitus (DM) group. The mice in the DM group were injected intraperitoneally with STZ (MCE, USA) at a dosage of 55 mg/kg daily for five consecutive days, whereas the mice in the control group were injected with citrate buffer alone (Meng et al., 2023). Blood glucose levels were measured using an Accu-Check Active Glucometer (Roche, Shanghai, China). Mice with random glucose levels higher than 16.67 mmol/L were defined as having diabetes. A total of 12 weeks after STZ injection, mice hearts and serum were used for assays. In the second part of the *in vivo* experiments (Figure 3A), eight-week-old male C57BL/6J mice were injected with STZ according to the above-described method and subsequently randomly divided into four groups: DM + shNC + saline, DM + shA17 + saline, DM + shNC + Epl, and DM + shA17 + Epl group. AAV9-A17 knock-down and AAV9-NC viruses were injected to diabetic mice through the tail vein 12 weeks after STZ

10.3389/fphar.2024.1364827

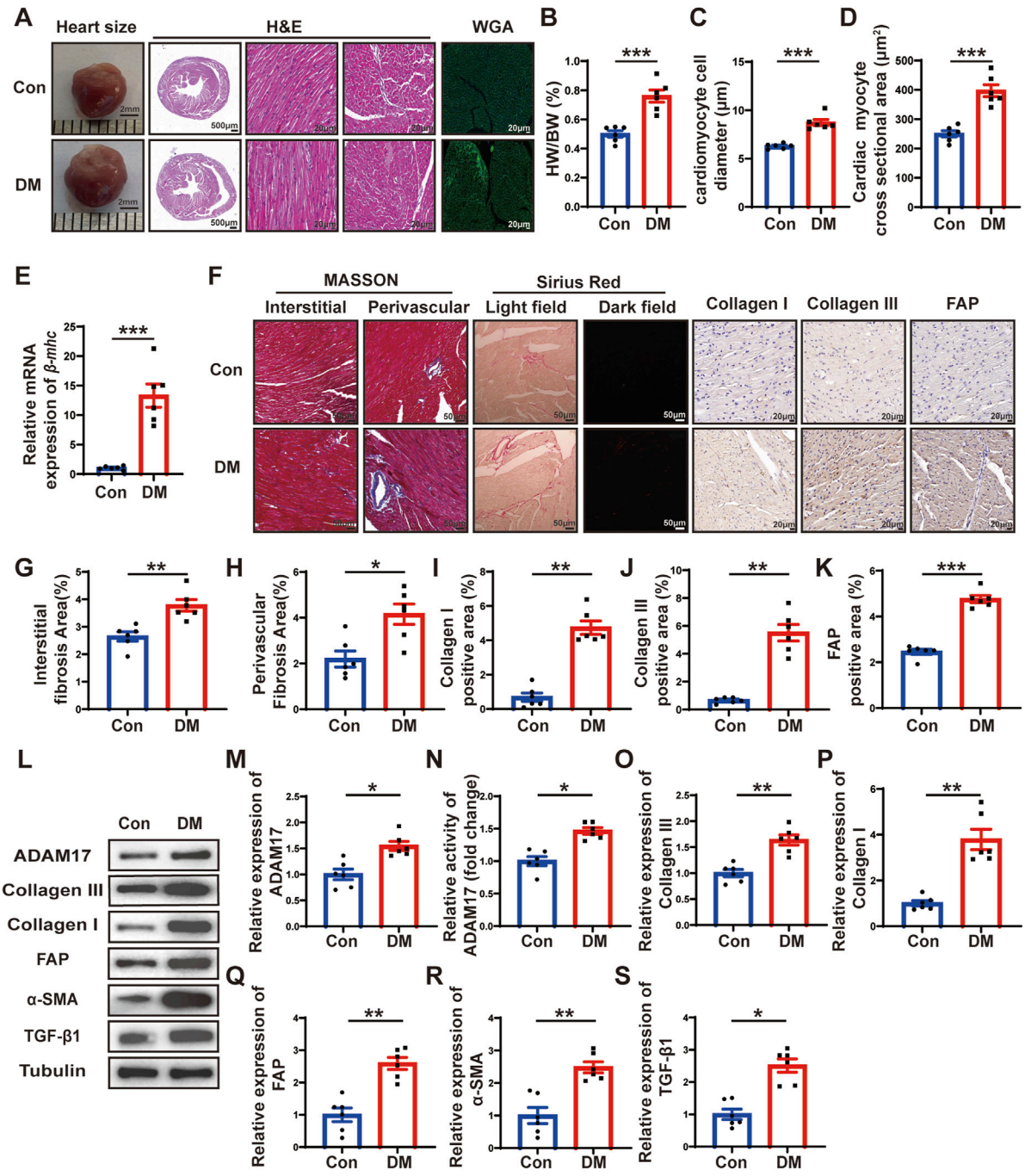


FIGURE 2
Histological staining and ADAM17 and cardiac fibrosis related molecular expression. **(A)** Representative images of heart sizes (scale bar = 2 mm), cardiac cross sections in hematoxylin and eosin (H&E) staining (scale bar = 500 μm), myocardial fiber tissue and cardiomyocyte cell diameter in H&E staining (scale bar = 20 μm), and cardiomyocyte cross-sectional areas in wheat germ agglutinin (WGA) staining (scale bar = 20 μm) in two groups of mice. **(B)** Measurements of heart weight/body weight (HW/BW) ratio in two groups of mice. **(C)** Quantification of the cardiomyocyte cell diameter in H&E staining in two groups of mice. **(D)** Quantification of cardiac myocyte cross-sectional area measured by WGA staining in two groups of mice. **(E)** Quantification of *β-mhc* mRNA expression in two groups of mice. **(F)** Representative Masson's trichrome staining for myocardial interstitial and perivascular fibrosis (scale bar = 50 μm), representative Sirius Red staining for myocardial fibrosis (scale bar = 50 μm), representative Collagen I, Collagen III, and fibroblast activation protein (FAP) staining (scale bar = 50 μm) in two groups of mice. **(G,H)** Quantification of the interstitial and perivascular fibrosis area in two groups of mice. **(I–K)** Quantification of the Collagen I, Collagen III, and FAP expression in two groups of mice. **(L)** Representative Western blotting images of ADAM17, Collagen III, Collagen I, FAP, α-SMA and TGF-β1 expression in two groups of mice. **(M)** Quantification of ADAM17 expression in two groups of mice. **(N)** Quantification of ADAM17 activity in two groups of mice. **(O–S)** Quantification of Collagen III, Collagen I, FAP, α-SMA and TGF-β1 expression in two groups of mice. Values shown were mean and SEM ($n$ = 6 in each group). *$p$ < 0.05; **$p$ < 0.01; ***$p$ < 0.001.

10.3389/fphar.2024.1364827

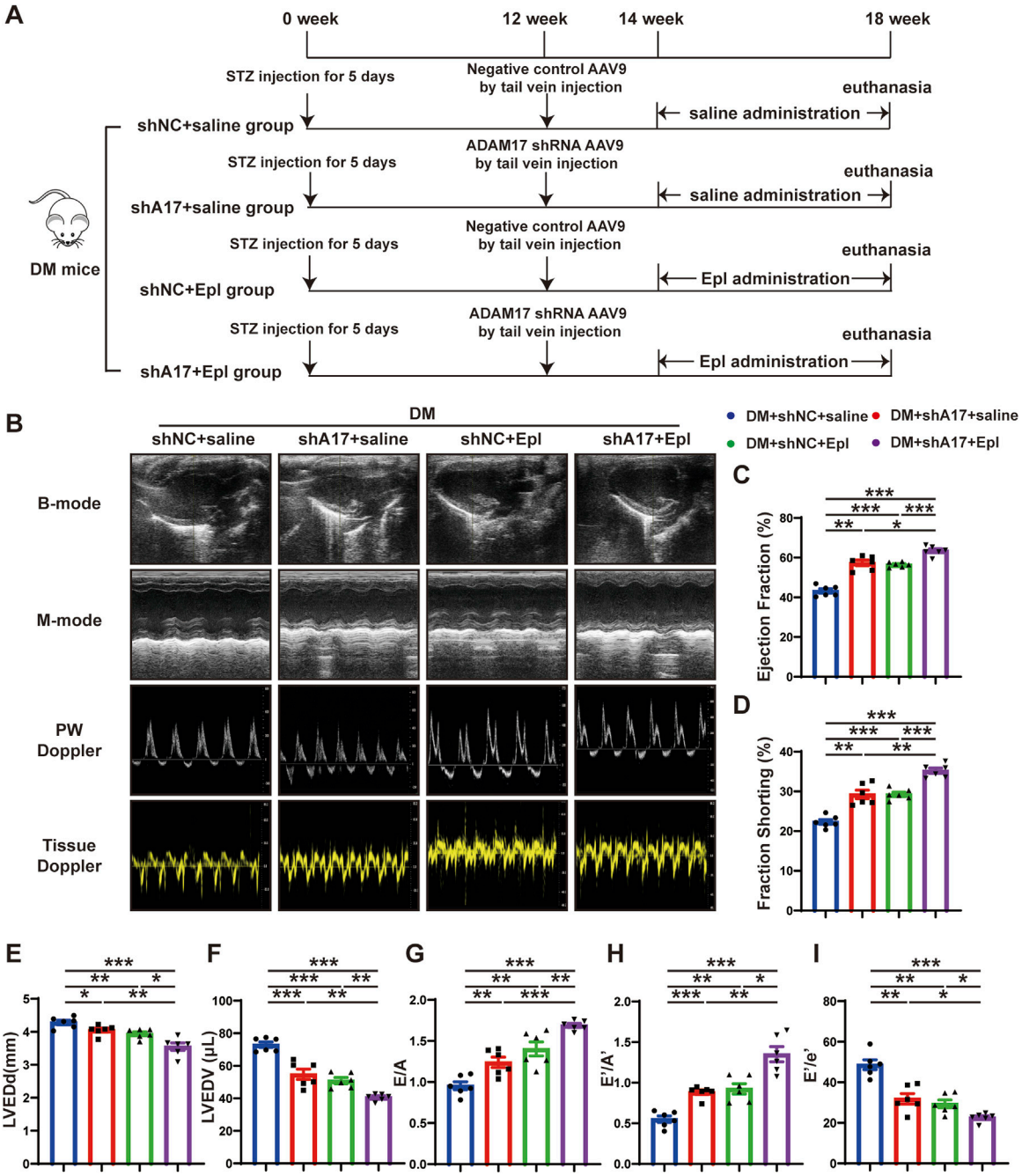


FIGURE 3
Time line of experimental studies *in vivo* and echocardiographic measurements in four groups of mice hearts. **(A)** Animal grouping and time line in second part of experimental studies *in vivo*. **(B)** Representative two-dimensional echocardiograms (first row), M-mode echocardiograms (second row), pulse-wave Doppler mode of mitral inflow (third row), and tissue Doppler mode of mitral annulus (fourth row). **(C)** Measurements of left ventricular ejection fraction (LVEF) in four groups of mice. **(D)** Measurements of fractional shortening (FS) in four groups of mice. **(E)** Measurements of left ventricular end-diastolic diameter (LVEDd) in four groups of mice. **(F)** Measurements of left ventricular end-diastolic volume (LVEDV) in four groups of mice. **(G)** Measurements of ratio of early to late left ventricular filling velocity (E/A) in four groups of mice. **(H)** Measurements of ratio of early to late diastolic peak annular velocity (E′/A′) in four groups of mice. **(I)** Measurements of the ratio of early diastolic transmittal inflow velocity to early diastolic mitral annulus velocity (E/E′) in four mice. Values shown were mean and SEM ($n$ = 6 in each group). *$p$ < 0.05; **$p$ < 0.01; ***$p$ < 0.001.

injection. Eplerenone, was administered at a dosage of 200 mg/kg per day for 1 month starting 2 weeks after AAV9 virus injection based on previous studies. These studies demonstrated that 200 mg/kg per day eplerenone effectively attenuated myocardial fibrosis in the angiotensin II induced hypertensive mouse and inhibited atrial fibrosis in mutant TGF-β1 transgenic mice (Nishioka et al., 2007; Chen XQ. et al., 2016). Consequently, our study employed 200 mg/kg per day dose of eplerenone to explore the

10.3389/fphar.2024.1364827

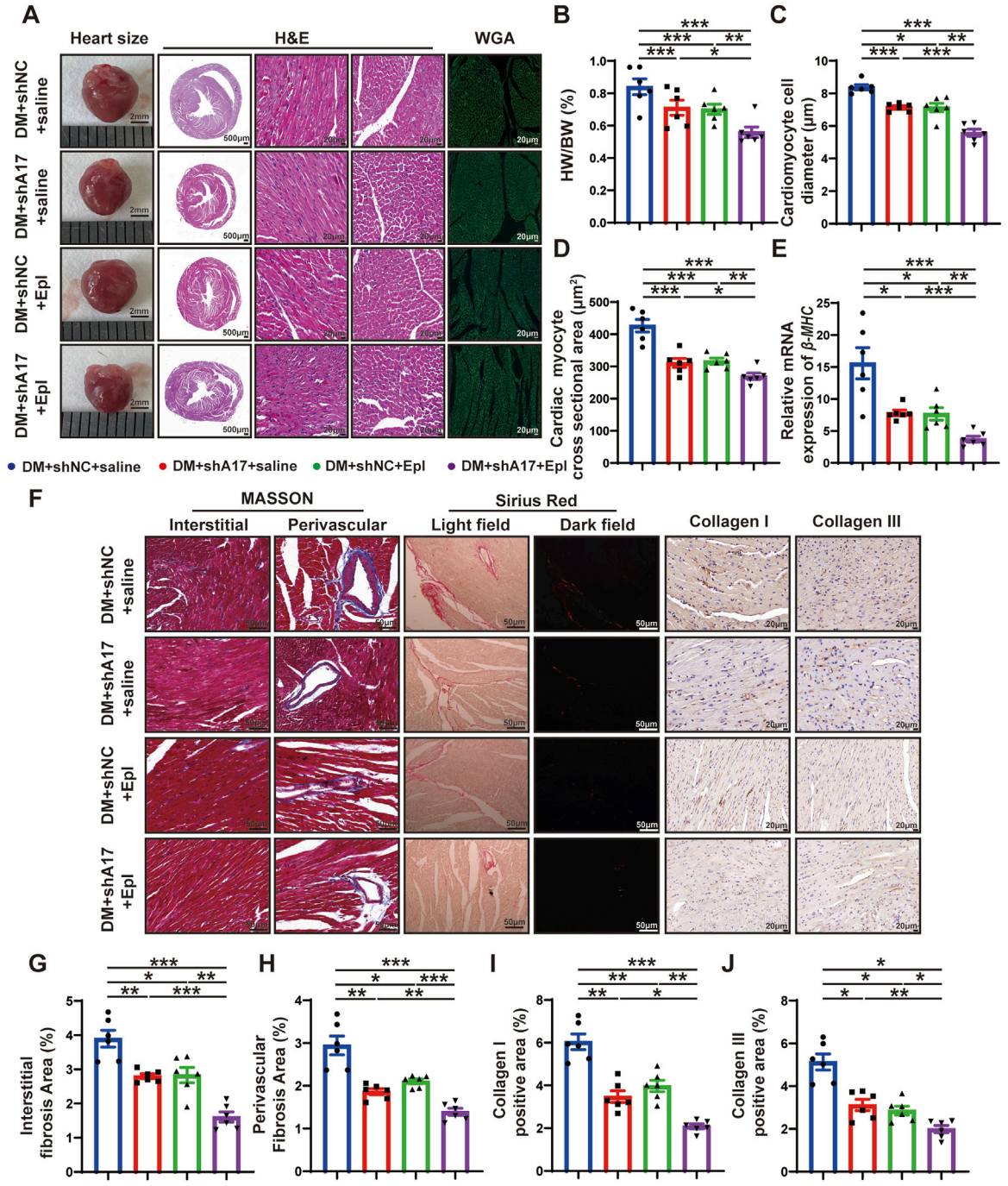


FIGURE 4
Histological staining in four groups of mice hearts. **(A)** Representative images of heart sizes (scale bar = 2 mm), cardiac cross sections in hematoxylin and eosin (H&E) staining (scale bar = 500 μm), myocardial fiber tissue and cardiomyocyte cell diameter in H&E staining (scale bar = 20 μm), and cardiomyocyte cross-sectional areas in wheat germ agglutinin (WGA) staining (scale bar = 20 μm) in four groups of mice. **(B)** Measurements of heart weight/body weight (HW/BW) ratio in four groups of mice. **(C)** Quantification of the cardiomyocyte cell diameter in H&E staining in four groups of mice. **(D)** Quantification of cardiac myocyte cross-sectional area measured by WGA staining in four groups of mice. **(E)** Quantification of *β-mhc* mRNA expression in four groups of mice. **(F)** Representative Masson's trichrome staining for myocardial interstitial and perivascular fibrosis (scale bar = 50 μm), representative Sirius Red staining for myocardial fibrosis (scale bar = 50 μm), representative Collagen I and Collagen III staining (scale bar = 50 μm) in four groups of mice. **(G,H)** Quantification of the interstitial and perivascular fibrosis area in four groups of mice. **(I,J)** Quantification of the Collagen I and Collagen III expression in four groups of mice. Values shown were mean and SEM ($n$ = 6 in each group). *$p$ < 0.05; **$p$ < 0.01; ***$p$ < 0.001.

effects on DCM. The DM + shNC + saline and DM + shA17 + saline mice were administered the same amount of normal saline. One month after eplerenone and saline administration, mice hearts and serum were collected for analysis. The experimental design detail of *in vivo* experiment in tabular form is listed in Supplementary Table S1.

10.3389/fphar.2024.1364827

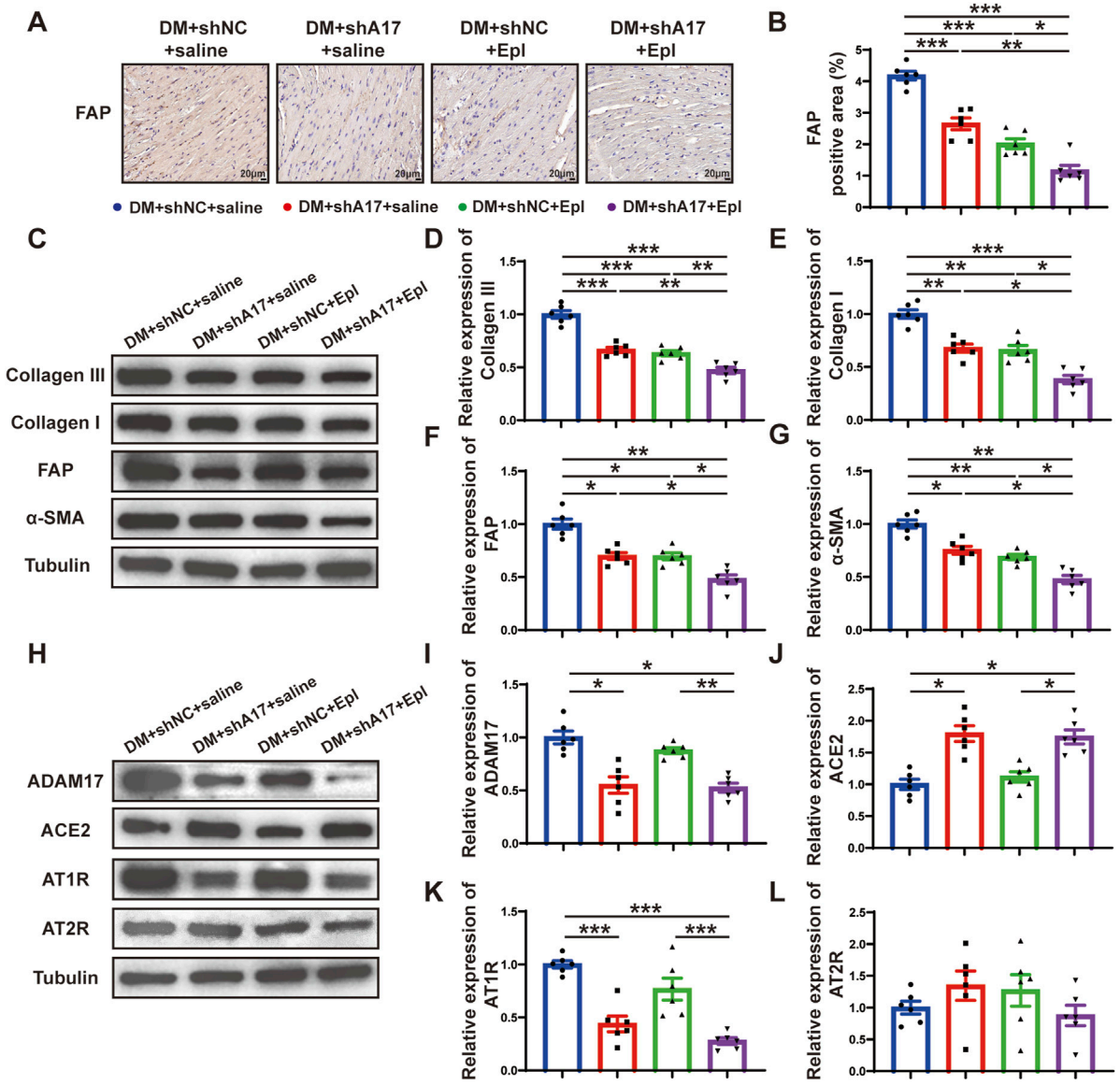


FIGURE 5
Cardiac fibroblasts transformation and RAAS activation following ADAM17 knockdown, eplerenone administration and combined treatment in DCM mice. **(A)** Representative of fibroblast activation protein (FAP) staining (scale bar = 20 μm) in four groups of mice. **(B)** Quantification of FAP expression in four groups of mice. **(C)** Representative Western blotting images of Collagen III, Collagen I, FAP and α-SMA expression in four groups of mice. **(D–G)** Quantification of Collagen III, Collagen I, FAP and α-SMA expression in four groups of mice. **(H)** Representative Western blotting images of ADAM17, ACE2, AT1R and AT2R expression in four groups of mice. **(I–L)** Quantification of ADAM17, ACE2, AT1R and AT2R expression in four groups of mice. Values shown were mean and SEM ($n$ = 6 in each group). *$p$ < 0.05; **$p$ < 0.01; ***$p$ < 0.001.

## Body weight and biochemical assay

The body weight of the mice was measured by an electronic balance (Shimadzu Corp., Japan). Blood glucose of the mice was measured in tail venous blood by an Accu-Chek glucose meter with matched blood glucose strips (Roche, Germany). Serum lipid levels, including serum total cholesterol (TC) and serum triglyceride (TG), serum potassium concentrations and serum albumin (ALB) levels, blood urea nitrogen (BUN) and serum creatinine (Scr) were measured by an automatic biochemical analyzer (Chemray 240, Shenzhen, China).

## Blood pressure and heart rate measurement

At the end of the experiment, the blood pressure and heart rate of the mice were measured using a mouse tail-cuff blood pressure analysis system (Softron BP-98A, Japan). All the mice were first acclimated to the device to ensure accurate and reproducible measurements. The measurements were recorded between 9 a.m. and 12 p.m. in a warm and quiet environment by the same investigator. The mice were warmed inside a hyperthermia cylinder at a temperature of about 36°C–40°C for 5 min according to the manufacturer's instructions, then the cuff sensor was placed at the base of the tail to record the measurements. At least three consecutive measurements were recorded to obtain the average values from each mouse.

10.3389/fphar.2024.1364827

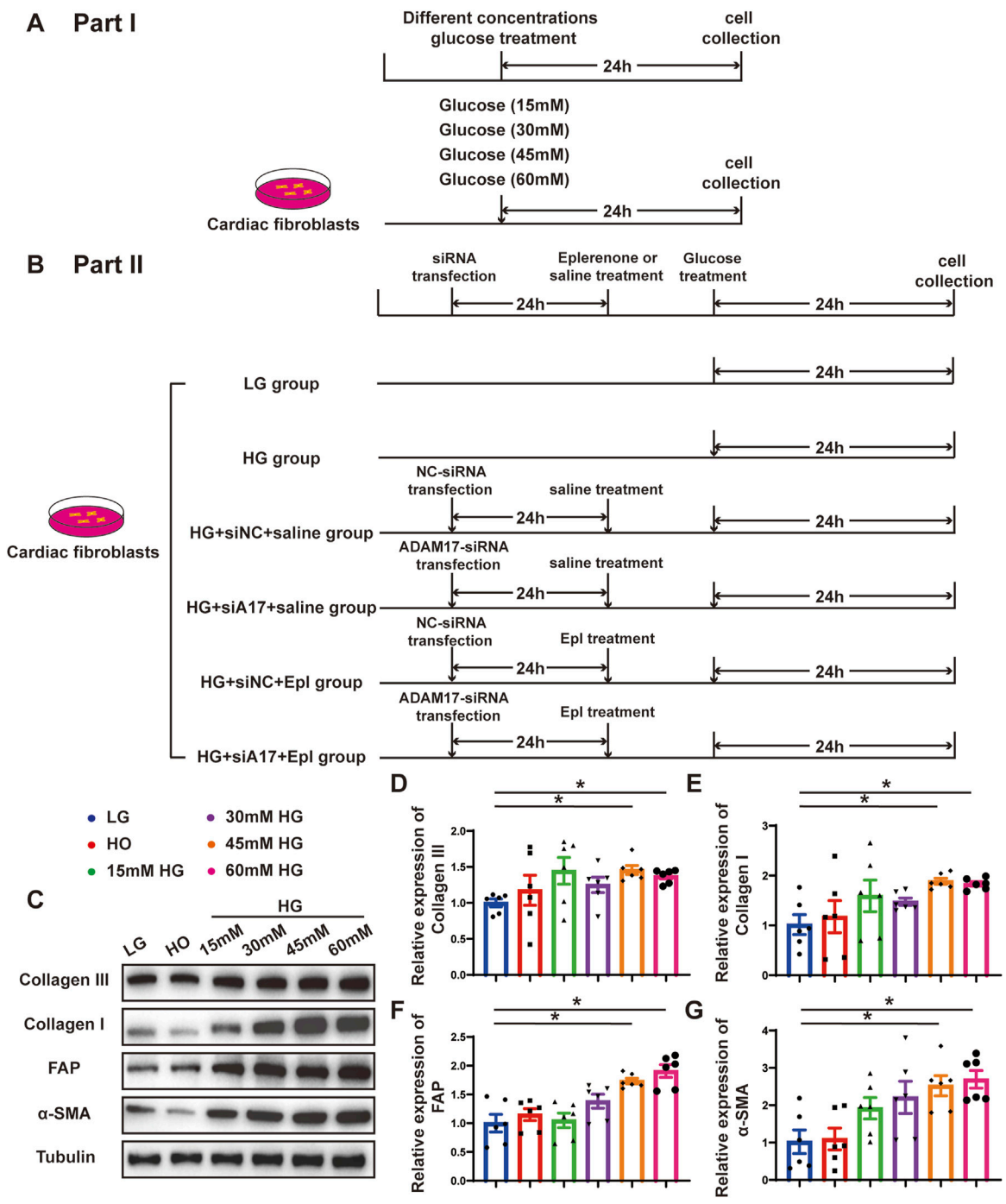


FIGURE 6
Time line of experimental studies *in vitro* and effect of glucose on primary cardiac fibroblasts transformation. **(A)** Cell treatment and time line in first part of experimental studies *in vitro*. **(B)** Cell treatment and time line in second part of experimental studies *in vitro*. **(C)** Representative Western blotting images of Collagen III, Collagen I, FAP and α-SMA expression in cardiac fibroblasts treated with different concentrations glucose. **(D–G)** Quantification of Collagen III, Collagen I, FAP and α-SMA expression in cardiac fibroblasts treated with different concentrations glucose. Values shown were mean and SEM ($n$ = 6 in each group). *$p$ < 0.05.

## Echocardiography

Transthoracic echocardiography was performed using Visual Sonics Vevo 770 machine using a 30 MHz high frequency MS400 transducer (Visual Sonics, Canada). Anesthesia (5% isoflurane) was administered, and the mice remained under general anesthesia with continuous administration of 2% isoflurane during echocardiogram acquisition. Indices of systolic function were obtained from long-axis M-mode scans. The collected parameters included left ventricular ejection fraction (LVEF), fractional shortening (FS), left ventricular end-diastolic diameter (LVEDd), left ventricular end-diastolic volume (LVEDV), ratio of

early to late diastolic mitral flow velocities (E/A), ratio of early to late diastolic mitral annular velocities (E'/A'), and ratio of early diastolic transmittal flow velocity to early diastolic mitral annular velocity (E/E') were calculated.

## Histology and immunohistochemistry

The hearts of mice were isolated and fixed in 4% paraformaldehyde, embedded in paraffin, and cut into 5 μm thick sections for subsequent analyses. Masson's trichrome, Sirius red and hematoxylin and eosin (H&E) staining were performed according to the manufacturer's instructions using staining kits. Fluorescein isothiocyanate-conjugated wheat germ agglutinin (FITC-conjugated WGA) staining was used to measure the cardiomyocyte cross-sectional size. For immunohistochemical staining of tissue sections, the sections were dewaxed and subjected to antigen retrieval with citrate buffer (pH 6.0), followed by treatment with 3% $H_2O_2$. The sections were then blocked with 5% goat serum for 30 min at 37°C and incubated with primary antibodies at 4°C overnight. The next day, the sections were incubated with horseradish peroxidase (HRP)-conjugated secondary antibodies (ZSGB-Bio, Beijing, China) for 30 min at room temperature, and detection was performed using a 3′-diaminobenzidine (DAB) kit (ZSGB-Bio, Beijing, China). Hematoxylin was used for nuclear staining. Sections reacting with nonimmune immunoglobulin G (IgG) as well as secondary antibodies were used as negative controls. All histological images were examined and photographed under a microscope (Ti-S, Nikon) and analyzed with the Image-Pro Plus 6.0 software (Media Cybernetics Inc., USA). The primary antibodies used are listed in Supplementary Table S3.

## TdT-mediated dUTP nick end-labeling (TUNEL) staining

Apoptotic cells in the myocardium were detected via TUNEL assay, performed using a commercially available kit (*In Situ* Cell Death Detection Kit, TMR red) following the manufacturer's instructions. Myocardial sections (5 μm thick) were permeabilized in PBS with 0.1% Triton X-100 and stained by TUNEL, subsequently sealed with DAPI tablet. The images were acquired with a fluorescence microscope (Ni-E, Nikon, Japan) with an excitation wavelength. The apoptosis ratio was expressed as the proportion of apoptotic cells to the total number of cells.

## Enzyme linked immunosorbent assay (ELISA)

Serum Hemoglobin A1c (HbA1c), IL-1β, IL-6, TNF-α, IL-4, and IL-10 levels in mice were measured using mouse HbA1c, IL-1β, IL-6, TNF-α, IL-4, and IL-10 ELISA kit following the manufacturer's instructions (ANRK, China).

## Cell treatment

Primary cardiac fibroblasts were extracted (Meng et al., 2023) and cultured in Dulbecco's modified Eagle's medium (DMEM) containing 10% fetal bovine serum at 37°C under 5% CO2. To examine the effect of different concentrations of glucose on ADAM17 expression in cardiac fibroblasts, cardiac fibroblasts at 60% confluence were randomly divided into 6 groups, which were exposed to different treatments in the first part of the *in vitro* experiments (Figure 6A): (1) 5.5 mM glucose (low-glucose control, LG); (2) a combination of 5.5 mM glucose and 54.5 mM mannitol (high-osmotic-pressure control, HO); (3) 15 mM glucose; (4) 30 mM glucose; (5) 45 mM glucose; (6) 60 mM glucose. In the second part of the *in vitro* experiments (Figure 6B), cardiac fibroblasts at 60% confluence were randomly divided into 6 groups, which were exposed to different treatments: (1) 5.5 mM glucose (low glucose, LG); (2) 60 mM glucose (high glucose, HG); (3) NC-siRNA prior to high-glucose treatment (HG + siNC + saline); (4) ADAM17-siRNA prior to high-glucose treatment (HG + siA17+saline); (5) NC-siRNA and eplerenone prior to high-glucose treatment (HG + siNC + Epl); and (6) ADAM17-siRNA and eplerenone prior to high-glucose treatment (HG + siA17 + Epl). Eplerenone (10 μM) was added 1 h before stimulation. The experimental design detail of *in vitro* experiment in tabular form is listed in Supplementary Table S2.

## Small interfering RNA (siRNA)-mediated gene silencing

The siRNA of ADAM17 or negative control siRNA were obtained from keyybio, Shandong, China. Cardiac fibroblasts were cultured in antibiotic-free medium. The ADAM17-siRNA and NC-siRNA were delivered to the cardiac fibroblasts by Lipofectamine iMAX reagent (Invitrogen, Carlsbad, CA) according to the manufacturer's protocol. After 24 h of transfection, the supernatant was replaced with fresh medium. ADAM17 siRNA sequence: 5′--3′: CGAGTTGATAGCAAAGAGA.

## ADAM17 activity assay

After treatment as previously described, mouse heart tissue and primary cardiac fibroblasts assayed each sample for ADAM17 activity according to the protocol of the SensoLyte 520 TACE (α-secretase) activity assay kit.

## Western blotting analysis

Total protein was extracted from heart tissues using the Total Protein Extraction Kit (Invent Biotechnologies, Plymouth, MN, United States), and protein was extracted from cardiac fibroblasts using RIPA lysis buffer. Equal amounts of extracted protein samples were separated using 10% sodium dodecyl sulfate-polyacrylamide gel electrophoresis; the resolved protein bands were transferred to a polyvinylidene fluoride membrane (Millipore, MA, United States). After incubation in 5% bovine serum albumin for 1 h at room temperature, the membranes were incubated with primary antibodies at 4°C overnight. Following incubation

10.3389/fphar.2024.1364827

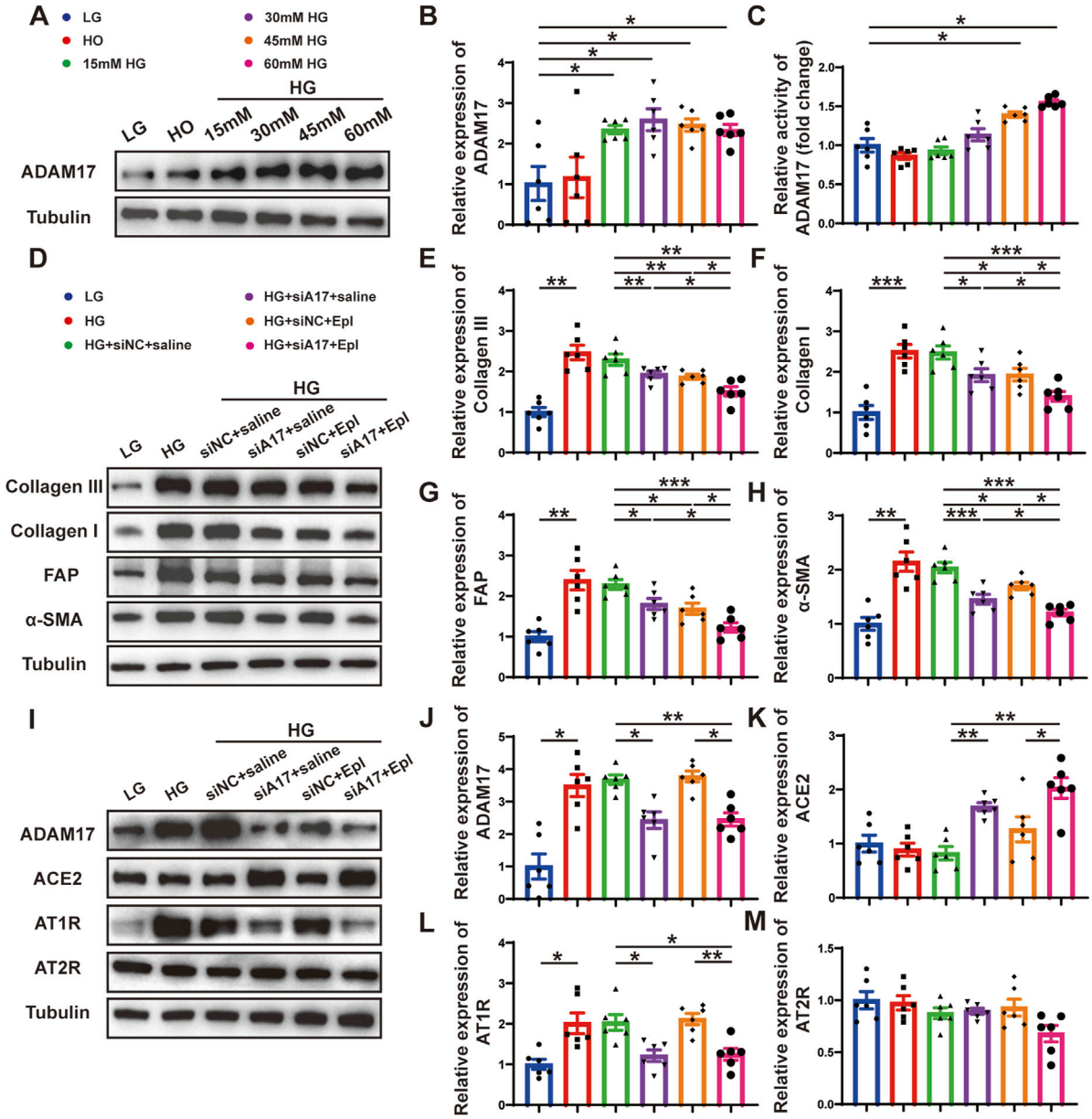


FIGURE 7
Cardiac fibroblasts transformation and RAAS activation following ADAM17 knockdown, eplerenone intervention and combined-administration in primary cardiac fibroblasts. **(A)** Representative Western blotting images of ADAM17 expression in cardiac fibroblasts treated with different concentrations glucose. **(B,C)** Quantification analysis of ADAM17 protein expression and activity in cardiac fibroblasts treated with different concentrations glucose. **(D)** Representative Western blotting images of Collagen III, Collagen I, FAP and α-SMA expression in cardiac fibroblasts treated with LG, HG, HG + siNC + saline, HG + siA17+saline, HG + siNC + Epl, HG + siA17+Epl, respectively. **(E–H)** Quantification of Collagen III, Collagen I, FAP and α-SMA expression in cardiac fibroblasts treated with LG, HG, HG + siNC + saline, HG + siA17+saline, HG + siNC + Epl, HG + siA17+Epl, respectively. **(I)** Representative Western blotting images of ADAM17, ACE2, AT1R and AT2R expression in cardiac fibroblasts treated with LG, HG, HG + siNC + saline, HG + siA17+saline, HG + siNC + Epl, HG + siA17+Epl, respectively. **(J–M)** Quantification of ADAM17, ACE2, AT1R and AT2R expression in cardiac fibroblasts treated with LG, HG, HG + siNC + saline, HG + siA17+saline, HG + siNC + Epl, HG + siA17+Epl, respectively. Values shown were mean and SEM ($n$ = 6 in each group). *$p$ < 0.05; **$p$ < 0.01; ***$p$ < 0.001.

with peroxidase-conjugated secondary antibodies (1:5000, Jackson ImmunoResearch Laboratories, PA, United States) at room temperature for 1 h, the protein bands were detected using a chemiluminescent substrate (Millipore, MA, United States) and exposure to a chemiluminescence instrument (GE, Amersham Imager 800RGB). The primary antibodies used are listed in Supplementary Table S3.

## Quantitative real-time polymerase chain reaction

Total RNA was extracted from isolated heart tissue by means of the RNeasy mini kit (Qiagen, 74704, Germany) which was reversed-transcribed using a PrimeScript RT reagent kit with gDNA Eraser (TaKaRa, Japan), and quantitative real-time RT-PCR was performed

utilizing Takara SYBR RT-PCR kits according to the manufacturer's instructions. Cycling conditions were: 95°C for 10 min, and 95°C for 15 s, 55°C for 15 s, and 72°C for 20 s for 40 cycles. Data were normalized by the level of *β-actin* expression in each individual sample, and the $2^{-\Delta\Delta CT}$ method was used to calculate relative expression changes. The primer sequences were listed in Supplementary Table S4.

## Statistical analysis

All data were presented as mean ± SEM. All analyses were performed with GraphPad Prism 8 (GraphPad, CA). Normality assumption of the data distribution was assessed using Shapiro-Wilk test. For normally distribution, data were analyzed by unpaired two-tailed Student's t-tests to determine the statistical difference between two groups, and one-way ANOVA were performed to determine the statistical difference between multiple groups. In all statistical comparisons, $p$-values < 0.05 was considered to denote statistically significance. Non-significant $p$-values were not shown.

# Results

## Cardiac systolic and diastolic function impaired in DCM mice

To investigate the mechanisms of DCM, we established a mouse model of DCM as described in the first part of the *in vivo* experiment (Figure 1A). We intraperitoneally injected streptozotocin (STZ) into eight-week-old C57BL/6J male mice for five consecutive days. The blood glucose levels of mice were markedly elevated in the DM group compared with those in the control group and remained high until the end of the experiment. Twelve weeks after STZ injection, the mice hearts and serum were harvested. The blood glucose and hemoglobin A1c (HbA1c) levels of the mice in the DM group were substantially higher than those in the control group (Supplementary Figure S1A, B), whereas the body weight was considerably lower (Supplementary Figure S1C). The heart rate (Supplementary Figure S1D) and blood pressure (Supplementary Figures S1E–G) of the mice in the DM group did not substantially differ from those in the control group. However, the serum total cholesterol (Supplementary Figure S1H) and serum triglyceride (Supplementary Figure S1I) level were higher in the DM mice than in the control mice; the potassium concentration (Supplementary Figure S1J), albumin (ALB) (Supplementary Figure S1K), blood urea nitrogen (BUN) (Supplementary Figure S1L), and serum creatinine (Scr) levels (Supplementary Figure S1M) did not significantly differ between the groups. The echocardiography and statistical results showed that compared with the control group, the cardiac systolic function of the mice in the DM group was deteriorated, which mainly manifested as decreased left ventricular ejection fraction (LVEF) and fractional shortening (FS), and increased left ventricular end-diastolic diameter (LVEDd) and left ventricular end-diastolic volume (LVEDV) (Figures 1B–F). The cardiac diastolic function of the mice in the DM group was worse than that of the control group, which manifested as decreased ratio of early to late diastolic mitral flow velocities (E/A), ratio of early to late diastolic mitral annular velocities (E'/A') and increased ratio of early diastolic transmittal flow velocity to early diastolic mitral annular velocity (E/E') (Figures 1G–I). These results showed that the diabetic mice experienced abnormal lipid metabolism and impaired cardiac function.

## DM promoted cardiac remodeling and increased myocardial ADAM17 expression and activity

To investigate the effects of DM on cardiac remodeling, heart size images were captured, and hematoxylin and eosin (H&E) staining and wheat germ agglutinin (WGA) staining were conducted. The results showed that the heart size, left ventricular cross-sectional area were larger in DM group than in the control group (Figure 2A). Moreover, the ratio of heart weight to body weight (HW/BW) of the mice in the DM group was markedly higher than that of the mice in the control group (Figure 2B). H&E staining showed that the diameter of cardiomyocytes in DM groups were significantly larger than that in control group (Figure 2C). WGA staining showed that cardiac myocyte cross sectional areas in DM group were significantly larger than that in control group (Figure 2D). In addition, qRT-PCR showed that *β-mhc* level in DM group was higher than that in the control group (Figure 2E). The results of Masson's trichrome staining and Sirius Red staining showed that the left ventricular fibrotic area in the DM group was dramatically larger than that in the control group, and the expressions of Collagen I, Collagen III and FAP in the left ventricle of the DM group were higher than those in the control group, as identified through histochemical staining (Figures 2F–K). In addition, compared with the control group, the myocardial ADAM17 protein expression and activity level were higher in the DM group; the levels of fibrosis-related molecules collagen III and collagen I were higher than those in the control group (Figures 2L–P). Cardiac fibroblasts play an important role in the pathology of myocardial fibrosis by differentiating into myofibroblasts. FAP is the marker of CMT and α-SMA is a marker of myofibroblasts, whereas TGF-β1, is a factor promoting CMT. The Western blotting results showed that the expressions of FAP, α-SMA and TGF-β1 were increased in the DM group, which proved that CMT can be promoted by hyperglycemic environment, thereby accelerating diabetic myocardial fibrosis (Figures 2Q–S). These results suggested that sustained hyperglycemia promoted cardiac hypertrophy, myocardial collagen deposition and CMT, which promoted cardiac remodeling and increased the expression and activity of ADAM17 in the myocardium, suggesting that ADAM17 played a role in the occurrence and development of DCM.

## Combination of ADAM17 knockdown and eplerenone treatment further attenuated cardiac dysfunction compared with single therapy in DM mice

Because the expression and activity of ADAM17 in the myocardium of the DCM mice were elevated, and cardiac fibroblast differentiation is a salient feature of DCM, we investigated the effects of ADAM17 deficiency in cardiac

10.3389/fphar.2024.1364827

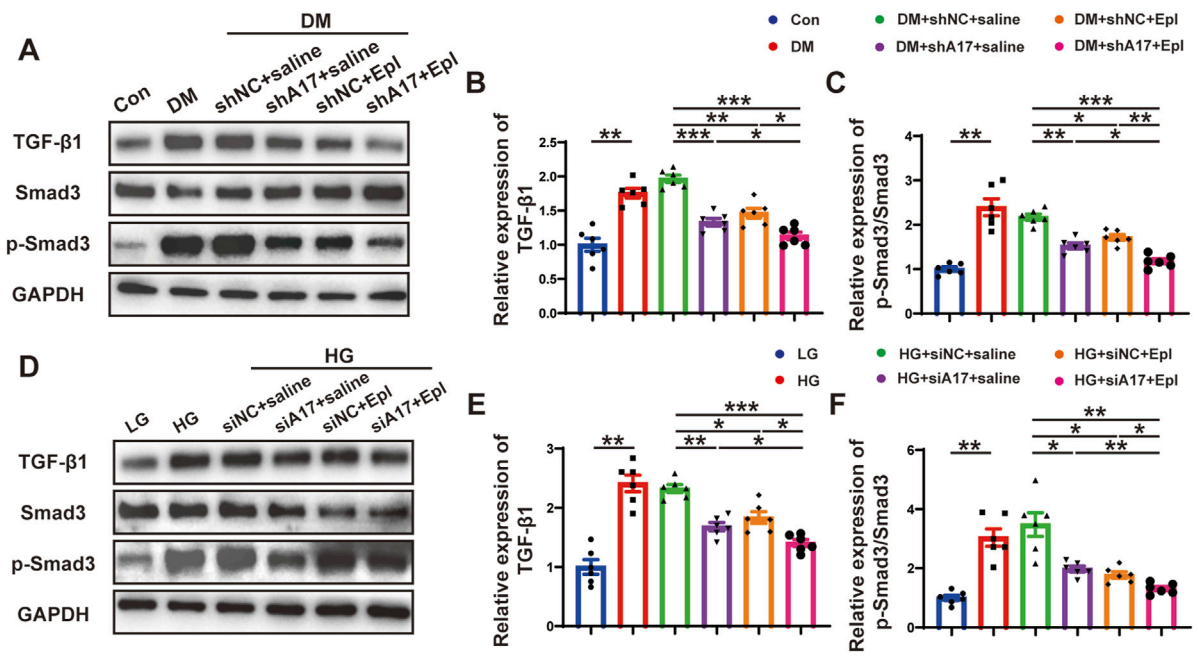


FIGURE 8
The activation of TGF-β1/Smad3 pathway and mechanism of the roles of combination of ADAM17 knockdown and eplerenone treatment in DCM-induced cardiac fibrosis. **(A)** Representative Western blotting images of TGF-β1, Smad3 and phospho-Smad3 expression in six groups of mice. **(B,C)** Quantification of TGF-β1 and the ratio of pSmad3/Smad3 in six groups of mice. **(D)** Representative Western blotting images of TGF-β1, Smad3 and phospho-Smad3 expression in cardiac fibroblasts treated with LG, HG, HG + siNC + saline, HG + siA17+saline, HG + siNC + Epl, HG + siA17+Epl, respectively. **(E,F)** Quantification of TGF-β1 and the ratio of pSmad3/Smad3 in cardiac fibroblasts treated with LG, HG, HG + siNC + saline, HG + siA17+saline, HG + siNC + Epl, HG + siA17+Epl, respectively. Values shown were mean and SEM ($n = 6$ in each group). *$p < 0.05$; **$p < 0.01$; ***$p < 0.001$.

fibroblasts and the use of the aldosterone receptor antagonist, eplerenone on the mice with DCM *in vivo*. The gene targeting ADAM17 is embryonic lethal (Liu et al., 2018). Our previous studies showed that mice with fibroblast conditional knockout of ADAM17 exhibit a strongly inflammatory state. Therefore, in this study, we used adeno-associated virus (AAV)9 to knock down ADAM17 expression and AAV9-shNC as a negative control, via tail vein injection. The results of the Western blotting analysis of the mouse heart tissues confirmed that ADAM17 protein expression was downregulated in AAV9-shA17 mice compared with that in the AAV9-shNC mice (Supplementary Figures S1N, O). Subsequently, the mice were administered eplerenone or saline, as described in the second part of the *in vivo* experiments (Figure 3A). The blood glucose level (Supplementary Figure S2A); HbA1c (Supplementary Figure S2B); body weight (Supplementary Figure S2C); heart rate (Supplementary Figure S2D); blood pressure (Supplementary Figures S2E–G); serum total cholesterol (Supplementary Figure S2H); serum triglyceride (Supplementary Figure S2I); serum potassium (Supplementary Figure S2J); serum albumin (ALB) (Supplementary Figure S2K); blood urea nitrogen (BUN) (Supplementary Figure S2L); and serum creatinine (Scr) levels (Supplementary Figure S2M) did not markedly differ among the four groups. At the end of the experiment, the echocardiography results showed that the LVEF and FS in the DM + shA17 + saline and DM + shNC + Epl groups were higher than those in the DM + shNC + saline group, whereas those in the DM + shA17 + Epl group were higher than those in the DM + shA17 + saline group and DM + shNC + Epl group (Figures 3B–D). In addition, the LVEDd and LVEDV in the DM + shA17 + saline and DM + shNC + Epl groups were lower than that in the DM + shNC + saline group, whereas that in the DM + shA17 + Epl group was lower than that in the DM + shA17 + saline and DM + shNC + Epl groups (Figures 3E, F). However, E/A and E'/A' were higher in the DM + shA17+saline and DM + shNC + Epl groups than in DM + shNC + saline group, but the E/E' was lower in the former than in the latter. The E/A and E'/A' levels in DM + shA17+Epl group were higher than those in DM + shA17 + saline and DM + shNC + Epl groups, whereas E/E' level was lower in DM + shA17 + Epl group than in those two groups (Figures 3G–I). These results demonstrated that ADAM17 knockdown in combination with eplerenone treatment can further improve the systolic and diastolic dysfunction of mice with DCM without affecting blood pressure and disturbing blood potassium levels.

## Combination of ADAM17 knockdown and eplerenone treatment further attenuated cardiac remodeling compared with single therapy in DM mice

To investigate the effects of ADAM17 knockdown and eplerenone on cardiac remodeling caused by DCM, heart size images were obtained, and H&E staining was conducted. The results showed that the heart size and cardiac cross-sectional area of the mice in the DM + shA17 + saline and DM + shNC + Epl groups were lower than those of the mice in the DM + shNC + saline

group. However, the heart size and cardiac cross-sectional area of the mice in the DM + shA17 + Epl group were further decreased compared with those of the mice in the DM + shA17 + saline and DM + shNC + Epl groups (Figure 4A). Moreover, compared with the DM + shNC + saline group, the HW/BW of the mice in the DM + shA17 + saline and DM + shNC + Epl groups were substantially lower; the levels were further decreased in the mice in the DM + shA17 + Epl group (Figure 4B).

H&E staining and WGA staining showed that the diameter of cardiomyocytes and cardiac myocyte cross sectional areas in the DM + shA17 + saline and DM + shNC + Epl groups were lower than those of the mice in the DM + shNC + saline group; the levels were further decreased in the mice in the DM + shA17 + Epl group (Figures 4C, D). In addition, qRT-PCR showed that the elevated *β-mhc* level in DM + shNC + saline group decreased in DM + shA17 + saline group and DM + shNC + Epl group, and further decreased in DM + shA17 + Epl group (Figure 4E). The results of Masson's trichrome and Sirius Red staining showed that the left ventricular fibrosis areas of the mice in the DM + shA17 + saline and DM + shNC + Epl groups were remarkably lower than those of the mice in the DM + shNC + saline group, whereas the left ventricular fibrosis induced by diabetes was further improved in the DM + shA17 + Epl group compared with that in the above two groups. The expression levels of collagen I and collagen III were also consistent with the fibrotic changes shown by Masson's trichrome and Sirius Red staining (Figures 4F–J). These results showed that cardiac hypertrophy and myocardial collagen deposition were considerably reduced by the combination of ADAM17 knockdown and eplerenone treatment compared with single therapy with ADAM17 deficiency or eplerenone administration.

## Combination of ADAM17 knockdown and eplerenone treatment further reduced CMT compared with single therapy in DM mice

We examined the effects of ADAM17 knockdown and eplerenone treatment on CMT and cardiac fibrosis in mice with DCM. The results of histochemical staining showed that the expression of FAP in the DM + shA17 + saline and DM + shNC + Epl groups were lower than that in the DM + shNC + saline group, whereas the expression of FAP in the DM + shA17 + Epl group was further decreased compared with that in the DM + shA17 + saline and DM + shNC + Epl groups (Figures 5A, B). The Western blotting results showed that the expressions of collagen III, collagen I, FAP, and α-SMA in DM + shA17 + saline and DM + shNC + Epl groups were downregulated compared with those in the DM + shNC + saline group, whereas those in DM + shA17+Epl group were further downregulated compared with those in DM + shA17+saline and DM + shNC + Epl groups (Figures 5C–G). Furthermore, the Western blotting results showed that ADAM17 and angiotensin type 1 receptor (AT1R) expression were decreased in the DM + shA17 + saline group compared with those in the DM + shNC + saline group; those in the DM + shNC + Epl group were not substantially different. Compared with those in the DM + shA17 + saline group, the expression of ADAM17 and AT1R in the DM + shA17 + Epl group did no substantially change, whereas the expressions of ADAM17 and AT1R in the DM + shA17 + Epl group were markedly decreased compared with those in the DM + shNC + Epl group. Compared with the DM + shNC + saline group, protein expression level of ACE2 was higher in the DM + shA17 + saline and DM + shA17 + Epl groups, whereas the level was not notably different in the DM + shNC + Epl group. However, we observed no substantial difference in the angiotensin type 2 receptor (AT2R) levels among the four groups (Figures 5H–L). These results suggested that ADAM17 knockdown reduced CMT and affected cardiac fibrosis by inhibiting the activation of the RAAS. Eplerenone also reduced CMT and improved the effects of cardiac fibrosis. Moreover, the combination of ADAM17 knockdown and eplerenone treatment can further reduce CMT and improve the effects of cardiac fibrosis compared with single therapy alone.

## High-glucose treatment promoted CMT and increased ADAM17 expression and activity in cardiac fibroblasts *in vitro*

To verify the effect of glucose on cardiac fibroblasts *in vitro*, we stimulated primary cardiac fibroblasts with different concentrations of glucose as described in the first part of the *in vitro* experiment (Figure 6A). The Western blotting results showed that the expressions of collagen III, collagen I, FAP, and α-SMA in cardiac fibroblasts gradually increased with the increase in glucose concentration (Figures 6C–G). Additionally, ADAM17 protein expression and activity in cardiac fibroblasts increased in a glucose-concentration- dependent manner (Figures 7A–C). These results suggested that high glucose levels promoted CMT *in vitro* and upregulated the expression and activity of ADAM17 in cardiac fibroblasts.

## Combination of ADAM17 knockdown and eplerenone treatment further reduced CMT compared with single therapy in cardiac fibroblasts *in vitro*

To further demonstrate the role of ADAM17 and eplerenone in CMT *in vitro*, we treated primary cardiac fibroblasts as described in the second part of the *in vitro* experiment (Figure 6B). The results of Western blotting showed that the expressions of collagen III, collagen I, FAP, and α-SMA were lower in the HG + siA17+saline and HG + siNC + Epl groups compared with HG + siNC + saline group. However, the expressions in the HG + siA17 + Epl group were event lower than those in the HG + siA17 + saline and HG + siNC + Epl groups (Figures 7D–H). Furthermore, the Western blotting results showed that ADAM17 and AT1R expressions were lower in the HG + siA17 + saline group than in the HG + siNC + saline group, but no notably different in the HG + siNC + Epl group. Compared with those in the HG + siA17 + saline group, the expression of ADAM17 and AT1R in the HG + siA17 + Epl group were not substantially different, whereas the expression of ADAM17 and AT1R in the HG + siA17 + Epl group were significantly lower than those in the HG + siNC + Epl group. Compared with the HG + siNC + saline group, the protein expression levels of ACE2 were higher in the HG +

siA17+saline group and HG + siA17 + Epl group, but no different in the HG + siNC + Epl group. However, no substantial difference was observed in AT2R expression among the six groups (Figures 7I–M). These results suggested that ADAM17 knockdown and eplerenone treatment inhibited CMT by inhibiting RAAS activation and ADAM17 knockdown combined with eplerenone further inhibited CMT *in vitro*.

### Combination of ADAM17 knockdown and eplerenone treatment affected CMT via regulating TGF-β1/Smad3 pathway *in vivo* and *in vitro*

We further examined the mechanisms underlying the effects of the combination of ADAM17 deficiency and eplerenone treatment in regulating CMT. TGF-β1 is a key profibrotic cytokine in DCM, and the TGF-β1/Smad3 pathway is a classic fibrosis pathway. Therefore, we examined the expression of phosphorylated Smad3 in the hearts of diabetic mice and found that phosphorylated Smad3 expression increased; however, ADAM17 knockdown and eplerenone treatment both decreased the expression of phosphorylation of Smad3. The combination of ADAM17 knockdown and eplerenone treatment further reduced the expressions of TGF-β1 and phosphorylated Smad3 *in vivo* (Figures 8A–C). Similarly, we found that high-glucose stimulation increased the expressions of TGF-β1 and phosphorylated Smad3 in cardiac fibroblasts *in vitro*, whereas ADAM17 deletion and eplerenone treatment decreased the expressions of TGF-β1 and phosphorylated Smad3 in cardiac fibroblasts. Consistent with the results of the *in vivo* experiments, ADAM17 knockdown combined with eplerenone treatment further reduced TGF-β1 and Smad3 phosphorylation in cardiac fibroblasts (Figures 8D–F). These results suggested that ADAM17 knockdown combined with eplerenone treatment inhibited fibroblast transformation by inhibiting TGF-β1/Smad3 pathway activation, thereby reducing cardiac fibrosis and improving cardiac remodeling in DCM.

## Discussion

The main finding of our study was that the combination of ADAM17 knockdown and eplerenone treatment can protect the heart by reversing left ventricular remodeling and dysfunction without changing blood pressure, blood glucose, or potassium levels in DCM mice. The underlying mechanism is that the overactivated RAAS is inhibited, which reduce the transformation of fibroblasts into myofibroblasts, mediated by the activated TGF-β1/Smad3 pathway, thereby leading to reducing the collagen synthesis and improving the cardiac remodeling induced by diabetes. In addition, the combination of ADAM17 inhibition and eplerenone administration reduced cardiac apoptosis and cardiac inflammation in diabetic mice, further improving diabetes-induced cardiac dysfunction (Supplementary Figure S3). The combined intervention including ADAM17 knockdown and eplerenone treatment provided an additional cardioprotective effect compared with that produced by monotherapy and produced no side effects, such as hyperkalemia, which was a crucial finding in the search for new treatments for DCM.

The primary pathological outcomes of DCM include cardiac hypertrophy, myocardial fibrosis, and extracellular collagen deposition. The activation of the RAAS plays vital role in the production and degradation of collagen (Agarwal et al., 2021), such as Ang II, which plays a key role in promoting myocardial fibrosis (Weber and Brilla, 1991). The renin-angiotensin system is the main regulator of aldosterone production, and Ang II acts through angiotensin receptors to stimulate aldosterone release. Aldosterone levels are higher in diabetic patients than in normal individuals, and the activation of aldosterone can lead to myocardial fibrosis. Therefore, the pharmacological disruption of aldosterone action at the tissue level may be particularly useful for patients with diabetes. Aldosterone binds to mineralocorticoid receptor (MR) to promote myocardial fibrosis; the specific mechanism may involve oxidative stress, inflammation, and apoptosis. MR is expressed in many tissues and cells including the kidney, heart, immune cells, and fibroblasts (Agarwal et al., 2021). The pathophysiological overactivation of MR leads to inflammation and fibrosis in cardiorenal disease. Cardiomyocyte-specific MR knockout also reduced inflammation and fibrosis in a mouse model of deoxycorticosterone acetate (DOCA)-salt-induced myocardial fibrosis (Fraccarollo et al., 2011). By blocking MR, eplerenone may attenuate cardiac steatosis and apoptosis and the subsequent remodeling and diastolic dysfunction in obese/type-II diabetic rats (Ramirez et al., 2013). Eplerenone, a selective aldosterone receptor antagonist, has been used in clinical studies to reduce morbidity and mortality in patients with acute myocardial infarction complicated by left ventricular dysfunction and heart failure (Pitt et al., 2023). In addition, a randomized controlled studies have shown that eplerenone reduces NT-proBNP levels in patients with worsening chronic heart failure and diabetes mellitus and/or chronic kidney disease (Filippatos et al., 2016).

Excessive RAAS activation leads to the excessive production of Ang II and aldosterone, playing an indispensable role in the pathogenesis of DCM. Aldosterone receptor antagonists are generally used in addition to administering ACEIs and ARBs to achieve the strongest therapeutic effect in diabetic patients with heart failure. Although aldosterone receptor antagonists in combination with ACEIs or ARBs can substantially improve cardiac remodeling and reduce adverse cardiovascular events in patients with heart failure; however, many limitations face their use. Firstly, ACEIs or ARBs in combination with aldosterone receptor antagonists may cause hyperkalemia and renal dysfunction to overrule the beneficial effects of this approach. In a randomized controlled trial designed to study the safety and efficacy of eplerenone in patients at a high risk of hyperkalemia and worsening renal function, eplerenone was effective in reducing the primary composite endpoint in all subgroups; however, the risks of hospitalization for hyperkalemia and discontinuation of investigational medication due to adverse events were increased (Eschalier et al., 2013). Secondly, although ACEIs inhibits Ang II production and ARBs inhibits Ang II binding to angiotensin receptors to inhibit the production of aldosterone, the so-called Ang II/aldosterone escape that often occurs for ACEIs cannot block the chymase-catalyzed Ang II, which usually produces more Ang II than the ACE process (Pitt et al., 1999). Finally, ARBs only block the

binding of Ang II to AT1R on the cell membrane, whereas the Ang II synthesized in the cell cannot be blocked, while intracellular Ang II still caused myocardial fibrosis.

Therefore, a treatment that may inhibit Ang II production without disturbing blood potassium concentration when combined with aldosterone receptor antagonists is urgently needed. Previous studies in our laboratory showed that ACE2/Ang1-7/MasR is a novel axis for the treatment of cardiovascular diseases. ACE2 cleaves Ang II to produce Ang-(1–7) and thus acts as a negative regulator of RAS (Simões e Silva and Teixeira, 2016). Overexpression of ACE2 improved left ventricular remodeling and function in DCM rats (Dong et al., 2012). As a transmembrane protein, ADAM17 cleaves ACE2 on the cell surface via proteolysis, causing ACE2 to fall off and lose its protective effects on the myocardium. *Wang X et al.* found that ADAM17 silencing can strongly inhibit the myocardial hypertrophy and myocardial fibrosis induced by Ang II stimulation in spontaneously hypertensive and hypertensive rats; however, the specific molecular mechanism of this effect is unknown (Wang et al., 2009). ADAM17 knockdown attenuated whereas ADAM17 overexpression aggravated cardiac fibrosis by regulating ACE2 shedding in diabetic mice (Cheng et al., 2022). However, Ang II can activate ADAM17 and increase ACE2 shedding, forming positive feedback in the RAAS; that is, Ang II stimulation inhibits the degradation of Ang II by ACE2, thereby reducing myocardial protection of ACE2 (Patel et al., 2014). In this study, ADAM17 knockdown reduced the shedding of ACE2, thereby increasing ACE2 expression in a high-glucose environment, which had an antagonistic effect on Ang II and improved cardiac function in DCM. In addition, the combined administration of eplerenone in mice with DCM further improved cardiac remodeling without causing potassium disturbances.

CMT plays an important role in myocardial fibrosis development. Fibroblasts transform into cells with secretory and contractile phenotypes called myofibroblasts (Liu et al., 2021). Myofibroblasts do not exist in normal myocardial tissues, and quiescent fibroblasts can only transition into myofibroblasts under pathological conditions, thereby promoting collagen synthesis during myocardial fibrosis. In heart failure, various pathological stimuli that lead to heart damage, such as mechanical stress, metabolic disorders, or inflammatory stimuli, may activate myofibroblasts (Chen C. et al., 2016). During myocardial fibrosis, myofibroblasts are activated through the synergistic action of growth factors and matrix proteins, which transmit pro-fibrotic signals into the cell and promote α-SMA transcription and translation (Shinde and Frangogiannis, 2017). FAP, a membrane-bound proline-specific serine protease, is not expressed in normal fibroblasts but is expressed in myofibroblasts. Myofibroblasts express α-SMA and FAP, whereas fibroblasts do not. Therefore, α-SMA and FAP can be used as myofibroblast markers. Ang II, aldosterone, and TGF-β1 can promote the transformation and proliferation of myofibroblasts, which are therapeutic targets for the treatment of myocardial fibrosis (Shinde and Frangogiannis, 2014).

The specific molecular mechanisms of myocardial fibrosis are very complex and involve a series of intracellular signaling pathways. TGF-β1 is a major cytokine that promotes fibrosis in the DCM. Ang II stimulates the expression of TGF-β1 in cardiac fibroblasts, and locally produced Ang II can exert a powerful stimulating effect on cardiac fibroblasts directly or through TGF-β1-mediated pathways (Kagami et al., 1994; Massagué, 2012). TGF-β1 may be the downstream molecule that MR induces and promotes fibrosis. Aldosterone stimulates TGF-β1 expression in rat mesangial cells by enhancing ERK1/2 and JNK activities and subsequent AP-1 activity, promoting proliferation and fibrosis in inflammatory kidney disease (Han et al., 2009). In this study, we found that a high-glucose environment substantially increased the expression of TGF-β1; after knocking down ADAM17, the shearing of ACE2 decreased, and the TGF-β1 pathway was inhibited to reduce the degree of myocardial fibrosis. In addition, eplerenone competes with aldosterone for the mineralocorticoid receptor, inhibited the effect of aldosterone, reduced TGF-β1 expression, and reduced the degree of fibrosis. Finally, the combination of ADAM17 knockdown and eplerenone treatment reduced the level of TGF-β1 expression and further reduced the degree of fibrosis compared with that achieved with single therapy alone.

Numerous studies have shown that RAAS members, especially Ang II and aldosterone, play a key role in the pathogenesis of myocardial fibrosis. In a number of large-scale randomized clinical trials, ACEIs, ARBs and aldosterone receptor antagonists have significantly reduced mortality in patients with chronic heart failure, partly as a result of improved myocardial fibrosis and left ventricular remodeling. By blocking MR, eplerenone may attenuate cardiac steatosis and apoptosis and the subsequent remodeling and diastolic dysfunction in obese/type-II diabetic rats without inhibiting the effect of Ang II (Ramirez et al., 2013). The combination of ACEIs or ARBs and aldosterone receptor antagonists may benefit significantly in patients with heart failure who have normal renal function and potassium levels. However, the combination of ACEIs or ARBs and aldosterone receptor antagonists may cause severe hyperkalemia and thus have limitations. Our previous study found that ADAM17 knockdown mitigates while ADAM17 overexpression aggravates cardiac fibrosis and dysfunction, but it is unclear whether ADAM17 inhibition in combination with eplerenone treatment is better than single therapy and has no side effects. Our study found that ADAM17 inhibition combined with eplerenone significantly improved myocardial fibrosis, apoptosis, and inflammation in diabetic mice by dual inhibition of Ang II and aldosterone, without affecting blood potassium concentration. In addition, due to the presence of intracellular RAAS in the heart, currently available RAAS inhibitors may not provide the expected cardiovascular benefits in diabetic cardiomyopathy. An interesting approach is to exploit the protective facet of RAAS. This alternative prong of RAAS constitutes of ACE2, which cleaves angiotensin II to form angiotensin (1–7), promotes the antifibrotic effects of DCM through AT2R and MasR, and ADAM17 knockdown plays a protective role in DCM by increasing ACE2 expression. Several small molecule inhibitors of ADAM17 have been screened for cancer research, which provides conditions for the future development of ADAM17 small molecule inhibitors for diabetic cardiomyopathy, with great clinical translational potential. Taken together, our findings highlight the potential translational value of ADAM17 inhibition in combination with eplerenone after diabetic cardiomyopathy.

## Conclusion

In summary, ADAM17 knockout reduced diabetes-induced collagen synthesis and ameliorated cardiac remodeling through the inhibition of RAAS overactivation when combined with eplerenone treatment, which reducing TGF-β1/Smad3 pathway activation-mediated CMT. The combined intervention of ADAM17 knockout and eplerenone therapy provided additional cardiac protection compared with a single therapy alone, and did not disturb potassium level. Therefore, this is be a novel and promising finding for the treatment of DCM.

## Data availability statement

The original contributions presented in the study are included in the article/Supplementary Material, further inquiries can be directed to the corresponding authors.

## Ethics statement

The animal study was approved by the Shandong University Animal Care Committee. The study was conducted in accordance with the local legislation and institutional requirements.

## Author contributions

LX: Methodology, Investigation, Data curation, Writing–original draft. DZ: Investigation, Data curation, Writing–review and editing. JY: Conceptualization, Writing–review and editing. FX: Supervision, Writing–review and editing. WS: Methodology, Writing–review and editing. YZ: Writing–review and editing, Funding acquisition, Conceptualization.

## Funding

The author(s) declare that financial support was received for the research, authorship, and/or publication of this article. This work was supported by grants of the National Natural Science Foundation of China (Nos 82030051 and 82000411), Key R&D Program of Shandong Province (2021SFGC0503, 2021ZDSYS05, and 2020ZLYS05), Shandong Provincial Natural Science Foundation (ZR2020QH023), Project funded by China Postdoctoral Science Foundation (2023M742124) and Postdoctoral Innovation Talents Support Program (BX20230210).

## Conflict of interest

The authors declare that the research was conducted in the absence of any commercial or financial relationships that could be construed as a potential conflict of interest.

## Publisher's note

All claims expressed in this article are solely those of the authors and do not necessarily represent those of their affiliated organizations, or those of the publisher, the editors and the reviewers. Any product that may be evaluated in this article, or claim that may be made by its manufacturer, is not guaranteed or endorsed by the publisher.

## Supplementary material

The Supplementary Material for this article can be found online at: https://www.frontiersin.org/articles/10.3389/fphar.2024.1364827/full#supplementary-material

## References

Adamo, M., Gardner, R. S., McDonagh, T. A., and Metra, M. (2022). The 'Ten Commandments' of the 2021 ESC Guidelines for the diagnosis and treatment of acute and chronic heart failure. *Eur. Heart J.* 43, 440–441. doi:10.1093/eurheartj/ehab853

Agarwal, R., Kolkhof, P., Bakris, G., Bauersachs, J., Haller, H., Wada, T., et al. (2021). Steroidal and non-steroidal mineralocorticoid receptor antagonists in cardiorenal medicine. *Eur. Heart J.* 42, 152–161. doi:10.1093/eurheartj/ehaa736

Boudina, S., and Abel, E. D. (2007). Diabetic cardiomyopathy revisited. *Circulation* 115, 3213–3223. doi:10.1161/CIRCULATIONAHA.106.679597

Brown, N. J. (2013). Contribution of aldosterone to cardiovascular and renal inflammation and fibrosis. *Nat. Rev. Nephrol.* 9, 459–469. doi:10.1038/nrneph.2013.110

Bugger, H., and Abel, E. D. (2014). Molecular mechanisms of diabetic cardiomyopathy. *Diabetologia* 57, 660–671. doi:10.1007/s00125-014-3171-6

Cai, B. S., Dongiovanni, P., Corey, K. E., Wang, X., Shmarakov, I. O., Zheng, Z., et al. (2020). Macrophage merTK promotes liver fibrosis in nonalcoholic steatohepatitis. *Cell Metab.* 31, 406–421. e7. doi:10.1016/j.cmet.2019.11.013

Cambier, L., Giani, J. F., Liu, W., Ijichi, T., Echavez, A. K., Valle, J., et al. (2018). Angiotensin II–induced end-organ damage in mice is attenuated by human exosomes and by an exosomal Y RNA fragment. *Hypertension* 72, 370–380. doi:10.1161/HYPERTENSIONAHA.118.11239

Chen, C., Li, R., Ross, R. S., and Manso, A. M. (2016b). Integrins and integrin-related proteins in cardiac fibrosis. *J. Mol. Cell. Cardiol.* 93, 162–174. doi:10.1016/j.yjmcc.2015.11.010

Chen, X. Q., Zhang, W., Wang, Q., Du, L., Yi, Y., Liu, Y., et al. (2016a). Eplerenone inhibits atrial fibrosis in mutant TGF-β1 transgenic mice. *Sci. China. Life Sci.* 59, 1042–1047. doi:10.1007/s11427-016-0037-y

Cheng, J., Xue, F., Cheng, C., Sui, W., Zhang, M., Qiao, L., et al. (2022). ADAM17 knockdown mitigates while ADAM17 overexpression aggravates cardiac fibrosis and dysfunction via regulating ACE2 shedding and myofibroblast transformation. *Front. Pharmacol.* 13, 997916. doi:10.3389/fphar.2022.997916

Collier, P., and McDonald, K. M. (2012). The role of renin angiotensin system intervention in stage B heart failure. *Heart Fail. Clin.* 8, 225–236. doi:10.1016/j.hfc.2011.11.006

Dannenberg, L., Weske, S., Kelm, M., Levkau, B., and Polzin, A. (2021). Cellular mechanisms and recommended drug-based therapeutic options in diabetic cardiomyopathy. *Pharmacol. Ther.* 228, 107920. doi:10.1016/j.pharmthera.2021.107920

Dillmann, W. H. (2019). Diabetic cardiomyopathy. *Circulation Res.* 124, 1160–1162. doi:10.1161/CIRCRESAHA.118.314665

Dong, B., Yu, Q. T., Dai, H. Y., Gao, Y. Y., Zhou, Z. L., Zhang, L., et al. (2012). Angiotensin-converting enzyme-2 overexpression improves left ventricular remodeling and function in a rat model of diabetic cardiomyopathy. *J. Am. Coll. Cardiol.* 59, 739–747. doi:10.1016/j.jacc.2011.09.071

Eschalier, R., McMurray, J. J. V., Swedberg, K., van Veldhuisen, D. J., Krum, H., Pocock, S. J., et al. (2013). Safety and efficacy of eplerenone in patients at high risk for hyperkalemia and/or worsening renal function: analyses of the EMPHASIS-HF study subgroups (Eplerenone in Mild Patients Hospitalization and SurvIval Study in Heart Failure). *J. Am. Coll. Cardiol.* 62, 1585–1593. doi:10.1016/j.jacc.2013.04.086

Filippatos, G., Anker, S. D., Böhm, M., Gheorghiade, M., Køber, L., Krum, H., et al. (2016). A randomized controlled study of finerenone vs eplerenone in patients with worsening chronic heart failure and diabetes mellitus and/or chronic kidney disease. *Eur. Heart J.* 37 (27), 2105–2114. doi:10.1093/eurheartj/ehw132

Fraccarollo, D., Berger, S., Galuppo, P., Kneitz, S., Hein, L., Schütz, G., et al. (2011). Deletion of cardiomyocyte mineralocorticoid receptor ameliorates adverse remodeling after myocardial infarction. *Circulation* 123, 400–408. doi:10.1161/CIRCULATIONAHA.110.983023

Goldsmith, E. C., Bradshaw, A. D., Zile, M. R., and Spinale, F. G. (2014). Myocardial fibroblast–matrix interactions and potential therapeutic targets. *J. Mol. Cell. Cardiol.* 70, 92–99. doi:10.1016/j.yjmcc.2014.01.008

Han, J. S., Choi, B. S., Yang, C. W., and Kim, Y. S. (2009). Aldosterone-induced TGF-beta1 expression is regulated by mitogen-activated protein kinases and activator protein-1 in mesangial cells. *J. Korean Med. Sci.* 24, S195–S203. doi:10.3346/jkms.2009.24.S1.S195

He, Y., Ling, S., Sun, Y., Sheng, Z., Chen, Z., Pan, X., et al. (2018). DNA methylation regulates α-smooth muscle actin expression during cardiac fibroblast differentiation. *J. Cell. Physiology* 234, 7174–7185. doi:10.1002/jcp.27471

Jia, G., Hill, M. A., and Sowers, J. R. (2018). Diabetic cardiomyopathy: an update of mechanisms contributing to this clinical entity. *Circulation Res.* 122, 624–638. doi:10.1161/CIRCRESAHA.117.311586

Johansen, M. L., Ibarrola, J., Fernández-Celis, A., Schou, M., Sonne, M. P., Refsgaard Holm, M., et al. (2021). The mineralocorticoid receptor antagonist eplerenone suppresses interstitial fibrosis in subcutaneous adipose tissue in patients with type 2 diabetes. *Diabetes* 70, 196–203. doi:10.2337/db20-0394

Kagami, S., Border, W. A., Miller, D. E., and Noble, N. A. (1994). Angiotensin II stimulates extracellular matrix protein synthesis through induction of transforming growth factor-beta expression in rat glomerular mesangial cells. *J. Clin. Investigation* 93, 2431–2437. doi:10.1172/JCI117251

Kefaloyianni, E., Muthu, M. L., Kaeppler, J., Sun, X., Sabbisetti, V., Chalaris, A., et al. (2016). ADAM17 substrate release in proximal tubule drives kidney fibrosis. *JCI Insight* 1, e87023. doi:10.1172/jci.insight.87023

Leung, M., Wong, V. W., Heritier, S., Mihailidou, A. S., and Leung, D. Y. (2013). Rationale and design of a randomized trial on the impact of aldosterone antagonism on cardiac structure and function in diabetic cardiomyopathy. *Cardiovasc. Diabetol.* 12, 139. doi:10.1186/1475-2840-12-139

Liu, B., Li, R., Zhang, J., Meng, C., Zhang, J., Song, X., et al. (2018). MicroRNA-708-3p as a potential therapeutic target via the ADAM17-GATA/STAT3 axis in idiopathic pulmonary fibrosis. *Exp. Mol. Med.* 50, e465. doi:10.1038/emm.2017.311

Liu, M., López de Juan Abad, B., and Cheng, K. (2021). Cardiac fibrosis: myofibroblast-mediated pathological regulation and drug delivery strategies. *Adv. Drug Deliv. Rev.* 173, 504–519. doi:10.1016/j.addr.2021.03.021

Mahajan, U. B., Chandrayan, G., Patil, C. R., Arya, D. S., Suchal, K., Agrawal, Y., et al. (2018). Eplerenone attenuates myocardial infarction in diabetic rats via modulation of the PI3K-Akt pathway and phosphorylation of GSK-3β. *Am. J. Transl. Res.* 10, 2810–2821.

Maron, B. A., and Leopold, J. A. (2010). Aldosterone receptor antagonists: effective but often forgotten. *Circulation* 121, 934–939. doi:10.1161/CIRCULATIONAHA.109.895235

Massagué, J. (2012). TGFβ signalling in context. *Nat. Rev. Mol. Cell Biol.* 13, 616–630. doi:10.1038/nrm3434

Meng, L. L., Lu, Y., Wang, X., Cheng, C., Xue, F., Xie, L., et al. (2023). NPRC deletion attenuates cardiac fibrosis in diabetic mice by activating PKA/PKG and inhibiting TGF-β1/Smad pathways. *Sci. Adv.* 9 (31), eadd4222. doi:10.1126/sciadv.add4222

Nagatomo, Y., Meguro, T., Ito, H., Koide, K., Anzai, T., Fukuda, K., et al. (2014). Significance of AT1 receptor independent activation of mineralocorticoid receptor in murine diabetic cardiomyopathy. *PLoS ONE* 9, e93145. doi:10.1371/journal.pone.0093145

Nishioka, T., Suzuki, M., Onishi, K., Takakura, N., Inada, H., Yoshida, T., et al. (2007). Eplerenone attenuates myocardial fibrosis in the angiotensin II-induced hypertensive mouse: involvement of tenascin-C induced by aldosterone-mediated inflammation. *J. Cardiovasc. Pharmacol.* 49, 261–268. doi:10.1097/FJC.0b013e318033dfd4

Pacak, C. A., Mah, C. S., Thattaliyath, B. D., Conlon, T. J., Lewis, M. A., Cloutier, D. E., et al. (2006). Recombinant adeno-associated virus serotype 9 leads to preferential cardiac transduction *in vivo*. *Circulation Res.* 99, e3–e9. doi:10.1161/01.RES.0000237661.18885.f6

Patel, V. B., Clarke, N., Wang, Z., Fan, D., Parajuli, N., Basu, R., et al. (2014). Angiotensin II induced proteolytic cleavage of myocardial ACE2 is mediated by TACE/ADAM-17: a positive feedback mechanism in the RAS. *J. Mol. Cell. Cardiol.* 66, 167–176. doi:10.1016/j.yjmcc.2013.11.017

Pitt, B., Remme, W., Zannad, F., Neaton, J., Martinez, F., Roniker, B., et al. (2023). Eplerenone, a selective aldosterone blocker, in patients with left ventricular dysfunction after myocardial infarction. *N. Engl. J. Med.* 348, 1309–1321. doi:10.1056/NEJMoa030207

Pitt, B., Stier, C. T., and Rajagopalan, S. (2003). Mineralocorticoid receptor blockade: new insights into the mechanism of action in patients with cardiovascular disease. *J. renin-angiotensin-aldosterone Syst. JRAAS* 4, 164–168. doi:10.3317/jraas.2003.025

Pitt, B., Zannad, F., Remme, W. J., Cody, R., Castaigne, A., Perez, A., et al. (1999). The effect of spironolactone on morbidity and mortality in patients with severe heart failure. Randomized Aldactone Evaluation Study Investigators. *N. Engl. J. Med.* 341, 709–717. doi:10.1056/NEJM199909023411001

Ramirez, E., Klett-Mingo, M., Ares-Carrasco, S., Picatoste, B., Ferrarini, A., Rupérez, F. J., et al. (2013). Eplerenone attenuated cardiac steatosis, apoptosis and diastolic dysfunction in experimental type-II diabetes. *Cardiovasc. Diabetol.* 12, 172. doi:10.1186/1475-2840-12-172

Rossello, A., Nuti, E., Ferrini, S., and Fabbi, M. (2016). Targeting ADAM17 sheddase activity in cancer. *Curr. Drug Targets* 17, 1908–1927. doi:10.2174/1389450117666160727143618

Scheller, J., Chalaris, A., Garbers, C., and Rose-John, S. (2011). ADAM17: a molecular switch to control inflammation and tissue regeneration. *Trends Immunol.* 32, 380–387. doi:10.1016/j.it.2011.05.005

Shinde, A. V., and Frangogiannis, N. G. (2014). Fibroblasts in myocardial infarction: a role in inflammation and repair. *J. Mol. Cell. Cardiol.* 70, 74–82. doi:10.1016/j.yjmcc.2013.11.015

Shinde, A. V., and Frangogiannis, N. G. (2017). Mechanisms of fibroblast activation in the remodeling myocardium. *Curr. Pathobiol. Rep.* 5, 145–152. doi:10.1007/s40139-017-0132-z

Simões e Silva, A. C., and Teixeira, M. M. (2016). ACE inhibition, ACE2 and angiotensin-(1-7) axis in kidney and cardiac inflammation and fibrosis. *Pharmacol. Res.* 107, 154–162. doi:10.1016/j.phrs.2016.03.018

Takayanagi, T., Forrester, S. J., Kawai, T., Obama, T., Tsuji, T., Elliott, K. J., et al. (2016). Vascular ADAM17 as a novel therapeutic target in mediating cardiovascular hypertrophy and perivascular fibrosis induced by angiotensin II. *Hypertension* 68, 949–955. doi:10.1161/HYPERTENSIONAHA.116.07620

Wang, X., Oka, T., Chow, F. L., Cooper, S. B., Odenbach, J., Lopaschuk, G. D., et al. (2009). Tumor necrosis factor-alpha-converting enzyme is a key regulator of agonist-induced cardiac hypertrophy and fibrosis. *Hypertension* 54, 575–582. doi:10.1161/HYPERTENSIONAHA.108.127670

Weber, K. T., and Brilla, C. G. (1991). Pathological hypertrophy and cardiac interstitium. Fibrosis and renin-angiotensin-aldosterone system. *Circulation* 83, 1849–1865. doi:10.1161/01.cir.83.6.1849

Wu, C. Y., Zhang, H., Zhang, J., Xie, C., Fan, C., Zhang, H., et al. (2018). Inflammation and fibrosis in perirenal adipose tissue of patients with aldosterone-producing adenoma. *Endocrinology* 159, 227–237. doi:10.1210/en.2017-00651

Zhou, Xl, Fang, Y. H., Wan, L., Xu, Q. R., Huang, H., Zhu, R. R., et al. (2018). Notch signaling inhibits cardiac fibroblast to myofibroblast transformation by antagonizing TGF-β1/Smad3 signaling. *J. Cell. Physiology* 234, 8834–8845. doi:10.1002/jcp.27543

frontiers | Frontiers in Pharmacology

TYPE Original Research
PUBLISHED 21 May 2024
DOI 10.3389/fphar.2024.1402782



OPEN ACCESS

EDITED BY
Ludwig Weckbach,
LMU Munich University Hospital, Germany

REVIEWED BY
Ioan Radu Lala,
Vasile Goldiș Western University of Arad, Romania
Adina Pop Moldovan,
Vasile Goldiș Western University of Arad, Romania

*CORRESPONDENCE
Celestino Sardu,
drsarducele@gmail.com

RECEIVED 18 March 2024
ACCEPTED 05 April 2024
PUBLISHED 21 May 2024

CITATION
Sardu C, Vittoria Marfella L, Giordano V, Lepre CC, D'Amico G, Volpicelli M, Contaldi C, Galiero R, Caturano A, Casolaro F, Sasso FC, Uran C, Cozzolino D, Nicoletti M, Signoriello G, Paolisso G and Marfella R (2024), Left bundle branch pacing and cardiac remodeling in HF patients with type 2 diabetes mellitus: epigenetic pathways and clinical outcomes. *Front. Pharmacol.* 15:1402782.
doi: 10.3389/fphar.2024.1402782



# Left bundle branch pacing and cardiac remodeling in HF patients with type 2 diabetes mellitus: epigenetic pathways and clinical outcomes

Celestino Sardu[1]*, Ludovica Vittoria Marfella[1], Valerio Giordano[2], Caterina Claudia Lepre[3], Giovanbattista D'Amico[4], Mario Volpicelli[5], Carla Contaldi[6], Raffaele Galiero[1], Alfredo Caturano[1], Flavia Casolaro[1], Ferdinando Carlo Sasso[1], Carlo Uran[7], Domenico Cozzolino[1], Maddalena Nicoletti[3], Giuseppe Signoriello[3], Giuseppe Paolisso[1,8] and Raffaele Marfella[1]

[1]Department of Advanced Medical and Surgical Sciences, University of Campania "Luigi Vanvitelli", Naples, Italy, [2]Department of Cardiovascular Disease, "Vallo Della Lucania" Hospital, Salerno, Italy, [3]Department of Experimental Medicine, University of Campania "Luigi Vanvitelli", Naples, Italy, [4]School of Geriatrics, University of L'Aquila, L'Aquila, Italy, [5]Cardiovascular Department, Santa Maria Delle Grazie Hospital, Nola, Italy, [6]Heart Failure Unit, Monaldi Hospital, Naples, Italy, [7]Department of Cardiovascular Diseases, San Giuseppe e Melorio Hospital, Santa Maria Capua Vetere, Italy, [8]UniCAMILLUS International Medical University, Rome, Italy

**Background:** Left bundle branch (LBB) pacing could achieve cardiac resynchronization therapy (CRT) in patients who cannot be resynchronized via the placement of the left ventricle (LV) lead into the coronary sinus. LBB pacing could improve cardiovascular outcomes in heart failure (HF) patients with LBB block who are affected by type 2 diabetes mellitus (T2DM).

**Study hypothesis:** LBB pacing could increase the number of CRT responders and lead to the best clinical outcomes in HF patients with T2DM, inducing cardiac remodeling and improving left ventricle ejection fraction (LVEF) via microRNA (miR) modulation.

**Methods:** In a multicenter observational study, we enrolled 334 HF patients with LBB block and an indication to receive LBB pacing for CRT. In these patients, we evaluated the CRT responder rate, clinical outcomes, and miR expression at 1 year of follow-up.

**Results:** At 1 year of follow-up, we had 223 responders (66.8%), 132 hospitalizations for HF (39.5%), 24 cardiac deaths (7.2%), and 37 all-cause deaths (11.1%), with a higher rate of HF hospitalizations (77 (69.4%) vs 55 (24.7%), $p < 0.05$), and cardiac deaths (13 (11.7% vs 11 (4.9%), $p < 0.05$) in non-responders vs responders. At the end of follow-up, we found the lowest expression of miR-26, miR-29, miR-30, miR-92, and miR-145 in LBB-pacing non-responders vs responders ($p < 0.05$), and a direct correlation between miR-30 (0.340, [0.833–1.915]; p 0.001), the 6-minute-walking test (6MWT; 0.168, [0.008–0.060]; p 0.011), angiotensin-receptor-neprilysin inhibitors (ARNI; 0.157, [0.183–4.877]; p 0.035), sodium-glucose-transporter-2 inhibitors (0.245,

[2.242–7.283]; p 0.001), and LVEF improvements. C reactive protein (CRP) inversely correlated with LVEF improvement (–0.220, [-(0.066–0.263)]; p 0.001). ARNI (1.373, CI 95% [1.007–1.872], p 0.045), miR-30 (2.713, CI 95% [1.543–4.769], p 0.001), and 6MWT (1.288, CI 95% [1.084–1.998], p 0.001) were predictors of LBB pacing responders at 1 year of follow-up.

**Conclusion:** LBB-pacing responders evidenced miR modulation, which was linked to significant improvement of the cardiac pump. Specifically, miR-30 was linked to cardiac pump improvement and predicted responders at 1 year of follow-up in patients with T2DM.

KEYWORDS

**heart failure, cardiac remodeling, reduced EF, T2DM, CRTd**

## Introduction

Cardiac resynchronization therapy (CRT) is recommended for patients with heart failure (HF) and left bundle branch (LBB) block (Glikson et al., 2021). Indeed, CRT could restore ventricular synchrony and improve LV hemodynamics by left ventricular lead placement through the coronary sinus (CS) (Glikson et al., 2021). These effects could improve exercise tolerance, reducing HF hospitalizations and mortality via LV reverse cardiac remodeling (Sardu et al., 2018a; Glikson et al., 2021). LV reverse cardiac remodeling is linked to the reduction of cardiac hypertrophy, fibrosis, and apoptosis via the modulation of specific microRNAs (miRs) (Marfella et al., 2013; Sardu et al., 2016). These effects are seen in patients defined as CRTd responders and linked to the modulation of a few miRs, which are differently expressed in non-responder vs responder patients (Marfella et al., 2013; Sardu et al., 2016). Notably, a higher percentage of CRT patients have type 2 diabetes mellitus (T2DM), which could negatively affect the responder rate and clinical outcomes (Marfella et al., 2013; Sardu et al., 2016; Sardu et al., 2018a; Glikson et al., 2021). Conversely, about 5%–7% of selected patients cannot receive CRT because of unsuccessful or complicated LV lead placement through CS and evidence of other limiting factors (Vijayaraman et al., 2021). The authors proposed CRT via LBB pacing in this setting, which is feasible and safe and provides an alternative treatment (Vijayaraman et al., 2021). Intriguingly, LBB pacing could lead to cardiac remodeling and the best clinical outcomes in HF patients who cannot receive CRT via CS pacing (Chen et al., 2022). On the other hand, the benefits of LBB pacing on cardiac remodeling and clinical outcomes are still under-investigated at the molecular and epigenetic levels in HF patients with T2DM. Therefore, here we evaluated the effects of LBB pacing on CRT response (responder rate) as the primary study endpoint and the rates of all causes of death, cardiac deaths, and HF hospitalizations in patients with T2DM as secondary study endpoints. Then, we evaluated the miRs differently expressed in LBB-pacing non-responders vs responders with T2DM at baseline and at 1 year of follow-up. Finally, we evaluated the miRs and other study variables correlated with echocardiographic indexes of cardiac pump improvement (increase of LV ejection fraction, LVEF> 10%) at 1 year of follow-up in LBB-pacing patients with T2DM.

## Methods

In all the participating centers, we enrolled consecutive HF patients with LBB, diagnosed T2DM, and indicated to receive CRT via LBB pacing (Glikson et al., 2021). The T2DM diagnosis was made according to the diagnostic criteria of the American Diabetes Association (Ref Moghissi et al., 2009). These patients did not receive the CRT via the placement of a left ventricular lead through the coronary sinus because it was not possible to reach the optimal LV pacing site via the right branch of the coronary sinus or by evidence of occlusion of the coronary sinus anatomy, phrenic nerve stimulation, and other anatomical constraints negatively influencing the CRT procedure (Vijayaraman et al., 2021; Chen et al., 2022). The screened T2DM patients answered a specific questionnaire about medicines used for diabetes treatment, the date of the beginning and end of treatment, the route of administration, and the duration of use (Ref Moghissi et al., 2009). These patients received CRT via the LBB pacing and met the following inclusion and exclusion criteria:

Inclusion criteria: age 18–80 years, sinus rhythm, LBB block, diagnosis of well-controlled T2DM (glycated hemoglobin (Hb1Ac) ≤7%), and clinical history of stable chronic HF under at least 3 months of guideline-directed medical anti-HF therapy (Gorcsan et al., 2008); NYHA functional class II or III, severe left ventricle ejection fraction reduction (LVEF <35%), stable sinus rhythm and indication to receive CRT (Glikson et al., 2021). The patients who respected the criteria received a CRT implant for LBB pacing (Vijayaraman et al., 2021).

Exclusion criteria: non-LBB QRS morphology, diagnosis of right bundle branch block (RBBB) or intraventricular conduction delay; T2DM with Hb1Ac>7%, unstable HF, NYHA functional class IV, persistent atrial fibrillation; patients previously treated with CRT, pacemakers, or internal cardioverter defibrillator implants; hyperkalemia, systolic hypotension (systolic blood pressure <90 mmHg); patients with an estimated glomerular filtration rate (eGFR) of at least 30 mL per minute per 1.73 $m^2$ of body surface area; pregnancy, inflammatory chronic systemic disease, or oncological disease; absence of informed patient consent, and any condition that would make survival for 1 year unlikely. The Institutional Review Boards at the enrolling hospitals approved the study, and all patients provided informed consent for the intervention (LBB-CRT pacing) and to participate in the study. Then, the enrolled study population was divided into two groups:

non-responders vs responders to CRT via LBB pacing according to trans thoracic echocardiographic evidence of a significant cardiac pump increase and LV reverse remodeling and significant change in functional HF class (NYHA class amelioration).

## Study design

We performed a multicenter, observational study with a follow-up of 1 year. We performed LBB pacing on all the study patients for CRT. In this cohort of patients with HF and T2DM, we evaluated the CRT responder rate as the primary study endpoint and all causes of death, cardiac deaths, and HF hospitalizations at 1 year of follow-up as secondary study endpoints. Finally, we evaluated the miRs expressed at baseline and at the end of follow-up in the LBB-pacing non-responders vs responders. Then, we correlated the clinical variables and the investigated miRs to the echocardiographic parameters of a significant increase in cardiac pump at the end of follow-up.

## Anthropometric and echocardiographic evaluations

The authors performed a physical examination of all enrolled patients, with evaluation of vital signs and revision of adverse events at follow-up. In the study cohorts, we performed a transthoracic two-dimensional echocardiogram with M-mode recordings, conventional Doppler, and pulsed-wave tissue Doppler imaging (TDI) measurements at baseline and then at 12 months of follow-up using a Philips iE33 echocardiograph (Eindhoven, Netherlands). The left ventricle end-diastolic diameters (LVEDD), end-diastolic volumes (LVEDV), end-systolic diameters (LVESD), and end-systolic volumes (LVESV) were measured. We calculated the LVEF with the Simpson method (Gorcsan et al., 2008). We classified the grading of mitral regurgitation as low (+), moderate (++), moderate-severe (+++), and severe (++++) (Jankowska et al., 2011). The diagnostic exam was performed by physicians fully trained in echocardiography, blinded to the study protocol. Finally, the authors analyzed all echocardiographic data.

## Implanting procedures and device programming

Experienced physicians in LBB pacing performed the implantation using the LBB pacing catheters (SelectSecure, model 3,830, Medtronic Inc., Minneapolis, United States; Solia S, Biotronik, Berlin, Germany) and dedicated delivery sheaths (C304 and C 315, Medtronic Inc., Minneapolis, United States; Selectra 3D, Biotronik, Berlin, Germany) available for use (Sardu et al., 2016; Vijayaraman et al., 2021). The LBB pacing lead was introduced into the right ventricle (RV) and placed on the right side of the interventricular septum (IVS), and here advanced deeply into the IVS until it reached the LV septal subendocardium and the RBBB morphology of the paced QRS complex was observed in electrocardiogram (ECG) lead V1 (Vijayaraman et al., 2021; Chen et al., 2022). We performed a pacing test during the procedure. Surface 12-lead ECG, intracardiac electrograms, and fluoroscopy were simultaneously monitored. We measured the pacing stimulus-to-LV activation time (LVAT) in lead V5 or V6 at low (<3 V/0.5 ms) and high (>5 V/0.5 ms) outputs. The lead tip was considered to be at the final position once LBB capture was confirmed by evidence of 1) the LBBB morphology disappearance, with a paced RBBB pattern (typical or atypical) observed in lead V1; 2) LVAT<100 ms at low pacing output (<3 V/0.5 ms), (Vijayaraman et al., 2021; Chen et al., 2022). We assessed the penetration depth in the IVS by injecting contrast medium through the sheath in the left anterior oblique 45-degree view during the procedure and by transthoracic echocardiography before discharge. Then, we used the CRT with a defibrillator (CRTd) device, then connecting the LBBP lead to the LV port of the device (Vijayaraman et al., 2021; Chen et al., 2022). We programmed the VV delay with devices in DDD mode to ensure exclusive LBBP with atrioventricular (AV) delay optimization for the shortest QRS interval duration. At the end of the procedure, we confirmed the final position of the CRT leads by catheter interrogation and cine fluoroscopy view.

## Laboratory analysis

After an overnight fast in all patients, we evaluated the plasma glucose, HbA1c, serum lipids, and B-type natriuretic peptide (BNP) by enzymatic assays. We evaluated serum levels of pro-inflammatory cytokines (tumor necrosis factor-alpha (TNFα), interleukin-1, (IL-1), and interleukin-6 (IL-6)), systemic inflammatory markers (C reactive protein, CRP), leucocytes and neutrophils count at baseline and 12-month follow-up (Sardu et al., 2018b; Adamo et al., 2020). We used commercially available enzyme-linked immunosorbent assays (ELISAs) kits to determine the TNFα, IL-1, IL-6, and CRP (TNFα: TNF alpha Human ELISA Kit KHC3011, Thermo Fisher Scientific; IL-1: Hu-man IL-1 α ELISA Kit RAB0269, Sigma-Aldrich; IL-6: Human IL-6 Quantikine ELISA Kit D6050, R&D Systems; CRP: CRP Human ELISA kit KHA0031, Thermo Fisher Scientific). An ice-cooled blood collection system was used to collect blood samples, which were immediately centrifuged for 10 min at 2,500 rpm at 4°C. Before proceeding with ELISAs, we isolated the supernatants containing serum samples and then stored them at −80°C.

## RNA serum extraction and miR analysis

We extracted 200 μL of serum from each enrolled CRT patient via peripheral venous blood samples at baseline and follow-up. We used the miRNeasy Mini kit to characterize the miR expression (Qiagen, 20124 Milan, Italy) (Marfella et al., 2013; Sardu et al., 2016). A single reaction for RNA isolation was carried out by pooling eight serum samples extracted from patients matched for sex, age, and clinical evaluations. Then, we assayed the miRs from blood samples at baseline and quarterly during 12 months of follow-up in LBB-responders vs LBB-non-responder patients. We evaluated the miRs implied in various processes of HF and previously evaluated and differently expressed in CRT defibrillator (CRTd) responders vs

non-responders (Marfella et al., 2013; Sardu et al., 2016). Thus, we spiked a 5-μL aliquot of 5 nM Syn-cel-miRNA-39 miScript miRNA-Mimic from the total RNA, including small RNAs, before nucleic acid preparation to monitor the efficiency of miR recovery and to normalize subsequent miR expression (Marfella et al., 2013; Sardu et al., 2016). We evaluated the serum expression of the miR-26b-5p, miR-29a-3p, miR-30e-5p, miR-92a-3p, and miR-145-5p, as previously seen in the CRT response (Marfella et al., 2013; Sardu et al., 2016). To date, we performed triplicate determinations of hsa-miR-26 (MIMAT0000083), miR-29 (MIMAT0000086), miR-30 (MIMAT0000692), miR-92 (MIMAT0000092), miR-145 (MIMAT0000437), and Ce_miR-39-3p (MIMAT0000010) through a CFX96 Real-Time System C1000 Touch Thermal Cycler (BioRad Laboratories, Inc), by using miScript SYBR Green PCR kit (218073, QIAGEN) and specific miScript primer assays (MS00003234, MS00003262, MS00009401, MS00006594, MS00003528, and MS00019789) (Lappegård et al., 2015; Vijayaraman et al., 2021; Chen et al., 2022). qRT-PCR data were analyzed by using the $2^{-\Delta\Delta Ct}$ method, where cycle threshold (Ct) values were determined by CFX Manager™ Software (BioRad Laboratories, Inc).

## Study endpoints

We evaluated the following primary and secondary study endpoints at 1 year of follow-up. Primary study endpoint: the rate of CRT responders to LBB pacing. We investigated the rate of CRT responders by the diagnosis of LV reverse remodeling (reduction in LVESV ≥10%) and significant increase of cardiac pump (assessment of LVEF ≥10%) assessed by transthoracic echocardiography, and significant change in functional HF class (improvement of the six min-walk test (6MWT) and Minnesota Living with HF scale improvement). Therefore, at follow-up, we re-evaluated the NYHA classification for each patient. The enrolled patients were instructed regularly to assess body weight, the occurrence of dyspnea, and any clinical symptoms. The patients graded their overall condition as unchanged or slightly, moderately, markedly worsened, or improved by global self-assessment (Sardu et al., 2018a).

-Secondary endpoints: all causes of death, cardiac deaths, and HF hospitalization events. Then, in these two groups of patients (responders vs non-responders), we selectively evaluated the miR expressions at baseline and 1 year of follow-up. Finally, we evaluated the miRs and study variables correlated to echocardiographic indexes of cardiac pump improvement (an increase of LVEF >10%) at 1 year of follow-up in LBB-pacing patients.

## Statistical methods

The data were collected and then analyzed by a qualified statistician. The HF patients treated by LBB pacing were then divided into non-responder vs responder cohorts. We performed the safety analyses on data from all HF and LBB-enrolled patients. Continuous variables were expressed as means and standard deviations and tested by a two-tailed Student's t-test. The categorical variables were compared using the chi-square or Fisher exact test where appropriate. We calculated the number of patients who showed echocardiographic evidence of significant improvement in cardiac pump (increase of LVEF ≥10%) at 1 year of follow-up. We reported this study event as a "yes" (score 1) or "not" (score 0). Then, we evaluated by multiple regression analysis its relationship with miRs and other study variables (after the evaluation of the normal distribution of model variables by residue analysis) at the end of follow-up. Finally, the predictors of the response (responder rate, as primary study endpoint) to CRT via LBB pacing at 1 year of follow-up were evaluated using Cox regression models in the study population adjusted for study variables: age, angiotensin-receptors-neprilysin inhibitors (ARNI), beta-blockers, BMI >30 kg/m$^2$, BNP, CRP, HbA1c, hypertension, LVEF, miR-30, miR-145, QRS at baseline, sodium-glucose-transporter 2 inhibitors (SGLT2i), II NYHA class, and 6MWT. A $p$-value < 0.05 was considered statistically significant. The statistical analysis was performed using the SPSS software package for Windows 17.0 (SPSS 23 Inc., Chicago, Illinois).

# Results

- Baseline findings: The characteristics of overall T2DM patients treated by LBB pacing (n = 334) and study cohorts divided as non-responders (n = 111) vs responders (n = 223) were reported in Table 1. At baseline, we did not find a significant difference between the LBB-pacing non-responders vs responders (p > 0.05) Table 1.
- Effects of LBB pacing on clinical parameters: At 1 year of follow-up, comparing LBB-pacing non-responders vs responders, we found significant differences regarding the clinical parameters of NYHA class (worsening of NYHA class), higher QRS duration, and BNP values, and lower values of 6MWT (p < 0.05); see Table 1. Non-responders showed higher values of inflammatory markers (p < 0.05) than responders; see Table 1. Conversely, non-responders showed the lowest values of LVEF (worsening of the cardiac pump) and highest values of end-diastolic and end-systolic diameters and volumes (p < 0.05); these study cohorts evidenced significant differences in the grade of mitral insufficiency (p < 0.05); see Table 1. Finally, at 1 year of follow-up, LBB-pacing non-responders vs responders showed a higher rate of patients receiving ARNI and SGLT2-I therapy (p < 0.05) Table 1.
- Primary and secondary study endpoints: at 1 year of follow-up, we reported 223 responder patients (66.8%) in the overall population, 132 hospitalizations for HF (39.5%), 24 cardiac deaths (7.2%), and 37 events of all-cause death (11.1%). We found a higher rate of HF hospitalizations (77 (69.4%) vs 55 (24.7%), p < 0.05) and cardiac deaths (13 (11.7%) vs 11 (4.9%), p < 0.05) in non-responders at 1 year of follow-up. The two groups did not differ in the rate of all causes of death (15 (13.5%) vs 22 (9.9%), p > 0.05) at 1 year of follow-up.
- MiR expression: In Figure 1, we reported the miR expression at baseline vs end of follow-up in LBB-pacing non-responders vs responders. At baseline (A part), we did not find significant differences in miR expression (miR-26, miR-29, miR-30, miR-92, and miR-145) in LBB-pacing non-responders vs

TABLE 1 Clinical characteristics of our study population at baseline and at the end of follow-up as CRT non-responders vs responders.

| Clinical parameter | Overall LBB pacing patients (n = 334) | Baseline | | *p*-value | 1-year follow-up | | *p*-value |
|---|---|---|---|---|---|---|---|
| | | Non-responders (n = 111) | Responders (n = 223) | | Non-responders (n = 111) | Responders (n = 223) | |
| Age, years | 70.7 ± 6.2 | 70.4 ± 5.9 | 70.8 ± 6.4 | 0.868 | 71.5 ± 5.9 | 71.8 ± 6.4 | 0.686 |
| Male, n (%) | 239 (71.5) | 75 (67.6) | 164 (73.5) | 0.260 | — | — | — |
| Smokers, n (%) | 175 (52.4) | 52 (46.8) | 123 (55.2) | 0.164 | 60 (54.1) | 134 (60.1) | 0.346 |
| BMI >30 kg/m$^2$ (%) | 24 (7.2) | 9 (8.1) | 15 (6.7) | 0.657 | 11 (9.9) | 19 (8.5) | 0.688 |
| Hypertension, n (%) | 237 (70.9) | 80 (72.1) | 157 (70.4) | 0.799 | 84 (75.7) | 162 (72.6) | 0.599 |
| Dyslipidemia, n (%) | 136 (40.7) | 49 (44.1) | 87 (39.0) | 0.408 | 45 (40.5) | 80 (35.9) | 0.472 |
| Ischemic heart failure, n (%) | 224 (67.1) | 73 (65.8) | 151 (67.7) | 0.803 | 84 (75.7) | 162 (72.6) | 0.599 |
| Plasma glucose (mg/dL) | 147.1 ± 23.2 | 146.3 ± 24.1 | 148.9 ± 22.7 | 0.388 | 141.6 ± 24.1 | 140.8 ± 20.7 | 0.356 |
| HbA1c (%) | 6.8 ± 0.36 | 6.8 ± 0.32 | 6.7 ± 0.41 | 0.084 | 6.6 ± 0.38 | 6.5 ± 0.41 | 0.113 |
| NYHA class, n (%) | | | | 0.402 | | | 0.001* |
| I NYHA class | | — | — | | 5 (4.2) | 22 (9.9) | |
| II NYHA class | | 25 (22.5) | 56 (25.1) | | 29 (26.1) | 99 (44.4) | |
| III NYHA class | | 86 (77.5) | 167 (74.9) | | 69 (62.2) | 96 (43.0) | |
| IV NYHA class | | — | — | | 8 (7.2) | 6 (2.7) | |
| QRS duration (ms) | 136.5 ± 8.5 | 135.9 ± 8.7 | 136.7 ± 8.5 | 0.187 | 130.8 ± 12.2 | 127.7 ± 11.6 | 0.022* |
| 6MWT | 240.32 ± 39.6 | 195.86 ± 32.53 | 190.46 ± 26.12 | 0.407 | 218.17 ± 44.15 | 247.17 ± 44.52 | 0.013* |
| BNP (pg/mL) | 420.73 [85.26–1,440.1] | 398.87 [58.10–1,398.87] | 464.66 [62.3–1,442.13] | 0.090 | 234.98 [83.12–751.15] | 157.98 [93.1–562.12] | 0.001* |
| **Inflammatory biomarkers** | | | | | | | |
| Lymphocytes | 7.47 ± 1.23 | 7.21 ± 1.08 | 7.65 ± 1.27 | 0.138 | 7.87 ± 1.68 | 7.30 ± 1.42 | 0.001* |
| Neutrophils | 5.94 ± 0.98 | 5.84 ± 1.02 | 5.99 ± 1.02 | 0.186 | 5.83 ± 0.98 | 5.50 ± 1.24 | 0.001* |
| CRP (mg/L) | 8.9 ± 0.98 | 8.66 ± 0.76 | 9.05 ± 0.51 | 0.734 | 6.29 ± 0.37 | 6.13 ± 0.40 | 0.001* |
| IL6 (pg/mL) | 6.53 ± 0.06 | 6.54 ± 0.07 | 6.48 ± 0.03 | 0.162 | 6.30 ± 0.09 | 5.99 ± 0.82 | 0.001* |
| TNFα (pg/mL) | 6.37 ± 0.04 | 6.35 ± 0.03 | 6.37 ± 0.04 | 0.744 | 6.36 ± 0.02 | 6.13 ± 0.02 | 0.001* |
| **Echocardiographic parameters** | | | | | | | |
| LVEF (%) | 30.1 ± 5.2 | 30.7 ± 4.2 | 29.7 ± 5.5 | 0.114 | 34.2 ± 9.3 | 46.1 ± 5.5 | 0.001* |
| LVEDd (mm) | 71.2 ± 3.9 | 71.5 ± 4.1 | 71.0 ± 3.8 | 0.276 | 69.5 ± 5.7 | 65.2 ± 3.8 | 0.001* |
| LVESd (mm) | 39.7 ± 2.4 | 41.5 ± 3.8 | 39.6 ± 2.4 | 0.289 | 39.9 ± 2.6 | 38.6 ± 4.8 | 0.152 |
| LVEDv (mL) | 240.9 ± 27.9 | 241.5 ± 14.7 | 243.9 ± 16.8 | 0.193 | 228.4 ± 19.7 | 210.5 ± 14.1 | 0.001* |
| LVESv (mL) | 131.3 ± 11.9 | 130.9 ± 19.3 | 133.3 ± 21.5 | 0.062 | 125.6 ± 15.8 | 104.9 ± 16.8 | 0.001* |
| Mitral insufficiency | | | | 0.812 | | | 0.046* |

(Continued on following page)

TABLE 1 (*Continued*) Clinical characteristics of our study population at baseline and at the end of follow-up as CRT non-responders vs responders.

| Clinical parameter | Overall LBB pacing patients (n = 334) | Baseline | | *p*-value | 1-year follow-up | | *p*-value |
|---|---|---|---|---|---|---|---|
| | | Non-responders (n = 111) | Responders (n = 223) | | Non-responders (n = 111) | Responders (n = 223) | |
| + (%) | | 53 (47.7) | 102 (45.7) | | 44 (39.6) | 112 (50.2) | |
| ++ (%) | | 41 (36.9) | 89 (39.9) | | 45 (40.5) | 98 (43.9) | |
| +++ (%) | | 17 (15.3) | 32 (14.3) | | 18 (16.2) | 13 (5.8) | |
| ++++ (%) | | | | | 3 (2.7) | — | |
| **Medications** | | | | | | | |
| Beta-blockers, n (%) | 220 (65.9) | 74 (66.7) | 146 (65.5) | 0.903 | 81 (73.0) | 162 (72.6) | 0.443 |
| Carvedilol | | 56 (75.7) | 105 (71.9) | | 60 (74.1) | 120 (74.1) | |
| Bisoprolol | | 18 (24.3) | 41 (28.1) | | 21 (25.9) | 42 (25.9) | |
| Calcium antagonist, n (%) | 16 (4.8) | 5 (4.5) | 11 (4.9) | 0.863 | 4 (3.6) | 9 (4.0) | 0.940 |
| Amiodarone, n (%) | 63 (18.9) | 20 (18.0) | 43 (19.3) | 0.882 | 27 (24.3) | 48 (21.5) | 0.443 |
| ACE inhibitors, n (%) | 84 (25.1) | 25 (22.5) | 59 (26.5) | 0.504 | 32 (28.8) | 60 (26.9) | 0.795 |
| ARS blockers, n (%) | 87 (26.0) | 33 (29.7) | 54 (24.2) | 0.292 | 35 (31.5) | 60 (26.9) | 0.440 |
| ARNI, n (%) | 101 (30.2) | 29 (26.1) | 72 (32.3) | 0.258 | 52 (46.8) | 78 (35.0) | 0.043* |
| Aspirin, n (%) | 124 (37.1) | 43 (38.7) | 81 (36.3) | 0.719 | 48 (43.2) | 84 (37.7) | 0.344 |
| Warfarin, n (%) | 99 (29.6) | 37 (33.3) | 62 (27.8) | 0.411 | 39 (35.1) | 66 (29.6) | 0.319 |
| NOAC, n (%) | 65 (19.5) | 25 (22.5) | 40 (17.9) | 0.379 | 26 (23.4) | 45 (20.2) | 0.270 |
| Ticlopidine, n (%) | 8 (2.4) | 2 (1.8) | 6 (2.7) | 0.724 | 4 (3.6) | 6 (2.7) | 0.736 |
| Ivabradine, n (%) | 103 (30.8) | 33 (29.7) | 70 (31.4) | 0.802 | 31 (27.9) | 70 (31.4) | 0.530 |
| Digoxin, n (%) | 98 (29.3) | 34 (30.6) | 64 (28.7) | 0.799 | 36 (32.4) | 68 (30.5) | 0.802 |
| Diuretics, n (%): loop diuretics | | 89 (80.2) | 188 (84.3) | 0.357 | 101 (91.0) | 196 (87.9) | 0.462 |
| Tiazides | | 13 (11.7) | 24 (10.8) | 0.517 | 14 (12.6) | 31 (13.9) | 0.865 |
| Aldosterone blockers | | 67 (60.4) | 129 (57.8) | 0.559 | 87 (78.4) | 155 (69.5) | 0.093 |
| Statins, n (%) | 234 (70.1) | 81 (73.0) | 153 (68.6) | 0.448 | 85 (76.6) | 160 (71.7) | 0.362 |
| SGLT2-I, n (%) | 71 (21.2) | 24 (21.6) | 47 (21.1) | 0.909 | 38 (34.2) | 50 (22.4) | 0.041* |
| Anti-DM medications, n (%) | | | | 0.631 | | | 0.813 |
| -oral hypoglycemic | 295 (88.3) | 96 (86.5) | 199 (89.2) | | 99 (89.2) | 202 (90.6) | |
| -insulin | 71 (21.3) | 25 (22.5) | 46 (20.6) | | 28 (25.2) | 53 (23.8) | |
| -DPP4i | 68 (20.4) | 24 (21.6) | 44 (19.7) | | 25 (22.5) | 52 (23.3) | |
| -GLP1-RA | 53 (15.9) | 17 (15.6) | 36 (16.1) | | 20 (18.0) | 39 (17.5) | |

responders; see Figure 1. At the end of follow-up (B part), we found the lowest expression of miR-26, miR-29, miR-30, miR-92, and miR-145 in the LBB-pacing non-responders vs responders ($p < 0.05$); see Figure 1.

- MiR changes and clinical parameters: The multiple variable regression analysis showed the relationship between study variables and cardiac pump (LVEF) improvement at 1 year follow-up post-LBB-pacing. Thus, we found a direct correlation

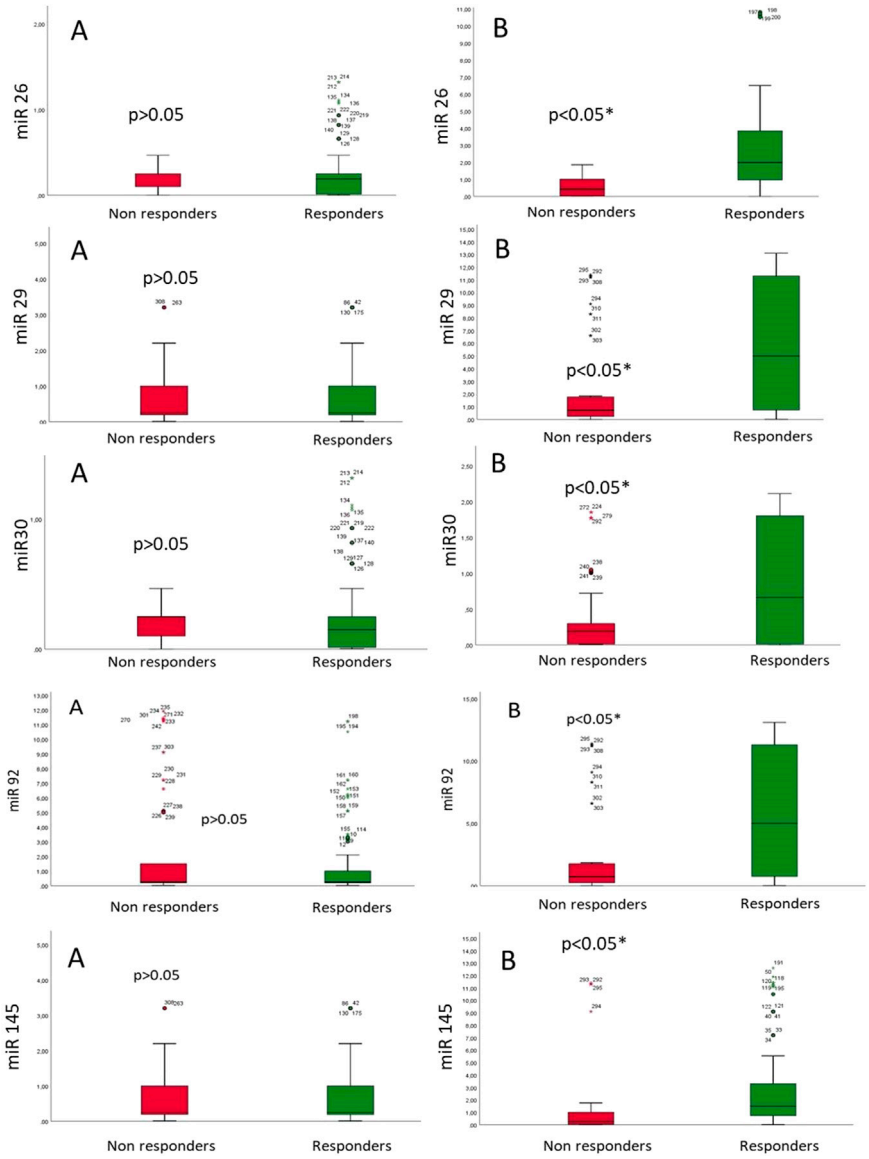


FIGURE 1
MicroRNA (miR) expression at baseline **(A)** and the end of follow-up **(B)** in patients with HF and T2DM in LBB-pacing non-responders vs. responders.

between miR-30 (0.340, [0.833–1.915]; p0.001), 6MWT (0.168, [0.008–0.060]; p 0.011), ARNI (0.157, [0.183–4.877]; p 0.035), and SGLT2i (0.245, [2.242–7.283]; p 0.001). In contrast, we found an inverse correlation between CRP (−0.220, [-(0.066–0.263)]; p 0.001) and LVEF improvement. Then, we used Cox regression analysis and found that ARNI therapy (1.373, CI 95% [1.007–1.872], p 0.045), miR-30 (2.713, CI 95% [1.543–4.769], p 0.001), and 6MWT (1.288, CI 95% [1.084–1.998], p 0.001), were predictors of LBB-pacing responders at 1 year of follow-up; see Table 2.

## Discussion

In our study, 223 T2DM patients (66.8%) were found to respond to CRT via LBB-pacing at 1 year of follow-up. LBB-pacing non-responders vs responders showed a worse NYHA class, higher QRS duration and BNP values, and the lowest values of 6MWT at 1 year of follow-up ($p < 0.05$). This negative clinical trend is linked to over-inflammation, worsening of the cardiac pump, and a more severe degree of mitral insufficiency ($p < 0.05$). Conversely, a higher rate of non-responders vs responders was found under ARNI and SGLT2-I therapy ($p < 0.05$) and showed the lowest expression of miRs ($p < 0.05$). Notably, miR-30 (β 0.340), 6MWT (β 0.168), ARNI (β 0.157), and SGLT2i therapy (β 0.245) correlated with significant improvements in LVEF ($p < 0.05$). In contrast, CRP values were inversely correlated (β-0.220) with significant improvements in the LVEF ($p < 0.05$). Intriguingly, miR-30 values (HR 2.7), ARNI therapy (HR 1.37), and the highest 6MWT values (HR 1.29) predicted the CRT responders via LBB pacing at 1 year of follow-up in T2DM patients ($p < 0.05$).

TABLE 2 Cox regression analysis for primary study endpoint (LBB-pacing responders) at 1 year of follow-up.

| | Univariate analysis | | | Multivariate analysis | | |
|---|---|---|---|---|---|---|
| Risk factor | HR | CI, 95% | *p*-value | HR | CI, 95% | *p*-value |
| Age | 1.007 | 0.983–1.031 | 0.565 | | | |
| ARNI | 1.375 | 1.054–1.795 | 0.019* | 1.373 | 1.007–1.872 | 0.045* |
| Beta-blockers | 1.041 | 0.789–1.372 | 0.777 | | | |
| BMI >30 kg/m$^2$ | 0.748 | 0.443–1.263 | 0.277 | | | |
| BNP | 1.015 | 0.989–1.102 | 0.277 | | | |
| CRP | 1.002 | 0.987–1.016 | 0.808 | | | |
| Glycemia | 0.852 | 0.650–1.117 | 0.248 | | | |
| Hb1Ac | 0.101 | −0.181–0.192 | 0.084 | | | |
| Hypertension | 1.053 | 0.789–1.404 | 0.726 | | | |
| LVEF | 0.950 | 0.847–0.973 | 0.047* | 0.956 | 0.927–1.126 | 0.104 |
| miR-30 | 1.954 | 1.109–3.441 | 0.020* | 2.713 | 1.543–4.769 | 0.001* |
| miR-145 | 1.015 | 0.859–1.199 | 0.863 | | | |
| QRS duration | 1.013 | 0.998–1.028 | 0.097 | | | |
| SGLT2i | 0.837 | 0.606–1.154 | 0.277 | | | |
| II NYHA class | 1.080 | 0.825–1.413 | 0.576 | | | |
| 6MWT | 1.192 | 1.018–1.996 | 0.001* | 1.288 | 1.084–1.998 | 0.001* |

CRT could improve myocardial ventricular geometry and cardiac pump in a comparable proportion of diabetic and non-diabetic patients, along with a similar functional status amelioration (Sardu et al., 2014). These clinical effects could link to significant modulation of the miRs implied in cardiac remodeling in the CRT responders via over-expression of miR 26, miR 29, miR 30, miR 92, and miR 145 (Marfella et al., 2013; Sardu et al., 2016). In this setting, we could first confirm that LBB pacing is an alternative treatment for patients who cannot be treated by positioning a left ventricular lead into the CS (Vijayaraman et al., 2021; Chen et al., 2022). Second, LBB pacing is equal to CS pacing for achieving the best clinical outcomes in CRT patients (Vijayaraman et al., 2021; Chen et al., 2022). We confirmed this trend in our population of LBB-pacing patients; in particular, we positively correlated the miR-30 values to improving the cardiac pump. Furthermore, the highest miR-30 values increased by about 2.7 fold in the responders to LBB-pacing at the end of follow-up. The miRs investigated here could be implied in failing heart adaptive processes and modulated (overexpressed) in CRT responders.

The reversion of these adaptive cardiac processes is linked to LV reverse remodeling and the improvement of the cardiac pump, with consequent improvement of symptoms and clinical outcomes. Furthermore, we might speculate that the LBB pacing might regulate cardiac apoptosis, fibrosis, and angiogenesis by modulation of miRs (and expression of genes) implied in these cardiac remodeling processes. In this scenario, the miR-30 regulated myocardial hypertrophy by decreasing cystathionine-γ-lyase expression, hydrogen sulfide production, and reducing hypoxic cardiomyocyte injury in a murine model (Marfella et al., 2013; Sardu et al., 2016). In humans treated with CRT, the miR-30 could control cardiac angiogenesis and apoptosis, and it is significantly overexpressed in CRT responders (Marfella et al., 2013; Sardu et al., 2016).

Similarly, 6MWT (β 0.168), ARNI (β 0.157), and SGLT2i (β 0.245) linked to LV reverse remodeling at the end of follow-up ($p < 0.05$). In contrast, the inflammation (CRP, β −0.220) is inversely correlated to LV reverse remodeling at the end of follow-up. The inflammation is a well-known negative prognostic and diagnostic marker and trigger of HF in overall patients (Lappegård et al., 2015; Dick and Epelman, 2016) and particularly in those treated with CRT (Sardu et al., 2022). Indeed, over-inflammation could lead to cardiac remodeling via enhanced cardiac fibrosis and an increase of cardiac volumetry in CRT patients, then conditioning a worse prognosis (Marfella et al., 2013; Sardu et al., 2016; Sardu et al., 2022). Intriguingly, over-inflammation and the altered glycemic status could cause the modification of circulating proteins and ionic channels, which are implied in the entity of CRT response in T2DM patients (Gambardella et al., 2022). Indeed, this could cause the ryanodine receptor 1 (RyR1) glycation in circulating lymphocytes (Gambardella et al., 2022). The RyR1 glycation could predict CRT responsiveness via pathologic intracellular calcium leakage (Gambardella et al., 2022). In this setting, the 6MWT is a diagnostic, monitoring, and prognostic test of clinical outcomes in CRT patients (Gorcsan et al., 2008; Sardu et al., 2018a; Glikson et al., 2021). Indeed, HF patients with the highest values of 6MWT have the best cardiovascular performance and clinical outcomes (Gorcsan et al., 2008; Sardu et al., 2018a; Glikson et al., 2021). In this setting, we found that higher 6MWT values at baseline could link to significant improvement of the cardiac pump. The highest

6MWT values at baseline resulted in a 1.288-fold higher responder rate at the end of follow-up. Conversely, anti-HF drugs with anti-remodeling properties, such as ARNI (0.157) and SGLT2i (0.245), are linked to improvement of the cardiac pump. Furthermore, ARNI therapy increased the odds of responders post LBB pacing at 1 year of follow-up about 1.37 times. In this scenario, ARNI is the gold standard and first-step therapeutic approach to induce LV reverse remodeling with improvement of cardiac pump and the best clinical outcomes in HF patients (Gorcsan et al., 2008). In line with this result, CRT non-responders are divided into ARNI users vs non-ARNI users; the ARNI therapy could promote functional and clinical improvement by modulating the epigenetics of adverse molecular remodeling (Sardu et al., 2023). Indeed, the ARNI promoted a beneficial effect on cardiac dysfunction, dyssynchrony, and clinical status in non-responder CRT patients via the changes in miR plasma levels (Sardu et al., 2023). Similarly, SGLT2i are anti-remodeling drugs and a first-step therapeutic approach and gold standard therapy for HF patients (Gorcsan et al., 2008). Indeed, the SGLT2i showed cardiovascular and systemic protective effects via anti-inflammatory properties (Sardu et al., 2023; Donofrio et al., 2021) and inducing cardiac pathways implied in the modulation of cardiac systolic and diastolic function in humans beyond the glycemic control (Marfella et al., 2022a; Marfella et al., 2022b). Our data showed that SGLT2i therapy positively correlated with cardiac pump improvements at the end of follow-up ($p < 0.05$).

## Study limitations

Further studies using large-scale microarray profiling are needed to address the association between CRT via LBB pacing and miR changes in non-responding vs responding T2DM patients. We did not find a correlation between the causative or mechanistic relationship between LV reverse remodeling after CRTd and LBB pacing in the T2DM population. On the other hand, as seen in previous studies (Sardu et al., 2016; Vijayaraman et al., 2021), we demonstrated the relationship between clinical, molecular, and echocardiographic parameters of LBB-pacing responders with miR changes. Thus, the findings could indirectly support the favorable epigenetic effects of CRT via LBB pacing in HF patients with T2DM who cannot be treated by CRT via CS pacing. Again, the LBB pacing could lead to LV reverse remodeling and best clinical outcomes via a reduction of the inflammatory burden. This suggests a correlation between over-inflammation, miR expression, and LV reverse remodeling in HF patients treated with LBB pacing.

Conversely, here, we did not provide an animal model of chronic HF with T2DM or an *ex-vivo* model of cultured cardiomyocyte cells. Both these models could help, from one side, to test the effects of LBB pacing on inflammation/miR expression LV reverse remodeling and clinical outcomes. On the other side, they could be used to test the effects of specific treatment with mimic-miR on inflammation and the different remodeling cardiac processes in patients treated with LBB pacing. This new approach could be used in the clinic to improve outcomes.

In this context, the miRs could be markers and potential targets of cardiovascular diseases and HF (Zhu and Fan, 2011; Mahjoob et al., 2022; Macvanin et al., 2023). Thus, specific anti-remodeling therapies could be used to modify the expression of miRs (Brioschi et al., 2023) and lead to the best clinical outcomes. In this setting, specifically, the miR-30 is implied in LV remodeling, with ameliorative effects on the cardiac pump and best clinical outcomes (Melman et al., 2015). The miR-30 is induced by CRT (Melman et al., 2015). Further studies will be designed to address this hypothesis and identify novel molecular markers of reversed remodeling after LBB pacing. Finally, but not less relevant, we might consider cardiac magnetic resonance imaging (MRI) added to late gadolinium enhancement (LGE) imaging to investigate the cardiac fibrosis and reverse remodeling in LBB pacing patients at baseline and at the end of follow-up. Indeed, in patients without contraindications to MRI, the combination of LGE imaging and cine imaging would make MRI the modality of choice in assessing LV remodeling and cardiac pump function in HF patients (Cohn et al., 2000).

# Conclusion

LBB pacing is an alternative CRT technique that provides ventricular synchrony, induces LV reverse remodeling, and improves clinical symptoms in HF patients with LBB and T2DM. Notably, the patients who responded to LBB pacing evidenced a selective miR modulation, which was linked to significant improvement of cardiac pump in T2DM patients. Specifically, we highlighted miR-30 as the miR directly linked to improvement of cardiac pump and predictor of responders event at 1 year of follow-up.

# Data availability statement

The raw data supporting the conclusions of this article will be made available by the authors, without undue reservation.

# Ethics statement

The studies involving humans were approved by the University of Campania "Luigi Vanvitelli." The studies were conducted in accordance with the local legislation and institutional requirements. Written informed consent for participation was obtained from the participants in accordance with the national legislation and institutional requirements. Written informed consent was obtained from the individual(s) for the publication of any potentially identifiable data included in this article.

# Author contributions

CS: writing–original draft. VL: writing–review and editing, writing–original draft, and investigation. VG: writing–review and editing, writing–original draft, validation, and investigation. CL: writing–review and editing, writing–original draft, investigation, and data curation. GD'A: writing–review and editing, writing–original draft, and conceptualization. MV: writing–review and editing, writing–original draft, and methodology. CC: writing–review and editing, writing–original draft, and methodology. RGa: writing–review and editing, writing–original

draft, and methodology. AC: writing–review and editing, writing–original draft, and methodology. FC: writing–review and editing, writing–original draft, and data curation. FS: writing–review and editing, writing–original draft, and validation. CU: writing–review and editing, writing–original draft, and investigation. DC: writing–review and editing and writing–original draft. MN: writing–review and editing, writing–original draft, and project administration. GSi: writing–review and editing, writing–original draft, and formal analysis. GP: writing–original draft and writing–review and editing. RM: writing–original draft and writing–review and editing.

## Funding

The author(s) declare that no financial support was received for the research, authorship, and/or publication of this article.

## Conflict of interest

The authors declare that the research was conducted in the absence of any commercial or financial relationships that could be construed as a potential conflict of interest.

The author(s) declared that they were an editorial board member of Frontiers, at the time of submission. This had no impact on the peer review process and the final decision.

## Publisher's note



## References

Adamo, L., Rocha-Resende, C., Prabhu, S. D., and Mann, D. L. (2020). Reappraising the role of inflammation in heart failure. *Nat. Rev. Cardiol.* 17 (5), 269–285. Epub 2020 Jan 22. Erratum in: Nat Rev Cardiol. 2021 Oct;18(10):735. doi:10.1038/s41569-019-0315-x

Brioschi, M., D'Alessandra, Y., Mapelli, M., Mattavelli, I., Salvioni, E., Eligini, S., et al. (2023). Impact of sacubitril/valsartan on circulating microRNA in patients with heart failure. *Biomedicines* 11 (4), 1037. doi:10.3390/biomedicines11041037

Chen, X., Ye, Y., Wang, Z., Jin, Q., Qiu, Z., Wang, J., et al. (2022). Cardiac resynchronization therapy via left bundle branch pacing vs. optimized biventricular pacing with adaptive algorithm in heart failure with left bundle branch block: a prospective, multi-centre, observational study. *Europace* 24 (5), 807–816. doi:10.1093/europace/euab249

Cohn, J. N., Ferrari, R., and Sharpe, N. (2000). Cardiac remodeling--concepts and clinical implications: a consensus paper from an international forum on cardiac remodeling. Behalf of an International Forum on Cardiac Remodeling. *J. Am. Coll. Cardiol.* 35 (3), 569–582. doi:10.1016/s0735-1097(99)00630-0

Dick, S. A., and Epelman, S. (2016). Chronic heart failure and inflammation: what do we really know? *Circ. Res.* 119 (1), 159–176. doi:10.1161/CIRCRESAHA.116.308030

D'Onofrio, N., Sardu, C., Trotta, M. C., Scisciola, L., Turriziani, F., Ferraraccio, F., et al. (2021). Sodium-glucose co-transporter2 expression and inflammatory activity in diabetic atherosclerotic plaques: effects of sodium-glucose co-transporter2 inhibitor treatment. *Mol. Metab.* 54, 101337. doi:10.1016/j.molmet.2021.101337

Gambardella, J., Jankauskas, S. S., D'Ascia, S. L., Sardu, C., Matarese, A., Minicucci, F., et al. (2022). Glycation of ryanodine receptor in circulating lymphocytes predicts the response to cardiac resynchronization therapy. *J. Heart Lung Transpl.* 41 (4), 438–441. doi:10.1016/j.healun.2021.12.008

Glikson, M., Nielsen, J. C., Kronborg, M. B., Michowitz, Y., Auricchio, A., Barbash, I. M., et al. (2021). 2021 ESC Guidelines on cardiac pacing and cardiac resynchronization therapy. *Eur. Heart J.* 42 (35), 3427–3520. doi:10.1093/eurheartj/ehab364

Gorcsan, J. I. I. I., Abraham, T., Agler, D. A., Bax, J. J., Derumeaux, G., Grimm, R. A., et al. (2008). Echocardiography for cardiac resynchronization therapy: recommendations for performance and reporting—a report from the American society of echocardiography dyssynchrony writing group endorsed by the heart rhythm society. *J. Am. Soc. Echocardiogr.* 21, 191–213. doi:10.1016/j.echo.2008.01.003

Jankowska, E. A., Filippatos, G. S., von Haehling, S., Papassotiriou, J., Morgenthaler, N. G., Cicoira, M., et al. (2011). Identification of chronic heart failure patients with a high 12-month mortality risk using biomarkers including plasma C-terminal pro-endothelin. *PLoS ONE* 6, e14506. doi:10.1371/journal.pone.0014506

Lappegård, K. T., Bjørnstad, H., Mollnes, T. E., and Hovland, A. (2015). Effect of cardiac resynchronization therapy on inflammation in congestive heart failure: a review. *Scand. J. Immunol.* 82 (3), 191–198. doi:10.1111/sji.12328

Macvanin, M. T., Gluvic, Z., Radovanovic, J., Essack, M., Gao, X., and Isenovic, E. R. (2023). Diabetic cardiomyopathy: the role of microRNAs and long non-coding RNAs. *Front. Endocrinol. (Lausanne)* 14, 1124613. doi:10.3389/fendo.2023.1124613

Mahjoob, G., Ahmadi, Y., Fatima Rajani, H., Khanbabaei, N., and Abolhasani, S. (2022). Circulating microRNAs as predictive biomarkers of coronary artery diseases in type 2 diabetes patients. *J. Clin. Lab. Anal.* 36 (5), e24380. doi:10.1002/jcla.24380

Marfella, R., Di Filippo, C., Potenza, N., Sardu, C., Rizzo, M. R., Siniscalchi, M., et al. (2013). Circulating microRNA changes in heart failure patients treated with cardiac resynchronization therapy: responders vs. non-responders. *Eur. J. Heart Fail* 15 (11), 1277–1288. doi:10.1093/eurjhf/hft088

Marfella, R., D'Onofrio, N., Trotta, M. C., Sardu, C., Scisciola, L., Amarelli, C., et al. (2022a). Sodium/glucose cotransporter 2 (SGLT2) inhibitors improve cardiac function by reducing JunD expression in human diabetic hearts. *Metabolism* 127, 154936. doi:10.1016/j.metabol.2021.154936

Marfella, R., Scisciola, L., D'Onofrio, N., Maiello, C., Trotta, M. C., Sardu, C., et al. (2022b). Sodium-glucose cotransporter-2 (SGLT2) expression in diabetic and non-diabetic failing human cardiomyocytes. *Pharmacol. Res.* 184, 106448. doi:10.1016/j.phrs.2022.106448

Melman, Y. F., Shah, R., Danielson, K., Xiao, J., Simonson, B., Barth, A., et al. (2015). Circulating MicroRNA-30d is associated with response to cardiac resynchronization therapy in heart failure and regulates cardiomyocyte apoptosis: a translational pilot study. *Circulation* 131 (25), 2202–2216. doi:10.1161/CIRCULATIONAHA.114.013220

Ref Moghissi, E. S., Korytkowski, M. T., DiNardo, M., Einhorn, D., Hellman, R., Hirsch, I. B., et al. (2009). American Association of Clinical Endocrinologists and American Diabetes Association consensus statement on inpatient glycemic control. *Diabetes Care* 32 (6), 1119–1131. doi:10.2337/dc09-9029

Sardu, C., Barbieri, M., Rizzo, M. R., Paolisso, P., Paolisso, G., and Marfella, R. (2016). Cardiac resynchronization therapy outcomes in type 2 diabetic patients: role of MicroRNA changes. *J. Diabetes Res.* 2016, 7292564. doi:10.1155/2016/7292564

Sardu, C., Marfella, R., Santamaria, M., Papini, S., Parisi, Q., Sacra, C., et al. (2018b). Stretch, injury and inflammation markers evaluation to predict clinical outcomes after implantable cardioverter defibrillator therapy in heart failure patients with metabolic syndrome. *Front. Physiol.* 9, 758. doi:10.3389/fphys.2018.00758

Sardu, C., Marfella, R., and Santulli, G. (2014). Impact of diabetes mellitus on the clinical response to cardiac resynchronization therapy in elderly people. *J. Cardiovasc Transl. Res.* 7 (3), 362–368. doi:10.1007/s12265-014-9545-9

Sardu, C., Massetti, M., Scisciola, L., Trotta, M. C., Santamaria, M., Volpicelli, M., et al. (2022). Angiotensin receptor/Neprilysin inhibitor effects in CRTd non-responders: from epigenetic to clinical beside. *Pharmacol. Res.* 182, 106303. doi:10.1016/j.phrs.2022.106303

Sardu, C., Paolisso, P., Sacra, C., Santamaria, M., de Lucia, C., Ruocco, A., et al. (2018a). Cardiac resynchronization therapy with a defibrillator (CRTd) in failing heart patients with type 2 diabetes mellitus and treated by glucagon-like peptide 1 receptor agonists (GLP-1 RA) therapy vs. conventional hypoglycemic drugs: arrhythmic burden, hospitalizations for heart failure, and CRTd responders rate. *Cardiovasc. Diabetol.* 17, 137. doi:10.1186/s12933-018-0778-9

Sardu, C., Trotta, M. C., Sasso, F. C., Sacra, C., Carpinella, G., Mauro, C., et al. (2023). SGLT2-inhibitors effects on the coronary fibrous cap thickness and MACEs in diabetic patients with inducible myocardial ischemia and multi vessels non-obstructive coronary artery stenosis. *Cardiovasc Diabetol.* 22 (1), 80. doi:10.1186/s12933-023-01814-7

Vijayaraman, P., Ponnusamy, S., Cano, Ó., Sharma, P. S., Naperkowski, A., Subsposh, F. A., et al. (2021). Left bundle branch area pacing for cardiac resynchronization therapy: results from the international LBBAP collaborative study group. *JACC Clin. Electrophysiol.* 7 (2), 135–147. doi:10.1016/j.jacep.2020.08.015

Zhu, H., and Fan, G. C. (2011). Extracellular/circulating microRNAs and their potential role in cardiovascular disease. *Am. J. Cardiovasc Dis.* 1 (2), 138–149.

frontiers | Frontiers in Pharmacology

TYPE Original Research
PUBLISHED 31 May 2024
DOI 10.3389/fphar.2024.1360177



OPEN ACCESS

EDITED BY
Ludwig Weckbach,
LMU Munich University Hospital, Germany

REVIEWED BY
Jiemei Wang,
Wayne State University, United States
Xin Xie,
Chengdu University of Traditional Chinese Medicine, China
Kang-Hoon Kim,
Monell Chemical Senses Center, United States

*CORRESPONDENCE
Hua Zhou,
htzh85@163.com
Gen Chen,
chengen86374062@126.com

†These authors have contributed equally to this work and share first authorship

RECEIVED 22 December 2023
ACCEPTED 10 May 2024
PUBLISHED 31 May 2024

CITATION
An N, Wang R, Li L, Wang B, Wang H, Peng G, Zhou H and Chen G (2024), Celastrol alleviates diabetic vascular injury via Keap1/Nrf2-mediated anti-inflammation.
*Front. Pharmacol.* 15:1360177.
doi: 10.3389/fphar.2024.1360177



# Celastrol alleviates diabetic vascular injury via Keap1/Nrf2-mediated anti-inflammation

Ning An[1†], Rixiang Wang[1†], Lin Li[1], Bingyu Wang[1], Huiting Wang[2], Ganyu Peng[2], Hua Zhou[1*] and Gen Chen[1,2*]

[1]The Affiliated Li Huili Hospital of Ningbo University, Health Science Center, Ningbo University, Ningbo, China, [2]Department of Pharmacology, Health Science Center, Ningbo University, Ningbo, China

**Introduction:** Celastrol (Cel) is a widely used main component of Chinese herbal medicine with strong anti-inflammatory, antiviral and antitumor activities. In the present study, we aimed to elucidate the cellular molecular protective mechanism of Cel against diabetes-induced inflammation and endothelial dysfunction.

**Methods:** Type 2 diabetes (T2DM) was induced by db/db mice, and osmotic pumps containing Cel (100 μg/kg/day) were implanted intraperitoneally and were calibrated to release the drug for 28 days. In addition, human umbilical vein endothelial cells (HUVECs) were cultured in normal or high glucose and palmitic acid-containing (HG + PA) media in the presence or absence of Cel for 48 h.

**Results:** Cel significantly ameliorated the hyperglycemia-induced abnormalities in nuclear factor (erythroid-derived 2)-like protein 2 (Nrf2) pathway activity and alleviated HG + PA-induced oxidative damage. However, the protective effect of Cel was almost completely abolished in HUVECs transfected with short hairpin (sh)RNA targeting Nrf2, but not by nonsense shRNA. Furthermore, HG + PA reduced the phosphorylation of AMP-activated protein kinase (AMPK), the autophagic degradation of p62/Kelch-like ECH-associated protein 1 (Keap1), and the nuclear localization of Nrf2. However, these catabolic pathways were inhibited by Cel treatment in HUVECs. In addition, compound C (AMPK inhibitors) and *AAV9-sh-Nrf2* reduced Cel-induced Nrf2 activation and angiogenesis in db/db mice.

**Discussion:** Taking these findings together, the endothelial protective effect of Cel in the presence of HG + PA may be at least in part attributed to its effects to reduce reactive oxygen species (ROS) and inflammation through p62/Keap1-mediated Nrf2 activation.

KEYWORDS

**dFUS, Nrf2, inflammation, celastrol, angiogenesis**

## Introduction

Diabetic foot ulcers (DFUs) are caused by diabetes-induced damage to deep tissues, including the blood vessels and nerve endings of the lower extremities. Specifically, chronic DFU is characterized by a highly active inflammatory state that is the result of, in part, poor pathogen control and high concentrations of pro-inflammatory cytokines. Furthermore, high levels of ROS and poor angiogenesis are present in patients with DFUs (Bowling et al.,

2015; Gallagher et al., 2024). Although wound care management is an established clinical field, the management of chronic diabetes-related skin lesions remains a major challenge.

Nuclear factor erythroid 2-related factor 2 (Nrf2) is a redox-sensitive transcription factor that regulates the transcription of many key antioxidant genes. Under conditions of oxidative stress, cysteine residues on Kelch-like ECH-associated protein 1 (Keap1) are oxidized by ROS, resulting in the release and activation of Nrf2, and its translocation to the nucleus (Dinkova-Kostova et al., 2002; Zhang and Hannink, 2003). In addition to the canonical pathway, p62 also interacts with the Nrf2-binding site of Keap1, competitively inhibiting the Keap1-Nrf2 interaction, which results in the expression of a series of genes encoding antioxidant proteins and anti-inflammatory enzymes (Komatsu et al., 2010; Lau et al., 2010). Nrf2 positively regulates *p62* gene expression, which suggests the existence of a positive feedback loop (Jain et al., 2010). Recently, an important role for Nrf2 in the prevention of DFUs has been reported (Xu et al., 2022). Nrf2-mediated antioxidant capacity appears to counteract the stress response that is induced by a highly active inflammatory state. Furthermore, the activation of Nrf2 protects against high glucose-induced apoptosis and cell damage in the kidney, heart, and blood vessels (Hashemi et al., 2023). Thus, the Nrf2 signaling pathway represents a therapeutic target for the cardiovascular complications of obesity and diabetes.

Substances derived from plants are an important source of new medicines. Thunder God Vine is an ancient herb that has been used in China for more than 2,000 years to treat chronic inflammatory diseases (Venkatesha and Moudgil, 2016). Celastrol (Cel, $C_{29}H_{38}O_4$), a pentacyclic triterpene, was originally extracted from *Trypterygium wilfordii Hook F.* and shows potential as a treatment for chronic diseases, such as Parkinson's disease, Alzheimer's disease, atherosclerosis, osteoarthritis, and rheumatoid arthritis (Allison et al., 2001; Pang et al., 2010; Gu et al., 2013; Kim et al., 2013; Choi et al., 2014). In addition, a recent study of Cel demonstrated that it ameliorates some metabolic diseases, such as obesity (Feng et al., 2019), insulin resistance (Ma et al., 2015), and suppresses cardiac and renal fibrosis (Guo et al., 2017; Ye et al., 2020). Cel has powerful antioxidant (Yuan et al., 2023) and anti-inflammatory effects (Hu et al., 2017; An et al., 2020; Shirai et al., 2023) that are mediated through upregulation of the Nrf2/antioxidant enzyme pathway (Nakayama et al., 2020; Qing et al., 2023). However, the effects of Cel on DFUs and the associated changes in angiogenesis have not been investigated. Therefore, in the present study, we aimed to determine whether Cel ameliorates hyperglycemia-induced endothelial dysfunction through the activation of Nrf2-related exogenous antioxidants, and to characterize its effects on the related signaling pathways.

# Materials and methods

## Animal procedures

Diabetic db/db mice and their control littermates, db/dm, were obtained from the GemPharmatech Co., Ltd. Before the commencement of the study, the mice were acclimated to their new environment for 4–6 days. They were housed at a temperature of 21°C ± 2°C and a relative humidity of 50% ± 15%, under a 12 h light-dark cycle. The fasting blood glucose concentrations of the mice were measured at the beginning of the study (Supplemental Table S1). AAV9 harbouring Nrf2 shRNA (*AAV9-CDH5-sh-Nrf2*) and control vector (*AAV9-CDH5-Scrambled*) were injected intravenously into tail veins of 7 weeks old male db/db or db/dm mice respectively. To ensure the effect of $1 \times 10^{12}$ vg of virus infection, we did the subsequent experiment 2 weeks later. ALZET® Osmotic Pumps (Model 2004) containing Cel (100 μg/kg/day, C0869, Sigma-Aldrich) (Fang et al., 2019) was implanted intraperitoneally, and then were calibrated to release the drug for 28 days (Figure 4E). The body mass and food intake of the mice were recorded every 3 days during the treatment period. All the mice were fasted for 12 h and subjected to glucose tolerance testing and insulin tolerance testing. For the analysis of signaling, bafilomycin A1 (10 mg/kg/2d, i. p., S1413, Selleck) and compound C (10 mg/kg/2d, i. p., S7306, Selleck) were administered. The procedures used in the study complied with the animal ethics guidelines of the institution and were approved by the Institutional Animal Care and Use Committee of Ningbo University, China.

## Cell culture

Human umbilical vein endothelial cells (HUVECs), widely used for the study of vascular function and repair (Guixé-Muntet et al., 2017; Cherubini et al., 2023), were purchased from Lonza (Basel, Switzerland) and cultured at 37°C in a 5% $CO_2$-containing humidified incubator using endothelial cell growth medium-2 (EGM-2, CC-3156, and CC-4176, Lonza) containing normal glucose (NG, 5.5 mM) or HG + PA (33 mM HG + 200 μM PA) (Alnahdi et al., 2019; Huang et al., 2021), with or without 100 nM Cel, for 48 h (Li et al., 2017; Ma et al., 2020). Fifth-to-seventh-generation subconfluent cells were used for the experiments. Mannitol (MAN, 33 mM: 5.5 mM of glucose +27.5 mM of D-mannitol; M4125, Sigma-Aldrich) was used as an osmolarity control for HG. For the analysis of the signaling pathways, MG132 (5 μM for 3 h), bafilomycin A1 (Baf A1, 10 nM for 12 h), or compound C (10 μM for 12 h) were added.

## Plasmids

HUVECs were transfected overnight with Nrf2-targeting shRNA (sc-37030, Santa Cruz) or nonsense shRNA at an MOI of 100× PFU/cell, and then the culture medium was replaced after 24 h. After 48 h, the expression of Nrf2 was measured by Western blot analysis.

## Immunoblotting analysis

Briefly, samples containing 30 μg protein were separated by SDS-PAGE on Tris-glycine gels and then transferred to polyvinylidene difluoride membranes. The membranes were blocked and incubated the primary antibody or secondary antibody [HRP-goat-anti-mouse (115-035-003, Jackson) or HRP-

goat-anti-rabbit (111-035-003, Jackson)]. Immunoreactive bands were visualized using Pierce ECL Western blotting substrate (WBKLS0500, Millipore).

The HUVECs were lysed and obtained cytoplasmic and nuclear lysates using the Keygen Nuclear-Cytosol Protein Extraction Kit from Nanjing KeyGen Biotech. Co., Ltd.

The primary antibodies used to probe the membranes were against p62 (sc-48402, 1:1,000), Lc3 (sc-271625, 1:1,000) (Santa Cruz Biotechnology), p-AMPK (2531S, 1:1,000), AMPK (2532S, 1:1,000) (Cell Signaling Technology), Nrf2 (66504-1, 1:1,000), Keap1 (10503-2, 1:1,000), β-actin (20536-1, 1:1,000), GAPDH (60004-1, 1:5,000), and Lamin b (66095-1, 1:1,000) (Proteintech). ImageQuant 5.2 software (Molecular Dynamics) was used to quantitatively analyze the expression of specific proteins, and β-actin was used as the loading control.

## Immunoprecipitation

IGEPAL CA-630 buffer [150 mM NaCl, 50 mM Tris-HCl, 2 mM EDTA, 1 μM leukopeptin (L5793, Sigma-Aldrich), 50 mM NaF, and 0.1 μM aprotinin (SRE0050, Sigma-Aldrich), 1% IGEPAL CA-630 (I8896, Sigma-Aldrich), pH 7.4] was used to lyse the HUVECs. After co-immunoprecipitation, the precipitates were washed five times with TBS. They were then eluted with glycine-HCl (0.1 M, pH 3.5) and the immunoprecipitates were subjected to immunoblotting using specific primary antibodies.

## RNA isolation and quantitative real-time-PCR (qRT-PCR)

RNA was extracted from HUVECs using TRIzol reagent (9,108, Takara Bio Inc.), according to the manufacturer's instructions. Next, total RNA (2 μg) was reverse transcribed into cDNA by using GoScript Reverse Transcription Kit (Promega, A5001). Quantitative RT-PCR analysis was performed using PowerUp SYBR Green Master Mix (Thermo Fisher Scientific, A25918). The relative expression of each gene was quantified using the $2^{-\Delta\Delta CT}$ method and normalized to the expression of *Actb*. The specific primer sequences used for qRT-PCR are listed in Supplementary Table S2.

## Cell counting kit (CCK)-8 assay

HUVECs ($1.0 \times 10^4$ per well) were cultured in 96-well plates for 24 h and treated with 25, 50, 75, 100, 200, 500, 750, or 1,000 nM Cel for 24 or 48 h, and their viability was assessed using the CCK-8 method. The absorbance of each well was measured using a microplate reader at 450 nm.

## Quantitative determination of oxidative stress (dihydroethidium assay)

HUVECs treated with HG + PA were stained with dihydroethidium (DHE, D7008, Sigma-Aldrich) probes to measure their ROS concentrations. DHE is cell permeable and able to react with superoxide to form ethidium, which in turn intercalates with DNA and produces nuclear fluorescence. HUVECs were seeded on 24-well plates and treated with HG in presence or absence Baicalin for 72 h and then incubated with 5 μM DHE in DMSO for 30 min at 37°C. Nuclear DHE positive staining indicates superoxide generation in cells. The fluorescence intensity was observed with a computer-assisted microscope (EVOS, Thermo Fisher Scientific).

## TUNEL staining

HUVECs were stained using an *In situ* Cell Death Detection kit (11684795910, Roche), according to the manufacturer's protocol. Cultured HUVECs were fixed (4% paraformaldehyde for 30 min) and permeabilized (0.1% Triton-X 100 for 10 min) in 6-well plates. After washing with PBS, cells were incubated with 50 μL tunel reaction mixture for 60 min at 37°C. After washing, the nuclei were stained with DAPI. The stained cells were then examined using a confocal laser scanning microscope (TCS SP8, Leica, Wetzlar, Germany).

## *In vitro* angiogenesis (tube formation) assay

The angiogenic activity of the HUVECs was assessed using a Matrigel tube formation assay. Briefly, HUVECs were scattered on the surface of Matrigel (Corning, 354234) and incubated in a cell incubator at 37°C for 24 h, followed by staining with the cell permeability dye Calcein AM (Corning, 354216) for 30 min. The formation of capillary-like tubes was identified using a computer-assisted microscope (EVOS, Thermo Fisher Scientific), the lengths of the tubes were calculated using ImageJ software (National Institutes of Health, Bethesda, MD, United States), and the mean values for the replicate wells were calculated.

## Aortic ring assays

To establish a direct action of Cel on vascular, thoracic aortae from db/db and db/dm mice infected with *AAV9-CDH5-sh-Nrf2* or *AAV9-CDH5-Scrambled* after 4-week treatment. Mice were surgically isolated, cleaned, and sectioned to form 0.5 mm rings. The lentivirus-mediated gene transfer (*Lv-CDH5-sh-Nrf2*) and vector (*Lv-sh-Scrambled*) were also respectively transfected with aortic rings from db/db and db/dm mice infected with *AAV9-CDH5-sh-Nrf2* or *AAV9-CDH5-Scrambled*. Next the rings were embedded and cultured in 96-well plates containing type I collagen (08-115, Millipore, 1 mg/mL) as previously described (Aplin et al., 2008; Baker et al., 2011). Then the medium was removed and replaced with either mannitol (33 mM: 5.5 mM of glucose +27.5 mM of D-mannitol) or HG + PA (33 mM HG + 200 μM PA) in the presence or absence of Cel (100 nM). Pre-treatment with Cel and VEGF were performed every day to analyze the role of the key signaling pathway. The number of endothelial microvessels that grew out of the rings was counted during the exponential growth phase to assess angiogenesis. Before the regression phase, the rings were fixed and immunofluorescence-stained for CD31 (ab281583, Abcam).

Photomicrographs were obtained after 12 days, and the total number of branches was counted using ImageJ.

## Scratch assay of wound healing

Cell migration was assessed using a scratch assay, as previously described (Das et al., 2018). Cells were seeded into six-well plates and cultured overnight until a confluent monolayer formed, which was then scratched using a 200 μL pipette tip. Before and 36 h after this injury, images of the damaged cell monolayers were captured using a microscope (EVOS, Thermo Fisher Scientific) and quantified using ImageJ software. All the experiments were performed in the presence of mitomycin-C (Jain et al., 2019) (10 μM, Selleck Chemicals, S8146), which inhibits cell proliferation.

## Wound healing assay in mice

General anesthesia was induced in mice by the inhalation of 2% isoflurane. Full-thickness wounds were created to the shaved dorsal skin of db/db and db/dm mice infected with *AAV9-CDH5-sh-Nrf2* or *AAV9-CDH5-Scrambled* using 8 mm skin biopsy punches. Skin wound edge injection of the *Lv-CDH5-sh-Nrf2* and control vector *Lv-Scramble*, and then each of the wounds were treated with DMSO, Cel (100 nM) with a diameter of 10 mm, and bandaged with sterile gauze. The subsequent wound closure was assessed daily (Li et al., 2015). The formula for calculating the remaining open wound area was as follows: wound area remaining open (%) = (open area on the indicated day/original wound area) × 100%. Five-micrometer-thick paraffin-embedded tissue sections were prepared, dewaxed, rehydrated, and stained with immunofluorescence of keratin 14 (ab119695, Abcam) and CD31 (ab281583, Abcam) respectively. After washing, the sections were incubated with secondary antibodies [AlexaFluor 647-conjugated anti-rabbit (ab150079, Abcam) in different tissue sections. The re-epithelialization ratio (leading edge ratio) was calculated as [(a + b)/c] × 100% (shown in Figure 4F; a and b are the lengths of the leading edges, and c is the initial length of the wound) (Safferling et al., 2013).

## Immunofluorescence

Immunofluorescence was used to identify areas of CD31, VCAM-1, and p65 expression in the aortic wall. Eight-micrometer-thick paraffin sections were prepared and incubated with anti-CD31 antibody (ab281583, Abcam), VCAM-1 antibody (ab134047, Abcam), or p65 antibody (66535-1, Proteintech). After washing, the sections were incubated with secondary antibodies [AlexaFluor 647-conjugated anti-rabbit (ab150079, Abcam) or AlexaFluor 488-conjugated anti-mouse (ab150113, Abcam)] at room temperature for 60 min. DAPI was used to label the nuclei. The CD31 or VCAM-1-stained area were examined using a confocal laser scanning microscope (TCS SP8, Leica, Wetzlar, Germany) and measured using ImageJ software. Data are presented as the percentages of the total area that was immunostained.

To quantitatively analyze the nuclear localization of Nrf2 in HUVECs. Cultured HUVECs were fixed (4% paraformaldehyde for 30 min), permeabilized (0.5% Triton-X 100 for 30 min) and blocked (5% BSA for 2 h) in 6-well plates. Then, cells were incubated with rabbit anti-Nrf2 primary antibody (1:200, 66504-1, Proteintech) overnight at 4°C. After washing, the cells were then incubated with secondary antibody (AlexaFluor 488-conjugated anti-mouse, ab150113, Abcam). The nuclei were stained with DAPI. The results were photographed via a confocal laser scanning microscope (TCS SP8, Leica, Wetzlar, Germany). The colocalization of Nrf2 and DAPI was assessed in randomly selected cells.

## Statistical analysis

All the analyses were performed with the investigator being blinded to the groups of mice or cultured cell treatments. Statistical comparisons were made using the two-tailed Student's *t*-test for two experimental groups or the one-way analysis of variance (ANOVA) for multiple groups. Statistical analyses were performed using GraphPad Prism.

# Results

## Celastrol attenuates HG + PA-induced inflammation and apoptosis in HUVECs

To determine the effects of Cel on the HG + PA-induced defects in HUVECs, we first evaluated the cytotoxicity of Cel *in vitro*. We found that concentrations of Cel <400 nmol/L caused no obvious cytotoxicity, whereas there was significantly lower cell viability when the concentration of Cel exceeded 750 nmol/L (Figure 1A). This is consistent with the effects of Cel to impair vascular growth in tumors at high concentrations (Pang et al., 2010). Furthermore, we found that the deleterious effect of HG + PA on the viability of HUVECs was significantly ameliorated by 100 nM Cel (Figure 1B). It has been reported that HG + PA-induced endothelial dysfunction is mediated through multiple mechanisms, including oxidative stress and pro-inflammatory responses (Xie et al., 2008). We demonstrated that HG + PA-induced inflammatory activity, reflected in the upregulation of the pro-inflammatory cytokines IL-1β, IL-6, IL-8, and TNF-α, was inhibited by Cel treatment (Figure 1C). In addition, we assessed the effect of Cel on oxidative stress in the endothelial cells using DHE. HG + PA treatment of HUVECs resulted in a significant increase in superoxide production, and this was attenuated by co-treatment with Cel (Figures 1D,E). HG + PA also induced a high level of apoptosis in HUVECs, as indicated by a larger proportion of TUNEL-positive cells. However, this HG + PA-induced apoptosis was significantly attenuated by Cel (Figures 1F,G). Furthermore, the migration of HG + PA-exposed HUVECs was significantly impaired, but this defect was significantly ameliorated by Cel (Figures 1H,I).

## Celastrol increases the activity of Nrf2 in HG + PA-treated HUVECs

Nrf2 plays a key role in the cellular response to oxidative stress (Jyrkkänen et al., 2008). Therefore, we speculated that Cel may

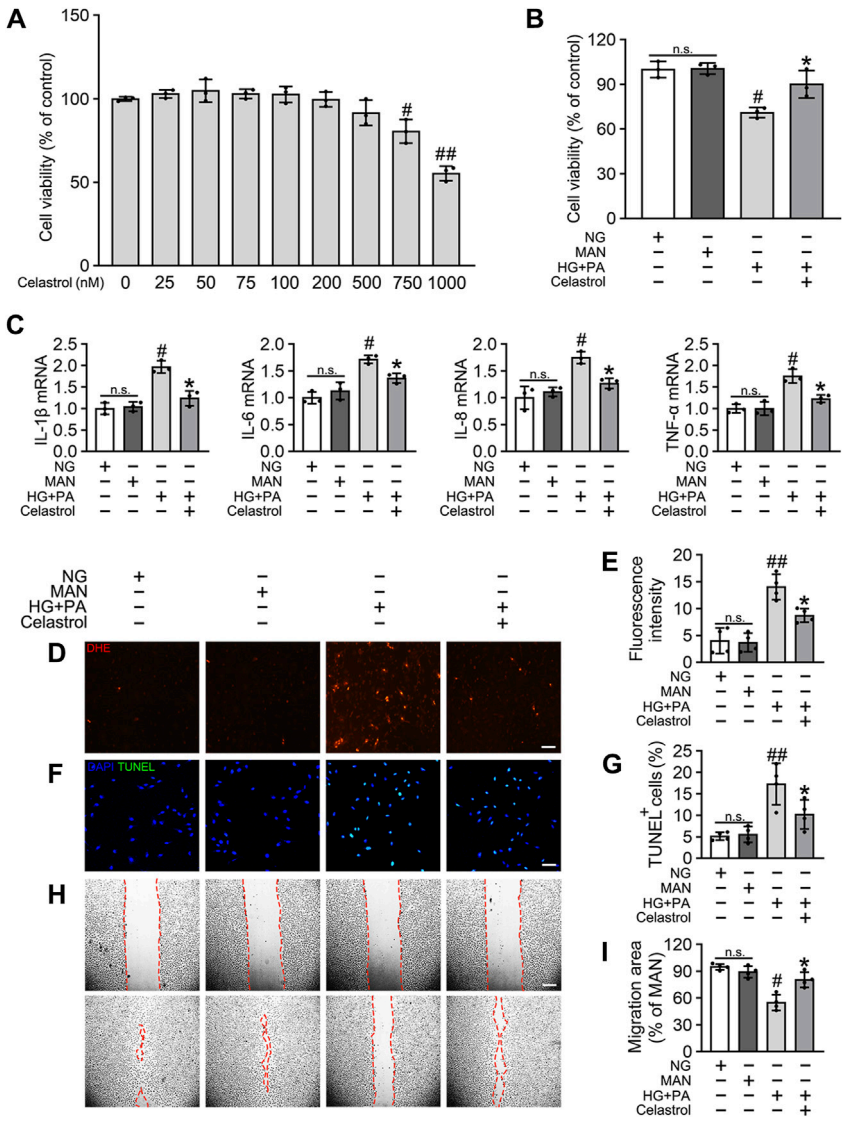


FIGURE 1
Cel attenuates HG + PA-induced inflammation and apoptosis in HUVECs. **(A)** The proliferation of HUVECs was monitored using a CCK-8 assay after exposure to different cultured conditions for 48 h. Values displayed are means ± SD of independent experiments. *$p < 0.05$ or **$p < 0.01$ vs. absence of Cel. **(B–I)** HUVECs cultured either in NG or HG + PA medium in the presence or absence of Cel for 48 h, MAN served as the osmotic control for the HG. **(B)** Shows cell viability of different groups. **(C)** The mRNA expression and quantitation of NF-κB downstream target genes were evaluated by sqRT-PCR. **(D)** Superoxide was determined with the fluorescent indicator DHE, Scale bars = 120 μm. **(E)** The quantitative analysis of fluorescent intensity in at least 4 separate fields. **(F)** TUNEL assay show that the apoptotic cells were labeled with green, and nuclei were stained with DAPI (blue). Scale bars = 100 μm. **(G)** The quantitative analysis of TUNEL$^+$ cells in at least 4 separate fields. **(H)** A scratch wound healing assay was performed in the presence of Mitomycin-C (10 μM). Cell monolayers were imaged at 0 and 36 h after wounding. Red vertical lines indicate the wound area borders. Scale bar = 65 μm. **(I)** Cell migration distances were measured based on the data. Data shown in graphs **(B–I)** represent the means ± SD of independent experiments. n. s = not significant, #$p < 0.05$ vs. HUVECs expose to MAN; *$p < 0.05$ vs. HUVECs expose to HG + PA.

ameliorate HG + PA-induced endothelial damage by activating Nrf2 and its downstream target genes. Nrf2 protein expression was downregulated by the HG + PA treatment, but consistent with previous findings (Li et al., 2017), the Nrf2 protein expression was significantly restored by Cel treatment (Figures 2A,B). Importantly, we found that the mRNA expression of the Nrf2 target genes *NQO1*, *NQO2*, *HO1*, *SOD2*, and *CAT* was significantly reduced by HG + PA treatment, but this was corrected by Cel treatment (Figures 2C–G). In addition, the nuclear localization of Nrf2 was significantly reduced by HG + PA treatment, but this did not occur in the presence of Cel (Figures 2H,I). The nuclear localization of Nrf2 in HUVECs was further characterized using immunofluorescence (Supplementary Figure S1A), which showed similar results. Overall, these results demonstrate that Cel restores Nrf2 protein expression and promotes the nuclear enrichment of Nrf2. Furthermore, consistent changes in Nrf2 target gene expression accompany the effects of Cel on Nrf2 nuclear localization, indicating that Cel activates the transcriptional function of Nrf2, ameliorates HG + PA-induced oxidative stress, and reduces the inflammatory response.

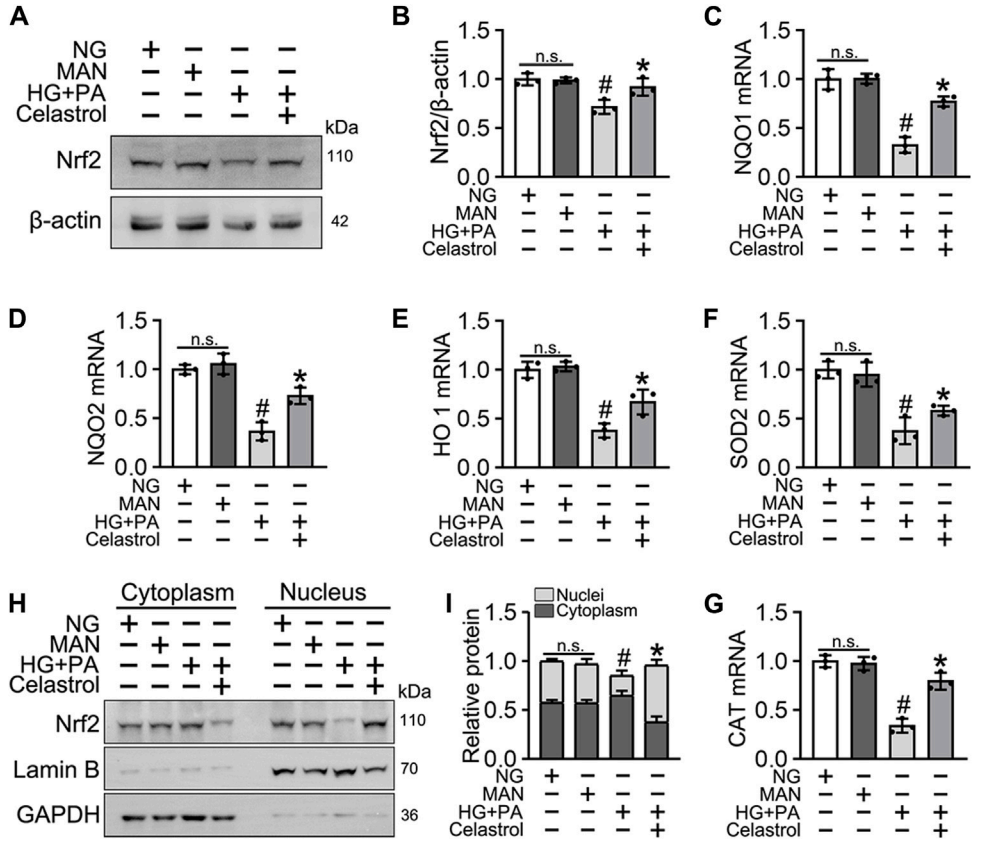


FIGURE 2
Cel enhanced the activity of Nrf2 in HG + PA-triggered HUVECs. HUVECs cultured either in NG or HG + PA medium in the presence or absence of Cel for 48 h, MAN served as the osmotic control for the HG. **(A)** The Nrf2 was evaluated by Western blot. **(B)** The quantitative analysis of immunoblots. **(C–G)** The mRNA expression and quantitation of Nrf2 downstream target genes were evaluated by sqRT-PCR. **(H)** Nuclear Nrf2 protein expression was measured using Western blotting. **(I)** The quantitative analysis of immunoblots. Data shown in the graphs represent the means ± SD of independent experiments. n. s = not significant, #$p < 0.05$ vs. HUVECs expose to MAN; *$p < 0.05$ vs. HUVECs expose to HG + PA.

## Celastrol ameliorates HG + PA-induced oxidative stress and inflammation through the activation of Nrf2 in HUVECs

To confirm the role of Nrf2 in the endothelial protective effects of Cel, we knocked down the expression of Nrf2 using specific shRNA. We found that even in the presence of Cel, Nrf2 shRNA treatment reduced the expression of a series of antioxidant-related genes (*NQO1*, *NQO2*, *HO1*, *CAT*, and *SOD2*) and increased the production of pro-inflammatory cytokines (IL-1β, IL-6, IL-8, and TNF-α) (Supplementary Figure S2). Notably, Cel significantly reduced HG + PA-induced superoxide generation (Figures 3A,B) and apoptosis (Figures 3C,D) in HUVECs, but this was impaired by Nrf2 shRNA co-treatment. In addition, the impairments in tube formation (Figures 3E,F) and migration (Figures 3G,H) of the HUVECs were also significantly ameliorated by Cel, but this effect was abrogated by Nrf2 shRNA co-administration. However, we found that Cel had a very small effect to enhance tube formation by the HUVECs under basal conditions (Supplementary Figure S3A). These results suggest that the Cel-induced activation of Nrf2 promotes cell proliferation and migration, and inhibits the apoptosis induced by HG + PA treatment.

## The Celastrol-induced activation of Nrf2 improves angiogenic function in the presence of T2DM-associated endothelial dysfunction

We next aimed to evaluate the effects of Cel and Nrf2 activity on the angiogenic function of endothelial cells in db/db mice (Figure 4E). Cel reduced the food intake and body mass of the diabetic mice (Figures 4A,B). It also rapidly reduced the circulating glucose concentrations (Figure 4C) and improved the insulin sensitivity (Figure 4D) of fasted diabetic mice, as demonstrated by glucose and insulin tolerance testing. However, transfected with *AAV9-sh-Nrf2* did not significantly impair the effects of Cel on body mass or blood glucose concentration (Figures 4B,D). To further assess the role of Nrf2 activity in the endothelial protection induced by Cel, we used an *in vivo* model of skin wound healing in mice, in which chronic inflammation inhibits endothelial function and subsequent wound healing (Safferling et al., 2013; Li et al., 2015). We found that *AAV9-sh-Nrf2* delayed the closure of wounds (Figures 4G,H) and was significantly less re-epithelialization in db/db mice than in the normal db/dm mice (Figures 4I,J). Furthermore, as model of skin wound healing in mice, we found that $CD31^+$ capillary density was lower in regenerated skin tissue from db/db mice than in skin from db/dm mice, and this was

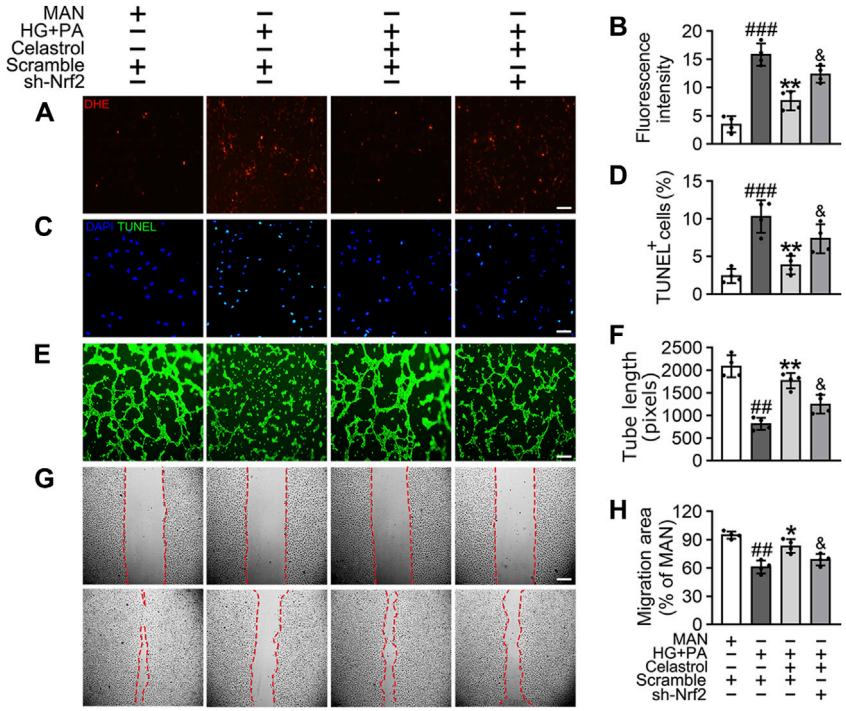


FIGURE 3
The protective effect of Cel on endothelial cells was mediated through Nrf2. HUVECs were transfected with or without Nrf2 shRNA (sh-Nrf2) or scramble shRNA (scramble) and then exposed to HG + PA medium in the presence or absence of Cel for 48 h. **(A)** Superoxide product test assay of HUVECs treated with the fluorescent indicator DHE, Scale bars = 120 μm. **(B)** The quantitative analysis of fluorescent intensity in at least 4 separate fields. **(C)** TUNEL assay: the apoptotic cells were labeled with green, and nuclei were stained with DAPI (blue). Scale bars = 100 μm. **(D)** The quantitative analysis of TUNEL$^+$ cells in at least 4 separate fields. **(E)** Capillary-like tube formation was assessed by matrigel angiogenesis assay in HUVECs. Scale bars = 85 μm. **(F)** Quantification of the tube length, and images of tube morphology were taken in four random microscopic fields per sample. **(G)** A scratch wound healing assay was performed in the presence of Mitomycin-C (10 μM). Cell monolayers were imaged at 0 and 36 h after wounding. Red vertical lines indicate the wound area borders. Scale bar = 65 μm. **(H)** Cell migration distances were measured based on the data. Data shown in the graphs represent the means ± SD of independent experiments. ###$p < 0.001$ vs. HUVECs expose to MAN; **$p < 0.01$ vs. HUVECs expose to HG + PA, and $p < 0.05$ vs. HUVECs expose to HG + PA treatment with Cel.

especially evident in db/db mice transfected with *AAV9-sh-Nrf2* (Figures 4K,L).

Subsequently, using vascular cell adhesion molecule (VCAM-1) as a marker of inflammatory stress, we showed that Cel treatment attenuated HG + PA-induced inflammation in HUVECs, whereas transfected with *AAV9-sh-Nrf2* worsened this (Figures 5A,B). In parallel, immunofluorescence analysis showed that the p65 expression in the aortic endothelial cell nuclei of diabetic mice was higher than that of normal mice. This effect was significantly ameliorated by Cel treatment, but the effect of Cel was abrogated by *AAV9-sh-Nrf2* administration (Figures 5C,D). The *ex vivo* aortic ring sprouting assay was used to further assess the protective effects of Cel on the endothelium. Aortic rings from male db/db or db/dm mice were firstly transfected with *Lv-sh-Nrf2* or *Lv-Scramble*, then cultured in HG + PA or MAN-containing medium in the presence or absence of Cel. In MAN medium, a well-structured microvessel network with clearly defined tubules and regular branching developed. By contrast, aortic rings cultured in HG + PA medium showed a significant impairment in budding, which was ameliorated by Cel, but this effect of Cel was abolished by *Lv-sh-Nrf2* (Figures 5E,F). Consistent with the *in vitro* findings, there was no significant improvement after Cel treatment in aortic ring sprout density under basal conditions (Supplementary Figure S3B). Taken together, these results indicate that the Cel-induced increase in Nrf2 activity inhibited oxidative stress and NFκB activity, thereby significantly ameliorating T2DM-associated endothelial dysfunction.

## Celastrol activates Nrf2 via the p62-Keap1 pathway, both *in vitro* and *in vivo*

Cel is thought to improve skeletal muscle and bone function through upregulation of the AMPK signaling pathway (Abu et al., 2020; Li et al., 2020), and it also ameliorates angiotensin II-mediated vascular smooth muscle cell senescence (Xu et al., 2017) and osteoarthritis (Feng et al., 2020) through the induction of autophagy. In addition, the function of Nrf2 has been reported to be regulated by the p62/Keap1/Nrf2 signaling pathway, the activation of which liberates Nrf2 from Keap1 and permits it to translocate to the nucleus (Zhang et al., 2021).

Consistent with this, we found that the low Nrf2 protein expression was restored (Figures 6A,C), and the expression of Keap1 remained unaffected by Cel and MG132 (a proteasome inhibitor) co-treatment (Figures 6A,D). Moreover, immunoprecipitation revealed that MG132 promotes the binding

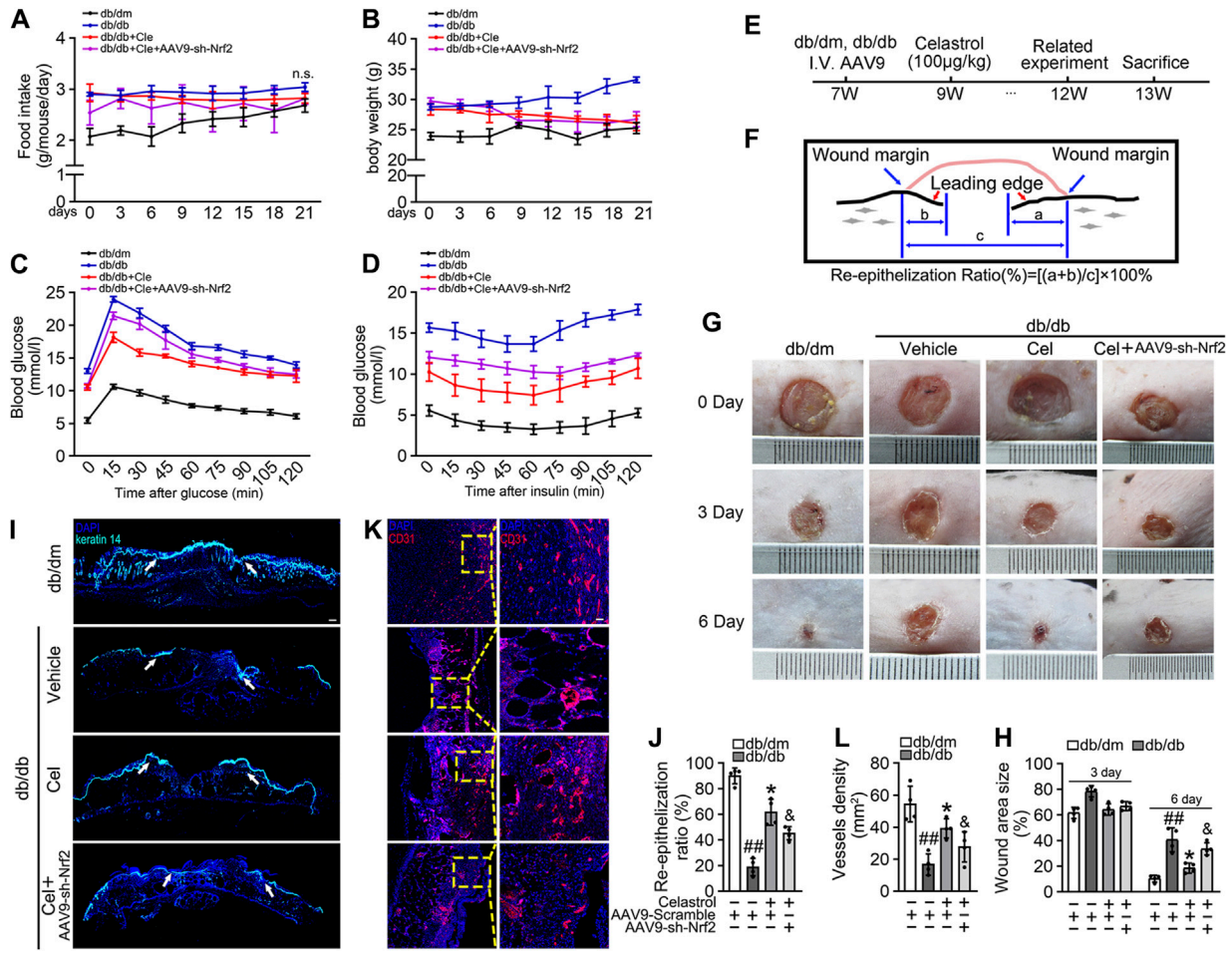


FIGURE 4
Celastrol-mediated Nrf2 ameliorates wound healing in db/db mice. **(A)** During the treatment period, the food intake of the mice was measured every 3 days **(B)** During the treatment period, the body weight of mice was measured every 3 days **(C)** Glucose tolerance test (GTT). After 21 days of administration of celastrol, the fasting hyperglycemia of the mice was reduced, and the glucose tolerance was also improved, which was related to the reduction of plasma glucose level in the fasting state and the response to glucose load. **(D)** Insulin tolerance tests (ITT). After 21 days of celastrol administration, mice showed improved insulin resistance and lowered blood glucose levels in response to glycemic load. **(E)** Design of the study. **(F)** Schematic diagram about **(I)**, the lengths of leading edges and the initial wound length were defined as indicated. **(G)** Images of skin wounds from db/dm mice and db/db mice ($n$ = 4). **(H)** The wound area size (%) was measured for 6 days **(G)**. **(I)** The skin sections were harvested and followed by immunofluorescence staining of keratin 14 (cyan). Scale bar = 1 mm. **(J)** Measurement of reepithelization ratio (leading edge ratio) in wound area **(I)**. **(K)** The skin sections were harvested and followed by immunofluorescence staining of CD31 (red). Scale bar = 25 μm. (L) Quantification of the CD31$^+$ capillary density in wound area **(K)**. Data shown in the graphs represent the means ± SD of independent experiments. ##$p$ < 0.01 vs. db/dm mice; *$p$ < 0.05 vs. db/db mice, and $p$ < 0.05 vs. db/db mice treatment with Cel.

of Nrf2 to Keap1 in cells treated with HG + PA, indicating that Keap1 accumulates in cells and binds to Nrf2, causing it to undergo ubiquitination degradation in response to HG + $p$A. However, MG132 did not significantly increase the association of Nrf2 and Keap1 in Cel-treated cells, indicating that Cel affects Keap1 protein levels through the regulation of the non-proteasomal degradation pathway, ultimately inhibiting the binding of Keap1 to Nrf2, causing the latter to undergo ubiquitination degradation (Figures 6A,B).

Given that the accumulation of Nrf2 is accompanied by abundant autophagosomal degradation (Komatsu et al., 2010; Ichimura et al., 2013; Zhang et al., 2021; Taguchi et al., 2012), we next analyzed whether Cel increases Nrf2 expression by modulating autophagy. Co-treatment with Baf-A1, an inhibitor of autophagic degradation, blocked the effect of Cel on Nrf2 accumulation (Figures 6E–G). A previous study showed that Keap1 interacts with p62 (an autophagic adapter) and frees Nrf2 translocate to the nucleus (Taguchi et al., 2012). Consistent with this, in the present study, we found that the interaction between Keap1 and p62 in HUVECs was increased by HG + PA treatment and restored to normal by Cel administration (Figures 6E,F). Interestingly, the interaction between Keap1 and Nrf2 was increased by co-treatment with Baf-A1, even in the presence of Cel (Figures 6E,F), indicating that Baf-A1 inhibits the autophagy pathway involving Keap1 and p62, but does not reduce the expression of Keap1 protein, and increases the probability of Keap1 and Nrf2 binding, thereby increasing the ubiquitination and degradation of Nrf2. Thus, Nrf2 protein expression is reduced by Baf-A1 (Figures 6E,F). We also found that the effects of Cel on the phosphorylation of AMPK and

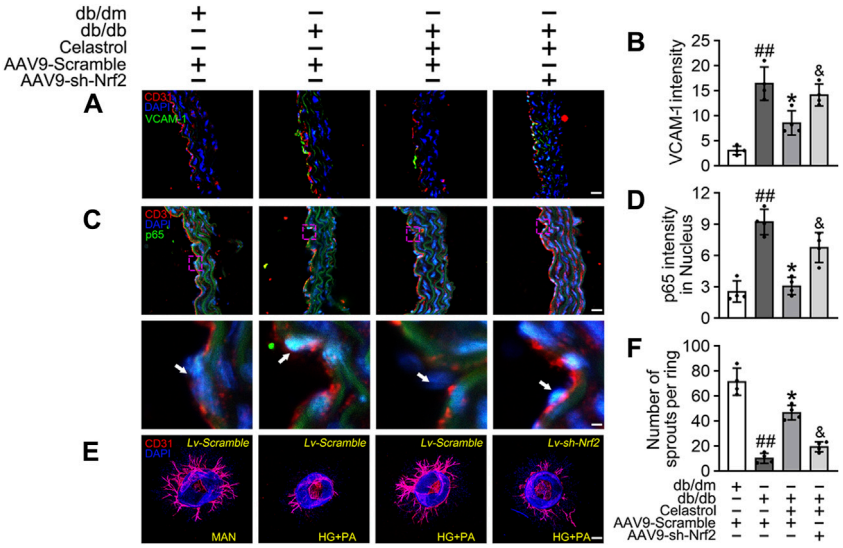


FIGURE 5
Cel attenuated inflammation and promoted angiogenesis in db/db mice. AAV9 harbouring Nrf2 shRNA (*AAV9-CDH5-sh-Nrf2*) and control vector (*AAV9-CDH5-Scrambled*) were injected intravenously into tail veins of 7 weeks old male db/db or db/dm mice respectively. Osmotic pumps containing Cel (100 μg/kg/day) was implanted intraperitoneally and were calibrated to release the drug for 28 days in db/db mice. **(A)** Representative confocal images of inflammation stress marker VCAM-1 in aortal vascular endothelium. The red area (CD31) represented endothelium, the green area represented VCAM-1 positive staining and the nucleus was blue. Scale bars = 40 μm. **(B)** Quantification of the number of VCAM-1 staining. **(C)** The presence of immunofluorescence with CD31 and p65 of aortal vascular endothelium. Scale bars = 40 μm. **(D)** The quantitative analysis of $p65^{+}$ in the nucleus of aortal vascular endothelium. **(E)** Representative images of aortic rings were transfected with *Lv-CDH5-sh-Nrf2* or *Lv-Scramble* and then exposed to MAN and HG + PA in the presence or absence of Cel (100 nM). All aortic rings cultured with VEGF (30 ng/mL). Scale bars = 350 μm. **(F)** Quantification of the number of sprouts. Data shown in the graphs represent the means ± SD of independent experiments. ##$p < 0.01$ vs. db/dm mice; *$p < 0.05$ vs. db/db mice, and $p < 0.05$ vs. db/db mice treatment with Cel.

autophagy were prevented by treatment with the specific pharmacological inhibitor of AMPK, compound C (Figures 6H–K). In addition, Cel had protective effects on tube formation (Figures 7A,B) and cell migration (Figures 7C,D), but these were abolished by compound C or Baf-A1 co-treatment.

To determine whether the protective effect of Cel against hyperglycemia-induced endothelial impairment is mediated via AMPK/p62-dependent autophagy in diabetic mice, compound C (10 mg/kg/2d, i. p.) or Baf-A1 (10 mg/kg/2d, i. p.) was administered. As expected, inhibition of the AMPK pathway or autophagy largely prevented the endothelial protective effect of Cel, as shown by a substantial increase in VCAM-1 expression in aortic vascular endothelium cells from db/db mice (Figures 7G,H) and an impairment in aortic ring sprouting (Figure 7E,F). These data suggest that Cel ameliorates the HG + PA-induced endothelial dysfunction by promoting the degradation of Keap1 in HUVECs, secondary to an effect on AMPK/p62-dependent autophagy, thereby liberating Nrf2 to translocate to the nucleus.

## Discussion

The 10th edition of the International Diabetes Federation Atlas estimated that there were 536.6 million people with diabetes in 2021 and that by 2045 there will be approximately 783.2 million adults with diabetes (Ogurtsova et al., 2022). The global prevalence of DFU has been reported to be 6.3%, higher in men than in women, and higher in patients with T2DM than in those with type 1 diabetes (6.4% vs. 5.5%, respectively) (Chen et al., 2023). Importantly, approximately 25% of patients with diabetes develop DFUs during their lifetime, and approximately 14%–24% of patients with DFUs ultimately require an amputation (Singh et al., 2005). In this study, the concomitant stimulation with high glucose (HG) and fatty acid (palmitic acid, PA) was used to mimic the *in vivo* T2DM-related hyperglycemia and hyperlipidemia condition on EC, as reported in different *in vitro* T2DM models (Alnahdi et al., 2019; Huang et al., 2021).

From a pathophysiological perspective, impaired wound healing in patients with diabetes is closely associated with inadequate angiogenesis (Okonkwo and DiPietro, 2017), which is caused by chronic inflammatory responses and impaired cellular responses to tissue hypoxia (Catrina and Zheng, 2016; Rehak et al., 2022). In addition, endothelial dysfunction, which includes endothelial cell dysfunction and a loss of endothelial cell barrier function, has also been reported in patients with DFUs (Zhang et al., 2022). Endothelial dysfunction is the most significant impairment affecting the microcirculation, and involves altered endothelial cell proliferation, thickening of the basement membrane, altered microvascular tone, and lower blood flow. Therefore, the effective treatment of chronic DFU necessitates improvements in endothelial function, angiogenesis, and immune function, and a reduction in inflammation, to promote tissue regeneration.

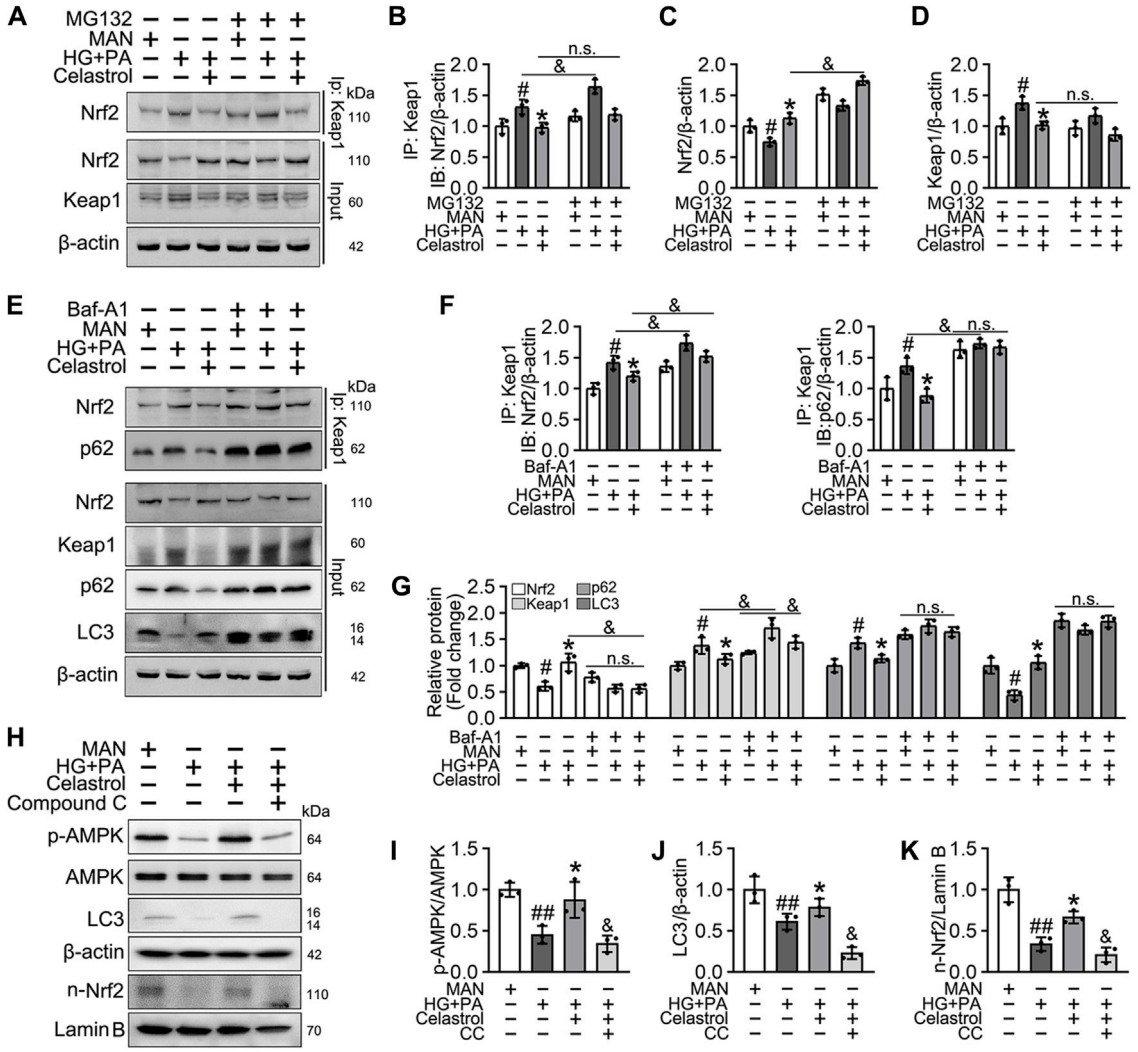


FIGURE 6
Cel activated Nrf2 via AMPK/p62/keap1 pathway *in vitro*. **(A–D)** HUVECs were cultured either in MAN (5.5 mM) and HG + PA (33 mM HG+200 μM PA) medium in the presence or absence of Cel (100 nM) or MG132 (5 μM) for 48 h. The cell lysates were subjected to immunoprecipitation with the Keap1 antibody, followed by immunoblotting with the indicated antibodies. The quantitative analysis of immunoprecipitation **(B)** and immunoblots **(C and D)**. Data shown in the graphs represent the means ± SD of independent experiments. #$p < 0.05$ vs. HUVECs expose to MAN; *$p < 0.01$ vs. HUVECs expose to HG + PA, and $p < 0.05$, n. s = not significant. **(E–G)** HUVECs were cultured either in MAN (5.5 mM) and HG + PA (33 mM HG+200 μM PA) medium in the presence or absence of Cel (100 nM) or Baf-A1 (20 nM) for 48 h. The cell lysates were subjected to immunoprecipitation with the Keap1 antibody, followed by immunoblotting with the indicated antibodies. The quantitative analysis of immunoprecipitation **(F)** and immunoblots **(G)**. Data shown in the graphs represent the means ± SD of independent experiments. #$p < 0.05$ vs. HUVECs expose to MAN; *$p < 0.01$ vs. HUVECs expose to HG + PA, and $p < 0.05$, n. s = not significant. **(H–K)** HUVECs were cultured either in MAN (5.5 mM) and HG + PA (33 mM HG+200 μM PA) medium in the presence or absence of Cel (100 nM) or Compound C (10 μM) for 48 h. The level of relative protein was evaluated by Western blot. The quantitative analysis of immunoblots **(I–K)**. Data shown in the graphs represent the means ± SD of independent experiments. #$p < 0.05$, ##$p < 0.01$ vs. HUVECs expose to MAN; *$p < 0.01$ vs. HUVECs expose to HG + PA, and $p < 0.05$ vs. HUVECs expose to Cel.

Cel is a quinone methide triterpenoid that is isolated from the traditional Chinese medicinal plant *Tripterygium wilfordii Hook f*. In recent years, Cel has received increasing attention for its potential therapeutic effects on inflammatory and metabolic disorders (Ma et al., 2015; Bian et al., 2016). Previous studies have shown that Cel reduces the obesity of HFD-fed diabetic obese (*db/db*) and leptin-deficient (*ob/ob*) mice by inhibiting endoplasmic reticulum stress and increasing STAT3-dependent leptin signaling (Liu et al., 2015). Furthermore, Cel reduces oxidative stress-related damage by increasing the activation of the Nrf2/antioxidase pathway (Divya et al., 2016). In addition, Cel has been shown to reduce the damage to vascular endothelial cells by reducing ROS production and the expression of pro-inflammatory molecules (Li et al., 2017). Therefore, Cel represents a potential treatment for DFUs. However, the detailed mechanism whereby Cel protects against DFU-associated endothelial cell dysfunction through the activation of Nrf2-associated extrinsic antioxidant defense mechanisms remains unclear.

Over the past few years, autophagy and oxidative stress have been shown to be intimately linked through complex signaling

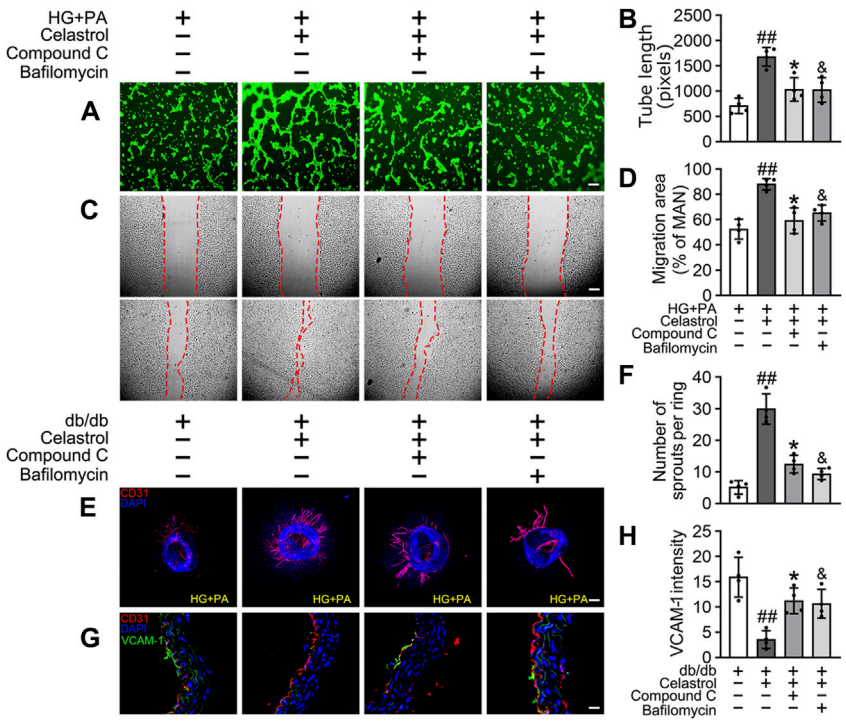


FIGURE 7
Cel ameliorates endothelial function via AMPK/autophagy pathway. **(A–D)** HUVECs were cultured in HG + PA (33 mM HG+200 μM PA) medium in the presence or absence of Cel (100 nM) or Compound C (10 μM) or Baf-A1 (20 nM) or MG132 (5 μM) for 48 h. **(A)** Capillary-like tube formation was assessed by matrigel angiogenesis assay in HUVECs. Scale bars = 85 μm. **(B)** Quantification of the tube length, and images of tube morphology were taken in four random microscopic fields per sample. **(C)** A scratch wound healing assay was performed in the presence of Mitomycin-C (10 μM). Cell monolayers were imaged at 0 and 36 h after wounding. Red vertical lines indicate the wound area borders. Scale bar = 65 μm. **(D)** Cell migration distances were measured based on the data. Data shown in the graphs represent the means ± SD of independent experiments. Data shown in the graphs represent the means ± SD of independent experiments. ##$p < 0.01$ vs. HUVECs expose to HG + PA; *$p < 0.01$, and $p < 0.05$ vs. HUVECs expose to HG + PA treatment with Cel. **(E–F)** Osmotic pumps containing Cel (100 μg/kg/day) was implanted intraperitoneally and were calibrated to release the drug for 28 days in db/db mice, and treatment with the absence or presence of Baf-A1 (10 mg/kg/2d) or Compound C (10 mg/kg/2d). **(E)** Representative images of aortic rings were pretreated with or without Baf A1 (20 nM) or Compound C (10 μM) for 2 h and then exposed to HG + PA in the presence or absence of Cel (100 nM). Scale bars = 350 μm. **(F)** Quantification of the number of sprouts. **(G)** Representative confocal images of inflammation stress marker VCAM-1 in aortal vascular endothelium. The red area (CD31) represented endothelium, the green area represented VCAM-1 positive staining and the nucleus was blue. Scale bars = 40 μm. **(H)** Quantification of the number of VCAM-1 staining. Data shown in the graphs represent the means ± SD of independent experiments. ##$p < 0.01$ vs. db/db mice; *$p < 0.05$, and $p < 0.05$ vs. db/db mice treatment with Cel.

pathways. In the present study, we found that p62 activates the antioxidant transcription factor Nrf2 through a non-canonical pathway. The mechanism of this is completely independent of redox status and involves the recruitment of Keap1, an adapter protein of the cul3-ubiquitin E3 ligase complex, which is responsible for the degradation of Nrf2 (Komatsu et al., 2010; Ichimura et al., 2013). Consistent with this model, p62 binds to ubiquitinated protein aggregates and its affinity for Keap1 increases when it is phosphorylated at Ser351 (Ichimura et al., 2013). The induction of Keap1 autophagic degradation (Taguchi et al., 2012) liberates Nrf2 translocate in the nucleus. In the present study, we found that Cel ameliorates HG + PA-induced HUVECs injury by increasing activation of the autophagy-related p62-Keap1-Nrf2 signaling pathway, thereby increasing the activity of Nrf2, and reducing ROS production and the expression of pro-inflammatory cytokines. Additionally, Nrf2 has also been shown to regulate multiple aspects of key metabolic pathways in a tissue-specific manner, including lipid, carbohydrate, and amino acid metabolism, as well as iron transport and storage (Eid et al., 2019). Intriguingly and inconsistently, $Nrf2^{-/-}$ mice have higher hepatic expression of Fgf21 than the wild type, resulting in improved glucose tolerance when fed a high-fat diet (Zhang et al., 2012; Slocum et al., 2016). In our study, endothelium-specific knockdown of Nrf2 had little effect on lipid and glucose metabolism in db/db mice treated with Cel. However, endothelium-specific Nrf2 deficiency abrogated the effect of Cel to ameliorate endothelial dysfunction and angiogenesis. Thus, we elucidate that Nrf2 in endothelial cells is a master regulator of vascular endothelial function improved by Cel.

Previous studies have shown that high glucose concentrations inhibit the activity of AMPK, which in turn stabilizes BCL2-BECN1, thereby inhibiting autophagy in cardiomyocytes (He et al., 2013). Interestingly, the atherosclerotic lesions of HFD-fed *Apoe*$^{-/-}$ mice are significantly worse than those of control mice because of impairment of endothelial autophagy, which implies that endothelial autophagy limits lipid accumulation in vessel walls (Torisu et al., 2016). However, several contradictory study found that cardiac-specific autophagy deficiency turned on Nrf2-mediated

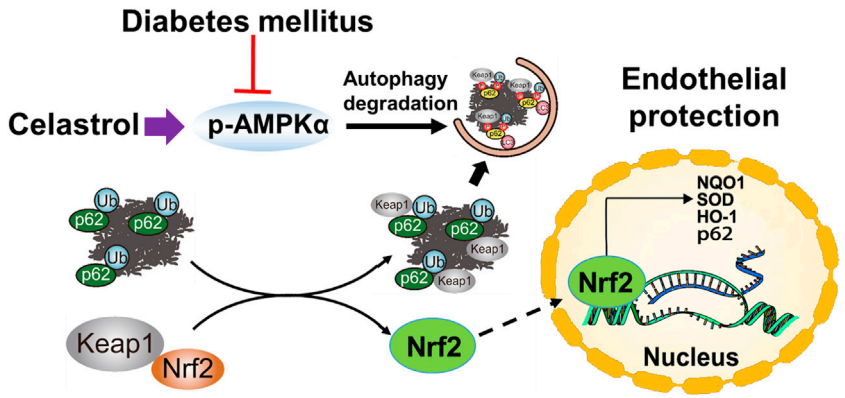


FIGURE 8
Schematic illustration of the protective effects of Cel on HUVECs under HG + PA conditions. HG + PA decreases the expression of Nrf2 in HUVECs and induces oxidative stress, which impairs the survival and angiogenic function of HUVECs. Under HG + PA conditions co-treatment with Cel improves HUVECs survival and function predominantly by Nrf2 activation mediated by increasing phosphorylation of AMPK and autophagic degradation of p62/Keap1.

myocardial damage in the pressure-overloaded heart (Qin et al., 1979) and cardiac autophagy inhibition was critical for driving Nrf2-mediated ferroptosis in type 1 diabetic cardiomyocytes (Zang et al., 2020). Overall, this is most likely attributed to the fact that acute/controlled Nrf2 activation is protective, whereas chronic activation, which occurs in an autophagy-deficient setting, is detrimental, which have documented extensively elsewhere (Dodson and Zhang, 2017; Dodson et al., 2022). In the present study, we found that Cel increases the phosphorylation of AMPK and activates the autophagy-related p62-Keap1-Nrf2 pathway in the presence of high glucose and lipid concentrations, thereby ameliorating the oxidative stress and inflammation, and improving tube formation by endothelial cells and budding from aortic rings. Therefore, we hypothesized that if the autophagic flow could be restored in time, the activated Nrf2 would still play a role in anti-oxidative stress and cell protection.

There were several limitations to our study. Firstly, although HUVECs was the most widely used cells for the study of vascular function and repair (Guixé-Muntet et al., 2017; Cherubini et al., 2023), it is worth exploring the function of the additional dermal microvascular endothelial cells *in vitro* studies of diabetic wounds, which may behave slightly differently from HUVECs under high glucose or lipotoxicity. Secondly, wound contraction usually seen in rodent wound healing but minimal/absent in human wound healing. Thus, it is better to use appropriate methods to prevent wound contraction (staying wet or using semi-occlusive wound dressing). Although we could confidently demonstrate the protective effect of Cel on diabetic wound healing through re-epithelialization, the contractive effect of skin wound healing may have increased the experimental uncertainty to some extent, even if the environment of each group in this study remained the same. Thirdly, although Cel could promote angiogenesis associated with anti-oxidative stress and anti-inflammation in T2D mice, it could not eliminate that completely. These results suggest that Cel has partial effect on improving wound healing following diabetic foot ulcers. It might be worth exploring whether Cel has better vascular protection on other complications of diabetes.

In summary, in the present study, we have shown for the first time that low-dose Cel does not affect the ability of cells to form tubes or angiogenesis under normal conditions. However, the protective effects of Cel against hyperglycemia and hyperlipidemia-induced endothelial injury may be at least in part the results of a maintenance of normal oxidative status and the consequent inhibition of inflammation. In addition, Cel was shown to reduce hyperglycemia/hyperlipidemia-induced inflammation through the AMPK-dependent p62-Keap1-Nrf2 signaling pathway (Figure 8). Although the poor water solubility, short plasma half-life, and high systemic toxicity of Cel greatly hinder its clinical use (Geng et al., 2022), these findings may suggest a new therapeutic approach for the short-term, targeted treatment of refractory diabetes-related skin ulcers and vascular defects in the future. Importantly, there have been many studies on the delivery of Cel by nanomaterials to ameliorate inflammation (An et al., 2020; Wu et al., 2022), we believe that the novel nanocomposites could overcome the poor bioavailability and short half-life of Cel and could be a good candidate for topical application in diabetic foot ulcers.

## Data availability statement

The original contributions presented in the study are included in the article/Supplementary Material, further inquiries can be directed to the corresponding authors.

## Ethics statement

The animal study was approved by Institutional Animal Care and Use Committee of Ningbo University, China. The study was conducted in accordance with the local legislation and institutional requirements.

## Author contributions

GC: Data curation, Funding acquisition, Investigation, Writing–original draft, Writing–review and editing. NA: Funding acquisition, Investigation, Resources, Writing–original draft, Writing–review and editing. RW: Writing–review and editing. LL: Software, Writing–review and editing. BW: Methodology, Writing–review and editing. HW: Writing–review and editing. GP: Writing–review and editing. HZ: Funding acquisition, Writing–review and editing.

## Funding

The author(s) declare that financial support was received for the research, authorship, and/or publication of this article. This work was supported by grants from the Medical Technology Program of Ningbo (2021Y04), National Natural Science Foundation of China (82300105), Natural Science Foundation of Zhejiang Province (LQ23H020003, LQ24H010001), Ningbo Natural Science Foundation (2022J265, 2023J374), the Project of Ningbo Leading Medical and Health Discipline (2022-F06) and National 111 Project of China (D16013).

## Conflict of interest

The authors declare that the research was conducted in the absence of any commercial or financial relationships that could be construed as a potential conflict of interest.

## Publisher's note



## Supplementary material

The Supplementary Material for this article can be found online at: https://www.frontiersin.org/articles/10.3389/fphar.2024.1360177/full#supplementary-material

## References

Abu, B. M., Shariff, K., Tan, J., and Lee, L. K. (2020). Celastrol attenuates inflammatory responses in adipose tissues and improves skeletal muscle mitochondrial functions in high fat diet-induced obese rats via upregulation of AMPK/SIRT1 signaling pathways. *Eur. J. Pharmacol.* 883, 173371. doi:10.1016/j.ejphar.2020.173371

Allison, A., Cacabelos, R., Lombardi, V., Alvarez, X. A., and Vigo, C. (2001). Celastrol, a potent antioxidant and anti-inflammatory drug, as a possible treatment for Alzheimer's disease. *Prog. neuro-psychopharmacology Biol. psychiatry* 25, 1341–1357. doi:10.1016/s0278-5846(01)00192-0

Alnahdi, A., John, A., and Raza, H. (2019). Augmentation of glucotoxicity, oxidative stress, apoptosis and mitochondrial dysfunction in HepG2 cells by palmitic acid. *Nutrients* 11, 1979. doi:10.3390/nu11091979

An, L., Li, Z., Shi, L., Wang, L., Wang, Y., Jin, L., et al. (2020). Inflammation-targeted celastrol nanodrug attenuates collagen-induced arthritis through NF-κB and Notch1 pathways. *Nano Lett.* 20, 7728–7736. doi:10.1021/acs.nanolett.0c03279

Aplin, A., Fogel, E., Zorzi, P., and Nicosia, R. F. (2008). The aortic ring model of angiogenesis. *Methods Enzym.* 443, 119–136. doi:10.1016/s0076-6879(08)02007-7

Baker, M., Robinson, S., Lechertier, T., Barber, P. R., Tavora, B., D'Amico, G., et al. (2011). Use of the mouse aortic ring assay to study angiogenesis. *Nat. Protoc.* 7, 89–104. doi:10.1038/nprot.2011.435

Bian, M., Du, X., Cui, J., Wang, P., Wang, W., Zhu, W., et al. (2016). Celastrol protects mouse retinas from bright light-induced degeneration through inhibition of oxidative stress and inflammation. *J. neuroinflammation* 13, 50. doi:10.1186/s12974-016-0516-8

Bowling, F., Rashid, S., and Boulton, A. (2015). Preventing and treating foot complications associated with diabetes mellitus. *Nat. Rev. Endocrinol.* 11, 606–616. doi:10.1038/nrendo.2015.130

Catrina, S., and Zheng, X. (2016). Disturbed hypoxic responses as a pathogenic mechanism of diabetic foot ulcers. *Diabetes/metabolism Res. Rev.* 32 Suppl 1, 179–185. doi:10.1002/dmrr.2742

Chen, L., Sun, S., Gao, Y., and Ran, X. (2023). Global mortality of diabetic foot ulcer: a systematic review and meta-analysis of observational studies. *Diabetes, Obes. metabolism* 25, 36–45. doi:10.1111/dom.14840

Cherubini, M., Erickson, S., Padmanaban, P., Haberkant, P., Stein, F., Beltran-Sastre, V., et al. (2023). Flow in fetoplacental-like microvessels *in vitro* enhances perfusion, barrier function, and matrix stability. *Sci. Adv.* 9, eadj8540. doi:10.1126/sciadv.adj8540

Choi, B., Kim, H., Lee, H., Sapkota, K., Park, S. E., Kim, S., et al. (2014). Celastrol from 'Thunder God Vine' protects SH-SY5Y cells through the preservation of mitochondrial function and inhibition of p38 MAPK in a rotenone model of Parkinson's disease. *Neurochem. Res.* 39, 84–96. doi:10.1007/s11064-013-1193-y

Das, A., Huang, G., Bonkowski, M., Longchamp, A., Li, C., Schultz, M. B., et al. (2018). Impairment of an endothelial $NAD^+$-$H_2S$ signaling network is a reversible cause of vascular aging. *Cell.* 173, 74–89.e20. doi:10.1016/j.cell.2018.02.008

Dinkova-Kostova, A., Holtzclaw, W., Cole, R., Itoh, K., Wakabayashi, N., Katoh, Y., et al. (2002). Direct evidence that sulfhydryl groups of Keap1 are the sensors regulating induction of phase 2 enzymes that protect against carcinogens and oxidants. *Proc. Natl. Acad. Sci. U. S. A.* 99, 11908–11913. doi:10.1073/pnas.172398899

Divya, T., Dineshbabu, V., Soumyakrishnan, S., Sureshkumar, A., and Sudhandiran, G. (2016). Celastrol enhances Nrf2 mediated antioxidant enzymes and exhibits anti-fibrotic effect through regulation of collagen production against bleomycin-induced pulmonary fibrosis. *Chemico-biological Interact.* 246, 52–62. doi:10.1016/j.cbi.2016.01.006

Dodson, M., Shakya, A., Anandhan, A., Chen, J., Garcia, J. G. N., and Zhang, D. D. (2022). NRF2 and diabetes: the good, the bad, and the complex. *Diabetes* 71, 2463–2476. doi:10.2337/db22-0623

Dodson, M., and Zhang, D. (2017). Non-canonical activation of NRF2: new insights and its relevance to disease. *Curr. Pathobiol. Rep.* 5, 171–176. doi:10.1007/s40139-017-0131-0

Eid, S., Sas, K., Abcouwer, S., Feldman, E. L., Gardner, T. W., Pennathur, S., et al. (2019). New insights into the mechanisms of diabetic complications: role of lipids and lipid metabolism. *Diabetologia* 62, 1539–1549. doi:10.1007/s00125-019-4959-1

Fang, P., He, B., Yu, M., Shi, M., Zhu, Y., Zhang, Z., et al. (2019). Treatment with celastrol protects against obesity through suppression of galanin-induced fat intake and activation of PGC-1α/GLUT4 axis-mediated glucose consumption. *Biochimica biophysica acta Mol. basis Dis.* 1865, 1341–1350. doi:10.1016/j.bbadis.2019.02.002

Feng, K., Chen, H., and Xu, C. (2020). Chondro-protective effects of celastrol on osteoarthritis through autophagy activation and NF-κB signaling pathway inhibition. *Inflamm. Res. official J. Eur. Histamine Res. Soc.* 69, 385–400. doi:10.1007/s00011-020-01327-z

Feng, X., Guan, D., Auen, T., Choi, J. W., Salazar Hernández, M. A., Lee, J., et al. (2019). IL1R1 is required for celastrol's leptin-sensitization and antiobesity effects. *Nat. Med.* 25, 575–582. doi:10.1038/s41591-019-0358-x

Gallagher, K., Mills, J., Armstrong, D., Conte, M. S., Kirsner, R. S., Minc, S. D., et al. (2024). Current status and principles for the treatment and prevention of diabetic foot ulcers in the cardiovascular patient population: a scientific statement from the American heart association. *Circulation* 149, e232–e253. doi:10.1161/cir.0000000000001192

Geng, Y., Xiang, J., Shao, S., Tang, J., and Shen, Y. (2022). Mitochondria-targeted polymer-celastrol conjugate with enhanced anticancer efficacy. *J. Control. release official J. Control. Release Soc.* 342, 122–133. doi:10.1016/j.jconrel.2022.01.002

Gu, L., Bai, W., Li, S., Zhang, Y., Han, Y., Gu, Y., et al. (2013). Celastrol prevents atherosclerosis via inhibiting LOX-1 and oxidative stress. *PloS one* 8, e65477. doi:10.1371/journal.pone.0065477

Guixé-Muntet, S., de Mesquita, F., Vila, S., Hernández-Gea, V., Peralta, C., García-Pagán, J. C., et al. (2017). Cross-talk between autophagy and KLF2 determines endothelial cell phenotype and microvascular function in acute liver injury. *J. hepatology* 66, 86–94. doi:10.1016/j.jhep.2016.07.051

Guo, L., Luo, S., Du, Z., Zhou, M., Li, P., Fu, Y., et al. (2017). Targeted delivery of celastrol to mesangial cells is effective against mesangioproliferative glomerulonephritis. *Nat. Commun.* 8, 878. doi:10.1038/s41467-017-00834-8

Hashemi, M., Zandieh, M., Ziaolhagh, S., Mojtabavi, S., Sadi, F. H., Koohpar, Z. K., et al. (2023). Nrf2 signaling in diabetic nephropathy, cardiomyopathy and neuropathy: therapeutic targeting, challenges and future prospective. *Biochimica biophysica acta Mol. basis Dis.* 1869, 166714. doi:10.1016/j.bbadis.2023.166714

He, C., Zhu, H., Li, H., Zou, M. H., and Xie, Z. (2013). Dissociation of Bcl-2-Beclin1 complex by activated AMPK enhances cardiac autophagy and protects against cardiomyocyte apoptosis in diabetes. *Diabetes* 62, 1270–1281. doi:10.2337/db12-0533

Hu, M., Luo, Q., Alitongbieke, G., Chong, S., Xu, C., Xie, L., et al. (2017). Celastrol-induced Nur77 interaction with TRAF2 alleviates inflammation by promoting mitochondrial ubiquitination and autophagy. *Mol. Cell.* 66, 141–153. doi:10.1016/j.molcel.2017.03.008

Huang, S., Chen, G., Sun, J., Chen, Y., Wang, N., Dong, Y., et al. (2021). Histone deacetylase 3 inhibition alleviates type 2 diabetes mellitus-induced endothelial dysfunction via Nrf2. *Cell. Commun. Signal. CCS* 19, 35. doi:10.1186/s12964-020-00681-z

Ichimura, Y., Waguri, S., Sou, Y., Kageyama, S., Hasegawa, J., Ishimura, R., et al. (2013). Phosphorylation of p62 activates the Keap1-Nrf2 pathway during selective autophagy. *Mol. Cell.* 51, 618–631. doi:10.1016/j.molcel.2013.08.003

Jain, A., Lamark, T., Sjøttem, E., Larsen, K. B., Awuh, J. A., Øvervatn, A., et al. (2010). p62/SQSTM1 is a target gene for transcription factor NRF2 and creates a positive feedback loop by inducing antioxidant response element-driven gene transcription. *J. Biol. Chem.* 285, 22576–22591. doi:10.1074/jbc.M110.118976

Jain, S., Gupta, R., and Sen, R. (2019). Rho-dependent transcription termination in bacteria recycles RNA polymerases stalled at DNA lesions. *Nat. Commun.* 10, 1207. doi:10.1038/s41467-019-09146-5

Jyrkkänen, H., Kansanen, E., Inkala, M., Kivelä, A. M., Hurttila, H., Heinonen, S. E., et al. (2008). Nrf2 regulates antioxidant gene expression evoked by oxidized phospholipids in endothelial cells and murine arteries *in vivo*. *Circulation Res.* 103, e1–e9. doi:10.1161/circresaha.108.176883

Kim, J., Lee, M., Nam, D., Song, H. K., Kang, Y. S., Lee, J. E., et al. (2013). Celastrol, an NF-κB inhibitor, improves insulin resistance and attenuates renal injury in db/db mice. *PloS one* 8, e62068. doi:10.1371/journal.pone.0062068

Komatsu, M., Kurokawa, H., Waguri, S., Taguchi, K., Kobayashi, A., Ichimura, Y., et al. (2010). The selective autophagy substrate p62 activates the stress responsive transcription factor Nrf2 through inactivation of Keap1. *Nat. Cell. Biol.* 12, 213–223. doi:10.1038/ncb2021

Lau, A., Wang, X., Zhao, F., Villeneuve, N. F., Wu, T., Jiang, T., et al. (2010). A noncanonical mechanism of Nrf2 activation by autophagy deficiency: direct interaction between Keap1 and p62. *Mol. Cell. Biol.* 30, 3275–3285. doi:10.1128/mcb.00248-10

Li, D., Wang, A., Liu, X., Meisgen, F., Grünler, J., Botusan, I. R., et al. (2015). MicroRNA-132 enhances transition from inflammation to proliferation during wound healing. *J. Clin. investigation* 125, 3008–3026. doi:10.1172/jci79052

Li, L., Wang, B., Li, Y., Li, L., Dai, Y., Lv, G., et al. (2020). Celastrol regulates bone marrow mesenchymal stem cell fate and bone-fat balance in osteoporosis and skeletal aging by inducing PGC-1α signaling. *Aging* 12, 16887–16898. doi:10.18632/aging.103590

Li, M., Liu, X., He, Y., Zheng, Q., Wang, M., Wu, Y., et al. (2017). Celastrol attenuates angiotensin II mediated human umbilical vein endothelial cells damage through activation of Nrf2/ERK1/2/Nox2 signal pathway. *Eur. J. Pharmacol.* 797, 124–133. doi:10.1016/j.ejphar.2017.01.027

Liu, J., Lee, J., Salazar Hernandez, M., Mazitschek, R., and Ozcan, U. (2015). Treatment of obesity with celastrol. *Cell.* 161, 999–1011. doi:10.1016/j.cell.2015.05.011

Ma, L., Cao, Y., Zhang, L., Li, K., Yan, L., Pan, Y., et al. (2020). Celastrol mitigates high glucose-induced inflammation and apoptosis in rat H9c2 cardiomyocytes via miR-345-5p/growth arrest-specific 6. *J. gene Med.* 22, e3201. doi:10.1002/jgm.3201

Ma, X., Xu, L., Alberobello, A., Gavrilova, O., Bagattin, A., Skarulis, M., et al. (2015). Celastrol protects against obesity and metabolic dysfunction through activation of a HSF1-pgc1α transcriptional Axis. *Cell. metab.* 22, 695–708. doi:10.1016/j.cmet.2015.08.005

Nakayama, T., Okimura, K., Shen, J., Guh, Y. J., Tamai, T. K., Shimada, A., et al. (2020). Seasonal changes in NRF2 antioxidant pathway regulates winter depression-like behavior. *Proc. Natl. Acad. Sci. U. S. A.* 117, 9594–9603. doi:10.1073/pnas.2000278117

Ogurtsova, K., Guariguata, L., Barengo, N., Ruiz, P. L. D., Sacre, J. W., Karuranga, S., et al. (2022). IDF diabetes Atlas: global estimates of undiagnosed diabetes in adults for 2021. *Diabetes Res. Clin. Pract.* 183, 109118. doi:10.1016/j.diabres.2021.109118

Okonkwo, U., and DiPietro, L. (2017). Diabetes and wound angiogenesis. *Int. J. Mol. Sci.* 18, 1419. doi:10.3390/ijms18071419

Pang, X., Yi, Z., Zhang, J., Lu, B., Sung, B., Qu, W., et al. (2010). Celastrol suppresses angiogenesis-mediated tumor growth through inhibition of AKT/mammalian target of rapamycin pathway. *Cancer Res.* 70, 1951–1959. doi:10.1158/0008-5472.Can-09-3201

Qin, Q., Qu, C., Niu, T., Zang, H., Qi, L., Lyu, L., et al. (1979). Nrf2-Mediated cardiac maladaptive remodeling and dysfunction in a setting of autophagy insufficiency. *Hypertens. Dallas, Tex* 67, 107–117. doi:10.1161/hypertensionaha.115.06062

Qing, T., Yan, L., Wang, S., Dai, X. Y., Ren, L. J., Zhang, J. Q. Z., et al. (2023). Celastrol alleviates oxidative stress induced by multi-walled carbon nanotubes through the Keap1/Nrf2/HO-1 signaling pathway. *Ecotoxicol. Environ. Saf.* 252, 114623. doi:10.1016/j.ecoenv.2023.114623

Rehak, L., Giurato, L., Meloni, M., Panunzi, A., Manti, G. M., and Uccioli, L. (2022). The immune-centric revolution in the diabetic foot: monocytes and lymphocytes role in wound healing and tissue regeneration-A narrative review. *J. Clin. Med.* 11, 889. doi:10.3390/jcm11030889

Safferling, K., Sütterlin, T., Westphal, K., Ernst, C., Breuhahn, K., James, M., et al. (2013). Wound healing revised: a novel reepithelialization mechanism revealed by *in vitro* and *in silico* models. *J. Cell. Biol.* 203, 691–709. doi:10.1083/jcb.201212020

Shirai, T., Nakai, A., Ando, E., Fujimoto, J., Leach, S., Arimori, T., et al. (2023). Celastrol suppresses humoral immune responses and autoimmunity by targeting the COMMD3/8 complex. *Sci. Immunol.* 8, eadc9324. doi:10.1126/sciimmunol.adc9324

Singh, N., Armstrong, D., and Lipsky, B. (2005). Preventing foot ulcers in patients with diabetes. *JAMA* 293, 217–228. doi:10.1001/jama.293.2.217

Slocum, S., Skoko, J., Wakabayashi, N., Aja, S., Yamamoto, M., Kensler, T. W., et al. (2016). Keap1/Nrf2 pathway activation leads to a repressed hepatic gluconeogenic and lipogenic program in mice on a high-fat diet. *Archives Biochem. biophysics* 591, 57–65. doi:10.1016/j.abb.2015.11.040

Taguchi, K., Fujikawa, N., Komatsu, M., Ishii, T., Unno, M., Akaike, T., et al. (2012). Keap1 degradation by autophagy for the maintenance of redox homeostasis. *Proc. Natl. Acad. Sci. U. S. A.* 109, 13561–13566. doi:10.1073/pnas.1121572109

Torisu, K., Singh, K., Torisu, T., Lovren, F., Liu, J., Pan, Y., et al. (2016). Intact endothelial autophagy is required to maintain vascular lipid homeostasis. *Aging Cell.* 15, 187–191. doi:10.1111/acel.12423

Venkatesha, S., and Moudgil, K. (2016). Celastrol and its role in controlling chronic diseases. *Adv. Exp. Med. Biol.* 928, 267–289. doi:10.1007/978-3-319-41334-1_12

Wu, Q., Wang, J., Wang, Y., Xiang, L., Tan, Y., Feng, J., et al. (2022). Targeted delivery of celastrol to glomerular endothelium and podocytes for chronic kidney disease treatment. *Nano Res.* 15, 3556–3568. doi:10.1007/s12274-021-3894-x

Xie, Z., Zhang, J., Wu, J., Viollet, B., and Zou, M. H. (2008). Upregulation of mitochondrial uncoupling protein-2 by the AMP-activated protein kinase in endothelial cells attenuates oxidative stress in diabetes. *Diabetes* 57, 3222–3230. doi:10.2337/db08-0610

Xu, X., Zhao, W., Feng, S., Sun, C., Chen, Q., Ni, B., et al. (2017). Celastrol alleviates angiotensin II-mediated vascular smooth muscle cell senescence via induction of autophagy. *Mol. Med. Rep.* 16, 7657–7664. doi:10.3892/mmr.2017.7533

Xu, Z., Liu, Y., Ma, R., Chen, J., Qiu, J., Du, S., et al. (2022). Thermosensitive hydrogel incorporating prussian blue nanoparticles promotes diabetic wound healing via ROS scavenging and mitochondrial function restoration. *ACS Appl. Mater. interfaces* 14, 14059–14071. doi:10.1021/acsami.1c24569

Ye, S., Luo, W., Khan, Z., Wu, G., Xuan, L., Shan, P., et al. (2020). Celastrol attenuates angiotensin II-induced cardiac remodeling by targeting STAT3. *Circulation Res.* 126, 1007–1023. doi:10.1161/circresaha.119.315861

Yuan, Z., Wang, J., Qu, Q., Zhu, Z., Xu, M., Zhao, M., et al. (2023). Celastrol combats methicillin-resistant *Staphylococcus aureus* by targeting $\Delta^1$ -Pyrroline-5-Carboxylate dehydrogenase. *Adv. Sci. Weinheim, Baden-Wurttemberg, Ger.* 10, e2302459. doi:10.1002/advs.202302459

Zang, H., Wu, W., Qi, L., Tan, W., Nagarkatti, P., Nagarkatti, M., et al. (2020). Autophagy inhibition enables Nrf2 to exaggerate the progression of diabetic cardiomyopathy in mice. *Diabetes* 69, 2720–2734. doi:10.2337/db19-1176

Zhang, D., and Hannink, M. (2003). Distinct cysteine residues in Keap1 are required for Keap1-dependent ubiquitination of Nrf2 and for stabilization of Nrf2 by chemopreventive agents and oxidative stress. *Mol. Cell. Biol.* 23, 8137–8151. doi:10.1128/mcb.23.22.8137-8151.2003

Zhang, F., Liu, Y., Wang, S., Yan, X., Lin, Y., Chen, D., et al. (2022). Interleukin-25-Mediated-IL-17RB upregulation promotes cutaneous wound healing in diabetic mice by improving endothelial cell functions. *Front. Immunol.* 13, 809755. doi:10.3389/fimmu.2022.809755

Zhang, L., Zou, L., Jiang, X., Cheng, S., Zhang, J., Qin, X., et al. (2021). Stabilization of Nrf2 leading to HO-1 activation protects against zinc oxide nanoparticles-induced endothelial cell death. *Nanotoxicology* 15, 779–797. doi:10.1080/17435390.2021.1919330

Zhang, Y., Wu, K., Liu, J., and Klaassen, C. D. (2012). Nrf2 deficiency improves glucose tolerance in mice fed a high-fat diet. *Toxicol. Appl. Pharmacol.* 264, 305–314. doi:10.1016/j.taap.2012.09.014

frontiers | Frontiers in Pharmacology

TYPE Original Research
PUBLISHED 05 June 2024
DOI 10.3389/fphar.2024.1362150



OPEN ACCESS

EDITED BY
Ludwig Weckbach,
LMU Munich University Hospital, Germany

REVIEWED BY
Prarambh S. R. Dwivedi,
Nitte Gulabi Shetty Memorial Institute of Pharmaceutical Sciences, India
Thilagavathi Ramasamy,
Karpagam Academy of Higher Education, India

*CORRESPONDENCE
Ching-Feng Weng,
cfwengcf@gmail.com

‡PRESENT ADDRESS
Ching-Feng Weng,
LEADTEK Research, INC., New Taipei City, Taiwan

§These authors have contributed equally to this work

RECEIVED 27 December 2023
ACCEPTED 29 April 2024
PUBLISHED 05 June 2024

CITATION
Huang X, Lin K, Liu S, Yang J, Zhao H, Zheng X-H, Tsai M-J, Chang C-S, Huang L and Weng C-F (2024), Combination of plant metabolites hinders starch digestion and glucose absorption while facilitating insulin sensitivity to diabetes.
*Front. Pharmacol.* 15:1362150.
doi: 10.3389/fphar.2024.1362150



# Combination of plant metabolites hinders starch digestion and glucose absorption while facilitating insulin sensitivity to diabetes

Xin Huang[1,2§], Kaihuang Lin[1,2§], Sinian Liu[1,2], Junxiong Yang[1,2], Haowei Zhao[1,2], Xiao-Hui Zheng[1,2], May-Jywan Tsai[3], Chun-Sheng Chang[4], Liyue Huang[1,2] and Ching-Feng Weng [1,2*‡]

[1]Functional Physiology Section, Department of Basic Medical Science, Xiamen Medical College, Xiamen, China, [2]Institute of Respiratory Disease, Department of Basic Medical Science, Xiamen Medical College, Xiamen, China, [3]Department of Neurosurgery, Neurological Institute, Taipei Veterans General Hospital, Taipei, Taiwan, [4]Department of Biotechnology and Food Technology, Southern Taiwan University of Science and Technology, Tainan, Taiwan

**Introduction:** Diabetes mellitus (DM) is a common endocrine disease resulting from interactions between genetic and environmental factors. Type II DM (T2DM) accounts for approximately 90% of all DM cases. Current medicines used in the treatment of DM have some adverse or undesirable effects on patients, necessitating the use of alternative medications.

**Methods:** To overcome the low bioavailability of plant metabolites, all entities were first screened through pharmacokinetic, network pharmacology, and molecular docking predictions. Experiments were further conducted on a combination of antidiabetic phytoactive molecules (rosmarinic acid, RA; luteolin, Lut; resveratrol, RS), along with *in vitro* evaluation (α-amylase inhibition assay) and diabetic mice tests (oral glucose tolerance test, OGTT; oral starch tolerance test, OSTT) for maximal responses to validate starch digestion and glucose absorption while facilitating insulin sensitivity.

**Results:** The results revealed that the combination of metabolites achieved all required criteria, including ADMET, drug likeness, and Lipinski rule. To determine the mechanisms underlying diabetic hyperglycemia and T2DM treatments, network pharmacology was used for regulatory network, PPI network, GO, and KEGG enrichment analyses. Furthermore, the combined metabolites showed adequate *in silico* predictions (α-amylase, α-glucosidase, and pancreatic lipase for improving starch digestion; SGLT-2, AMPK, glucokinase, aldose reductase, acetylcholinesterase, and acetylcholine M2 receptor for mediating glucose absorption; GLP-1R, DPP-IV, and PPAR-γ for regulating

**Abbreviations:** DIO, diet-induced obese; GT, glucose tolerance; IGT, insulin intolerance test; Lut, luteolin; MAPK, mitogen-activated protein kinase; OGTT, oral glucose tolerance test; OSTT, oral starch tolerance test; RA, rosmarinic acid; RS, resveratrol.

insulin sensitivity), *in vitro* α-amylase inhibition, and *in vivo* efficacy (OSTT versus acarbose; OGTT versus metformin and insulin) as nutraceuticals against T2DM.

**Discussion:** The results demonstrate that the combination of RA, Lut, and RS could be exploited for multitarget therapy as prospective antihyperglycemic phytopharmaceuticals that hinder starch digestion and glucose absorption while facilitating insulin sensitivity.

KEYWORDS

**antihyperglycemia, combinatory chemistry, phytopharmaceutical, polyphenol, *in silico*, multitarget**

# 1 Introduction

Diabetes mellitus (DM) is a widespread metabolic disease with a rapidly growing global population; it is characterized by chronic hyperglycemia resulting from inadequate insulin secretion and/or insulin action (Ozougwu et al., 2013; Thompson and Kanamarlapudi, 2013) and is attributable to the interactions between genetic and environmental factors. Type II DM (T2DM) is also designated as non-insulin-dependent DM (NIDDM) and is often known to occur as a consequence of excess blood glucose (hyperglycemia) caused by dysfunctional β-cells and insulin resistance. T2DM is the major form of diabetes, as an estimated 90% of DM patients are diagnosed with this form. The global incidence of DM continues to increase, and it is expected that there will be more than 590 million patients with this disorder by 2035 (Ozougwu et al., 2013; Guariguata et al., 2014). It is known that DM can cause several other complications, such as cardiovascular diseases, ischemic heart disease, obesity, peripheral vascular disease, stroke, retinopathy, neuropathy, nephropathy, diabetic foot ulcers, and a variety of heterogeneous diseases, based on abnormalities in the relative metabolic pathways (Boulton et al., 2005; Punthakee et al., 2018; Swilam et al., 2022), with T2DM causing over 95% of these comorbidities (Punthakee et al., 2018). Although various types of oral hyperglycemic drugs (e.g., acarbose, miglitol, voglibose, metformin, and sulfonylureas) are available for the treatment of diabetes (Spínola et al., 2019), these approved synthetic drugs cannot be applied for long-term glycemic control or reversal of comorbidity progression; their side effects or adverse reactions are also usually downplayed, coupled with the cost, which makes their access especially challenging for the low-income population in developing and underdeveloped countries. Therefore, there is an urgency for developing alternative therapeutics with limited associated shortcomings (Takayanagi et al., 2011). This is a major health issue in today's society and is significantly linked with the socioeconomic difficulties experienced worldwide.

The documentation of natural products that moderate blood glucose levels can possibly accelerate exploitation of mild interventions like folk or herbal medicines as well as functional foods in the treatment of chronic diseases, including diabetes. In comparison, active metabolites from synthetic sources, extracts, or natural products from natural sources such as botanical drugs and plant metabolites that are commonly safe, easy to locate, easily accessible, and reasonably inexpensive, with low incidence of adverse effects must be prioritized to facilitate the surging diversion into phytomedicine (Wais et al., 2012; Bizzarri et al., 2020). Polyphenols are a large class of metabolites deemed to have multiple biological properties, such as antioxidant, cytotoxic, anti-inflammatory, antihypertensive, and antidiabetic functions (Rana et al., 2022). For instance, curcumin has been widely shown to be a popular antidiabetic, but its limitations like poor absorption, rapid metabolism and elimination, and low concentrations in the plasma and target tissue are considered to be obstacles in treatment (Pivari et al., 2019). It has been noted that monotarget therapy with natural polyphenols failed to manage blood glucose levels and other comorbidities; therefore, the combined use (polytherapy) of polyphenols has become a common practice (Boonrueng et al., 2022).

The flavone luteolin (3′, 4′, 5, 7-tetrahydroxyflavone, Lut) is a naturally occurring secondary metabolite present in various plants, such as celery, chrysanthemum flowers, sweet bell peppers, carrots, onion leaves, broccoli, and parsley. It has anti-inflammatory and antioxidant activities, and it increases glucose metabolism by potentiating insulin sensitivity while enhancing β-cell function and mass during a hyperglycemic clamp (Daily et al., 2021). However, one study revealed that Lut has limited bioavailability that consequently affects its biological properties and efficacy (Taheri et al., 2021). Resveratrol (3,5,4′-trihydroxy-trans-stilbene, RS) is a naturally occurring polyphenolic stilbene compound found in more than 70 plant species and their products, such as grapes, peanuts, mulberries, bilberries, blueberries, cranberries, and spruce, as well as other plant roots, leaves, and fruits in response to biotic and abiotic factors. It has been shown to have numerous biological activities, such as antitumor, antioxidant, antiviral, and phytoestrogenic properties. The effective use of RS is restricted by its poor solubility, photosensitivity, and rapid metabolism, which strongly undermine its bioavailability and bioactivity (Santos et al., 2019). Rosmarinic acid (ester of caffeic acid, RA) is a secondary metabolite and polyphenol present in many culinary plants, such as rosemary, mint, basil, and perilla, that presents various well-documented biological effects, such as anti-inflammatory, antioxidant, antidiabetic, and antitumor properties. Despite the high therapeutic potential of RA, its intrinsic properties of poor water solubility and low bioavailability have limited its translation to clinical settings (Chung et al., 2020). Based on the low bioavailability and bioactivity of the abovementioned compounds, a putative reconstitution (combinatory chemistry) of RA, Lut, and RS could enhance the bioavailability and efficiency to achieve maximal response against the limitations. This combination is worth investigating as it can potentially help lower blood glucose levels in diabetes.

In recent times, researchers have been keen on developing methods to induce antihyperglycemia by eliminating starch digestion, promoting metabolism (glucose uptake, absorption,

TABLE 1 (A) Physicochemical properties and (B) *in silico* ADME/toxicity profiles of rosmarinic acid, luteolin, and resveratrol.

| Property name | Luteolin | Resveratrol | Rosmarinic acid |
|---|---|---|---|
| (A) Physicochemical properties | | | |
| Molecular weight | **286.24** | **228.24** | **360.3** |
| XLogP3 | **1.4** | **3.1** | **2.4** |
| Hydrogen bond donor count | **4** | **3** | **5** |
| Hydrogen bond acceptor count | **6** | **3** | **8** |
| Rotatable bond count | **1** | **2** | **7** |
| Topological polar surface area (TPSA) | **107 Å²** | **60.7 Å²** | **145 Å²** |
| Heavy atom count | **21** | **17** | **26** |
| Formal charge | **0** | **0** | **0** |
| Complexity | **447** | **246** | **519** |
| Defined atom stereocenter count | **0** | **0** | **1** |
| Defined bond stereocenter count | **0** | **1** | **1** |
| Covalently bonded unit count | **1** | **1** | **1** |
| Compound is canonicalized | **Yes** | **Yes** | **Yes** |
| (B) ADMET | | | |
| Human intestinal absorption | **HIA-** | **HIA+** | **HIA-** |
| Human oral bioavailability | **HOB+** | **HOB-** | **HOB+** |
| Blood–brain barrier | **BBB+** | **BBB+** | **BBB+** |
| Caco2 permeability | **Caco2+** | **Caco2+** | **Caco2+** |
| Acute oral tox log (1 mol/kg) | **Nil** | **Nil** | **Nil** |
| Carcinogenic | - | - | - |
| CYP2C9 | - | + | - |
| CYP2D6 | + | - | - |
| CYP1A2 | + | + | - |
| CYP2C19 | - | - | - |
| CYP3A4 | + | + | - |
| Hepatotoxicity | - | - | - |
| Lipinski rule violation | **Nil** | **Nil** | **Nil** |
| Lead likeness violation | **Nil** | **1** | **1** |
| Solubility LogS | **−2.588** | **−2.439** | **−3.154** |

Footnote: ADMET, Absorption, Distribution, Metabolism, Excretion, Toxicity; +, positive; -, negative; solubility normal range: −6.5 to 0.5.
HIA% < 30% = HIA-; HIA% > 30% = HIA+; CYP2C9 inhibitor, CYP2D6 inhibitor, CYP1A2 inhibitor, CYP2C19 inhibitor.

and utilization), and triggering insulin sensitivity; approaches have been employed to explore good metabolite candidates and further determine the best combination ratio for phytotherapeutics. In this study, the best or gold combination of known antidiabetic metabolites, specially RA, Lut, and RS, was tailored on the basis of $IC_{50}$, solubility, and network pharmacology studies. Then, molecular docking of these selected metabolites was examined toward diabetic multitarget proteins, such as α-amylase, α-glucosidase, pancreatic lipase, SGLT-2, AMPK, glucokinase, aldose reductase, acetylcholinesterase, acetylcholine M2 receptor, GLP-1R, DPP-IV, and PPAR-γ, which are extensively considered therapeutic targets in clinical treatments for maximal response to reducing blood glucose levels. Furthermore, *in vitro* α-amylase inhibition assays with the lone metabolites and combination as well as *in vivo* tests (oral starch tolerance test, OSTT, and oral glucose tolerance test, OGTT) in diet-induced obese diabetic mice were conducted to verify the combination for putative antidiabetic effects. Finally, the molecular mechanism of the combination was predicted through a network pharmacology study.

TABLE 2 Solubility and $IC_{50}$ (*in vitro* and *in vivo*) values of rosmarinic acid, luteolin, and resveratrol. DMSO: dimethyl sulfoxide, DMF: dimethyl formamide.

| Ligands | Solubility | $IC_{50}$ (μM) | | | | | | $EC_{50}$ (μM) | |
|---|---|---|---|---|---|---|---|---|---|
| | | α-Amylase[1–4] | α-Glucosidase[2,5–9] | DPP-IV[2,10] | PTP-1B[11,12] | Aldose reductase[13,14] | Pancreatic lipase[15,16] | SIRT1[17] | PPAR-γ[18] |
| Luteolin<br>$C_{15}H_{10}O_6$<br>CID: 5280445 | In methanol and alkaline solutions; slightly in water, DMSO (57 mg/mL), and ethanol (6 mg/mL) | 147–360 | 26.41–172 | 0.12 | 136.3 | 0.6 | 63 | - | 2.3 |
| Resveratrol<br>$C_{14}H_{12}O_3$<br>CID: 445154 | In water (3 mg/100 mL); in ethanol, DMSO, and DMF (65 mg/mL) | 32.23 | 47.93–123 | 5.638 | - | 117.6 | - | 7 | - |
| Rosmarinic acid<br>$C_{18}H_{16}O_8$<br>CID: 5281792 | In ethanol, DMSO, and DMF (25 mg/mL) | 103 | 33 | - | 137 | 11.2 | 51.28 | - | - |

References: 1. Kusano G, Takahira M, Shibano M, et al. Studies on inhibitory activities of fukiic acid esters on germination, alpha-amylase and carboxypeptidase A. *Biol Pharm Bull*. 1998; 21(9): 997-999. doi: 10.1248/bpb.21.997.

2. Khalid MF, Rehman K, Irshad K, Chohan TA, Akash MSH. Biochemical investigation of inhibitory activities of plant-derived bioactive compounds against carbohydrate and glucagon-like peptide-1 metabolizing enzymes. *Dose Resp*. 2022; 20(2):15593258221093276. doi: 10.1177/15593258221093275.

3. Yang Y, Wang Y, Zeng W, et al. A strategy based on liquid-liquid-refining extraction and high-speed counter-current chromatography for the bioassay-guided separation of active compound from *Taraxacum mongolicum*. *J Chromatogr A*. 2020; 1614:460727. doi: 10.1016/j.chroma.2019.460727.

4. Tadera K, Minami Y, Takamatsu K, Matsuoka T. Inhibition of alpha-glucosidase and alpha-amylase by flavonoids. *J Nutr Sci Vitaminol (Tokyo)*. 2006; 52(2):149-153. doi: 10.3177/jnsv.52.149.

5. Yan J, Zhang G, Pan J, Wang Y. α-Glucosidase inhibition by luteolin: Kinetics, interaction and molecular docking. *Int J Biol Macromol*. 2014; 64:213-223. doi: 10.1016/j.ijbiomac.2013.12.007.

6. Wagle A, Seong SH, Shrestha S, Jung HA, Choi JS. Korean thistle (*Cirsium japonicum* var. maackii (Maxim.) Matsum.): A potential dietary supplement against diabetes and Alzheimer's disease. *Molecules*. 2019; 24(3):E649. doi: 10.3390/molecules24030649.

7. Kubínová R, Pořízková R, Navrátilová A, et al. Antimicrobial and enzyme inhibitory activities of the constituents of *Plectranthus madagascariensis* (Pers.) Benth. *J Enzyme Inhib Med Chem*. 2014; 29(5):749-752. doi: 10.3109/14756366.2013.848204.

8. Ablat A, Halabi MF, Mohamad J, et al. Antidiabetic effects of *Brucea javanica* seeds in type 2 diabetic rats. *BMC Complement Altern Med*. 2017; 17(1):94. doi: 10.1186/s12906-017-1610-x.

9. Zhang CC, Geng CA, Huang XY, Zhang XM, Chen JJ. Antidiabetic stilbenes from peony seeds with PTP1B, α-glucosidase, and DPPIV inhibitory activities. *J Agri Food Chem*. 2019; 67(24): 6765-6772. doi: 10.1021/acs.jafc.9b01193.

10. Fan J, Johnson MH, Lila MA, Yousef G, de Mejia EG. Berry and citrus phenolic compounds inhibit dipeptidyl peptidase IV: Implications in diabetes management. *Evid Based Complement Altern Med*. 2013; 2013:479505. doi: 10.1155/2013/479505.

11. Huang Q, Chen JJ, Pan Y, et al. Chemical profiling and antidiabetic potency of *Paeonia delavayi*: Comparison between different parts and constituents. *J Pharm Biomed Anal*. 2021; 198: 113998. doi: 10.1016/j.jpba.2021.113998.

12. Salinas-Arellano E, Pérez-Vásquez A, Rivero-Cruz I, et al. Flavonoids and terpenoids with PTP-1B inhibitory properties from the infusion of *Salvia amarissima Ortega*. *Molecules*. 2020; 25(15):E3530. doi: 10.3390/molecules25153530.

13. Kim SB, Hwang SH, Wang Z, Yu JM, Lim SS. Rapid identification and isolation of inhibitors of rat lens aldose reductase and antioxidant in *Maackia amurensis*. *Biomed Res Int*. 2017; 2017: 4941825. doi: 10.1155/2017/4941825.

14. Ha TJ, Lee JH, Lee MH, et al. Isolation and identification of phenolic compounds from the seeds of *Perilla frutescens* (L.) and their inhibitory activities against α-glucosidase and aldose reductase. *Food Chem*. 2012; 135(3):1397-1403. doi: 10.1016/j.foodchem.2012.05.104.

15. Afifi FU, Kasabri V, Litescu S, Abaza IF, Tawaha K. Phytochemical and biological evaluations of *Arum hygrophilum Boiss*. (Araceae). *Pharmacogn Mag*. 2017; 13(50):275-280. doi: 10.4103/0973-1296.204551.

16. Ramirez G, Zamilpa A, Zavala M, Perez J, Morales D, Tortoriello J. Chrysoeriol and other polyphenols from *Tecoma stans* with lipase inhibitory activity. *J Ethnopharmacol*. 2016; 185:1-8. doi: 10.1016/j.jep.2016.03.014.

17. Sharma S, Misra CS, Arumugam S, et al. Antidiabetic activity of resveratrol, a known SIRT1 activator in a genetic model for type-2 diabetes. *Phytother Res*. 2011; 25(1):67-73. doi: 10.1002/ptr.3221.

18. Liu Q, Yang QM, Hu HJ, et al. Bioactive diterpenoids and flavonoids from the aerial parts of *Scoparia dulcis*. *J Nat Prod*. 2014; 77(7):1594-1600. doi: 10.1021/np500150f.

# 2 Materials and methods

## 2.1 Materials

Purified Lut (98% purity), RS (98%), and RA (98%) were obtained from Shaanxi Dongshuo Biotechnology Co., Ltd. (Shaanxi, China).

## 2.2 Pharmacokinetics and ADME/toxicity profiling

The pharmacokinetic properties of the materials, such as ADMET behaviors of the ligands in the human body, were screened using the SwissADME (http://www.swissadme.ch/index.php) and admetSAR prediction tool webserver (http://lmmd.ecust.

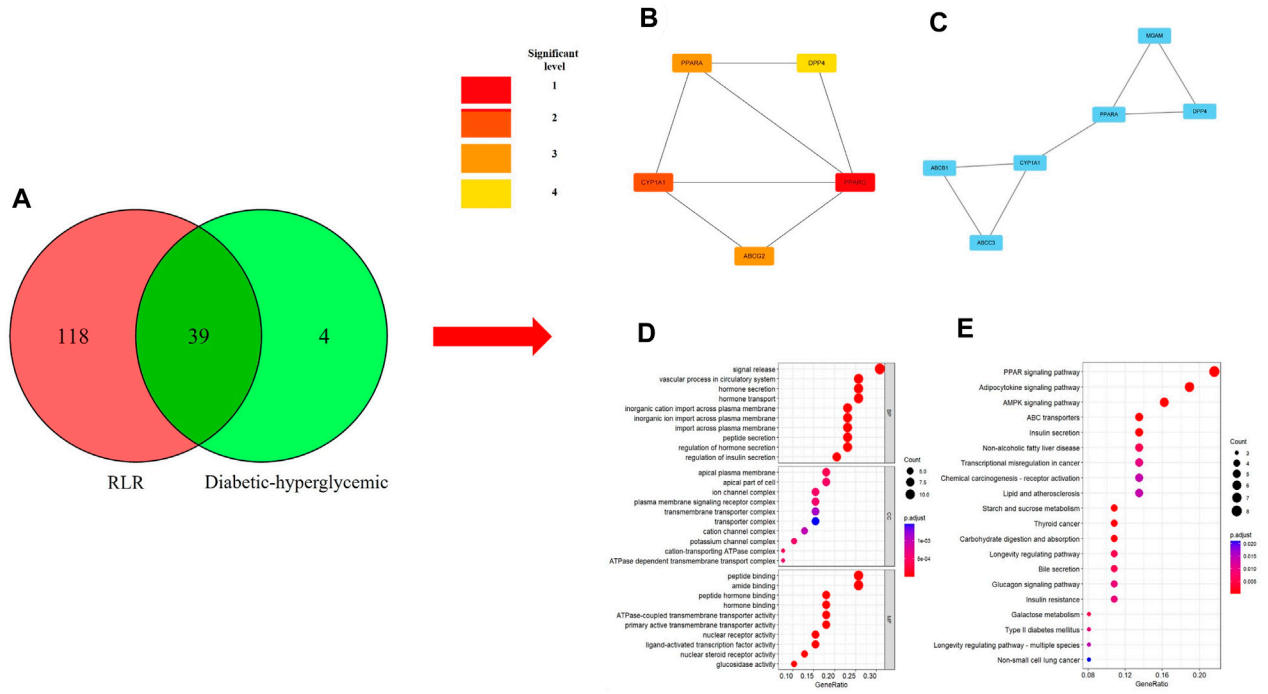


FIGURE 1
**(A)** Intersecting targets between rosmarinic acid, luteolin, and resveratrol (RLR) and diabetic hyperglycemia. **(B)** PPI network analysis. Nodes with red labels are the top-5 hub targets as analyzed by Cytohubba, and darker node colors represent higher scores. **(C)** Blue nodes represent nodes in the most crucial module analyzed by MCODE. **(D)** GO enrichment analysis of 39 intersecting targets. The top-10 GO functional terms were selected finally. **(E)** KEGG pathway enrichment analysis of 39 intersecting targets. The top-20 pathways were identified (adjusted p ≤0.05). The colors represent the adjusted p values, and spot sizes represent the gene counts.

edu.cn/admetsar2). This step is significant for identifying the drug likeness, medicinal chemistry, lead likeness, and toxicity potential of new candidate drugs, phytochemicals, food additives, and industrial chemicals; it is also a prerequisite for establishing valid complementary methods before *in vivo*/*in vitro* analyses (Cheng et al., 2012; Sharma et al., 2020; Suchitra et al., 2020).

## 2.3 Exploring the potential targets of RA, Lut, and RS

The Traditional Chinese Medicine Systems Pharmacology Database and Analysis Platform (TCMSP) (https://tcmsp-e.com/) (Liu et al., 2013) were used to obtain the potential targets of RA, Lut, and RS (RLR). The target names were standardized using the UniProt database (https://www.uniprot.org/) for the status criterion of "Reviewed" and organism category of "Human".

## 2.4 Acquisition of diabetic hyperglycemia and T2DM related targets as well as construction of Venn diagrams

Diabetic hyperglycemia targets were screened using the DrugBank database; further, the RCSB database was searched for the target protein database (PDB) using qualifiers such as "*Homo sapiens*," "X-ray," and "no mutation." These targets were compared with the RLR targets, and Venn diagrams were constructed to identify the targets related to both diabetic hyperglycemia and RLR. T2DM-related targets were obtained from four databases, namely, the Comparative Toxicogenomics Database (CTD) (http://ctdbase.org/), GeneCards (https://www.genecards.org/), OMIM (https://www.omim.org), and DisGeNET (https://www.disgenet.org/). Threshold scores were simultaneously set in the CTD, GeneCards, and DisGeNET to filter the targets; all targets from the four databases were merged, and duplicate values were deleted to obtain the corresponding T2DM targets. Venn diagrams were also constructed for the T2DM targets using the tools in Hiplot Pro (https://hiplot.com.cn/), a comprehensive web service for biomedical data analysis and visualization. The common targets between RLR and T2DM (i.e., T2DM-related targets treated by RLR) were obtained from the Venn diagrams.

## 2.5 Construction of regulatory networks between RLR and the intersecting targets

Cytoscape (version 3.9.1; https://cytoscape.org/) (Shannon et al., 2003) was used to visualize the interactions of RLR with diabetic hyperglycemia and T2DM as a regulatory network. The intersecting targets and different types of metabolites were displayed using various shapes. The degree value represents the number of interactions generated by a node, and a higher degree value denotes a more significant status in the network. These higher degree values were represented using deeper colors.

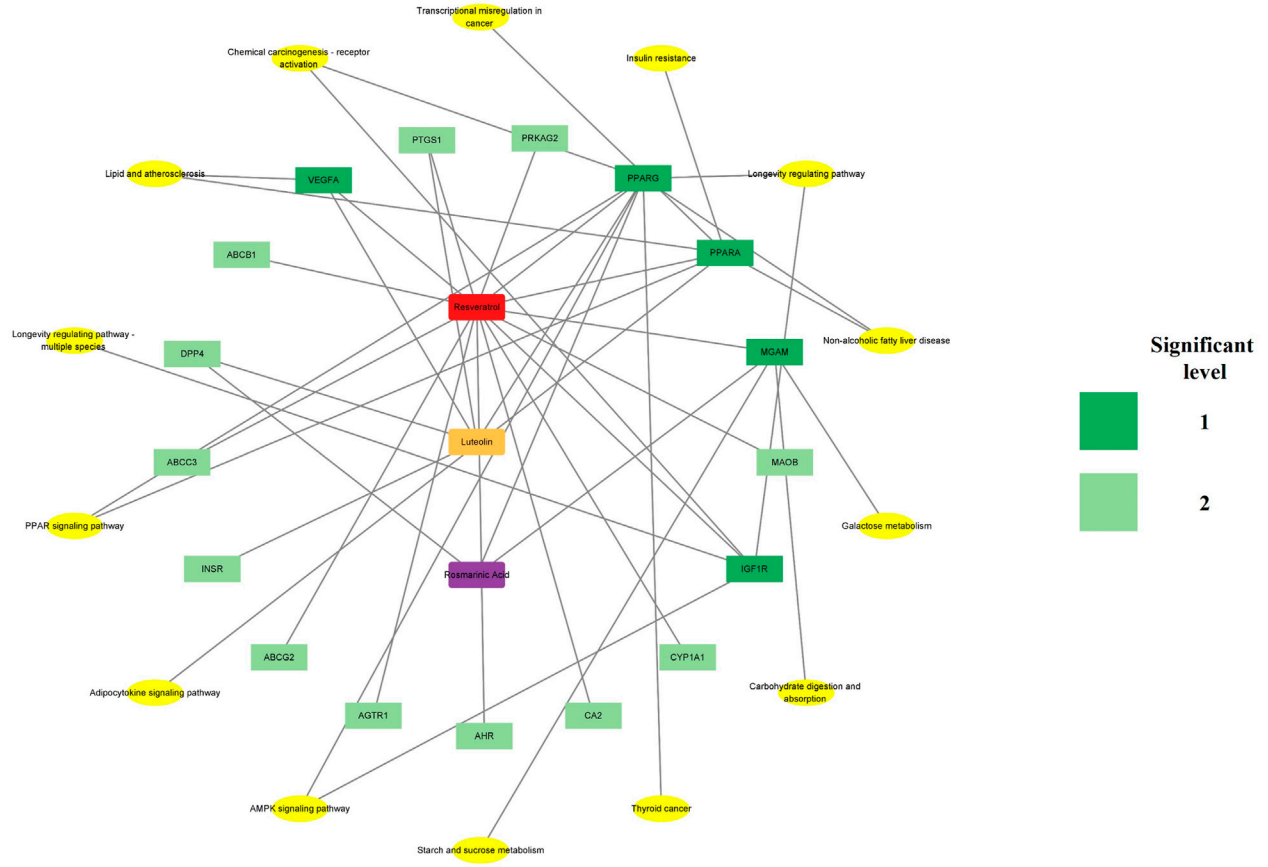


FIGURE 2
Metabolite–target–pathway network of rosmarinic acid (RA), luteolin (Lut), and resveratrol (RS) (RLR) showing the diabetic–hypoglycemic effects. The red, orange, and purple nodes represent RS, Lut, and RA, respectively. The dark and light green colors indicate the significance of the targets for the related core pathways, and the yellow nodes represent the pathways.

## 2.6 Network analysis of protein–protein interactions (PPIs) of the intersecting targets

The intersecting targets were imported into the STRING 11.0 platform and visualized using Cytoscape 3.9.1 software to construct the PPI network. The CytoHubba plugin was applied to analyze and obtain the top-10 hub genes ranked by degree value (Chin et al., 2014). The MCODE plugin was then used to analyze the most significant module and determine the top-10 hub targets ranked on the basis of the MCODE score in the module (Saito et al., 2012). The K-means clustering algorithm was used with the MCODE plugin, and the module with the highest score was considered to be the most significant module. Nodes with higher MCODE scores were assigned more significant statuses in the general PPI network.

## 2.7 GO and KEGG pathway enrichment analyses

The R packages "clusterProfiler," "org.Hs.eg.db," "ggplot2," and "DOSE" were used to perform gene ontology (GO) and Kyoto encyclopedia of genes and genomes (KEGG) pathway enrichment analyses, and the results were visually displayed using R 4.2.3 software. The statistical significance for the enrichment analysis was an adjusted p value ≤0.05. Three aspects of the GO analysis, namely, molecular function (MF), biological process (BP), and cellular component (CC), which were most significantly associated with the top-10 GO functional terms were selected in each field. Correspondingly, the KEGG pathway enrichment analysis was conducted to investigate the intersecting genes, and results were obtained for the top-20 pathways.

## 2.8 Molecular docking

All structures of the tested target proteins were first downloaded from the RCSB repository with PDB numbers (https://www.rcsb.org/), namely, α-amylase (5U3A; 4GQR), α-glucosidase (3TOP; 3L4Y), pancreatic lipase (1LPA), SGLT-2 (7VSI), AMPK (6C9F), glucokinase (3A0I), aldose reductase (1IEI), acetylcholinesterase (4BDT), acetylcholine M2 receptor (4MQT), GLP-1R (7C2E), DPP-IV (4N8D), and PPAR-γ (1WM0; 4CI5). The criteria for target selection were as follows: "*H. sapiens*" and "no mutation." The key residues used as constituents of the putative binding pockets were found from the corresponding literature in the RCSB

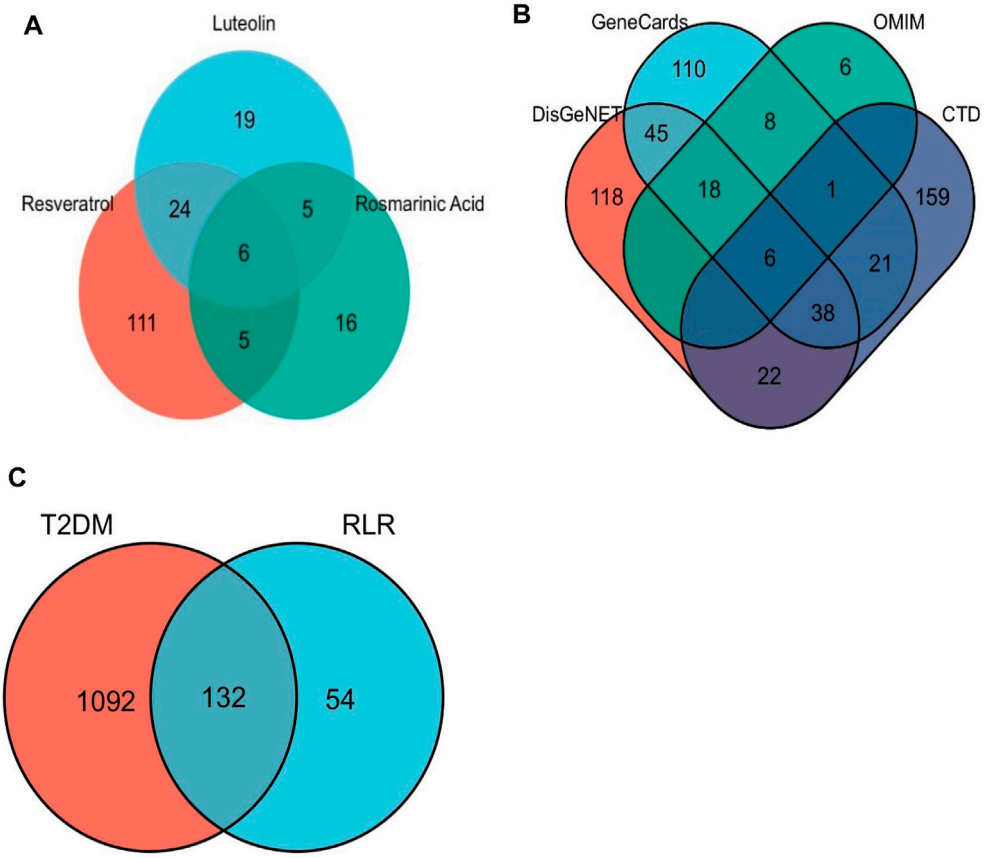


FIGURE 3
Venn diagrams of **(A)** rosmarinic acid, luteolin, and resveratrol (RLR) targets from TCMSP. **(B)** T2DM-related targets obtained from four databases. **(C)** Intersecting targets between T2DM and RLR.

repository based on PDB numbers. For each protein structure, the selected key residues were applied to constitute the putative binding pocket (Supplementary Table S1 footnotes).

Originally, the ligands and water molecules were removed from the protein crystal, to which hydrogen and the desired electric charge were added using Discovery Studio 2019. Next, the protein structures were subjected to energy minimization before docking. In the Simulation | Change Forcefield tools, CHARMM36 was one of the versions applied to minimize the energy. Second, the test chemicals (ligands) were sourced from PubChem (https://pubchem.ncbi.nlm.nih.gov/; RA (5281792), Lut (5280445), and RS (445154)) and were also charged with hydrogen atoms. Finally, molecular simulations were performed, whose results showed that the ligand was located inside the grid box of the receptor. The lowest binding energy (kcal/mol) was calculated using AutoDock Vina 1.2.0, and the 2D and 3D images were visualized and analyzed using Discovery Studio 2019.

## 2.9 α-Amylase activity assay

The α-amylase inhibitory evaluations of the selected metabolites (RA, Lut, and RS) were performed using the 3,5 dinitrosalicylic acid (DNSA) colorimetric assay (Chen T.-H. et al., 2021; Chen S.-P. et al., 2021). The α-amylase activity was quantified based on the reduction of sugars from the breakdown of starch, using DNSA dissolved in 2 M NaOH/5.3 M $Na^+$-$K^+$-tartaric acid, as previously described (Luyen et al., 2018). In brief, the substrate solution was prepared by dissolving starch (4 mg/mL) in 20 mM of phosphate-buffered saline (PBS 1×, pH 6.8). Approximately 50 µL of each sample solution (various concentrations in each of the test chemicals) and 100 µL of 16 unit/mL α-amylase were added to 1.5-mL Eppendorf tubes and incubated for 10 min. Next, 100 µL of the substrate solution was added to each mixture and incubated at 37°C for an additional 30 min. Finally, 50 µL of the DNS reagent was added to each mixture and boiled for 10 min. The optical densities of the samples were detected at 540 nm ($OD_{540}$) using the Infinite® M200 PRO multimode microplate reader (Tecan, Switzerland) with acarbose as the positive control.

## 2.10 Diet-induced diabetic model preparation

### 2.10.1 Animal care and diet-induced obesity induction

Sixty male ICR mice (6 weeks old) were obtained from Wu's Laboratory Animals (Fujian, China) and housed in controlled environmental conditions at room temperature (22°C ± 2°C) and humidity (50% ± 10%). A 12/12 h light/dark (6 a.m. to 6 p.m.) cycle

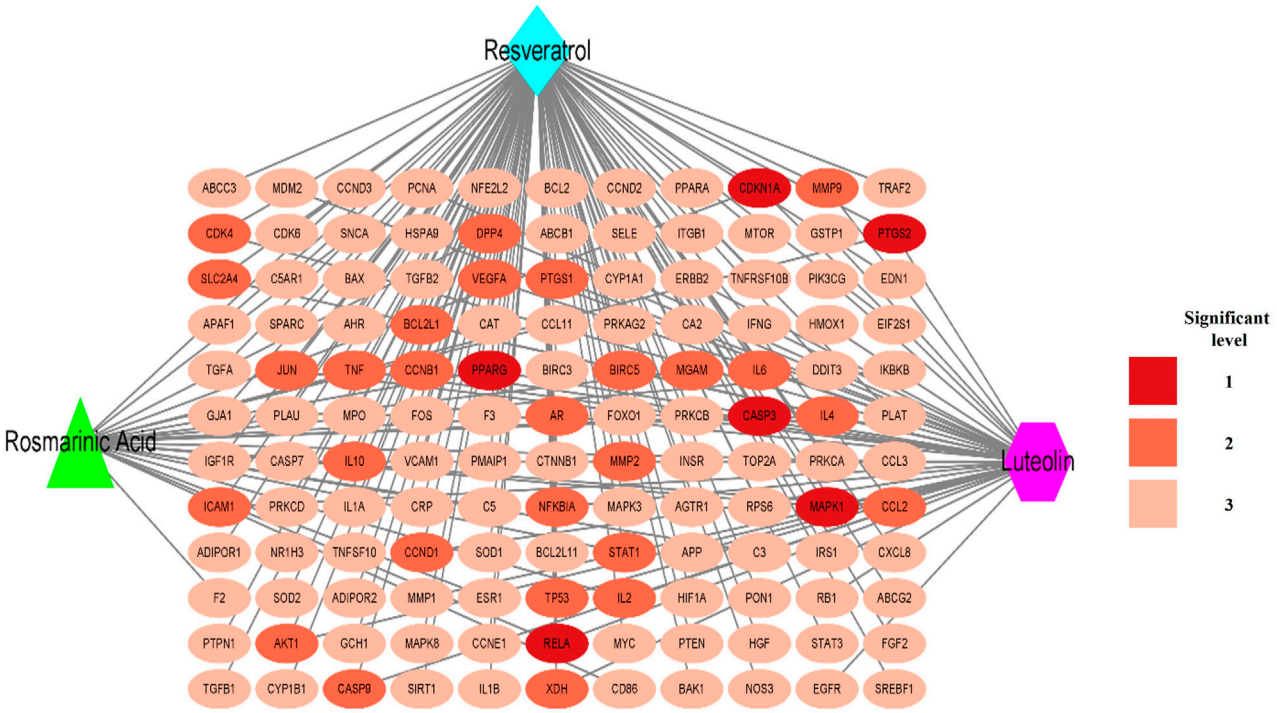


FIGURE 4
Establishment of the component–target–interaction network. The red elliptical nodes represent the intersecting targets, while the blue diamond, green triangle, and purple hexagon nodes represent rosmarinic acid, luteolin, and resveratrol (RLR), respectively. The connecting lines represent the interactions between the metabolites and targets.

was maintained throughout the study period. The mice had free access to food as well as tap water and were maintained on a standard laboratory diet (Rodent feed 1022, BEIJING HFK BIOSCIENCE Co., Ltd., Beijing, China). The animal experiments were approved by the Xiamen Medical College Animal Ethics Committee (SYXK, 2018-0010) and were conducted in accordance with the "Guide for the Care and Use of Laboratory Animals" of Xiamen Medical College.

### 2.10.2 Insulin intolerance test (IGT) and determination of diabetic mice

The protocols for the diet-induced obese (DIO) mice and glucose tolerance (GT) were followed as per our previous study (Huang et al., 2019a). First, DIO mice were fasted for 10 h prior to oral gavage of 4 g/kg bodyweight (Bwt) glucose solution. At the beginning of the test, the fasting blood glucose levels of the mice were measured from tail-vein samples using an Accu-Chek blood glucose analyzer (Hoffmann-La Roche AG, Basel, Switzerland).

### 2.10.3 OGTT

The OGTT of the diabetic mice were performed as per the procedures described in a previous report (Huang et al., 2019a), with slight modifications. For this test, a total of 48 DIO diabetic mice were divided into eight groups (n = 6) as control (water), positive control (125 mg/kg Bwt of metformin dissolved in water), Lut (12.5 mg/kg Bwt dissolved in edible oil), RA (66.0 mg/kg Bwt dissolved in edible oil), RS (91.0 mg/kg Bwt dissolved in edible oil), RLR mixture (RA: Lut: RS = 5:1:4; fasting blood glucose >7 mmol/L; 100 mg/kg Bwt), RLR-H (fasting blood glucose >10 mmol/L; 100 mg/kg Bwt), and insulin (0.2 U/kg intraperitoneally). Then, 4 g/kg Bwt of glucose solution (fresh preparation, dissolved in water) was provided during the test at various times (30, 60, 90, and 120 min). The blood glucose levels of the mice were lastly measured from tail-vein samples using a blood analyzer.

### 2.10.4 OSTT

For this test, a total of 24 DIO diabetic mice were divided into four groups (n = 6) as control (water only), positive control (10 mg/kg acarbose dissolved in water), RLR mixture (fasting blood glucose >7 mmol/L; 100 mg/kg Bwt), and RLR-H (fasting blood glucose >10 mmol/L; 100 mg/kg Bwt). The protocols for the OSTT were the same as those for OGTT but with three modifications: a) 3 g/kg Bwt of corn starch solution (fresh preparation, dissolved in water) was administered; b) the positive control used was acarbose (10 mg/kg); c) the test time was extended to 180 min. The blood glucose levels of the mice were again measured from tail-vein samples using a blood analyzer.

## 2.11 Statistical analysis

The data were expressed in terms of means ± SEM for the *in vivo* results and means ± SD for all other cases. Statistical comparisons of the results were conducted using one-way analysis of variance

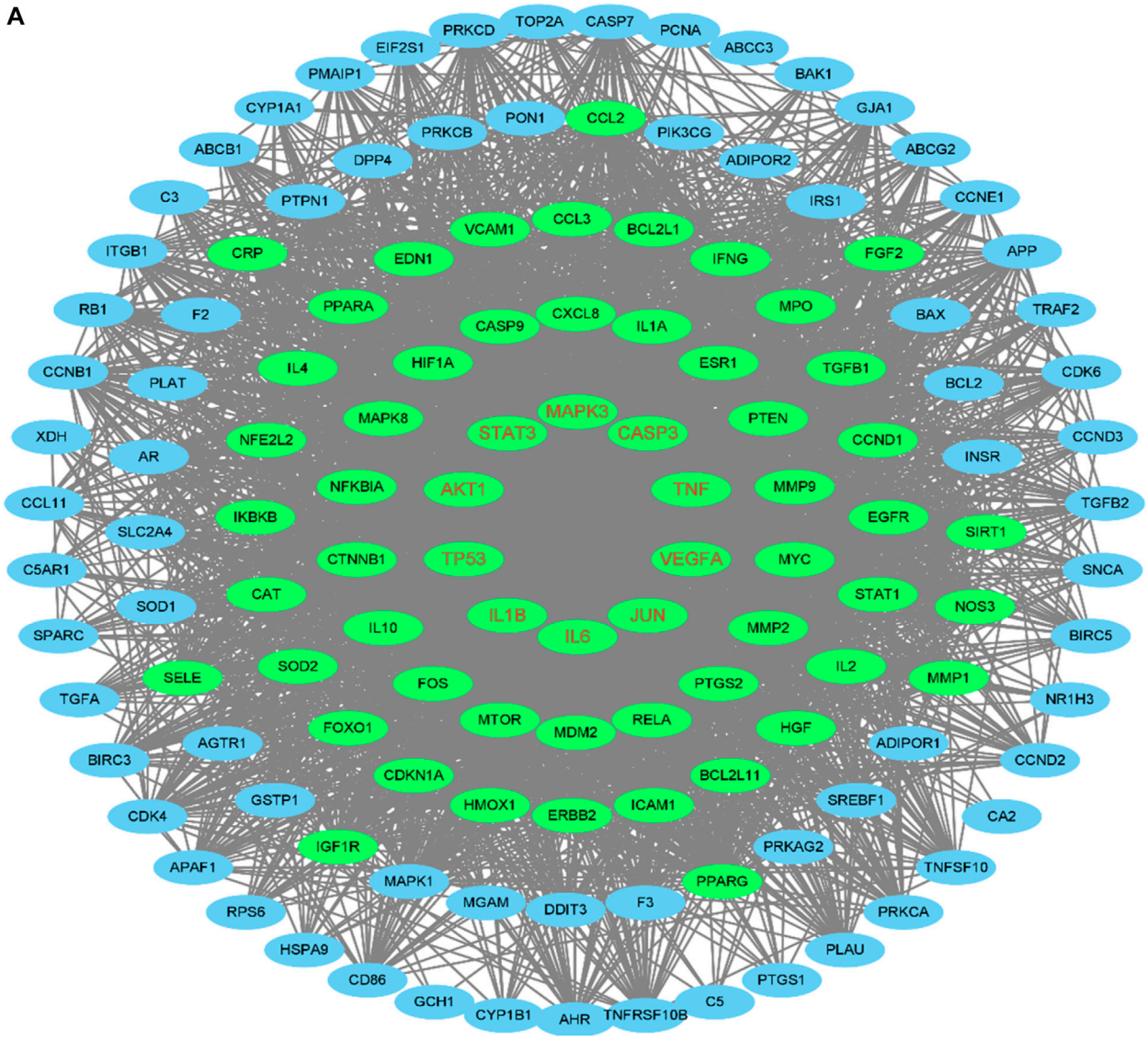


FIGURE 5
(Continued).

(ANOVA). The means in each column followed by different letters indicate the significant differences at $p < 0.05$ based on the *post hoc* Tukey's test.

# 3 Results

## 3.1 ADMET

The *in silico* ADMET profiling of metabolites characteristically illustrates the latent to be profitable interactions between the potential drug candidates with specific protein targets for successful drug discovery and development. In this study, the deviations of RA, Lut, and RS are all within acceptable ranges. It was found that two of the chemicals, Lut and RA, behaved as HOB+, while RS behaved as HOB-. Therefore, the drug candidates reflect this blood–brain barrier (BBB) crossing with a topological polar surface area (TPSA) values as follows: RS <60.7 $Å_2$; RA, Lut >90 $Å_2$. All of the WLogP values were also found to be less than 6 (Ishola et al., 2021). Thus, the three phytochemical candidates examined in this study (RA, Lut, and RS) can cause transversion of the BBB; however, two of the candidates exhibit carcinogenic properties. The BBB is essential for restricting in/outflux to the CNS microenvironment to ensure adequate neuronal function (Ishola et al., 2020). Although RA, Lut, and RS possess considerable binding affinities to the three antidiabetic protein targets, their significant BBB transversion could be employed to develop drugs against neurodegenerative diseases. Caco2 cells are widely used as a model of the intestinal epithelial cells exposed to the intestinal lumen, which is the location of action for pancreatic α-amylase and α-glucosidase (Lea, 2015). Furthermore, all three candidates are readily absorbed at the intestine and are negative. The accessibility of

10.3389/fphar.2024.1362150

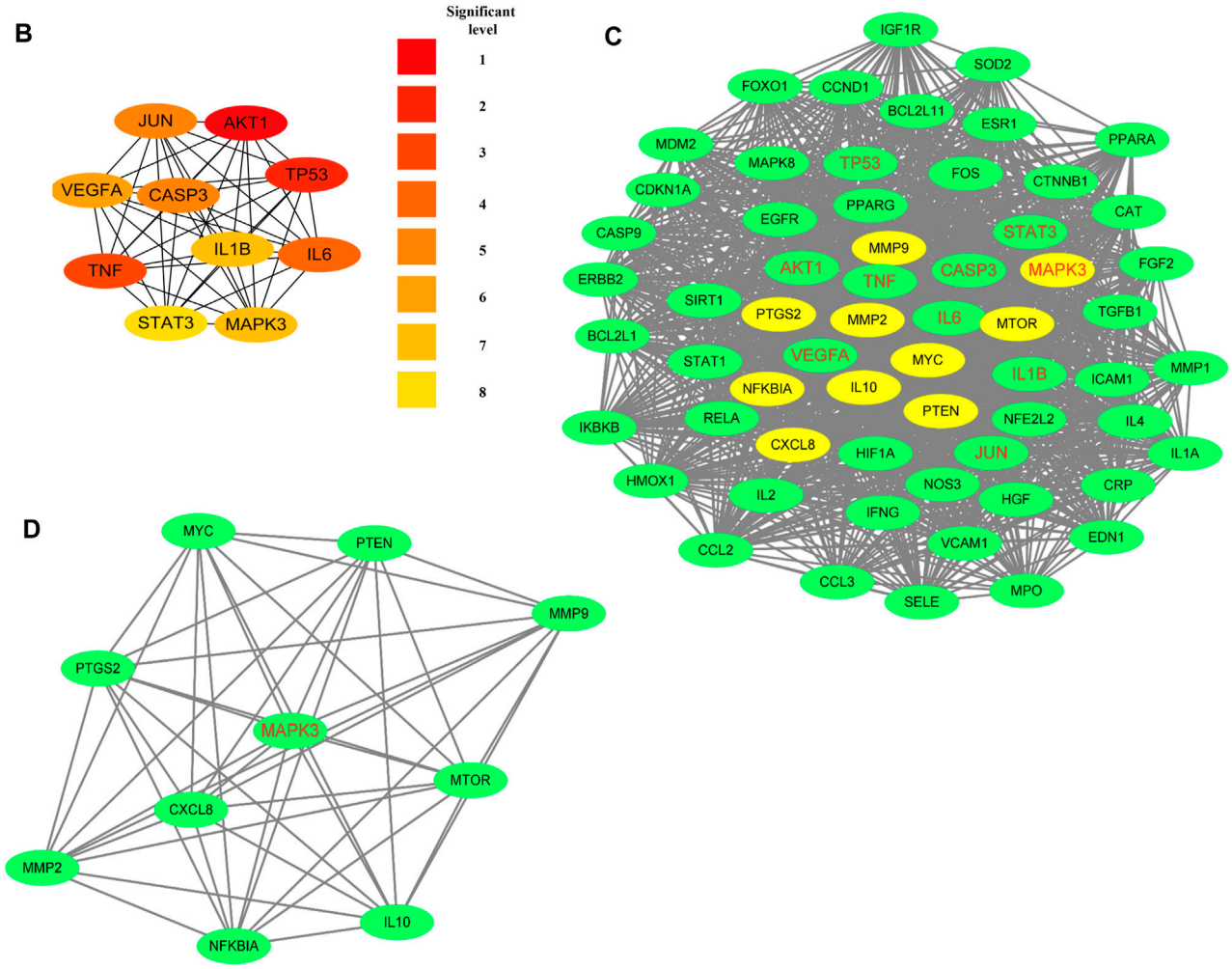


FIGURE 5
(Continued). PPI networks: nodes with red labels are the top-10 hub targets obtained using Cytohubba, and the green nodes represent the nodes in the most crucial module analyzed using MCODE. **(A)** PPI network of T2DM-related targets that can be treated by rosmarinic acid, luteolin, and resveratrol (RLR). **(B)** Top-10 hub targets screened using CytoHubba, where the darker node colors represent higher scores. **(C)** Analysis of the most significant module using MCODE, where the yellow nodes represent the top-10 hub targets ranked on the basis of the MCODE score. **(D)** Top-10 hub targets ranked by MCODE score.

a drug candidate through a membrane is determined by its Caco2 permeation, and this attribute is especially notable in the case of RA, Lut, and RS. These three phytochemicals as potential drug candidates therefore substantially pass the profiling tests (Table 1). We assessed the bioavailability and toxicity of the metabolites using Lipinski's rule-of-five and ADMET analysis, and the metabolites fulfil all the listed criteria, similar to the findings of a previous study (Sharma et al., 2020), suggesting their suitability for the development of potent antidiabetic drugs.

## 3.2 $IC_{50}$ and solubility

Based on a review of the half-maximal inhibitory concentrations ($IC_{50}$) from literature, the solubility and $IC_{50}$ (*in vitro* and *in vivo*) are determined for the various proteins of RA, Lut, and RS (Table 2). Based on the retrieved $IC_{50}$ and solubility values, the ratio of RA: Lut: RS is determined to be 5:1:4 for the subsequent experiments.

## 3.3 Acquisition of the targets of RLR, diabetic hyperglycemia, and T2DM

The screening results from the TCMSP provided 146 targets of RS, 54 of Lut, 32 of RA, and 186 targets in total (Figure 3A). There were 43 related targets of diabetic hyperglycemia, as screened from the DrugBank database. The screening of T2DM targets showed 937 from the CTD, 336 from GeneCards, 247 from DisGeNET, and 39 from OMIM (Figure 3B). Pathway annotations and component–target–interaction (CTI) network constructions were performed for the subsequent assays.

## 3.4 Metabolite–target–pathway network analysis between active targets of diabetic hyperglycemia and RLR

Cytoscape 3.9.1 was used to construct the PPI and CTI networks. Venn diagrams of the related targets were used for the PPI analysis as

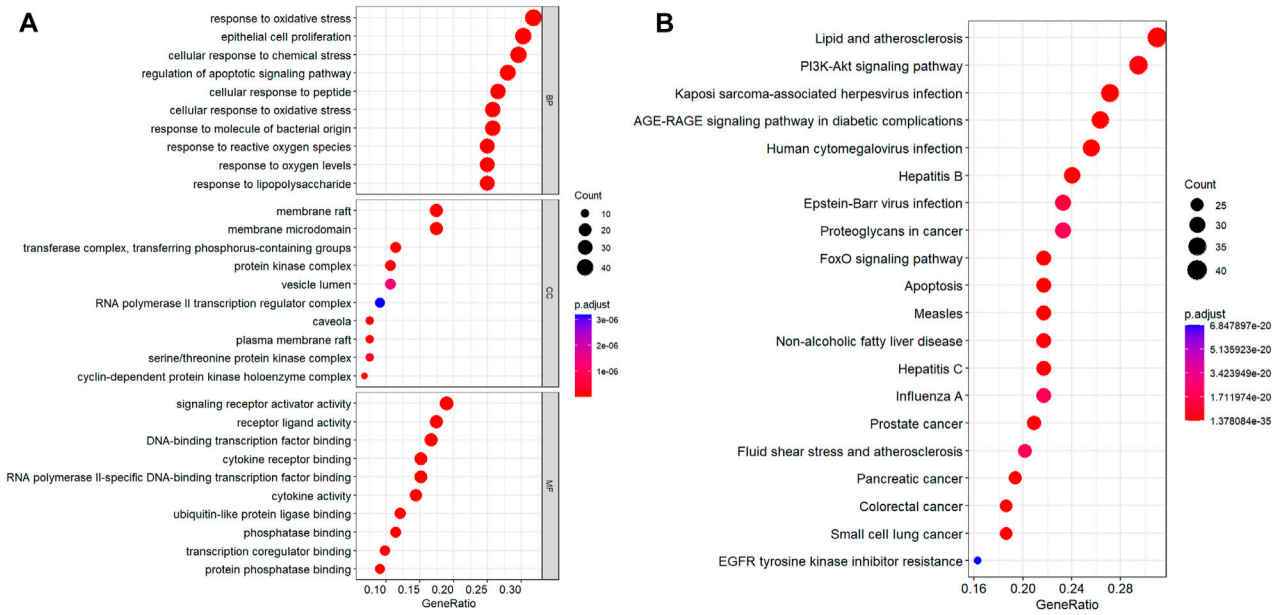


FIGURE 6
Color representations of the adjusted p scores and spot sizes indicating gene counts. **(A)** GO enrichment results of 132 intersecting targets, from which the top-10 GO functional terms were selected. **(B)** KEGG pathway enrichment results of 129 intersecting targets, from which the top-20 pathways were identified. (adjusted p ≤0.05).

well as GO and KEGG pathway enrichment analyses (Figure 1A). The PPI network comprised 13 nodes and 25 edges. The top-5 hub targets in Cytohubba ranked by degree value were PPARG, ABCG2, CYP1A1, PPARA, and DPP4. The top-5 hub targets ranked by MCODE score were PPARA, MGAM, ABCC3, CYP1A1, and DPP4. The PPI results showed that PPARA and DPP4 were critical genes based on the two algorithms (Figures 1B, C). The KEGG and GO enrichment analyses showed that the core signaling pathway was the PPAR signaling pathway (Figures 1D, E). To identify the relationship between RLR and diabetic hyperglycemia, a metabolite–target–pathway network diagram was constructed using the results of the above analyses (Figure 2).

## 3.5 Intersection between RLR- and T2DM-related targets

A Venn diagram was used to obtain 132 intersecting targets between RLR and T2DM, as shown in Figure 3C. Accordingly, all three candidates (RA, Lut, and RS) have good links with the T2DM targets.

## 3.6 Establishment and analysis of CTI network between RLR and intersecting targets

The CTI network (Cytoscape 3.9.1) encompasses 135 nodes and 171 edges. As shown in Figure 4, all three components (RLR) had broad interactions with the corresponding targets of T2DM that are treatable by RLR. RS had 104, Lut had 44, and RA had 23 interactions with the intersecting targets. The degree values of the intersecting targets range from 1 to 3 with a red-colored gradient. According to the CTI results, PPARG, CDKN1A, PTGS2, CASP3, MAPK1, and RELA had interactions with the three components (RLR).

## 3.7 Prediction of RLR hub targets using PPI network of the intersecting targets

The PPI network comprised 132 nodes and 3140 edges (Figure 5A). The top-10 hub targets in Cytohubba ranked by degree value were AKT1, TP53, TNF, IL6, CASP3, JUN, VEGFA, IL1B, MAPK3, and STAT3 (Figure 5B). The most significant cluster with a score of 49.97 contained 61 nodes and 1499 edges, as obtained from MCODE analysis (Figure 5C). The top-10 hub targets ranked by MCODE score were NFKBIA, IL10, CXCL8, MMP9, MMP2, PTGS2, MAPK3, MYC, MTOR, and PTEN (Figure 5D). Remarkably, MAPK3 was found to be a critical gene under both methods.

## 3.8 Prediction of RLR molecular mechanism via GO and KEGG pathway enrichment analyses

A total of 132 intersecting targets were analyzed by GO enrichment, and the results comprised 2584 BPs, 50 CCs, and 201 MFs obtained using R studio (Figure 6A). When sorted by the degree of significance, the top-3 BPs were responses to oxidative stress, epithelial cell proliferations, and cellular responses to chemical stress; the top-3 CCs were membrane rafts, membrane microdomains, and transferase complexes transferring phosphorus-containing groups; the top-3 MFs were signaling receptor activator

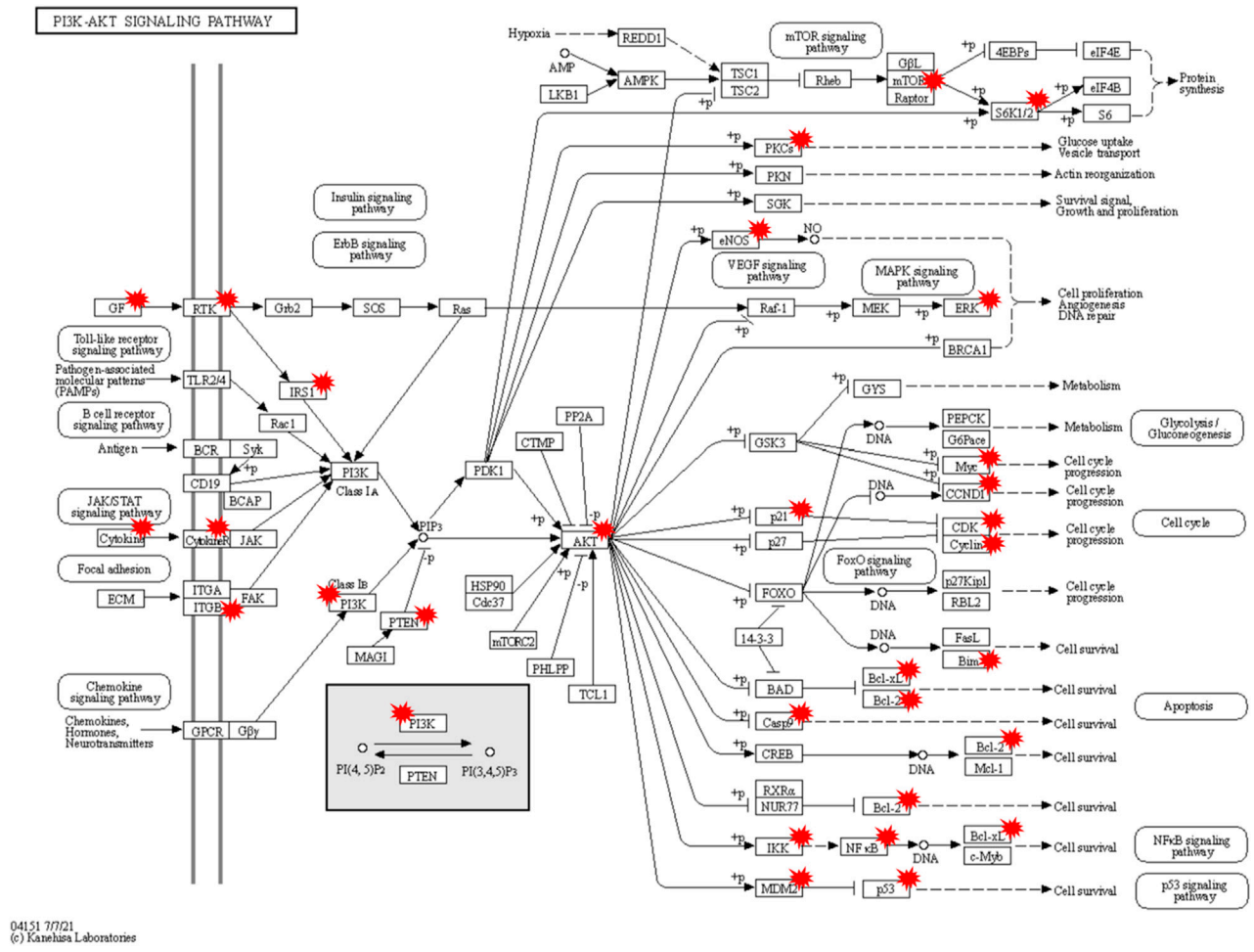


FIGURE 7
Potential molecular mechanisms of rosmarinic acid, luteolin, and resveratrol (RLR) in T2DM treatment via regulation of the PI3K-AKT signaling pathway. The targets with red markers can be treated by RLR.

activity, receptor ligand activity, and DNA-binding transcription factor binding. Furthermore, 129 KEGG enrichment pathways related to T2DM were obtained, of which the top-30 signaling pathways of significance were selected for visual presentation (Figure 6B). Among the enriched pathways, the PI3K-AKT signaling pathway has great significance in T2DM treatment, and RLR acted on multiple targets of the PI3K-AKT signaling pathway, as shown in Figure 7.

## 3.9 *In silico* docking

Nowadays, the application of computational techniques offers several advantages in rationalizing the route toward the discovery of novel drugs or identification of the biological properties of compounds (both natural and synthetic origins) for use in the treatment or supplementation of several diseases (Gelmini et al., 2018; Grande et al., 2021). In particular, molecular docking allows fitting a ligand to a binding site by combining and optimizing the steric, hydrophobic, and electrostatic complementarity variables. Furthermore, one of the main goals of molecular docking is the identification of the most energetically favorable conformation of a ligand at the binding site of the target molecule (the more negative binding energy is the better ligand–target stability). An absolute value greater than 4.25 indicates certain binding activity, a value exceeding 5.0 indicates good binding activity, and a value exceeding 7.0 indicates strong binding activity (Hsin et al., 2013). To clarify the intermolecular affinity between the metabolites (RA, Lut, and RS) and specific targets, molecular docking simulations were performed. The docking analysis revealed that twelve therapeutic molecular targets, namely, α-amylase, α-glucosidase, pancreatic lipase, SGLT-2, AMPK, glucokinase, aldose reductase, acetylcholinesterase, acetylcholine M2 receptor, GLP-1R, DPP-IV, and PPAR-γ, showed good binding affinities and better binding modes (as shown in Supplementary Figure S1 of the Supplementary Material).

Supplementary Table S1 and Figure 8A show the targets controlling starch digestion. The α-amylase (PDB: 5U3A) modeling results revealed that RA formed H-bonds with ARG195, GLU233, and HIS201; Lut formed H-bonds with GLN63, ASP197, and GLU233; and RS formed H-bonds with ASP197. The reference drug acarbose is a catalytic inhibitor that formed H-bonds with

10.3389/fphar.2024.1362150

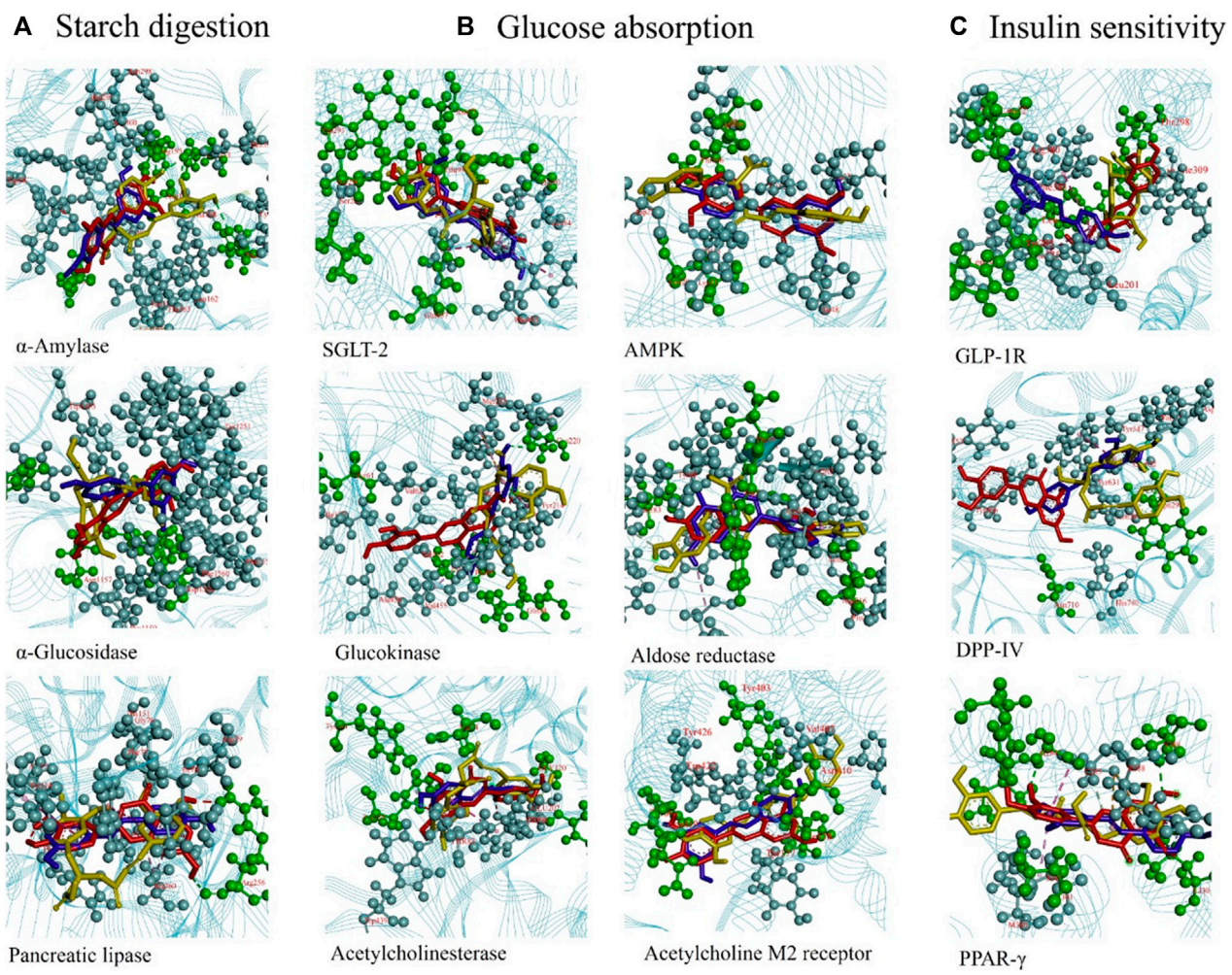


FIGURE 8
**(A)** Rosmarinic acid (RA), luteolin (Lut), and resveratrol (RS) binding with the diabetes-related proteins α-amylase, α-glucosidase, and pancreatic lipase to control starch digestion. **(B)** Lut, RA, and RS binding with proteins SGLT-2, AMPK, glucokinase, aldose reductase, acetylcholinesterase, and acetylcholine M2 receptor to mediate glucose absorption. **(C)** Lut, RA, and RS binding with proteins GLP-1R, DPP-IV, and PPAR-γ to regulate insulin sensitivity. RA: yellow; Lut: red; RS: blue.

GLU233, HIS201, TRP58, and THR163. For α-glucosidase (PDB: 3TOP), RA had H-bonds with ASP1526, TRP1369, ARG1510, and ASP1420; Lut had H-bonds with ASP1526; and RS had H-bonds with ASP1526. The H-bond interactions of RA and RS against α-glucosidase occur at the same amino acid residue (ASP1526). When comparing the binding affinities of five standard inhibitor drugs (acarbose, miglitol, voglibose, emiglitate. and 1-deoxynojirimycin) with three ligands (RA, Lut, RS) of α-glucosidase, Lut possessed the best binding affinity (−9.3 kcal/mol) out of the five standard inhibitor drugs. When compared with acarbose as the reference drug, the binding affinities of RA, Lut, and RS on α-amylase and α-glucosidase were higher (Lut > RA > RS > Acarbose), suggesting that they can be used as competitive inhibitors. For pancreatic lipase (PDB: 1GPL), RA did not form any H-bonds with amino acid residues, while Lut formed H-bonds with ARG256 and RS formed H-bonds with ARG256.

The targets involved in the mediation of glucose absorption are illustrated in Supplementary Table S1 and Figure 8B. For the sodium-dependent glucose transporter 2 (SGLT-2) (PDB:7VSI), RA formed H-bonds with ASN75, HIS80, GLU99, TYP290, TYP291, and GLN457; Lut formed H-bonds with SER286; and RS formed H-bonds with ASN75. For adenosine 5'-monophosphate (AMP)-activated protein kinase (AMPK; PDB: 6C9F), RA formed H-bonds with THR106 and ASP108; Lut formed H-bonds with LEU20; and RS did not form any H-bonds. For glucokinase (PDB: 3A0I), RA formed H-bonds with GLN98; Lut formed H-bonds with TYR61; and RS formed H-bonds with CYS220, GLN98, and LEU451 amino acid residues. For aldose reductase (PDB: 1IEI), RA formed H-bonds with SER210, TRP20, and THR19; Lut formed H-bonds with ASP216 and GLN183; and RS formed H-bonds with GLN183 amino acid residue. For acetylcholinesterase (PDB: 4BDT), RA formed H-bonds with TYR337, ASP74, THR283, GLY120, and TYR133; Lut formed H-bonds with TYR341 and ASP74; and RS formed H-bonds with GLY120 and TYR341. For acetylcholine M2 receptor (PDB: 4MQT), RA did not form any H-bonds; Lut formed H-bonds with TYR80, ASN419, and ASN410; and RS formed H-bonds with LEU98 amino acid residue.

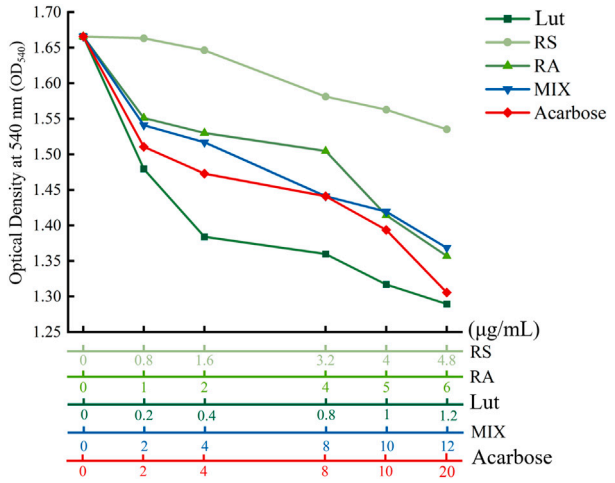


FIGURE 9
Inhibitory profiles of rosmarinic acid (RA), luteolin (Lut), resveratrol (RS), RLR mixture (MIX), and acarbose on α-amylase activity.

The targets involved in the regulation of insulin sensitivity are presented in Supplementary Table S1 and Figure 8C. The modeling results of the glucagon-like peptide-1 receptor (GLP-1R; PDB: 7C2E) revealed that RA formed H-bonds with ARG310 and THR298; Lut formed H-bonds with ARG310, LEU384, and THR298; and RS formed H-bonds with LEU32 and TYR298 amino acid residues. For dipeptidyl peptidase-4 (DPP-IV; PDB: 4N8D), RA formed H-bonds with ASP545, VAL546, TRP629, and TYR631; Lut formed H-bonds with TYP631 and ASN710; and RS formed H-bonds with TRP629 and VAL546 amino acid residues. For PPAR-γ (PDB: 1WM0), RA formed H-bonds with SER289, SER342, and GLY284; Lut formed H-bonds with HIS266, ILE281, and SER289; and RS formed H-bonds with LEU330. The 2D- and 3D-binding features of α-amylase, α-glucosidase, pancreatic lipase, SGLT-2, AMPK, glucokinase, aldose reductase, acetylcholinesterase, acetylcholine M2 receptor, GLP-1R, DPP-IV, and PPAR-γ are also shown for Lut (Supplementary Figure S2), RA (Supplementary Figure S3), and RS (Supplementary Figure S4). The grid box coordinates for the specific proteins are presented in Supplementary Table S2 of the Supplementary Material.

## 3.10 *In vitro* enzymatic measurement of α-amylase activity

To corroborate the *in vivo* observations, RA, RS, Lut, acarbose, and RLR were tested as the metabolites to measure the alteration of α-amylase activity for understanding the suppressive effects of the RLR mixture on α-amylase activity. The inhibitory patterns of α-amylase activity are shown in Figure 9. Compared to the untreated control, the inhibition of α-amylase activities by RA, RS, Lut, acarbose, and RLR revealed different patterns depending on the concentration used. Furthermore, compared with the reference drug acarbose (a widely prescribed α-glucosidase and α-amylase inhibitor in the clinic), the inhibitory concentration of α-amylase activity for an RLR mixture of 12 μg/mL was equivalent to that of 13.7 μg/mL of acarbose. Additionally, the inhibitory profiles of RA, Lut, and RS on α-amylase activity are associated with the binding ranks of the docking results (kcal/mol) (Supplementary Table S1). This experiment suggests that the RLR mixture possesses an appropriate inhibitory potential for α-amylase activity. It is noted that α-amylase and α-glucosidase are important therapeutic targets for the management of T2DM; the inhibition of these enzymes can result in decrease of postprandial hyperglycemia. This evidence provides an opportunity for a food-based strategy to modulate starch breakdown to glucose, which could contribute to the management of hyperglycemia- and diabetes-related complications.

## 3.11 OSTT

To investigate the effect of the RLR mixture for starch digestion, two fasting blood glucose levels (RLR, RLR-H) and acarbose were evaluated via the OSTT to determine the inhibitory efficacy. Acarbose was used as the positive control. Compared to the untreated group, the RLR, RLR-H, and acarbose groups showed good trends for reducing blood glucose levels with time, particularly the acarbose group (Figure 10A, 10B). Interestingly, the suppressive efficacy on blood glucose for fasting blood glucose >7 mmol/L in RLR group was similar to that for fasting blood glucose >10 mmol/L in RLR-H group. Moreover, the results showed that the efficacy of the RLR mixture (100 mg/kg) was equipotent to 48.5% of acarbose (10 mg/kg). The blood glucose levels in the OSTT after administering, the RLR mixture demonstrate maximal responses regardless of the fasting blood glucose levels.

## 3.12 OGTT

The OSTT findings revealed that the RLR mixture significantly inhibited starch digestion. To further understand the hypoglycemic efficacies, RA, Lut, RS, RLR, RLR-H, metformin, and insulin were evaluated via the OGTT. The experimental data indicated that RLR and metformin had similar trends for reducing postprandial blood glucose levels compared to the untreated control. Compared to the reference drug metformin, the impact of RLR was generally equipotent to 78.5% of metformin (125 mg/kg Bwt) (Figures 10C, D). Interestingly, the results illustrated that the RLR mixture lowered blood glucose levels without causing hypoglycemia, implying that this phytomixture would be a good fit for antidiabetes. Here, the abilities of RA, Lut, and RS to bind effectively with the twelve protein targets (α-amylase, α-glucosidase, pancreatic lipase, SGLT-2, AMPK, glucokinase, aldose reductase, acetylcholinesterase, acetylcholine M2 receptor, GLP-1R, DPP-IV, and PPAR-γ) could be pivotal in the treatment of T2DM, in addition to the link capabilities of the metabolites to interact more strongly than the standard drugs with the individual receptors.

# 4 Discussion

This study presents proof-of-concept evaluations for the use of network pharmacology studies and multitarget *in silico*

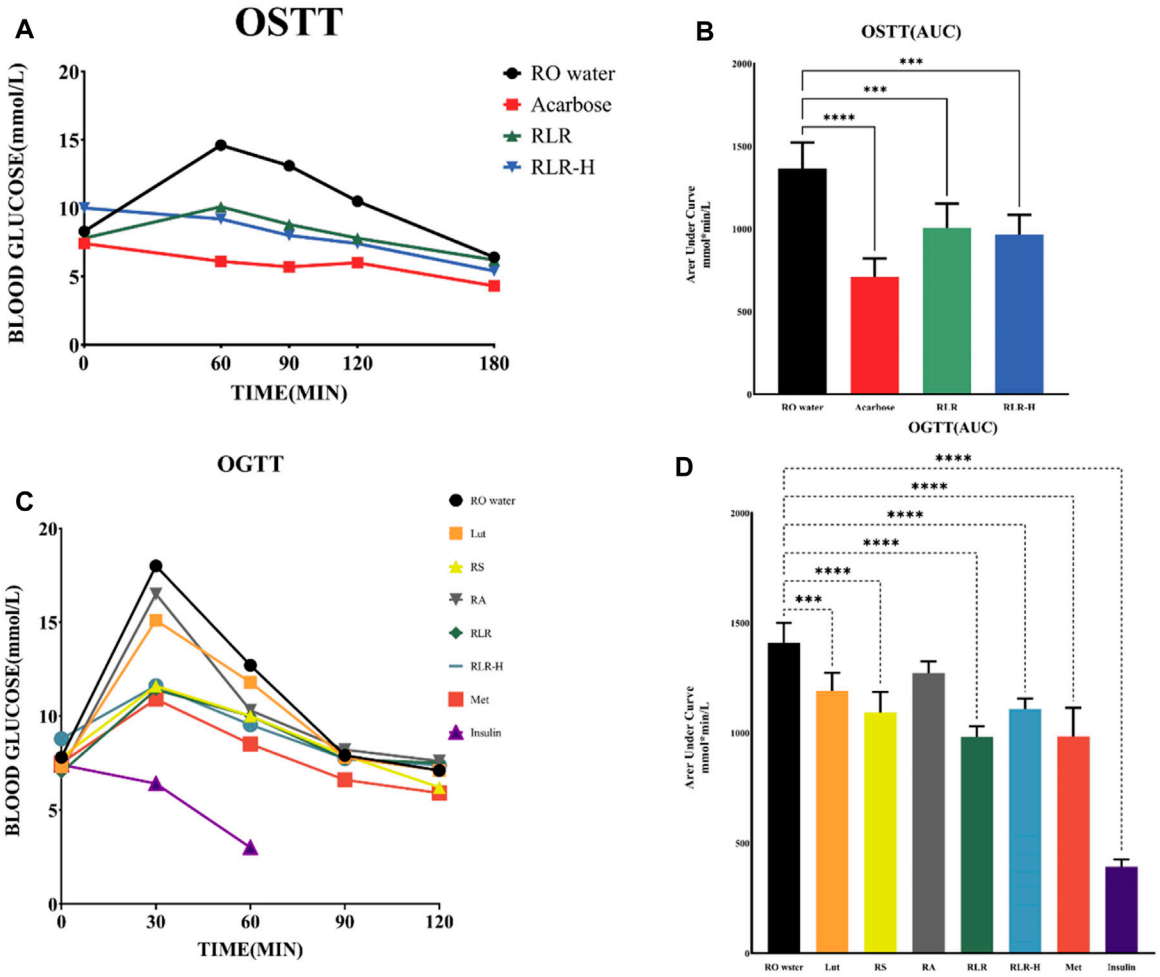


FIGURE 10
Alteration of blood glucose levels in treatments using rosmarinic acid, luteolin, and resveratrol (RLR) mixture: **(A,B)** oral starch tolerance test (OSTT) and **(C,D)** oral glucose tolerance test (OGTT). Acarbose: 10 mg/kg, Lut: 6.5 mg/kg bodyweight (Bwt), RS: 88 mg/kg Bwt, RA: 50.5 mg/kg Bwt, RLR: 100 mg/kg Bwt, metformin (Met): 125 mg/kg, insulin: 0.2 U/mL. ***$p < 0.001$; ****$p < 0.0001$ compared with the control.

screening to reveal that the RLR mixture has proven hypoglycemic effects. Notably, by reevaluating the blood glucose lowering efficacy of the RLR mixture along with *in vitro* and *in vivo* (OSTT and OGTT) validations for the combined metabolites, this study demonstrates that the mixture has satisfactory performance against diabetes. RA, Lut, and RS are all hydrophobic and water-insoluble natural polyphenolic compounds that frequently show low bioavailability, poor systemic delivery, and low efficacy. Generally, the poor water solubility, rapid decomposition, and short serum half-life (low stability) significantly limit their potential in pharmacological applications, particularly in the treatment of DM. Given these defects, several reports have focused on nanoparticle coatings (Imam et al., 2022), metabolite-based nanodrug delivery (Intagliata et al., 2019; Taghipour et al., 2019; Saleem et al., 2022), and chemical modifications like derivative production to enhance the bioavailability when using natural products. Nonetheless, this process usually takes a long time; therefore, developing combinations with other metabolites in the same solubility range while preventing toxicity can help to meet the treatment goals. It is well known that DM is a complex disease involving the alterations of multiple signaling pathways and that hypoglycemic induction is the preferred treatment for diabetes (Niu et al., 2022). To determine the potential antihyperglycemic mechanisms of RLR, a metabolite–target–pathway network was constructed and five candidate target proteins (PPAR, MGAM, DPP4, VEGFA, and IGF1R) were identified. Despite the widespread pharmacological activities of RA, Lut, and RS, particularly in a mixture, we performed molecular dynamics (MD) simulations on the top-3 complexes identified via network analysis and molecular docking to confirm the lowest binding affinity of metabolite–target interactions. Additionally, the synergistic effects of the RLR mixture are under consideration for exploration in a future study. The ligand–protein interactions and molecular mechanism of the signal pathway via Western blot analysis are also under investigation for understanding the pharmacological value of the mixture in preclinical tests.

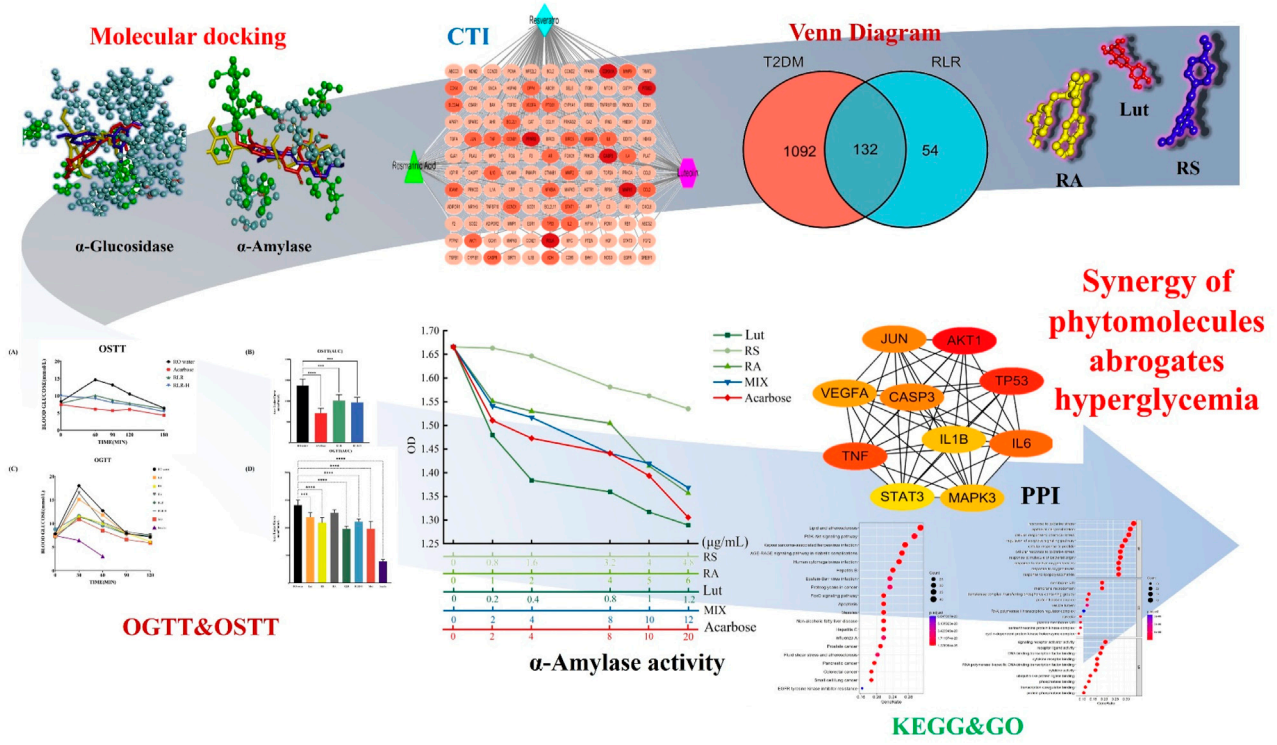


FIGURE 11
Schematic illustration depicting the synergy of rosmarinic acid (RA), luteolin (Lut), and resveratrol (RS) in the abrogation of hyperglycemia.

## 4.1 Antihyperglycemic effects of RA, Lut, and RS via suppression of digestive enzymes

Given the high prevalence of T2DM, various therapeutic approaches have been attempted for its management, including inhibition of key enzymes such as α-glucosidase and α-amylase. Starch is absorbed by the hydrolytic action of α-amylase, followed by the action of the intestinal α-glucosidase enzyme. Consequently, α-amylase inhibitors that modulate blood glucose levels after meals may be considered effective chemotherapeutic tools to treat diabetes. α-Glucosidase is a carbohydrate-hydrolyzing enzyme secreted by the intestinal chorionic epithelium; the inhibition of this enzyme promotes delayed carbohydrate digestion, thereby preventing excessive glucose absorption (You et al., 2012). Currently, α-glucosidase inhibitors, such as acarbose and nojirimycin, are successfully used to control the glucose levels of diabetic patients. Acarbose has been reported to cause several undesirable side effects, such as abdominal pain, flatulence, and diarrhea (Israili, 2011). The usefulness of many synthetic antidiabetic agents is constrained by their side effects and limited effectiveness. The main advantages of using natural metabolites as alternatives to prescription hypoglycemic drugs include fewer side effects, easy availability, presence of numerous bioactive compounds, and possible multiple protein targets in a single compound that can lower blood glucose levels (Pereira et al., 2019). α-Amylase and α-glucosidase are important therapeutic targets for the management of T2DM; the inhibition of these enzymes through phytochemicals such as RA can reduce postprandial hyperglycemia (Tolmie et al., 2021). RA has been shown to have α-glucosidase inhibitory activity ($IC_{50}$ of 0.23 ± 0.01 mg/mL) (Zhu et al., 2014). The $IC_{50}$ value for Lut is 339.4 ± 16.3 μM against α-glucosidase activity (Zhang et al., 2017). RS having an $IC_{50}$ value of 47.93 ± 5.21 μM has been observed to have a weaker effect on α-amylase than the effect of acarbose (4.60 ± 1.26 μM); however, RS has been found a significant effect on the inhibition of α-glucosidase (32.23 ± 0.56 μM). The $IC_{50}$ value of RS (5.64 ± 0.01 μM) compared to that of Diprotin A (7.21 ± 0.02 μM) indicates that RS may have significantly inhibitory effects on the DPP-IV enzyme (Khalid et al., 2022). The RLR mixture showed good inhibition of α-amylase activity in the present work (Figure 10), revealing the antihyperglycemic potential of this combination.

## 4.2 Antihyperglycemic effects of RA, Lut, and RS

RA is a secondary metabolite and polyphenol that demonstrates antioxidant, anti-inflammatory, anticancer, immunomodulatory, neuroprotective, and other beneficial effects on insulin sensitization and skin afflictions (Alagawany et al., 2017). Lut can work against α-amylase and α-glucosidase proteins by inhibiting starch and digesting disaccharides into glucose (Christian and Nagar, 2021; Jugran et al., 2021). Many preclinical reports reveal that Lut has excellent antioxidant, anticancer, neuroprotective, cardioprotective, and anti-inflammatory effects, and various clinical trials have been designed to investigate its therapeutic potential in humans (Taheri et al., 2021).

RS is a member of the stilbene family and a well-known polyphenolic metabolite found in grapes, apples, blueberries, mulberries, peanuts, pistachios, plums, and red wine; it has been found to potentially exhibit antitumor, antiangiogenic, antidiabetic, antiaging, glucose metabolism, antiobesity, immunomodulatory, and cardioprotective activities, in addition to being an antioxidant (Zhang L.-X. et al., 2021). Although there are various *in vitro* and *in vivo* studies illustrating the effectiveness of RS in DM, many clinical trials show that RS has latent benefits in DM patients (Öztürk et al., 2017). RS may improve insulin resistance, lower fasting blood glucose and insulin levels, and attenuate oxidative stress in patients with T2DM (Zhang T. et al., 2021). RS also protects the pancreatic β-cells, increases insulin secretion and glucose homeostasis, decreases insulin resistance, and ameliorates metabolic disorders (Szkudelski and Szkudelska, 2015). A systematic review and meta-analysis has demonstrated that RS has a statistically significant dose–response effect on blood glucose, glycated hemoglobin/hemoglobin (HbA1c), and insulin levels; however, there is insufficient scientific evidence to propose a therapeutic dose in human subjects (García-Martínez et al., 2022). The most potent DPP-IV inhibitors have been found to be RS, Lut, apigenin, and flavones that exhibit hypoglycemic activities at nanomolar concentrations (Singla et al., 2019). Our previous works have demonstrated the antihyperglycemic effects of botanical drugs, plant sources, and natural products based on *in silico* docking relevant to antidiabetic target proteins (α-amylase, α-glucosidase, AMPK, PPAR-γ, DPP-IV, and GLP-1R), which have been further validated by *in vitro* assays and diabetic mice tests (Huang et al., 2019b; Chen T.-H. et al., 2021; Chen S.-P. et al., 2021). In this study, RA, Lut, and RS were found to dock with more clinically therapeutic targets (Supplementary Table S1; Figure 8), suggesting that RLR could be a latent candidate for antihyperglycemic nutraceuticals.

## 4.3 Signal pathways in the antihyperglycemic effects of RA, Lut, and RS

Mitochondrial biogenesis dysfunction has been associated with metabolic disorders, such as obesity and T2DM. A decline in the PGC-1α/AMPK/SIRT-1 signaling pathway seems to be the underlying mechanism for reduced mitochondrial biogenesis in diabetes. The proliferator-activated receptor gamma coactivator-1α (PGC-1α) protein is regulated by two enzymes, namely, AMPK and silent information regulator 1 (SIRT1), which are important in mitochondrial biogenesis.

The current study shows the effects of RA as a regulatory glucose homeostasis agent to increase muscle glucose uptake and AMPK phosphorylation as the targeted approach for combating insulin resistance (Vlavcheski et al., 2017). RA can reduce hyperglycemia and ameliorate insulin sensitivity by decreasing PEPCK expression and increasing GLUT4 expression for glucose uptake (Runtuwene et al., 2016). The levels of blood glucose, HbA1c, advanced glycation end products (AGE), TNF-α, IL-1β, IL-6, NO, p-JNK, P38MAPK, and NF-κB are significantly reduced with concomitant elevation in the plasma insulin level for oral administration of RA (100 mg/kg Bwt) in diabetic rats (Govindaraj and Sorimuthu Pillai, 2015). Supplementation with RA increases the expressions of the mitochondrial biogenesis genes like PGC-1α, SIRT1, and TFAM through activation of AMPK in the skeletal muscles of rats with insulin resistance as well as in L6 myotubes. Furthermore, RA treatment increases glucose uptake and decreases the phosphorylation of serine IRS-1 while increasing the translocation of GLUT 4 (Jayanthy et al., 2017).

Lut prevents the expression of the transcription factor FOXO1 (Christian and Nagar, 2021); when the FOXO1 transcript is blocked, gluconeogenesis is inhibited through the PI3K-AKT pathway (Christian and Nagar, 2021). Recently, Lut has been shown to inhibit DPP-IV, thus prolonging insulin activity by increasing GLP-1 (Singla et al., 2019). In addition, Lut improves glucose intolerance and reduces the expression of gluconeogenesis-associated enzymes in a liver X receptor (LXR) α-dependent manner (Park et al., 2020). The protective effects of RS include regulation of multiple signaling pathways, such as inhibition of oxidative stress and inflammation, enhancement of insulin sensitivity, induction of autophagy, regulation of lipid metabolism, promotion of GLUT4 expression and translocation, and activation of the SIRT1/AMPK signaling axis (Su et al., 2022). RS treatment significantly decreases the levels of proinflammatory cytokines, HbA1c, IL-6, TNF-α, and IL-1β in diabetes in the elderly (Ma and Zhang, 2022). Previous research has shown that RS could relieve insulin resistance through the Sirt1-p-AMPK-p-AKT and Sirt1-p-IRS-1-p-AKT pathways in adipocytes (Chen et al., 2018), thereby promoting glucose uptake through increased membrane accumulation of Glut4.

For the RLR mixture (100 mg/kg Bwt; RA: Lut: RS = 5:1:4), *in vivo* experiments (Figures 10A, B) have shown the potential to relieve insulin resistance by suppressing starch digestion, stimulating metabolism (glucose uptake, absorption, and utilization), and activating insulin sensitivity. Based on literature, it is clear that dietary metabolites can impede diabetic diseases by 1) blocking oxidative stress-inhibiting inflammatory mediators by suppressing Keap1 or activating Nrf2 expression and their downstream targets in the nucleus, including HO-1, SOD, and CAT; 2) mediating Nrf2 signaling through various kinases like GSK3β, PI3/AKT, and MAPK; and 3) modifying epigenetic modulations, such as methylation, at the Nrf2 promoter region. However, further investigations into other upstream signaling molecules like Nrf2 and the effects of metabolites are needed (Thiruvengadam et al., 2021).

According to the data from the PPI analysis (Figure 5), mitogen-activated protein kinase (MAPK) 3 was the hub target of RLR in T2DM treatment. MAPK3 is a common target for T2DM (Maradesha et al., 2023), and evidence has shown that overactivation of MAPK3 can lead to insulin sensitivity impairment, while MAPK3 knockout can undo insulin resistance (Jiao et al., 2013). GO enrichment analysis predicted that RLR alleviated T2DM through multiple BPs, CCs, and MFs, such as responses to oxidative stress, membrane rafts, and signaling receptor activator activities (Figure 6A). KEGG enrichment analysis predicted that RLR could play a therapeutic role in T2DM by regulating the PI3K-AKT signaling pathway (Figures 6B, 7), which plays key roles in essential cellular processes, such as glucose homeostasis and lipid metabolism (Abeyrathna and Su, 2015). Phosphatidylinositol 3'-kinase (PI3K) is initially activated by several signal molecules, such as growth factors and cytokines.

The activated PI3K catalyzes phosphatidylinositol 4,5-biphosphate (PIP2) to phosphatidylinositol 3,4,5-triphosphate (PIP3) and subsequently activates RAC serine/threonine–protein kinase (AKT) for further signal cascade (Franke et al., 1997). Under physiological conditions, insulin mediates glucose uptake and reduces gluconeogenesis through the PI3K-AKT signaling pathway. Nevertheless, in energy excessive conditions, the PI3K-AKT signaling pathway is impaired, causing insulin resistance (Huang et al., 2018). The aforementioned network pharmacology study indicates that RLR has great therapeutic potential for T2DM by regulating the PI3K-AKT signaling pathway, especially MAPK3.

## 5 Conclusion

Historically, folk and traditional herbal medicines have been popularly used all over the world regardless of the region. Recently, evidence-based, personalized, and precision medicines have become crucial for remedying human diseases through the ethnomedicinal functions of numerous botanical drugs or plant species on diseases (e.g., cancer, diabetes, metabolic syndrome, and microbial infections), free-radical scavengers, and antioxidative stress. In this study, network pharmacology studies, multitarget *in silico* screening, as well as *in vitro* and *in vivo* validations of a combination of metabolites are used to counteract diabetes instead of exploiting synthetic drugs (Figure 11). Multiple predictions obtained via network and docking analyses accompanied by investigation of the underlying mechanisms indicate the potential of the proposed RLR mixture in diabetes treatment. A comprehensive analysis of the efficacy of the RLR mixture on diabetes demonstrated that the mixture holds promising clues regarding the hypoglycemic effect. Furthermore, this study is expected to direct future clinical trials, with important implications for human health.

## Data availability statement

The raw data supporting the conclusions of this article will be made available by the authors, without undue reservation.

## Ethics statement

The animal experiments were approved by the Xiamen Medical College Animal Ethics Committee (SYXK, 2018-0010) and conducted in accordance with the "Guide for the Care and Use of Laboratory Animals" of Xiamen Medical College. The study was also conducted in accordance with the local legislation and institutional requirements.

## Author contributions

XH: conceptualization, data curation, formal analysis, investigation, methodology, project administration, resources, software, supervision, validation, visualization, writing–original draft. KL: conceptualization, data curation, formal analysis, investigation, methodology, project administration, resources, software, supervision, validation, visualization, writing–original draft. SL: data curation, resources, software, validation, writing–original draft. JY: data curation, formal analysis, software, writing–original draft. HZ: data curation, formal analysis, software, and writing–original draft. X-HZ: investigation, writing–review and editing, and writing–original draft. M-JT: investigation, writing–review and editing, and writing–original draft. C-SC: investigation, writing–review and editing, and writing–original draft. LH: supervision, validation, visualization, writing–review and editing, and writing–original draft. C-FW: conceptualization, data curation, formal analysis, funding acquisition, investigation, methodology, project administration, resources, software, supervision, validation, visualization, writing–original draft, and writing–review and editing.

## Funding

The author(s) declare that financial support was received for the research, authorship, and/or publication of this article. This work was supported by Xiamen Medical College (No. K2019-01 for C-FW) and SINOLOOK HONGKONG LIMITED Company (address: Room 604, 6/F., Easey Comme).

## Acknowledgments

The authors sincerely thank Professor Max K. Leong and Mr. Ting-Shu Chen for providing technical help with the molecular docking study.

## Conflict of interest

The authors declare that the research was conducted in the absence of any commercial or financial relationships that could be construed as a potential conflict of interest.

## Publisher's note



## Supplementary material

The Supplementary Material for this article can be found online at: https://www.frontiersin.org/articles/10.3389/fphar.2024.1362150/full#supplementary-material

# References


Abeyrathna, P., and Su, Y. (2015). The critical role of Akt in cardiovascular function. *Vasc. Pharmacol.* 74, 38–48. doi:10.1016/j.vph.2015.05.008

Alagawany, M., Abd El-Hack, M. E., Farag, M. R., Gopi, M., Karthik, K., Malik, Y. S., et al. (2017). Rosmarinic acid: modes of action, medicinal values and health benefits. *Anim. Health Res. Rev.* 18, 167–176. doi:10.1017/S1466252317000081

Bizzarri, M., Giuliani, A., Monti, N., Verna, R., Pensotti, A., and Cucina, A. (2020). Rediscovery of natural compounds acting via multitarget recognition and noncanonical pharmacodynamical actions. *Drug Discov. Today* 25, 920–927. doi:10.1016/j.drudis.2020.02.010

Boonrueng, P., Wasana, P. W. D., Hasriadi, null, Vajragupta, O., Rojsitthisak, P., and Towiwat, P. (2022). Combination of curcumin and piperine synergistically improves pain-like behaviors in mouse models of pain with no potential CNS side effects. *Chin. Med.* 17, 119. doi:10.1186/s13020-022-00660-1

Boulton, A. J. M., Vileikyte, L., Ragnarson-Tennvall, G., and Apelqvist, J. (2005). The global burden of diabetic foot disease. *Lancet* 366, 1719–1724. doi:10.1016/S0140-6736(05)67698-2

Chen, S., Zhao, Z., Ke, L., Li, Z., Li, W., Zhang, Z., et al. (2018). Resveratrol improves glucose uptake in insulin-resistant adipocytes via Sirt1. *J. Nutr. Biochem.* 55, 209–218. doi:10.1016/j.jnutbio.2018.02.007

Chen, S.-P., Lin, S.-R., Chen, T.-H., Ng, H.-S., Yim, H.-S., Leong, M. K., et al. (2021b). Mangosteen xanthone γ-mangostin exerts lowering blood glucose effect with potentiating insulin sensitivity through the mediation of AMPK/PPARγ. *Biomed. Pharmacother.* 144, 112333. doi:10.1016/j.biopha.2021.112333

Chen, T.-H., Fu, Y.-S., Chen, S.-P., Fuh, Y.-M., Chang, C., and Weng, C.-F. (2021a). Garcinia linii extracts exert the mediation of anti-diabetic molecular targets on anti-hyperglycemia. *Biomed. Pharmacother.* 134, 111151. doi:10.1016/j.biopha.2020.111151

Cheng, F., Li, W., Zhou, Y., Shen, J., Wu, Z., Liu, G., et al. (2012). admetSAR: a comprehensive source and free tool for assessment of chemical ADMET properties. *J. Chem. Inf. Model* 52, 3099–3105. doi:10.1021/ci300367a

Chin, C.-H., Chen, S.-H., Wu, H.-H., Ho, C.-W., Ko, M.-T., and Lin, C.-Y. (2014). cytoHubba: identifying hub objects and sub-networks from complex interactome. *BMC Syst. Biol.* 8 (Suppl. 4), S11. doi:10.1186/1752-0509-8-S4-S11

Christian, A., and Nagar, K. (2021). Understanding patients experiences living with diabetes mellitus: a qualitative study, Gujarat, India. *J. Pharm. Res. Int.* 33, 464–471. doi:10.9734/jpri/2021/v33i58A34139

Chung, C. H., Jung, W., Keum, H., Kim, T. W., and Jon, S. (2020). Nanoparticles derived from the natural antioxidant rosmarinic acid ameliorate acute inflammatory bowel disease. *ACS Nano* 14, 6887–6896. doi:10.1021/acsnano.0c01018

Daily, J. W., Kang, S., and Park, S. (2021). Protection against Alzheimer's disease by luteolin: role of brain glucose regulation, anti-inflammatory activity, and the gut microbiota-liver-brain axis. *Biofactors* 47, 218–231. doi:10.1002/biof.1703

Franke, T. F., Kaplan, D. R., Cantley, L. C., and Toker, A. (1997). Direct regulation of the Akt proto-oncogene product by phosphatidylinositol-3,4-bisphosphate. *Science* 275, 665–668. doi:10.1126/science.275.5300.665

García-Martínez, B. I., Ruiz-Ramos, M., Pedraza-Chaverri, J., Santiago-Osorio, E., and Mendoza-Núñez, V. M. (2022). Influence of age and dose on the effect of resveratrol for glycemic control in type 2 diabetes mellitus: systematic review and meta-analysis. *Molecules* 27, 5232. doi:10.3390/molecules27165232

Gelmini, F., Grande, F., Rizzuti, B., Ioele, G., Casacchia, T., Guzzi, R., et al. (2018). Identification by molecular docking of homoisoflavones from leopoldia comosa as ligands of estrogen receptors. *Molecules* 23, 894. doi:10.3390/molecules23040894

Govindaraj, J., and Sorimuthu Pillai, S. (2015). Rosmarinic acid modulates the antioxidant status and protects pancreatic tissues from glucolipotoxicity mediated oxidative stress in high-fat diet: streptozotocin-induced diabetic rats. *Mol. Cell Biochem.* 404, 143–159. doi:10.1007/s11010-015-2374-6

Grande, F., Occhiuzzi, M., Perri, M., Ioele, G., Rizzuti, B., Statti, G., et al. (2021). Polyphenols from Citrus Tacle® extract endowed with HMGCR inhibitory activity: an antihypercholesterolemia natural remedy. *Molecules* 26, 5718. doi:10.3390/molecules26185718

Guariguata, L., Whiting, D. R., Hambleton, I., Beagley, J., Linnenkamp, U., and Shaw, J. E. (2014). Global estimates of diabetes prevalence for 2013 and projections for 2035. *Diabetes Res. Clin. Pract.* 103, 137–149. doi:10.1016/j.diabres.2013.11.002

Hsin, K.-Y., Ghosh, S., and Kitano, H. (2013). Combining machine learning systems and multiple docking simulation packages to improve docking prediction reliability for network pharmacology. *PLoS One* 8, e83922. doi:10.1371/journal.pone.0083922

Huang, P.-K., Lin, S.-R., Riyaphan, J., Fu, Y.-S., and Weng, C.-F. (2019a). Polyalthia clerodane diterpene potentiates hypoglycemia via inhibition of Dipeptidyl peptidase 4. *Int. J. Mol. Sci.* 20, E530. doi:10.3390/ijms20030530

Huang, P.-K., Lin, S.-R., Riyaphan, J., Fu, Y.-S., and Weng, C.-F. (2019b). Polyalthia clerodane diterpene potentiates hypoglycemia via inhibition of Dipeptidyl peptidase 4. *Int. J. Mol. Sci.* 20, E530. doi:10.3390/ijms20030530

Huang, X., Liu, G., Guo, J., and Su, Z. (2018). The PI3K/AKT pathway in obesity and type 2 diabetes. *Int. J. Biol. Sci.* 14, 1483–1496. doi:10.7150/ijbs.27173

Imam, S. S., Alshehri, S., Altamimi, M. A., Hussain, A., Alyahya, K. H., Mahdi, W. A., et al. (2022). Formulation and evaluation of luteolin-loaded nanovesicles: *in vitro* physicochemical characterization and viability assessment. *ACS Omega* 7, 1048–1056. doi:10.1021/acsomega.1c05628

Intagliata, S., Modica, M. N., Santagati, L. M., and Montenegro, L. (2019). Strategies to improve resveratrol systemic and topical bioavailability: an update. *Antioxidants (Basel)* 8, E244. doi:10.3390/antiox8080244

Ishola, A. A., Oyinloye, B. E., Ajiboye, B. O., and Kappo, A. P. (2020). Molecular docking studies of flavonoids from andrographis paniculata as potential acetylcholinesterase, butyrylcholinesterase and monoamine oxidase inhibitors towards the treatment of neurodegenerative diseases. *Biointerface Res. Appl. Chem.* 11, 9871–9879. doi:10.33263/BRIAC113.98719879

Ishola, A. A., Oyinloye, B. E., Ajiboye, B. O., and Kappo, A. P. (2021). Molecular docking studies of flavonoids from andrographis paniculata as potential acetylcholinesterase, butyrylcholinesterase and monoamine oxidase inhibitors towards the treatment of. *Neurodegener. Dis.* 11, 9871–9879. doi:10.33263/BRIAC113.98719879

Israili, Z. H. (2011). Advances in the treatment of type 2 diabetes mellitus. *Am. J. Ther.* 18, 117–152. doi:10.1097/MJT.0b013e3181afbf51

Jayanthy, G., Roshana Devi, V., Ilango, K., and Subramanian, S. P. (2017). Rosmarinic acid mediates mitochondrial biogenesis in insulin resistant skeletal muscle through activation of AMPK. *J. Cell Biochem.* 118, 1839–1848. doi:10.1002/jcb.25869

Jiao, P., Feng, B., Li, Y., He, Q., and Xu, H. (2013). Hepatic ERK activity plays a role in energy metabolism. *Mol. Cell Endocrinol.* 375, 157–166. doi:10.1016/j.mce.2013.05.021

Jugran, A. K., Rawat, S., Devkota, H. P., Bhatt, I. D., and Rawal, R. S. (2021). Diabetes and plant-derived natural products: from ethnopharmacological approaches to their potential for modern drug discovery and development. *Phytother. Res.* 35, 223–245. doi:10.1002/ptr.6821

Khalid, M. F., Rehman, K., Irshad, K., Chohan, T. A., and Akash, M. S. H. (2022). Biochemical investigation of inhibitory activities of plant-derived bioactive compounds against carbohydrate and glucagon-like peptide-1 metabolizing enzymes. *Dose Response* 20, 15593258221093275. doi:10.1177/15593258221093275

Lea, T. (2015) *Caco-2 cell line*. Berlin, Germany: Springer. doi:10.1007/978-3-319-16104-4_10

Liu, H., Wang, J., Zhou, W., Wang, Y., and Yang, L. (2013). Systems approaches and polypharmacology for drug discovery from herbal medicines: an example using licorice. *J. Ethnopharmacol.* 146, 773–793. doi:10.1016/j.jep.2013.02.004

Luyen, N. T., Dang, N. H., Binh, P. T. X., Hai, N. T., and Dat, N. T. (2018). Hypoglycemic property of triterpenoid saponin PFS isolated from Polyscias fruticosa leaves. *Acad Bras Cienc* 90, 2881–2886. doi:10.1590/0001-3765201820170945

Ma, N., and Zhang, Y. (2022). Effects of resveratrol therapy on glucose metabolism, insulin resistance, inflammation, and renal function in the elderly patients with type 2 diabetes mellitus: a randomized controlled clinical trial protocol. *Med. Baltim.* 101, e30049. doi:10.1097/MD.0000000000030049

Maradesha, T., Martiz, R. M., Patil, S. M., Prasad, A., Babakr, A. T., Silina, E., et al. (2023). Integrated network pharmacology and molecular modeling approach for the discovery of novel potential MAPK3 inhibitors from whole green jackfruit flour targeting obesity-linked diabetes mellitus. *PLoS One* 18, e0280847. doi:10.1371/journal.pone.0280847

Niu, B., Xie, X., Xiong, X., and Jiang, J. (2022). Network pharmacology-based analysis of the anti-hyperglycemic active ingredients of roselle and experimental validation. *Comput. Biol. Med.* 141, 104636. doi:10.1016/j.compbiomed.2021.104636

Ozougwu, J., Obimba, K. C., Belonwu, C. D., and Unakalamba, C. B. (2013). The pathogenesis and pathophysiology of type 1 and type 2 diabetes mellitus. *Acad. Journals* 4, 46–57. doi:10.5897/jpap2013.0001

Öztürk, E., Arslan, A. K. K., Yerer, M. B., and Bishayee, A. (2017). Resveratrol and diabetes: a critical review of clinical studies. *Biomed. Pharmacother.* 95, 230–234. doi:10.1016/j.biopha.2017.08.070

Park, H.-S., Lee, K., Kim, S.-H., Hong, M. J., Jeong, N.-J., and Kim, M.-S. (2020). Luteolin improves hypercholesterolemia and glucose intolerance through LXRα-dependent pathway in diet-induced obese mice. *J. Food Biochem.* 44, e13358. doi:10.1111/jfbc.13358

Pereira, A. S. P., Banegas-Luna, A. J., Peña-García, J., Pérez-Sánchez, H., and Apostolides, Z. (2019). Evaluation of the anti-diabetic activity of some common herbs and spices: providing new insights with inverse virtual screening. *Molecules* 24, E4030. doi:10.3390/molecules24224030

Pivari, F., Mingione, A., Brasacchio, C., and Soldati, L. (2019). Curcumin and type 2 diabetes mellitus: prevention and treatment. *Nutrients* 11, 1837. doi:10.3390/nu11081837

Punthakee, Z., Goldenberg, R., and Katz, P. (2018). Definition, classification and diagnosis of diabetes, prediabetes and metabolic syndrome. *Can. J. Diabetes* 42 (Suppl. 1), S10–S15. doi:10.1016/j.jcjd.2017.10.003

Rana, A., Samtiya, M., Dhewa, T., Mishra, V., and Aluko, R. E. (2022). Health benefits of polyphenols: a concise review. *J. Food Biochem.* 46, e14264. doi:10.1111/jfbc.14264

Runtuwene, J., Cheng, K.-C., Asakawa, A., Amitani, H., Amitani, M., Morinaga, A., et al. (2016). Rosmarinic acid ameliorates hyperglycemia and insulin sensitivity in diabetic rats, potentially by modulating the expression of PEPCK and GLUT4. *Drug Des. Devel Ther.* 10, 2193–2202. doi:10.2147/DDDT.S108539

Saito, R., Smoot, M. E., Ono, K., Ruscheinski, J., Wang, P.-L., Lotia, S., et al. (2012). A travel guide to Cytoscape plugins. *Nat. Methods* 9, 1069–1076. doi:10.1038/nmeth.2212

Saleem, Z., Rehman, K., and Hamid Akash, M. S. (2022). Role of drug delivery system in improving the bioavailability of resveratrol. *Curr. Pharm. Des.* 28, 1632–1642. doi:10.2174/1381612828666220705113514

Santos, A. C., Pereira, I., Pereira-Silva, M., Ferreira, L., Caldas, M., Collado-González, M., et al. (2019). Nanotechnology-based formulations for resveratrol delivery: effects on resveratrol *in vivo* bioavailability and bioactivity. *Colloids Surf. B Biointerfaces* 180, 127–140. doi:10.1016/j.colsurfb.2019.04.030

Shannon, P., Markiel, A., Ozier, O., Baliga, N. S., Wang, J. T., Ramage, D., et al. (2003). Cytoscape: a software environment for integrated models of biomolecular interaction networks. *Genome Res.* 13, 2498–2504. doi:10.1101/gr.1239303

Sharma, P., Joshi, T., Joshi, T., Chandra, S., and Tamta, S. (2020). *In silico* screening of potential antidiabetic phytochemicals from Phyllanthus emblica against therapeutic targets of type 2 diabetes. *J. Ethnopharmacol.* 248, 112268. doi:10.1016/j.jep.2019.112268

Singla, R. K., Kumar, R., Khan, S., Mohit, null, Kumari, K., and Garg, A. (2019). Natural products: potential source of DPP-IV inhibitors. *Curr. Protein Pept. Sci.* 20, 1218–1225. doi:10.2174/1389203720666190502154129

Spínola, V., Llorent-Martínez, E. J., and Castilho, P. C. (2019). Polyphenols of Myrica faya inhibit key enzymes linked to type II diabetes and obesity and formation of advanced glycation end-products (*in vitro*): potential role in the prevention of diabetic complications. *Food Res. Int.* 116, 1229–1238. doi:10.1016/j.foodres.2018.10.010

Su, M., Zhao, W., Xu, S., and Weng, J. (2022). Resveratrol in treating diabetes and its cardiovascular complications: a review of its mechanisms of action. *Antioxidants (Basel)* 11, 1085. doi:10.3390/antiox11061085

Suchitra, K. P., Jha, A., Bhatt, R., and Kumar, A. (2020). Molecular docking and ADMET-based mining of terpenoids against targets of type-II diabetes. *Netw. Model. Analysis Health Inf. Bioinforma.* 9, 21. doi:10.1007/s13721-020-00229-8

Swilam, N., Nawwar, M. A. M., Radwan, R. A., and Mostafa, E. S. (2022). Antidiabetic activity and *in silico* molecular docking of polyphenols from ammannia baccifera L. subsp. aegyptiaca (willd.) koehne waste: structure elucidation of undescribed acylated flavonol diglucoside. *Plants (Basel)* 11, 452. doi:10.3390/plants11030452

Szkudelski, T., and Szkudelska, K. (2015). Resveratrol and diabetes: from animal to human studies. *Biochim. Biophys. Acta* 1852, 1145–1154. doi:10.1016/j.bbadis.2014.10.013

Taghipour, Y. D., Hajialyani, M., Naseri, R., Hesari, M., Mohammadi, P., Stefanucci, A., et al. (2019). Nanoformulations of natural products for management of metabolic syndrome. *Int. J. Nanomedicine* 14, 5303–5321. doi:10.2147/IJN.S213831

Taheri, Y., Sharifi-Rad, J., Antika, G., Yılmaz, Y. B., Tumer, T. B., Abuhamdah, S., et al. (2021). Paving luteolin therapeutic potentialities and agro-food-pharma applications: emphasis on *in vivo* pharmacological effects and bioavailability traits. *Oxid. Med. Cell Longev.* 2021, 1987588. doi:10.1155/2021/1987588

Takayanagi, R., Inoguchi, T., and Ohnaka, K. (2011). Clinical and experimental evidence for oxidative stress as an exacerbating factor of diabetes mellitus. *J. Clin. Biochem. Nutr.* 48, 72–77. doi:10.3164/jcbn.11-014FR

Thiruvengadam, M., Venkidasamy, B., Subramanian, U., Samynathan, R., Ali Shariati, M., Rebezov, M., et al. (2021). Bioactive compounds in oxidative stress-mediated diseases: targeting the NRF2/ARE signaling pathway and epigenetic regulation. *Antioxidants (Basel)* 10, 1859. doi:10.3390/antiox10121859

Thompson, A., and Kanamarlapudi, V. (2013). Type 2 diabetes mellitus and glucagon like peptide-1 receptor signalling, clinical and experimental. *Pharmacology* 3, 138. doi:10.4172/2161-1459.1000138

Tolmie, M., Bester, M. J., and Apostolides, Z. (2021). Inhibition of α-glucosidase and α-amylase by herbal compounds for the treatment of type 2 diabetes: a validation of *in silico* reverse docking with *in vitro* enzyme assays. *J. Diabetes* 13, 779–791. doi:10.1111/1753-0407.13163

Vlavcheski, F., Naimi, M., Murphy, B., Hudlicky, T., and Tsiani, E. (2017). Rosmarinic acid, a rosemary extract polyphenol, increases skeletal muscle cell glucose uptake and activates AMPK. *Molecules* 22, E1669. doi:10.3390/molecules22101669

Wais, M., Nazish, I., Samad, A., Beg, S., Abusufyan, S., Ajaj, S. A., et al. (2012). Herbal drugs for diabetic treatment: an updated review of patents. *Recent Pat. Antiinfect Drug Discov.* 7, 53–59. doi:10.2174/157489112799829701

You, Q., Chen, F., Wang, X., Jiang, Y., and Lin, S. (2012). Antidiabetic activities of phenolic compounds in muscadine against alpha-glucosidase and pancreatic lipase. *Lwt - Food Sci. Technol.* 46, 164–168. doi:10.1016/j.lwt.2011.10.011

Zhang, B.-W., Li, X., Sun, W.-L., Xing, Y., Xiu, Z.-L., Zhuang, C.-L., et al. (2017). Dietary flavonoids and acarbose synergistically inhibit α-glucosidase and lower postprandial blood glucose. *J. Agric. Food Chem.* 65, 8319–8330. doi:10.1021/acs.jafc.7b02531

Zhang, L.-X., Li, C.-X., Kakar, M. U., Khan, M. S., Wu, P.-F., Amir, R. M., et al. (2021a). Resveratrol (RV): a pharmacological review and call for further research. *Biomed. Pharmacother.* 143, 112164. doi:10.1016/j.biopha.2021.112164

Zhang, T., He, Q., Liu, Y., Chen, Z., and Hu, H. (2021b). Efficacy and safety of resveratrol supplements on blood lipid and blood glucose control in patients with type 2 diabetes: a systematic review and meta-analysis of randomized controlled trials. *Evid. Based Complement. Altern. Med.* 2021, 5644171. doi:10.1155/2021/5644171

Zhu, F., Asada, T., Sato, A., Koi, Y., Nishiwaki, H., and Tamura, H. (2014). Rosmarinic acid extract for antioxidant, antiallergic, and α-glucosidase inhibitory activities, isolated by supramolecular technique and solvent extraction from Perilla leaves. *J. Agric. Food Chem.* 62, 885–892. doi:10.1021/jf404318j

frontiers | Frontiers in Pharmacology

TYPE Opinion
PUBLISHED 12 June 2024
DOI 10.3389/fphar.2024.1419729



OPEN ACCESS

EDITED BY
Ludwig Weckbach,
LMU Munich University Hospital, Germany

REVIEWED BY
Aditya Yashwant Sarode,
Columbia University, United States

*CORRESPONDENCE
HaiTao Zou,
haitao_zou@yeah.net

RECEIVED 18 April 2024
ACCEPTED 29 May 2024
PUBLISHED 12 June 2024

CITATION
Huang L, Hu R and Zou H (2024), Relative efficacy of five SGLT2 inhibitors: a network meta-analysis of 20 cardiovascular and respiratory outcomes.
*Front. Pharmacol.* 15:1419729.
doi: 10.3389/fphar.2024.1419729



# Relative efficacy of five SGLT2 inhibitors: a network meta-analysis of 20 cardiovascular and respiratory outcomes

LiGang Huang[1], Rong Hu[2] and HaiTao Zou[2]*

[1]Department of Cardiovascular Medicine, Dianjiang People's Hospital of Chongqing, Chongqing, China, [2]Department of Respiratory and Critical Care Medicine, Dianjiang People's Hospital of Chongqing, Chongqing, China

KEYWORDS

**SGLT2 inhibitors (gliflozins), heart failure, myocardial infarction, pneumonia, asthma, complete atrioventricular block, acute respiratory failure, hypertensive crisis**

## Background

More and more clinical guidelines have recommended use of sodium-glucose cotransporter-2 (SGLT2) inhibitors, also known as gliflozins, to prevent major adverse cardiovascular and renal events in patients with type 2 diabetes, heart failure, and/or chronic kidney disease. The mechanisms by which SGLT2 inhibitors exert cardiovascular and renal benefits include but are not limited to: the anti-inflammatory effects by the potential pathways (e.g., mitochondrial, oxidative stress, and inflammasome pathways) (Mashayekhi et al., 2024), the modulation of cellular energy metabolism, and housekeeping mechanisms (Preda et al., 2024). Since there have not been head-to-head cardiovascular outcome randomized controlled trials (RCTs) comparing a gliflozin with one other gliflozin, the relative efficacy of various gliflozins on cardiovascular outcomes has not been established. Several published network meta-analyses (Kanie et al., 2021; Lin et al., 2021; Giugliano et al., 2022; Zhang et al., 2022; Brønden et al., 2023) assessing the cardiovascular outcomes of SGLT2 inhibitors have compared SGLT2 inhibitors with non-gliflozin drugs, such as glucagon-like peptide-1 receptor agonists, dipeptidyl peptidase-4 inhibitors, and finerenone; but have not performed the comparisons among various gliflozins. Moreover, these studies (Kanie et al., 2021; Lin et al., 2021; Giugliano et al., 2022; Zhang et al., 2022; Brønden et al., 2023) of network meta-analysis have focused on evaluating those composite cardiovascular outcomes, such as major adverse cardiovascular events (defined as a composite of cardiovascular death, myocardial infarction, and stroke), but have evaluated a limited number of individual cardiovascular outcomes. Some important individual outcomes, such as complete atrioventricular block and hypertensive crisis, have not been evaluated in any of these studies (Kanie et al., 2021; Lin et al., 2021; Giugliano et al., 2022; Zhang et al., 2022; Brønden et al., 2023). Therefore, we included those large-scale placebo-controlled RCTs of

**Abbreviations:** CI, confidence interval; COPD, chronic obstructive pulmonary disease; LRTI, lower respiratory tract infection; SGLT2, sodium-glucose cotransporter-2; RR, risk ratio; SUCRA, surface under the cumulative ranking curve; RCTs, randomized controlled trials; PRISMA, Preferred Reporting Items for Systematic Reviews and Meta-Analyses; SAEs, serious adverse events.

SGLT2 inhibitors to carry out a network meta-analysis, aiming to assess the relative efficacy of various gliflozins on various individual cardiovascular outcomes.

In recent years, more and more real-world studies have revealed the obvious benefits of SGLT2 inhibitors against many respiratory diseases, such as chronic obstructive pulmonary disease (COPD) (Pradhan et al., 2022), pneumonia (Wu et al., 2022), obstructive airway disease (Au et al., 2023), pulmonary edema (Jeong et al., 2023), and respiratory failure (Jeong et al., 2023). Similar with these real-world evidences, several meta-analyses (Yin et al., 2021; Li et al., 2022; Wang et al., 2022; Wang and Zhou, 2024; Xiao et al., 2024) based on RCTs have also revealed the respiratory system benefits of SGLT2 inhibitors. A meta-analysis (Yin et al., 2021) of 9 RCTs showed that use of gliflozins was significantly associated with the lower risks of multiple respiratory diseases, such as COPD, and asthma. One other meta-analysis (Xiao et al., 2024) of 14 RCTs and another meta-analysis (Wang and Zhou, 2024) of 32 RCTs produced the substantially consistent findings. Moreover, two other studies (Li et al., 2022; Wang et al., 2022) of meta-analysis based on RCTs revealed that use of gliflozins was significantly associated with less pneumonia and asthma, respectively. These aforementioned findings seem to suggest that it is relatively certain for gliflozins to exert the effects against relevant respiratory diseases. However, it has been unclear whether there are obvious differences among various gliflozins in the effects against respiratory diseases. Therefore, in this network meta-analysis we would also assess the relative efficacy of different gliflozins on various respiratory outcomes.

## Methods

This network meta-analysis was done according to the Preferred Reporting Items for Systematic Reviews and Meta-Analyses (PRISMA) extension statement for network meta-analyses (Hutton et al., 2015). A systematic search was performed using PubMed and ClinicalTrials.gov for relevant articles published before 21 August 2023. Our search strategy used in this network meta-analysis was as follows: ((Canagliflozin [TIAB] OR Dapagliflozin [TIAB] OR Empagliflozin [TIAB] OR Ertugliflozin [TIAB] OR Sotagliflozin [TIAB] OR Canagliflozin [MH] OR Dapagliflozin [Supplementary Concept] OR Empagliflozin [Supplementary Concept] OR Ertugliflozin [Supplementary Concept] OR LX4211 [TIAB] OR LX-4211 [TIAB]) AND (randomized controlled trial [PT] OR randomized controlled trial [TI] OR clinical trial [PT] OR clinical trial [TI] OR random* [TIAB] OR trial* [TIAB] OR placebo [TIAB] OR drug therapy [MH] OR drug therapy [SH]) AND humans [MH]) NOT (review* [TI] OR review* [PT] OR meta-analysis [TI] OR meta-analysis [PT]). Our search strategy had no limit on literature language.

In this network meta-analysis, we included those studies that were the RCTs having enrolled ≥ four hundred subjects, having compared any of the five SGLT2 inhibitors (i.e., canagliflozin, dapagliflozin, empagliflozin, ertugliflozin, and sotagliflozin) with placebo, and having reported any of the serious adverse events (SAEs) of interest. The SAEs of interest in this network meta-analysis were 20 kinds of cardiovascular and respiratory diseases, consisting of 10 cardiovascular diseases (namely, Myocardial infarction, Cardiac failure, Cardiac failure chronic, Cardiac failure congestive, Atrioventricular block complete, Cardiac failure acute, Coronary artery disease, Hypertensive crisis, Hypertensive emergency, and Hypertension) and 10 respiratory diseases (namely, Acute respiratory failure, Pulmonary oedema, COPD, Pulmonary hypertension, Dyspnoea, Asthma, Respiratory tract infection, Lower respiratory tract infection [LRTI], Pneumonia, and Pneumonia bacterial). We excluded those RCTs published in Letter to the Editor or Research Letter, but did not exclude those published in Short Original Article, Brief Report, or Rapid Communications. Two authors independently extracted the outcome data from ClinicalTrials.gov and extracted the other information (e.g., first author, publication year, and participant characteristics) from the full texts of included studies. Furthermore, two authors independently evaluated the quality of included RCTs according to the Cochrane risk of bias assessment tool (Higgins et al., 2011). Any disagreements between them would be addressed by discussion between them and a third author.

Using the two-category data (i.e., the numbers of events and subjects in each study arm), we did network meta-analyses on all of the 20 outcomes of interest. In order to derive the conservative results, we used a random-effects model to perform network meta-analysis. The effect sizes for pairwise comparisons among various SGLT2 inhibitors were given in the forest plots showing risk ratios (RRs) and their 95% confidence intervals (CIs). We drew network plots to present the network of comparisons, and drew funnel plots to assess the potential publication bias. We drew surface under the cumulative ranking curve (SUCRA) plots to present the relative rankings of various gliflozins for each outcome. More importantly, we also drew radar plots, in order that a radar plot could present lots of SUCRA values for many outcomes, with a greater SUCRA value meaning a greater probability for reducing adverse events. $p < 0.05$ represented for statistical significance. All of the statistical analyses and the statistical plots were done using the Stata/MP 16.0 software.

## Results

At first, we identified 2704 records. After study selection (Supplementary Figure S1), we finally included 28 articles reporting a total of 29 RCTs. The ClinicalTrials.gov identification numbers of these included trials were NCT03594110 [EMPA-KIDNEY] (Herrington et al., 2023), NCT03242252 [SOTA-CKD3] (Cherney et al., 2023), NCT03521934 [SOLOIST-WHF] (Bhatt et al., 2021a), NCT04157751 [EMPULSE] (Voors et al., 2022), NCT03315143 [SCORED] (Bhatt et al., 2021b), NCT04252287 [CHIEF-HF] (Spertus et al., 2022), NCT03619213 [DELIVER] (Solomon et al., 2022), NCT01986855 [VERTIS RENAL] (Grunberger et al., 2018), NCT03057951 [EMPEROR-Preserved] (Anker et al., 2021), NCT00528879 (Bailey et al., 2010), NCT03036124 [DAPA-HF] (McMurray et al., 2019), NCT00673231 (Wilding et al., 2012), NCT03036150 [DAPA-CKD] (Heerspink et al., 2020), NCT02384941 [inTandem1] (Buse et al., 2018), NCT03057977 [EMPEROR-Reduced] (Packer et al., 2020), NCT01210001 [EMPA-REG EXTEND] (Kovacs et al., 2015), NCT01730534 [DECLARE–TIMI 58] (Wiviott et al., 2019),

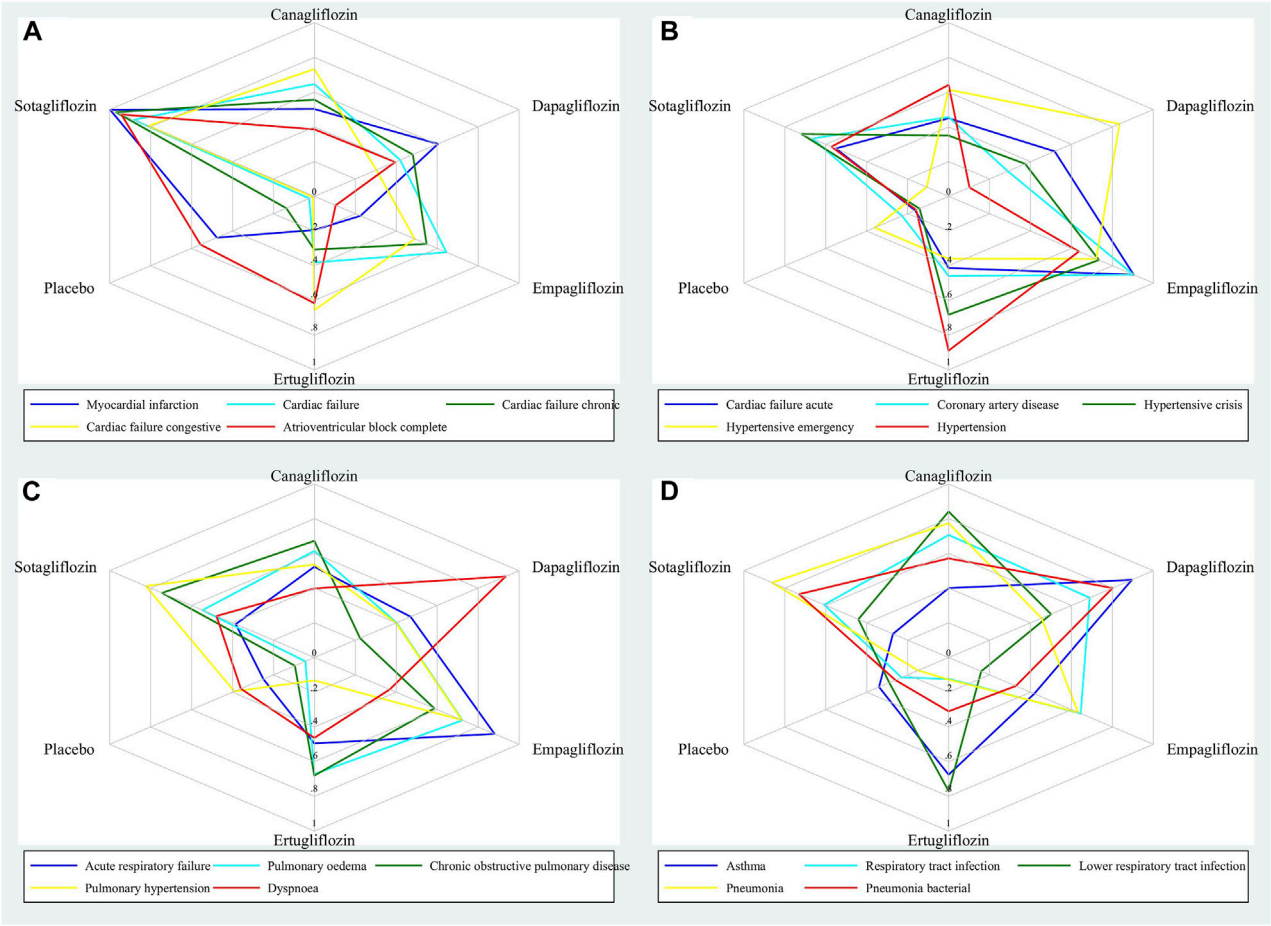


FIGURE 1
Radar plots showing the SUCRA values of five gliflozins for 20 cardiovascular and respiratory outcomes.

NCT01011868 (Tuttle et al., 2022), NCT02065791 [CREDENCE] (Perkovic et al., 2019), NCT01031680 (Cefalu et al., 2015), NCT04350593 [DARE-19] (Kosiborod et al., 2021), NCT01131676 [EMPA-REG OUTCOME] (Zinman et al., 2015), NCT01042977 (Leiter et al., 2016), NCT01032629 [CANVAS] (Neal et al., 2017), NCT01989754 [CANVAS-R] (Neal et al., 2017), NCT01106651 (Januzzi et al., 2017), NCT01164501 [EMPA-REG RENAL] (Barnett et al., 2014), NCT01986881 [VERTIS CV] (Cannon et al., 2020), and NCT01106625 [CANTATA-MSU] (Polidori et al., 2014), respectively. The detailed characteristics of these included trials are shown in Supplementary Table S1. These included RCTs were with low risk of bias in general, and enrolled a total of 100740 participants, including 54735 taking SGLT2 inhibitors and 46005 taking placebo. A total of five gliflozins were involved in this network meta-analysis, and they were dapagliflozin (N = 18791), empagliflozin (N = 14186), canagliflozin (N = 9004), ertugliflozin (N = 5806), and sotagliflozin (N = 6948), respectively.

Figure 1 shows the SUCRA values of five gliflozins for the 20 cardiovascular and respiratory outcomes assessed in this network meta-analysis. Sotagliflozin had the greatest SUCRA values for reducing Myocardial infarction, Cardiac failure, Cardiac failure chronic, Cardiac failure congestive, and Atrioventricular block complete (Figure 1A). Empagliflozin had the greatest SUCRA values for reducing Cardiac failure acute, Coronary artery disease, and Hypertensive crisis; dapagliflozin had the greatest SUCRA value for reducing Hypertensive emergency; and ertugliflozin had the greatest SUCRA value for reducing Hypertension (Figure 1B). Empagliflozin had the greatest SUCRA values for reducing Acute respiratory failure, and Pulmonary oedema; sotagliflozin had the greatest SUCRA values for reducing COPD, and Pulmonary hypertension; and dapagliflozin had the greatest SUCRA value for reducing Dyspnoea (Figure 1C). Dapagliflozin had the greatest SUCRA values for reducing Asthma, and Pneumonia bacterial; canagliflozin had the greatest SUCRA values for reducing Respiratory tract infection, and LRTI; and sotagliflozin had the greatest SUCRA value for reducing Pneumonia (Figure 1D). The detailed SUCRA plots of five gliflozins for all outcomes are provided in Supplementary Figures S2–S21.

The results of network meta-analyses on 20 cardiovascular and respiratory outcomes are presented in the forest plots (Supplementary Figures S22–S41). Sotagliflozin significantly reduced Myocardial infarction compared with placebo (RR 0.49, 95% CI 0.32-0.74), ertugliflozin (RR 0.41, 95% CI 0.23-0.70), empagliflozin (RR 0.43, 95% CI 0.27-0.70), dapagliflozin (RR

0.52, 95% CI 0.32-0.84), and canagliflozin (RR 0.50, 95% CI 0.29-0.85) (Supplementary Figure S22). Sotagliflozin (RR 0.62, 95% CI 0.51-0.76), empagliflozin, dapagliflozin, and canagliflozin significantly reduced Cardiac failure compared with placebo (Supplementary Figure S23). Sotagliflozin significantly reduced Cardiac failure chronic compared with placebo (RR 0.33, 95% CI 0.17-0.64), ertugliflozin (RR 0.35, 95% CI 0.14-0.90), empagliflozin (RR 0.45, 95% CI 0.20-0.97), and dapagliflozin (RR 0.42, 95% CI 0.20-0.90) (Supplementary Figure S24). Sotagliflozin (RR 0.57, 95% CI 0.37-0.86), empagliflozin, dapagliflozin, and canagliflozin significantly reduced Cardiac failure congestive compared with placebo (Supplementary Figure S25). Sotagliflozin significantly reduced Atrioventricular block complete compared with placebo (RR 0.36, 95% CI 0.13-0.99), empagliflozin (RR 0.17, 95% CI 0.05-0.61), and dapagliflozin (RR 0.30, 95% CI 0.10-0.94) (Supplementary Figure S26). Empagliflozin and dapagliflozin significantly reduced Cardiac failure acute compared with placebo (Supplementary Figure S27). Empagliflozin significantly reduced Coronary artery disease compared with placebo (Supplementary Figure S28). Empagliflozin significantly reduced Hypertensive crisis compared with placebo (Supplementary Figure S29). Dapagliflozin significantly reduced Hypertensive emergency compared with placebo and sotagliflozin (Supplementary Figure S30). Ertugliflozin significantly reduced Hypertension compared with dapagliflozin (RR 0.30, 95% CI 0.11-0.83) and placebo (Supplementary Figure S31). Empagliflozin significantly reduced Acute respiratory failure compared with placebo (Supplementary Figure S32). Empagliflozin, dapagliflozin, and canagliflozin significantly reduced Pulmonary oedema compared with placebo (Supplementary Figure S33). Empagliflozin significantly reduced COPD compared with placebo (Supplementary Figure S34). Empagliflozin significantly reduced Pulmonary hypertension compared with placebo (Supplementary Figure S35). Dapagliflozin significantly reduced Dyspnoea compared with placebo and empagliflozin (Supplementary Figure S36). Dapagliflozin significantly reduced Asthma compared with placebo (Supplementary Figure S37). Canagliflozin significantly reduced Respiratory tract infection compared with placebo (Supplementary Figure S38). Canagliflozin significantly reduced LRTI compared with placebo and empagliflozin (Supplementary Figure S39). Sotagliflozin (RR 0.69, 95% CI 0.50-0.97), empagliflozin, and canagliflozin significantly reduced Pneumonia compared with placebo (Supplementary Figure S40). Sotagliflozin (RR 0.43, 95% CI 0.25-0.75) and dapagliflozin significantly reduced Pneumonia bacterial compared with placebo (Supplementary Figure S41).

The network plots of 20 outcomes are given in Supplementary Figures S42–S61. These plots suggested that all of the included studies were placebo-controlled trials and there was no direct evidence among various gliflozins. Therefore, there was no need to perform inconsistency test. Furthermore, the funnel plots of 20 outcomes (Supplementary Figures S62–S81) showed that many of the included studies were located at the top of the funnel plots, suggesting that many of the included studies had a relatively large sample size. Meanwhile, all of funnel plots were substantially symmetrical. This suggested, it was unlikely that there was any potential publication bias in this network meta-analysis.

## Discussion

This is the first network meta-analysis which aimed to assess the relative efficacy of various SGLT2 inhibitors on various cardiovascular and respiratory outcomes. This network meta-analysis produced several key findings as follows.

First, sotagliflozin *versus* placebo significantly reduced Myocardial infarction, Cardiac failure, Cardiac failure chronic, Cardiac failure congestive, Atrioventricular block complete, and Pneumonia; and sotagliflozin had the greatest SUCRA values for reducing these six outcomes. These suggest that sotagliflozin may be the best gliflozin for preventing these cardiopulmonary outcomes. The findings regarding heart failure and myocardial infarction in our network meta-analysis are consistent with those in previous network meta-analyses (Qiu et al., 2022; Tornyos et al., 2022; Kongmalai et al., 2023; Li et al., 2023): Li et al. (Li et al., 2023) identified that sotagliflozin had the best efficacy in reducing heart failure events; Kongmalai et al. (Kongmalai et al., 2023) identified that sotagliflozin had the highest probability of reducing the composite outcome of heart failure hospitalization and cardiovascular death; Tornyos et al. (Tornyos et al., 2022) identified that sotagliflozin seemed to be more effective regarding composite heart failure outcome and myocardial infarction than ertugliflozin; and Qiu et al. (Qiu et al., 2022) identified that the maximum SUCRA value accompanied sotagliflozin in reducing myocardial infarction.

Second, empagliflozin *versus* placebo significantly reduced Cardiac failure acute, Coronary artery disease, Hypertensive crisis, Acute respiratory failure, Pulmonary oedema, COPD, and Pulmonary hypertension; and empagliflozin had the greatest SUCRA values for reducing the former five outcomes. These suggest that empagliflozin may be the best gliflozin for preventing these cardiopulmonary outcomes. The findings regarding acute heart failure in our network meta-analysis are similar with the results of the EMPULSE trial (Kosiborod et al., 2022; Voors et al., 2022): initiation of empagliflozin in patients hospitalized for acute heart failure was safe in general and led to significant clinical benefit (Voors et al., 2022), and that benefit was not affected by the degree of symptomatic impairment at baseline (Kosiborod et al., 2022). In spite of this, the efficacy of empagliflozin in acute heart failure on long-term cardiovascular outcomes (e.g., cardiovascular death, worsening heart failure, and rehospitalization for heart failure) needs further investigation. Similar with the findings regarding pulmonary hypertension and COPD in our study, an animal study (Chowdhury et al., 2020) showed that empagliflozin attenuated maladaptive pulmonary remodeling, reduced right ventricle systolic pressure, and lowered the risk of death in experimental rats with pulmonary arterial hypertension. Furthermore, gliflozins could exert the beneficial effects against COPD and $CO_2$ retention by reducing serum glucose level and then reducing the generation of endogenous $CO_2$ (Brikman and Dori, 2020).

Third, dapagliflozin *versus* placebo significantly reduced Hypertensive emergency, Asthma, Dyspnoea, and Pneumonia bacterial; and dapagliflozin had the greatest SUCRA values for reducing these four outcomes. These suggest that dapagliflozin may be the best gliflozin for preventing these cardiopulmonary outcomes. What supports the anti-asthma activity of dapagliflozin

is, Tabaa and others (Tabaa et al., 2022) carried out a rigorous animal experiment, and came to the following conclusion: since dapagliflozin had anti-oxidant, anti-inflammatory, and bronchodilator properties, this gliflozin might present a novel promising possibility for the treatment of asthma.

Last, canagliflozin *versus* placebo significantly reduced Respiratory tract infection and LRTI; and canagliflozin had the greatest SUCRA values for reducing these two outcomes. These suggest that canagliflozin may be the best gliflozin for preventing these respiratory outcomes. Meanwhile, ertugliflozin significantly reduced Hypertension compared with dapagliflozin and placebo; and ertugliflozin had the greatest SUCRA value for reducing this outcome. These suggest that ertugliflozin may be the best gliflozin for preventing Hypertension. Similarly, a *post hoc* pooled analysis of three phase 3 RCTs of ertugliflozin identified that ertugliflozin *versus* placebo resulted in statistically significant reductions in systolic blood pressure and diastolic blood pressure (Liu et al., 2019). Moreover, one of the underlying mechanisms for the effect of canagliflozin against LRTI (e.g., pneumonia) is that: canagliflozin ameliorates NLRP3 (i.e., NOD-, LRR-, and pyrin domain-containing protein 3) inflammasome-mediated inflammation through inhibiting NF-κB signaling and upregulating Bif-1 (i.e., Bax-interacting factor 1) (Niu et al., 2022).

This network meta-analysis has two main strengths. First, this network meta-analysis possessed a large sample size: the included RCTs involved a total of 100740 subjects, and the sample size of each drug intervention of our interest ranged from 5806 to 18791. This suggested that this study had a relatively sufficient statistical power to assess each intervention of interest. Second, there was no any potential publication bias observed for all of the 20 cardiovascular and respiratory outcomes assessed in this study. In contrast, this network meta-analysis has two main weaknesses. First, this network meta-analysis only assessed the five gliflozins: canagliflozin, dapagliflozin, empagliflozin, ertugliflozin, and sotagliflozin; whereas this study did not assess the other gliflozins, such as, bexagliflozin, tofogliflozin, and ipragliflozin. This is because the former five gliflozins have been evaluated in large-scale cardiovascular outcome RCTs, whereas the other gliflozins have not until now. Therefore, there is a need for an update for this network meta-analysis when possible. Second, due to the absence of large-scale head-to-head RCTs performing the comparisons among various gliflozins, we only included placebo-controlled trials in this network meta-analysis. It is meaningful to conduct relevant head-to-head trials to confirm our findings.

In conclusion, our network meta-analysis, for the first time, reveals that different gliflozins have different impacts on various cardiovascular and respiratory outcomes. Among the five gliflozins assessed, sotagliflozin may be the best gliflozin for preventing heart failure, myocardial infarction, complete atrioventricular block, and pneumonia; empagliflozin may be the best gliflozin for preventing acute heart failure, acute respiratory failure, and hypertensive crisis; and dapagliflozin may be the best gliflozin for preventing asthma, and hypertensive emergency. However, further research, including head-to-head trials, is needed to confirm and expand upon these findings.

## Author contributions

LH: Data curation, Formal Analysis, Writing–original draft, Writing–review and editing. RH: Data curation, Writing–original draft, Writing–review and editing. HZ: Conceptualization, Data curation, Writing–original draft, Writing–review and editing.

## Funding

The author(s) declare that no financial support was received for the research, authorship, and/or publication of this article.

## Conflict of interest

The authors declare that the research was conducted in the absence of any commercial or financial relationships that could be construed as a potential conflict of interest.

## Publisher's note



## Supplementary material

The Supplementary Material for this article can be found online at: https://www.frontiersin.org/articles/10.3389/fphar.2024.1419729/full#supplementary-material

## References

Anker, S. D., Butler, J., Filippatos, G., Ferreira, J. P., Bocchi, E., Böhm, M., et al. (2021). Empagliflozin in heart failure with a preserved ejection fraction. *New Engl. J. Med.* 385 (16), 1451–1461. doi:10.1056/NEJMoa2107038

Au, P., Tan, K., Lam, D., Cheung, B. M. Y., Wong, I. C. K., Kwok, W. C., et al. (2023). Association of sodium-glucose cotransporter 2 inhibitor vs dipeptidyl peptidase-4 inhibitor use with risk of incident obstructive airway disease and exacerbation events among patients with type 2 diabetes in Hong Kong. *Jama Netw. Open* 6 (1), e2251177. doi:10.1001/jamanetworkopen.2022.51177

Bailey, C. J., Gross, J. L., Pieters, A., Bastien, A., and List, J. F. (2010). Effect of dapagliflozin in patients with type 2 diabetes who have inadequate glycaemic control with metformin: a randomised, double-blind, placebo-controlled trial. *Lancet* 375 (9733), 2223–2233. doi:10.1016/S0140-6736(10)60407-2

Barnett, A. H., Mithal, A., Manassie, J., Jones, R., Rattunde, H., Woerle, H. J., et al. (2014). Efficacy and safety of empagliflozin added to existing antidiabetes treatment in patients with type 2 diabetes and chronic kidney disease: a randomised, double-blind, placebo-controlled trial. *Lancet Diabetes Endo* 2 (5), 369–384. doi:10.1016/S2213-8587(13)70208-0

Bhatt, D. L., Szarek, M., Pitt, B., Cannon, C. P., Leiter, L. A., McGuire, D. K., et al. (2021b). Sotagliflozin in patients with diabetes and chronic kidney disease. *New Engl. J. Med.* 384 (2), 129–139. doi:10.1056/NEJMoa2030186

Bhatt, D. L., Szarek, M., Steg, P. G., Cannon, C. P., Leiter, L. A., McGuire, D. K., et al. (2021a). Sotagliflozin in patients with diabetes and recent worsening heart failure. *New Engl. J. Med.* 384 (2), 117–128. doi:10.1056/NEJMoa2030183

Brikman, S., and Dori, G. (2020). Sodium glucose cotransporter2 inhibitor-possible treatment for patients with diabetes, pulmonary disease and CO(2) retention. *Med. Hypotheses* 139, 109631. doi:10.1016/j.mehy.2020.109631

Brønden, A., Christensen, M. B., Glintborg, D., Snorgaard, O., Kofoed-Enevoldsen, A., Madsen, G. K., et al. (2023). Effects of DPP-4 inhibitors, GLP-1 receptor agonists, SGLT-2 inhibitors and sulphonylureas on mortality, cardiovascular and renal outcomes in type 2 diabetes: a network meta-analyses-driven approach. *Diabet. Med.* 40 (8), e15157. doi:10.1111/dme.15157

Buse, J. B., Garg, S. K., Rosenstock, J., Bailey, T. S., Banks, P., Bode, B. W., et al. (2018). Sotagliflozin in combination with optimized insulin therapy in adults with type 1 diabetes: the north American inTandem1 study. *Diabetes Care* 41 (9), 1970–1980. doi:10.2337/dc18-0343

Cannon, C. P., Pratley, R., Dagogo-Jack, S., Mancuso, J., Huyck, S., Masiukiewicz, U., et al. (2020). Cardiovascular outcomes with ertugliflozin in type 2 diabetes. *New Engl. J. Med.* 383 (15), 1425–1435. doi:10.1056/NEJMoa2004967

Cefalu, W. T., Leiter, L. A., de Bruin, T. W., Gause-Nilsson, I., Sugg, J., and Parikh, S. J. (2015). Dapagliflozin's effects on glycemia and cardiovascular risk factors in high-risk patients with type 2 diabetes: a 24-week, multicenter, randomized, double-blind, placebo-controlled study with a 28-week extension. *Diabetes Care* 38 (7), 1218–1227. doi:10.2337/dc14-0315

Cherney, D., Ferrannini, E., Umpierrez, G. E., Peters, A. L., Rosenstock, J., Powell, D. R., et al. (2023). Efficacy and safety of sotagliflozin in patients with type 2 diabetes and stage 3 chronic kidney disease. *Diabetes Obes. Metab.* 25 (6), 1646–1657. doi:10.1111/dom.15019

Chowdhury, B., Luu, A. Z., Luu, V. Z., Kabir, M. G., Pan, Y., Teoh, H., et al. (2020). The SGLT2 inhibitor empagliflozin reduces mortality and prevents progression in experimental pulmonary hypertension. *Biochem. Bioph Res. Co.* 524 (1), 50–56. doi:10.1016/j.bbrc.2020.01.015

Giugliano, D., Longo, M., Signoriello, S., Maiorino, M. I., Solerte, B., Chiodini, P., et al. (2022). The effect of DPP-4 inhibitors, GLP-1 receptor agonists and SGLT-2 inhibitors on cardiorenal outcomes: a network meta-analysis of 23 CVOTs. *Cardiovasc Diabetol.* 21 (1), 42. doi:10.1186/s12933-022-01474-z

Grunberger, G., Camp, S., Johnson, J., Huyck, S., Terra, S. G., Mancuso, J. P., et al. (2018). Ertugliflozin in patients with stage 3 chronic kidney disease and type 2 diabetes mellitus: the VERTIS RENAL randomized study. *Diabetes Ther.* 9 (1), 49–66. doi:10.1007/s13300-017-0337-5

Heerspink, H., Stefánsson, B. V., Correa-Rotter, R., Chertow, G. M., Greene, T., Hou, F. F., et al. (2020). Dapagliflozin in patients with chronic kidney disease. *New Engl. J. Med.* 383 (15), 1436–1446. doi:10.1056/NEJMoa2024816

Herrington, W. G., Staplin, N., Wanner, C., Green, J. B., and Hauske, S. J. (2023). Empagliflozin in patients with chronic kidney disease. *New Engl. J. Med.* 388 (2), 117–127. doi:10.1056/NEJMoa2204233

Higgins, J. P., Altman, D. G., Gøtzsche, P. C., Jüni, P., Moher, D., Oxman, A. D., et al. (2011). The Cochrane Collaboration's tool for assessing risk of bias in randomised trials. *Bmj-Brit Med. J.* 343, d5928. doi:10.1136/bmj.d5928

Hutton, B., Salanti, G., Caldwell, D. M., Chaimani, A., Schmid, C. H., Cameron, C., et al. (2015). The PRISMA extension statement for reporting of systematic reviews incorporating network meta-analyses of health care interventions: checklist and explanations. *Ann. Intern Med.* 162 (11), 777–784. doi:10.7326/M14-2385

Januzzi, J. J., Butler, J., Jarolim, P., Sattar, N., Vijapurkar, U., Desai, M., et al. (2017). Effects of canagliflozin on cardiovascular biomarkers in older adults with type 2 diabetes. *J. Am. Coll. Cardiol.* 70 (6), 704–712. doi:10.1016/j.jacc.2017.06.016

Jeong, H. E., Park, S., Noh, Y., Bea, S., Filion, K. B., Yu, O. H. Y., et al. (2023). Association of adverse respiratory events with sodium-glucose cotransporter 2 inhibitors versus dipeptidyl peptidase 4 inhibitors among patients with type 2 diabetes in South Korea: a nationwide cohort study. *Bmc Med.* 21 (1), 47. doi:10.1186/s12916-023-02765-2

Kanie, T., Mizuno, A., Takaoka, Y., Suzuki, T., Yoneoka, D., Nishikawa, Y., et al. (2021). Dipeptidyl peptidase-4 inhibitors, glucagon-like peptide 1 receptor agonists and sodium-glucose co-transporter-2 inhibitors for people with cardiovascular disease: a network meta-analysis. *Cochrane Db Syst. Rev.* 10 (10), CD13650. doi:10.1002/14651858.CD013650.pub2

Kongmalai, T., Hadnorntun, P., Leelahavarong, P., Kongmalai, P., Srinonprasert, V., Chirakarnjanakorn, S., et al. (2023). Comparative cardiovascular benefits of individual SGLT2 inhibitors in type 2 diabetes and heart failure: a systematic review and network meta-analysis of randomized controlled trials. *Front. Endocrinol.* 14, 1216160. doi:10.3389/fendo.2023.1216160

Kosiborod, M. N., Angermann, C. E., Collins, S. P., Teerlink, J. R., Ponikowski, P., Biegus, J., et al. (2022). Effects of empagliflozin on symptoms, physical limitations, and quality of life in patients hospitalized for acute heart failure: results from the EMPULSE trial. *Circulation* 146 (4), 279–288. doi:10.1161/CIRCULATIONAHA.122.059725

Kosiborod, M. N., Esterline, R., Furtado, R., Oscarsson, J., Gasparyan, S. B., Koch, G. G., et al. (2021). Dapagliflozin in patients with cardiometabolic risk factors hospitalised with COVID-19 (DARE-19): a randomised, double-blind, placebo-controlled, phase 3 trial. *Lancet Diabetes Endo* 9 (9), 586–594. doi:10.1016/S2213-8587(21)00180-7

Kovacs, C. S., Seshiah, V., Merker, L., Christiansen, A. V., Roux, F., Salsali, A., et al. (2015). Empagliflozin as add-on therapy to pioglitazone with or without metformin in patients with type 2 diabetes mellitus. *Clin. Ther.* 37 (8), 1773–1788.e1. doi:10.1016/j.clinthera.2015.05.511

Leiter, L. A., Cefalu, W. T., de Bruin, T. W., Xu, J., Parikh, S., Johnsson, E., et al. (2016). Long-term maintenance of efficacy of dapagliflozin in patients with type 2 diabetes mellitus and cardiovascular disease. *Diabetes Obes. Metab.* 18 (8), 766–774. doi:10.1111/dom.12666

Li, H. L., Tse, Y. K., Chandramouli, C., Hon, N. W. L., Cheung, C. L., Lam, L. Y., et al. (2022). Sodium-glucose cotransporter 2 inhibitors and the risk of pneumonia and septic shock. *J. Clin. Endocr. Metab.* 107 (12), 3442–3451. doi:10.1210/clinem/dgac558

Li, J., Zhu, C., Liang, J., Liu, H., and Wang, Z. (2023). Cardiovascular benefits and safety of sotagliflozin in type 2 diabetes mellitus patients with heart failure or cardiovascular risk factors: a Bayesian network meta-analysis. *Front. Pharmacol.* 14, 1303694. doi:10.3389/fphar.2023.1303694

Lin, D. S., Lee, J. K., Hung, C. S., and Chen, W. J. (2021). The efficacy and safety of novel classes of glucose-lowering drugs for cardiovascular outcomes: a network meta-analysis of randomised clinical trials. *Diabetologia* 64 (12), 2676–2686. doi:10.1007/s00125-021-05529-w

Liu, J., Pong, A., Gallo, S., Darekar, A., and Terra, S. G. (2019). Effect of ertugliflozin on blood pressure in patients with type 2 diabetes mellitus: a *post hoc* pooled analysis of randomized controlled trials. *Cardiovasc Diabetol.* 18 (1), 59. doi:10.1186/s12933-019-0856-7

Mashayekhi, M., Safa, B. I., Gonzalez, M., Kim, S. F., and Echouffo-Tcheugui, J. B. (2024). Systemic and organ-specific anti-inflammatory effects of sodium-glucose cotransporter-2 inhibitors. *Trends Endocrin Met.* 35 (5), 425–438. doi:10.1016/j.tem.2024.02.003

McMurray, J., Solomon, S. D., Inzucchi, S. E., Køber, L., Kosiborod, M. N., Martinez, F. A., et al. (2019). Dapagliflozin in patients with heart failure and reduced ejection fraction. *New Engl. J. Med.* 381 (21), 1995–2008. doi:10.1056/NEJMoa1911303

Neal, B., Perkovic, V., Mahaffey, K. W., de Zeeuw, D., Fulcher, G., Erondu, N., et al. (2017). Canagliflozin and cardiovascular and renal events in type 2 diabetes. *New Engl. J. Med.* 377 (7), 644–657. doi:10.1056/NEJMoa1611925

Niu, Y., Zhang, Y., Zhang, W., Lu, J., Chen, Y., Hao, W., et al. (2022). Canagliflozin ameliorates NLRP3 inflammasome-mediated inflammation through inhibiting NF-κB signaling and upregulating bif-1. *Front. Pharmacol.* 13, 820541. doi:10.3389/fphar.2022.820541

Packer, M., Anker, S. D., Butler, J., Filippatos, G., Pocock, S. J., Carson, P., et al. (2020). Cardiovascular and renal outcomes with empagliflozin in heart failure. *New Engl. J. Med.* 383 (15), 1413–1424. doi:10.1056/NEJMoa2022190

Perkovic, V., Jardine, M. J., Neal, B., Bompoint, S., Heerspink, H. J. L., Charytan, D. M., et al. (2019). Canagliflozin and renal outcomes in type 2 diabetes and nephropathy. *New Engl. J. Med.* 380 (24), 2295–2306. doi:10.1056/NEJMoa1811744

Polidori, D., Mari, A., and Ferrannini, E. (2014). Canagliflozin, a sodium glucose co-transporter 2 inhibitor, improves model-based indices of beta cell function in patients with type 2 diabetes. *Diabetologia* 57 (5), 891–901. doi:10.1007/s00125-014-3196-x

Pradhan, R., Lu, S., Yin, H., Yu, O. H. Y., Ernst, P., Suissa, S., et al. (2022). Novel antihyperglycaemic drugs and prevention of chronic obstructive pulmonary disease exacerbations among patients with type 2 diabetes: population based cohort study. *Bmj-Brit Med. J.* 379, e071380. doi:10.1136/bmj-2022-071380

Preda, A., Montecucco, F., Carbone, F., Camici, G. G., Lüscher, T. F., Kraler, S., et al. (2024). SGLT2 inhibitors: from glucose-lowering to cardiovascular benefits. *Cardiovasc Res.* 120 (5), 443–460. doi:10.1093/cvr/cvae047

Qiu, M., Wei, W., Wei, X. B., and Liu, S. Y. (2022). Updated network meta-analysis assessing the relative efficacy of 13 GLP-1 RA and SGLT2 inhibitor interventions on cardiorenal and mortality outcomes in type 2 diabetes. *Eur. J. Clin. Pharmacol.* 78 (4), 695–697. doi:10.1007/s00228-021-03261-3

Solomon, S. D., McMurray, J., Claggett, B., de Boer, R. A., DeMets, D., Hernandez, A. F., et al. (2022). Dapagliflozin in heart failure with mildly reduced or preserved ejection fraction. *New Engl. J. Med.* 387 (12), 1089–1098. doi:10.1056/NEJMoa2206286

Spertus, J. A., Birmingham, M. C., Nassif, M., Damaraju, C. V., Abbate, A., Butler, J., et al. (2022). The SGLT2 inhibitor canagliflozin in heart failure: the CHIEF-HF remote, patient-centered randomized trial. *Nat. Med.* 28 (4), 809–813. doi:10.1038/s41591-022-01703-8

Tabaa, M., Fattah, A., Shaalan, M., Rashad, E., and El, M. N. (2022). Dapagliflozin mitigates ovalbumin-prompted airway inflammatory-oxidative successions and associated bronchospasm in a rat model of allergic asthma. *Expert Opin. Ther. Tar* 26 (5), 487–506. doi:10.1080/14728222.2022.2077723

Tornyos, D., Meuer, M., Lukács, R., El Alaoui El Abdallaoui, O., Kupó, P., Faludi, R., et al. (2022). Cardiovascular outcomes in patients treated with sodium-glucose transport protein 2 inhibitors, a network meta-analysis of randomized trials. *Front. Cardiovasc Med.* 9, 1041200. doi:10.3389/fcvm.2022.1041200

Tuttle, K. R., Levin, A., Nangaku, M., Kadowaki, T., Agarwal, R., Hauske, S. J., et al. (2022). Safety of empagliflozin in patients with type 2 diabetes and chronic kidney disease: pooled analysis of placebo-controlled clinical trials. *Diabetes Care* 45 (6), 1445–1452. doi:10.2337/dc21-2034

Voors, A. A., Angermann, C. E., Teerlink, J. R., Collins, S. P., Kosiborod, M., Biegus, J., et al. (2022). The SGLT2 inhibitor empagliflozin in patients hospitalized for acute heart failure: a multinational randomized trial. *Nat. Med.* 28 (3), 568–574. doi:10.1038/s41591-021-01659-1

Wang, A., Tang, H., Zhang, N., and Feng, X. (2022). Association between novel Glucose-Lowering drugs and risk of Asthma: a network Meta-Analysis of cardiorenal outcome trials. *Diabetes Res. Clin. P. R.* 183, 109080. doi:10.1016/j.diabres.2021.109080

Wang, Y., and Zhou, X. (2024). The relationship between use of SGLT2is and incidence of respiratory and infectious diseases and site-specific fractures: a meta-analysis based on 32 large RCTs. *Eur. J. Clin. Pharmacol.* 80, 563–573. doi:10.1007/s00228-024-03631-7

Wilding, J. P., Woo, V., Soler, N. G., Pahor, A., Sugg, J., Rohwedder, K., et al. (2012). Long-term efficacy of dapagliflozin in patients with type 2 diabetes mellitus receiving high doses of insulin: a randomized trial. *Ann. Intern Med.* 156 (6), 405–415. doi:10.7326/0003-4819-156-6-201203200-00003

Wiviott, S. D., Raz, I., Bonaca, M. P., Mosenzon, O., Kato, E. T., Cahn, A., et al. (2019). Dapagliflozin and cardiovascular outcomes in type 2 diabetes. *New Engl. J. Med.* 380 (4), 347–357. doi:10.1056/NEJMoa1812389

Wu, M. Z., Chandramouli, C., Wong, P. F., Chan, Y. H., Li, H. L., Yu, S. Y., et al. (2022). Risk of sepsis and pneumonia in patients initiated on SGLT2 inhibitors and DPP-4 inhibitors. *Diabetes Metab.* 48 (6), 101367. doi:10.1016/j.diabet.2022.101367

Xiao, Y., Peng, S., and Liu, C. (2024). Association of SGLT2is with respiratory and skin diseases. *Endocrine*. doi:10.1007/s12020-024-03739-x

Yin, D. G., Qiu, M., and Duan, X. Y. (2021). Association between SGLT2is and cardiovascular and respiratory diseases: a meta-analysis of large trials. *Front. Pharmacol.* 12, 724405. doi:10.3389/fphar.2021.724405

Zhang, Y., Jiang, L., Wang, J., Wang, T., Chien, C., Huang, W., et al. (2022). Network meta-analysis on the effects of finerenone versus SGLT2 inhibitors and GLP-1 receptor agonists on cardiovascular and renal outcomes in patients with type 2 diabetes mellitus and chronic kidney disease. *Cardiovasc Diabetol.* 21 (1), 232. doi:10.1186/s12933-022-01676-5

Zinman, B., Wanner, C., Lachin, J. M., Fitchett, D., Bluhmki, E., Hantel, S., et al. (2015). Empagliflozin, cardiovascular outcomes, and mortality in type 2 diabetes. *New Engl. J. Med.* 373 (22), 2117–2128. doi:10.1056/NEJMoa1504720

frontiers | Frontiers in Pharmacology

TYPE Review
PUBLISHED 14 June 2024
DOI 10.3389/fphar.2024.1422740



OPEN ACCESS

EDITED BY
Anca Hermenean,
Vasile Goldis Western University of Arad, Romania

REVIEWED BY
Danila Gurgone,
University of Glasgow, United Kingdom
Era Gorica,
University of Zurich, Switzerland

*CORRESPONDENCE
Donato Cappetta,
donato.cappetta@unisalento.it

†These authors have contributed equally to this work

RECEIVED 24 April 2024
ACCEPTED 21 May 2024
PUBLISHED 14 June 2024

CITATION
Riemma MA, Mele E, Donniacuo M, Telesca M, Bellocchio G, Castaldo G, Rossi F, De Angelis A, Cappetta D, Urbanek K and Berrino L (2024), Glucagon-like peptide-1 receptor agonists and sodium-glucose cotransporter 2 inhibitors, anti-diabetic drugs in heart failure and cognitive impairment: potential mechanisms of the protective effects.
*Front. Pharmacol.* 15:1422740.
doi: 10.3389/fphar.2024.1422740



# Glucagon-like peptide-1 receptor agonists and sodium-glucose cotransporter 2 inhibitors, anti-diabetic drugs in heart failure and cognitive impairment: potential mechanisms of the protective effects

Maria Antonietta Riemma[1†], Elena Mele[1†], Maria Donniacuo[2], Marialucia Telesca[1], Gabriella Bellocchio[1], Giuseppe Castaldo[3,4], Francesco Rossi[1], Antonella De Angelis[1], Donato Cappetta[2*], Konrad Urbanek[3,4†] and Liberato Berrino[1†]

[1]Department of Experimental Medicine, University of Campania "Luigi Vanvitelli", Naples, Italy, [2]Department of Biological and Environmental Sciences and Technologies, University of Salento, Lecce, Italy, [3]Department of Molecular Medicine and Medical Biotechnologies, University of Naples "Federico II", Naples, Italy, [4]CEINGE-Advanced Biotechnologies, Naples, Italy

Heart failure and cognitive impairment emerge as public health problems that need to be addressed due to the aging global population. The conditions that often coexist are strongly related to advancing age and multimorbidity. Epidemiological evidence indicates that cardiovascular disease and neurodegenerative processes shares similar aspects, in term of prevalence, age distribution, and mortality. Type 2 diabetes increasingly represents a risk factor associated not only to cardiometabolic pathologies but also to neurological conditions. The pathophysiological features of type 2 diabetes and its metabolic complications (hyperglycemia, hyperinsulinemia, and insulin resistance) play a crucial role in the development and progression of both heart failure and cognitive dysfunction. This connection has opened to a potential new strategy, in which new classes of anti-diabetic medications, such as glucagon-like peptide-1 receptor (GLP-1R) agonists and sodium-glucose cotransporter 2 (SGLT2) inhibitors, are able to reduce the overall risk of cardiovascular events and neuronal damage, showing additional protective effects beyond glycemic control. The pleiotropic effects of GLP-1R agonists and SGLT2 inhibitors have been extensively investigated. They exert direct and indirect cardioprotective and neuroprotective actions, by reducing inflammation, oxidative stress, ions

**Abbreviations:** DPP-4, protease dipeptidyl peptidase 4; GIP, glucose-dependent insulinotropic polypeptide; GLP-1, glucagon-like peptide-1; GLP-1R, glucagon-like peptide-1 receptor; HF, heart failure; HFpEF, heart failure with preserved ejection fraction; HFrEF, heart failure with reduced ejection fraction; IL, interleukin; INa, sodium current; mTOR, mammalian target of rapamycin; NCX, sodium/calcium exchanger; NF-κB, nuclear factor-κB; **NHE-1**, sodium/hydrogen exchanger-1; **NLRP3**, NLR family pyrin domain containing 3 inflammasome; **RAAS**, renin-angiotensin-aldosterone system; **ROS**, reactive oxygen species; **SGLT2**, sodium-glucose cotransporter 2; **TNF-α**, tumor necrosis factor-α.

overload, and restoring insulin signaling. Nonetheless, the specificity of pathways and their contribution has not been fully elucidated, and this underlines the urgency for more comprehensive research.

KEYWORDS

heart failure, cognitive impairment, type 2 diabetes, glucagon-like peptide-1 receptor agonists, sodium-glucose cotransporter 2 inhibitors

# 1 Introduction

Heart failure (HF) and cognitive impairment are two common health conditions that often coexist in the general population (Virani et al., 2021). Both syndromes affecting cardiac and cognitive functions loom as public health problems in the coming decades due to the aging global population (Patnode et al., 2020; Díez-Villanueva et al., 2021).

HF is a clinical syndrome with symptoms and/or signs caused by a structural and/or functional cardiac abnormality affecting more than 60 million people worldwide (Groenewegen et al., 2020). Nearly half of the patients with HF are diagnosed with HF with preserved ejection fraction (HFpEF), a subclass of HF in which patients are more likely to be older and female, with multiple chronic comorbidities, such as hypertension, type 2 diabetes, and obesity (Owan et al., 2006; Dunlay et al., 2017). In addition to traditional comorbidities, cognitive impairment, which represents an independent risk factor for HF, significantly increases the hospitalization and mortality, and decreases quality of life of patients with HF (Dodson et al., 2013; Vellone et al., 2020).

Epidemiological evidence indicates that neurodegenerative processes share similar profiles with HF, in term of prevalence, age distribution, and mortality (Pappolla et al., 2003; Razay et al., 2007). Cognitive impairment encompasses a range of cognitive functions, including memory, attention, understanding, reasoning, problem-solving, decision-making, and language production (Murman, 2015). Interestingly, HF represents *per se* a risk factor for developing dementia (Qiu et al., 2006). Particularly prevalent in those over 70, where it reaches up to 10%, HF has long been recognized as a potential cause of cognitive dysfunction, sometimes referred to as cardiogenic dementia (Cardiogenic dementia, 1977; Liu et al., 2024). On the other hand, these syndromes can occur independently. The relationship between HF and cognitive impairment stems from partly common background. Age, metabolic disorders, genetic profile, or dysfunctional neuroendocrine systems are capable to affect both systems (Packer, 2018; Nguyen et al., 2020).

In this review, we will provide an overview of physiological connections between heart and brain. In particular, we will discuss the impact of metabolic disorders in affecting HF and cognitive function, and the implication of clinical treatments, focusing on paramount effects of new antidiabetic drugs.

# 2 A common milieu of metabolic disorders in heart failure and cognitive impairment

## 2.1 Heart failure

According to epidemiologic analyses, HF is highly prevalent in patients with type 2 diabetes, who are at a higher risk (up to 2-fold in men and 4-fold in women) of developing HF than patients without diabetes (Dunlay et al., 2019). However, it is important to note that type 2 diabetes, obesity, and metabolic dysfunction may specifically increase the likelihood of developing HFpEF more than HF with reduced ejection fraction (HFrEF) (Samson et al., 2016). Evidence from community-based cohorts has shown that higher body mass index and insulin resistance may be strongly associated with future HFpEF, especially among women (Savji et al., 2018). Furthermore, a sedentary lifestyle is associated with a greater risk of HFpEF compared with HFrEF (Pandey et al., 2016).

Several pathophysiological mechanisms linking type 2 diabetes and HF are recognized, with hyperglycemia, hyperinsulinemia, and insulin resistance known to initiate and perpetuate disease progression. Impairment in glucose metabolism, alterations of nitric oxide signaling, and reactive oxygen species (ROS) accumulation with mounting oxidative stress are among mechanisms underlying both micro- and macrovasculopathy, and diabetic cardiomyopathy with cardiac hypertrophy and fibrosis (Kolwicz and Tian, 2011; Piperi et al., 2015). Of note, insulin resistance is emerging as a major risk factor for the development of HF (Aroor et al., 2012a).

In this context, a prominent feature is functional alteration of mitochondria—the major source of intracellular ROS that compromise insulin signaling (Kim et al., 2008; Aroor et al., 2012b). In diabetic patients, ATP production relies even more on fatty acid oxidation rather than glycolysis (Lopaschuk, 2016). This process disrupts the oxidative phosphorylation and produces more ROS causing oxidative damage to cellular proteins and lipids (Gollmer et al., 2020). Changes in mitochondrial bioenergetics also affect myocardial ion handling resulting in cytosolic sodium and calcium overload (Trost et al., 2002; Bers, 2006). Abnormalities in the expression or activity of ryanodin receptor, sarcoplasmic endoplasmic reticulum $Ca^{2+}$-ATPase, and sodium/calcium exchanger (NCX), reported in HF and diabetic cardiomyopathy, contribute to myocardial cell death, cardiac fibrosis, and diastolic dysfunction (Lebeche et al., 2008; Tuunanen and Knuuti, 2011).

In patients with type 2 diabetes, systemic chronic inflammation, caused by hyperglycemia and insulin resistance, participates in the development of vascular complications, and contributes to HF (Tsalamandris et al., 2019). Activation of nuclear factor-κB (NF-κB) results in downstream pro-inflammatory cytokine release, such as tumor necrosis factor-α (TNF-α), interleukin (IL)-6, and IL-1β, which amplify ROS-induced myocardial stress further promoting adverse remodeling, fibrosis, and myocardial dysfunction (Brasier, 2010; Jia et al., 2018).

The activation of renin-angiotensin-aldosterone system (RAAS) is associated with insulin resistance as well (Lastra et al., 2010). Upregulation of angiotensin II can activate NADPH oxidase enzyme

complex in vascular smooth muscle cells and cardiomyocytes, further increasing the generation of ROS and participating in the progression of HF (Doughan et al., 2008). In addition, aldosterone, released upon the action of angiotensin II and sympathetic nervous system hyperactivation, reduces insulin sensitivity in several cell types triggering maladaptive responses in type 2 diabetes, hypertension, and HF (Aroor et al., 2012a). This is only a general outline, and excellent detailed reviews are available. However, the effective role of key pathways in the pathogenesis of cardiometabolic HF is still understudied and require further investigation. Understanding these mechanisms is crucial, as it can lead to the development of targeted interventions aimed at preserving cardiovascular health in individuals with type 2 diabetes.

## 2.2 Cognitive impairment

Cognitive impairment is generally referred to Alzheimer's disease and vascular dementia, recognized as the two most prevalent causes of dementia that affects about 50 million people worldwide, with cases projected to triple by 2050 (GBD, 2016 Dementia Collaborators, 2019; Ou et al., 2024). Type 2 diabetes has increasingly represented a risk factor associated not only to cardiometabolic pathologies but also to neurological conditions, highlighting its negative impact on cognitive function (Banday et al., 2020; Tomic et al., 2022). Hyperglycemia in diabetic patients is a risk factor for Alzheimer's disease that is also called "type 3 diabetes" (Barone et al., 2021).

The relationship between type 2 diabetes and cognitive impairment is multifaceted and intricate. Although exact mechanisms are still unknown, several potential pathways have emerged. The combination of vascular damage and neurodegeneration represents the main postulated mechanism underlying the development of cognitive impairment in patients with type 2 diabetes or HF (Dao et al., 2023). Chronic hyperglycemia and hyperinsulinemia drive a metabolic imbalance promoting oxidative stress, inflammation, and endothelial damage, responsible for non-enzymatic biomolecule glycation, accelerating cerebrovascular atherosclerosis and neurodegenerative damage that further promote cognitive dysfunction and dementia (Barone et al., 2021; Kopp et al., 2022). Under physiologic conditions, insulin promotes amyloid-β protein clearance thereby preventing its accumulation (Mullins et al., 2017). Alteration in insulin signaling may accelerate the onset of Alzheimer's disease, by changing the intracellular concentration of neurotransmitters involved in memory formation and functioning, and influencing on amyloid-β-related processes and amyloid clearance (Craft, 2007; Spinelli et al., 2019; Rizzo et al., 2022). Additionally, insulin resistance increases the number of neuritic plaques by affecting tau phosphorylation, widely considered a pivotal pathological hallmark in Alzheimer's disease (Wegmann et al., 2021).

Experimental studies provide strong evidence that insulin resistance-related neuroinflammation feeds cognitive impairment neuropathology, leading to a raised-up brain levels of pro-inflammatory cytokines (Mullins et al., 2017; Denver et al., 2018). Hyperphosphorylation of tau triggers pro-inflammatory signaling cascades, as a consequence of vascular inflammation and vasoconstriction (Paris et al., 2000). Activated microglia drive the immune response to the inflammatory state releasing immune signaling molecules (cytokines, and chemokines), and inducing neuronal cell death (Calsolaro and Edison, 2016).

These data underline the importance of optimal glycemic control and call for major pharmacological interventions to reduce the risk of cardiometabolic-related cognitive impairment.

The pathophysiological overlap between cardiometabolic HF and cognitive impairment opens to reasonable possibility that new successful pharmacological approaches used in type 2 diabetes may be beneficial for cardiovascular and neurological diseases. Indeed, there is growing interest in the potential of new classes of anti-diabetic medications such as glucagon-like peptide-1 receptor (GLP-1R) agonists and sodium-glucose cotransporter 2 (SGLT2) inhibitors, to reduce the risk of cardiovascular events and slow down the progression of neuronal damage. Notably, these drugs not only act on the glycemic control, but also show protective effects independently of their anti-diabetic effect (Table 1, Figure 1).

# 3 Glucagon-like peptide-1 receptor agonists

Glucagon-like peptide-1 (GLP-1) represents a particular incretin that has generated a lot of interest. Discovered for the first time in 1987, GLP-1 is an intestinal gut hormone that is secreted in response to food intake and potentiates the glucose-dependent insulin secretion from pancreatic β-cells (Drucker et al., 1987). It acts by binding to the G protein-coupled receptor GLP-1 receptor (GLP-1R). In addition to metabolic effects (promotion of insulin secretion, inhibition of appetite, reduction of gastric emptying, and increase of natriuretic and diuretic processes), experimental studies have pointed out the cardio- and neuroprotective effects of GLP-1 (During et al., 2003; Bendotti et al., 2022; Yang et al., 2022). GLP-1 is a labile peptide and is rapidly removed from circulation by enzymatic degradation by the serine protease dipeptidyl peptidase (DPP)-4. The therapeutic approach to target the incretin system for the treatment of type 2 diabetes involves the use of GLP-1 agonists or DPP-4 inhibitors to increase the levels of endogenous GLP-1 (Cosentino et al., 2020).

In addition to pancreatic localization, GLP-1R has been found in the gastrointestinal system, kidneys, central nervous system, and cardiovascular system (Pyke et al., 2014). The additional non-glycemic effect related to incretins may be linked to extra-pancreatic tissue localization of GLP-1R.

GLP-1R agonists are classified on their molecular backbone derived either from human GLP-1 (liraglutide, semaglutide, and dulaglutide) or from exendin-4 (exenatide and lixisenatide), a salivary gland hormone from the Gila monster lizard (Colin et al., 2023). In addition, a dual GLP-1/glucose-dependent insulinotropic polypeptide (GIP) co-agonist, tirzepatide, has been recently developed for the treatment of type 2 diabetes and obesity (Jakubowska et al., 2024). GIP is an incretin hormone secreted by small intestine in response to luminal presence of nutrients (Deacon and Ahrén, 2011). It stimulates insulin secretion, facilitates fat deposition, promotes bone formation and may be involved in memory formation and control of appetite (Seino et al., 2010). Changes in GIP secretion could contribute to the loss of incretin effect observed in patients with type 2 diabetes (Holst et al., 2011).

TABLE 1 Summary of cardioprotective and neuroprotective mechanisms by GLP-1R agonists and SGLT2 inhibitors.

| Site of action | GLP-1R agonists | SGLT2 inhibitors |
|---|---|---|
| **Heart** | Increasing of atrial natriuretic peptide and nitric oxide, reduction of blood pressure (Kim et al., 2013; Richards et al., 2014; Drucker, 2016; Baggio et al., 2018; Pandey et al., 2023) | Increasing of diuresis and natriuresis, reduction of blood pressure (Mazidi et al., 2017; Dominguez Rieg and Rieg, 2019) |
| | Suppression of oxidative stress (Drucker, 2016; Helmstädter et al., 2020; Baylan et al., 2022) | Suppression of oxidative stress (Frati et al., 2017; Checa and Aran, 2020; Chen et al., 2022; Elrakaybi et al., 2022) |
| | Inhibition of pro-inflammatory cytokines, NLRP3 inflammasome, promotion of M2 macrophage phenotype (Hogan et al., 2014; Bułdak et al., 2016; Bruen et al., 2017; Luo et al., 2019; Yu et al., 2019; Püschel et al., 2022) | Inhibition of pro-inflammatory cytokines, NLRP3 inflammasome, promotion of M2 macrophage phenotype (Lee et al., 2017; Ye et al., 2017; Byrne et al., 2020; Kim et al., 2020) |
| | Energetic shift from fatty acid to glucose oxidation (Bao et al., 2011) | Modulation of myocardial hypertrophy and fibrosis (Bay et al., 2013; Croteau et al., 2021) |
| | Activation of SIRT1 signaling (Luo et al., 2019) | Regulation of sodium and calcium homeostasis (Cappetta et al., 2020; Uthman et al., 2022) |
| | Inhibition of RAAS pathway (Kim et al., 2013; Jensen et al., 2020; Martins et al., 2020) | Inhibition of RAAS and sympathetic neurohormonal pathways (Salvatore et al., 2022) |
| **Brain** | Reduction of neuroinflammation, decrease of microglia activation, promotion of M2 macrophage phenotype (Hogan et al., 2014; Bułdak et al., 2016; Bruen et al., 2017; Yu et al., 2019; Zhang et al., 2021a; Püschel et al., 2022) | Reduction of NLRP3 inflammasome, decrease of microglia activation, promotion of M2 macrophage phenotype (Lin et al., 2014; Iannantuoni et al., 2019; Xu et al., 2019; Lee et al., 2020; Lonnemann et al., 2020; Lee et al., 2021; Khedr et al., 2024) |
| | Reduction of amyloid-β plaque deposition and tau hyperphosphorylation (Li et al., 2012; Long-Smith et al., 2013; McClean and Hölscher, 2014; McClean et al., 2015; Cai et al., 2018) | Reduction of amyloid-β plaque deposition and tau hyperphosphorylation (Huang et al., 2016; Cenini and Voos, 2019; Lonnemann et al., 2020) |
| | Activation of brain-derived neurotrophic factor (Du et al., 2022) | Activition of brain-derived neurotrophic factor (Arab et al., 2021) |
| | Enhancement glucose metabolism (Bomba et al., 2013; Zheng et al., 2021) | Interference with mTOR signaling (Packer, 2020; Stanciu et al., 2021; Samman et al., 2023) |

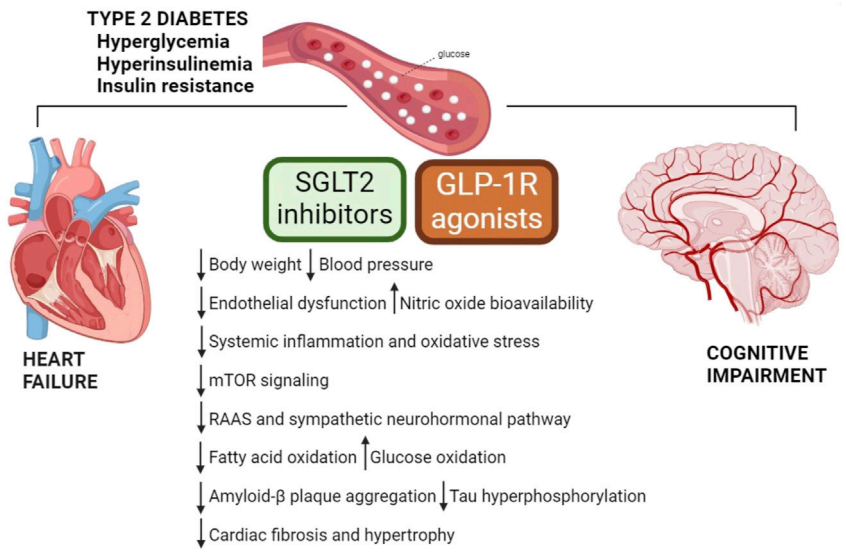


FIGURE 1
Mechanisms underlying favorable effects of GLP-1R agonists and SGLT2 inhibitors. Metabolic complications play a crucial role in the development and progression of HF and cognitive dysfunction. GLP-1R agonists and SGLT2 inhibitors exert direct and indirect cardioprotective and neuroprotective actions, and their benefits lay beyond glycemic control. GLP-1R, glucagon-like peptide-1 receptor; mTOR, mammalian target of rapamycin; RAAS, renin-angiotensin-aldosterone system; SGLT2, sodium-glucose cotransporter 2.

GLP-1R agonists are known to significantly decrease the cardiovascular risk of diabetic patients, while they are currently being investigated to determine their potential efficacy for neurodegenerative diseases associated to cardiometabolic pathology.

## 3.1 GLP-1R agonists in the cardiovascular system

GLP-1R is expressed in the heart and vasculature, raising the possibility that GLP-1 might have both direct and indirect actions on the cardiovascular system (Ussher and Drucker, 2023). GLP-1R expression has been found in both the atria and ventricles (Baggio et al., 2018). Its regulation contributes to the reduction of blood pressure through the secretion of atrial natriuretic peptide or by regulating the availability of nitric oxide (Pandey et al., 2023). GLP-1 and its receptor agonists have been shown to reduce endothelial inflammation and oxidative stress, through the activation of nitric oxide production, crucial for maintaining healthy vascular tone and function (Drucker, 2016).

Incretin-based therapies has evidenced a reduced cardiovascular risk in high-risk individuals with type 2 diabetes, independent of the need for additional glucose control. Among GLP-1R agonists, liraglutide, semaglutide, and dulaglutide are widely available with licensed indications for the prevention of cardiovascular disease (Marx et al., 2022).

However, understanding how activation of the GLP-1R contributes to myocardial protection and decreases cardiac injury is challenging.

GLP-1R activation reduces blood pressure, as shown in experimental models of hypertension (Hirata et al., 2009; Laugero et al., 2009). The anti-hypertensive effect of GLP-1R agonists has been observed with liraglutide that is able to mediate atrial natriuretic peptide secretion from atrial cardiomyocytes, thus lowering systolic and diastolic blood pressure increased by angiotensin II (Kim et al., 2013). In addition, it has been demonstrated the specific involvement of endothelial GLP-1R in contributing to the anti-hypertensive effects by controlling nitric oxide bioavailability (Richards et al., 2014; Baggio et al., 2018). Liraglutide shows efficacy in experimental arterial hypertension, independently of glycemic control. Mechanistically, liraglutide suppresses the angiotensin II-induced inflammatory cascade and oxidative stress in the vascular wall, leading to reduced expression of adhesion molecules at endothelial level. As a result, function of endothelial nitric oxide synthase is preserved, thus restoring nitric oxide level (Helmstädter et al., 2020; Baylan et al., 2022). Additionally, the relevant effect of GLP-1R signaling on blood pressure control may be attributable to the action of agonists on sodium reabsorption in the proximal tubule, and interference with intrarenal angiotensin II, thus augmenting renal blood flow and promoting natriuresis (Jensen et al., 2020; Martins et al., 2020).

Reduced cardiac and vascular inflammation has been well documented for GLP-1R agonists in experimental and human studies (Drucker, 2016). Liraglutide lowers vascular dysfunction and systemic inflammation in a lipopolysaccharide-induced sepsis model, by normalizing the expression of adhesion molecules and cytokines (Steven et al., 2015). Interestingly, in GLP-1R-deficient mice, liraglutide loses its beneficial effects (Steven et al., 2017). In regulating the response to inflammation of the endothelium, dulaglutide counteracts high glucose-induced activation of the NLR family pyrin domain containing 3 (NLRP3) inflammasome and suppresses maturation and release of IL-1β and IL-18; the lack of effects of dulaglutide on endothelial inflammation by SIRT1 siRNA evidences the involvement of SIRT1 pathway in this process (Luo et al., 2019). In human peripheral blood cells, liraglutide has been reported to decrease the production of pro-inflammatory cytokines (TNF-α, IL-1β, and IL-6), and activation of macrophages (Hogan et al., 2014; Bruen et al., 2017). Under pathological stress, the role of macrophages in inflammatory responses, which drive insulin resistance and diabetes, is significant (Püschel et al., 2022). In this regard, GLP-1R agonists (i.e., exenatide) improve insulin resistance suppressing pro-inflammatory phenotypes of monocytes/macrophages, and directly modulating NF-κB activation and IL-1β, IL-6, and TNF-α expression (Bułdak et al., 2016; Yu et al., 2019).

Data suggests that GLP-1R-dependent cardioprotection may also result from effects on cardiac energetic metabolism. In ischemia–reperfusion model, albiglutide promotes energetic shift from fatty acid to glucose oxidation, reducing myocardial infarct size and improving contractile function (Bao et al., 2011). Likewise, liraglutide increases myocardial glucose oxidation, and alleviates diastolic dysfunction in mice subjected to experimental diabetic cardiomyopathy (Almutairi et al., 2021).

Dual GLP-1R/GIP receptor agonists co-stimulate both GLP-1R and GIP receptor, and enhance insulinotropic and antihyperglycemic effects compared with selective GLP-1R agonists (Finan et al., 2013). Tirzepatide is the only approved incretin multi-agonist. It has been proven superior to single GLP-1R agonist or insulin analog treatments in reducing blood glucose, body mass index, and weight (Dutta et al., 2021). Tirzepatide has been associated with improvements in lipoprotein profiles, blood pressure, and inflammation, although favorable effects on cardiovascular risk factors have been reported in only a single clinical trial (Wilson et al., 2020; Del et al., 2021).

Triple agonists are unimolecular peptide drugs that target GLP-1R, GIP receptor, and glucagone receptor, developed primarily for treating metabolic diseases (Knerr et al., 2022). Preclinical data available so far have highlighted metabolic efficacy and its superior performance to dual agonists in reducing cardiovascular risk factors, such as plasma glucose levels, and body weight (Finan et al., 2015; Knerr et al., 2022).

The above findings underscore the potential of GLP-1R agonists as efficacious and safe drugs with pleiotropic activities on cardiovascular system that are independent of their glycemic control effects emphasizing cardiovascular outcomes as one of the primary goals in the management of type 2 diabetes.

## 3.2 GLP-1R agonists in the central nervous system

GLP-1R, expressed in endothelial cells, microglia, astrocytes, and neurons, is widely distributed in the hypothalamus, cortex, subventricular zone, and substantia nigra (Hamilton and Holscher, 2009; Cork et al., 2015; Reich and Hölscher, 2022). GLP-1R overexpression has been found in neurons, microglia, and

endothelial cells, where is correlated to low level of inflammation and improved cognitive function (Du et al., 2022). GLP-1R activation, by stimulating adenylyl cyclase and consequently elevating cyclic adenosine monophosphate levels, enhance neuroprotective signaling through upregulation of anti-inflammatory and anti-apoptotic signaling (Holz, 2004; Delghandi et al., 2005; Robichaux and Cheng, 2018; Wicinski et al., 2019; Mehdi et al., 2023).

Pharmacological approaches able to promote healthy incretin and insulin signaling in the brain may represent a potential direction for neurodegenerative disease treatment. Clinical trials have pointed out a neuroprotective effect and an improvement of clinical outcome for some anti-diabetic treatments, translating them into new therapies against neurodegenerative conditions, such as Alzheimer's disease, dementia, or Parkinson's disease (Green et al., 2019; Kopp et al., 2022; Colin et al., 2023).

GLP-1R agonists cross the blood-brain barrier and have been widely tested in preclinical studies as therapeutic option for neuroinflammation and neurodegeneration. In an experimental model of Alzheimer's disease, liraglutide exerts neuronal anti-inflammatory effects, decreasing the number of activated microglia cells in the hippocampus, and astrocyte in the cortex as well as reducing the expression of pro-inflammatory cytokines (IL-6, IL-12, and IL-1β). It also shows properties as growth and differentiation factor, increasing stem cell proliferation and differentiation into mature neurons (Parthsarathy and Holscher, 2013; Batista et al., 2018). In a model of cognitive impairment associated to neuropathic pain, the inhibition of GLP-1/GLP-R axis increases the expression of pro-inflammatory cytokines IL-1β and TNF-α, while exenatide treatment prevents the phosphorylation of NF-κB and decreases inflammatory burden (Zhang LQ. et al., 2021).

GLP-1 activation can reduce the pathological process of amyloid-β plaque aggregation/deposition and tau hyperphosphorylation enhanced by neuroinflammation, thus preventing age-related neurodegenerative changes, such as decline of learning and memory (Li et al., 2012). Lixisenatide is a long-lasting GLP-1R agonist that crosses blood-brain barrier at very low doses (Hunter and Holscher, 2012). In a mouse model of Alzheimer's disease, it reduces amyloid-β plaques, tau neurofibrillary tangles, and neuroinflammation, by activating CREB pathway and inhibiting p38/MAPK signaling (Cai et al., 2018). A large body of evidence reports a beneficial effect of liraglutide on amyloid pathology. The drug, as prophylactic or long-term treatments, significantly reduces amyloid-β plaque size, number, and load (Long-Smith et al., 2013; McClean and Hölscher, 2014; McClean et al., 2015). Both liraglutide and dulaglutide ameliorate impaired learning and memory ability limiting tau hyperphosphorylation and neurofilament aggregates through the modulation of JNK or Akt activity (Qi et al., 2016; Chen et al., 2017; Zhou et al., 2019).

Neuronal apoptosis, induced by plaque deposition and stress, is a pathophysiological marker in cognitive impairment (Engidawork et al., 2001). In a mouse model of Parkinson's disease, both lixisenatide and liraglitude are associated with neuroprotective benefits and reduced motor impairment by decreasing pro-apoptotic BAX signaling and increasing expression of anti-apoptotic Bcl-2 (Liu et al., 2015). Likewise, the neuroprotective effect of semaglutide involves modulation of apoptotic signaling (Chang et al., 2020).

GLP-1R agonists may also exert their neuroprotective action increasing level and activity of brain-derived neurotrophic factor, regulating calcium homeostasis, promoting glycolysis, and reducing vascular damage (Du et al., 2022). Of note, it has been shown that liraglutide improves learning and memory as well as cognitive function by regulating intracellular calcium homeostasis in cortical or hippocampal pyramidal cells (Wang et al., 2013). Moreover, both exenatide and liraglutide enhance glucose metabolism and aerobic glycolysis by increasing brain lactate dehydrogenase activity (Bomba et al., 2013; Zheng et al., 2021).

Dual GLP-1R/GIP receptor agonists exert anti-neuroinflammatory and anti-neurodegenerative benefits in preclinical studies and improve memory function, synaptic health, and neurogenesis (Pathak et al., 2018; Zhang et al., 2020). Interestingly, the dual agonist tirzepatide has shown efficacy in neuroprotection, by counteracting hyperglycemia and insulin resistance-related effects at the neuronal level (Fontanella et al., 2024).

Also triple agonists have demonstrated to possess anti-neurodegenerative properties, indicating a potential for treating Alzheimer's disease by reducing neuroinflammation and oxidative stress, enhancing neuronal health and viability, and minimizing glutamate excitotoxicity (Kopp et al., 2022). In mouse models of Alzheimer's disease, triple agonists play a neuroprotective role and ameliorate cognitive deficits by significantly reducing hippocampal amyloid-β, phosphorylated tau aggregates, and neuroinflammation, and stimulating neurogenesis and brain-derived neurotrophic factor expression (Li et al., 2018; Tai et al., 2018).

All these experimental data support the potential benefit of this drug class to translate neuroprotective properties from cellular and animal studies to humans. Although several clinical trials have been completed or are currently underway, repurposing GLP-1R agonists to treat cardiometabolic syndrome-related neurodegenerative diseases will require additional research to confirm safety and efficacy.

## 4 Sodium/glucose co-transporter 2 inhibitors

Sodium/glucose co-transporter 2 (SGLT2) inhibitors or gliflozins represent a new class of approved oral anti-hyperglycemic drugs widely used in clinical practice for the treatment of type 2 diabetes, alone or in association with metformin (Kalra, 2014; Nauck, 2014). Their main mechanism of action consists in the inhibition of SGLT receptors, of which two different isoforms are known, SGLT1 and SGLT2. SGLTs are membrane proteins that act as co-transporters of glucose and sodium in the cell, and their expression and function have been detected in many organs of the body (Pandey and Tamrakar, 2019; Koepsell, 2020). Selective SGLT2 inhibitors block glucose reabsorption in the proximal renal tubule, increasing glucose elimination and reducing hyperglycemia. They improve both insulin secretion by β-cells and peripheral insulin sensitivity (Ni et al., 2020).

Dapagliflozin, empagliflozin, and ertugliflozin are the most selective SGLT2 inhibitors (Ferrannini, 2017). Sotagliflozin,

referred to as a dual SGLT1/2 inhibitor, has the highest affinity for SGLT1 (Markham and Keam, 2019), while canagliflozin can act as a dual SGLT1/2 inhibitor and is able to inhibit intestinal glucose absorption by blocking intestinal SGLT1 (Dominguez Rieg and Rieg, 2019). Although these drugs were initially developed for the treatment of type 2 diabetes, clinical studies have largely demonstrated their beneficial effects in metabolic, renal, and cardiovascular diseases that go beyond glucose control (Minze et al., 2018; Mascolo et al., 2022a; Urbanek et al., 2023).

Based on the results of clinical data, empagliflozin and dapagliflozin are now recommended for the treatment of HFpEF, as well as for HFrEF also in the absence of diabetes (McDonagh et al., 2021; McDonagh et al., 2023).

## 4.1 SGLT2 inhibitors in the cardiovascular system

Numerous studies have proved that SGLT2 inhibitors reduce the combined risk of cardiovascular death and hospitalization in HF patients with or without diabetes. The benefits include osmotic diuresis and natriuresis, weight loss and lipid metabolism shift, blood pressure reduction, decrease in uric acid, oxidative stress, and inflammation with a lower risk of hypoglycaemia or pancreatic β-cell overstimulation. They represent a new therapeutic approach able to act directly on the heart or kidneys, independently of insulin sensitivity (Lopaschuk and Verma, 2020; Goldberg, 2021). SGLT2 inhibitor effects have been established on cardiomyocytes, endothelial cells, fibroblasts, and smooth muscle cells (Uthman et al., 2018a; Cappetta et al., 2021).

Oxidative stress and inflammation significantly and interdependently contribute to the onset and progression of cardiovascular diseases (Frati et al., 2017). Inflammation can induce acute or chronic oxidative stress via cytosolic protein kinase C and calcium release; *vice versa*, oxidative stress is a positive modulator of the inflammatory response through NLRP3 inflammasome and NF-κB (Checa and Aran, 2020; Chen et al., 2022). SGLT2 inhibitors exhibit considerable potential as anti-inflammatory agents, through indirect mechanisms that involve metabolic improvement, oxidative stress reduction, as well as direct modulation of inflammatory pathways (Elrakaybi et al., 2022). In obese mice with diabetes, dapagliflozin reduces cardiac dysfunction interfering with activation of NLRP3 inflammasome and affects cardiac fibrosis by attenuating collagen 1 and collagen 3 deposition (Ye et al., 2017). Similarly, empagliflozin suppresses NLRP3 inflammasome activation in macrophages of diabetic patients (Kim et al., 2020). Furthermore, it has been shown that empagliflozin attenuates the decline of cardiac function in mice with HF in the absence of diabetes and that this is associated with reduced priming of NLRP3 inflammasome in the heart (Byrne et al., 2020). In post-ischemic rat hearts, treatment with dapagliflozin results in higher level of IL-10, a cytokine that facilitates the conversion of macrophages from a pro-inflammatory M1 to anti-inflammatory M2 phenotype, thereby inhibiting myofibroblast differentiation and extracellular matrix formation (Lee et al., 2017).

Cardiomyocytes and endothelial cells are major targets for SGLT2 inhibitors in the heart (Chen et al., 2022). Studies support that intracellular sodium and calcium overload induce signaling cascades that lead to dysregulation of mitochondrial homeostasis, with energy impairment and elevated free radical production, and consequent increase in cardiac hypertrophy and remodeling (Bay et al., 2013). In mice with diabetic cardiomyopathy, ertugliflozin prevents myocardial hypertrophy, fibrosis, and diastolic dysfunction by preserving mitochondrial function and improving myocardial energetics (Croteau et al., 2021). Activation of NCX and sodium/hydrogen exchanger-1 (NHE-1), at cardiac and vascular level, mediate the maladaptive neurohormonal stimulation (sympathetic nervous system, RAAS, and natriuretic peptide system) during the pathophysiological course toward HF (Baartscheer et al., 2003; Packer, 2017). SGLT2 inhibitors show a strict interaction with human and murine cardiomyocytes through direct inhibition of the myocardial isoform of NHE (Uthman et al., 2018b; Trum et al., 2020). Moreover, both dapagliflozin and empagliflozin have been shown to directly inhibit NHE-1 activity in human endothelial cells (Cappetta et al., 2020; Uthman et al., 2022). Another factor in the development of HF is the late component of the cardiac voltage-gated sodium current, termed late-INa (Horvath and Bers, 2014). *In silico* approach confirms a reduction of late-INa by empagliflozin demonstrating that SGLT2 inhibitors may be the ligands for the cardiac sodium channel Nav1.5 isoform that drives late-INa (Philippaert et al., 2021). Amelioration of dysfunctional sodium and calcium homeostasis in cardiomyocytes from diabetic hearts is able to reverse cardiac remodeling and counteract the development of diabetic cardiomyopathy (Lee et al., 2019; Philippaert et al., 2021). Moreover, the regulation of sodium and calcium homeostasis in cardiomyocytes and coronary endothelium is directly translated into improved contractility and relaxation of the heart (Cappetta et al., 2020).

Diuretic and natriuretic effects of SGLT2 inhibitors contribute to the reduction of intravascular volume and decrease in blood pressure, lowering afterload, improving cardiac efficiency, and reducing ventricular mass index (Mazidi et al., 2017; Dominguez Rieg and Rieg, 2019). SGLT2 inhibitors can reduce natriuretic peptides leading to a reduction in ventricular pressure and distention, and both pulmonary and systemic decongestion (Mascolo et al., 2022b). Moreover, the favorable hemodynamic effects seem to be related with an attenuated endothelial cell activation and improved vasorelaxation *via* voltage-gated potassium channels (Dimitriadis et al., 2023). Additionally, benefits include the capacity to decrease the RAAS and sympathetic neurohormonal pathways and a positive pharmacodynamic interaction with RAAS inhibitors (Salvatore et al., 2022).

The above cardiac and extracardiac effects outline the cardioprotective mechanisms of SGLT2 inhibitors that stay behind the success of these drugs in the cardiovascular field.

## 4.2 SGLT2 inhibitors in the central nervous system

SGLT1 is localized in the pyramidal cells of the brain cortex, Purkinje cerebellum cells, hippocampus pyramidal, and granular cells (Pawlos et al., 2021). SGLT2 brain expression is lower compared to SGLT1, and it is localized mainly in the

microvessels of the blood-brain barrier, in the amygdala, hypothalamus, periaqueductal gray, and in the dorsomedial medulla (Enerson and Drewes, 2006). Both co-transporters are also described in the membrane of the capillary endothelium (Koepsell, 2020). Interestingly, the presence of SGLT1/2 co-transporters has been found mainly in areas involved in processes such as learning, food intake, energy and glucose homeostasis, and central cardiovascular and autonomic regulation (Wiciński et al., 2020).

Growing evidence suggests that SGLT2 inhibitors have a neuroprotective potential and may improve the impaired cognitive function of diabetic patients by exerting pleiotropic effects and modulating numerous molecular mechanisms.

Chronic inflammation negatively affects the blood-brain barrier and leads to a pro-inflammatory phenotype of astrocytes and microglia (Rochfort and Cummins, 2015). Pro-inflammatory M1 polarization associates with neurodegeneration and cognitive impairment (Zhang Z. et al., 2021). SGLT2 inhibitors (i.e., dapagliflozin) have been proven to strongly promote macrophage polarization towards a M2 phenotype, thus alleviating inflammation and atherosclerotic processes (Lee et al., 2020). Similarly, empagliflozin can mitigate inflammation and macrophage stimulation by downregulating JAK2/STAT1 pathway and optimize energy expenditure (Xu et al., 2019; Lee et al., 2021). SGLT2 inhibitors may also regulate macrophage activation by decreasing the generation of free radicals and enhancing the expression of antioxidant enzymes (Lin et al., 2014; Iannantuoni et al., 2019). In Alzheimer's disease, NLRP3 inflammasome has emerged as a pathological component participating in the impaired removal of amyloid-β by microglia (Lonnemann et al., 2020). Notably, SGLT2 inhibitors empagliflozin and canagliflozin act on macrophages and attenuate NLRP3 inflammasome in atherosclerosis and cognitive impairment, respectively (Kim et al., 2020; Khedr et al., 2024).

The inflammatory state may contribute to the overproduction of ROS or the decrease in antioxidant defense by compromising mitochondrial function (Guo et al., 2013). Oxidative stress is associated with amyloid-β- or tau-induced neurotoxicity, which results in impaired synaptic plasticity, neurotransmitter imbalance, and neuronal loss, leading to cognitive impairment (Huang et al., 2016; Cenini and Voos, 2019). Interestingly, the administration of dapagliflozin in obese mice is associated with a significant improvement in brain mitochondrial function and decreased ROS production, preventing cognitive decline (Sa-Nguanmoo et al., 2017).

Another crucial target involved in metabolic diseases and cognitive impairment is the mammalian target of rapamycin (mTOR). Hyperglycemia-induced mTOR upregulation leads to blood-brain barrier disruption and endothelial dysfunction, and contributes to tau hyperphosphorylation and amyloid-β aggregation in Alzheimer's disease (Van Skike and Galvan, 2018; Uddin et al., 2020). SGLT2 inhibitors contribute to switching energy metabolism and reinstate mTOR activity in cardiovascular system, and by restoring mTOR cycle may interfere with a cognitive impairment (Packer, 2020; Stanciu et al., 2021).

Brain insulin resistance is heavily implicated in the pathogenesis of Alzheimer's disease, and takes part in amyloid-β- and tau phosphorylation-mediated neuronal damage (Mullins et al., 2017). In a murine model of Alzheimer's disease and type 2 diabetes, empagliflozin has been shown to ameliorate metabolic alterations and glucose levels lowering senile plaque burden; these effects are accompanied by an improvement of cognitive deficits (Hierro-Bujalance et al., 2020). In an experimental model of Alzheimer's disease induced by aluminum chloride, dapagliflozin shows neuroprotective effects by suppressing brain amyloid-β protein deposition; improved cognition is mediated through different mechanisms, such as attenuation of oxidative stress, enhancement of glucose metabolism, and regulation of mTOR signaling (Samman et al., 2023). Moreover, dapagliflozin markedly alleviates neuronal oxidative stress, tau phosphorylation and amyloid-β production due to the ability to counteract neuronal apoptosis and upregulating glial cell-derived neurotrophic factor (Arab et al., 2021).

Alzheimer's disease is also characterized by a reduced level of neuronal acetylcholine and the first line pharmacological treatment is based on the use of acetylcholinesterase inhibitors (Ferreira-Vieira et al., 2016). In an experimental model of cognitive impairment induced by scopolamine, the beneficial effect of canagliflozin on cognitive function has been attributed to the capacity to inhibit acetylcholinesterase and increase acetylcholine M1 receptor expression (Arafa et al., 2017). These results have been confirmed by molecular docking studies evaluating the binding energy of dapagliflozin to the catalytic site of SGLT2 and acetylcholinesterase enzymes, thus suggesting that dapagliflozin might act as a dual inhibitor to treat diabetes-associated neurological disorders (Shaikh et al., 2016).

## 5 Future directions

The mechanisms underlying HF and cognitive impairment have been extensively investigated although studies to provide a comprehensive view of the pathophysiological aspects at stake are needed. At this regard, epigenetic signature, observed in type 2 diabetes as well as in chronic cardiovascular and neurological diseases, is emerging as an innovative research field and a potential pharmacological target. Future research should explores the capability of GLP-1R agonists and SGLT2 inhibitors to modulate epigenetic writers, readers and erasers in the context of cardiovascular and brain homeostasis (Scisciola et al., 2020; Donniacuo et al., 2023).

The effectiveness of these anti-diabetic drugs in HF patients has been clearly established. Instead, the use of GLP-1R agonists and SGLT2 inhibitors as a potential therapeutic option for cognitive dysfunction is a relatively new area of investigation, and clinical studies are still limited. Therefore, more research is needed to understand the underlying mechanisms and to determine long-term safety and efficacy in humans. Intriguingly, the association of these pharmacological classes may represent a promising therapeutic strategy, and some clinical studies have already shown adjunctive benefits of the combination therapy.

Given the impact of type 2 diabetes on cardiovascular and neurological diseases, GLP-1 agonists and SGLT2 inhibitors represent a valid pharmacological tool for improving cardiometabolic profile and diabetes-related cognitive impairment. Because the vast array of molecular and cellular mechanisms modulated by these two new drug classes often intercept in pathophysiological background of chronic

cardiovascular and neurodegenerative diseases, it is possible that any future new anti-diabetic drug may be also relevant for cardiometabolic and cognitive decline, independently from the anti-diabetic action.

## Author contributions

MR: Writing–original draft, Conceptualization. EM: Investigation, Writing–original draft. MD: Writing–original draft, Investigation. MT: Writing–original draft, Investigation. GB: Investigation, Writing–original draft. GC: Writing–review and editing, Supervision. FR: Writing–review and editing, Supervision. AD: Writing–review and editing, Supervision. DC: Writing–review and editing, Conceptualization, Writing–original draft. KU: Writing–review and editing, Funding acquisition. LB: Writing–review and editing, Supervision, Funding acquisition.

## Funding

The author(s) declare that financial support was received for the research, authorship, and/or publication of this article. Work supported by #NEXTGENERATIONEU (NGEU) and funded by the Ministry of University and Research (MUR), National Recovery and Resilience Plan (NRRP), project MNESYS (PE0000006)—A Multiscale integrated approach to the study of the nervous system in health and disease (DN. 1553 11.10.2022).

## Conflict of interest

Authors GC and KU were employed by CEINGE-Advanced Biotechnologies.

The remaining authors declare that the research was conducted in the absence of any commercial or financial relationships that could be construed as a potential conflict of interest.

The author(s) declared that they were an editorial board member of Frontiers, at the time of submission. This had no impact on the peer review process and the final decision.

## Publisher's note



## References

Almutairi, M., Gopal, K., Greenwell, A. A., Young, A., Gill, R., Aburasayn, H., et al. (2021). The GLP-1 receptor agonist liraglutide increases myocardial glucose oxidation rates via indirect mechanisms and mitigates experimental diabetic cardiomyopathy. *Can. J. Cardiol.* 37 (1), 140–150. doi:10.1016/j.cjca.2020.02.098

Arab, H. H., Safar, M. M., and Shahin, N. N. (2021). Targeting ROS-dependent AKT/GSK-3β/NF-κB and DJ-1/nrf2 pathways by dapagliflozin attenuates neuronal injury and motor dysfunction in rotenone-induced Parkinson's disease rat model. *ACS Chem. Neurosci.* 12 (4), 689–703. doi:10.1021/acschemneuro.0c00722

Arafa, N. M. S., Ali, E. H. A., and Hassan, M. K. (2017). Canagliflozin prevents scopolamine-induced memory impairment in rats: comparison with galantamine hydrobromide action. *Chem. Biol. Interact.* 277, 195–203. doi:10.1016/j.cbi.2017.08.013

Aroor, A. R., Mandavia, C., Ren, J., Sowers, J. R., and Pulakat, L. (2012b). Mitochondria and oxidative stress in the cardiorenal metabolic syndrome. *Cardiorenal Med.* 2, 87–109. doi:10.1159/000335675

Aroor, A. R., Mandavia, C. H., and Sowers, J. R. (2012a). Insulin resistance and heart failure: molecular mechanisms. *Heart Fail Clin.* 8 (4), 609–617. doi:10.1016/j.hfc.2012.06.005

Baartscheer, A., Schumacher, C. A., van Borren, M. M., Belterman, C. N., Coronel, R., and Fiolet, J. W. (2003). Increased Na+/H+-exchange activity is the cause of increased [Na+]i and underlies disturbed calcium handling in the rabbit pressure and volume overload heart failure model. *Cardiovasc Res.* 57 (4), 1015–1024. doi:10.1016/s0008-6363(02)00809-x

Baggio, L. L., Yusta, B., Mulvihill, E. E., Cao, X., Streutker, C. J., Butany, J., et al. (2018). GLP-1 receptor expression within the human heart. *Endocrinology* 159 (4), 1570–1584. doi:10.1210/en.2018-00004

Banday, M. Z., Sameer, A. S., and Nissar, S. (2020). Pathophysiology of diabetes: an overview. *Avicenna J. Med.* 10, 174–188. doi:10.4103/ajm.ajm_53_20

Bao, W., Aravindhan, K., Alsaid, H., Chendrimada, T., Szapacs, M., Citerone, D. R., et al. (2011). Albiglutide, a long lasting glucagon-like peptide-1 analog, protects the rat heart against ischemia/reperfusion injury: evidence for improving cardiac metabolic efficiency. *PLoS One* 6 (8), e23570. doi:10.1371/journal.pone.0023570

Barone, E., Di Domenico, F., Perluigi, M., and Butterfield, D. A. (2021). The interplay among oxidative stress, brain insulin resistance and AMPK dysfunction contribute to neurodegeneration in type 2 diabetes and Alzheimer disease. *Free Radic. Biol. Med.* 176, 16–33. doi:10.1016/j.freeradbiomed.2021.09.006

Batista, A. F., Forny-Germano, L., Clarke, J. R., Lyra, E. S. N. M., Brito-Moreira, J., Boehnke, S. E., et al. (2018). The diabetes drug liraglutide reverses cognitive impairment in mice and attenuates insulin receptor and synaptic pathology in a non-human primate model of Alzheimer's disease. *J. Pathol.* 245 (1), 85–100. doi:10.1002/path.5056

Bay, J., Kohlhaas, M., and Maack, C. (2013). Intracellular $Na^+$ and cardiac metabolism. *J. Mol. Cell Cardiol.* 61, 20–27. doi:10.1016/j.yjmcc.2013.05.010

Baylan, U., Korn, A., Emmens, R. W., Schalkwijk, C. G., Niessen, H. W. M., Krijnen, P. A. J., et al. (2022). Liraglutide treatment attenuates inflammation markers in the cardiac, cerebral and renal microvasculature in streptozotocin-induced diabetic rats. *Eur. J. Clin. Invest.* 52 (9), e13807. doi:10.1111/eci.13807

Bendotti, G., Montefusco, L., Lunati, M. E., Usuelli, V., Pastore, I., Lazzaroni, E., et al. (2022). The anti-inflammatory and immunological properties of GLP-1 Receptor Agonists. *Pharmacol. Res.* 182, 106320. doi:10.1016/j.phrs.2022.106320

Bers, D. M. (2006). Altered cardiac myocyte Ca regulation in heart failure. *Physiol. (Bethesda)* 21, 380–387. doi:10.1152/physiol.00019.2006

Bomba, M., Ciavardelli, D., Silvestri, E., Canzoniero, L. M., Lattanzio, R., Chiappini, P., et al. (2013). Exenatide promotes cognitive enhancement and positive brain metabolic changes in PS1-KI mice but has no effects in 3xTg-AD animals. *Cell Death Dis.* 4, e612. doi:10.1038/cddis.2013.139

Brasier, A. R. (2010). The nuclear factor-kappaB-interleukin-6 signalling pathway mediating vascular inflammation. *Cardiovasc Res.* 86 (2), 211–218. doi:10.1093/cvr/cvq076

Bruen, R., Curley, S., Kajani, S., Crean, D., O'Reilly, M. E., Lucitt, M. B., et al. (2017). Liraglutide dictates macrophage phenotype in apolipoprotein E null mice during early atherosclerosis. *Cardiovasc Diabetol.* 16 (1), 143. doi:10.1186/s12933-017-0626-3

Bułdak, Ł., Machnik, G., Bułdak, R. J., Łabuzek, K., Bołdys, A., and Okopień, B. (2016). Exenatide and metformin express their anti-inflammatory effects on human monocytes/macrophages by the attenuation of MAPKs and NFκB signaling. *Naunyn-Schmiedeberg's archives Pharmacol.* 389 (10), 1103–1115. doi:10.1007/s00210-016-1277-8

Byrne, N. J., Matsumura, N., Maayah, Z. H., Ferdaoussi, M., Takahara, S., Darwesh, A. M., et al. (2020). Empagliflozin blunts worsening cardiac dysfunction associated with reduced NLRP3 (Nucleotide-Binding domain-like receptor protein 3) inflammasome activation in heart failure. *Circ. Heart Fail* 13 (1), e006277. doi:10.1161/CIRCHEARTFAILURE.119.006277

Cai, H. Y., Yang, J. T., Wang, Z. J., Zhang, J., Yang, W., Wu, M. N., et al. (2018). Lixisenatide reduces amyloid plaques, neurofibrillary tangles and neuroinflammation in an APP/PS1/tau mouse model of Alzheimer's disease. *Biochem. Biophys. Res. Commun.* 495 (1), 1034–1040. doi:10.1016/j.bbrc.2017.11.114

Calsolaro, V., and Edison, P. (2016). Neuroinflammation in Alzheimer's disease: current evidence and future directions. *Alzheimers Dement.* 12, 719–732. doi:10.1016/j.jalz.2016.02.010

Cappetta, D., De Angelis, A., Bellocchio, G., Telesca, M., Cianflone, E., Torella, D., et al. (2021). Sodium-glucose cotransporter 2 inhibitors and heart failure: a bedside-to-bench journey. *Front. Cardiovasc Med.* 8, 810791. doi:10.3389/fcvm.2021.810791

Cappetta, D., De Angelis, A., Ciuffreda, L. P., Coppini, R., Cozzolino, A., Miccichè, A., et al. (2020). Amelioration of diastolic dysfunction by dapagliflozin in a non-diabetic model involves coronary endothelium. *Pharmacol. Res.* 157, 104781. doi:10.1016/j.phrs.2020.104781

Cardiogenic dementia (1977). Cardiogenic dementia. *Lancet.* 1, 27–28. doi:10.1016/S0140-6736(77)91660-9

Cenini, G., and Voos, W. (2019). Mitochondria as potential targets in alzheimer disease therapy: an update. *Front. Pharmacol.* 10, 902. doi:10.3389/fphar.2019.00902

Chang, Y. F., Zhang, D., Hu, W. M., Liu, D. X., and Li, L. (2020). Semaglutide-mediated protection against Aβ correlated with enhancement of autophagy and inhibition of apotosis. *J. Clin. Neurosci.* 81, 234–239. doi:10.1016/j.jocn.2020.09.054

Checa, J., and Aran, J. M. (2020). Reactive oxygen species: drivers of physiological and pathological processes. *J. Inflamm. Res.* 13, 1057–1073. doi:10.2147/JIR.S275595

Chen, S., Coronel, R., Hollmann, M. W., Weber, N. C., and Zuurbier, C. J. (2022). Direct cardiac effects of SGLT2 inhibitors. *Cardiovasc Diabetol.* 21 (1), 45. doi:10.1186/s12933-022-01480-1

Chen, S., Sun, J., Zhao, G., Guo, A., Chen, Y., Fu, R., et al. (2017). Liraglutide improves water maze learning and memory performance while reduces hyperphosphorylation of tau and neurofilaments in APP/PS1/tau triple transgenic mice. *Neurochem. Res.* 42 (8), 2326–2335. doi:10.1007/s11064-017-2250-8

Colin, I. M., Szczepanski, L. W., Gérard, A. C., and Elosegi, J. A. (2023). Emerging evidence for the use of antidiabetic drugs, glucagon-like peptide 1 receptor agonists, for the treatment of alzheimer's disease. *touchREV Endocrinol.* 19 (1), 16–24. doi:10.17925/EE.2023.19.1.16

Cork, S. C., Richards, J. E., Holt, M. K., Gribble, F. M., Reimann, F., and Trapp, S. (2015). Distribution and characterisation of glucagon-like peptide-1 receptor expressing cells in the mouse brain. *Mol. Metab.* 4, 718–731. doi:10.1016/j.molmet.2015.07.008

Cosentino, F., Grant, P. J., Aboyans, V., Bailey, C. J., Ceriello, A., Delgado, V., et al. (2020). 2019 ESC Guidelines on diabetes, pre-diabetes, and cardiovascular diseases developed in collaboration with the EASD. *Eur. Heart J.* 41 (2), 255–323. doi:10.1093/eurheartj/ehz486

Craft, S. (2007). Insulin resistance and alzheimer's disease pathogenesis: potential mechanisms and implications for treatment. *Curr. Alzheimer Res.* 4, 147–152. doi:10.2174/156720507780362137

Croteau, D., Luptak, I., Chambers, J. M., Hobai, I., Panagia, M., Pimentel, D. R., et al. (2021). Effects of sodium-glucose linked transporter 2 inhibition with ertugliflozin on mitochondrial function, energetics, and metabolic gene expression in the presence and absence of diabetes mellitus in mice. *J. Am. Heart Assoc.* 10 (13), e019995. doi:10.1161/JAHA.120.019995

Dao, L., Choi, S., and Freeby, M. (2023). Type 2 diabetes mellitus and cognitive function: understanding the connections. *Curr. Opin. Endocrinol. Diabetes Obes.* 30 (1), 7–13. doi:10.1097/MED.0000000000000783

Deacon, C. F., and Ahrén, B. (2011). Physiology of incretins in health and disease. *Rev. Diabet. Stud.* 8 (3), 293–306. doi:10.1900/RDS.2011.8.293

Del, P. S., Kahn, S. E., Pavo, I., Weerakkody, G. J., Yang, Z., Doupis, J., et al. (2021). Tirzepatide versus insulin glargine in type 2 diabetes and increased cardiovascular risk (SURPASS-4): a randomised, open-label, parallel-group, multicentre, phase 3 trial. *Lancet* 398 (10313), 1811–1824. doi:10.1016/S0140-6736(21)02188-7

Delghandi, M. P., Johannessen, M., and Moens, U. (2005). The cAMP signalling pathway activates CREB through PKA, p38 and MSK1 in NIH 3T3 cells. *Cell Signal* 17 (11), 1343–1351. doi:10.1016/j.cellsig.2005.02.003

Denver, P., English, A., and McClean, P. L. (2018). Inflammation, insulin signaling and cognitive function in aged APP/PS1 mice. *Brain Behav. Immun.* 70, 423–434. doi:10.1016/j.bbi.2018.03.032

Díez-Villanueva, P., Jiménez-Méndez, C., and Alfonso, F. (2021). Heart failure in the elderly. *J. Geriatr. Cardiol.* 18 (3), 219–232. doi:10.11909/j.issn.1671-5411.2021.03.009

Dimitriadis, K., Adamopoulou, E., Pyrpyris, N., Sakalidis, A., Leontsinis, I., Manta, E., et al. (2023). The effect of SGLT2 inhibitors on the endothelium and the microcirculation: from bench to bedside and beyond. *Eur. Heart J. Cardiovasc Pharmacother.* 9 (8), 741–757. doi:10.1093/ehjcvp/pvad053

Dodson, J. A., Truong, T. T., Towle, V. R., Kerins, G., and Chaudhry, S. I. (2013). Cognitive impairment in older adults with heart failure: prevalence, documentation, and impact on outcomes. *Am. J. Med.* 126 (2), 120–126. doi:10.1016/j.amjmed.2012.05.029

Dominguez Rieg, J. A., and Rieg, T. (2019). What does sodium-glucose co-transporter 1 inhibition add: prospects for dual inhibition. *Diabetes Obes. Metab.* 21 (Suppl. 2), 43–52. doi:10.1111/dom.13630

Donniacuo, M., De Angelis, A., Telesca, M., Bellocchio, G., Riemma, M. A., Paolisso, P., et al. (2023). Atrial fibrillation: epigenetic aspects and role of sodium-glucose cotransporter 2 inhibitors. *Pharmacol. Res.* 188, 106591. doi:10.1016/j.phrs.2022.106591

Doughan, A. K., Harrison, D. G., and Dikalov, S. I. (2008). Molecular mechanisms of angiotensin II-mediated mitochondrial dysfunction: linking mitochondrial oxidative damage and vascular endothelial dysfunction. *Circ. Res.* 102 (4), 488–496. doi:10.1161/CIRCRESAHA.107.162800

Drucker, D. J. (2016). The cardiovascular biology of glucagon-like peptide-1. *Cell Metab.* 24 (1), 15–30. doi:10.1016/j.cmet.2016.06.009

Drucker, D. J., Philippe, J., Mojsov, S., Chick, W. L., and Habener, J. F. (1987). Glucagon-like peptide I stimulates insulin gene expression and increases cyclic AMP levels in a rat islet cell line. *Proc. Natl. Acad. Sci. U. S. A.* 84, 3434–3438. doi:10.1073/pnas.84.10.3434

Du, H., Meng, X., Yao, Y., and Xu, J. (2022). The mechanism and efficacy of GLP-1 receptor agonists in the treatment of Alzheimer's disease. *Front. Endocrinol. (Lausanne)* 13, 1033479. doi:10.3389/fendo.2022.1033479

Dunlay, S. M., Givertz, M. M., Aguilar, D., Allen, L. A., Chan, M., Desai, A. S., et al. (2019). Type 2 diabetes mellitus and heart failure: a scientific statement from the American heart association and the heart failure society of America: this statement does not represent an update of the 2017 ACC/AHA/HFSA heart failure guideline update. *Circulation* 140 (7), e294–e324. doi:10.1161/CIR.0000000000000691

Dunlay, S. M., Roger, V. L., and Redfield, M. M. (2017). Epidemiology of heart failure with preserved ejection fraction. *Nat. Rev. Cardiol.* 14 (10), 591–602. doi:10.1038/nrcardio.2017.65

During, M. J., Cao, L., Zuzga, D. S., Francis, J. S., Fitzsimons, H. L., Jiao, X. Y., et al. (2003). Glucagon-like peptide-1 receptor is involved in learning and neuroprotection. *Nat. Med.* 9, 1173–1179. doi:10.1038/nm919

Dutta, D., Surana, V., Singla, R., Aggarwal, S., and Sharma, M. (2021). Efficacy and safety of novel twincretin tirzepatide a dual GIP and GLP-1 receptor agonist in the management of type-2 diabetes: a Cochrane meta-analysis. *Indian J. Endocrinol. Metab.* 25 (6), 475–489. doi:10.4103/ijem.ijem_423_21

Elrakaybi, A., Laubner, K., Zhou, Q., Hug, M. J., and Seufert, J. (2022). Cardiovascular protection by SGLT2 inhibitors - do anti-inflammatory mechanisms play a role? *Mol. Metab.* 64, 101549. doi:10.1016/j.molmet.2022.101549

Enerson, B. E., and Drewes, L. R. (2006). The rat blood-brain barrier transcriptome. *J. Cereb. Blood Flow. Metab.* 26 (7), 959–973. doi:10.1038/sj.jcbfm.9600249

Engidawork, E., Gulesserian, T., Seidl, R., Cairns, N., and Lubec, G. (2001). Expression of apoptosis related proteins in brains of patients with Alzheimer's disease. *Neurosci. Lett.* 303 (2), 79–82. doi:10.1016/s0304-3940(01)01618-4

Ferrannini, E. (2017). Sodium-glucose Co-transporters and their inhibition: clinical physiology. *Cell Metab.* 26 (1), 27–38. doi:10.1016/j.cmet.2017.04.011

Ferreira-Vieira, T. H., Guimaraes, I. M., Silva, F. R., and Ribeiro, F. M. (2016). Alzheimer's disease: targeting the cholinergic system. *Curr. Neuropharmacol.* 14 (1), 101–115. doi:10.2174/1570159x13666150716165726

Finan, B., Ma, T., Ottaway, N., Muller, T. D., Habegger, K. M., Heppner, K. M., et al. (2013). Unimolecular dual incretins maximize metabolic benefits in rodents, monkeys, and humans. *Sci. Transl. Med.* 5, 209ra151. doi:10.1126/scitranslmed.3007218

Finan, B., Yang, B., Ottaway, N., Smiley, D. L., Ma, T., Clemmensen, C., et al. (2015). A rationally designed monomeric peptide triagonist corrects obesity and diabetes in rodents. *Nat. Med.* 21 (1), 27–36. doi:10.1038/nm.3761

Fontanella, R. A., Ghosh, P., Pesapane, A., Taktaz, F., Puocci, A., Franzese, M., et al. (2024). Tirzepatide prevents neurodegeneration through multiple molecular pathways. *J. Transl. Med.* 22 (1), 114. doi:10.1186/s12967-024-04927-z

Frati, G., Schirone, L., Chimenti, I., Yee, D., Biondi-Zoccai, G., Volpe, M., et al. (2017). An overview of the inflammatory signalling mechanisms in the myocardium underlying the development of diabetic cardiomyopathy. *Cardiovasc Res.* 113 (4), 378–388. doi:10.1093/cvr/cvx011

GBD 2016 Dementia Collaborators (2019). Global, regional, and national burden of Alzheimer's disease and other dementias, 1990-2016: a systematic analysis for the Global Burden of Disease Study 2016. *Lancet Neurol.* 18 (1), 88–106. doi:10.1016/S1474-4422(18)30403-4

Goldberg, L. R. (2021). The pleiotropic effects of SGLT2 inhibitors: remodeling the treatment of heart failure. *J. Am. Coll. Cardiol.* 77, 256–258. doi:10.1016/j.jacc.2020.11.029

Gollmer, J., Zirlik, A., and Bugger, H. (2020). Mitochondrial mechanisms in diabetic cardiomyopathy. *Diabetes Metab. J.* 44 (1), 33–53. doi:10.4093/dmj.2019.0185

Green, H., Tsitsi, P., Markaki, I., Aarsland, D., and Svenningsson, P. (2019). Novel treatment opportunities against cognitive impairment in Parkinson's disease with an emphasis on diabetes-related pathways. *CNS Drugs* 33, 143–160. doi:10.1007/s40263-018-0601-x

Groenewegen, A., Rutten, F. H., Mosterd, A., and Hoes, A. W. (2020). Epidemiology of heart failure. *Eur. J. Heart Fail* 22 (8), 1342–1356. doi:10.1002/ejhf.1858

Guo, C., Sun, L., Chen, X., and Zhang, D. (2013). Oxidative stress, mitochondrial damage and neurodegenerative diseases. *Neural Regen. Res.* 8 (21), 2003–2014. doi:10.3969/j.issn.1673-5374.2013.21.009

Hamilton, A., and Holscher, C. (2009). Receptors for the incretin glucagon-like peptide-1 are expressed on neurons in the central nervous system. *Neuroreport* 20, 1161–1166. doi:10.1097/WNR.0b013e32832fbf14

Helmstädter, J., Frenis, K., Filippou, K., Grill, A., Dib, M., Kalinovic, S., et al. (2020). Endothelial GLP-1 (Glucagon-Like peptide-1) receptor mediates cardiovascular

protection by liraglutide in mice with experimental arterial hypertension. *Arterioscler. Thromb. Vasc. Biol.* 40 (1), 145–158. doi:10.1161/atv.0000615456.97862.30

Hierro-Bujalance, C., Infante-Garcia, C., Del Marco, A., Herrera, M., Carranza-Naval, M. J., Suarez, J., et al. (2020). Empagliflozin reduces vascular damage and cognitive impairment in a mixed murine model of Alzheimer's disease and type 2 diabetes. *Alzheimers Res. Ther.* 12 (1), 40. doi:10.1186/s13195-020-00607-4

Hirata, K., Kume, S., Araki, S., Sakaguchi, M., Chin-Kanasaki, M., Isshiki, K., et al. (2009). Exendin-4 has an anti-hypertensive effect in salt-sensitive mice model. *Biochem. Biophys. Res. Commun.* 380 (1), 44–49. doi:10.1016/j.bbrc.2009.01.003

Hogan, A. E., Gaoatswe, G., Lynch, L., Corrigan, M. A., Woods, C., O'Connell, J., et al. (2014). Glucagon-like peptide 1 analogue therapy directly modulates innate immune-mediated inflammation in individuals with type 2 diabetes mellitus. *Diabetologia* 57 (4), 781–784. doi:10.1007/s00125-013-3145-0

Holst, J. J., Knop, F. K., Vilsbøll, T., Krarup, T., and Madsbad, S. (2011). Loss of incretin effect is a specific, important, and early characteristic of type 2 diabetes. *Diabetes Care* 34 (Suppl. 2), S251–S257. doi:10.2337/dc11-s227

Holz, G. G. (2004). EPAC: a new cAMP-binding protein in support of glucagon-like peptide 1 receptor mediated signal transduction in the pancreatic beta-cell. *Diabetes* 53 (1), 5–13. doi:10.2337/diabetes.53.1.5

Horvath, B., and Bers, D. M. (2014). The late sodium current in heart failure: pathophysiology and clinical relevance. *Esc. Heart Fail* 1 (1), 26–40. doi:10.1002/ehf2.12003

Huang, W. J., Zhang, X., and Chen, W. W. (2016). Role of oxidative stress in Alzheimer's disease. *Biomed. Rep.* 4 (5), 519–522. doi:10.3892/br.2016.630

Hunter, K., and Holscher, C. (2012). Drugs developed to treat diabetes, liraglutide and lixisenatide, cross the blood brain barrier and enhance neurogenesis. *BMC Neurosci.* 13, 33. doi:10.1186/1471-2202-13-33

Iannantuoni, F., M de Marañon, A., Diaz-Morales, N., Falcon, R., Bañuls, C., Abad-Jimenez, Z., et al. (2019). The SGLT2 inhibitor empagliflozin ameliorates the inflammatory profile in type 2 diabetic patients and promotes an antioxidant response in leukocytes. *J. Clin. Med.* 8 (11), 1814. doi:10.3390/jcm8111814

Jakubowska, A., Roux, C. W. L., and Viljoen, A. (2024). The road towards triple agonists: glucagon-like peptide 1, glucose-dependent insulinotropic polypeptide and glucagon receptor - an update. *Endocrinol. Metab. Seoul.* 39 (1), 12–22. doi:10.3803/EnM.2024.1942

Jensen, E. P., Møller, S., Hviid, A. V., Veedfald, S., Holst, J. J., Pedersen, J., et al. (2020). GLP-1-induced renal vasodilation in rodents depends exclusively on the known GLP-1 receptor and is lost in prehypertensive rats. *Am. J. Physiol. Ren. Physiol.* 318 (6), F1409–F1417. doi:10.1152/ajprenal.00579.2019

Jia, G., Hill, M. A., and Sowers, J. R. (2018). Diabetic cardiomyopathy: an update of mechanisms contributing to this clinical entity. *Circ. Res.* 122, 624–638. doi:10.1161/CIRCRESAHA.117.311586

Kalra, S. (2014). Sodium glucose Co-Transporter-2 (SGLT2) inhibitors: a review of their basic and clinical Pharmacology. *Diabetes Ther.* 5 (2), 355–366. doi:10.1007/s13300-014-0089-4

Khedr, L. H., Rahmo, R. M., Eldemerdash, O. M., Helmy, E. M., Ramzy, F. A., Lotfy, G. H., et al. (2024). Implication of M2 macrophage on NLRP3 inflammasome signaling in mediating the neuroprotective effect of Canagliflozin against methotrexate-induced cognitive impairment. *Int. Immunopharmacol.* 130, 111709. doi:10.1016/j.intimp.2024.111709

Kim, J., Wei, Y., and Sowers, J. R. (2008). Role of mitochondrial dysfunction in insulin resistance. *Circ. Res.* 102, 401–414. doi:10.1161/CIRCRESAHA.107.165472

Kim, M., Platt, M. J., Shibasaki, T., Quaggin, S. E., Backx, P. H., Seino, S., et al. (2013). GLP-1 receptor activation and Epac2 link atrial natriuretic peptide secretion to control of blood pressure. *Nat. Med.* 19 (5), 567–575. doi:10.1038/nm.3128

Kim, S. R., Lee, S. G., Kim, S. H., Kim, J. H., Choi, E., Cho, W., et al. (2020). SGLT2 inhibition modulates NLRP3 inflammasome activity via ketones and insulin in diabetes with cardiovascular disease. *Nat. Commun.* 11 (1), 2127. doi:10.1038/s41467-020-15983-6

Knerr, P. J., Mowery, S. A., Douros, J. D., Premdjee, B., Hjollund, K. R., He, Y., et al. (2022). Next generation GLP-1/GIP/glucagon triple agonists normalize body weight in obese mice. *Mol. Metab.* 63, 101533. doi:10.1016/j.molmet.2022.101533

Koepsell, H. (2020). Glucose transporters in the small intestine in health and disease. *Pflugers Arch.* 472 (9), 1207–1248. doi:10.1007/s00424-020-02439-5

Kolwicz, S. C., and Tian, R. (2011). Glucose metabolism and cardiac hypertrophy. *Cardiovasc Res.* 90 (2), 194–201. doi:10.1093/cvr/cvr071

Kopp, K. O., Glotfelty, E. J., Li, Y., and Greig, N. H. (2022). Glucagon-like peptide-1 (GLP-1) receptor agonists and neuroinflammation: implications for neurodegenerative disease treatment. *Pharmacol. Res.* 186, 106550. doi:10.1016/j.phrs.2022.106550

Lastra, G., Dhuper, S., Johnson, M. S., and Sowers, J. R. (2010). Salt, aldosterone, and insulin resistance: impact on the cardiovascular system. *Nat. Rev. Cardiol.* 7, 577–584. doi:10.1038/nrcardio.2010.123

Laugero, K. D., Stonehouse, A. H., Guss, S., Landry, J., Vu, C., and Parkes, D. G. (2009). Exenatide improves hypertension in a rat model of the metabolic syndrome. *Metab. Syndr. Relat. Disord.* 7 (4), 327–334. doi:10.1089/met.2008.0095

Lebeche, D., Davidoff, A. J., and Hajjar, R. J. (2008). Interplay between impaired calcium regulation and insulin signaling abnormalities in diabetic cardiomyopathy. *Nat. Clin. Pract. Cardiovasc Med.* 5, 715–724. doi:10.1038/ncpcardio1347

Lee, N., Heo, Y. J., Choi, S. E., Jeon, J. Y., Han, S. J., Kim, D. J., et al. (2021). Anti-inflammatory effects of empagliflozin and gemigliptin on LPS-stimulated macrophage via the IKK/NF-κB, MKK7/JNK, and JAK2/STAT1 signalling pathways. *J. Immunol. Res.* 2021, 9944880. doi:10.1155/2021/9944880

Lee, S. G., Lee, S. J., Lee, J. J., Kim, J. S., Lee, O. H., Kim, C. K., et al. (2020). Anti-inflammatory effect for atherosclerosis progression by sodium-glucose cotransporter 2 (SGLT-2) inhibitor in a normoglycemic rabbit model. *Korean Circ. J.* 50 (5), 443–457. doi:10.4070/kcj.2019.0296

Lee, T. I., Chen, Y. C., Lin, Y. K., Chung, C. C., Lu, Y. Y., Kao, Y. H., et al. (2019). Empagliflozin attenuates myocardial sodium and calcium dysregulation and reverses cardiac remodeling in streptozotocin-induced diabetic rats. *Int. J. Mol. Sci.* 20 (7), 1680. doi:10.3390/ijms20071680

Lee, T. M., Chang, N. C., and Lin, S. Z. (2017). Dapagliflozin, a selective SGLT2 Inhibitor, attenuated cardiac fibrosis by regulating the macrophage polarization via STAT3 signaling in infarcted rat hearts. *Free Radic. Biol. Med.* 104, 298–310. doi:10.1016/j.freeradbiomed.2017.01.035

Li, L., Zhang, Z. F., Holscher, C., Gao, C., Jiang, Y. H., and Liu, Y. Z. (2012). ($Val^8$) glucagon-like peptide-1 prevents tau hyperphosphorylation, impairment of spatial learning and ultra-structural cellular damage induced by streptozotocin in rat brains. *Eur. J. Pharmacol.* 674 (2-3), 280–286. doi:10.1016/j.ejphar.2011.11.005

Li, T., Jiao, J. J., Hölscher, C., Wu, M. N., Zhang, J., Tong, J. Q., et al. (2018). A novel GLP-1/GIP/Gcg triagonist reduces cognitive deficits and pathology in the 3xTg mouse model of Alzheimer's disease. *Hippocampus* 28 (5), 358–372. doi:10.1002/hipo.22837

Lin, B., Koibuchi, N., Hasegawa, Y., Sueta, D., Toyama, K., Uekawa, K., et al. (2014). Glycemic control with empagliflozin, a novel selective SGLT2 inhibitor, ameliorates cardiovascular injury and cognitive dysfunction in obese and type 2 diabetic mice. *Cardiovasc Diabetol.* 13, 148. doi:10.1186/s12933-014-0148-1

Liu, J., Xiao, G., Liang, Y., He, S., Lyu, M., and Zhu, Y. (2024). Heart-brain interaction in cardiogenic dementia: pathophysiology and therapeutic potential. *Front. Cardiovasc Med.* 11, 1304864. doi:10.3389/fcvm.2024.1304864

Liu, W., Jalewa, J., Sharma, M., Li, G., Li, L., and Holscher, C. (2015). Neuroprotective effects of lixisenatide and liraglutide in the 1-methyl-4-phenyl-1,2,3,6-tetrahydropyridine mouse model of Parkinson's disease. *Neuroscience* 303, 42–50. doi:10.1016/j.neuroscience.2015.06.054

Long-Smith, C. M., Manning, S., McClean, P. L., Coakley, M. F., O'Halloran, D. J., Holscher, C., et al. (2013). The diabetes drug liraglutide ameliorates aberrant insulin receptor localisation and signalling in parallel with decreasing both amyloid-β plaque and glial pathology in a mouse model of Alzheimer's disease. *Neuromolecular Med.* 15 (1), 102–114. doi:10.1007/s12017-012-8199-5

Lonnemann, N., Hosseini, S., Marchetti, C., Skouras, D. B., Stefanoni, D., D'Alessandro, A., et al. (2020). The NLRP3 inflammasome inhibitor OLT1177 rescues cognitive impairment in a mouse model of Alzheimer's disease. *Proc. Natl. Acad. Sci. U. S. A.* 117 (50), 32145–32154. doi:10.1073/pnas.2009680117

Lopaschuk, G. D. (2016). Fatty acid oxidation and its relation with insulin resistance and associated disorders. *Ann. Nutr. Metab.* 68 (3), 15–20. doi:10.1159/000448357

Lopaschuk, G. D., and Verma, S. (2020). Mechanisms of cardiovascular benefits of sodium glucose Co-transporter 2 (SGLT2) inhibitors: a state-of-the-art review. *JACC Basic Transl. Sci.* 5 (6), 632–644. doi:10.1016/j.jacbts.2020.02.004

Luo, X., Hu, Y., He, S., Ye, Q., Lv, Z., Liu, J., et al. (2019). Dulaglutide inhibits high glucose-induced endothelial dysfunction and NLRP3 inflammasome activation. *Arch. Biochem. Biophys.* 671, 203–209. doi:10.1016/j.abb.2019.07.008

Markham, A., and Keam, S. J. (2019). Sotagliflozin: first global approval. *Drugs* 79 (9), 1023–1029. doi:10.1007/s40265-019-01146-5

Martins, F. L., Bailey, M. A., and Girardi, A. C. C. (2020). Endogenous activation of glucagon-like peptide-1 receptor contributes to blood pressure control: role of proximal tubule Na+/H+ exchanger isoform 3, renal angiotensin II, and insulin sensitivity. *Hypertension* 76 (3), 839–848. doi:10.1161/HYPERTENSIONAHA.120.14868

Marx, N., Husain, M., Lehrke, M., Verma, S., and Sattar, N. (2022). GLP-1 receptor agonists for the reduction of atherosclerotic cardiovascular risk in patients with type 2 diabetes. *Circulation* 146 (24), 1882–1894. doi:10.1161/CIRCULATIONAHA.122.059595

Mascolo, A., di Mauro, G., Cappetta, D., De Angelis, A., Torella, D., Urbanek, K., et al. (2022b). Current and future therapeutic perspective in chronic heart failure. *Pharmacol. Res.* 175, 106035. doi:10.1016/j.phrs.2021.106035

Mascolo, A., Di Napoli, R., Balzano, N., Cappetta, D., Urbanek, K., De Angelis, A., et al. (2022a). Safety profile of sodium glucose co-transporter 2 (SGLT2) inhibitors: a brief summary. *Front. Cardiovasc Med.* 9, 1010693. doi:10.3389/fcvm.2022.1010693

Mazidi, M., Rezaie, P., Gao, H. K., and Kengne, A. P. (2017). Effect of sodium-glucose cotransport-2 inhibitors on blood pressure in people with type 2 diabetes mellitus: a systematic review and meta-analysis of 43 randomized control trials with 22 528 patients. *J. Am. Heart Assoc.* 6 (6), e004007. doi:10.1161/JAHA.116.004007

McClean, P. L., and Hölscher, C. (2014). Liraglutide can reverse memory impairment, synaptic loss and reduce plaque load in aged APP/PS1 mice, a model of Alzheimer's disease. *Neuropharmacology* 76 Pt A, 57–67. doi:10.1016/j.neuropharm.2013.08.005

McClean, P. L., Jalewa, J., and Hölscher, C. (2015). Prophylactic liraglutide treatment prevents amyloid plaque deposition, chronic inflammation and memory impairment in APP/PS1 mice. *Behav. Brain Res.* 293, 96–106. doi:10.1016/j.bbr.2015.07.024

McDonagh, T. A., Metra, M., Adamo, M., Gardner, R. S., Baumbach, A., Böhm, M., et al. (2021). 2021 ESC Guidelines for the diagnosis and treatment of acute and chronic heart failure. *Eur. Heart J.* 42 (36), 3599–3726. doi:10.1093/eurheartj/ehab368

McDonagh, T. A., Metra, M., Adamo, M., Gardner, R. S., Baumbach, A., Böhm, M., et al. (2023). 2023 Focused Update of the 2021 ESC Guidelines for the diagnosis and treatment of acute and chronic heart failure. *Eur. Heart J.* 44 (37), 3627–3639. doi:10.1093/eurheartj/ehad195

Mehdi, S. F., Pusapati, S., Anwar, M. S., Lohana, D., Kumar, P., Nandula, S. A., et al. (2023). Glucagon-like peptide-1: a multi-faceted anti-inflammatory agent. *Front. Immunol.* 14, 1148209. doi:10.3389/fimmu.2023.1148209

Minze, M. G., Will, K. J., Terrell, B. T., Black, R. L., and Irons, B. K. (2018). Benefits of SGLT2 inhibitors beyond glycemic control - a focus on metabolic, cardiovascular and renal outcomes. *Curr. Diabetes Rev.* 14 (6), 509–517. doi:10.2174/1573399813666170816142351

Mullins, R. J., Diehl, T. C., Chia, C. W., and Kapogiannis, D. (2017). Insulin resistance as a link between amyloid-beta and Tau pathologies in Alzheimer's disease. *Front. Aging Neurosci.* 9, 118. doi:10.3389/fnagi.2017.00118

Murman, D. L. (2015). The impact of age on cognition. *Semin. Hear* 36 (3), 111–121. doi:10.1055/s-0035-1555115

Nauck, M. A. (2014). Update on developments with SGLT2 inhibitors in the management of type 2 diabetes. *Drug Des. Devel Ther.* 8, 1335–1380. doi:10.2147/DDDT.S50773

Nguyen, T. T., Ta, Q. T. H., Nguyen, T. K. O., Nguyen, T. T. D., and Giau, V. V. (2020). Type 3 diabetes and its role implications in alzheimer's disease. *Int. J. Mol. Sci.* 21 (9), 3165. doi:10.3390/ijms21093165

Ni, L., Yuan, C., Chen, G., Zhang, C., and Wu, X. (2020). SGLT2i: beyond the glucose-lowering effect. *Cardiovasc Diabetol.* 19 (1), 98. doi:10.1186/s12933-020-01071-y

Ou, Y. N., Zhang, Y. B., Li, Y. Z., Huang, S. Y., Zhang, W., Deng, Y. T., et al. (2024). Socioeconomic status, lifestyle and risk of incident dementia: a prospective cohort study of 276730 participants. *Geroscience* 46 (2), 2265–2279. doi:10.1007/s11357-023-00994-0

Owan, T. E., Hodge, D. O., Herges, R. M., Jacobsen, S. J., Roger, V. L., and Redfield, M. M. (2006). Trends in prevalence and outcome of heart failure with preserved ejection fraction. *N. Engl. J. Med.* 355 (3), 251–259. doi:10.1056/NEJMoa052256

Packer, M. (2017). Activation and inhibition of sodium-hydrogen exchanger is a mechanism that links the pathophysiology and treatment of diabetes mellitus with that of heart failure. *Circulation* 136 (16), 1548–1559. doi:10.1161/CIRCULATIONAHA.117.030418

Packer, M. (2018). Heart failure: the most important, preventable, and treatable cardiovascular complication of type 2 diabetes. *Diabetes Care* 41 (1), 11–13. doi:10.2337/dci17-0052

Packer, M. (2020). SGLT2 inhibitors produce cardiorenal benefits by promoting adaptive cellular reprogramming to induce a state of fasting mimicry: a paradigm shift in understanding their mechanism of action. *Diabetes Care* 43 (3), 508–511. doi:10.2337/dci19-0074

Pandey, A., Salahuddin, U., Garg, S., Ayers, C., Kulinski, J., Anand, V., et al. (2016). Continuous dose-response association between sedentary time and risk for cardiovascular disease: a meta-analysis. *JAMA Cardiol.* 1 (5), 575–583. doi:10.1001/jamacardio.2016.1567

Pandey, J., and Tamrakar, A. K. (2019). SGLT2 inhibitors for the treatment of diabetes: a patent review (2013-2018). *Expert Opin. Ther. Pat.* 29 (5), 369–384. doi:10.1080/13543776.2019.1612879

Pandey, S., Mangmool, S., and Parichatikanond, W. (2023). Multifaceted roles of GLP-1 and its analogs: a review on molecular mechanisms with a cardiotherapeutic perspective. *Pharm. (Basel)* 16 (6), 836. doi:10.3390/ph16060836

Pappolla, M. A., Bryant-Thomas, T. K., Herbert, D., Pacheco, J., Fabra Garcia, M., Manjon, M., et al. (2003). Mild hypercholesterolemia is an early risk factor for the development of Alzheimer amyloid pathology. *Neurology* 61 (2), 199–205. doi:10.1212/01.wnl.0000070182.02537.84

Paris, D., Town, T., Mori, T., Parker, T. A., Humphrey, J., and Mullan, M. (2000). Soluble beta-amyloid peptides mediate vasoactivity via activation of a pro-inflammatory pathway. *Neurobiol. Aging* 21 (2), 183–197. doi:10.1016/s0197-4580(99)00111-6

Parthsarathy, V., and Holscher, C. (2013). The type 2 diabetes drug liraglutide reduces chronic inflammation induced by irradiation in the mouse brain. *Eur. J. Pharmacol.* 700 (1-3), 42–50. doi:10.1016/j.ejphar.2012.12.012

Pathak, N. M., Pathak, V., Gault, V. A., McClean, S., Irwin, N., and Flatt, P. R. (2018). Novel dual incretin agonist peptide with antidiabetic and neuroprotective potential. *Biochem. Pharmacol.* 155, 264–274. doi:10.1016/j.bcp.2018.07.021

Patnode, C. D., Perdue, L. A., Rossom, R. C., Rushkin, M. C., Redmond, N., Thomas, R. G., et al. (2020). Screening for cognitive impairment in older adults: updated evidence report and systematic review for the US preventive services task force. *JAMA* 323 (8), 764–785. doi:10.1001/jama.2019.22258

Pawlos, A., Broncel, M., Woźniak, E., and Gorzelak-Pabiś, P. (2021). Neuroprotective effect of SGLT2 inhibitors. *Molecules* 26 (23), 7213. doi:10.3390/molecules26237213

Philippaert, K., Kalyaanamoorthy, S., Fatehi, M., Long, W., Soni, S., Byrne, N. J., et al. (2021). Cardiac late sodium channel current is a molecular target for the sodium/glucose cotransporter 2 inhibitor empagliflozin. *Circulation* 143 (22), 2188–2204. doi:10.1161/CIRCULATIONAHA.121.053350

Piperi, C., Goumenos, A., Adamopoulos, C., and Papavassiliou, A. G. (2015). AGE/RAGE signalling regulation by miRNAs: associations with diabetic complications and therapeutic potential. *Int. J. Biochem. Cell Biol.* 60, 197–201. doi:10.1016/j.biocel.2015.01.009

Püschel, G. P., Klauder, J., and Henkel, J. (2022). Macrophages, low-grade inflammation, insulin resistance and hyperinsulinemia: a mutual ambiguous relationship in the development of metabolic diseases. *J. Clin. Med.* 11 (15), 4358. doi:10.3390/jcm11154358

Pyke, C., Heller, R. S., Kirk, R. K., Ørskov, C., Reedtz-Runge, S., Kaastrup, P., et al. (2014). GLP-1 receptor localization in monkey and human tissue: novel distribution revealed with extensively validated monoclonal antibody. *Endocrinology* 155 (4), 1280–1290. doi:10.1210/en.2013-1934

Qi, L., Ke, L., Liu, X., Liao, L., Ke, S., Liu, X., et al. (2016). Subcutaneous administration of liraglutide ameliorates learning and memory impairment by modulating tau hyperphosphorylation via the glycogen synthase kinase-3β pathway in an amyloid β protein induced alzheimer disease mouse model. *Eur. J. Pharmacol.* 783, 23–32. doi:10.1016/j.ejphar.2016.04.052

Qiu, C., Winblad, B., Marengoni, A., Klarin, I., Fastbom, J., and Fratiglioni, L. (2006). Heart failure and risk of dementia and Alzheimer disease: a population-based cohort study. *Arch. Intern Med.* 166 (9), 1003–1008. doi:10.1001/archinte.166.9.1003

Razay, G., Vreugdenhil, A., and Wilcock, G. (2007). The metabolic syndrome and Alzheimer disease. *Arch. Neurol.* 64 (1), 93–96. doi:10.1001/archneur.64.1.93

Reich, N., and Hölscher, C. (2022). The neuroprotective effects of glucagon-like peptide 1 in Alzheimer's and Parkinson's disease: an in-depth review. *Front. Neurosci.* 16, 970925. doi:10.3389/fnins.2022.970925

Richards, P., Parker, H. E., Adriaenssens, A. E., Hodgson, J. M., Cork, S. C., Trapp, S., et al. (2014). Identification and characterization of GLP-1 receptor-expressing cells using a new transgenic mouse model. *Diabetes* 63 (4), 1224–1233. doi:10.2337/db13-1440

Rizzo, M. R., Di Meo, I., Polito, R., Auriemma, M. C., Gambardella, A., di Mauro, G., et al. (2022). Cognitive impairment and type 2 diabetes mellitus: focus of SGLT2 inhibitors treatment. *Pharmacol. Res.* 176, 106062. doi:10.1016/j.phrs.2022.106062

Robichaux, W. G., and Cheng, X. (2018). Intracellular cAMP sensor EPAC: physiology, pathophysiology, and therapeutics development. *Physiol. Rev.* 98 (2), 919–1053. doi:10.1152/physrev.00025.2017

Rochfort, K. D., and Cummins, P. M. (2015). The blood-brain barrier endothelium: a target for pro-inflammatory cytokines. *Biochem. Soc. Trans.* 43 (4), 702–706. doi:10.1042/BST20140319

Salvatore, T., Galiero, R., Caturano, A., Rinaldi, L., Di Martino, A., Albanese, G., et al. (2022). An overview of the cardiorenal protective mechanisms of SGLT2 inhibitors. *Int. J. Mol. Sci.* 23 (7), 3651. doi:10.3390/ijms23073651

Samman, W. A., Selim, S. M., El Fayoumi, H. M., El-Sayed, N. M., Mehanna, E. T., and Hazem, R. M. (2023). Dapagliflozin ameliorates cognitive impairment in aluminum-chloride-induced alzheimer's disease via modulation of AMPK/mTOR, oxidative stress and glucose metabolism. *Pharm. (Basel)* 16 (5), 753. doi:10.3390/ph16050753

Samson, R., Jaiswal, A., Ennezat, P. V., Cassidy, M., and Le Jemtel, T. H. (2016). Clinical phenotypes in heart failure with preserved ejection fraction. *J. Am. Heart Assoc.* 5 (1), e002477. doi:10.1161/JAHA.115.002477

Sa-Nguanmoo, P., Tanajak, P., Kerdphoo, S., Jaiwongkam, T., Pratchayasakul, W., Chattipakorn, N., et al. (2017). SGLT2-inhibitor and DPP-4 inhibitor improve brain function via attenuating mitochondrial dysfunction, insulin resistance, inflammation, and apoptosis in HFD-induced obese rats. *Toxicol. Appl. Pharmacol.* 333, 43–50. doi:10.1016/j.taap.2017.08.005

Savji, N., Meijers, W. C., Bartz, T. M., Bhambhani, V., Cushman, M., Nayor, M., et al. (2018). The association of obesity and cardiometabolic traits with incident HFpEF and HFrEF. *JACC Heart Fail* 6 (8), 701–709. doi:10.1016/j.jchf.2018.05.018

Scisciola, L., Rizzo, M. R., Cataldo, V., Fontanella, R. A., Balestrieri, M. L., D'Onofrio, N., et al. (2020). Incretin drugs effect on epigenetic machinery: new potential therapeutic implications in preventing vascular diabetic complications. *FASEB J.* 34 (12), 16489–16503. doi:10.1096/fj.202000860RR

Seino, Y., Fukushima, M., and Yabe, D. (2010). GIP and GLP-1, the two incretin hormones: similarities and differences. *J. Diabetes Investig.* 1 (1-2), 8–23. doi:10.1111/j.2040-1124.2010.00022.x

Shaikh, S., Rizvi, S. M., Shakil, S., Riyaz, S., Biswas, D., and Jahan, R. (2016). Forxiga (dapagliflozin): plausible role in the treatment of diabetes-associated neurological disorders. *Biotechnol. Appl. Biochem.* 63 (1), 145–150. doi:10.1002/bab.1319

Spinelli, M., Fusco, S., and Grassi, C. (2019). Brain insulin resistance and hippocampal plasticity: mechanisms and biomarkers of cognitive decline. *Front. Neurosci.* 31, 788. doi:10.3389/fnins.2019.00788

Stanciu, G. D., Rusu, R. N., Bild, V., Filipiuc, L. E., Tamba, B. I., and Ababei, D. C. (2021). Systemic actions of SGLT2 inhibition on chronic mTOR activation as a shared pathogenic mechanism between alzheimer's disease and diabetes. *Biomedicines* 9 (5), 576. doi:10.3390/biomedicines9050576

Steven, S., Hausding, M., Kröller-Schön, S., Mader, M., Mikhed, Y., Stamm, P., et al. (2015). Gliptin and GLP-1 analog treatment improves survival and vascular inflammation/dysfunction in animals with lipopolysaccharide-induced endotoxemia. *Basic Res. Cardiol.* 110 (2), 6. doi:10.1007/s00395-015-0465-x

Steven, S., Jurk, K., Kopp, M., Kröller-Schön, S., Mikhed, Y., Schwierczek, K., et al. (2017). Glucagon-like peptide-1 receptor signalling reduces microvascular thrombosis, nitro-oxidative stress and platelet activation in endotoxaemic mice. *Br. J. Pharmacol.* 174 (12), 1620–1632. doi:10.1111/bph.13549

Tai, J., Liu, W., Li, Y., Li, L., and Holscher, C. (2018). Neuroprotective effects of a triple GLP-1/GIP/glucagon receptor agonist in the APP/PS1 transgenic mouse model of Alzheimer's disease. *Brain Res.* 1678, 64–74. doi:10.1016/j.brainres.2017.10.012

Tomic, D., Shaw, J. E., and Magliano, D. J. (2022). The burden and risks of emerging complications of diabetes mellitus. *Nat. Rev. Endocrinol.* 18, 525–539. doi:10.1038/s41574-022-00690-7

Trost, S. U., Belke, D. D., Bluhm, W. F., Meyer, M., Swanson, E., and Dillmann, W. H. (2002). Overexpression of the sarcoplasmic reticulum Ca(2+)-ATPase improves myocardial contractility in diabetic cardiomyopathy. *Diabetes* 51, 1166–1171. doi:10.2337/diabetes.51.4.1166

Trum, M., Riechel, J., Lebek, S., Pabel, S., Sossalla, S. T., Hirt, S., et al. (2020). Empagliflozin inhibits Na+/H+ exchanger activity in human atrial cardiomyocytes. *Esc. Heart Fail* 7, 4429–4437. doi:10.1002/ehf2.13024

Tsalamandris, S., Antonopoulos, A. S., Oikonomou, E., Papamikroulis, G. A., Vogiatzi, G., Papaioannou, S., et al. (2019). The role of inflammation in diabetes: current concepts and future perspectives. *Eur. Cardiol. Rev.* 14 (1), 50–59. doi:10.15420/ecr.2018.33.1

Tuunanen, H., and Knuuti, J. (2011). Metabolic remodelling in human heart failure. *Cardiovasc Res.* 90, 251–257. doi:10.1093/cvr/cvr052

Uddin, M. S., Rahman, M. A., Kabir, M. T., Behl, T., Mathew, B., Perveen, A., et al. (2020). Multifarious roles of mTOR signaling in cognitive aging and cerebrovascular dysfunction of Alzheimer's disease. *IUBMB Life* 72 (9), 1843–1855. doi:10.1002/iub.2324

Urbanek, K., Cappetta, D., Bellocchio, G., Coppola, M. A., Imbrici, P., Telesca, M., et al. (2023). Dapagliflozin protects the kidney in a non-diabetic model of cardiorenal syndrome. *Pharmacol. Res.* 188, 106659. doi:10.1016/j.phrs.2023.106659

Ussher, J. R., and Drucker, D. J. (2023). Glucagon-like peptide 1 receptor agonists: cardiovascular benefits and mechanisms of action. *Nat. Rev. Cardiol.* 20 (7), 463–474. doi:10.1038/s41569-023-00849-3

Uthman, L., Baartscheer, A., Bleijlevens, B., Schumacher, C. A., Fiolet, J. W. T., Koeman, A., et al. (2018b). Class effects of SGLT2 inhibitors in mouse cardiomyocytes and hearts: inhibition of Na+/H+ exchanger, lowering of cytosolic Na+ and vasodilation. *Diabetologia* 61, 722–726. doi:10.1007/s00125-017-4509-7

Uthman, L., Baartscheer, A., Schumacher, C. A., Fiolet, J. W. T., Kuschma, M. C., Hollmann, M. W., et al. (2018a). Direct cardiac actions of sodium glucose cotransporter 2 inhibitors target pathogenic mechanisms underlying heart failure in diabetic patients. *Front. Physiol.* 9, 1575. doi:10.3389/fphys.2018.01575

Uthman, L., Li, X., Baartscheer, A., Schumacher, C. A., Baumgart, P., Hermanides, J., et al. (2022). Empagliflozin reduces oxidative stress through inhibition of the novel inflammation/NHE/[Na+]c/ROS-pathway in human endothelial cells. *Biomed. Pharmacother.* 146, 112515. doi:10.1016/j.biopha.2021.112515

Van Skike, C. E., and Galvan, V. (2018). A perfect sTORm: the role of the mammalian target of rapamycin (mTOR) in cerebrovascular dysfunction of alzheimer's disease: a mini-review. *Gerontology* 64 (3), 205–211. doi:10.1159/000485381

Vellone, E., Chialà, O., Boyne, J., Klompstra, L., Evangelista, L. S., Back, M., et al. (2020). Cognitive impairment in patients with heart failure: an international study. *Esc. Heart Fail* 7 (1), 46–53. doi:10.1002/ehf2.12542

Virani, S. S., Alonso, A., Aparicio, H. J., Benjamin, E. J., Bittencourt, M. S., Callaway, C. W., et al. (2021). Heart disease and stroke statistics-2021 update: a report from the American heart association. *Circulation* 143 (8), e254–e743. doi:10.1161/CIR.0000000000000950

Wang, X. H., Yang, W., Holscher, C., Wang, Z. J., Cai, H. Y., Li, Q. S., et al. (2013). Val$^{8}$-GLP-1 remodels synaptic activity and intracellular calcium homeostasis impaired by amyloid β peptide in rats. *J. Neurosci. Res.* 91 (4), 568–577. doi:10.1002/jnr.23181

Wegmann, S., Biernat, J., and Mandelkow, E. (2021). A current view on Tau protein phosphorylation in Alzheimer's disease. *Curr. Opin. Neurobiol.* 69, 131–138. doi:10.1016/j.conb.2021.03.003

Wicinski, M., Socha, M., Malinowski, B., Wodkiewicz, E., Walczak, M., Gorski, K., et al. (2019). Liraglutide and its neuroprotective properties-focus on possible biochemical mechanisms in alzheimer's disease and cerebral ischemic events. *Int. J. Mol. Sci.* 20 (5), 1050. doi:10.3390/ijms20051050

Wiciński, M., Wódkiewicz, E., Górski, K., Walczak, M., and Malinowski, B. (2020). Perspective of SGLT2 inhibition in treatment of conditions connected to neuronal loss: focus on alzheimer's disease and ischemia-related brain injury. *Pharm. (Basel)* 13 (11), 379. doi:10.3390/ph13110379

Wilson, J. M., Nikooienejad, A., Robins, D. A., Roell, W. C., Riesmeyer, J. S., Haupt, A., et al. (2020). The dual glucose-dependent insulinotropic peptide and glucagon-like peptide-1 receptor agonist, tirzepatide, improves lipoprotein biomarkers associated with insulin resistance and cardiovascular risk in patients with type 2 diabetes. *Diabetes Obes. Metab.* 22 (12), 2451–2459. doi:10.1111/dom.14174

Xu, L., Nagata, N., Chen, G., Nagashimada, M., Zhuge, F., Ni, Y., et al. (2019). Empagliflozin reverses obesity and insulin resistance through fat browning and alternative macrophage activation in mice fed a high-fat diet. *BMJ Open Diabetes Res. Care* 7 (1), e000783. doi:10.1136/bmjdrc-2019-000783

Yang, X., Qiang, Q., Li, N., Feng, P., Wei, W., and Hölscher, C. (2022). Neuroprotective mechanisms of glucagon-like peptide-1-based therapies in ischemic stroke: an update based on preclinical research. *Front. Neurol.* 13, 844697. doi:10.3389/fneur.2022.844697

Ye, Y., Bajaj, M., Yang, H. C., Perez-Polo, J. R., and Birnbaum, Y. (2017). SGLT-2 inhibition with dapagliflozin reduces the activation of the Nlrp3/ASC inflammasome and attenuates the development of diabetic cardiomyopathy in mice with type 2 diabetes. Further augmentation of the effects with saxagliptin, a DPP4 inhibitor. *Cardiovasc Drugs Ther.* 31 (2), 119–132. doi:10.1007/s10557-017-6725-2

Yu, H., Rimbert, A., Palmer, A. E., Toyohara, T., Xia, Y., Xia, F., et al. (2019). GPR146 deficiency protects against hypercholesterolemia and atherosclerosis. *Cell* 179 (6), 1276–1288.e14. doi:10.1016/j.cell.2019.10.034

Zhang, L. Q., Zhang, W., Li, T., Yang, T., Yuan, X., Zhou, Y., et al. (2021a). GLP-1R activation ameliorated novel-object recognition memory dysfunction via regulating hippocampal AMPK/NF-κB pathway in neuropathic pain mice. *Neurobiol. Learn Mem.* 182, 107463. doi:10.1016/j.nlm.2021.107463

Zhang, L. Y., Zhang, L. P., Li, Y. W., Li, L., Melchiorsen, J. U., Rosenkilde, M., et al. (2020). The novel dual GLP-1/GIP receptor agonist DA-CH5 is superior to single GLP-1 receptor agonists in the MPTP model of Parkinson?s disease. *J. Park. Dis.* 10 (2), 523–542. doi:10.3233/JPD-191768

Zhang, Z., Li, X. G., Wang, Z. H., Song, M., Yu, S. P., Kang, S. S., et al. (2021b). δ-Secretase-cleaved Tau stimulates Aβ production via upregulating STAT1-BACE1 signaling in Alzheimer's disease. *Mol. Psychiatry* 26 (2), 586–603. doi:10.1038/s41380-018-0286-z

Zheng, J., Xie, Y., Ren, L., Qi, L., Wu, L., Pan, X., et al. (2021). GLP-1 improves the supportive ability of astrocytes to neurons by promoting aerobic glycolysis in alzheimer's disease. *Mol. Metab.* 47, 101180. doi:10.1016/j.molmet.2021.101180

Zhou, M., Chen, S., Peng, P., Gu, Z., Yu, J., Zhao, G., et al. (2019). Dulaglutide ameliorates STZ induced AD-like impairment of learning and memory ability by modulating hyperphosphorylation of tau and NFs through GSK3β. *Biochem. Biophys. Res. Commun.* 511 (1), 154–160. doi:10.1016/j.bbrc.2019.01.103

frontiers | Frontiers in Pharmacology

TYPE Original Research
PUBLISHED 30 July 2024
DOI 10.3389/fphar.2024.1424544



OPEN ACCESS

EDITED BY
Ludwig Weckbach,
LMU Munich University Hospital, Germany

REVIEWED BY
Sze Wa Chan,
Saint Francis University, China
Andrea Elia,
Temple University, United States

*CORRESPONDENCE
Chen Lin,
clin@ncu.edu.tw
Men-Tzung Lo,
mzlo@ncu.edu.tw

RECEIVED 28 April 2024
ACCEPTED 15 July 2024
PUBLISHED 30 July 2024

CITATION
Chen J-J, Lin C, Lo M-T, Lin L-Y, Chang H-C and Liu G-C (2024), Autonomic modulation by SGLT2i or DPP4i in patients with diabetes favors cardiovascular outcomes as revealed by skin sympathetic nerve activity.
*Front. Pharmacol.* 15:1424544.
doi: 10.3389/fphar.2024.1424544



# Autonomic modulation by SGLT2i or DPP4i in patients with diabetes favors cardiovascular outcomes as revealed by skin sympathetic nerve activity

Jien-Jiun Chen[1], Chen Lin[2]*, Men-Tzung Lo[2]*, Lian-Yu Lin[3], Hsiang-Chih Chang[2] and Geng-Chi Liu[2]

[1]Department of Internal Medicine, Division of Cardiology, Yunlin Branch of National Taiwan University Hospital, Yunlin, Taiwan, [2]Department of Biomedical Sciences and Engineering, National Central University, Taoyuan, Taiwan, [3]Department of Internal Medicine, Division of Cardiology, College of Medicine, National Taiwan University and Hospital, Taipei, Taiwan

**Background:** Sodium-glucose cotransporter 2 inhibitors (SGLT2i) and dipeptidyl peptidase-4 inhibitors (DPP4i) are important second-line treatments for patients with type 2 diabetes mellitus (T2DM). Patients taking SGLT2i have favorable cardiovascular outcomes via various mechanisms, including autonomic nervous system (ANS) modulation. This study aimed to use neuro-electrocardiography (neuECG) to test the effects of SGLT2i or DPP4i on the ANS.

**Methods:** Patients with T2DM, who did not reach target hemoglobin (Hb)A1C levels despite metformin treatment, were enrolled. SGLT2i or DPP4i were prescribed randomly unless a compelling indication was present. NeuECG and heart rate were recorded for 10 min before and after a 3-month treatment. The patients were treated according to standard practice and the obtained data for skin sympathetic nerve activity (SKNA) and ANS entropy were analyzed offline.

**Results:** We enrolled 96 patients, of which 49 received SGLT2i and 47 received DPP4i. The baseline parameters were similar between the groups. No adverse event was seen during the study period. In the burst analysis of SKNA at baseline, all parameters were similar. After the 3-month treatment, the firing frequency was higher in SGLT2i group (0.104 $\pm$ 0.045 vs 0.083 $\pm$ 0.033 burst/min, $p < 0.05$), with increased long firing duration (7.34 $\pm$ 3.66 vs 5.906 $\pm$ 2.921, $p < 0.05$) in 3-s aSKNA scale; the other parameters did not show any significant change. By symbolic entropy, the most complex patterns (Rank 3) were found to be significantly higher in SGLT2i-treated patients than in DDP4i-treated group (0.084 $\pm$ 0.028 vs 0.07 $\pm$ 0.024, $p = 0.01$) and the direction of change in Rank 3, after SGLT2i treatment, was opposite to that observed in the DDP4i group (0.012 $\pm$ 0.036 vs. −0.005 $\pm$ 0.037, $p = 0.024$). Our findings demonstrated the favorable autonomic modulation by SGLTi and the detrimental effects of DPP4i on ANS.

**Abbreviations:** T2DM, type 2 diabetes mellitus; SGLT2i, sodium glucose co-transporter 2 inhibitor; DPP4i, Dipeptidyl peptidase-4 inhibitor; CV, cardiovascular; SNS, sympathetic nervous system; AMI, acute myocardial infarction; HRV, heart rate variability; ECG, electrocardiography; SKNA, sympathetic nerve activity; iSKNA, integrated SKNA; aSKNA, averaged iSKNA; HbA1C, hemoglobin A1C; Hz, Hertz; ANS, autonomic nervous system; AF, atrial fibrillation.

**Conclusion:** We demonstrated the autonomic modulation by SGLTi and DPP4i using SKNA in patients with DM, which might provide insights into the favorable outcomes of SGLT2i. Furthermore, we refined the analytical methods of neuECG, which uses SKNA to evaluate autonomic function.

KEYWORDS

**NeuECG, skin sympathetic nerve activity, autonomic modulation, entropy analysis, sodium-glucose cotransporter 2 inhibitor**

## Introduction

Patients with type 2 diabetes mellitus (T2DM) have to take oral hypoglycemic agents in addition to lifestyle modifications (Cheng and Fantus, 2005). According to the current guidelines, the first-line therapy for T2DM uses metformin, followed by either sodium-glucose cotransporter 2 inhibitor (SGLT2i), dipeptidyl peptidase-4 inhibitor (DPP4i), α-glucosidase inhibitor, or sulfonylureas (Qaseem et al., 2017; Flory and Lipska, 2019; Grant and Cosentino, 2019; Dong et al., 2023). Of the second-line drugs, SGLT2i and DPP4i have no side effect of hypoglycemia (Molina-Vega et al., 2018), and have a positive effect (SGLT2i) on cardiovascular (CV) outcomes, including CV mortality, heart failure hospitalization, and myocardial infarction, regardless of the glycemic status (Zelniker et al., 2019; Chan and Chan, 2023; He et al., 2023; Talha et al., 2023). Although the CV effect of DPP4i is controversial, most studies have shown neutral effects (Scheen, 2018; Rosenstock et al., 2019; Subrahmanyan et al., 2021). The mechanisms underlying SGLT2i have favorable CV outcomes, including natriuresis, diuresis, glycemic control, improved cardiac metabolism, prevention of adverse cardiac remodeling and ischemia-reperfusion injury, and inhibition of sympathetic nervous system (SNS) activity (Cowie and Fisher, 2020; Lopaschuk and Verma, 2020). A previous study had compared heart rate variability (HRV) outcomes in patients with acute myocardial infarction (AMI) taking SGLT2i or placebo and showed that early SGLT2i administration in patients with AMI and T2DM might be effective in improving cardiac nerve activity without any adverse event (Shimizu et al., 2020). The study used traditional HRV to evaluate the SNS activity. Many theories have been postulated regarding this phenomenon, one such suggested that a reduction in renal stress results in the inhibition of renal afferent sympathetic activation (Sano, 2018; Herat et al., 2020; Sano, 2020).

We consider signals with frequencies beyond 150 Hz in the electrocardiography (ECG) as noise (Uradu et al., 2017). However, studies have shown that such signals can convey information about the skin sympathetic nerve activity (SKNA) (Jiang et al., 2015), and SKNA elevation or bursts have been found to trigger ventricular arrhythmia and initiate and terminate atrial arrhythmia (Kusayama et al., 2019). SKNA can be directly and noninvasively measured using conventional ECG electrodes with a high-band-pass amplifier (Kusayama et al., 2019). Validation was performed by recording stellate ganglion and thoracic invasion, which showed consistent data (Jiang et al., 2015). Standard methods for recording and analyzing these complex signals, including iSKNA and aSKNA, have already been published and formally named as neuECG (Kusayama et al., 2020). Although SKNA has been demonstrated to accurately estimate sympathetic nerve activity and be potent for clinical applications, there has been no report concerning the direct measurement of sympathetic activity in patients with T2DM taking second-line medication for which decreased cardiovascular morbidity and mortality and improved renal outcomes due to sympathetic inhibition have been emphasized (Karakas et al., 2013; Cowie and Fisher, 2020; Lopaschuk and Verma, 2020).

In this study, we considered that SKNA detected by neuECG can provide information on the sympathetic control of the cardiovascular and renal systems, resulting in favorable outcomes. We analyzed SKNA data using published methods and developed entropy analyses. To balance glycemic control as a possible confounding factor, we recruited patients taking DPP4i for comparison. We hypothesized that SGLT2i has favorable sympathetic modulation effects, which could be proven by SKNA using neuECG.

## Materials and methods

From December 2020 to August 2022, we recruited patients with T2DM who had hemoglobin A1C (HbA1C) levels higher than the therapeutic goal (6.5%) despite treatment with metformin or those who could not tolerate metformin. Patient was screened for eligibility and were excluded if he/she had heart failure symptoms or severe chornic kidney disease. The patients were prescribed SGLT2i (empagliflozin 25 mg once daily) or DPP4i (linagliptin 5 mg once daily) as second-line treatment for their DM per treating physician's judgement (in a random manner unless compelling indication or contraindication existed).

### Data acquisition

SKNA parameters were obtained using traditional bipolar electrodes, and Lead II signals were recorded for 10 min and digitized at 10,000 Hz by a fully programmable amplifier/data acquisition unit (MP36, BIOPAC, USA). Both ECG and SKNA data were filtered through two distinct filter types. Before treatment, we recorded the SKNA for 10 min, and after 3 months of treatment, we recorded the SKNA again. (Figure 1). All recordings were performed at an outpatient clinic in a small private room after the patient had rested fully. Drug compliance was confirmed by direct confrontation. Patient baseline characteristics, including underlying disease, glucose level, HbA1C level, renal function, and medication, were reviewed. Patients received usual care for their diseases. Offline analysis of the SKNA data was performed using custom-developed MATLAB programs. The study was

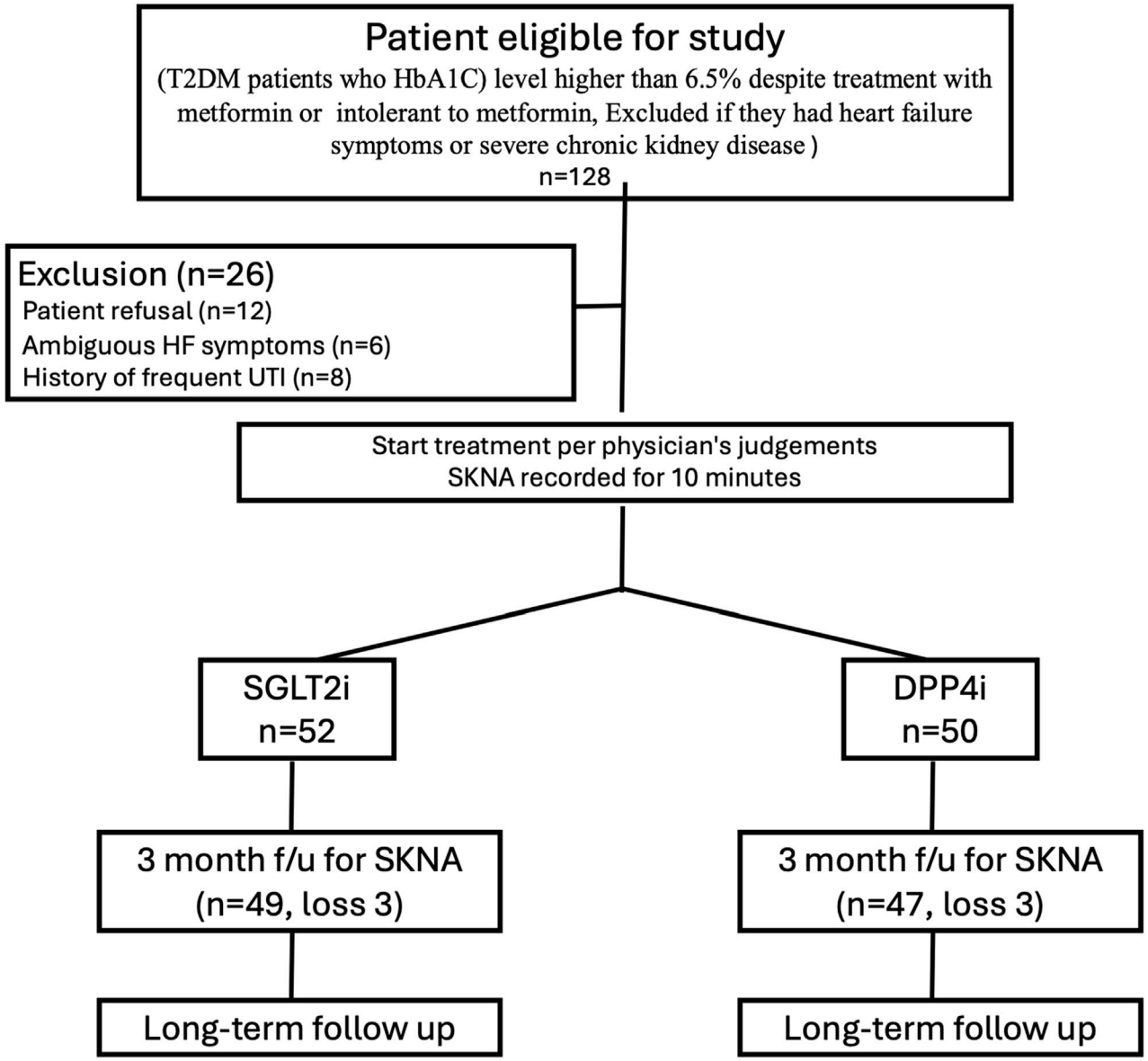


FIGURE 1
Study protocol. The figure showed the study protocol. After assessment of eligibility (Patients with T2DM, who had hemoglobin A1C (HbA1C) levels higher than the therapeutic goal (6.5%) despite treatment with metformin or those who could not tolerate metformin. Patient were excluded if he/she had heart failure symptoms or severe chornic kidney disease). We excluded some patients before prescription and performing SKNA recording. We excluded patients with symptoms that might be related to heart failure and patients with frequent urinary tract infection. Some patients were excluded because he/she did not want to take part in the study.

conducted in compliance with the Declaration of Helsinki. This study was approved by the Research Ethics Committee of the National Taiwan University Hospital (202107096RINA).

## Data preprocessing

ECG recordings in adults were extracted using a band-pass filter ranging from 0.05 to 150 Hz, with amplitudes measured in millivolts. For the SKNA signal, a high-pass filter with a cutoff frequency of 500 Hz was employed to differentiate electrical signals from sources such as the electrocardiogram and myopotential signals. In addition, a 1000-Hz low-pass filter was used to attenuate the electrical noise caused by radio frequency interference (Kusayama et al., 2020; Chen et al., 2022). The filtered signals (SKNA) were then rectified. Summation of the instantaneous rectified SKNA over a 100-m time window was denoted as the integrated SKNA (iSKNA) (Kusayama et al., 2020; Chen et al., 2022). Averaging the iSKNA (aSKNA) signal over a less-than-2-s window significantly correlated with heart rate (i.e., heart rates significantly affected aSKNA amplitude due to similar frequency). Consequently, we considered only time windows of 3 s or longer as potential signals for further analysis, aiming to quantify time-dependent sympathetic nerve activity. Drawing inspiration from

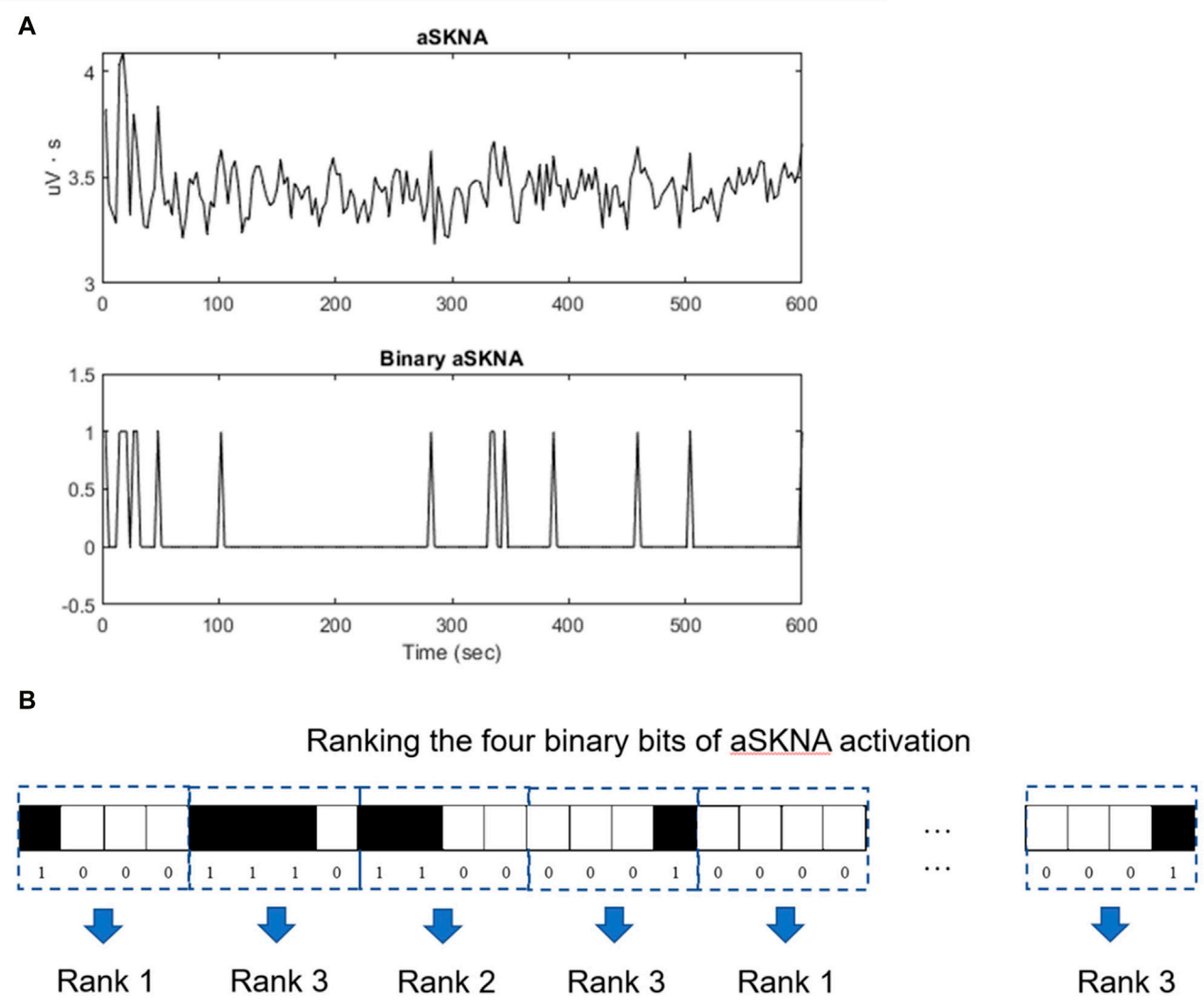


FIGURE 2
Entropy analysis of the aSKNA signals. **(A)** The aSKNA signal is transformed into a binary sequence by applying a specific threshold, "1" denoting activation, and "0" denoting non-activation. **(B)** Subsequently, the binary sequence is segmented into numerous non-overlapping blocks, each of uniform length, denoted by "m" (for instance, m = 4). These segments are classified into distinct categories according to their conditional probabilities, ensuring that segments within the same category possess identical conditional probabilities. Comprehensive categorization is performed for all conceivable 4-bit sequences, which are then arranged according to their conditional probabilities. For instance, a category ranked '3' represents sequences with the highest complexity, whereas a rank of '1' corresponds to sequences that are the most predictable.

the frequency-domain analysis in heart rate variability tests, we hypothesized that shorter time windows are more likely to evaluate the interaction between sympathetic and parasympathetic activities. Time windows of 10 s or longer were deemed inapplicable for further analysis owing to the limited recording time. Additionally, the peak of each QRS wave in the ECG data was annotated using an automated algorithm and carefully corrected by experienced technicians.

## Burst analysis

The presence of aSKNA bursts may be related to the initiation and termination of cardiac arrhythmias (Sano, 2020). Burst activity can be differentiated from baseline activity, which consists of random single spikes with large amplitudes and durations. To differentiate between the baseline and burst, we used the k-means algorithm to cluster the unsupervised data (aSKNA) into two groups (Kusayama et al., 2020). The mean value plus three times the standard deviation of the group with a relatively low amplitude was used as the threshold for burst determination of each subject (Kusayama et al., 2020). A complete burst starts at the point where the amplitude of an aSKNA signal exceeds the threshold and ends at the point where the amplitude of the signal is below the threshold. The aSKNA parameters were calculated as follows:

- Burst amplitude (μV) is the average voltage during burst within the time frame being evaluated;
- Burst frequency (bursts/min) is the total number of "On," amplitudes of aSKNA that exceed the threshold, in every minute;

- Burst duration (%) = $\frac{\text{total span of burst (min)}}{\text{total span of the time frame being evaluated (min)}} \times 100$;
  - ◆ The study duration was divided into short and long periods. Long firing duration in 1-s window means >2 s and in 5-s window means > 10 s.
- Total burst area (μV · min) is the sum total of burst area (μV · min) within the time frame being evaluated.

## Symbolic entropy analysis

To quantify the predictability or complexity of a highly fluctuating time series, we denoted the aSKNA signal as a binary sequence based on an individual threshold (1 for activation and 0 for non-activation). This sequence was then divided into multiple nonoverlapping segments of equal length m (in this study, m was set to 4). These m-bit sequences were categorized based on their temporal patterns using the concept of approximate/sample entropy (Lake et al., 2002; Lo et al., 2015). For instance, a 4-bit sequence was dissected into multiple single-bit vectors, and vectors with identical binary codes in the sequence were collected. Conditional probability of the subsequent bit was ascertained, given the same preceding status (Figure 2). Sequences were allocated to different categories based on their conditional probabilities, meaning that sequences within a category shared identical conditional probabilities. Categories were established for all possible 4-bit sequences and were ranked according to their conditional probabilities. For example, the highest rank 3 signified the most complex pattern, whereas rank 1 indicated the most predictable pattern.

## Statistical analysis

Continuous variables with a normal distribution are expressed as mean ± standard deviation. Categorical variables are expressed as percentages. The demographics, comorbid diseases, and medication use of the surviving and expired patients were compared. Normality of the variables was tested using the Shapiro-Wilk test, and the between-group differences of continuous variables with normal distribution were tested using the Student's t-test; the Mann-Whitney U test was used for non-normally distributed variables. Categorical variables were compared between the patients with different outcomes using Fisher's exact test. The hazard ratios of variables with significant between-group differences were further estimated using the Cox proportional hazard regression model. The optimal dichotomization cutoff points of the variables were determined by the best results of the log-rank test sought from the 30th to 70th percentile in fifth percentile increments each time. All statistical analyses were performed using R software, version 3.5.0. Statistical significance was set at $p < 0.05$.

## Sample size calculation

The sample size for our study was determined through a power analysis. Previous research by Hynninen P. indicated a strong correlation between skin sympathetic nerve activity (SKNA) and sudomotor activity (Hynninen, 2020). Additionally, Syngle A et al. identified a large effect size in alterations of submotor activity after 12 weeks of DPP4i treatment (Syngle et al., 2021). In our study, we anticipated a medium to large effect size of 0.65 for changes in SKNA post-medication. We set the significance level (alpha) at 0.05 and aimed for a power of 85%, using a two-tailed paired t-test to evaluate this effect. Based on these parameters, the calculated sample size required for our study was determined to be approximately 44 participants per group.

# Results

We enrolled 96 patients in our study, general characteristics of whom are listed in Table 1. For treatment, 49 patients took SGLT2i, and 47 patients took DPP4i. No significant difference was seen in the underlying diseases, AC sugar, HbA1C, renal function, or medications (Table 2). Some patients had past medical history of heart failure but at the moment of study, they were asymptomatic, and their heart failure were heart failure with preserved ejection fraction or heart failure with recovered ejection fraction. No major adverse cardiovascular outcome occurred during this period, and no patient experienced urinary tract infections, pancreatitis, or hypoglycemic episodes. After 3 months of treatment, AC sugar and HbA1C decreased numerically (Table 2), though only in the SGLT2i group; the HbA1C reached statistical significance (for AC sugar, 138 ± 26 vs 126 ± 51, p = 0.154 for SGLTi group; 152 ± 55 vs 135 ± 48, p = 0.112 for DPP4i group; for HbA1C, 7.5 ± 1.3 vs 6.9 ± 1.0, p = 0.03for SGLT2i group, 7.8 ± 1.7 vs vs 7.1 ± 1.7, p = 0.07 for DPP4i group). Renal function was stable in both the groups during this period. During follow up, only one patient experienced major adverse cardiovascular outcome. The patient had ST-segment elevation myocardial infarction, which was treated by primary angioplasty. She was taking DPP4i for the treatment of diabetes mellitus, and has been doing well till date. HRV parameters between patients using SGLT2i and DDP4i exhibited no differences at baseline or after treatment, as shown in Supplementary Table S1. Additionally, there were no significant changes in HRV parameters from baseline to post-treatment in either group.

The results of aSKNA within a 3-s time window for each group, both before and after treatment, are presented in Table 3. Additionally, we compared the changes in the derived parameters before and after treatment in the SGLT2i and DPP4i groups to assess the direction and magnitude of the effects of the drugs on these parameters. Figures 3, 4 display the typical changes observed in the burst and symbolic entropy analyses of SKNA in patients treated with DDP4i and SGLT2i, respectively. Table 3 shows that at baseline, all aSKNA parameters measured over a 3-s window were similar between the groups. After a 3-month treatment period, the firing frequency significantly increased in SGLT2i inhibitor group, but decreased in the DDP4i group (baseline firirng frequency: 0.091 ± 0.048 vs 0.091 ± 0.038, p = 0.972; post treatment 0.104 ± 0.045, 0.083 ± 0.033; difference 0.013 ± 0.051 vs. −0.007 ± 0.049, p = 0.044 in SGLT2i and DPP4i group respectively). Furthermore, post-treatment measurements indicated a longer firing duration in the SGLT2i group (baseline 6.309 ± 4.266 vs 6.274 ± 3.125, p = 0.963; post treatment 7.34 ± 3.66 vs 5.906 ± 2.921, p = 0.034 in SGLT2i and DPP4i group respectively). However, no significant change was observed in other SKNA parameters following the treatments.

TABLE 1 Baseline characteristics of the study participants.

| Basic characteristics | SLGT2i | DPP4i | P-value |
|---|---|---|---|
| | N = 49 | N = 47 | |
| Age (year) | 68 ± 10 | 67 ± 14 | 0.82 |
| Male, no. (%) | 31 (63) | 25 (53) | 0.32 |
| Atrial fibrillation, no. (%) | 8 (16) | 9 (19) | 0.72 |
| History of heart failure no. (%) | 12 (24) | 11 (23) | 0.96 |
| Hypertension no. (%) | 43 (87) | 42 (89) | 0.80 |
| Coronary artery disease no. (%) | 24 (50) | 27 (57) | 0.41 |
| Medication | | | |
| ACEi/ARB, % | 35 (71) | 27 (57) | 0.76 |
| Beta-blocker, % | 33 (67) | 33 (70) | 0.86 |
| Statins, % | 30 (61) | 25 (53) | 0.43 |

Values are expressed as mean ± standard deviation, median (interquartile range), or number (percentage).
Abbreviations: SGLT2i, sodium-glucose co-transporter 2 inhibitor; DPP4i, Dipeptidyl peptidase-4, inhibitor; HbA1c, hemoglobin A1C; eGFR, estimated glomerular filtration rate; ACEi/ARB, angiotensin-converting enzyme inhibitor/angiotensin receptor blocker.

TABLE 2 Changes in clinical measurements.

| Changes in parameters | Pre-treatment | Post-treatment | p |
|---|---|---|---|
| SGT2i group; N = 49 | | | |
| AC sugar, mg/dL | 138 ± 26 | 126 ± 51 | 0.154 |
| HbA1C (%) | 7.5 ± 1.3 | 6.9 ± 1.0 | 0.03 |
| eGFR (ml/min/1.73 $m^2$) | 83 ± 27 | 83 ± 31 | 0.83 |
| DPP4i group; N = 47 | | | |
| AC sugar, mg/dL | 152 ± 55 | 135 ± 48 | 0.112 |
| HbA1C (%) | 7.8 ± 1.7 | 7.1 ± 1.3 | 0.07 |
| eGFR (ml/min/1.73 $m^2$) | 74 ± 30 | 77 ± 32 | 0.62 |

Abbreviations as Table 1.

By symbolic entropy analysis (Table 4), no significant difference was found between the DDP4i and SGLT2i groups before and after treatment in terms of the components of the most predictive to complex patterns (Ranks 1–3). However, the most complex patterns (Rank 3) were significantly higher post-SGLT2i treatment than post-DDP4i therapy (0.084 ± 0.028 vs 0.07 ± 0.024, p = 0.01). Furthermore, the direction of change in Rank 3 following SGLT2i treatment was opposite to that observed in the DDP4i group (0.012 ± 0.036 vs. −0.005 ± 0.037, p = 0.024). Representative figures describing pre-and post treatment changes in DPP4i and SGLT2i were showed in Figures 3, 4 respectively.

## Discussion

In this study, we reported that neuECG is a feasible tool for evaluating sympathetic nerve activity in patients with DM in an outpatient clinical setting. After a 3-month treatment with SGLT2 inhibitors, there was a notable decrease in firing frequency and a significant increase in the duration of long firing episodes using 3-s aSKNA window. Entropy analysis revealed that complex activation patterns may indicate effective modulation dynamics in the SGLT2 inhibitor group. The above findings supported the sympathetic modulation of these drugs, provided a pharmacological basis for favorable cardiovascular and renal outcomes in patients taking SGLT2i, and showed the powerful application of neuECG in delineating changes in the autonomic nervous system.

Autonomic nervous system (ANS) activation plays a crucial role in cardiovascular outcomes (Karakas and Koenig, 2013), including myocardial infarction, heart failure (Wu and Vaseghi, 2020), and arrhythmia initiation and termination (Kusayama et al., 2019; Tsai et al., 2023). Compared to age-matched healthy controls (Supplementary Table S2), DM patients displayed significantly higher aSKNA threshold, mean amplitude, and burst amplitude over a timescale of 1–5 s. This suggests marked autonomic

TABLE 3 aSKNA in 3-s time window.

| SKNA | SGLT2i N = 49 | DPP4i N = 47 | P-value |
|---|---|---|---|
| Pre-treatment | | | |
| Baseline (μV) | 1.812 ± 0.159 | 1.837 ± 0.121 | 0.388 |
| Threshold (μV) | 1.909 ± 0.123 | 1.928 ± 0.096 | 0.401 |
| Frequency (b/m) | 0.091 ± 0.048 | 0.091 ± 0.038 | 0.972 |
| Duration (%) | 17.819 ± 14.207 | 15.849 ± 6.658 | 0.388 |
| Duration, long (%) | 6.309 ± 4.266 | 6.274 ± 3.125 | 0.963 |
| Duration, short (%) | 11.511 ± 14.696 | 9.575 ± 6.493 | 0.408 |
| Burst amplitude (μV) | 1.863 ± 0.129 | 1.877 ± 0.112 | 0.564 |
| Mean amplitude (μV) | 1.948 ± 0.098 | 1.961 ± 0.083 | 0.477 |
| Area (μV*mins) | 0.328 ± 0.805 | 0.199 ± 0.158 | 0.286 |
| Post-treatment | | | |
| Baseline (μV) | 1.798 ± 0.198 | 1.839 ± 0.108 | 0.217 |
| Threshold (μV) | 1.894 ± 0.168 | 1.937 ± 0.083 | 0.116 |
| Frequency (b/m) | 0.104 ± 0.045 | 0.083 ± 0.033 | 0.011* |
| Duration (%) | 17.947 ± 6.322 | 16.491 ± 8.343 | 0.325 |
| Duration, long (%) | 7.34 ± 3.66 | 5.906 ± 2.921 | 0.034* |
| Duration, short (%) | 10.606 ± 6.476 | 10.585 ± 9.224 | 0.989 |
| Burst amplitude (μV) | 1.841 ± 0.192 | 1.886 ± 0.092 | 0.15 |
| Mean amplitude (μV) | 1.932 ± 0.146 | 1.969 ± 0.076 | 0.121 |
| Area (μV*mins) | 0.228 ± 0.138 | 0.245 ± 0.264 | 0.681 |
| Difference | | | |
| Baseline (μV) | −0.013 ± 0.221 | 0.002 ± 0.106 | 0.678 |
| Threshold (μV) | −0.015 ± 0.185 | 0.009 ± 0.089 | 0.584 |
| Frequency (b/m) | 0.013 ± 0.051 | −0.007 ± 0.049 | 0.044* |
| Duration (%) | 0.128 ± 15.229 | 0.642 ± 10.086 | 0.954 |
| Duration, long (%) | 1.032 ± 4.383 | −0.368 ± 3.834 | 0.113 |
| Duration, short (%) | −0.904 ± 15.873 | 1.009 ± 9.797 | 0.698 |
| Burst amplitude (μV) | −0.022 ± 0.196 | 0.008 ± 0.098 | 0.438 |
| Mean amplitude (μV) | −0.016 ± 0.155 | 0.008 ± 0.085 | 0.475 |
| Area (μV*min) | −0.1 ± 0.821 | 0.046 ± 0.232 | 0.409 |

All values are expressed as mean ± SD. *denotes $p < 0.05$.
Abbreviations: SKNA, skin sympathetic nerve activity; please refer to text for definition.

dysfunction in individuals with DM. In our previous study, we found that in patients undergoing ablation for atrial fibrillation, post-ablation firing for a long duration in the aSKNA 5-s window was a significant predictor of recurrence (Chen et al., 2022). Patients free of AF after ablation had a longer firing duration in the 5-s aSKNA analyses. Although the mechanism of recurrence was complex, given that higher SNS activity initiated AF, we believe that proper modulation of the autonomic nervous system is crucial for AF treatment. Likewise, we found that treatment with SGLT2i had similar effects on the SNS, which might explain the effects of SNS modulation translating into favorable cardiovascular outcomes.

The onset of T2DM is becoming earlier in population (Pan and Jia, 2018). In addition to the consequences of hyperglycemia, T2DM has severe adverse cardiovascular and renal outcomes (Lo et al., 2020), and SGLT2i could be a potential medication to reverse these outcomes (Zelniker et al., 2019). Our study provided solid evidence for SNS modulation by SGLT2i in patients with DM. In our previous studies, SNS played a crucial role in determining mortality in critically ill patients (Chen et al., 2021) and could predict AF ablation outcomes (Chen et al., 2022). We believe that we provided mechanistic evidence to treat young patients with SGLT2i, which might improve their health condition, especially CV and renal function. Syngle A et al. observed significantly higher sudomotor activity after 12 weeks of DPP4 inhibitor treatment, indicating an increase in sympathetic activity. Additionally, there were significant reductions in both blood pressure and heart rate responses to standing and the Valsalva maneuver compared to baseline measurements ((Syngle et al., 2021). In our study, we found that HRV parameters were less sensitive in a resting state compared to their response under stimuli. Moreover, most HRV parameters did not show significant changes in patients treated with SGLT2i, even after 1 year (Sardu et al., 2022). Given the strong association between SKNA and sudomotor activity, SKNA may serve as a more sensitive surrogate for evaluating autonomic function.

Entropy analysis was used to assess the predictability and dynamics of neural activities. Research has demonstrated that a reduction in entropy may serve as an indicator of various diseases, including cardiovascular diseases (Costa et al., 2005; Ho et al., 2011; Chiu et al., 2017) and type I diabetes (Trunkvalterova et al., 2008). The observed increase in the most complex patterns (Rank 3) following SGLT2 inhibitor (SGLT2i) treatment, as compared to DDP4 inhibitor (DDP4i) therapy, not only indicated an increase in the complexity of autonomic nerve activity but also pointed to an adaptive improvement in modulation dynamics following SGLT2i treatment. This was in addition to the changes in firing characteristics, such as frequency and duration. These findings go beyond cardiac autonomic regulation, suggesting a wider physiological and therapeutic importance of SGLT2 inhibitors. These insights underscored the importance of incorporating symbolic entropy analysis into the assessment of neuECG dynamics to provide a deeper understanding of the behavior of the autonomic nervous system in health and disease. Our findings indicate that the complexity of autonomic system modulation can be quantified using entropy analysis. Furthermore, the cardio-renal protective effects of SGLT2 inhibitors may be attributed to the restoration of autonomic modulation in patients with DM.

SGLT2i show some contraindications in patients with ketoacidosis, advanced chronic kidney disease (CKD), or frequent urinary tract infection after treatment with SGLT2i (Seidu et al., 2022). However, in continuous usage of SGLT2i in advanced CKD DPP4i has been advocated (Yau et al., 2022). DPP4i, especially linagliptin, can be used in all patients, including those with liver or renal dysfunction and DM, except for patients with pancreatitis after DPP4i (Scott, 2011). From pharmacological point of view (including SNS modulation and other effects) and current clinical evidence,

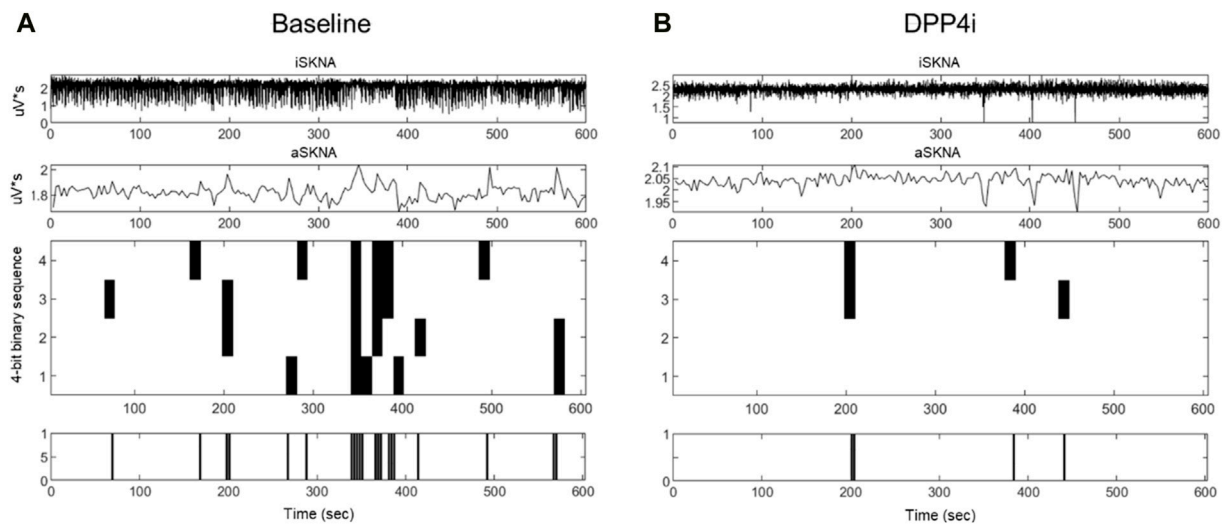


FIGURE 3
Typical characteristic activation patterns of aSKNA in patients before **(A)** and after **(B)** DDP4 inhibitor treatment. The traces from top to bottom represent iSKNA, aSKNA with a 3-s window, and 4-bit activation patterns, respectively. Each vertical line indicates a 4-bit binary sequence of activation patterns, with activation depicted in white and non-activation in black. Decreased activation frequency and an increase in less complex patterns (rank 1) were observed.

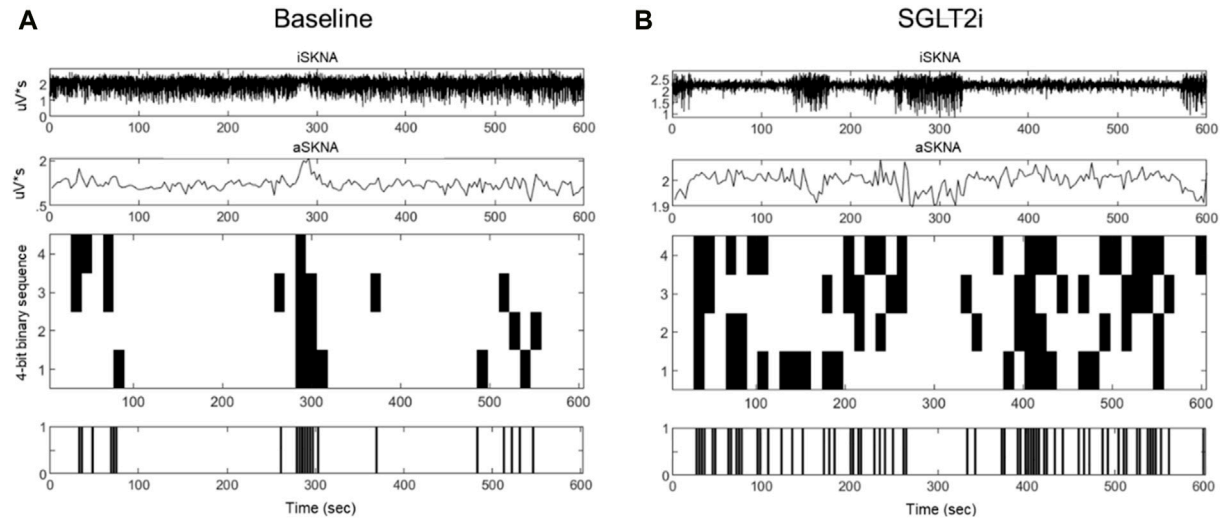


FIGURE 4
Typical characteristic activation patterns of aSKNA in patients before **(A)** and after **(B)** SGLT2 inhibitor treatment. The traces from top to bottom represent iSKNA, aSKNA with a 3-swindow, and 4-bit activation patterns, respectively. Each vertical line indicates a 4-bit binary sequence of activation patterns, with activation depicted in white and non-activation in black. Patients receiving SGLT2 inhibitors demonstrated patterns of greater complexity and extended durations of activation.

given that SGLT2i reduced major cardiovascular events and improved renal outcome in patients with T2DM or heart failure regardless of glycemic control, and based on our data from neuECG analyses on autonomic modulation, we would recommend SGLT2i as a second-line medication or even first-line medication in patients with T2DM and as a standard treatment in patients with HF.

This study has several limitations. The number of recruited patients was limited, and the recording was performed at an outpatient clinic. Environmental and seasonal effects cannot be ignored. While the study period was 3 months only, the patients used the drugs continuously and could have changed to combination therapy (SGLT2i and DPP4i). However, the long-term effects of these drugs and their combinations would require further elucidation. All patients were managed by a single cardiologist and, although the number of cases was limited, the treatment policies for their underlying diseases were similar. We believe that unnecessary changes in medication or other interventions that interfere with the outcomes in different

TABLE 4 Entropy parameters.

| SKNA | SGLT2i | DPP4i | P-value |
|---|---|---|---|
| | N = 49 | N = 47 | |
| Pre-treatment | | | |
| Rank 1 | 0.737 ± 0.123 | 0.736 ± 0.104 | 0.981 |
| Rank 2 | 0.192 ± 0.096 | 0.189 ± 0.081 | 0.853 |
| Rank 3 | 0.071 ± 0.031 | 0.075 ± 0.026 | 0.497 |
| Post-treatment | | | |
| Rank 1 | 0.702 ± 0.117 | 0.756 ± 0.088 | 0.011* |
| Rank 2 | 0.215 ± 0.092 | 0.174 ± 0.067 | 0.015* |
| Rank 3 | 0.084 ± 0.028 | 0.07 ± 0.024 | 0.01* |
| Difference | | | |
| Rank 1 | −0.035 ± 0.138 | 0.02 ± 0.138 | 0.088 |
| Rank 2 | 0.023 ± 0.106 | −0.014 ± 0.104 | 0.146 |
| Rank 3 | 0.012 ± 0.036 | −0.005 ± 0.037 | 0.024* |

All values are expressed as mean ± SD. *denotes $p < 0.05$.
Abbreviation: HR, heart rate.

scenarios can be avoided. We intentionally performed a randomized study; however, the use of SGLT2i and DPP4i had compelling indications or contraindications and there are complex reimbursement issues in Taiwan (approval of SGLT2i for heart failure were later than publish of randomized controlled trials and international guidelines). Moreover, during the study period, new clinical evidences for SGLT2i were published. Therefore, this study was not fully randomized. We belived that HbA1C/Age/Sex/Ethnicity might affect autonomic function. The study population were all East-Asian and their age/sex and baslineline HbA1C were matched in study groups. We found there's no difference in SKNA parameters between men and women except firing frequency (Supplementary Table S3). However futher large scale study might be conducted to address these concerns. Our study showed entropy analysis was a powerful tool to evaluate autonomic function in DM patients; however, we were not sure the application could be generalized to other diseases.

In conclusion, our study demonstrated that improved autonomic regulation, as evidenced by SKNA analyses, including burst and symbolic entropy analyses, could be a plausible explanation for the favorable cardiovascular and renal outcomes associated with SGLT2i observed in numerous clinical trials. Furthermore, we refined neuECG analyses to enhance the ability of the method to evaluate autonomic modulation under different scenarios. We would recommend considering SGLT2i as a second- or even first-line medication for patients with type 2 diabetes mellitus (T2DM), even in the absence of heart failure, unless there are compelling contraindications.

## Data availability statement

The raw data supporting the conclusions of this article will be made available by the authors, without undue reservation.

## Ethics statement

The studies involving humans were approved by Research ethics committee of National Taiwan University Hospital. The studies were conducted in accordance with the local legislation and institutional requirements. The participants provided their written informed consent to participate in this study.

## Author contributions

J-JC: Data curation, Writing–original draft, Visualization, Resources, Methodology, Investigation, Funding acquisition, Formal Analysis, Conceptualization. CL: Writing–review and editing, Writing–original draft, Validation, Investigation, Formal Analysis, Data curation. M-TL: Writing–review and editing, Validation, Resources, Formal Analysis. L-YL: Writing–review and editing, Validation, Supervision. H-CC: Writing–review and editing, Formal Analysis, Data curation. G-CL: Writing–review and editing, Formal Analysis.

## Funding

The author(s) declare that financial support was received for the research, authorship, and/or publication of this article. J-JC was supported by the National Science and Technology Council (NSTC; Taiwan, ROC) [grant number 110-2314-B-002 -217 -MY2]. CL and M-TL were supported by NSTC [grant numbers 110-2221-E-008 -093, 108-2221-E-008-095-MY2, and 109-2823-8-008-002-CV].

## Acknowledgments

We thank Prof. Shien-Fong Lin and Dr. Chun Liu for recording and setting the parameters. We thank all the patients who participated in this study.

## Conflict of interest

The authors declare that the research was conducted in the absence of any commercial or financial relationships that could be construed as a potential conflict of interest.

## Publisher's note



## Supplementary material

The Supplementary Material for this article can be found online at: https://www.frontiersin.org/articles/10.3389/fphar.2024.1424544/full#supplementary-material

# References


Chan, J. C. H., and Chan, M. C. Y. (2023). SGLT2 inhibitors: the next blockbuster multifaceted drug? *Med. Kaunas.* 59, 388. doi:10.3390/medicina59020388

Chen, J. J., Lin, C., Chuang, Y. C., Lee, S. F., Lin, T. Y., Yu, C. C., et al. (2022). Alterations of sympathetic dynamics after atrial fibrillation ablation by analysis sympathetic nerve activity provide prognostic value for recurrence and mechanistic insights into ablation. *Front. Cardiovasc. Med.* 9, 1024156. doi:10.3389/fcvm.2022.1024156

Chen, J. J., Lin, C., Lo, M. T., and Lin, L. Y. (2021). Complex dynamics of skin sympathetic nerve activities provides mechanistic insights into critical-illness and are prognostic predictors. *J. Formos. Med. Assoc.* 120, 1041–1042. doi:10.1016/j.jfma.2020.10.010

Cheng, A. Y. Y., and Fantus, I. G. (2005). Oral antihyperglycemic therapy for type 2 diabetes mellitus. *CMAJ* 172, 213–226. doi:10.1503/cmaj.1031414

Chiu, H. C., Ma, H. P., Lin, C., Lo, M. T., Lin, L. Y., Wu, C. K., et al. (2017). Serial heart rhythm complexity changes in patients with anterior wall ST segment elevation myocardial infarction. *Sci. Rep.* 7, 43507. doi:10.1038/srep43507

Costa, M., Goldberger, A. L., and Peng, C. K. (2005). Multiscale entropy analysis of biological signals. *Phys. Rev. E Stat. Nonlin. Soft Matter Phys.* 71, 021906. doi:10.1103/PhysRevE.71.021906

Cowie, M. R., and Fisher, M. (2020). SGLT2 inhibitors: mechanisms of cardiovascular benefit beyond glycaemic control. *Nat. Rev. Cardiol.* 17, 761–772. doi:10.1038/s41569-020-0406-8

Dong, Y., Qi, Y., Jiang, H., Mi, T., Zhang, Y., Peng, C., et al. (2023). The development and benefits of metformin in various diseases. *Front. Med.* 17, 388–431. doi:10.1007/s11684-023-0998-6

Flory, J., and Lipska, K. (2019). Metformin in 2019. *JAMA* 321, 1926–1927. doi:10.1001/jama.2019.3805

Grant, P. J., and Cosentino, F. (2019). The 2019 ESC guidelines on diabetes, pre-diabetes, and cardiovascular diseases developed in collaboration with the EASD: new features and the "ten commandments" of the 2019 guidelines are discussed by professor peter J. Grant and professor francesco Cosentino, the task force chairmen. *Eur. Heart J.* 40, 3215–3217. doi:10.1093/eurheartj/ehz687

He, G., Yang, G., Huang, X., Luo, D., Tang, C., and Zhang, Z. (2023). SGLT2 inhibitors for prevention of primary and secondary cardiovascular outcomes: a meta-analysis of randomized controlled trials. *Heart Lung* 59, 109–116. doi:10.1016/j.hrtlng.2023.02.009

Herat, L. Y., Magno, A. L., Rudnicka, C., Hricova, J., Carnagarin, R., Ward, N. C., et al. (2020). SGLT2 inhibitor-induced sympathoinhibition: a novel mechanism for cardiorenal protection. *JACC Basic Transl. Sci.* 5, 169–179. doi:10.1016/j.jacbts.2019.11.007

Ho, Y. L., Lin, C., Lin, Y. H., and Lo, M. T. (2011). The prognostic value of non-linear analysis of heart rate variability in patients with congestive heart failure–A pilot study of multiscale entropy. *PLOS ONE* 6, e18699. doi:10.1371/journal.pone.0018699

Hynninen, P. (2020). Studies of sympathetic nerve activity in cutaneous nerves in healthy subjects using intraneural microneurography (Accession No. 2013420395). Doctoral dissertation. Uppsala: Uppsala University Publications.

Jiang, Z., Zhao, Y., Doytchinova, A., Kamp, N. J., Tsai, W. C., Yuan, Y., et al. (2015). Using skin sympathetic nerve activity to estimate stellate ganglion nerve activity in dogs. *Heart Rhythm* 12, 1324–1332. doi:10.1016/j.hrthm.2015.02.012

Karakas, M., and Koenig, W. (2013). Sympathetic nervous system: a crucial player modulating residual cardiovascular risk. *Circ. Res.* 112, 13–16. doi:10.1161/CIRCRESAHA.112.281097

Kusayama, T., Wan, J., Doytchinova, A., Wong, J., Kabir, R. A., Mitscher, G., et al. (2019). Skin sympathetic nerve activity and the temporal clustering of cardiac arrhythmias. *JCI Insight* 4, e125853. doi:10.1172/jci.insight.125853

Kusayama, T., Wong, J., Liu, X., He, W., Doytchinova, A., Robinson, E. A., et al. (2020). Simultaneous noninvasive recording of electrocardiogram and skin sympathetic nerve activity (neuECG). *Nat. Protoc.* 15, 1853–1877. doi:10.1038/s41596-020-0316-6

Lake, D. E., Richman, J. S., Griffin, M. P., and Moorman, J. R. (2002). Sample entropy analysis of neonatal heart rate variability. *Am. J. Physiol. Regul. Integr. Comp. Physiol.* 283, R789–R797. doi:10.1152/ajpregu.00069.2002

Lo, K. B., Gul, F., Ram, P., Kluger, A. Y., Tecson, K. M., McCullough, P. A., et al. (2020). The effects of SGLT2 inhibitors on cardiovascular and renal outcomes in diabetic patients: a systematic review and meta-analysis. *Cardiorenal Med.* 10, 1–10. doi:10.1159/000503919

Lo, M. T., Chang, Y. C., Lin, C., Young, H. W. V., Lin, Y. H., Ho, Y. L., et al. (2015). Outlier-resilient complexity analysis of heartbeat dynamics. *Sci. Rep.* 5, 8836. doi:10.1038/srep08836

Lopaschuk, G. D., and Verma, S. (2020). Mechanisms of cardiovascular benefits of sodium glucose co-transporter 2 (SGLT2) inhibitors: a state-of-the-art review. *JACC Basic Transl. Sci.* 5, 632–644. doi:10.1016/j.jacbts.2020.02.004

Molina-Vega, M., Muñoz-Garach, A., Fernández-García, J. C., and Tinahones, F. J. (2018). The safety of DPP-4 inhibitor and SGLT2 inhibitor combination therapies. *Expert Opin. Drug Saf.* 17, 815–824. doi:10.1080/14740338.2018.1497158

Pan, J., and Jia, W. (2018). Early-onset diabetes: an epidemic in China. *Front. Med.* 12, 624–633. doi:10.1007/s11684-018-0669-1

Qaseem, A., Barry, M. J., Humphrey, L. L., Forciea, M. A., Fitterman, N., Horwitch, C., et al. (2017). Oral pharmacologic treatment of type 2 diabetes mellitus: a clinical practice guideline update from the American College of Physicians. *Ann. Intern. Med.* 166, 279–290. doi:10.7326/M16-1860

Rosenstock, J., Perkovic, V., Johansen, O. E., Cooper, M. E., Kahn, S. E., Marx, N., et al. (2019). Effect of linagliptin vs placebo on major cardiovascular events in adults with type 2 diabetes and high cardiovascular and renal risk: the Carmelina randomized clinical trial. *JAMA* 321, 69–79. doi:10.1001/jama.2018.18269

Sano, M. (2018). A new class of drugs for heart failure: SGLT2 inhibitors reduce sympathetic overactivity. *J. Cardiol.* 71, 471–476. doi:10.1016/j.jjcc.2017.12.004

Sano, M. (2020). Sodium glucose cotransporter (SGLT)-2 inhibitors alleviate the renal stress responsible for sympathetic activation. *Ther. Adv. Cardiovasc. Dis.* 14, 1753944720939383. doi:10.1177/1753944720939383

Sardu, C., Massimo Massetti, M., Rambaldi, P., Gatta, G., Cappabianca, S., Sasso, F. C., et al. (2022). SGLT2-inhibitors reduce the cardiac autonomic neuropathy dysfunction and vaso-vagal syncope recurrence in patients with type 2 diabetes mellitus: the SCAN study. *Metabolism* 137, 155243. doi:10.1016/j.metabol.2022.155243

Scheen, A. J. (2018). Cardiovascular effects of new oral glucose-lowering agents: DPP-4 and SGLT-2 inhibitors. *Circ. Res.* 122, 1439–1459. doi:10.1161/CIRCRESAHA.117.311588

Scott, L. J. (2011). Linagliptin: in type 2 diabetes mellitus. *Drugs* 71, 611–624. doi:10.2165/11207400-000000000-00000

Seidu, S., Kunutsor, S. K., Topsever, P., and Khunti, K. (2022). Benefits and harms of sodium-glucose co-transporter-2 inhibitors (SGLT2-I) and renin-angiotensin-aldosterone system inhibitors (RAAS-I) versus SGLT2-Is alone in patients with type 2 diabetes: a systematic review and meta-analysis of randomized controlled trials. *Endocrinol. Diabetes Metab.* 5, e00303. doi:10.1002/edm2.303

Shimizu, W., Kubota, Y., Hoshika, Y., Mozawa, K., Tara, S., Tokita, Y., et al. (2020). Effects of empagliflozin versus placebo on cardiac sympathetic activity in acute myocardial infarction patients with type 2 diabetes mellitus: the EMBODY trial. *Cardiovasc. Diabetol.* 19, 148. doi:10.1186/s12933-020-01127-z

Subrahmanyan, N. A., Koshy, R. M., Jacob, K., and Pappachan, J. M. (2021). Efficacy and cardiovascular safety of DPP-4 inhibitors. *Curr. Drug Saf.* 16, 154–164. doi:10.2174/1574886315999200819150544

Syngle, A., Chahal, S., and Vohra, K. (2021). Efficacy and tolerability of DPP4 inhibitor, teneligliptin, on autonomic and peripheral neuropathy in type 2 diabetes: an open label, pilot study. *Neurol. Sci.* 42, 1429–1436. doi:10.1007/s10072-020-04681-2

Talha, K. M., Anker, S. D., and Butler, J. (2023). SGLT-2 inhibitors in heart failure: a review of current evidence. *Int. J. Heart Fail* 5, 82–90. doi:10.36628/ijhf.2022.0030

Trunkvalterova, Z., Javorka, M., Tonhajzerova, I., Javorkova, J., Lazarova, Z., Javorka, K., et al. (2008). Reduced short-term complexity of heart rate and blood pressure dynamics in patients with diabetes mellitus type 1: multiscale entropy analysis. *Physiol. Meas.* 29, 817–828. doi:10.1088/0967-3334/29/7/010

Tsai, W. C., Hung, T. C., Kusayama, T., Han, S., Fishbein, M. C., Chen, L. S., et al. (2023). Autonomic modulation of atrial fibrillation. *JACC Basic Transl. Sci.* 8, 1398–1410. doi:10.1016/j.jacbts.2023.03.019

Uradu, A., Wan, J., Doytchinova, A., Wright, K. C., Lin, A. Y. T., Chen, L. S., et al. (2017). Skin sympathetic nerve activity precedes the onset and termination of paroxysmal atrial tachycardia and fibrillation. *Heart Rhythm* 14, 964–971. doi:10.1016/j.hrthm.2017.03.030

Wu, P., and Vaseghi, M. (2020). The autonomic nervous system and ventricular arrhythmias in myocardial infarction and heart failure. *Pacing Clin. Electrophysiol.* 43, 172–180. doi:10.1111/pace.13856

Yau, K., Dharia, A., Alrowiyti, I., and Cherney, D. Z. I. (2022). Prescribing SGLT2 inhibitors in patients with CKD: expanding indications and practical considerations. *Kidney Int. Rep.* 7, 2546–2547. doi:10.1016/j.ekir.2022.08.016

Zelniker, T. A., Wiviott, S. D., Raz, I., Im, K., Goodrich, E. L., Bonaca, M. P., et al. (2019). SGLT2 inhibitors for primary and secondary prevention of cardiovascular and renal outcomes in type 2 diabetes: a systematic review and meta-analysis of cardiovascular outcome trials. *Lancet* 393, 31–39. doi:10.1016/S0140-6736(18)32590-X

# Frontiers in Pharmacology

**Explores the interactions between chemicals and living beings**

The most cited journal in its field, which advances access to pharmacological discoveries to prevent and treat human disease.

---

## Discover the latest Research Topics

See more →


**Frontiers**

Avenue du Tribunal-Fédéral 34
1005 Lausanne, Switzerland
frontiersin.org

**Contact us**

+41 (0)21 510 17 00
frontiersin.org/about/contact